Poly(lactide):

From Hyperbranched Copolyesters to New Block Copolymers with Functional Methacrylates

Florian Karsten Wolf

geboren in Mainz

Mainz, den 26.05.2010

Dekan:

Prodekan:

1. Berichterstatter:

2. Berichterstatter:

Tag der Mündlichen Prüfung: 01.07.2010

Hiermit versichere ich gemäß § 10 Abs. 3d der Promotionsordnung vom 24.07.2007, dass ich die als Dissertation vorgelegte Arbeit selbst angefertigt und alle benutzten Hilfsmittel (Literatur, Apparaturen, Material) in der Arbeit angegeben habe.

Die als Dissertation vorgelegte Arbeit wurde in der Zeit von April 2007 bis Mai 2010 am Institut für Organische und Makromolekulare Chemie an der Johannes Gutenberg-Universität Mainz im Arbeitskreis von Univ.-Prof. Dr. Holger Frey angefertigt.

„Ich bin immer noch verwirrt, aber auf einem höheren Niveau.“

Enrico Fermi, Kernphysiker (1901-1954)

Table of Contents

Motivation and Objectives

The recent progress in materials for medical and environmental applications largely relies on the development of biocompatible polymers. Among these, the group of biodegradable aliphatic poly(ester) represents a synthetically well accessible species. Especially poly(lactide), poly(glycolide), and poly(ε-caprolactone) have found practical application in bone fixation devices and surgical sutures for almost 30 years and represent the most successful and versatile members of their class. The production of poly(lactide) from renewable resources renders it highly interesting for the replacement of commodity polymers in e.g. packaging applications. Increased synthetic control of polymer properties now permits the production of more sophisticated polymer systems for therapeutic applications. The recent successes in controlled ring-opening polymerization of lactones, especially those related to highly efficient and metal free organocatalysis, are very promising and should expand the synthetic possibilities tremendously.

Particularly the advent of non linear polymer structures has found increasing attention in recent years. The introduction of dendritic units in the poly(lactide) backbone represents a promising method to alter the polymers' physical properties and thus compensate the shortcomings of the linear analog. Objectives are tailoring of degradability and increase in the number of accessible endgroups.

An elemental drawback of conventional aliphatic poly(ester)s hampering their use in physiological and hence water-based environment is their lack of diversity regarding polarity and functionality. Hydrophilicity is a central issue in the design of amphiphilic, poly(ester)-based block copolymers. Therefore, the development and polymerization of new monomers is thus vital for creating high performance polymers for biomedical applications.

Besides ring-opening polymerization of lactones, several polymerization mechanisms can be exploited: One of contemporary interest with excellent tolerance towards functional groups as well as the poly(ester) backbone is controlled radical polymerization. This method should allow for a flexible combination of poly(ester)s with functionally diverse methacrylates resulting in amphiphilic block copolymers.

The objective of this work is the development of novel pathways to poly(lactide) topologies. Star-shaped and branched poly(lactide)s are of particular interest. The latter

represent a great synthetic challenge which shall be approached in a one-step strategy. Besides the materials' properties, the investigation of the development of branching in the course of the copolymerization is of central interest. The development of hydroxyl-functional lactone monomers and inimers shall be pursued to create branched and/or functional poly(ester)s. The combination of poly(lactide) with other, non-poly(ester) based, hydrophilic, functional, and biocompatible building blocks to copolymers shall be explored. This approach benefits from the good degradability, natural hydrophobicity, and interesting stereochemistry of lactide as well as the easy functionalization of epoxides and methacrylate-monomers which represent flexible hydrophilic building blocks. Different living polymerization methods shall be combined to provide easy access to well-defined (multi)block copolymers. The self-aggregation and superstructure formation of these block copolymers are of particular interest with regard to their application in targeted drug delivery systems.

Abstract

The prologue of this thesis (**Chapter 1.0**) gives a general overview on lactone based poly(ester) chemistry with a focus on advanced synthetic strategies for ring-opening polymerization, including the emerging field of organo catalysis. This section is followed by a presentation of the state-of the art regarding the two central fields of the thesis: (i) polyfunctional and branched poly(ester)s as well as (ii) the development of new poly(ester) based block copolymers with functional methacrylates. Several examples for the synthesis of functional lactone and carbonate monomers are presented in **Chapter 1.1**. These are particularly interesting for the realization of a lactone-based "inimer" concept which provides access to branched structures. The pathways to dendritic, as well as hyperbranched polymers are presented, highlighting the principles of ring-opening multibranching, as well as self condensing vinyl polymerization. **Chapter 1.2** illuminates the vast potential of block copolymers composed of poly(ester)s and poly(methacrylate)s. Several synthetic approaches are being discussed. Furthermore, the perspective of these structures in biomedical applications, particularly as drug delivery systems and raw materials for tissue engineering scaffolds, is highlighted.

Chapter 2 deals with the synthesis of non-linear poly(ester) structures. In **Chapter 2.1**, the synthesis of poly(lactide)-based multiarm stars, prepared via a grafting-from method, is described. The hyperbranched poly(ether)-polyol poly(glycerol) is employed as a hydrophilic core molecule. The resulting star block copolymers exhibit potential as phase transfer agents and can stabilize hydrophilic dyes in a hydrophobic environment. These partially biodegradable polymers are particularly attractive for the stabilization of the hydrophilic drugs in emulsified solutions for intravenous applications. In **Chapter 2.2**, this approach is expanded to poly(glycolide) multiarm star polymers. Generally, the problem of the poor solubility of poly(glycolide)s in common organic solvents is approached by the reduction of the total chain length. These poly(glycolide)-poly(glycerol) multiarm star block copolymers exhibit solubility in DMF and DMSO up to a glycolide weight fraction exceeding 90%, which corresponds to a molecular weight of 16.000 g/mol. Furthermore, the problematically high melting temperatures of poly(glycolide) could be significantly reduced and thus allow for

facilitated processing conditions of the polymer melt. In **Chapter 2.3**, the first successful synthesis of hyperbranched poly(lactide)s is presented. The ring-opening, multibranching copolymerization of lactide with the "inimer" 5HDON (a hydroxyl-functional lactone monomer) was carefully examined by NMR spectroscopy, SEC, and MALDI-ToF MS. Up to 50% of the employed inimer were incorporated as dendritic units. Besides a precise molecular characterization involving the determination of the degree of branching, we were able to put forward a conclusive reaction model for the formation of branching during the copolymerization. A selective functionalization of the focal unit of the branched copolymers was accomplished. Organo base mediated polymerization proved to be equally successful and additionally allowed the synthesis of branched and linear lactone-functionalized species.

Several innovative approaches to amphiphilic poly(ester)/poly(methacrylate)-based block copolymers are presented in the third part of this thesis (**Chapter 3**). Block copolymer build-up especially relies on the combination of ring-opening and living radical polymerization. Atom transfer radical polymerization has been successfully combined with lactide ring-opening, using the "double headed" initiator 2-hydroxyethyl-2-bromo-isobutyrate. This strategy allowed for the realization of poly(lactide)-*block*-poly(2-hydroxyethyl methacrylate) copolymers, which represent promising materials for tissue engineering scaffolds with anti-fouling properties (**Chapter 3.1**). The block copolymer build-up was achieved via a two-step/one-pot strategy. This approach forgoes the use of protecting groups for HEMA by a careful selection of polymerization sequence and solvents. The oxidative deactivation of the Sn(II) transesterification catalyst of the first block by addition of a Cu(II) species allowed the circumvention of intermediate purification steps.

A series of potentially biocompatible and partially biodegradable homo- and block copolymers is described in **Chapter 3.2**. In order to create block copolymers with a comparably strong hydrophilic character, a new acetal-protected glycerol monomethacrylate monomer (*cis*-1,3- benzylidene glycerol methacrylate/BGMA) was designed. ATRP of BGMA yielded well-defined poly(methacrylate)s with pendant benzylidene acetal groups and high glass transition temperatures (115-130 °C). This hydrophobic PBGMA could be readily transformed into the hydrophilic and water-soluble poly(*iso*-glycerol methacrylate) (PIGMA) by mild acidic hydrolysis. Block copolymers of PIGMA and poly(lactide) exhibited interesting spherical aggregates in aqueous environment. Because of the unique feature of

stereocomplex formation of poly(lactide), the corresponding aggregate morphology could be adjusted by mixing two nearly identical PIGMA-b-PLA copolymers with enantiomeric poly(lactide) blocks in a 1:1 ratio. In this case the uniformly shaped micelles (20 nm) changed to large vesicles with diameters ranging from 600 to 1400 nm. In **Chapter 3.3**, poly(ethylene glycol)-*b*-PBGMA copolymers are described. Here, BGMA provides the hydrophobic block which allows the incorporation of water-insoluble fluorescent dye Nile Red in the corresponding aggregates in aqueous solution. Under physiological conditions, the aggregates are stable. At slightly acidic pH values (pH 4/37°C), they decompose due to a polarity change of the BGMA block caused by progressing acetal cleavage. The controlled release of the hydrophilic dye could be followed by fluorescence spectroscopy. This stimuli-responsive behavior renders the system highly attractive for the targeted delivery of anti-cancer drugs. In **Chapter 3.4**, which was realized in cooperation, the concept of biocompatible, amphiphilic poly(lactide) based polymer drug conjugates, was persued. This was accomplished in the form of fluorescently labeled poly(HPMA)-*b*-poly(lactide) copolymers. Ring-opening polymerization of L-lactide was followed by conversion into a chain transfer agent (CTA) and reversible addition - fragmentation and chain transfer (RAFT) polymerization of pentafluorophenyl methacrylate. Selective aminolysis of this precursor block with 2-hydroxypropylamine and dye afforded the labeled amphiphile. Fluorescence correlation spectroscopy (FCS) of the block copolymer aggregates exhibited fast cellular uptake by human cervix adenocarcinoma cells without showing toxic effects in the examined concentration range (**Chapter 4.1**).

The current state of further projects which are subject of ongoing studies is addressed in **Chapter 4**. This covers the synthesis of biocompatible star block copolymers (**Chapter 4.2**), the development of new methacrylate monomers for biomedical applications (**Chapters 4.3** and **4.4**). Finally, further investigation of hydroxyl-functional lactones and carbonates which are promising candidates for the synthesis of new hydrophilic linear or hyperbranched biopolymers, is addressed in **Chapter 4.5**.

Graphical Abstract

20

Chapter 1: Introduction

1.0 Poly(lactide), a Special Poly(ester) for Medical and Environmental Applications

Poly(lactone)s: An Interesting Familiy

Aliphatic poly(ester)s provide versatile biocompatible and biodegradable polymers with good mechanical properties. Their application as biodegradable substitutes for conventional commodity thermoplastics and applications in the biomedical field is the driving force behind their rapid development. As a consequence of the easy metabolization of the degradation products among the family of biodegradable polymers, aliphatic poly(ester)s possess a leading position. Poly(lactide)s (PLA) are the most prominent and successful example of this family.
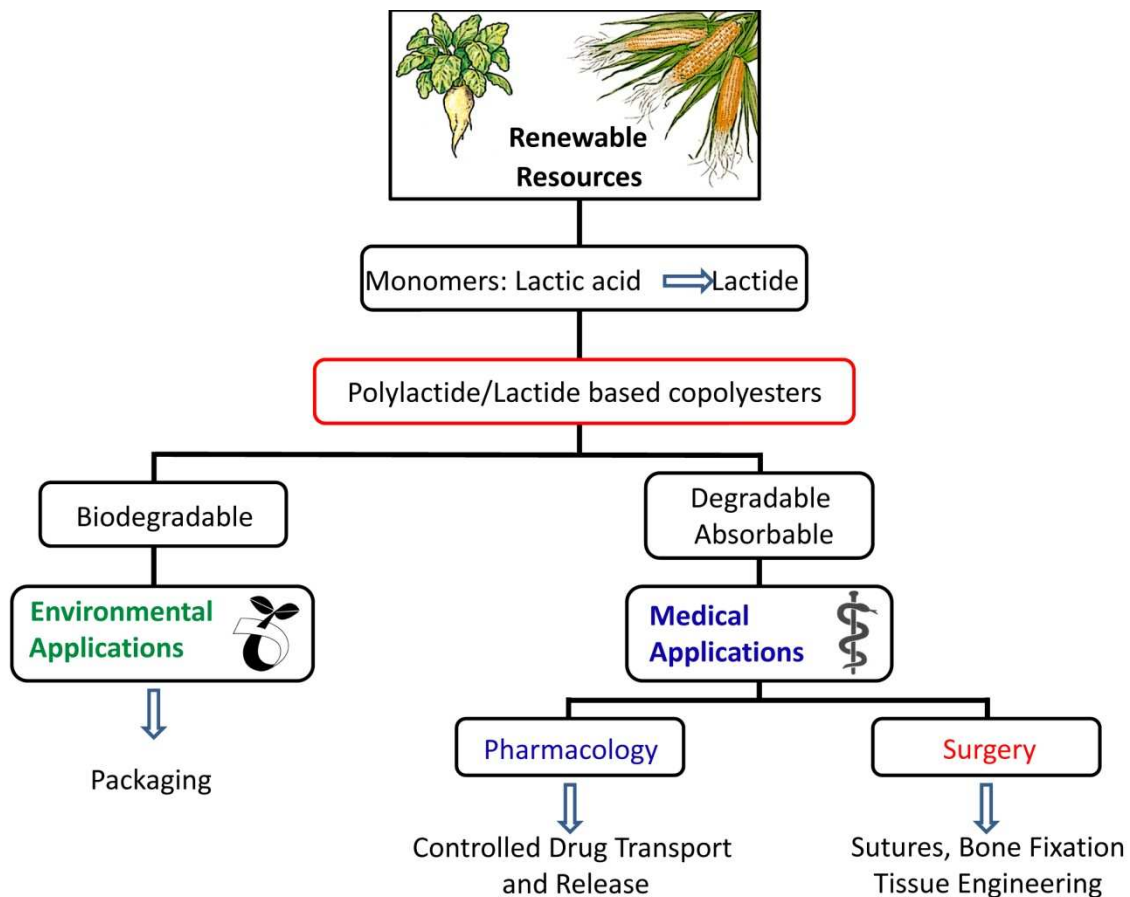
Figure 1: Production and application of poly(lactide).

Poly(ester)s generally degrade through a bulk erosion mechanism which is facilitated by diffusion of water into the polymer matrix.[1] The polarity of the poly(ester) therefore significantly influences its degradation rate (e.g. poly(glycolide) (PGA) decomposes

significantly faster than poly(ε-caprolactone) (PεCl)).[2] Thereby, the initial molecular weight of the polymer chains decreases as a result of more or less random chain scission throughout the polymer matrix.[3] Interestingly, the decrease in molecular weight initially leads to an increase in chain flexibility and therefore promotes crystallization. Throughout this process, degradation is significantly accelerated by the formation of carboxylic acid groups within the polymer matrix in an autocatalytic process. Monomeric and oligomeric material diffuses out of the amorphous regions of the polymer matrix. This stage underlines the bulk erosion character of the process.[4] The composition of the migrating species is of fundamental importance since monomeric hydroxyl acids from implanted poly(ester) material are a potential cause of inflammatory responses in the surrounding tissue and can even cause osteolysis in the affected bone.[5] Although the approach toward phase equilibrium between water and polymer is fast (adsorption), the approach toward chemical equilibrium (hydrolysis) is sufficiently slow so that a shelf life can be defined for a particular resin or article.[6] Degradation can be accelerated through the action of a range of enzymes as well as chemically through both transesterification and hydrolysis in either acidic or basic solutions.[7]

Poly(ε-caprolactone) and poly(δ-valerolactone) are both tough and flexible polymers, a consequence of melting temperatures (T_m) around 60 °C that result largely from the crystalline domains within the polymers, and glass transition temperatures (T_g) well below room temperature.[8] PεCl has a highly flexible polymer chain which favors mobility and thus a high degree of crystallinity.

Poly(glycolide), PGA, is also highly crystalline and displays a high melting point (225-230 °C) which can be attributed to a high carboxylic group density per carbon. These characteristics also result in a relatively poor solubility. Only a small range of fluorinated solvents can break up the crystalline domains (e.g. hexafluoro isopropanol). This problem can be overcome via the copolymerization with other lactone monomers such as lactide. Poly(lactic acid) (PLA) bears an additional methyl group which sterically shields the ester group. The increase in hydrophobicity results in slower degradation rates compared to poly(glycolide).

The two stereo centers of lactide provide a multitude of possibilities. Three possible configurations exist: The enantiomeric L,L- and D,D-Lactide form and the identical D,L- or L,D-

meso compound. The racemic or equimolar mixture of the L and D enantiomers (*racemo*-lactide) froms a stereocomplex and shows an increased melting point.

Among the lactide isomers reactivity is slightly different: Due to a higher ring-strain *meso*-lactide has an elevated rate of hydrolysis and a greater tendency to polymerize. The L- and D-enantiomers have identical rates. ROP (ring-opening polymerization) of the pure *racemo* compounds in the absence of epimerization reactions enables synthesis of the isotactic, highly crystalline PLLA or PDLA (T_m = 170-180°C). Both *meso*- and D-lactide induce twists in the otherwise very regular poly(L-lactide) molecular architecture and therefore influence the crystallization tendency. PLA derived from more than 93% L- lactic acid can be semi-crystalline whereas PLA composed of 50 to 93% L-lactic acid is strictly amorphous. Molecular imperfections are responsible for the decrease in both the rate and extent of poly(L-lactide) crystallization and therefore lead to increased degradation rates. However, the glass transition temperatures are less affected by the PLAs tacticity (T_g=50-60 °C).

Fascinatingly, homo-chiral PLLA and PDLA polymers form a crystalline polymer upon mixing. This stereocomplexation between enantiomeric, isotactic PLLA and PDLA chains was first observed in 1987.[9] The resulting blends show improved mechanical properties, thermal-(T_m = 220-230°C) and hydrolysis-resistance compared to the single compounds.

Table 1: Thermal behavior of lactone derived poly(esters) (taken from reference [10]).

Polymer	Tacticity	$T_g/°C^a$	$T_m/°C^b$
Poly(ε-caprolactone)^c	—	−60	65
Poly(δ-valerolactone)^c	—	−63	60
Poly(γ-butyrolactone)^c	—	−59	65
Poly(β-butyrolactone)^c	Atactic	−2	—
Poly(β-butyrolactone)^c	Isotactic	5	180
Poly(β-propriolactone)^c	—	−24	93
Poly(glycolic acid)^c	—	34	225
Poly(lactic acid)^c	Atactic	45–55	—
Poly(lactic acid)^c	Isotactic	55–60	170
Poly(lactic acid)^d	Syndiotactic	34	151
Poly(lactic acid)^e	Heterotactic	<45	—
Poly(lactic acid)^d	Stereocomplex	65–72	220–230

Industrial Production

Polymer grade L-lactide is produced industrially by metal-catalyzed intramolecular transesterification of low molecular weight poly(L-lactic acid) (PLLA) in a solvent free, continuous process. The corn to be used as the raw material is estimated to be less than 0.2% of the total U.S. corn crop.

Poly(lactide) can be synthesized in two different ways: either the step polycondensation of lactic acid or the ring opening polymerization (ROP) of the cyclic diester lactide. The more traditional polycondensation[11] usually requires high temperatures, long reaction times and a continuous removal of water to finally recover quite low molecular weight polymers with poor mechanical properties. Material properties of low molecular weight PLAs can be improved by (diol) chain coupling with isocyanates.[12]

The ring opening polymerization provides a direct and easy access to the corresponding high molecular weight poly(lactide). ROP of lactide is known to be promoted by Lewis acid type catalysts such as metals, metal halogenides, oxides, aryls and carboxylates. The main representative of this group of catalysts is tin(II)bis(2-ethylhexanoate). The ring opening polymerisation is initiated by protic compounds such as water, alcohols, thiols and amines, which are either present as impurities in the lactide dimer or can be added on demand. Recent developments in lactone polymerization will be dicussed in the following paragraph.

In comparison to some commodity polymers, PLA based products perform less good in terms of their impact strength and show a low elongation at break, a poor melt strength, a low heat deflection temperature (HDT), a narrow processing window and low thermal stability. These problems can be overcome by copolymerization with other lactones and the appropriate choice of processing conditions. High molecular weight PLA is a stiff, colorless and glossy thermoplastic having properties similar to polystyrene (PS) and can be processed by injection molding, fiber spinning, thermoforming and film casting.[13] Where poly(propylene) (PP) and poly(ethylene) (PE) can be blended with other polymers, PLA is not compatible with other resins. Alternatively it can be coextruded with other resins with the option of choosing an appropriate tie resin to enhance interlayer adhesion.[14]

Especially *Nature Works*, a joint venture Company founded by Cargill and DOW Chemicals and now completely owned by Cargill has driven forward the commercial production of poly(lactide) based products (Ingeo®). The manufacturing facility, located in Blair, Nebraska, USA, came online in 2002 and has an annual name plate capacity of 140,000 tons of polymer (Figure 2). Production on this scale has lifted PLA into the olymp of commodity polymers. The current resin price is situated at approx. 4.8 US $/kg (at a minimum order of 1000 kg).

In Germany, a plant with an annual capacity of 60.000/year shall be completed until mid 2012 by a German/Swiss joint venture company (Pyramid Bioplastics Guben GmbH).[15]

Figure 2: Nature Works® Production facility of poly(lactide) surrounded by corn fields in Blair, Nebraska (USA).

Although slightly more expensive than comparable poly(olefine)s 1.5-4 US $/kg it is cheaper than e.g. PET/PBT (poly(ethylene or butylene terephtalate) (approx. 5-6 US $/kg). Food packaging and agricultural applications are currently the main field of application (In the form of fibers and nonwovens, films, extruded and thermoformed containers, and extrusion and emulsion coatings).[16] Next to a better carbon dioxide balance, complete biodegradation of the environmentally benign PLA is a key advantage. Films made with PLA shows no detectable permeation of flavor and aroma into or out of food products. PLA film is also resistant to most oils and fats found in food products including dry foods such as cake mixes.

Bottles can be made from PLA by injection stretch blow-molding (ISBM) with characteristics similar to PET. In contrast to oxygen, PLA's carbon dioxide transfer rate is high so it cannot

retain carbonation found in soft drinks or beer. Consequently, bottles made with PLA are best suited for dairy, juices or water products. Film made from PLA has similar characteristics as cellophane, oriented poly(propylene) (OPP) or oriented poly(ehthylene) (OPE). The polymer offers a combination of performance properties in film applications, including high clarity and gloss.[17]

ROP of Lactide and other Lactones: General Aspects

There has been much research directed toward the controlled ROP of commercially available cyclic esters including glycolide, lactide, caprolactone, valerolactone and propiolactones since it allows the preparation of aliphatic poly(ester)s with highly controlled molecular parameters. Despite of the reversibility, ROP of lactones can reflect many aspects of living polymerization. Particularly polymerization control and rate are not necessarily concuring factors. A variety of catalytic systems have been investigated to mediate the ROP process more efficiently including the development of well-defined metal complexes, organic catalysts and the study of enzymatic catalysis.[18] These will be reviewed in the following.

The synthesis of PLA by ROP was first reported by Carothers et al. in 1932.[19] Low-molecular-weight polymer was produced and the synthesis of high molecular weight materials was not possible until the development of effective lactide purification techniques in the 1950s[20]:
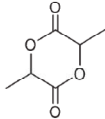
Darstellung von Lactid

Aus dem Forschungslaboratorium für makromolekulare Chemie
Dr. J. Kleine, München (1958)

*„Für die Depolymerisation wurden im allgemeinen **Polykondensate** der Milchsäure verwendet, die ohne Kondensationskatalysatoren hergestellt waren. Die verhaltnismäßig niedermolekularen Poly(lactide) wurden im Allgemeinen unter Zusatz von 0,1-1,0 g Zinkstaub der Vakuumdestillation unterworfen, wobei die Temperatur des Kolbeninhaltes langsam von 200 auf 260°C gesteigert wurde. Sdp.: 148-150°C. Zweckmäßig erwies sich eine kontinuierliche Zuführung des Polylactid in geschmolzener Form während der Vakuumdestillation. Das übergegangene Lactid erstarrte im Auffanggefäß, welches mit Eiswasser gekühlt wurde, zu weißen Kristallen, welche teilweise gelblich verfärbt waren. Ausbeute über 90 % d. Th. Das Rohlactid enthält noch eine Reihe von Verunreinigungen wie Trilactylsäure) und Wasser. Zwecks Entfernung der Verunreinigungen wurde das Lactid mehrmals **umkristallisiert**. Im Allgemeinen wurde hierfür wasserfreies Äthylacetat verwendet. Eine ungenügende Reinigung führt bei der Polymerisation zu Kettenabbruch resp. wechselnden Viskositäten, die einen Vergleich über die Wirksamkeit der einzelnen Katalysatoren unmöglich machen."*

During the last half century many different catalysts have been studied to increase the reaction productivity. Among them, 2-ethylhexanoic acid tin(II) salt (Sn(Oct)$_2$) is the most widely used catalyst in both scientific research and industrial production and is the only one that has been accepted by the U.S. Food and Drug Administration (FDA).

Table 2: Enthalpy and entropy of ROP for selected lactones (298 K) [(taken from reference 21)]

Ring size					
	β-Propiolactone	γ-Butyrolactone	δ-Valerolactone	Lactide	ε-Caprolactone
ΔH/kJ mol^{-1}	−82.3	5.1	−27.4	−22.9	−28.8
ΔS/J mol^{-1} K^{-1}	−74^a	−29.9^a	−65.0^a	−25.0^b	−53.9^a

^{a} [Monomer] = 10 M, conducted in liquid monomer. ^{b} [Monomer] = 1 M, conducted in solution. The values are taken from ref. 14.

Monomers such as ε-caprolactone, δ-valerolactone, β-butyrolactone and the cyclic diesters, lactide and glycolide, are typically used for poly(ester) synthesis via ROP as a consequence of their good polymerizability arising primarily from their ring strain. The enthalpic contribution (Table 2 & Table 3) is very important, since ring-opening is coupled to a loss in entropy and the monomer/polymer equilibrium increases with rising temperature until the ceiling temperature is reached.

$$\Delta G_P = \Delta H_P - T\Delta S_P$$

The equilibrium monomer concentration can be easily obtained from the thermodynamic parameters using the equation from Daiton and Ivins, which was originally developed for the reversible addition polymerization.[22]

$$\ln [M]_{eq} = \Delta H_P/RT - \Delta S^0{}_P/R$$

Especially, when melt polymerization or simple processing of the poly(ester) is desired and elevated temperatures are required to suppress crystallization and achieve sufficient fluidity, this term has to be considered carefully. Conversely, this means that the experimentally determined equilibrium monomer concentrations $[M]_{eq}$, allows a determination of the monomers thermodynamic parameters. On the other hand, this thermodynamic

phenomenon allows the simple production of lactones from the polymer melt – which is therefore common praxis.

Table 3: Enthalpy and entropy of ROP for selected lactones at 373 K: PL= β-Propiolactone, LA= Lactide, DX =1,4-Dioxane-2-on; CL= ε-Caprolactone

Monomer	Ring size	Monomer Polymer States[a]	$\dfrac{\Delta H_p}{\text{kJ/mol}}$	$\dfrac{\Delta S_p^0}{\text{J/mol K}}$	$\dfrac{[M]_{cq}}{\text{mol/L}}$	
PL[11]	4	ll	-74.4	-51	2.45×10^{-7} [b]	
LA[12]	6	ss	-22.9	-41	0.09 [c]	
DX[13]	6	ll	-13.8	-45	2.5 [c]	
CL[14]	7	ll	-13.9	-10.4	$0.37^{[b]}$ (≈0) [c]	

[a] l – liquid, s-solution
[b] calculated from equation 4
[c] observed experimentally
[d] estimated from data in ref.[15]

The formation of strainless cyclic oligomers is a special form of transesterification based depolymerization. This intramolecular back biting reaction is in particular pronounced for caprolactone and dioxanone. This phenomenon can nowadays be visualized with the help of MALDI-ToF (matrix assisted laser desorption/ionization - time of flight) mass spectrometry.[23] The corresponding species can be readily identified since they lack the employed initiator/endgroup, compared to linear polymer chains.[24,25]

Metal Catalyzed Polymerization[26]

Practical Aspects
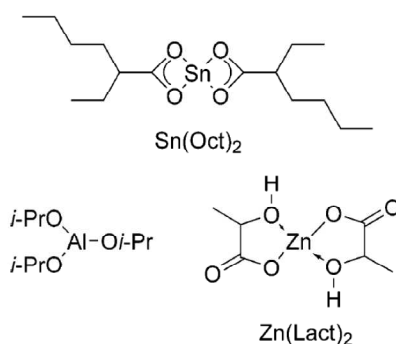
Figure 3: Structures of the most prominent metal based transesterification catalysts: Tin(II) octanoate [Sn(Oct)$_2$], aluminum(III) isopropoxide [Al(Oi-Pr)$_3$] and zinc(II) lactate [Zn(Lact)$_2$].

The most widely used complex for the industrial preparation of PLA (poly(L-lactide) and PLGA (poly(L-lactide-co-glycolide) is tin(II) bis(2-ethylhexanoate) (Sn(Oct)$_2$)(Figure 3). It has to be emphasized, that Sn(Oct)$_2$ is not the actual initating species and a protic co-initiator is necessary. If used without the addition of protic compounds, initiation usually takes place by trace contaminations of water, forming a carboxylic acid end-group. In a moisture-rich environment the poly(lactide) polymer of high molecular mass is thermodynamically unstable, as explained by the small equilibrium constant for the condensation reaction of lactic acid to poly(lactic acid).

Aluminum alkoxides have also proven to be catalysts for the ROP of cyclic esters. The archetypal example, namely, Al(Oi-Pr)$_3$, has also been intensively used for mechanistic studies but has not found industrial relevance since it is significantly less active than Sn(Oct)$_2$ and long reaction times are required under similar polymerization conditions.[27]

Even though Sn(Oct)$_2$ can promote quite fast lactide polymerisation, it is also known to have adverse effects on the PLA molecular weight and properties, as a result of back-biting and intermolecular transesterification reactions, not only during the lactide polymerisation, but also during any further melt processing. Intramolecular transesterification reactions are responsible for the formation of cyclic compounds of various sizes. Furthermore, polymerization of cyclic esters such as lactide is also perturbed by intermolecular transesterification: A growing chain attacks another chain and segmental exchange occurs (Figure 4).
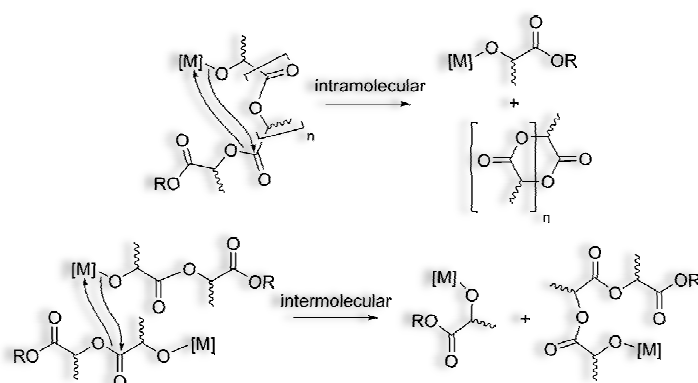
Figure 4: Intra- and intermolecular transesterification reactions in lactide polymerization.
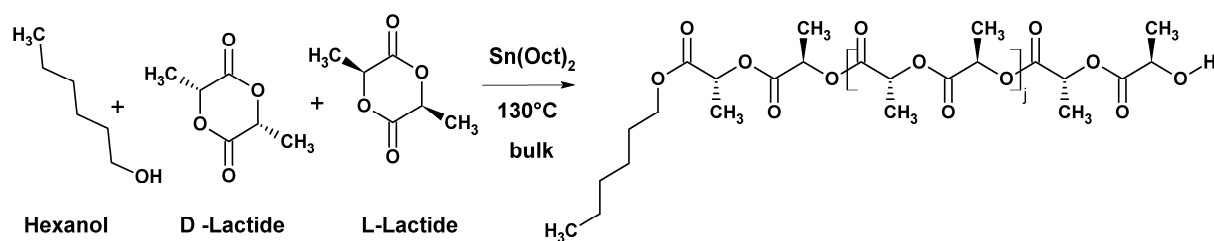
Figure 5: Polymerization of a 1:1 mixture of D- and L-Lactide with 0.1 mole% Sn(Oct)$_2$ in bulk at 130°C (M/I= 40/1). Samples were harvested in logarithmically increasing intervals and analyzed via SEC and MALDI-Tof. The polymerization was continued beyond the monomer/polymer equilibrium.
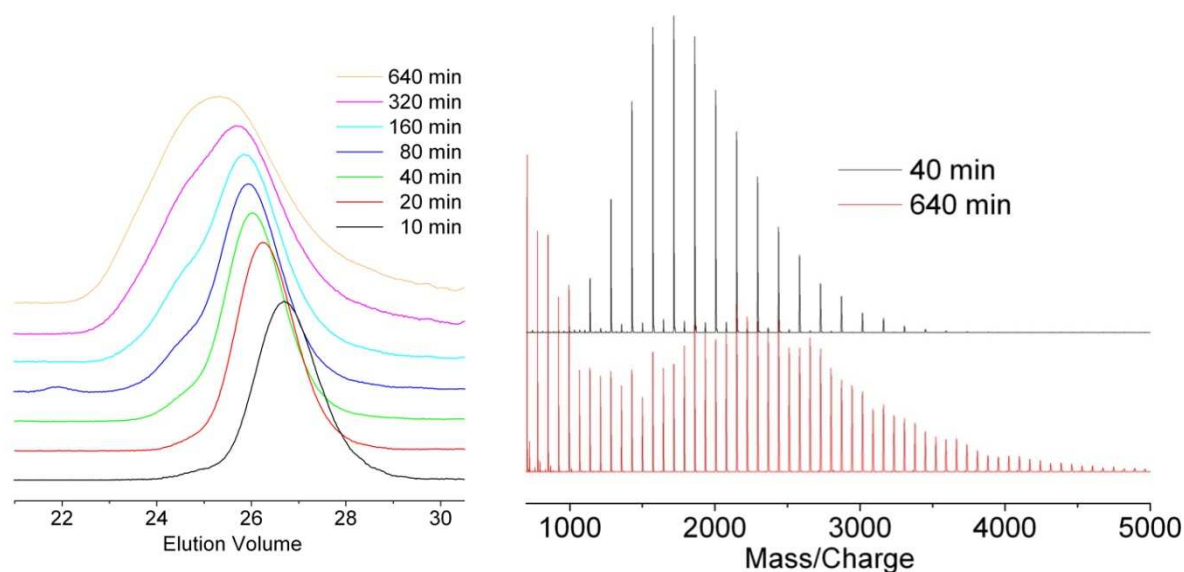
Figure 6: left: SEC (in THF) – significant broadening of the traces can be observed; right, MALDI-ToF spectra of the sample before and after reaching the equilibrium monomer concentration.

Since the rate of transesterifiction is significantly slower than the rate of propagation, well-defined polymers are accessible with most transesterification catalysts, when the polymerization time does not significantly exceed the time needed for an (almost) complete consumption of the monomer. This is illustrated by a model experiment depicted in Figure 5. A mixture of D- and L-Lactide (to prevent crystallization) was copolymerized in bulk under Sn(Oct)$_2$ catalysis (0.1 mol%) and 1-hexanol as initiator at 130°C (Figure 5).[28] Under these conditions, the monomer is known to be consumed rapidly within minutes. Nevertheless, the polymerization kinetics were followed over a time scale, reflecting a multitude of the "optimal" polymerization time, i.e. for 11 h. In Figure 7, the evolution of molecular weight and polydispersity show an interesting correlation. In the beginning (below 100 min) we

observe only a small increase in polydispersity and the molecular weight passes through a maximum and decreases beyond the time required to reach the maximum monomer conversion. Transesterifcation reactions are accompanied by the appearance of poly(lactide) chains with an odd number of lactice acid units – a phenomenon that is easily confirmed via MALDI-ToF spectroscopy (Figure 6).
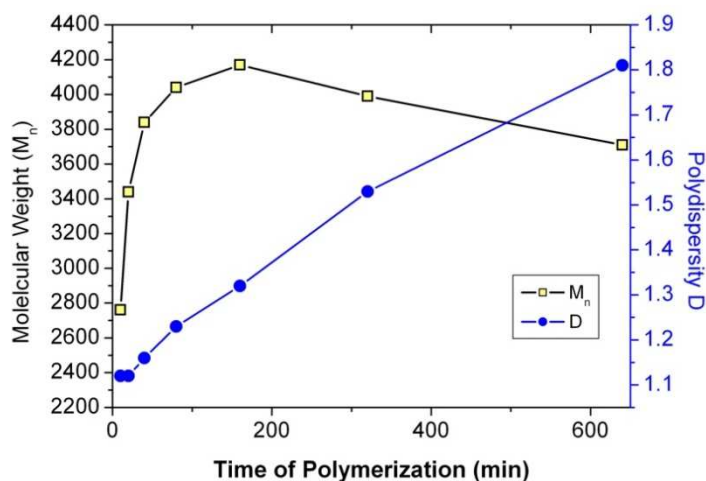
Figure 7: Evolution of molecular weight (SEC, THF-PS-standards) and polydispersity for $Sn(Oct)_2$ catalyzed lactide polymerization at 130°C.

Although the polymerization rate increases with temperature, the maximum molecular weight observed substantially decreases due to increased transesterifications reactions. This effect is enhanced particularly in the case of temperatures exceeding 150°C. Generally, the monomer conversion levels off at 98% in the 110–150°C range, but decreases down to 95% above 180°C. This can be confirmed via depolymerization experiments. In fact, this principle is used for the depolymerization of low molecular weight (condensation-type) PLA for the production of lactide. In summary, lactide polymerization data suggest a reversible rate form with a propagation term that is first order in monomer and catalyst.[29] It has to be emphasized that the catalyst concentration is affecting the reaction rate, whereas OH-bearing species (such as co-catalyst and impurities) are controlling both reaction rate and polymer molecular weight.[30] Monomer/polymer equilibriums are significantly complicated in the copolymerization of different lactones.[31,32]

Mechanism

The mechanism of ROP of lactide catalyzed by Sn(Oct)$_2$ has been investigated by many researchers. Hitherto literature is still at loss for an unequivocal description. The reaction mechanism is very difficult to determine by kinetic studies or from end groups analysis of the reaction products. Above all, it is difficult to elucidate the structure of the actual initiating and propagating species during ROP by spectroscopic or chromatographic methods. Generally, there are two popular rival (initiation) mechanisms which have debated this reaction step heavily:

The first mechanism (mainly from Kricheldorf et al.[33,34]) is based on a kind of "monomer activation", where monomer, OH-bearing species, and catalyst form a ternary complex. Accordingly, Sn- atoms are not bond to the active chains, and the corresponding polymerization rate is simply first order with respect to the initial amounts of catalyst and alcohol.

The second one was proposed by Penczek et al. and is based on the "alkoxide initiation mechanism". Accordingly, stannous octoate actually reacts with OH-bearing species to form an alkoxide that is the species initiating the polymerization.

"The appropriate experiments were carried out to show that some "mechanisms" put forward during the past few decades by several research groups were not sufficiently substantiated."

(Penczek, S. et al. in Macromolecules 2000)[35]

Therefore, Sn(Oct)$_2$ and OH groups are initiator and co-initiator, respectively, often indicated as catalyst and "co-catalyst". The direct observation of macromolecules (some might say, "oligomers") containing Oct-Sn-O-R end groups by MALDI-TOF and the dependences of the polymerization rate upon monomer, catalyst, and "co-catalyst" concentrations are solid evidence in favor of the second mechanism. Moreover, the same authors proposed a comprehensive kinetic scheme of the reaction, also involving reversible chain transfer and "polymer-interchange reactions" (i.e. trans-esterifications).[36] As described above, such reactions are responsible for the fast interchange of active endgroups among the polymer chains and directly affect the molecular weight distribution of the final polymer. The resulting polymerization mechanism is currently the most accepted (Figure 8).
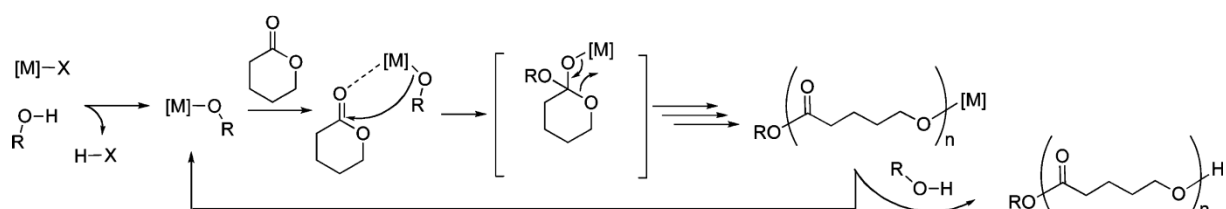
Figure 8: General mechanism for transition metal catalyzed polymerization as proposed by Penzcek et al.: It is based on the reversible formation of Sn-alkoxide species, which coordinate and insert the lactone.

Theoretical studies strongly support a coordination insertion mechanism for the lactone polymerization with Sn(II)-Salts.[37] The mechanism operates via the coordination of the lactone to the above discussed Lewis acidic metal alkoxide complex, which activates and attacks the lactone at the carbonyl carbon. Acyl bond cleavage results in ring opening and the generation of a novel metal alkoxide species from which the cycle can re-initiate. Many metals apart from Sn (i.e. Al, Mg, Zn, Ca, Fe, Y, Sm, Lu, Ti, and Zr)[38] have potential in the catalysis of the coordination–insertion polymerization. Their common features are a sufficient Lewis acidity and the possibility to form a labile metal alkoxide or amide bond.[39]

Anionic and Cationic Polymerization

Cationic

 Kricheldorf et al. demonstrated the feasibility of this cationic route with alkylating agents, acylating agents, Lewis acids, and protic acids (methyl triflate) in the late 1980s, but the polymerization was far from matching "living-criteria".[40,41] Bourissou et al. reported the controlled cationic polymerization of lactide using a combination of triflic acid (as the catalyst) and a protic reagent (water or an alcohol) as an initiator in 2005.[42]

The controlled cationic ring-opening polymerization is believed to proceed by an "activated cationic polymerization" mechanism as described by Penczek for cyclic ethers in 2000,[43] where the acid would activate the cyclic ester monomer (e.g. via protonation or alkylation) and the alcohol would be the (nucleophilic) initiator of polymerization (Figure 9). Therefore Polymerization is thought to proceed by protonation of LA by triflic acid followed by nucleophilic attack by the initiating alcohol or the end of the growing polymer chain (under

acyl-oxygen cleavage). Studies by Kricheldorf and Penczek showed that the presence of a protic coinitiator is important for the controlled character of the polymerization.
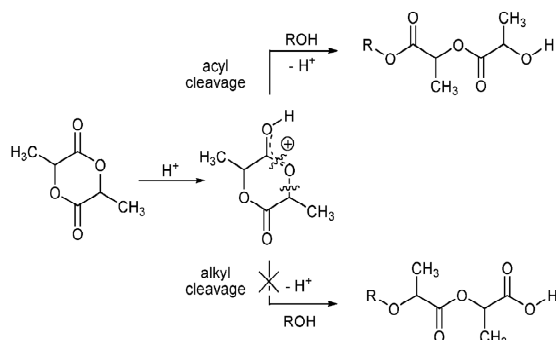
Figure 9: CROP-Mechanism (activated monomer type) as described by Bourrisou et al. (Macromolecules 2005)

Anionic

The anionic polymerization of lactones with Li or K alkoxides is well-known.[44] At increased temperature, this methods leads to significant side reactions and racemisation of the polymer due to α-H-abstractions at monomer and polymer.[45] This is also a significant problem, when alkyl-lithium compounds are used for initiation.[46] Lithium-alkoxides are efficient in initating the ROP of lactides with less pronounced side reactions.[47] However, polymerization at room temperature (20°C) with potassium counter-ion produces well-defined poly(ester)s. This technique is especially useful when block copolymers with epoxides are desired (e.g. EO–ethylene oxide) since a change of the catalyst system is not necessary. After complete consumption of the epoxide monomer, lactide can be added (after lowering the temperature).[48]

Organocatalytic Approaches[49]

The trend towards environmentally sound organocatalysts has stimulated "greener" versions of classic synthetic asymmetric reactions in organic chemistry. Next to enzymatic approaches, the extension of organic catalysis to controlled polymerization procedures is an interesting and in some aspects desirable alternative to the above presented traditional organometallic approaches. The organocatalyzed ROP of lactide clearly proceeds very

differently to ROP promoted by metal complexes as will be illustrated in the following, although not all aspects are fully understood yet.

Enzymatic ROP

The groups of Kobayashi[50] and Knani[51] independently developed the concept of enzyme-catalyzed ring-opening polymerization and polycondensation. Lipase is an enzyme class which generally catalyzes the hydrolysis of fatty acid esters in an aqueous environment in living organisms. Nevertheless, some lipases are stable in organic solvents, even at elevated temperature, and can be used for the *in vitro* formation and hydrolysis of ester bonds.[52] A remarkable feature of lipase catalyzed polymerization is their good performance in the ROP of larger lactone rings exceeding seven units, i.e. processes with no significant enthalpic contribution.[53] Hereby, the reaction even accelerates with an increase in ring size.[54] This can be explained with the decreasing polarity of the lactones with increasing ring-size which favors the rate-determining step: According to the assumed activated monomer mechanism, this is the formation of the lactone-enzyme complex.[55] Enzymes generally exhibit high stereo-, reaction-, and substrate specificity and come from renewable resources that can be easily recycled.[56] Selective α- and ω-end-functionalization is possible via the addition of functional acids.[57] This can be exploited for the formation of block copolymers via orthogonal polymerization techniques.[58] The capability to simultaneously catalyze the condensation of alcohols with acids and the ROP of esters was used in our group to create branched poly(ε-caprolactone) copolymers with 2,2-bishydroxymethyl propionic acid as branching agent.[59]

Bases: Pyridines, Amidines and Guanidines

Pyridine and dimethyl aminopyridine (DMAP) are moderate bases and good nucleophiles. They have found intense application as acylation and alkylation catalysts. This potential triggered Hedrick et al. to examine their potential in ROP of Lactide. Especially the latter, more nucleophilic compound has shown good activity in the ring-opening polymerization of lactide in melt and in solution. This was in fact the first successful organic catalytic approach for the ROP of Lactide (not including enzymes).[60] The key element is the role of the pyridine derivative. It could primarily act as a base or nucleophile.
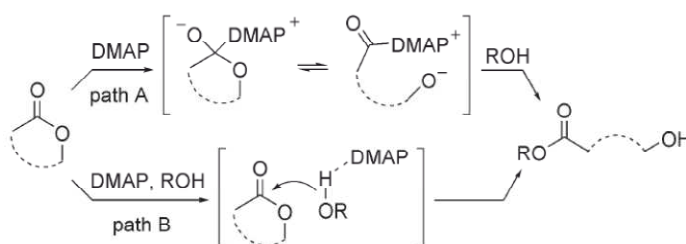
Figure 10: Nucleophilic (A) vs. base- mechanism (B) for the ROP of Lactones with DMAP

Bonduelle et al. found a higher stability of tetrahedral versus acyl-pyridinium intermediates. Their calculations therefore favor the basic mechanism (Figure 10 B) and polymerization most likely proceeds via a concerted alcohol activation process.[61] DMAP possibly acts as a bifunctional catalyst through its basic nitrogen center and the acidic ortho-hydrogen atom. This is energetically possible but not yet provable. Generally, this discussion can be extended to other organic bases, where, in the presence of OH-compounds, the base mechanism is energetically favored.
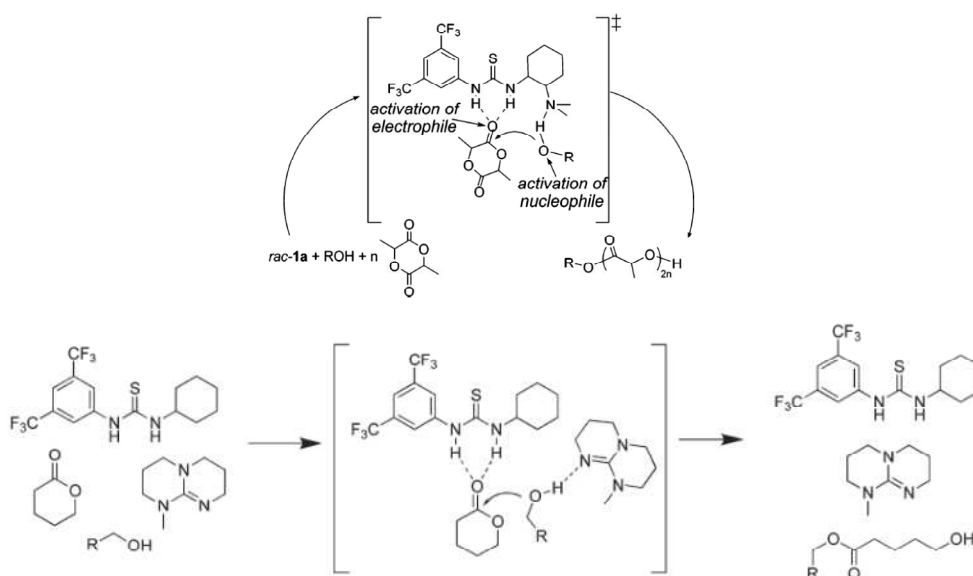
Scheme 1: ROP of VL by the dual activation of monomer and initiator by a thiourea/amine combinations[62].

"*Despite its low monomer scope and slow reaction times, DMAP marked two fundamental advances in the development of polymerization catalysts: (1) these catalysts show a high selectivity for transesterification of the monomer (propagation) relative to the open chain esters of the polymer (chain shuttling), and (2) these catalysts are compatible with a range of different initiators and cocatalysts. DMAP does not catalyze the transesterification of esters with*

secondary alcohols, which mitigates transesterification of the PLA backbone by the propagating alcohol end groups, resulting in narrow polydispersities"[63,64]

Cooperative activation of the monomer and propagating moiety is also believed to play a significant role in the polymerization with thiourea/amine (TU/A) combinations. The simple presence of nitrogen (super-) bases such as 7-methyl-(1,5,7-triazabicyclo[4.4.0]dec-5-ene) (MTBD, $^{MeCN}pK_a$ MTBDH$^+$ = 25.5) and 1,8-diazabicyclo[5.4.0]undec-7-ene (DBU, $^{MeCN}pK_a$ DBUH$^+$= 24.3) are believed to solely activate the alcohol. They show sufficient catalytic activity for lactide and trimethylene carbonate (TMC) while butyro-, valero- and caprolactone are hardly polymerized at all - although basicities are similar to those of the strong neutral phosphazene bases.[65] These have been developed by Schwesinger and Schlemper and are more universal in application. Due to their complementary character, thiourea/amine combinations are more comparable to the multiple hydrogen bonding sides, present in enzyme catalysis. Only the combination of the hydrogen bonding capabilities of the thiourea H-bond donor and the amine base is effective in catalysis (Scheme 1). It has to be emphasized that covalent connection of the components is unnecessary, although it is beneficial. An increase in basicity is also accompanied by an increase in reactivity. Although not the most reactive, (thiourea/amine)s are highly selective in the ROP of lactones transesterifications are hardly observed - even after prolonged reaction times and hence complete conversion of the monomer.[66] 1,5,7-Triazabicyclodecene (TBD) is a special guanidine superbase and shows superior catalytic activity compared to MTBD, DBU and TU/As, completes ROP of lactide within seconds and shows activity to virtually all six- and seven- membered lactones and TMCs.[67,68] Today, several mechanisms of the TBD transacetylation reaction appear to be feasible. For the ROP of lactide, nucleophilic as well as basic H-bond activation are plausible candidates (Scheme 2 & Scheme 3). The latter has been favored by theoretical calculations: "*Binding of the alcohol to TBD simultaneously activates the alcohol and creates an incipient guanidinium ion, which can function as an H-bond donor to the lactone carbonyl (analogous to a thiourea)."* [69] It is highly plausible that inter- and intramolecular transesterification reactions are influenced/promoted by the nucleophilic character of the catalyst.
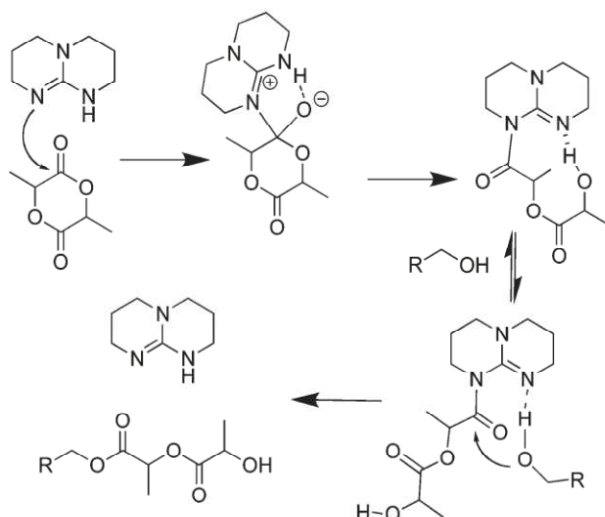
Scheme 2: Nucleophilic mechanism for the TBD-catalyzed ROP of lactide.
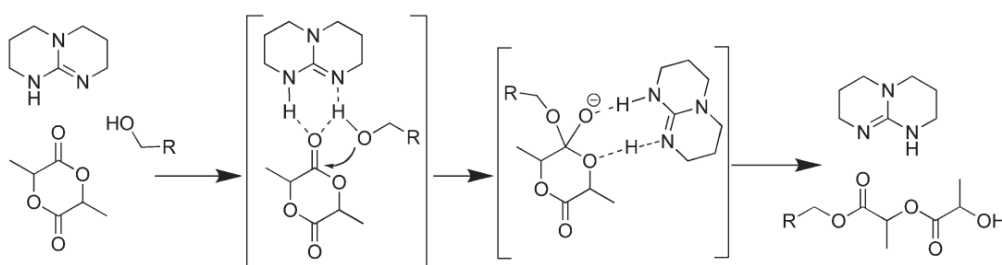
Scheme 3: TBD-catalyzed ROP of LA by the hydrogen-bonding, "basic" dual activation mechanism.

N-Heterocyclic Carbenes (NHCs): Sensitive but Versatile

Singlet-carbenes are known to be highly reactive, unstable compounds. Their stabilization and isolation were not achieved until 1991 by Arduengo and coworkers. This was made possible by pioneering studies from Breslow and Wanzlik. While Breslow proposed the special catalytic activity of deprotonated imidazilium derivates in vitamin B1 chemistry[70], Wanzlik even succeeded in the preparation of the imidazilium based carbenes[71], although the isolation was not possible back then.[72]

*"We report the synthesis, structure, and characterization of the first crystalline carbene. Carbene I, 1,3-di-l-adamantylimidazol- 2-ylidene. It forms colorless crystals with sufficient kinetic and thermodynamic stability to be easily isolated and characterized. The deprotonation of **1.3-di-l-adamantylimidazolium chloride 2** in THF at room temperature with catalytic dimsyl anion (TH,S(O)CH,) in the presence of 1 equiv. of sodium hydride produces carbene **1** (Figure 11). This deprotonation can also be accomplished with potassium tert-butoxide in THF to give a 96% yield of **1**. Carbene **1** is stable in the*
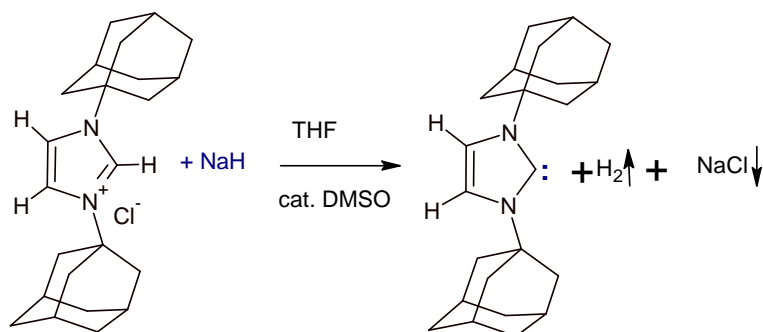
Figure 11: The first crystalline carbene, realized by Anthony J. Arduengo III, 1991

In contrast to highly unstable alkyl-carbenes, the $\pi-$ and σ-donors of the carbenes hetero-atoms stabilize the free p-Orbital. Since their first preparation carbenes have been realized in great diversity, varying in the incorporated heteroatoms and substituents. They are strong bases and, similar to phosphines, good ligands in organometallic chemistry and played an important role in the development of the second generation Grubbs catalyst for olefin metathesis.[74,75]

In general, NHCs are basic, soft, and nucleophilic species and recognized as good σ-donors and poor π-acceptors. In 2002 it was discovered that NHCs are effective organocatalysts for transesterification reactions.[76,77] In the following, this discovery lead to their investigation as catalysts for the ring-opening polymerization of lactones.[78,79]

The generation of imidazolium carbenes is generally accomplished via reaction of the respective N,N'-substituted ethylenediamines with aldehydes. Subsequent reaction of the corresponding salts/adducts with the appropriate bases or thermolysis releases the carbene[80]. Imidazole-based catalysts are significantly more active towards ROP than the thiazolium-based analogs. Less sterically demanding carbenes were found to be more active towards ring-opening polymerization (ROP) than their shielded analogs.

Catalytic activity generally shows little solvent dependence. Practically, Hedrick et. al. found that catalyst ratios of 0.25–1.5 equiv. relative to the initiating alcohol for targeted DP's of > 100 produced narrowly dispersed poly(lactide)s in 1–2 M THF/lactide solutions.[81] This

catalyst amount is significantly less comparable to pyridine, DBU, and thiourea catalyst and comparable to TBD.

Analogous to pyridine, amidine and guanidine bases, a "nucleophilic"- and a "basic" H-bonding alcohol activation mechanism are being discussed for the NHC-catalyzed transesterifications and ring-opening polymerizations of lactones. Mechanistic studies to test for the viability of the nucleophilic mechanism demonstrated that in the absence of alcohol initiators the carbene IMes (mesitylene subst.) could mediate the zwitterionic ring-opening polymerization of lactide to generate cyclic poly(lactide)s (Figure 12). This was readily evidenced via ^{1}H NMR and MALDI-ToF spectrometry and generally represents a new, fascinating and promising route to cyclic structures via ROP which will certainly be explored further.

Zwitterionic polymerizations generally are ionic polymerizations where both the anion and the cation are attached to the same polymer chain. Despite of the fact that theoretical calculations predicted that the H-bond alcohol activation mechanism has a lower barrier than the nucleophilic mechanism[82], experimental studies evidence the zwitterionic character of the polymerization:

> *"The kinetic and mechanistic investigations indicate that the NHC acts as a catalyst/initiator; because of a slower rate of initiation relative to propagation, only a small fraction (approximately 30-50%) of the carbenes is converted to active zwitterions which propagate rapidly and extrude the carbene to generate cyclic macrolactones. The proposed mechanism (Figure 12) for these reactions involves nucleophilic attack of the carbene initiator (IMes) to generate a zwitterionic intermediate (Z_1). Addition of monomers to the zwitterions (Z_1) leads to chain growth by generation of higher zwitterions (Z_n); macrocyclization of the zwitterions (Z_n) generates cyclic poly(lactide)s (C_n) with liberation of the carbene."[83]*
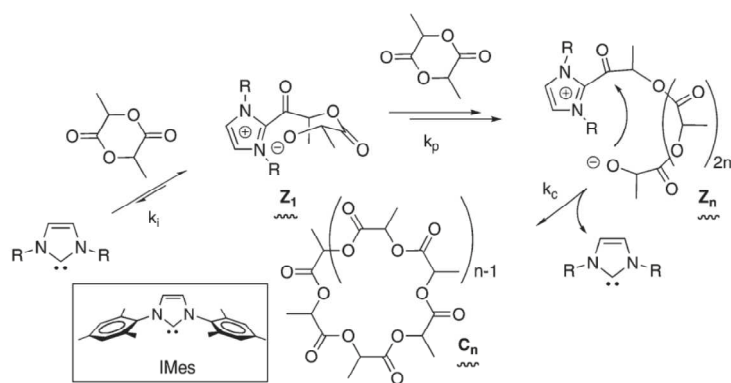
Figure 12: Synthesis of cyclic poly(lactide) via a nucleophilic zwitterionic mechanism promoted by carbene catalysis. Essential is the absence of co-nucleophiles.

While IMes **1** is very active for the ring-opening polymerization of lactide, it is less active for the ROP of ε-caprolactone (ε-CL).

The extreme potential and versatility of N-heterocyclic carbenes in living polymerization is illustrated by recent successes described by Daniel Taton and Yves Gnanoux. They employed these compounds for the ROP of epoxides, for the group transfer polymerization (GTP)[84,85,86] of acrylates and methacrylates and for the ROP of esters.[87]

Precision Synthesis

Although the presented ROP catalysts allow access to well-defined poly(ester)s (PDIs below 1.1 are possible in routine synthesis) monodisperse poly(ester) systems are generally desirable to study fundamental structure/property relations without detrimental polydispersity effect. A reasonable but elaborate method is their isolation and fractionation from conventionally prepared polydisperse samples.[88] An innovative synthetic approach, introduced by Hawker and co-workers, allows the "generation-wise" build-up of precisely defined linear ε-caprolactone oligomers (Figure 13). Orthogonal protecting groups, *t*-butyldimethylsilyl (TBDMS) ether for the hydroxyl group and benzyl (Bn) ester for the carboxylic acid group allowed the build-up of monodisperse poly(ester)s which represent important model compounds for the study of structure-property relations. This iterative approach has also been applied for lactic acid by the same group and proved equally successful.[89]
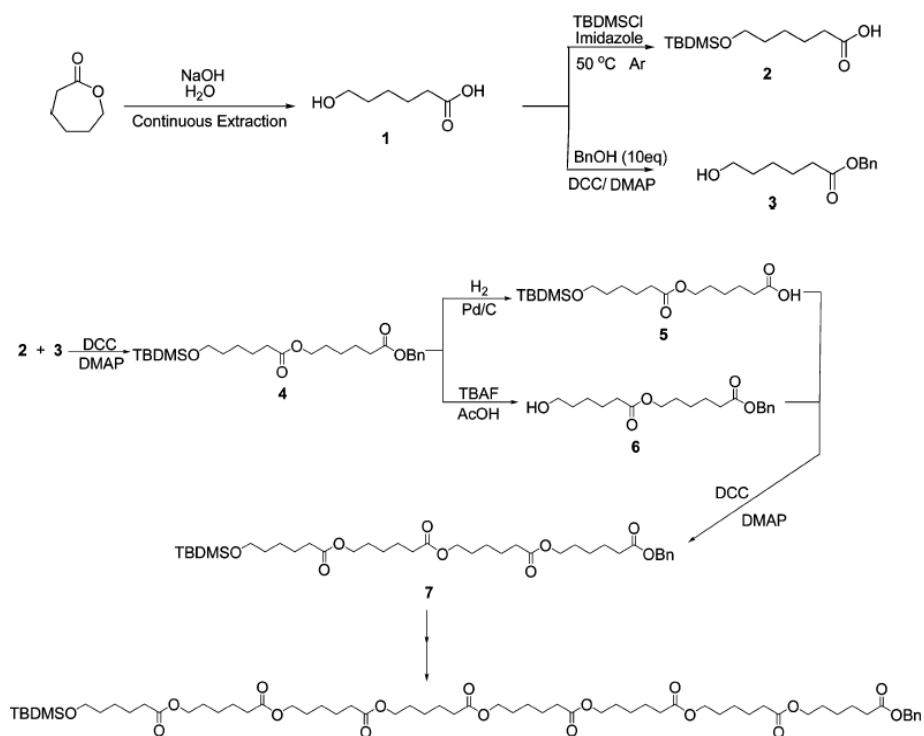
Figure 13: Synthesis of molecularly defined *ε*-caprolactone oligomers and polymers up to the 64-mer, via an exponential growth strategy as presented by Hedrick and coworkers.[90]

In summary, ROP of lactones and cyclic diacids displays many characteristics of a living polymerization enabling the synthesis of poly(ester)s that display predictable molecular weights (from the monomer to initiator ratio), narrow molecular weight distributions, end-group control and the ability to access block copolymers by chain extension. Furthermore, application of readily available stereo-pure monomers in cooperation with controlled ROP has enabled the facile manipulation of the tacticity of the resulting polymers, greatly affecting their properties. Spectacular progress has been achieved over the last ten years regarding the preparation of PLAs under mild conditions with a high level of control via organocatalytic ring-opening polymerization. Monodisperse poly(ester)s are accessible via a cascade coupling approach and have been realized up to the 64-mer.

1.1 Polyfunctional and Branched Poly(ester)s and Polycarbonates

Introduction of Functional Groups in Lactones and Cyclic Carbonates:

Although branched and hyperbranched poly(ester)s will be discussed in the following section (1.2) functionalized lactone derivates, especially those with free hydroxyl groups, represent important intermediate building blocks for their realization via ROMBP (ring-opening, multi-branching polymerization). Nevertheless, also general functionalization strategies will be discussed, since they significantly enhance the value of poyl(ester)s in biomedical and material science applications. The availability of functional pendant groups along the polymer backbone can be considered a highly efficient mean to tailor the properties of poly(ester)s - including features like hydrophilicity, biodegradation rates, bioadhesion, drug attachment, etc. Even more important is the combination of biodegradability and water solubility since it can significantly expand the possible applications for polymers in biomedical applications.[91] In addition, some functionalized lactones are potential inimer systems which can provide access to branched poly(ester)s.

Lactones

Emrick et al. realized a cyclic lactone (α-cyclopentene-δ-valerolactone) for the synthesis of aliphatic copoly(ester)s (comonomer: ε-caprolactone) with pendant cyclic olefins, followed by conversion of the olefins to 1,2-diols, and coupling of the hydroxyl groups to PEG-carboxylic acid derivatives.[92] Alkine and azide functionalized lactones[93] allow pre- or post polymerization functionalization reactions via click-chemistry, as recently summarized in a review by Jerome et al.[94]
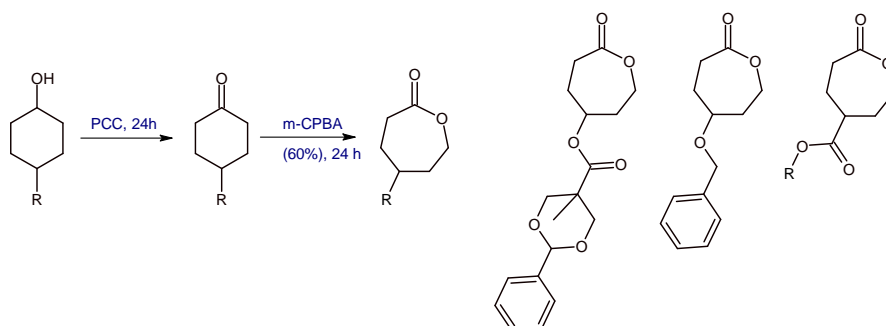
Figure 14: Synthetic pathway to 5-substituted caprolactone derivates as published by Trollsas et al. in 2000[95]: Key element is the Bayer-Villiger oxidation method.

Various chemical approaches have been developed to present carboxyl[96] and hydroxyl groups[97,98] onto such poly(ester)s via ring-opening polymerization (ROP) of lactones or lactides with appropriate functional monomers. While useful, these methods generally require a complex multistep synthesis of the protected monomer before polymerization and removal of the protective groups prior to further chemical manipulation which can result in degradation of the polymer. A selective reaction between a ketone-bearing aliphatic poly(ester) and amino oxy-terminated functional groups (Figure 15) is used for the grafting to approach. Jérôme and co-workers first described the chemical synthesis of **1** (Figure 15) in which the authors reported that reduction of the ketone to the corresponding alcohol gave a functional poly(ester) in high yield.[99,100,101]
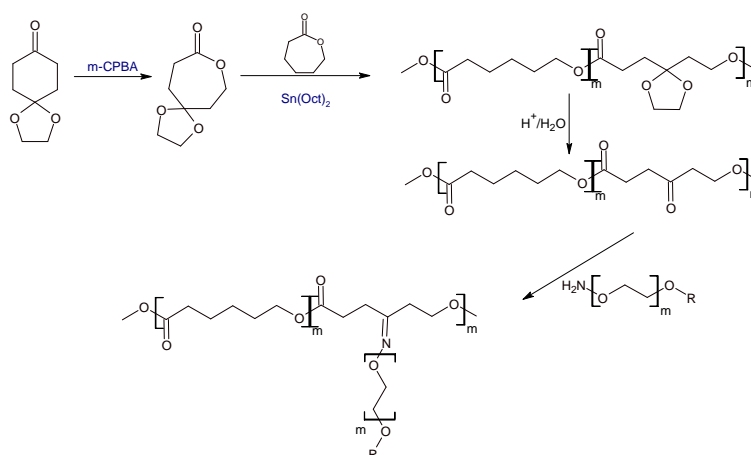
Figure 15: An unconventional synthetic approach to PCL-graft-PEO: The spiro-acetal (left: note the B.-V. oxidation step) was hydrolyzed after polymerization to yield the poly(5-keto-ε-caprolactone), which can alternatively be reduced to the hydroxyl-functionality.[102]

An interesting strategy to modify a lactone is the deprotonation of the α-H with a strong base (which is hardly nucleophilic, e.g. LDA.) and to subject it to a nucleophilic substitution with an activated alkyl-halide.[103] Bis-allyl-valerolactone has been realized in this manner.[104,105]

Next to pure lactone systems, another special class of cyclic monomers has to be mentioned when it comes to the synthesis of functionalized copoly(ester)s: **Esteramides/Depsipeptides** can be polymerized via ROP under the acyl-oxygen cleavage of a morpholine-2,5-dione derivative while the amide bond remains intact. Polydepsipeptides (peptolides) generally represent copolymers of a hydroxy acid and an amino acid. The synthesis and polymerization

of cyclic esteramides/depsipeptides was achieved in seminal work more than two decades ago by Pieter Dijkstra and Jan Feijen.[106] Copolymerization with lactide and other lactones was soon found to be possible.[107] In elegant work, Langer and coworkers used a protected lysine functionalized depsipeptide to form an aminofunctional poly(lactide) which was subsequently coupled with the RGD tripeptide recognition sequence.[108] The synthetic procedure shown in Figure 16 represents the general pathway to a substituted esteramide monomer and its subsequent copolymerization with lactide.
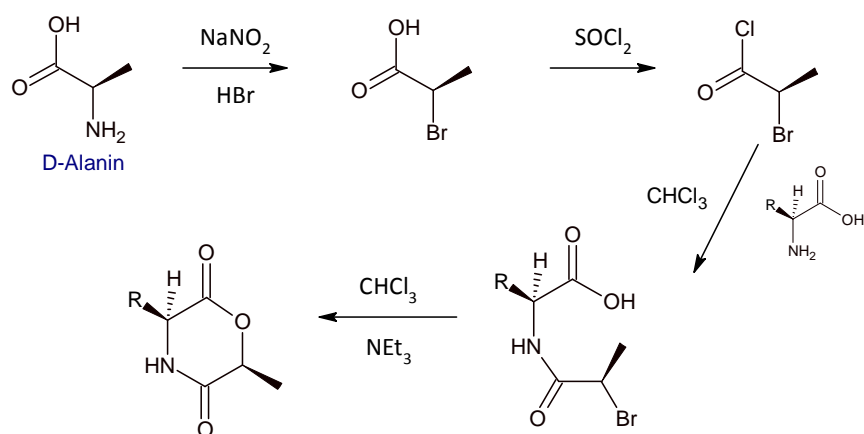
Figure 16: Left: Synthesis of a substituted morpholine-2,5-dione derivative as introduced by Feijen et al.

Cyclic Diesters: Substituted Glycolide Derivates

The synthesis of glycolide derivates is slightly more difficult compared to lactones and six-membered carbonates. Lactonization cannot be achieved via the Bayer-Villiger oxidation for obvious reasons. The two substituents in the dilactone can be equal (homodimers) or different (heterodimers) requiring dissimilar synthetic pathways. Homodimers are usually prepared by thermal catalytic depolymerization of low molecular weight polycondensates with transition metal complexes as transesterification catalysts (e.g. synthesis of lactide and glycolide). This route is hardly applicable to homodimers with molecular weights significantly exceeding that of lactide. Due to the lack of the lactones volatility, the introduction of larger substituents in the α-postion requires another cyclisation strategy.[109] Cyclisation is then achieved under (diluted) Ruggli-Ziegler conditions in toluene with p-TsOH (Figure 17a).[110,111] Nevertheless, yields are often unsatisfactory and scale up is difficult to achieve. Work up is tedious and requires chromatographic methods if selective crystallization of the cyclic dimer is not possible. Mixtures of D,L-substituted α-hydroxyl acid reactants yield a distribution of *R,R*; *S,S* and the meso-compound (which often shows no tendency to crystallize).
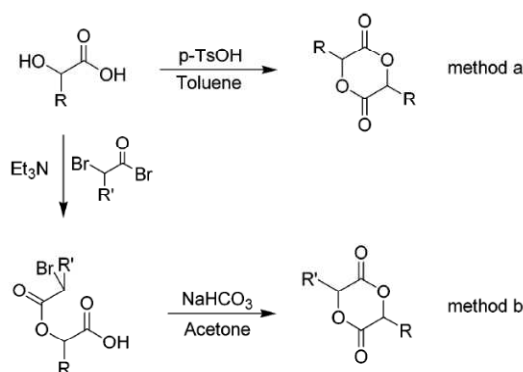
Figure 17: Cyclisation strategies for homo (a) and hetero substituted (b) glycolide derivatives.

Heterosubstituted monomers generally carry one α-H or α-methyl group, while the second substituent carries a desirable functionality. They are obtained by reaction of the substitute α-hydroxy acid with 2-bromoacetly bromide or 2-bromo-2-methyl-acetylbromide and subsequent lactonization in refluxing acetone (Figure 17b).[112] Alternatively, lactonization can be achieved from the diacid via cyanuric chloride, acetone and Et_3N.[113] If the acid bromide or chloride is not available, Steglich type reactions with DCC or HOBt are the method of choice for the dimer formation. The required alpha hydroxyl acids are often obtained in their

enantiomerically pure form from the structurally similar amino acids after diazotation with NaNO$_2$ and treatment with H$_2$SO$_4$. Alternatively, Baker and coworkers illustrated interesting routes from ethyl glyoxylate[114] and diethyl oxalate[115] to yield special lactide monomers (Figure 18).
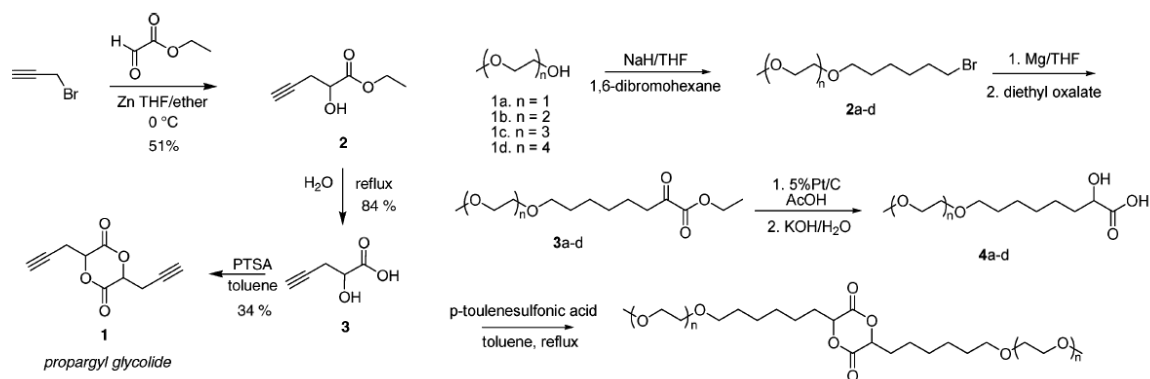
Figure 18: Innovative glycolide monomers, realized by Baker et al. Left: Propargyl glycolide for the synthesis of "clickable poly(lactide)", right: PEG-modified glycolide for poly(lactide)s" with "tunable LCST".

The direct functionalization of lactide and glycolide is hardly described in literature. Nevertheless, Hillmayer and coworkers recently described a very elegant way to norbornen functionalized lactide via α-bromination, elimation and cyclo-addtion (of cyclopentadiene).[116]

Especially hydroxyl-functional glycolides are of interest for biomedical applications.[117,118] Noga et al. recently demonstrated the synthesis of a poly(lactide) copolymer with pendant benzyloxy groups.[119] This has been realized by the copolymerization of a benzyl-ether di-substituted monomer with lactide (Figure 19). This monomer has been developed in parallel by Wolf and Frey via a different synthetic procedure. Synthesis and polymerization will be discussed in chapter 4.5. Debenzylation of the polymer to provide pendant hydroxyl groups was followed by modification with succinic anhydride and afforded the corresponding carboxylic acid functionalized copolymer that was amenable to standard carbodiimide coupling conditions. An amino-substituted biotin derivative was coupled to the carboxyl groups of copolymer films as proof-of-concept. In a demonstration of the function of these new materials, an RGD-containing peptide sequence was tethered to copolymer films at various densities. This enhanced the selective adhesion of epithelia cells significantly.
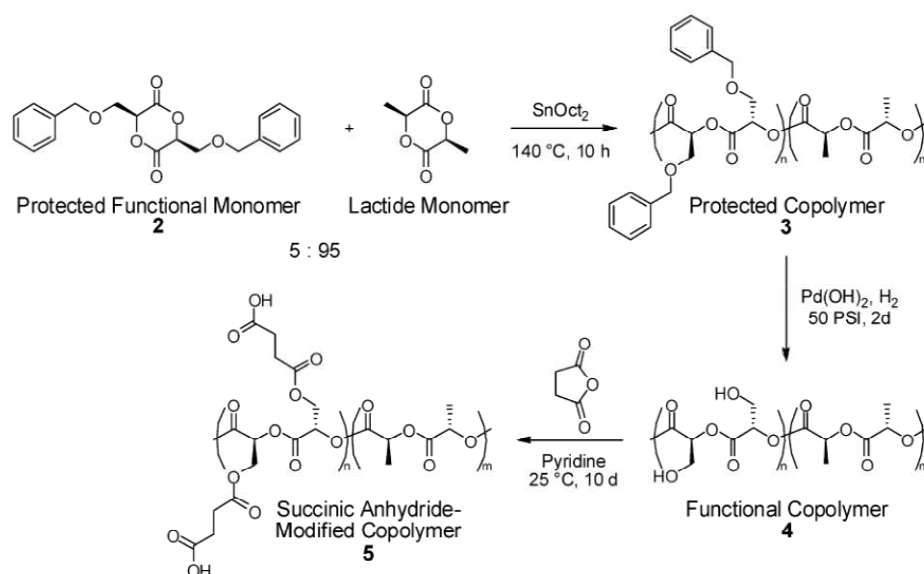
Figure 19: Synthesis of hydroxyl-functionalized poly(lactide) (4) via a benzyloxy-substituted lactide monomer (2). After conversion with succinic anhydride, a RGD-peptide could be coupled to the backbone to improve performance and adhesion selectivity in tissue engineering applications.

An excellent review on the synthesis of functional poly(ester)s has just been published by Dove and Pounder which is highly recommended for further reading on the topic of functionalized lactones.[120]

Cyclic Carbonates

Cyclic, six membered carbonates represent attractive monomer systems with a field of application comparable to that of lactide. Trimethylene carbonate (TMC) embodies the simplest form of this class and has found widespread attention.[121,122] In general, the introduction of pendant groups is desirable to improve the thermal properties of PTMC (T_g= 19 °C, T_m= 36 °C). The carbonates' architecture is very amenable for the introduction of functional groups since cyclization of the respective 2-substituted propanediol is less challenging than that of comparable α-hydroxy-acids. While TMC is often realized in a transesterification process with diethyl carbonate (and subsequent distillation in vacuo), the conversion of heavier, 2-modified propanediols is usally conducted with a more reactive equivalent: Ethyl-chloroformiate (sometimes even phosgene). The monomer can then be obtained in good yields (approx. 80%) in its pure form via (re-)crystallization. The presence of only one substituent at the most distant position from the carbonate group has advantageous effects on its reactivity in ROP. Different strategies for the modification of six membered carbonates have thus been developed in recent years:

Hydroxyl-functionalized polycarbonates were first realized by Vandenberg et al. in 1999 via a ketal-protected intermediate based on pentaerythritol.[123] Rockicki et. al. synthesized and polymerized 5-allyloxy-1,3-dioxan-2-one. They also used a thiol-ene "click" reaction with 2-mercaptoethanol to produce a hydroxyl-functional "inimer" carbonate for the ROMBP to form branched polycarbonates.[124] Grinstaff et al. realized an interesting precursor to glycerol-1,3-carbonate. The secondary hydroxyl-functionality of the six membered ring was protected as benzylether which could be cleaved via hydrogenation after polymerization.[125] Jing et al realized 5-methyl-5-(2-nitro-benzoxycarbonyl)-1,3-dioxan-2-one. After copolymerization with lactide, the nitro-benzoxygroups could be cleaved via UV-irradiation and carboxylic acid groups, carrying poly(carbonate ester)s, were obtained.[126] The same group succeeded in the introduction and modification of free amino groups via the carbonate motive.[127]
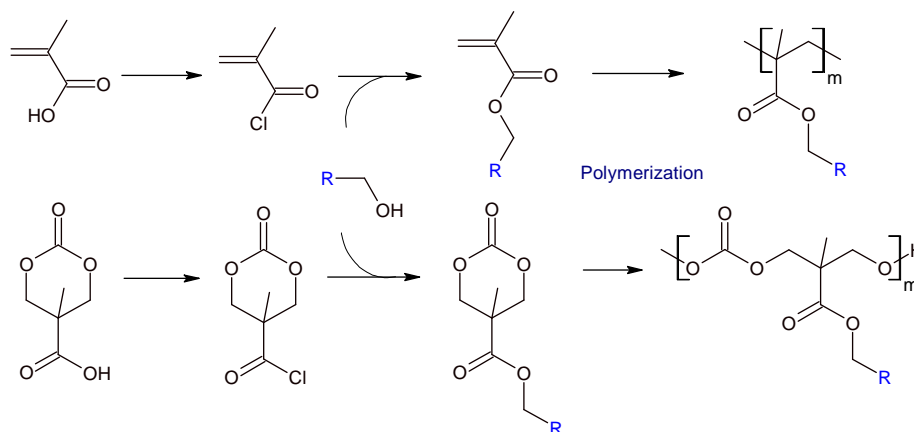
Figure 20: Derivatization of (meth)acrylates for radical polymerization (top) and cyclic carbonates for ring-opening polymerization (bottom) as proposed by Pratt et al.[128]

In the recent past the group of Hedrick and Waymouth has demonstrated that 2,2-bis-(methylol)propionic acid (Bis-MPA) (also termed BHP = bis(hydroxymethyl)propionic acid can produce a six-membered cyclic carbonate ring bearing free carboxylic acid group. This monomer can be readily esterified with a suitable alcohol (Figure 20) and thus represent a versatile building block, comparable to methacrylates. They demonstrated that even guanidinium groups can be bound to the respective monomer motive. Polymerization with thiourea catalysts yielded oligomers which mimic the TAT-petide *"HIV-TAT"* (*Trans-Activator of Transcription)* of the HIV virus. They are highly promising vectors to facilitate the passage of drugs through the highly selective blood/brain barrier.[129]

Alkin- functionalized carbonate monomers allow the highly versatile post-polymerization modification via azide based "click"-chemistry (Figure 21).[130]
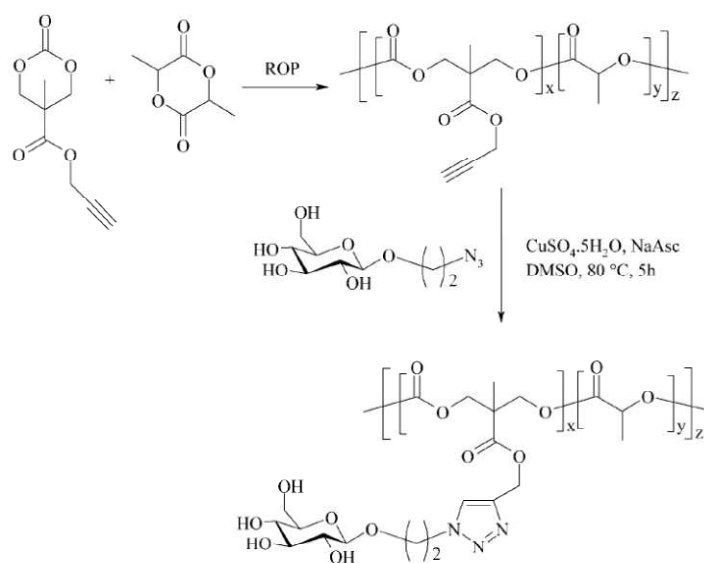
Figure 21: Grafting of glucose onto a terminal alkine containing PLA.

In a similar approach acryloyl carbonate and methacryloyl carbonate monomers were synthesized in four steps from 1,1,1-tris(hydroxymethyl)ethane and copolymerized with ε-caprolactone (ε-CL) and D,L-lactide (LA).[131] The acryloyl groups could be functionalized via the Michael-type conjugate addition with varying thiol-containing molecules such as 2-mercaptoethanol, 3-mercaptopropanoic acid, cysteamine, cysteine, and arginine-glycine-aspartic acid-cysteine (RGDC) peptide (Figure 22).
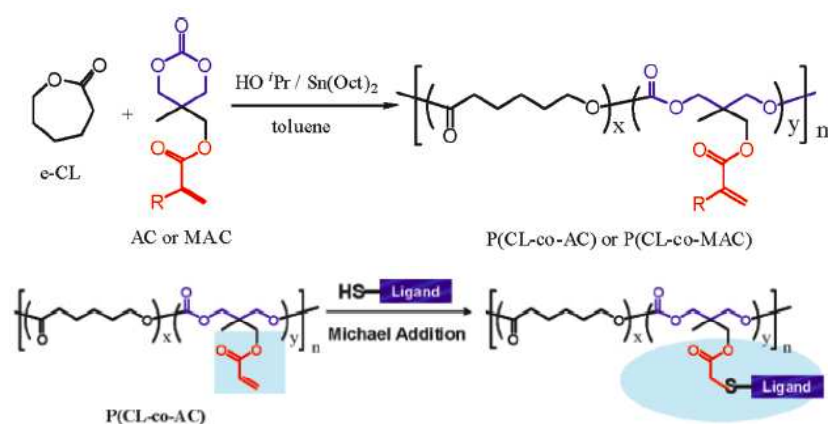
Figure 22: Copolymer with thiol-containing molecules by michael-type conjugate addition.

Branched and Hyperbranched Polymers

Poly(ester) Dendrimers

Dendrimers are built up from AB_n monomers via a generation wise build up. Each reaction ideally achieves full conversion of the accessible reactive groups. Hence dendrimers are monodisperse, perfectly branched polymers that adopt a globular three-dimensional shape as the generation number increases.[132,133] Tomalia,[134] Newkome[135] as well as Fréchet and Hawker[136] provided groundbreaking works in this field. Dendritic macromolecules generally possess a well-defined core, interior region layers, and a high surface-area to volume ratio. With each successive generation, the number of end groups doubles and the properties of the dendrimer are more and more influenced by the end group. These chemical and structural attributes of dendrimers translate to unique chemical and physical properties (e.g. solubility, chemical reactivity, viscosity, glass transition temperature). Thus, opportunities exist to control both the three dimensional structure and material properties of dendrimers through specific adaptation at the molecular level. Their synthesis is generally based on two orthogonal protecting groups – a concept known from peptide synthesis. The generation wise build up can be performed in either a convergent (from surface to core)[137], or a divergent (from core to surface) manner.
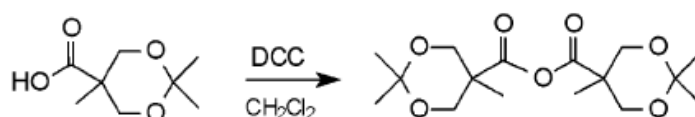
Figure 23: Acetonide-protected 2,2-bis(hydroxymethyl)propionic acid and the more reactive anhydride, which is primarily used in dendrimer construction.

Poly(ester) dendrimers are based on AB_2-building blocks with two hydroxyl and one carboxylic acid functionalities. 2,2-bis(hydroxymethyl)propionic aci (BHP), pioneered by the groups of Hult and Fréchet is the most prominent building block for the condensation based formation of branched poly(ester) structures. The convergent approach was first realized by protecting the focal point of BHP by a benzyl ester group and deprotection by catalytic hydrogenolysis. The esterifications were performed by conversion of the acid into the

corresponding acid chloride and followed by reaction with the hydroxyl groups in the presence of triethylamine and dimethylamino-pyridine.[138] An alternative route to BHP dendrimers was designed using a direct coupling strategy of the free acid via a Steglich type reaction. Here acetonide formation was used for hydroxyl protection of the first generation (important to yield a polyhydroxyl-functional dendrimer).[139] Nevertheless, incomplete conversions lead to imperfect dendritic build up. This could be largely overcome by the use of the respective anhydrides which provided better yields and showed excellent performance (Figure 23).[140,141,142] Due to its chemical build up, acetonide-protected 2,2-bis(hydroxymethyl)propionic acid is determined to be employed in divergent coupling reactions (or combinations of both[143]). This synthetic concept has been dominant ever since (Figure 24).[144,145]
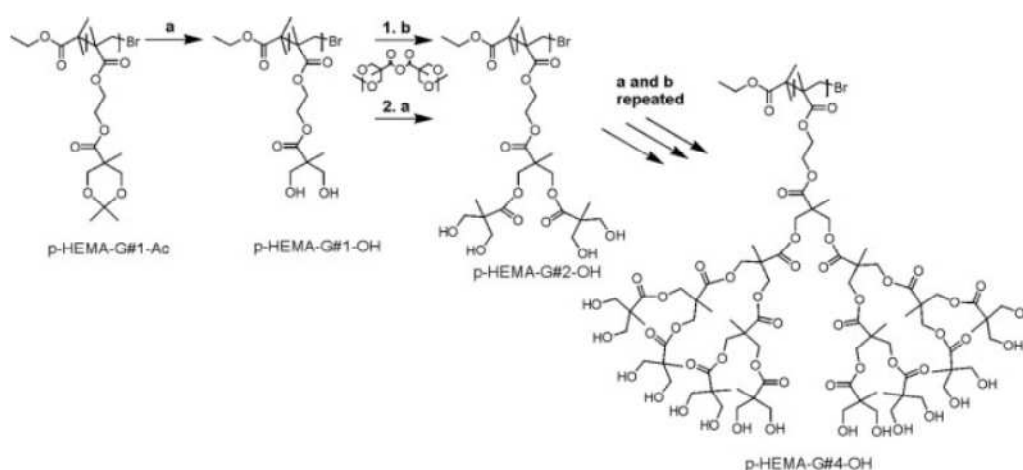
Figure 24: BHP dendrimers prepared via the divergent approach from a Poly(HEMA) backbone.

An innovative use of BHP dendrons was presented by Hawker et al. They were functionalized at the focal point with a single α-bromoisobutyrate group, thus forming a functional dendron macroinitiator. A library of highly branched, 3-dimensional, dendron functional core cross-linked star (CCS) polymers were prepared from these macro initiators by varying generation number and polystyrene chain length, followed by reaction with divinyl benzene, utilizing the "arm first" approach (Figure 25). The number of arms of the star polymer was shown to decrease with increasing dendron size..[146]
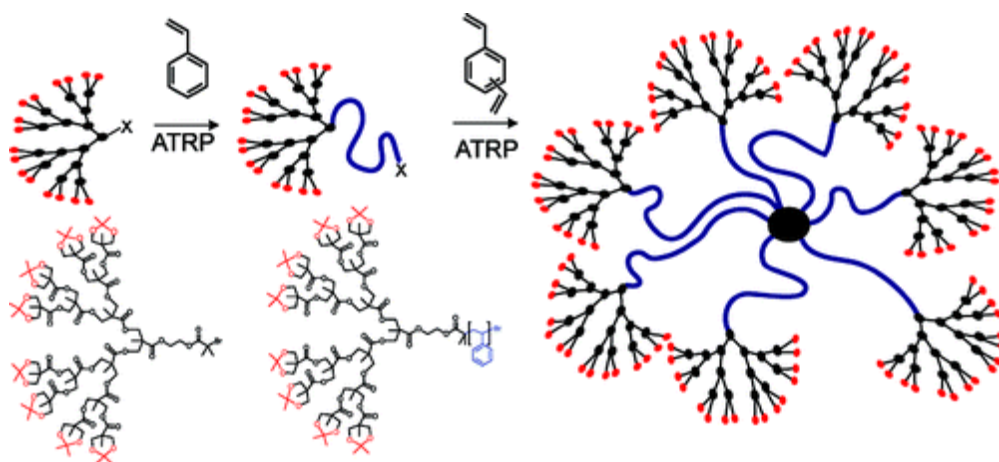
Figure 25: Poly(ester) dendrimers as ATRP-macroinitiators.

Aliphatic ester dendrimers based on acetonide protected 2,2-bis(hydroxymethyl)propionic acid anhydride growth units were successfully synthesized as a form of dendritic hybrids up to G4 (Figure 26). First ATRP with an appropriate initiator yielded benzyl alcohol functionalized linear polystyrene.[147] The dendritic repeating units were grown from the benzyl alcohol end group of the support via a typical esterification process. In the final step, the dendrimers were obtained via the selective cleavage of the benzyl ester group using a palladium(II) acetate catalyst in DMF.
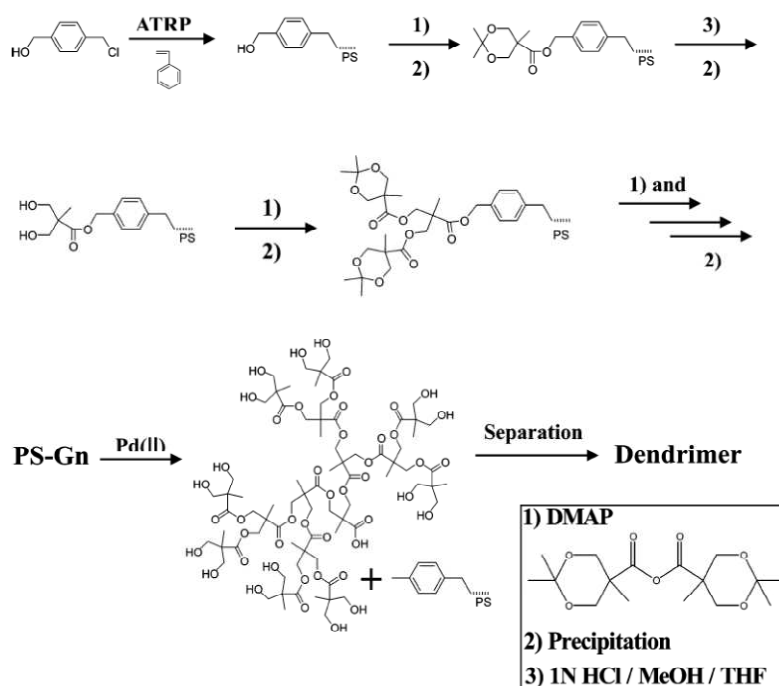
Figure 26: Divergent generation wise build up of dendritic BHP from a linear polystyrene polymer support. 1) Anhydride promoted coupling with DMAP and 2) mild acidic hydrolysis.

Other biopoly(ester) dendrimers have been described be Grinnstaff et al.[148] Their design emphasizes a possible use as advanced material for biomedical applications (Figure 27). The AB$_2$-monomer units, possessing one carboxylic acid and two hydroxyl groups incorporate structural motives which are known to be biocompatible. Glycerol is the other key molecular structure constituting the branching unit required for the dendritic architecture.
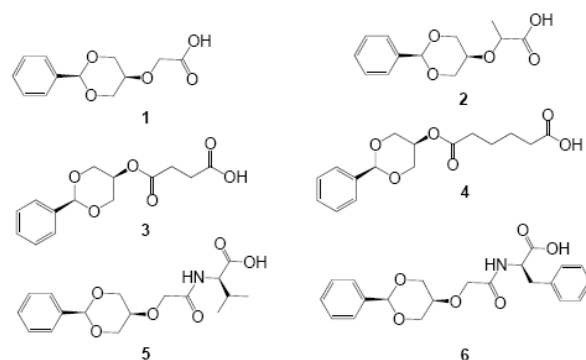
Figure 27: Modular approach by Grinstaff et al: Building blocks for the divergent syntheses of poly(ester) dendrimers composed of glycerol, lactic acid, glycolic acid, phenylalanine, succinic acid etc.

Degree of Branching: A Measure for the Compromise in Perfection
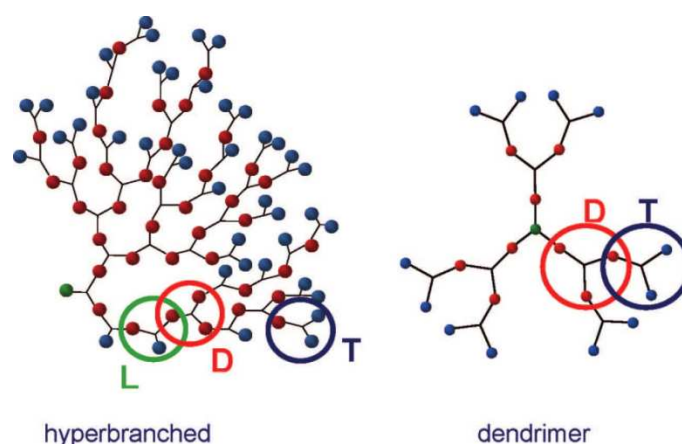
Figure 28 Schematic representation of the different polymer units in hyperbranched polymers compared to dendrimers: L) linear; D) dendritic; and T) terminal units (taken from Voit., B. I.; Lederer, A. *Chem. Rev.* **2009,** *109,* 5924–5973)

Interestingly perfectly branched polymers, i.e. dendrimers preceded the systematic research on polymers with an imperfectly branched structure although Flory already developed the

theoretical fundamentals for "random" A-R-B$_{(f-1)}$* polycondensates in the 1950s.[149] These structures were termed (hyper-) branched polymers and contain a certain amount of linear repeat units (L). In an approach to quantify their extent of branching[150] Hawker and Fréchet introduced the degree of branching (DB)[151] which is hence a universal, topological measure for presence of dendritic units (D) in branched molecules realized via cascade like reactions (without crosslinks). It hence correlates directly to the density of the polymer structure and the number and of terminal units (T).

$$DB_{Fréchet} = \frac{D + T}{D + T + L}$$

Fréchets initial definition has been refined by Hölter and Frey.[152] Their version conforms more stringent to simple boundary conditions: While perfectly branched dendrimers reach a DB of 1, strictly linear polymers have a DB of 0. This form is more suitable for the calculation of the DB in the low and medium molecular mass region. Since $T = D+1$, the DB$_{Fréchet}$ approximates the DB$_{Frey}$ with increasing degree of polymerization (DP$_n$= D+T+L).

$$DB_{Frey} = \frac{2D}{2D + L}$$

In general, hyperbranched polymers are characterized by a random distribution of functional groups throughout their structure. This leads to low average chain lengths between the branching points. Hence, chain-entanglements are considerably suppressed. The resulting reduction in solution and melt viscosities, as well as the high density of functional groups renders these materials highly interesting for industrial applications.

---

* Step-growth polycondensation of multifunctional AB$_m$-type monomers, containing one A group and m (m≥ 2) complementary B groups.

Polycondensation of AB$_2$-Monomers: Aliphatic Bis-hydroxyl-acids

Hyperbranched polymers are advantageous because they encompass highly branched nanoscopic structures with dense peripheral functionality. They are polydisperse and can be prepared using one-pot synthesis, unlike dendrimers, making the former less costly.

> *In the classical approach toward hyperbranched polymers, which goes back to Flory's early description as a special type of polycondensation, AB$_X$ monomers with equal reactivity of the B functionalities are reacted. The reaction involves the typical features of a step-growth reaction of multifunctional monomers and the formed oligomers but without the possibility of crosslinking. Dendritic (fully reacted B functions), terminal (no reacted B function), and linear (one reacted B function) units and one focal unit (A function) should be present in the resulting, highly branched macromolecule.*[153]

Apart from the tedious dendrimer build up based on the AB$_2$-monomer bis-MPA, Hult et al. also investigated its straight forward polycondensation reaction. First attempts of the polymerization in bulk using acid catalyst afforded highly disperse poly(ester)s.[154,155] By copolymerizing bis-MPA with a polyol core the risk of gelation was greatly reduced and the dispersity lowered.[156] In addition to a discontinuous monomer addition, this technique was the foundation of the commercially available hyperbranched poly(ester) Boltorn®, provided by Perstorp. In contrast to dendrimer synthesis, the simple reaction procedure allows a commercial production on a multi ton scale. The manufacturer claims manifold fields of application for Boltorn as *"Precursor for UV-curing acrylate oligomers with exceptional relationship between viscosity, molecular weight and functionality. The acrylate of Boltorn® P500 yields: high reactivity, high chemical resistance, high scratch resistance, tough coatings, low shrinkage."*[157] Furthermore it is used as cross-linking polyol for flexible polyurethane foams. In a systematic study, Fradet and coworkers found that the AB- and B-branching factors were significantly lower than expected for random polymerizations, reflecting the existence of both negative A-B and B-B substitution effects, i.e. lower reaction rate of a given A or B group after reaction of the other groups present on the same monomer unit.[158] Parzukowski et al. recently presented a new aliphatic poly(ester)/polyether derived from glycerol and based on AB$_2$ polycondensation.[159]

Combinations of ROP and Polycondensation

In 2002 Frey et al. used a combination of the step-growth AB$_2$-approach with the chain-growth ROMBP for the synthesis of branched poly(ester). This was realized via a one-pot reaction in bulk from ε-caprolactone and 2,2-bis(hydroxylmethyl) butyric acid (BHB) via an enzyme catalyst.[160] The concept could later be expanded to other transesterification catalysts, namely HfCl$_4$(THF)$_2$ and diphenylammonium trifluoromethanesulfonate (DPAT).[161] Although water is released as condensation byproduct the branching agent was not fully incorporated. Nevertheless, the resulting polymers showed a certain excess molecular weight compared to their theoretical M/I ratio, which is a strong indicator for branched structures.
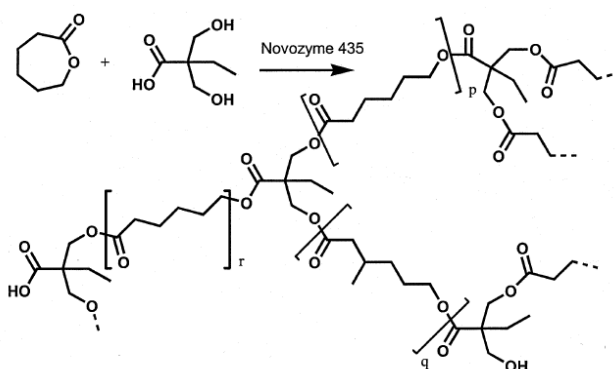
Figure 29: Combination of ROP and AB$_2$-step polycondensation as introduced by Frey et al. for ε-caprolactone and BHB.

It has to be emphasized that similar approaches in producing a branched topology failed when lactide was employed.[162] They resulted primarily in the formation of mid-chain carboxylic acid functional poly(lactide) by chain growth from the diol.[163] It was recently shown by Feijen[164], that these P(ε–Cl) and PLA AB$_2$-macromonomers can be produced via controlled ring-opening polymerization with Sn(Oct)$_2$. A condensation type reaction is absent under the employed reaction conditions (no water removal). Frey et al. succeeded in a post polymerization coupling of this kind of macromonomer via a Steglich type condensation.[165] The at least partial success of the in situ formation of dendritic units with caprolactone could be attributed to the higher transesterification tendency of a primary-, compared to a secondary alcohol/ester linkage.

Initiating Monomers for Living Polymerization Methods – Towards Branched Poly(ester)s

In 1995 Fréchet et al. introduced for the first time a chain growth mechanism for the preparation of branched polymers.[166] His initiating monomer concept was based on the just recently developed ATRP and became known as self condensing vinyl polymerization (SCVP). This concept was soon expanded to lactone and epoxide based monomers: i.e. the self-condensing ring-opening polymerization SCROP (also known as ring-opening multibranching polymerization) (ROMBP) or the proton transfer polymerization. These processes have the advantage of producing and not consuming reactive sites during polymerization. In contrast to dendrigraft approaches, the branching units are formed throughout polymerization according to the same mechanism and in a random order that is just defined by the reactivity constants of the respective monomers and inimers. Especially the balance between initiation and propagation significantly influences the degree of branching, the molecular weight and the weight distribution.

Self-Condensing Vinyl Polymerization (SCVP)

The SCVP is based on the CRP of a vinyl monomer that bears an additional initiating group ("inimer"= initiator + monomer) suitable for the respective polymerization method (Figure 31). This can be a nitroxyl group,[167] an activated halogen (Figure 30) or a chain transfer agent. These monomers allow propagation through the double bond (chain growth) and the initiation and propagation of a second chain, originating from the intiator site of the respective monomer. The reaction of both groups leads to the formation of hyperbranched polymers in a one-pot reaction.
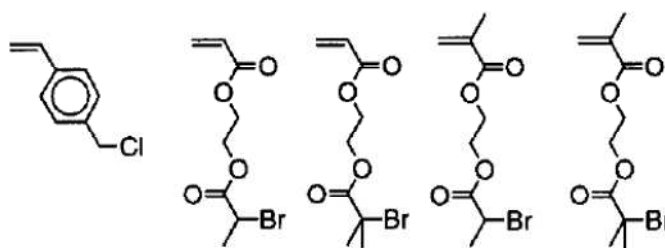
Figure 30: Different acrylate and methacrylate inimers as used in the ATRP based SCVP.

Müller et al. showed that even group transfer polymerization can be adapted according to the principles of SCVP (Figure 31).[168] Only a small amount of inimer can thereby significantly alter the solution viscosity of the copolymer[169] and the copolymerization of monomers and inimers allows access to a plethora of material properties.[170] The kinetics of growth resemble a step-growth polymerization even though the polymerization occurs by a radical mechanism (hence the term "self condensing").
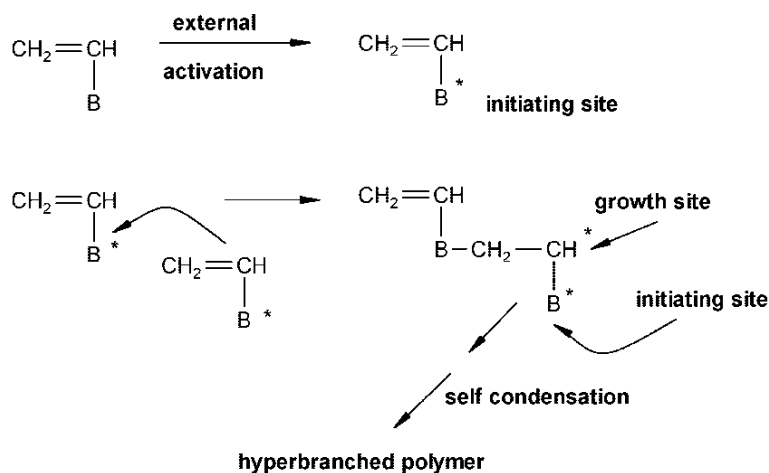
Figure 31: Concept of the SCVP.

Müller et al. concluded from theoretical and experimental studies on SCVP that the effect of the two different active centers, namely initiating ones, B*, and propagating ones, A*, with nonequal reactivities of the two centers (k_A and k_B) have a strong effect on kinetics and MWD. The MWD narrows down to 2 for $k_A > k_B$ (corresponding to the common polycondensation of AB monomers) but broadens for $k_B > k_A$.[171] This is also valid for the DB, which therefore often deviates from the theoretical 0.5.[172,173] Generally, the polydispersity is relatively high and often significantly exceeds 2 for high conversions.

So called macroinimers have been prepared by Müller et al. The subsequent SCVP step raised the molecular weight from aprox. 3000 to 80000 g/mol.[174] Heise et al. introduced the synthesis of branched polymers by SCVP of fully enzymatically generated and therefore biodegradable poly(ε-caprolactone) macroinimers by radical polymerization (Figure 32).**[175]** Apart from ATRP and GTP, NMP and RAFT[176] have also been successfully employed in SCVP.
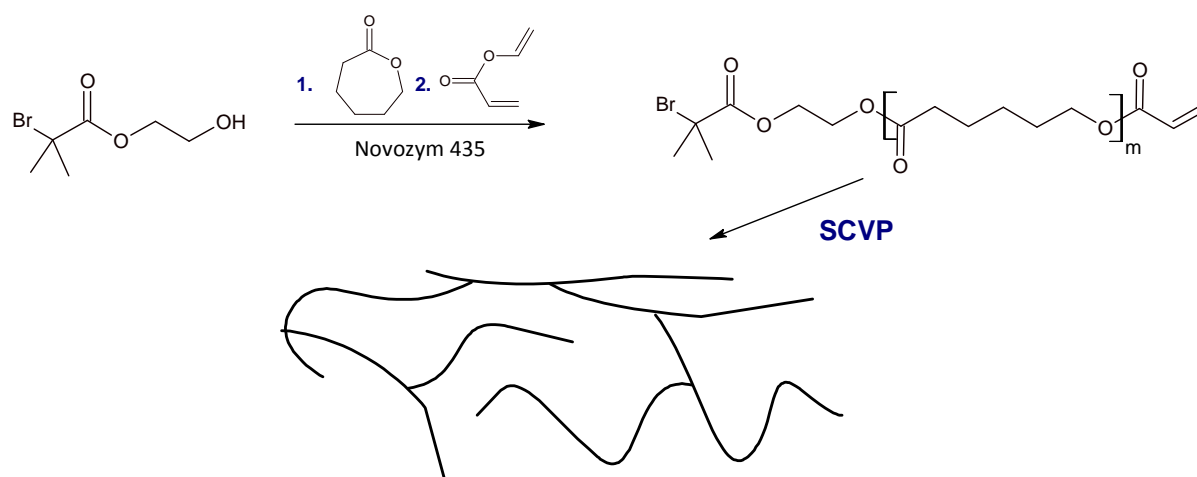
Figure 32: Sequence of enzymatic ROP of ε-Cl to a telechelic macromonomer which is converted to a branched structure via ATRP/SCVP.

Ring-Opening Multi-Branching Polymerization (ROMBP)

Fréchet and coworkers transferred the concept of the self condensing cyclic ester polymerization to poly(ester) synthesis via ROP.[177] In ring-opening multi branching Polymerization (ROMBP), the monomer function is a heterocyclic group and a cationic, coordinative or anionic mechanism is applied. Potential inimers are therefore hydroxy-functional lactones and cyclic esters. These monomers resemble a bifunctional AB monomer and are converted to an AB$_2$ type after ring-opening and are therefore often termed "latent AB$_2$ monomers" (Figure 33).
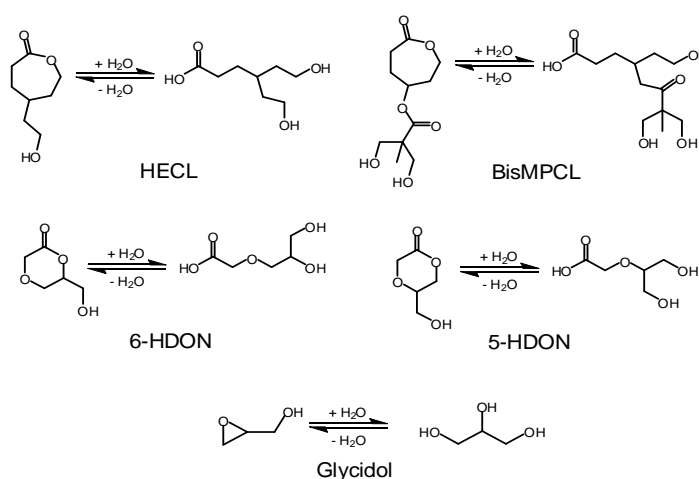
Figure 33: "Latent AB$_2$ monomers": Lactone and epoxide based inimers in their cyclic and open form.

Poly(glycerol), a highly branched polyether/polyol is the most prominent example of an inimer based polyether material. This milestone in ROMBP of epoxides was achieved by Frey and Sunder in 1999. The slow monomer addition was their key concept to achieve hyperbranched but well-defined poly(glycidol) (= poly(glycerol)) .[178] Theoretical studies predicted that the polydispersity in SCVP and ROMP would behave reciprocal to the number of functional groups in the core (PDI≈1+1/f with f = core functionality).[179,180] In combination, the slow monomer addition technique and the use of a polyfunctional initiator can be a powerful means to achieve well-defined molecular structures.[181] Thereby, a sufficiently high reactivity of the added monomer towards the core is a fundamental requirement. A problem is however the final end group dilution of growing chains/per chain end which limits the molecular weight to approx. 6000 g/mol. This can be partially overcome by using macroinitiators with higher degrees of deprotonation/core of the core forming molecule (up to 25,000 g/mol).[182]

The ROMBP of lactone-inimers features a more complex kinetic scheme. Whereas in SCVP usually irreversible reactions are involved, in ROMBP also reversible preconditions have to be considered. Apart from Fréchets work on caprolactone inimers,[183] only few further examples followed thus far. Since then, 6-[184] and 5-hydroxmethyl-1,4-dioxanone[185] have been prepared and polymerized to hyperbranched poly(ester)s/polyethers.

The first copolymerization of a lactone inimer (mevalonolactone, 10 mol%) with lactide has been conducted by Ouchi et al. in bulk.[186] Reviewing their presented results, it has to be underlined that the formation of branching points could not be evidenced clearly. The evolution of the elution traces in combination with ^{1}H NMR spectroscopy revealed a rapid lactide polymerization to an α-lactone functionalized PLA after 1 day. The disappearance of the respective lactone signal after 8 days could also be explained with a polyaddition type reaction between hydroxyl-end group and lactone moiety. Especially since the lactide monomer has long been consumed at this stage of the reaction.

Carbonate based inimers and their hyperbranched polymers are hard to find in literature so far and the only example known to us has been realized in elegant work by Parzuchowski et al.[187] In an interesting "mixed" inimer approach, linear-hyperbranched block copolymers

were realized by the simultaneous SCVP and ROMBP of HEMA and an alkylbromide functionalized caprolactone.[188]

Knauss et al. reported on the successful ROMBP of an epoxide inimer and a lactone, namely glycidol and lactide.[189] The long chain branched polymers revealed excess molecular weights and reduced viscosities. However, a precise structural characterization via NMR was not conducted. This is a general problem with polymer prepared via SCVP and ROMBP of suitable inimers. A precise structural elucidation and quantification of subunits is very hard to achieve. Application and "squeamish" evaluation of modern NMR-spectroscopy in combination with other analytic methods are inevitable in achieving this goal. Thus far, we only have a immature understanding of the lactone based ROMBP and detailed studies on the crucial molecular parameters are still to be done. Another interesting issue is the design of new lactone inimers. The balance between the concurring ROP-, initiation- and transesterification reactions have to be taken into account, when it comes to their demanding design and synthesis.

1.2 New Poly(ester) Based Block Copolymers with Functional Methacrylates

Connecting two distinct polymer segments at their ends covalently results in the formation of a class of hybrid macromolecules called block copolymers.[190] Block copolymers represent fascinating materials which offer interesting features often based on their microphase separation and self-organization properties. Especially living polymerization methods offer access to chemically and physically heterogenous systems. Block copolymers of lactone based poly(esters) with poly(acrylates) are thus accessible via different and orthogonal polymerization methods. Their combination benefits from the degradability and the hydrophobic nature of the poly(ester) backbone and the simple attachment and variation of functional groups along the (meth)acrylate backbone.

The different synthetic strategies resulting in well-defined block like structures are reviewed and compared. They involve several living polymerization methods for lactones as well as acrylic systems which have been developed in recent years and decades. A special focus is directed on their aggregation behavior in solution and numerous applications in biomedicine are addressed.

Controlled Radical Polymerization (CRP) Methods for the Synthesis of Polymethacrylate Block Copolymers

Derivatization of aliphatic poly(ester)s is particularly delicate compared to non degradable polymers. Many reaction conditions cleave the ester bond and thus result in the premature degradation of the polymer. As we have seen in the previous section, the synthesis of functional lactones is often demanding – especially hydrophilic monomers are hardly accessible in sufficient quantities and often require the use of protecting groups. Pure lactone/carbonate based amphiphiles are therefore a great preparative challenge and hence hardly described in literature.[191,192,193] A far more viable route is the combination of hydrophobic, but highly degradable and biocompatible poly(ester)s with hydrophilic, biocompatible but non-degradable polyethers or polymethacrylates. The design of acrylates

and epoxides allows for a simple modification of their pendant functional groups. The following chapter will therefore discuss synthetic strategies which deal with the combination of poly(lactone)s and polymethacrylates.

As opposed to conventional free radical polymerization techniques, controlled radical polymerization methods moderate the concentration of radicals in solution by reversible activation/deactivation processes to maintain excellent control over polymer molecular weight and polydispersity. The respective initiators and chain transfer agents generally allow for an efficient chain extension in a grafting from approach and thus the simple preparation of block copolymers. Additionally, it is orthogonal to a plethora of functional groups such as alcohols and amines.

The atom transfer radical polymerization (ATRP) is especially suitable for the formation of block copolymers with lactones. The radical polymerization process in general is compatible with other lactone systems because the initiating moiety (eg. alkylhalides) can be readily introduced and even multifunctional initiators are accessible with low synthetic effort. Cu(I) salts and multidentate amine ligands are the most established ATRP agents, [194195,196] although other metal/ligand combinations have been successfully applied.[197,198] Generally, the halide is reversibly transferred to the metal complex which is thus oxidized formally. This is accompanied by the formation of an active alkyl radical, permitting chain growth. While the ATRP polymerization kinetics are widely independent of the absolute catalyst amount, the ratio of the copper (I) to the inactive copper (II) species has a significant influence. Polymerization activity and control are largely affected by the redox potential (salt, ligand, solvent, concentration and temperature dependent) of the respective complex and the reactivity of the monomer. Generally, acrylates, methacrylates, methacrylamides, and styrenics are susceptible for polymerization via ATRP. An innovative approach for the reduction of the amount of the employed copper is the addition of environmentally benign reducing agents like ascorbinic acid. This AGET (Activators Regenerated by Electron Transfer)[199200] continuously reduces inactive copper (II) species and thus prevents a depletion of the active species by the omnipresent (oxidative) termination reactions.[201] Percec and coworkers recently presented a new, promising variant of copper based LRP. Here copper (0) is considered as the highly active catalytic species reacting via single electron transfer (hence

SET-LRP).[202] Here, disproportionation of Cu (I) to Cu(II) and very reactive, nascent Cu(0) takes place at room temperature and below, resulting in an ultrafast synthesis of ultrahigh molecular weight polymers. Apart from standard monomers (styrenics, methacrylates, etc.) even vinylchloride can now be polymerized in a fast and controlled manner.

The early nitroxide mediated polymerization (NMP) had significant disadvantages compared to the ATRP/CRP techniques presented above and was applicable virtually only on a very small set of styrene based monomers. Nevertheless, systematic work has led to variety of nitroxide compounds which are suitable for the polymerization of a much broader range of vinyl monomers.[203] Control and livingness of the polymerization are separate aspects and can only be achieved by careful tailoring of the reaction parameters for a given monomer/nitroxide combination.[204] The mechanism is based entirely on the persistent radical effect.[205] The major reactions in NMP are (i) the cleavage of the initiator and of the intermediate alkoxyamine capped chains into propagating alkyl and persistent aminoxyl radicals, (ii) the reformation of the alkoxyamine capped chains by radical cross-coupling and (iii) the irreversible self-termination of the alkyl species and their addition to the monomer. Irreversible termination by alkyl-alkyl coupling leads to an increase in the persistent radical concentration and therefore to a decrease in free alkyl radicals – a process with self regulating character. In comparison with 2,2,6,6-tetramethylpiperidinoxyl (TEMPO), a couple of newly developed systems led to a dramatic increase in the applicability of NMP for the controlled synthesis of block copolymers. Especially the SG1-Nitroxide has found intense application and was commercialized by Archema.[206] It can be readily introduced via its NHS-activated ester form.[207]

Several strategies for the coupling of poly(ester) blocks via the above presented CRP methods can be envisioned: Especially the chain-end functionalization of the first block with the suitable moiety to initiate the second polymerization type (macro-initiatior approach) or the use of a hetero-bifunctional initiator, able to initiate both polymerizations, are efficient approaches and shall be reviewed in the following paragraph.[208]

70

Synthetic Strategies: Combining CRP and ROP

The combination of disparate polymerization techniques has attracted considerable attention over the past decade since it allows the generation of materials from monomers that react by fundamentally different mechanisms. Various strategies, including the use of dual initiators, chain-end or pendent group transformations to produce block,[209] graft,[210] brush,[211] star, miktoarm star[212,213] shell-crosslinked nanoparticles[214] and even branched copoylmers have been employed.
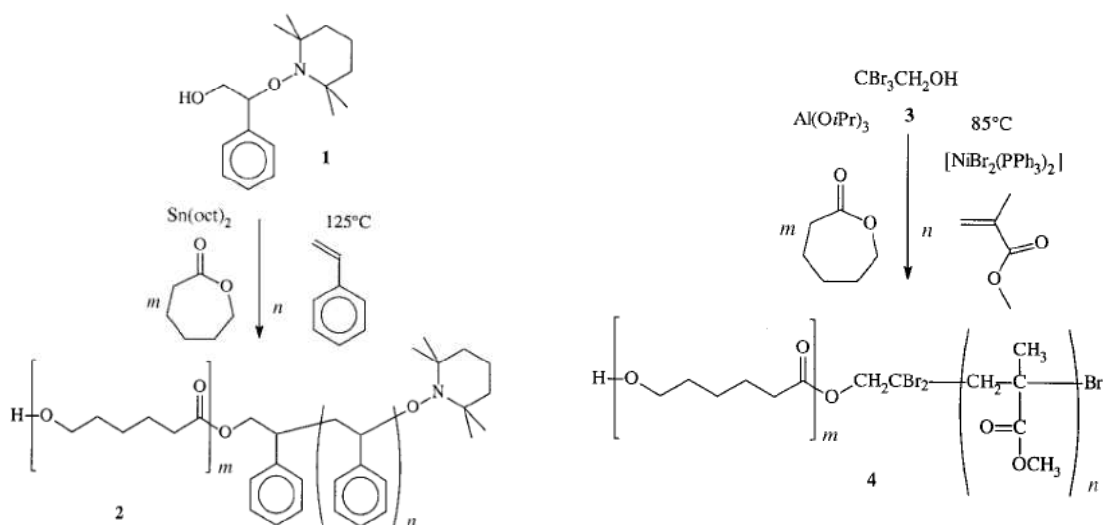
Figure 34: Pioneering works by Hawker and Hedrick introducing the concept of dual headed initiators for the synthesis of block copolymers by ROP and CRP.

Block Copolymers

Traditional formation of block copolymers requires a two-step procedure, either through the coupling of preformed polymers with functional groups at the chain ends or through macromolecular initiators for the polymerization of a second monomer. Especially the concept of performing dual living polymerizations from a single initiating molecule with no intermediate activation or transformation is of great significance. Polymer analoguous reactions can thus be avoided to realize a suitable link for the mechanistic transformation from one block to the other. [215] This has first been presented in pioneering work by Hawker et al. in 1997 combining ROP and NMP[216] and ROP and ATRP[217](Figure 34). Poly(D,L-lactide)-*b*-poly(*N,N*-dimethylamino-2-ethyl methacrylate) (PDLLA-*b*-PDMAEMA) were realized in a two step lactide first sequence by Hadjichristidis et al. to encapsulate the hydrophobic drug

Dipyridamole.[218] Nevertheless, they used a polymer analogous modification to form the PLA-macroinitiator in this case. A similar approach had been previously realized by Lazzaroni et al. for Poly(ε-CL-*b*-DMAEMA) copolymers.[219]

Heise et al. illustrated that even the combination of enzyme mediated ROP of ε-capolactone with subsequent ATRP of styrene can be employed to form well-defined diblock copolymers.[220] In a similar manner, E.W. Meijer et al. realized a cascade approach to a chiral block copolymer combining enantioselective ROP of 4-methyl-ε-caprolactone (Novozyme 435) and ATRP of methyl methacrylate.[221]
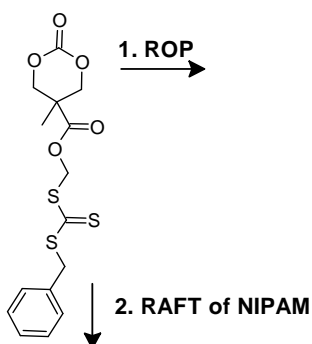
Figure 35: An orthogonal inimer for degradable brush-polymers.

Hedrick et al prepared a cyclic carbonate 2,2-bishydroxymethyl propionic acid with a pendant RAFT agent (Figure 35).[222] This orthogonal inimer was converted to environmentally sensitive graft copolymers via ROP and subsequent grafting from of N-Isopropylacrylamide (NIPAM).

Akiyoshi and coworkers prepared biodegradable amphiphilic polymers composed of hydrophobic polyphosphate grafted with well-defined hydrophilic poly[2-ethacryloyloxyethyl phosphorylcholine (MPC)]. 2-Isopropyl-2-oxo-1,3,2-dioxaphospholane and 2-(2-oxo-1,3,2-dioxaphosphoroyloxyethyl-2-bromoisobutyrate) (OPBB) were copolymerized by ring-opening polymerization using triisobutylaluminum as an initiator and catalyst. The hydrophilic arms were then grafted from the 2-bromoisobutyrate groups alongside the backbone. The graft copolymer associated and formed nanosize-hydrogels (nanogels).[223]

Multiblock Copolymers

On the way to more complex structures, also triblock copolymers have been realized. Here two subsequent ATRP cascades afforded the blocks 1 and 2 in an example from Pan et al.[224] Starting with the more reactive monomer styrene and a CuBr based catalyst, the second block follows and is realized by chain extension with MMA and a CuCl based catalyst. Lactide is polymerized from the pendant hydroxyl group of the ω-chain end.

Also multiarm star shaped multi-block copolymers could be realized (Figure 36). Herby the ATRP of MMA is used in the final reaction step after the buildup of a G-3 Fréchet Dendron, the grafting from of PLA and the end group modification into an ATPR-macroinitiator.
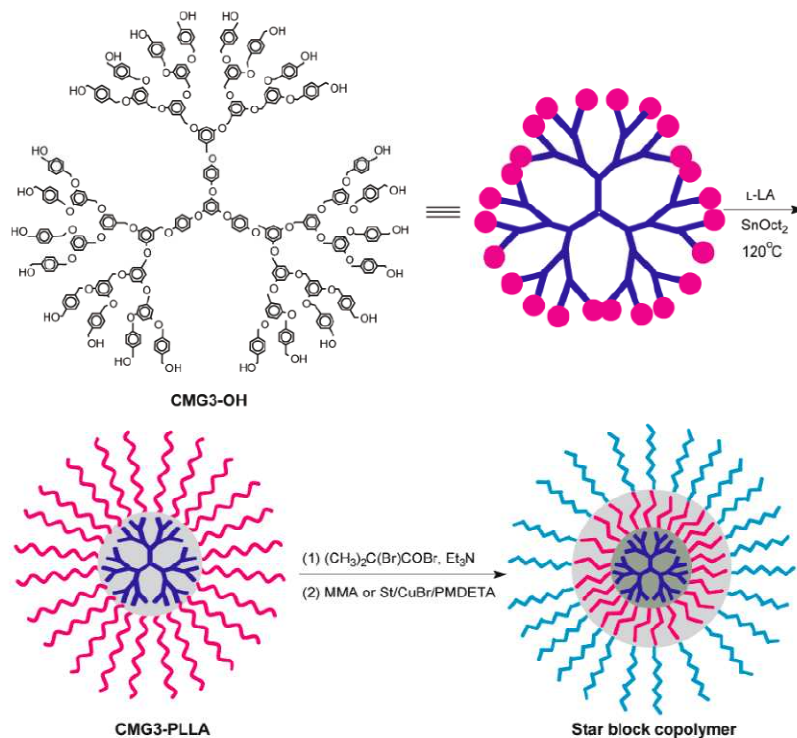
Figure 36: Synthesis of Star Block Copolymers by Mechanism Transformation as presented by Xi et al. using a Fréchet Dendron, Lactide and MMA.[225]

Miktoarm Stars

In 2004, Zhao and coworkers presented a new method to synthesize ABC 3-mictoarm star terpolymers. A trifunctional initiator bearing a hydroxy group, an ATRP initiator, and a nitroxide-mediated radical polymerization (NMP) initiator were designed and used in the preparation of star terpolymers composed of poly(ε-caprolactone) (PCL), PMMA, and PS

arms by sequential living ring-opening polymerization (ROP) of ε-caprolactone (CL), ATRP of MMA, and NMP of styrene (Figure 37).
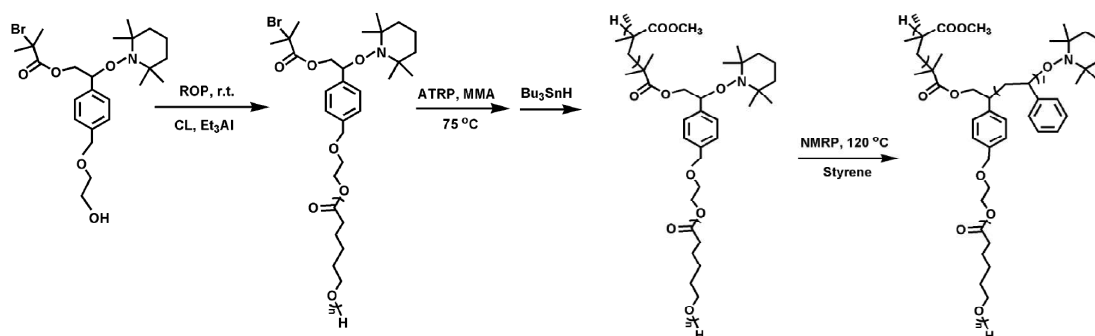
Figure 37: Synthesis of star-terpolymers by combining ring-opening polymerization (ROP), atom transfer radical polymerization (ATRP), and nitroxide-mediated radical polymerization (NMP) from a trifunctional initiator.

PS terminated with three functional groups, hydroxyl, RAFT-agent, and acetylene groups, has been synthesized successfully by the reaction of the RAFT agent with a functionalized styrene derivate. This multifunctional macroinitiator could be used for the subsequent ROP of ε-CL, RAFT polymerization of MMA, and a ''click'' reaction with PEO-N$_3$ to yield a four-mictoarm star (Figure 38).
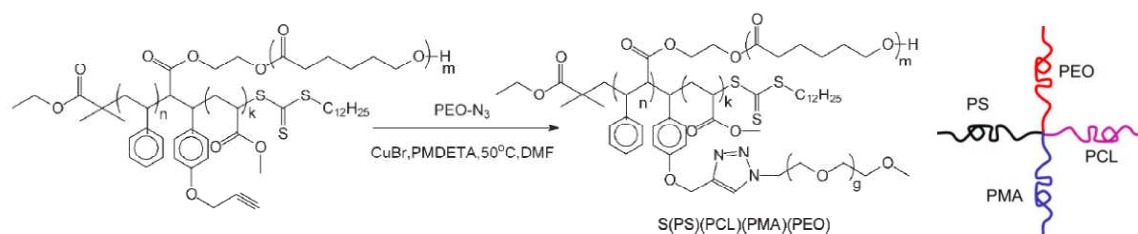
Figure 38: ABCD 4-mictoarm star polymer realized by Yang et al.: After CRP and ROP, the last arm is clicked to the center of the 3-arm star.[226]

Branched Polymers

In the previous section, the SCVP approach to hyperbranched polymers has been discussed. A special combination of ROP and CRP has been introduced by Hedrick et al[227] via the concurrent polymerizations of an ABC monomer: (ε-caprolactone), substituted with 2-bromo-2-dimethylpropionate) with a BCD monomer: (2-hydroxyethyl methacrylate) (HEMA). This concept allows the preparation of branched copolymers. The two monomers that polymerize by different mechanism, i.e. ring-opening polymerization (ROP) and atom transfer radical polymerization (ATRP) bear initiating centers that are compatible to the

opposite monomer. Adding un-functionalized comonomers such as CL and/or MMA in alters the molecular architecture.
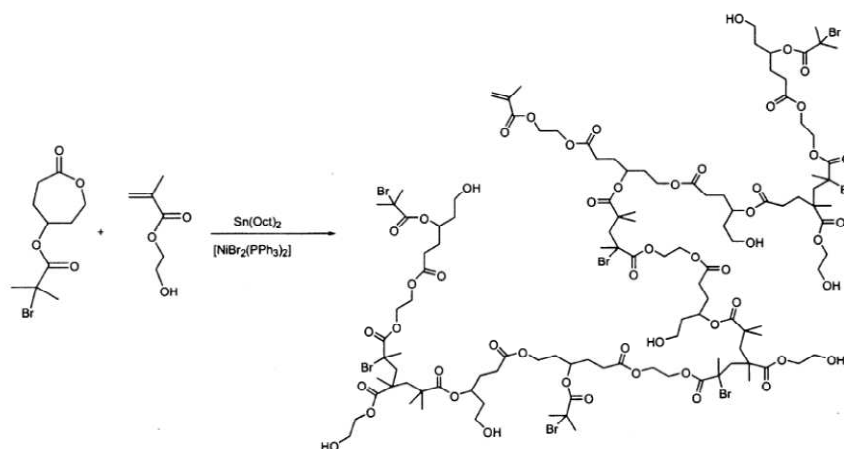
Figure 39: Combination of ROP and CRP by Hedrick et al. by the use of two orthogonal catalyst systems NiBr$_2$(PPh$_2$)$_2$ and Sn(Oct)$_2$ in one pot.

Biomedical Applications

Controlled Drug Delivery

The general principles of controlled polymer mediated drug delivery have been further developed since the early descriptions of Helmut Ringsdorf.[228,229] His concepts of polymer/drug conjugates have been realized in pioneering work by Ruth Duncan and coworkers[230] followed by many other research groups.[231] The target is the creation of a drug vehicle (or carrier) that permits the slow release of the drug (temporal control) or delivers the drug to the preferred site of activity (distribution control).[232] The controlled assembly of block copolymers in solution can be exploited for this purpose.[233] Especially block copolymer micelles and polymersomes are promising drug delivery and release vehicles.[234] The hydrophobic micelle core, which acts as a drug reservoir, is surrounded by a hydrophilic corona that provides a protective inter-phase between the core and the external environment (Figure 40).[235] Polymersomes form a nano-container with an aqueous core which can be used as a transport system for water-soluble therapeutic agents.[236,237] Current research objectives are focusing on the stability of the micellar assembly, prolonged circulation times, efficient drug absorption and the controlled release of the drug for optimal targeting.[238] Release triggers and mechanisms promoting the targeted delivery of drugs from polymer-drug conjugates or micelles at the desired site of action can be variations in pH, temperature, enzyme concentration, or attachment of targeting ligands.[239,240,241] Biodegradable poly(ester)s in general and particularly poly(lactide) are highly promising candidates as hydrophobic, core-forming species. Combinations of these well established poly(ester)s with innovative, shell-forming polymer species as well as their nanoscopic design and synthesis are subject of intense studies.

Important factors influencing drug release are the length of the core-forming polymer segment, the affinity between drug and core (i.e. partition coefficient between the core and the aqueous phase), and the amount of the loaded drug. Most stable drug loading can be achieved when the affinity, e.g. assessed by the Flory–Huggins interaction parameter between the drug and the core-forming segment of the block copolymer, is high.
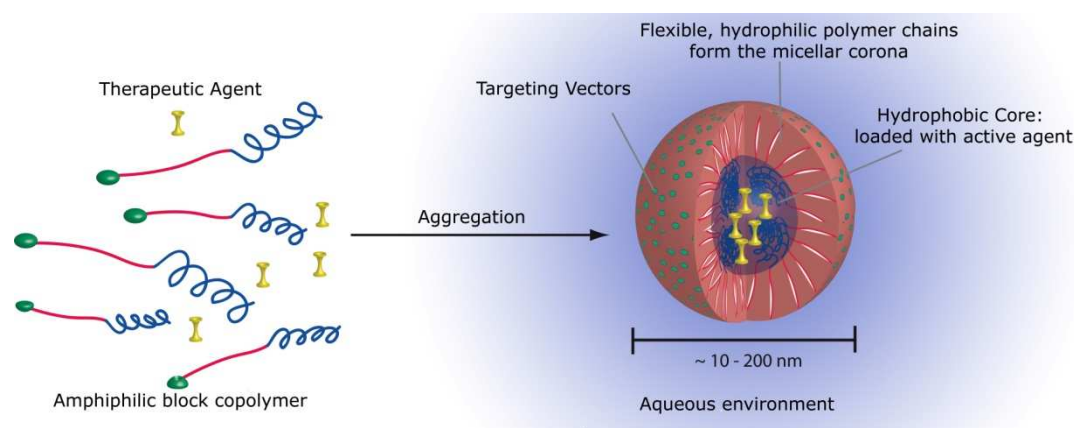
Figure 40: Encapsulation of therapeutic agents in micellar drug delivery systems.

Especially chemotherapy could benefit from polymer supported delivery. The widely used anti cancer drug Paclitaxel, which is extracted from the bark of the Pacific Yew tree (Taxus brevifolia), has limited solubility in water (0.3 mg/L at 37 °C) and requires a hydrophobic environment.[242] It is a natural taxane and highly effective against various tumors like ovarian and breast cancer and prevents cancer cells from dividing by binding and stabilizing the microtubules and inhibiting the disassembly into tubulins at the end of the mitosis process.[243]

Poly(ester)s in Micellar Drug Delivery Applications

In experiment polymeric micelles are very often cleared from the systemic circulation of animals within the first 8 to 10 h after intravenous administration. [244,245] Compared to other core-forming blocks, PLA based micelles (e.g. poly(ethylene glycol)-*b*-poly(D,L-lactide) showed superior circulation times (25% of the injected dose was still detected in the blood after 24 h).[246] Because of the degradability and hydrophobicity, poly(lactide) based block copolymers have moved into the center of attention for drug delivery applications.[247]

A great deal of work has focused on the use of PEG di- and triblock copolymers with poly(ester)s (these polymers can be easily obtained by using the terminal hydroxyl-chain end from the epoxide to initiate ROP of cyclic ester monomers). A number of studies has appeared on poly(ethylene glycol)-*b*-PLA copolymers which provide access to micelles[248,249] and polymersomes.[250] Leroux et al. produced micelles (40 nm) from amphiphilic poly(*N*-vinylpyrrolidone)-*block*-poly(D,L-lactide) (PVP-*b*-PDLLA) diblock copolymer.[251] Also poly-

electrolytes, like poly(vinylsulfonate) have been combined with lactide to create aggregate forming amphiphiles.[252]

Stereocomplex Stabilization of the Micellar Core

The isotactic character of poly(lactide) after controlled polymerization of the enantiomerically pure L- or D- isomer is the key to a special crystalline form. Upon blending in a similar weight ratio, poly(D- and L-Lactide) can form a special $3_1\alpha$-helical crystal conformation which shows increased stability compared to the standard form. This is reflected by increased melting temperatures and enthalpies. Crucial parameters affecting stereocomplexation are the mixing ratio and the molecular weight of L-lactide and D-lactide unit sequences.

> *"When the interaction between polymers having different tacticities or configurations prevails over that one between polymers with the same tacticity or configuration, a stereo-selective association of the former polymer pair takes place."*[253]

This increased, non covalent stabilization has recently come into focus for the additional stabilization of PLA-based micelles with intended applications in pharmacology.[254,255] This is particularly of importance since polymeric micelles are equilibrium systems that are susceptible to infinite dilution arising from the time of their administration. Using an innovative synthetic strategy PEO-*b*-PLA mictoarmstars, featuring two enantiomeric PLA arms were realized by Nederberg et al. for the fabrication of micelles with improved Paclitaxel release performance (almost zero order).[256] The concept of sterocomplexation is thereby used to stabilize the micelle against premature deterioration in the blood stream.[257] Hedrick and Yang could produce exceedingly elongated cylindrical micelles by loading enantiomeric poly(lactide)-*b*-PEO copolymers with Paclitaxel. Only the stereo-block copolymer/Paclitaxel mixture forms a long fiber-like assembled structure, while complexes formed from the block copolymer mixture without Paclitaxel had a spherical shape.[258] PLA stereocomplexation can also be used to fabricate mixed micelles with different shell forming species such as PEG and thermoresponsive PNIPAM.[259]

Innovative Hydrophilic Block Builders: Functional (Meth-)Acrylates

The design of the polar shell is of fundamental importance: The avoidance of opsonin-adsorption is a primary objective because this protein promotes the subsequent uptake of the aggregate by the reticuloendothelial system (RES) in the liver and spleen. PEG is performing quite well in this discipline and is therefore considered the gold standard[260] – yet there is still room for improvement. In order to increase the functionality of these systems and hence potentially improve their performance, the combination of poly(ester)s with other readily tunable functional polymers is required.

Especially hydrophilic methacrylates are promising candidates for this task and combination with a hydrophobic poly(ester) such as PLA have rarely been described. CRP methods like ATRP and RAFT have been approved for the formation of poly(ester)/poly(methacrylate) block copolymers.[261] Sufficiently hydrophilic methacrylate candidates could be glycerol methacrylate (GMA)[262,263] and oligoethylene glycol methacrylate (OEGMA)[264,265,266,267]. Poly(2-hydroxypropyl methacrylamide) (PHPMA) has an almost 30 year old history in drug delivery and has been a forerunner in terms of clinical testing and approval. Yet its potential in the combination with poly(ester)s has not been fully explored.[268,269] 2-Methacryloyloxyethyl phosphorylcholine (MPC) has been polymerized from various ATRP macroinitiators and could be a highly interesting hydrophile for a combination with poly(ester)s. Its polymers are remarkably resistant to protein adsorption and bacterial/cellular adhesion.[270,271,272] Especially methacrylate-based macromonomers appear as a promising means to stimuli responsive brushes.[273,274]

In summary we can say that the combination of poly(ester)s with new hydrophilic methacryates is highly desirable for the formation of stable, biodegradable micelles with a good loading performance and long circulation times. This strategy takes advantage of the properties of the poly(ester) blocks such as facile degradability and crystallinity and the fact that functional (meth)acrylates can be easily modified or copolymerized. Both factors are beneficial for the attachment of targeting vectors. A number of external stimuli can be applied to induce physical-chemical phase transitions, which can be used as release triggers.

Amphiphilic Block Copoly(ester)s for Tissue Engineering Applications

Scaffolds used in tissue engineering are three-dimensional structures which provide a template for cell organization, guide cell differentiation, and give protection to the delivered cells (mechanical and/or chemical) from the surrounding tissue over an appropriate period of time, while enabling exchange of nutrients and waste products.[275] These devices may not induce an intense or prolonged inflammatory response in vivo and must degrade in a controlled manner without releasing toxic byproducts. Cell scaffolds used in current research are typically open cell foams[276,277] or nonwoven fiber meshes[278,279] with pores ranging from a few tens to several hundreds of micrometers in diameter, depending on the application, with porosities of 95 vol. %.

Many polymers that have been studied for medical applications share certain properties that are essential to their use as biomaterials. Their application in tissue engineering requires them to be biocompatible, non-toxic, and non-inflammatory, which is particularly important when designing degradable polymers as the degradation products as well have to meet these criteria.

The use of degradable polymers is desirable because surgical removal is not required; however, care must be taken to ensure the compatibility of both intermediate and final degradation products, the timing of the degradation process, and how each of these affects the regenerative process. A significant bio-resorbable material used in the generation of degradable scaffolds is therefore a class of poly(ester)s belonging to the family of poly(α-hydroxy acids) since they match the above mentioned requirements.[280]

The family of poly(α-hydroxy acids), poly(carbonate)s and poly(caprolactone)s offer excellent compatibility and cell adhesion properties. Despite the great success of these polymers, tissue engineering faces a major challenge, i.e. the problem of non-specific protein adsorption on these highly compatible materials (one might say: "almost too compatible"). Such non-fouling properties can be supplemented with the enhanced adsorption of specific proteins, or immobilization of cell recognition motives to control the interaction between

cells and synthetic substrates. A range of materials can be rendered resistant to non-specific protein adsorption by the surface modification or grafting of PEG to the substrate.
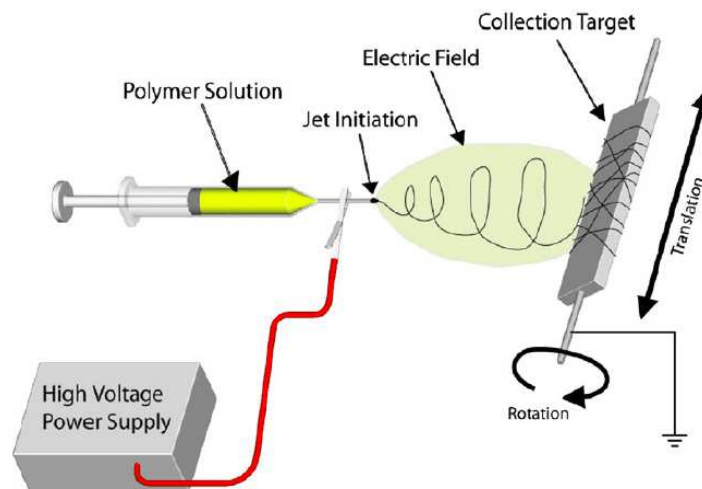
Figure 41: Illustration of the electrospinnig process of a polymer solution.[281]

Especially electrospun nanofibers have attracted interest in the generation of biomedical scaffolds based on fiber meshes and offer a tool to construct nanometer scale dimensions. There has been a surge in the use of electrospinning techniques[282] to create nanofibre scaffolds as substrates from a wide range of different polymers. They mimic the size scale of fibrous proteins (fibrils) found in extracellular matrices and the three dimensional nature of the matrix allows for cells to infiltrate the interporous matrix. Proliferation is therefore promoted by the formation of an interpenetrated network, enabling the diffusion of nutrients and the formation of vessels.
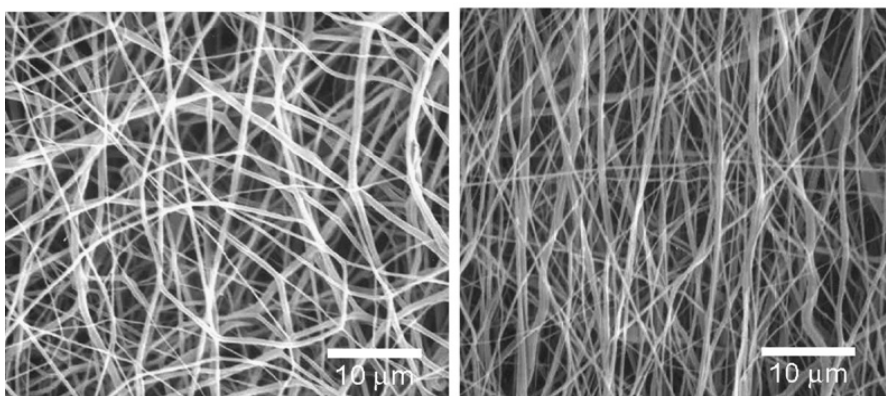
Figure 42: Poly(ester) fibres produced by electrospinning.[283]

Besides the small fiber diameter, nanofiber scaffolds offer high surface to volume ratios and the potential for high porosity and interconnected pores. The functionalization with biologically active ligands as well as the minimization of unspecific protein adsorption remain challenging tasks for the preparation of electrospun fiber constructs. However, while all proteins are known to have an inherent tendency to deposit rapidly onto surfaces, it is generally accepted that cell adhesion and subsequent cellular events are controlled by proteins adsorbed onto artificial surfaces.[284] It is therefore reasonable to assume that the surface properties determine the organization of the adsorbed protein layer, and the nature of this layer in turn determines the cellular response to the implant. Many different surface preparations based on poly(ethylene glycol) (PEG) have been developed to prevent non-specific adsorption of proteins and cells. "Non-fouling" tissue engineering scaffolds could be realized by the use of amphiphilic block copolymers if controlled microphase separation can be induced during the spinning process.

The combination of amphiphilic poly(ester) based block copolymers with the advanced electrospinning technique offers the chance to realize fibres with a hydrophilic and protein repellant shell. Microphase separation of the block copolymer during the electrospinning process is therefore a key element on the way to these structures. Special functionalization with peptide sequences could promote the adhesion of cells with complementary receptors (Figure 43).

The arginine-glycine-aspartic acid (RGD) cell adhesion sequence was discovered in fibronectin 26 years ago (Pierschbacher & Ruoslahti 1984). The surprising finding that only three amino acids would form an essential recognition site for cells in a very large protein was initially received with some skepticism. The class of integrins, cell surface receptors that recognize the RGD sequence of various proteins, has given RGD a central role in cell adhesion biology as the prototype adhesion signal. Short peptides containing the RGD sequence can mimic cell adhesion proteins in two ways: When coated onto a surface, they promote cell adhesion, whereas in solution they act as decoys, preventing adhesion.[285]
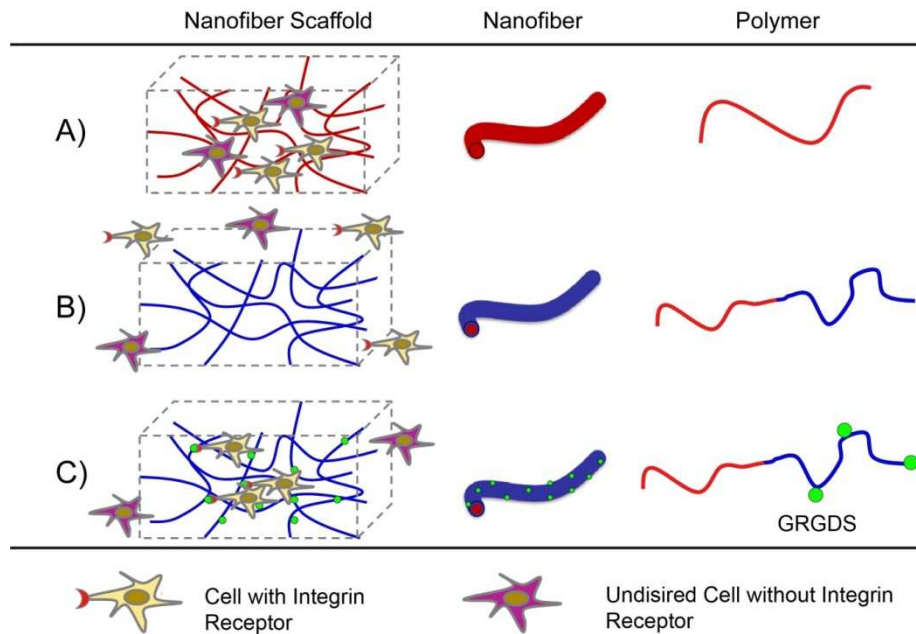
Figure 43: Evolution of a tissue engineering scaffold: A) conventional design made from a degradable poly(ester) B) Scaffold with a hydrophobic, protein repellent shell, realized by microphase separation during the electrospinning process. C) Hydrophilic Scaffold with peptide marker for specific cell adhesion.

Klee et al. recently realized homogenous GRGDS (a cell adhesive peptide sequence for integrin receptors incorporating the RGD sequence, H-Gly-Arg-Gly-Asp-Ser-OH)[286] functionalized and non functionalized electrospun fibres of PEG-*b*-P(ε-CL) with a dominant hydrophilic block.[287] Contact angle measurements (30°) confirmed the hydrophilicity of the fibers and suggested that the hydrophilic block is oriented towards the fiber surface. Similar results were obtained with PEG-PLLA block copolymers.[288] The general design principle is presented in Figure 43. Functional hydrophilic substitutes for PEG which should allow for a better receptor conjugation by the addition of available functional groups: A synthetic approach is presented in chapter 3.1 in the form of Poly(lactide)-*b*-Poly(hydroxymethyl methacrylate) copolymers.

References

[1] Lyu, S.-P.; Schley, J.; Loy, B.; Lind, D.; Hobot, Ch.; Sparer, R.; Untereker, D. Kinetics and Time-Temperature Equivalence of Polymer Degradation *Biomacromolecules* **2007,** *8*, 2301-2310.

[2] Hakkarainen, M.; Adamus, G.; Höglund, A.; Kowalczuk, M.; Albertsson, A. C. ESI-MS Reveals the Influence of Hydrophilicity and Architecture on the Water-Soluble Degradation Product Patterns of Biodegradable Homo- and Copoly(ester)s of 1,5-dioxepan-2-one and ε-Caprolactone *Macromolecules* **2008**, *41*, 3547-3554.

[3] Albertsson, A. C. Varma, I. K. Aliphatic poly(ester)s: Synthesis, properties and applications *Adv. Polym. Sci.,* **2002**, *157*, 1–40.

[4] Hofmann, D.; Entrialgo-Castano, M.; Kratz, K.; Lendlein, A. Knowledge-Based Approach towards Hydrolytic Degradation of Polymer-Based Biomaterials *Adv. Mater.* **2009**, *21*, 3237–3245.

[5] Hakkarainen, M.; Höglund, A.; Odelius, K.; Albertsson, A. C. Tuning the Release Rate of Acidic Degradation Products through Macromolecular Design of Caprolactone-Based Copolymers *J. Am. Chem. Soc.* **2007**, 129, 6308-6312.

[6] Witzke, D. R. Introduction to Properties, Engineering, and Prospects of Poly(lactide) Polymers *Ph.D. Dissertation*, Michigan State University, East Lansing, MI, 1997.

[7] Hakkarainen, M.; Karlsson, S.; Albertsson, A.-C. Rapid (bio)degradation of poly(lactide) by mixed culture of compost microorganisms—low molecular weight products and matrix changes *Polymer* **2000***, 41, 2331–2338.

[8] Coulembiera, O.; Degea, Ph.; Hedrick, J. L.; Dubois, Ph. From controlled ring-opening polymerization to biodegradable aliphatic poly(ester): Especially poly(b-malic acid) derivatives *Prog. Polym. Sci.* **2006,** *31,* 723–747.

[9] Ikada, Y.; Jamshidi, K.; Tsuji, H.; Hyon, S.-H. Stereocomplex Formation between Enantiomeric Poly(lactides) *Macromolecules* **1987**, *20*, 904-906.

[10] Dove, A. P. Controlled ring-opening polymerisation of cyclic esters: polymer blocks in self-assembled nanostructures Chem. Commun. **2008**, 6446–6470.

[11] Hiltunen, K.; Seppala , J. V.; Harkonen, M. Effect of Catalyst and Polymerization Conditions on the Preparation of Low Molecular Weight Lactic Acid Polymers *Macromolecules* **1997,** *30,* 373-379.

[12] Gu, S. Y.; Yang, M.; Yu, T.; Ren, T. B.; Ren, J.; Synthesis and characterization of biodegradable lactic acid-based polymers by chain extension *Polym. Int.* ***2008, 57***, 982–986.

[13] Drumright, R. E.; Gruber, P. R.; Henton, D. E. Poly(lactic Acid) Technology *Adv. Mater.* **2000**, *12*, 1841-1846.

[14] Martin, O.; Schwach, E.; Avérous, L.; Couturier, Y. Properties of Biodegradable Multilayer Films Based on Plasticized Wheat Starch *Starch/Stärke* **2001,** *53*, 372–380.

[15] Web source: www.pyraplast.com

[16] Web source: www.natureworksllc.com

[17] Barry, Ch. Bio-based plastics still say "green" -but now performance is key: poly(lactide)'s packaging characteristics put corn-based plastic in the ballpark with polyethylene, polypropylene *Food & Drug Packaging* **2001**.

[18] Jérôme, Ch.; Lecomte, Ph. Recent advances in the synthesis of aliphatic poly(ester)s by ring-opening polymerization *Adv. Drug Del. Rev.* **2008**, *60*, 1056–1076.

[19] Carothers, W. H.; Dorough, G. L.; van Natta, F. J. Studies of Polymerization and Ring Formation. X. The Reversible Polymerization of Six-Membered cyclic Esters *J. Am. Chem. Soc.* **1932**, *54*, 761–772.

[20] Kleine, J.; Kleine, H. H.; Über hochmolekulare, insbesondere optisch aktive Poly(ester) der Milchsäure, ein Beitrag zur Stereochemie Makromolekularer Verbindungen *Die Makromolekulare Chemie* **1959**; *30*, 23-38.

[21] Duda, A; Kowalski, A Thermodynamic and kinetic polymerizability of cyclic esters Libiszowski, J *Macromol. Symp.* **2005**, *224,* 71-83.

[22] Dainton, F. S., Ivin, K. J. Some Thermodynamic and Kinetic Aspects of Addition Polymerization *Q. Rev. Chem. Soc.* **1958**, *12*, 61-92.

[23] Nielen, M. W. F. Maldi time-of-flight mass spectrometry of synthetic polymers *Mass Spectrometry Reviews* **1999**, *18*, 309-344.

[24] Libiszowski, J.; Kowalski, A.; Szymanski, R.; Duda, A.; Raquez, J. M.; Degee P.; Dubois, P. Monomer-Linear Macromolecules-Cyclic Oligomers Equilibria in the Polymerization of 1,4-Dioxan-2-one *Macromolecules* **2004,** *37,* 52-59.

[25] Montaudo. G.; Montaudo, M. S.; Puglisi, C.; Samperi, F.; Spassky, N.; LeBorgne, A.; Wisniewski, M. Evidence for Ester-Exchange Reactions and Cyclic Oligomer Formation in the Ring-Opening Polymerization of Lactide with Aluminum Complex Initiators *Macromolecules* **1996,** *29,* 6461-6465.

[26] Wu, J.; Yu, T.-L.; Chen, Ch.-T.; Lin, Ch.-Ch. Recent developments in main group metal complexes catalyzed/initiated polymerization of lactides and related cyclic esters *Coordination Chemistry Reviews* **2006** *250*, 602–626.

[27] Dubois, Ph.; Jacobs, C.; Jerome, R. Teyssié, Ph. Macromolecular Engineering of Polylactones and Poly(lactide)s. 4. Mechanism and Kinetics of Lactide Homopolymerization by Aluminum Isopropoxide *Macromolecules* **1991**, *24,* 2266-2270.

[28] Wofl, F., Frey, H. *unpublished results.*

[29] Witzke, D. R.; Narayan, R.; Kolstad, J. J Reversible Kinetics and Thermodynamics of the Homopolymerization of L-Lactide with 2-Ethylhexanoic Acid Tin(II) Salt *Macromolecules* **1997,** *30,* 7075-7085.

[30] Yu, Y.; Storti, G.; Morbidelli, M. Ring-Opening Polymerization of L,L-Lactide: Kinetic and Modeling Study *Macromolecules* **2009**, 42, 8187–8197.

[31] Duda A, Libiszowski J, Mosnacek J, Penczek S Copolymerization of cyclic esters at the living polymer-monomer equilibrium *Macromol. Symp.* **2005**, *226,* 109-119.

[32] Mosnácek, J.; Duda, A.; Libiszowski, J.; Penczek, S. Copolymerization of L-Lactide at Its Living Polymer-Monomer Equilibrium with ℇ-Caprolactone as Comonomer *Macromolecules* **2005,** *38,* 2027-2029.

[33] Kricheldorf, H. R.; Kreiser-Saunders, I.; Boettecher, C. Polylactones: 31. Sn(II)octoate-initiated polymerization of L-lactide: a mechanistic study *Polymer* 1995, *36*, 1253–1250.

[34] Kricheldorf, H. R.; Kreiser-Saunders, I.; Stricker, A. Polylactones 48. SnOct$_2$-Initiated Polymerizations of Lactide: A Mechanistic Study *Macromolecules* **2000**, *33*, 702–709.

[35] Kowalski, A.; Duda, A.; Penczek, S. Kinetics and Mechanism of Cyclic Esters Polymerization Initiated with Tin(II) Octoate. 3. Polymerization of L,L-Dilactide *Macromolecules* **2000**, *33*, 7359–7370.

[36] Penczek, S. et al. On the Mechanism of Cyclic-Ester Polymerization induced by Tin(II) Octanoate *Macromol. Symp.* **2000,** *157,* 61–70.

[37] Ryner, M.; Stridsberg, K.; Albertsson, A.-C. Mechanism of Ring-Opening Polymerization of 1,5-Dioxepan-2-one and L-Lactide with Stannous 2-Ethylhexanoate. A Theoretical Study *Macromolecules* **2001,** *34,* 3877-3881.

[38] Dechy-Cabaret, O.; Martin-Vaca, B.; Bourissou, D. Controlled Ring-Opening Polymerization of Lactide and Glycolide *Chem. Rev.* **2004,** *104*, 6147-6176.

[39] Degée, Ph.; Dubois, Ph.; Jacobson, S., Fritz, H.-G.; Jérôme, R. Beneficial Effect of Triphenylphosphine on the Bulk Polymerization of L,L-Lactide Promoted by 2-Ethylhexanoic Acid Tin (II) Salt *J. Polym. Sci.: Part A: Polym. Chem.* **1999**, *37*, 2413–2420.

[40] Kricheldorf, H. R.; Dunsing, R. Polylactones, 8 Mechanism of the cationic polymeriztion of L,L-dilactide *Makromol. Chem.* **1986**, *187*, 1611-1625.

[41] Kricheldorf, H. R.; Kreiser, I. Polylactones, 11 Cationic copolymerization of glycolide with L,L-dilactide *Makromol. Chem.* **1987**, *188*, 1861-1873.

[42] Bourissou, D.; Martin-Vaca, B.; Dumitrescu, A.; Graullier, M.; Lacombe, F. Controlled Cationic Polymerization of Lactide *Macromolecules* **2005,** *38,* 9993-9998.

[43] Penczek, S. Cationic Ring-Opening Polymerization (CROP) Major Mechanistic Phenomena *J. Polym. Sci., Part A: Polym. Chem.* **2000**, *38*, 1919.

[44] Jedlinski, Z.; Walach, W.; Kurcok, P.; Adamus, G. Polymerization of lactones, 12. Polymerization of L,L-dilactide and L,D-dilactide in the presence of potassium methoxide *Makromol. Chem.* **1991**, *192*, 2051-2057.

[45] Kricheldorf, H.R.; Serra, A. Polylactones 6. Influence of Various Metal Salts on the Optical Purity of Poly(L-Lactide) *Polym. Bull.* **1985***, 14***,** 497-502.

[46] Kricheldorf, H. R.; Kreiser-Saunders, I. Makromol. Chem. **1990***, 191*, 1057.

[47] Kricheldorf H. R.; Boettcher, C*.* Polylactones 26 Lithium alkoxide-initiated polymerizations of L-lactide *Makromol. Chem.* **1993,** *194*, 1665-1669.

[48] Gadzinowski, M. Sosnowski, S. Biodegradable/Biocompatible ABC Triblock Copolymer Bearing Hydroxyl Groups in the Middle Block *J. Polym. Sci. Part A: Polym. Chem.* **2003**, 41: 3750–3760.

[49]Nahrain E. Kamber, Wonhee Jeong, and Robert M. Waymouth Organocatalytic Ring-Opening Polymerization Chem. Rev. **2007,** 107, 5813-5840.

[50] Uyama, H.; Kobayashi, S. Enzymatic Ring-Opening Polymerization of Lactones Catalyzed by Lipase *Chem. Lett.* **1993**, 1149-1150.

[51] Knani, D.; Gutman, A. L.; Kohn, D. H. Enzymatic Poly(ester)ification in Organic Media. Enzyme-Catalyzed Synthesis of Linear Poly(ester)s. 1. Condensation Polymerization of linear Hydroxyesters. II. Ring-Opening Polymerization of c-Caprolactone *J. Polym. Sci., Part A: Polym. Chem.* **1993**, *31*, 1221.

[52] Kobayashi, S.; Uyama, H.; Kimura, S. Enzymatic Polymerization *Chem. Rev.* **2001,** *101,* 3793-3818.

[53] Kobayashi, S. Makino, A. Enzymatic Polymer Synthesis: An Opportunity for Green Polymer Chemistry *Chem. Rev.* **2009,** *109,* 5288–5353.

[54] van der Meulen, I.; de Geus, M.; Antheunis, H.; Deumens, R.; Joosten, E. A. J.; Koning, C. E.; Heise, A. Polymers from Functional Macrolactones as Potential Biomaterials: Enzymatic Ring Opening Polymerization, Biodegradation, and Biocompatibility *Biomacromolecules* **2008,** *9,* 3404–3410.

[55] Takwa, M.; Simpson, N.; Malmström, E.; Hult, K.; Martinelle, M. One-Pot Difunctionalization of Poly(⊠-pentadecalactone) with Thiol-Thiol or Thiol-Acrylate Groups, Catalyzed by *Candida antarctica* Lipase B *Macromol. Rapid Commun.* **2006**, *27*, 1932.

[56] Hiroshi Uyama, H. Kobayashi, S. Enzyme-catalyzed polymerization to functional polymers *Journal of Molecular Catalysis B: Enzymatic* **2002**, *19*, 117–127.

[57] Hedfors, C.; Ostmark, E.; Malmström, E.; Hult, K.; Martinelle M. Thiol End-Functionalization of Poly(omega-caprolactone), Catalyzed by *Candida antarctica* Lipase B *Macromolecules* **2005***, 38,* 647-649.

[58] de Geus, M.; Peeters, J.; Wolffs, M.; Hermans, Th.; Palmans, A. R. A.; Koning, C. E.; Heise, A. Investigation of Factors Influencing the Chemoenzymatic Synthesis of Block Copolymers *Macromolecules* **2005,** *38,* 4220-4225.

[59] Frey, H.; Neuner, I. T.; Ursu, M. *Abstracts of Papers of the American chemical Society* **2003**, *226*, 437-POLY, U421-U421.

[60] Nederberg, F.; Connor, E. F.; Moller, M.; Glauser, T.; Hedrick,J. L. New Paradigms for Organic Catalysts: The First Organocatalytic Living Polymerization Angew. Chem., Int. Ed. **2001**, *40*, 2712–2715.

[61] Bonduelle, C.; Martin-Vaca, B.; Cossio, F. P.; Bourissou, D. Monomer versus Alcohol Activation in the 4-Dimethylaminopyridine- Catalyzed Ring-Opening Polymerization of Lactide and Lactic O-CarboxylicAnhydride *Chem.: Eur. J.* **2008**, *14*, 5304–5312.

[62] Pratt, R. C.; Lohmeijer, B. G. G.; Long, D. A.; Lundberg, P.N. P.; Dove, A. P.; Li, H.; Wade, C. G.; Waymouth, R. M.; Hedrick, J. L. Exploration, Optimization, and Application of Supramolecular Thiourea-Amine Catalysts for the Synthesis of Lactide (Co)polymers *Macromolecules* **2006**, *39,* 7863-7871.

[63] Kiesewetter, M. K.; Shin, E. J.; Hedrick, J. L.; Waymouth, R. M. Organocatalysis: Opportunities and Challenges for Polymer Synthesis *Macromolecules* **2010**, 43, 2093–2107.

[64] Nederberg, F.; Connor, E. F.; Glausser, T.; Hedrick, J. L. Organocatalytic chain scission of poly(lactides): a general route to controlled molecular weight, functionality and macromolecular architecture *Chem. Commun.* **2001**, 2066–2067.

[65] Zhang, L.; Nederberg, F.; Pratt, R. C.; Waymouth, R. M.; Hedrick, J. L.; Wade, C. G. Phosphazene Bases: A New Category of Organocatalysts for the Living Ring-Opening Polymerization of Cyclic Esters *Macromolecules* **2007,** *40,* 4154-4158.

[66] Lohmeijer, B. G. G.; Pratt, R. C.; Leibfarth, F.; Logan, J. W.; Long, D. A.; Dove, A. P.; Nederberg, F.; Choi, J.; Wade, C.; Waymouth,R. M.; Hedrick, J. L. Guanidine and Amidine Organocatalysts for Ring-Opening Polymerization of Cyclic Esters *Macromolecules* **2006,** *39,* 8574-8583.

[67] Nederberg, F.; Lohmeijer, B. G. G.; Leibfarth, F.; Pratt, R. C.; Choi, J.; Dove, A. P.; Waymouth, R. M.; Hedrick, J. L. Organocatalytic Ring-Opening Polymerization of Trimethylene Carbonate *Biomacromolecules* **2007,** *8*, 153-160.

[68] Pratt, R. C.; Lohmeijer, B. G. G.; Long, D. A.; Waymouth, R. M.; Hedrick, J. L. Triazabicyclodecene: A Simple Bifunctional Organocatalyst for Acyl Transfer and Ring-Opening Polymerization of Cyclic Esters *J. Am. Chem. Soc.* **2006**, 128, 4556-4557.

[69] Simón, L.; Goodman, J. M. The Mechanism of TBD-Catalyzed Ring-Opening Polymerization of Cyclic Esters *J. Org. Chem.* **2007**, *72*, 9656-9662.

[70] Breslow, R. On the Mechanism of Thiamine Action. 1 V.l Evidence from Studies on Model Systems *J. Am. Chem. Soc.* **1958**, *80*, 3719.

[71] Wanzlick, H. W.; Schikora, E. Ein neuer Zugang zur Carben-Chemie *Angew. Chem.* **1960**, *72*, 494.

[72] Wanzlick, H. W.; Schikora, E Ein nucleophiles Carben *Chem. Ber*. **1961,** *94*, 2389-2393.

[73] Arduengo, A. J., III; Harlow, R. L.; Kline, M A Stable Crystalline Carbene *J. Am. Chem. Soc.* **1991**, *113*, 361-363.

[74] Arduengo, A. J. Looking for Stable Carbenes: The Difficulty in Starting Anew *Acc. Chem. Res.* **1999**, *32*, 913-921.

[75] Scholl, M.; Ding, Sh.; Lee, Ch. W.; Grubbs, R. H. Synthesis and Activity of a New Generation of Ruthenium-Based Olefin Metathesis Catalysts Coordinated with 1,3-Dimesityl-4,5-dihydroimidazol-2-ylidene Ligands *Org. Lett.*, 1999, 1, 953–956.

[76] Grasa, G. A.; Kissling, R. M.; Nolan, S. P. *N-Heterocyclic Carbenes as Versatile Nucleophilic Catalysts for Transesterification/Acylation Reactions Org. Lett.* 2002, 4, 3583–3586.

[77] Nyce, G. W.; Lamboy, J. A.; Connor, E. F.; Waymouth, R. M.; Hedrick, J. L. *Org. Lett.* 2002, 4, 3587–3590.

[78] Connor, E. F.; Nyce, G. W.; Myers, M.; Mock, A.; Hedrick, J. L. First Example of N-Heterocyclic Carbenes as Catalysts for Living Polymerization: Organocatalytic Ring-Opening Polymerization of Cyclic Esters *J. Am. Chem. Soc.* **2002**, *124*, 914–915

[79] Nyce, G. W.; Glauser, T.; Connor, E. F.; Mock, A.; Waymouth, R. M.; Hedrick, J. L. In Situ Generation of Carbenes: A General and VersatilePlatform for Organocatalytic Living Polymerization *J. Am. Chem. Soc.* 2003, 125, 3046–3056.

[80] Nyce, G. W.; Csihony, S.; Waymouth, R. W; Hedrick, J. L. A General and Versatile Approach to Thermally Generated N-Heterocyclic Carbenes *Chem. Eur. J.* **2004**, 10, 4073 – 4079.

[81] Dove, A. P.; Pratt, R. C.; Lohmeijer, B. G. G.; Culkin, D. A.; Hagberg, E. C.; Nyce, G. W.; Waymouth, R. M.; Hedrick, J. L. N-Heterocyclic carbenes: Effective organic catalysts for living polymerization *Polymer* **2006**, 47, 4018-4025.

[82] Lai, C.-L.; Lee, H. M.; Hu, C.-H. Theoretical study on the mechanism of *N*-heterocyclic carbene catalyzed transesterification reactions *Tetrahedron Lett*. **2005**, *46*, 6265–6270.

[83] Jeong, W.; Shin, E. J.; Culkin, D. A.; Hedrick, J. L.; Waymouth, R. M. Zwitterionic Polymerization: A Kinetic Strategy for the Controlled Synthesis of Cyclic Poly(lactide) *J. Am. Chem. Soc.* **2009**, *131*, 4884–4891.

[84] Raynaud, J.; Ciolino, A.; Baceiredo, A.; Destarac, M.; Bonnette, F.; Kato, T.; Gnanou, Y.; Taton, D. Harnessing the potential of N-heterocyclic carbenes for the rejuvenation of group-transfer polymerization of (meth)acrylics *Angew. Chem., Int. Ed.* **2008**, 47, 5390–5393.

[85] Scholten, M. D.; Hedrick, J. L.; Waymouth,R.M. *Macromolecules* **2008**, *41*, 7399–7404.

[86] Raynaud, J.; Gnanou, Y.; Taton, D. Group Transfer Polymerization of (Meth)acrylic Monomers Catalyzed by N-Heterocyclic Carbenes and Synthesis of All Acrylic Block Copolymers: Evidence for an Associative Mechanism *Macromolecules* **2009**, *42*, 5996–6005.

[87] Raynaud, J.; Absalon, Ch.; Gnanou, Y.; Taton, D. N-Heterocyclic Carbene-Induced Zwitterionic Ring-Opening Polymerization of Ethylene Oxide and Direct Synthesis of r,ω-Difunctionalized Poly(ethylene oxide)s and Poly(ethylene oxide)-b-poly(ε-caprolactone) Block Copolymers *J. Am. Chem. Soc.* **2009**, *131*, 3201–3209

[88] de Jong, S. J.; van Dijk-Wolthuis, W. N. E.; Kettenes-van den Bosch, J. J. Schuyl, P. J. W.; Hennink, W. E. Monodisperse Enantiomeric Lactic Acid Oligomers: Preparation, Characterization, and Stereocomplex Formation *Macromolecules* **1998**, *31*, 6397–6402.

[89] Takizawa, K.; Nulwala, H.; Hu, J., Yoshinaga, K.; Hawker, C. J. Molecularly Defined (*L*)-Lactic Acid Oligomers and Polymers: Synthesis and Characterization *Journal of Polymer Science: Part A: Polymer Chemistry* **2008**; *46*, 5977–5990.

[90] Takizawa, K.; Tang, Ch. Hawker, C. J. Molecularly Defined Caprolactone Oligomers and Polymers: Synthesis and Characterization *J. Am. Chem. Soc.* **2008**, *130*, 1718–1726.

[91] Lou, X.; Detrembleur, Ch.; Jérôme, R. Novel Aliphatic Poly(ester)s Based on Functional Cyclic (Di)Esters *Macromol. Rapid Commun.* **2003**, *24*, 161-172.

[92] Parrish, B.; Emrick, T. Aliphatic Poly(ester)s with Pendant Cyclopentene Groups: Controlled Synthesis and Conversion to Poly(ester)-*graft*-PEG Copolymers *Macromolecules* **2004,** *37,* 5863-5865.

[93] Bryan Parrish, Rebecca B. Breitenkamp, and Todd Emrick PEG- and Peptide-Grafted Aliphatic Poly(ester)s by Click Chemistry *J. Am. Chem. Soc.* **2005,** *120*, 7404-7410*.*

[94] Lecomte, Ph.; Riva, R.; Jérôme, Ch.; Jérôme, R. Macromolecular Engineering of Biodegradable Poly(ester)s by Ring-Opening Polymerization and 'Click' Chemistry *Macromol. Rapid Commun.* **2008**, *29*, 982–997.

[95] Trollsås, M.; Lee, V.Y.; Mecerreyes, D.; Löwenhielm, P.; Möller, M.; Miller, R. D.; Hedrick, J.L. Hydrophilic Aliphatic Poly(ester)s: Design, Synthesis, and Ring-Opening Polymerization of Functional Cyclic Esters *Macromolecules* **2000**, *33,* 4619-4627.

[96] Kimura, Y.; Shirotani, K.; Yamane, H.; Kitao, T. Ring-Opening Polymerization of 3(*S*)-[Benzyloxycarbonyl)methyl]-1,4-dioxane-2,5-dione: A New Route to a Poly(☐-hydroxy acid) with Pendant Carboxyl Groups *Macromolecules* **1988**, *21,* 3338-3340.

[97] Seyednejad, H.; Vermonden, T.; Fedorovich, N. E.; van Eijk, R.; van Steenbergen, E.M. J ;Dhert, W. J. A.; Nostrum; C.F.; Hennink, W. E. Synthesis and Characterization of Hydroxyl-Functionalized Caprolactone Copolymers and Their Effect on Adhesion, Proliferation, and Differentiation of Human Mesenchymal Stem Cells *Biomacromolecules* **2009,** *10,* 3048–3054.

[98] Wang, L.; Jia, X.;Yuan, Zh. Synthesis and characterization of novel functionalized poly(lactide)s with pendent hydroxyl arms *Polymer* **2006**, *47*, 6978-6985.

[99] Tian, D.; Dubois, P.; Grandfils, C.; Jerome, R. Ring-Opening Polymerization of 1,4,8-Trioxaspiro[4.6]-9-undecanone: A New Route to Aliphatic Poly(ester)s Bearing Functional Pendent Groups *Macromolecules* **1997,** *30,* 406-409.

[100] Tian, D.; Dubois, P.; Jerome, R. Macromolecular Engineering of Polylactones and Poly(lactide)s. 23. Synthesis and Characterization of Biodegradable and Biocompatible Homopolymers and Block Copolymers Based on 1,4,8-Trioxa[4.6]spiro-9-undecanone *Macromolecules* **1997,** *30,* 1947-1954.

[101] Tian, D.; Dubois, P.; Jerome, R. Macromolecular Engineering of Polylactones and Poly(lactide)s. 22. Copolymerization of ☐-Caprolactone and 1,4,8-Trioxaspiro[4.6]-9-undecanone Initiated by Aluminum Isopropoxide *Macromolecules* **1997,** *30,* 2575-2581.

[102] Taniguchi I.; Mayes, A.M.; Chan, E. W. L.; Griffith, L.G. A Chemoselective Approach to Grafting Biodegradable Poly(ester)s *Macromolecules* **2005,** *38,* 216-219.

[103] Herrmann, J. L.; Schlessinger, R. H. Method for Alkylating Lactones *J. Chem. Soc., Chem. Commun.* **1973**, 711-712.

[104] Molander, G. A.; Harris, C. R. Sequenced Reactions with Samarium(II) Iodide. Tandem Intramolecular Nucleophilic Acyl Substitution/Intramolecular Barbier Cyclizations *J. Am. Chem. Soc.* **1995,** *117,* 3705-3716.

[105] Parrish, B.; Emrick, T. Aliphatic Poly(ester)s with Pendant Cyclopentene Groups: Controlled Synthesis and Conversion to Poly(ester)-*graft*-PEG Copolymers *Macromolecules* **2004**, *37*, 5863-5865.

[106] in 't Veld, P.J.A.; Dijkstra, P. J.; van Lochem, J.H.; Feijen, J. Synthesis of alternating polydepsipeptides by ring-opening polymerization of morpholine-2,5-dione derivatives *Makromol. Chem.* **1990**, *191*, 1813 -1825.

[107] *Yonezawa, N.; Todaa, F.; Hasegawa, M.* Synthesis of polydepsipeptides: Ring-opening polymerization of 6-isopropylmorpholine-2,5-dione and 6-isopropyl-4-methylmorpholine-2,5-dione *Makromol. Chem. /Macromol. Rapid. Commun.* **1985**, *6,* 607-611.

[108] Barrera, D. A.; Zylstra, E.; Lansbury, P.T.; Langer, R. Synthesis and RGD Peptide Modification of a New Biodegradable Copolymer: Poly (lactic acid-celysine) *J. Am. Chem. Soc.* **1993**, *115 ,* 11010-11011.

[109] Yin, M.; Baker, G. L. Preparation and Characterization of Substituted Poly(lactide)s *Macromolecules* **1999**, *32*, 7711–7718.

[110] Jing, F.; Smith, M. R. III, Baker, G. L. Cyclohexyl-Substituted Polyglycolides with High Glass Transition Temperatures *Macromolecules* **2007**, *40,* 9304-9312.

[111] Simmons, T. L.; Baker, G. L. Poly(phenyllactide): Synthesis, Characterization, and Hydrolytic Degradation *Biomacromolecules* **2001,** *2*, 658-663.

[112] Leemhuis, M.; van Nostrum, C. F.; Kruijtzer, J. A. W. ;Zhong, Z. Y.;ten Breteler, M.R.; Dijkstra, P.J.; Feijen, J.; Hennink, W. E. Functionalized Poly(*R*-hydroxy acid)s via Ring-Opening Polymerization: Toward Hydrophilic Poly(ester)s with Pendant Hydroxyl Groups *Macromolecules* **2006,** *39,* 3500-3508.

[113] Leemhuis, M.; van Steenis, J. H.; van Uxem, M.J.; van Nostrum, C. F.; Hennink, W. E**.** A Versatile Route to Functionalized Dilactones as Monomers for the Synthesis of Poly(α-hydroxy) Acids *Eur. J. Org. Chem.* **2003**, 3344-3349.

[114] Jiang, X., Vogel, E. B.; Smith III, M. R.; Baker, G. L. "Clickable" Polyglycolides: Tunable Synthons for Thermoresponsive, Degradable Polymers *Macromolecules* **2008,** *41,* 1937-1944

[115] Jiang, X.; Smith III, M. R.; Baker, G. L. Water-Soluble Thermoresponsive Poly(lactide)s *Macromolecules* **2008,** *41,* 318-324.

[116] Jing, F.; Hillmyer, M. A. A Bifunctional Monomer Derived from Lactide for Toughening Poly(lactide) *J. Am. Chem. Soc.* **2008**, *130*, 13826–13827.

[117] Benabdillah, K. M.; Coudane, J.; Boustta, M.; Engel, R.; Vert, M. Synthesis and Characterization of Novel Degradable Poly(ester)s Derivedfrom D-Gluconic and Glycolic Acids *Macromolecules* **1999**, *32,*8774–8780.

[118] Benabdillah, K.M.; Boustta, M.; Coudane J.; Vert, M. Novel Degradable Polymers Combining D-Gluconic Acid, a Sugar of Vegetal Origin, with Lactic and Glycolic Acids *Biomacromolecules* **2001**, *2*, 1279–1284.

[119]Noga, D. E.; Petrie, T. A.; Kumar, A.; Weck, M.; García, A.J.; Collard, D. M.; Synthesis and Modification of Functional Poly(lactide) Copolymers: Toward Biofunctional Materials *Biomacromolecules* **2008**, *9,* 2056–2062.

120 Pounder R. J.; Dove, A. P. Towards poly(ester) nanoparticles: recent advances in the synthesis of functional poly(ester)s by ring-opening polymerization *Polym. Chem.* **2010** DOI: 10.1039/b9py00327d.

[121] Zhu, K. J., Hendren, R. W., Jensen, K.; Pitt, C. G. Synthesis, Properties, and Biodegradation **of** Poly(1,3-trimethylene carbonate) *Macromolecules* **1991**, 24, 1736–1740.

[122] Rokicki, G. Aliphatic cyclic carbonates and spiroorthocarbonates as monomers *Progress in Polymer Science* **2000**, *25*, 259-342.

[123] Vandenberg E. J.; Tian, D. A New, Crystalline High Melting Bis(hydroxymethyl)polycarbonate and Its Acetone Ketal for Biomaterial Applications *Macromolecules* **1999,** *32,* 3613-3619.

[124] Parzuchowski, P. G.; Jaroch, M.; Tryznowski, M.; Rokicki, G. Synthesis of New Glycerol-Based Hyperbranched Polycarbonates *Macromolecules* **2008**, *41*, 3859-3865.

[125] Ray, W. C.; III Grinstaff, M. W. Polycarbonate and Poly(carbonate-ester)s Synthesized from Biocompatible Building Blocks of Glycerol and Lactic Acid *Macromolecules* **2003,** *36,* 3557-3562.

[126] Xie, Zh.; Hu, X.; Chen, X.; Sun, J.; Shi, Q.; Jing, X. Synthesis and Characterization of Novel Biodegradable Poly(carbonate ester)s with Photolabile Protecting Groups *Biomacromolecules* **2008,** *9,* 376–380.

[127] Hu, X.; chen, X.; Xie, Z.; Cheng, H.; Jing, X. Aliphatic Poly(ester-carbonate)s Bearing Amino Groups and Its RGD Peptide Grafting *J. Polym. Sci., Part A: Polym. Chem* **2008,** *46*, 7022–7032.

[128] Pratt, R. C.; Nederberg, F.; Waymouth, R. M.; Hedrick, J. L. Tagging alcohols with cyclic carbonate: a versatile equivalent of (meth)acrylate for ring-opening polymerization *Chem. Commun.* **2008**, 114–116.

[129] Cooley, C. B.; Trantow, B. M.; Nederberg, F.; Kiesewetter, M. K.; Hedrick, J. L.; Waymouth, R. M.; Wender, P. A. Oligocarbonate Molecular Transporters: Oligomerization-Based Syntheses and Cell-Penetrating Studies *J. Am. Chem. Soc***. 2009**, *131*, 16401–16403.

[130] Lu, C.; Shi, Q.; Chen, X.; Lu, T.; Xie, Z.; Hu, X.; Ma, J.; Jing, X. Sugars-grafted aliphatic biodegradable poly(L-lactide-*co*-carbonate)s by click reaction and their specific interaction with lectin molecules *J. Polym. Sci., Part A: Polym. Chem.* **2007**, *45*, 3204.

[131] Chen, W.; Yang, H.; Wang, R.; Cheng, R.; Meng, F.; Wei, W.; Zhong, Zh. Versatile Synthesis of Functional Biodegradable Polymers by Combining Ring-Opening Polymerization and Postpolymerization Modification via Michael-Type Addition Reaction *Macromolecules* **2010**, *43*, 201–207.

[132] Tomalia, D. A.; Naylor, A. M.; Goddard, W. A., III. Starburst Dendrimers: Molecular-Level Control of Size, Shape, Surface Chemistry, Topology, and Flexibility from Atoms to Macroscopic Matter *Angew. Chem., Int. Ed. Engl*. **1990**, *29*, 138-175.

[133] Kim, Y. H.; Webster, O. W. Watersoluble hyperbranched polyphenylene: A unimolecular micelle *J. Am. Chem. Soc.* **1990**, *112*, 4592–4593.

[134] Tomalia, D. A.; Baker, H.; Dewald, J.; Hall, M.; Kallos, G.; Martin, S.; Roeck, J.; Ryder, J.; Smith, P. A new class of Polymers: Star-burst Dendritic macromolecules *Polym. J.* **1985**, *17,* 117-132.

[135] Roush, W. R.; Adam, M. A.; Harris, D. J. Cascade Molecules: A New Approach to Micelles. A [27]-Arbor *J. Org. Chem.* **1985,** *50***,** 2004-2006.

[136] Hawker, C. J.; Frechét, J. M. J. Preparation of Polymers with Controlled Molecular Architecture. A New Convergent Approach to Dendritic *J. Am. Chem. Soc.* **1990**, *112,* 7638-7647.

[137] Grayson, S. M.; Fréchet, J. M. J Convergent Dendrons and Dendrimers: from Synthesis to Applications *Chem. Rev.* **2001,** *101,* 3819-3867.

[138] Ihre, H.; Hult, A.; Söderlind, E. Synthesis, Characterization, and ^{1}H NMR Self-Diffusion Studies of Dendritic Aliphatic Poly(ester)s Based on 2,2-Bis(hydroxymethyl)propionic Acid and 1,1,1-Tris(hydroxyphenyl)ethane *J. Am. Chem. Soc.* **1996**, *118*, 6388-6395.

[139] Fréchet, J. M. J.; Gitsov, M.; Ihre, H. ; Hult, A. Double-Stage Convergent Approach for the Synthesis of Functionalized Dendritic Aliphatic Poly(ester)s Based on 2,2-Bis(hydroxymethyl)propionic Acid *Macromolecules* **1998,** *31,* 4061-4068.

[140] Ihre, H.; Padilla de Jesús, O. L.; Fréchet, J. M. J. Fast and Convenient Divergent Synthesis of Aliphatic Ester Dendrimers by Anhydride Coupling *J. Am. Chem. Soc.* **2001***, 123,* 5908-5917*.*

[141] Hecht, S.; Fréchet, J. M. J. Light-Driven Catalysis within Dendrimers: Designing Amphiphilic Singlet Oxygen Sensitizers *J. Am. Chem. Soc.* **2001,** *123,* 6959-6960.

[142] Malkoch,M.; Malmström, E.; Hult, A. Rapid and Efficient Synthesis of Aliphatic Ester Dendrons and Dendrimers *Macromolecules* **2002,** *35,* 8307-8314.

[143] Gillies, E. R. Fréchet, J. M. J. Designing Macromolecules for Therapeutic Applications: Poly(ester) Dendrimers Poly(ethylene oxide) "Bow-Tie" Hybrids with Tunable Molecular Weight and Architecture *J. Am. Chem. Soc.* **2002**, *124*, 14137-14146.

[144] Malkoch, M.; Claesson, H.; Loewenhielm, P.; Malmström, E.; Hult, A. Synthesis and characterization of 2,2-bis(methylol)propionic acid dendrimers with different cores and terminal groups *J. Polym. Sci., Part A: Polym. Chem.* **2004**, *42*, 1758-1767.

[145] Nyström, A.; Hult, A. Dendronized Polymers with Tailored Surface Groups *J.Polym. Sci., Part A: Polym. Chem.* **2005**, *43*, 3852-3867.

[146] Connal, L. A.; Vestberg, R.; Hawker, C. J.; Qiao, G. G Synthesis of Dendron Functionalized Core Cross-linked Star Polymers *Macromolecules* **2007,** *40,* 7855-7863.

[147] Yim, S.-H.; Huh, J.; Ahn, Ch.-H.; Park, T. G. Development of a Novel Synthetic Method for Aliphatic Ester Dendrimers *Macromolecules* **2007,** *40,* 205-210

[148] Grinstaff, M. W.; Biodendrimers: New Polymeric Biomaterials for Tissue Engineering *Chem. Eur. J.* **2002**, *8*, 2838-2846.

[149] Flory, P. J. Molecular size-distribution in three dimensional polymers. VI. Branched polymers containing A-R-Bf-1 type units *J. Am. Chem. Soc.* 1952, *74*, 2718–2723.

[150] Kim, Y. H. Highly Branched Aromatic Polymers Prepared by Single-Step Syntheses *Macromol. Symp.* **1994**, *77*, 21- 33.

[151] Hawker, C. J.; Lee, R.; Frechét, J. M. J. One-step synthesis of hyperbranched dendritic poly(ester)s *J. Am. Chem. Soc.* **1991**, *113*, 4583–4588.

[152] Hölter, D., Burgath, A.; Frey, H. Degree of branching in hyperbranched polymers *Acta Polymer.* **1997,** *48,* 30-35.

[153] Voit., B. I.; Lederer, A. Hyperbranched and Highly Branched Polymer ArchitecturessSynthetic Strategies and Major Characterization Aspects *Chem. Rev.* **2009,** *109,* 5924–5973.

[154] Malmstrtöm, E.; Johansson, M.; Hult, A. Hyperbranched Aliphatic Poly(ester)s *Macromolecules* **1995,** *28***,** 1698-1703.

[155] Magnusson, H.; Malmström, E.; Hult, A. Structure Buildup in Hyperbranched Polymers from 2,2-Bis(hydroxymethyl)propionic Acid *Macromolecules* **2000,** *33,* 3099-3104.

[156] Malmström, E.; Hult, A. Kinetics of Formation of Hyperbranched Poly(ester)s Based on 2,2-Bis(hydroxymethyl)propionic Acid *Macromolecules* **1996**, *29*, 1222-1228.

[157] Boltorn® P500 *Product Data Sheet* **2010** www.perstorp.com

[158] Chikh, L.; Tessier, M.; Fradet, A: Polydispersity of Hyperbranched Poly(ester)s Based on 2,2-Bis(hydroxymethyl)propanoic Acid: SEC/MALDI-TOF MS and 13C NMR/Kinetic-Recursive Probability Analysis *Macromolecules* **2008**, *41*, 9044-9050.

[159] Parzuchowski, P. G.; Grabowska, M.; Jaroch, M.; Kusznerczuk, M. *J. Polym. Sci., Part A: Polym. Chem.* **2009**, 47, 3860–3868.

[160] Skaria, S.; Mario Smet, M.; Frey, H. Enzyme-Catalyzed Synthesis of Hyperbranched Aliphatic Poly(ester)s *Macromol. Rapid Commun.* **2002**, *23*, 292-296.

[161] Smet, M.; Gottschalk, C.; Skaria, S.; Frey, F. Aliphatic Hyperbranched Copoly(ester)s by Combination of ROP and AB$_2$-Polycondensation *Macromol. Chem. Phys.* **2005**, *206*, 2421–2428.

[162] Gottschalk, C.; Frey, H. Hyperbranched Poly(lactide) Copolymers *Macromolecules*, 2006, 39, 1719–1723

[163] Cooper, T. R.; Storey, R. F**.** Poly(lactic Acid) and Chain-Extended Poly(lactic acid)-Polyurethane Functionalized with Pendent Carboxylic Acid Groups *Macromolecules* **2008**, *41,* 655-662.

[164] Velthoen, I. W.; Dijkstra, P. D.; Feijen, J. AB$_2$ Functional Poly(ester)s via Ring Opening Polymerization: Synthesis and Characterization *Macromol. Chem. Phys.* **2009**, *210*, 689–697.

[165] Fischer, A., Wolf, F. K.; Frey, H. **2010** *unpublished results.*

[166] Fréchet, J. M. J.; Henmi, H.; Gitsov, I.; Aoshima, S.; Leduc, M. R.; Grubbs, R. B. Self-Condensing Vinyl Polymerization: An Approach to Dendritic Materials *Science* **1995**, *269*, 1080-1083.

[167] Hawker, C. J.; Fréchet, J. M. J.; Grubbs, R. B.; Dao, J. Preparation of Hyperbranched and Star Polymers by a "Living", Self-condensing Free Radical Polymerization *J. Am. Chem. Soc.* **1995**, *117*, 10763-10764.

[168] Simon, P. F. W.; Radke, W.; Müller, A. H. E. Hyperbranched methacrylates by self-condensing group transfer polymerization *Macromol. Rapid Commun.* **1997**, *18*, 865.

[169] Simon, P. F. W.; Müller, A. H. E. Synthesis of Hyperbranched and Highly Branched Methacrylates by Self-Condensing Group Transfer Copolymerization *Macromolecules* **2001**, *34*, 6206-6213.

[170] Powell, K. T.; Cheng, C.; Wooley, K. L. Complex Amphiphilic Hyperbranched Fluoropolymers by Atom Transfer Radical Self-Condensing Vinyl (Co)polymerization *Macromolecules* **2007**, *40*, 4509–4515.

[171] Müller, A.H.E.; Yan, D.; Wulkow, M. Molecular Parameters of Hyperbranched Polymers Made bySelf-Condensing Vinyl Polymerization. 1. Molecular Weight Distribution *Macromolecules* **1997**, *30*, 7015-7023.

[172] Yan, D. Y.; Müller, A. H. E.; Matyjaszewski, K. Molecular Parameters of Hyperbranched Polymers Made by Self-Condensing Vinyl Polymerization. 2. Degree of Branching *Macromolecules* **1997**, *30*, **7024–7033.**

[173] Weimer, M. W.; Fréchet, J. M. J.; Gitsov, I. Importance of Active-Site Reactivity and Reaction Conditions in the Preparation of Hyperbranched Polymers by Self-Condensing Vinyl Polymerization: Highly Branched vs. Linear Poly[4-(chloromethyl) styrene] by Metal-Catalyzed ''Living'' Radical Polymerization *J. Polym. Sci., Part A: Polym. Chem.* **1998**, *36*, 955.

[174] Cheng, G.; Simon, P. F. W.; Hartenstein, M.; Müller, A. H. E. Synthesis of hyperbranched poly(*tert*-butyl acrylate) by self-condensing atom transfer radical polymerization of a macroinimer *Macromol. Rapid. Commun.* **2000**, *21*, 846–852.

[175] Peeters, J. W.; Palmans, A. R. A.; Meijer, E. W.; Koning, C.E.; Heise, A. Chemoenzymatic Synthesis of Branched Polymers *Macromol. Rapid Commun.* **2005**, *26*, 684–689.

[176] Vogt, A. P.; Condi, S. R.; Sumerlin, B. S. Hyperbranched Polymers via RAFT Copolymerization of an Acryloyl Trithiocarbonate *Aust. J. Chem.* **2007**, *60*, 396–399.

[177] Trollsas, M.; Löwenhielm, P.; Lee, V. Y.; Möller, M.; Miller, R. D.; Hedrick, J. L. New Approach to Hyperbranched Poly(ester)s: Self-Condensing Cyclic Ester Polymerization of Bis(hydroxymethyl)-Substituted ⱶ-Caprolactone *Macromolecules* **1999**, *32*, 9062-9066.

[178] Sunder, A.; Hanselmann, R.; Frey, H.; Mülhaupt, R. Controlled Synthesis of Hyperbranched Polyglycerols by Ring-Opening Multibranching Polymerization *Macromolecules* **1999**, *32*, 4240-4246.

[179] Radke, W.; Litvinenko, G.; Müller, A. H. E. Effect of Core-Forming Molecules on Molecular Weight Distribution and Degree of Branching in the Synthesis of Hyperbranched Polymers *Macromolecules* **1998**, *31*, 239-248.

[180] Hanselmann, R.; Hölter, D.; Frey, H. Hyperbranched Polymers Prepared via the Core-Dilution/Slow Addition Technique: Computer Simulation of Molecular Weight Distribution and Degree of Branching *Macromolecules* **1998**, *31*, 3790-3801.

[181] Wilms, D.; Stiriba., S.; Frey, H. Hyperbranched Polyglycerols: From the Controlled Synthesis of Biocompatible Polyether Polyols to Multipurpose Applications *Accounts of Chemical Research* **2010**, *43*, 129-141

[182] Wilms, D.; Wurm, F.; Nieberle, J.; Böhm, P.; Kemmer-Jonas, U.; Frey, H. Hyperbranched Polyglycerols with Elevated Molecular Weights: A Facile Two-Step Synthesis Protocol Based on Polyglycerol Macroinitiators M*acromolecules* 2009, *42*, 3230–3236.

[183] Liu, M., Vladimirov, N.; Fréchet. J. M. J. A New Approach to Hyperbranched Polymers by Ring-Opening Polymerization of an AB Monomer: 4-(2-Hydroxyethyl)-ε-caprolactone *Macromolecules* **1999**, *32*, 6881-6884.

[184] Yu, X.- H.; Feng, J.; Zhuo, R.- X. Preparation of Hyperbranched Aliphatic Poly(ester) Derived from Functionalized 1,4-Dioxan-2-one *Macromolecules* **2005**, *38,* 6244-6247.

[185] Parzuchowski, P. G.; Grabowska, M.; Tryznowski, M.; Rokicki, G. Synthesis of Glycerol Based Hyperbranched Poly(ester)s with Primary Hydroxyl Groups *Macromolecules* **2006**, *39*, 7181–7186.

[186] Tasaka, F.; Ohya, Y.; Ouchi, T. One-Pot Synthesis of Novel Branched Poly(lactide) Through the Copolymerization of Lactide with Mevalonolactone *Macromol. Rapid Commun.* **2001**, *22*, 820-824.

[187] Parzuchowski, P. G.; Jaroch, M.; Tryznowski, M.; Rokicki, G. Synthesis of New Glycerol-Based Hyperbranched Polycarbonates *Macromolecules* **2008**, *41*, 3859-3865

[188] Zou, P.; Yang, L.-P.; Pan, C.- Y. One-Pot Synthesis of Linear-Hyperbranched Diblock Copolymers via Self-Condensing Vinyl Polymerization and Ring Opening Polymerization *J. Polym. Sci., Part A: Polym. Chem.* **2008,** *46*, 7628–7636.

[189] Pitet, L. M.; Hait S. B.; Lanyk T. J.; Knauss, D. M. Linear and branched architectures from the polymerization of lactide with glycidol *Macromolecules* **2007**, *40*, 2327–2334.

[190] Hadjichristidis, N.; Pispas, S. Floudas, G. Block Copolymers: Synthetic Strategies, Physical Properties, and Applications **2002***,* Wiley-Interscience, New York.

[191] Ray, W. C.; III Grinstaff, M. W. Polycarbonate and Poly(carbonate-ester)s Synthesized from Biocompatible Building Blocks of Glycerol and Lactic Acid *Macromolecules* **2003,** *36,* 3557-3562.

[192] Zhang, X. J.; Mei, H. J.; Hu, C.; Zhong, Z. L.; Zhuo, R. X. Amphiphilic Triblock Copolycarbonates with Poly(glycerol carbonate) as Hydrophilic Blocks *Macromolecules* **2009**, *42*, 1010-1016.

[193] Wolinsky, J. B.; Ray III, W. C.; Colson, Y. L.; Grinstaff, M. W. Poly(carbonate ester)s Based on Units of 6-Hydroxyhexanoic Acid and Glycerol *Macromolecules* **2007,** *40,* 7065-7068.

[194] Xia, J.; Matyjaszewski, K. Controlled/"Living" Radical Polymerization. Atom Transfer Radical Polymerization Using Multidentate Amine Ligands *Macromolecules* **1997,** *30,* 7697-7700.

[195] Matyjaszewski, K.; Xia, J.; Atom Transfer Radical Polymerization *Chem. Rev.* **2001,** *101,* 2921-2990.

[196] Pintauer, T., Matyjaszewski, K. Structural aspects of copper catalyzed atom transfer radical polymerization *Coord. Chem. Rev.* **2005**, *249*, 1155–1184.

[197] Kamigaito, M.; Ando, T.; Sawamoto M.; Metal-Catalyzed Living Radical Polymerization *Chem. Rev.* **2001,** *101,* 3689-3745.

[198] Ouchi, M.; Terashima, T.; Sawamoto; M. Transition Metal-Catalyzed Living Radical Polymerization: Toward Perfection in Catalysis and Precision Polymer Synthesis *Chem. Rev.* **2009,** *109,* 4963–5050.

[199] Jakubowski, W.; Matyjaszewski, K. Activator Generated by Electron Transfer for Atom Transfer Radical Polymerization *Macromolecules* **2005,** *38,* 4139-4146.

[200] Jakubowski, W.; Matyjaszewski, K. Activators Regenerated by Electron Transfer for Atom-Transfer Radical Polymerization of (Meth)acrylates and Related Block Copolymers *Angew. Chem. Int. Ed.* **2006**, *45*, 4482 –4486.

[201] Tsarevsky, N. V.; Matyjaszewski, K. "Green" Atom Transfer Radical Polymerization: From Process Design to Preparation of Well-Defined Environmentally Friendly Polymeric Materials *Chem. Rev.* **2007**, *107*, 2270-2299.

[202] Percec, V.; Guliashvili, T.; Ladislaw, J. S.; Wistrand, A.; Stjerndahl, A.; Sienkowska, M. J.; Monteiro, M. J.; Sahoo, S. Ultrafast Synthesis of Ultrahigh Molar Mass Polymers by Metal-Catalyzed Living Radical Polymerization of Acrylates, Methacrylates, and Vinyl Chloride Mediated by SET at 25 °C *J. Am. Chem. Soc.* **2006**, *128*, 14156-14165.

[203] Benoit,D.; Chaplinski, V.; Braslau, R.; Hawker, C. J. Development of a Universal Alkoxyamine for "Living" Free Radical Polymerizations *J. Am. Chem. Soc.* **1999,** *121,* 3904-3920.

[204] Chauvin, F.;Dufils, P.- E.; Gigmes, D.; Guillaneuf, Y.; Marque, S. R. A.; Tordo, P.; Bertin, D. Nitroxide-Mediated Polymerization: The Pivotal Role of the k_d Value of the Initiating Alkoxyamine and the Importance of the Experimental Conditions *Macromolecules* **2006,** *39,* 5238-5250.

[205] Kothe, T.; Marque, S.; Martschke, R.; Popov, M.; Fischer, H. Radical reaction kinetics during homolysis of *N*-alkoxyamines: verification of the persistent radical effect *J. Chem. Soc., Perkin Trans. 2* **1998**, 1553-1559.

[206] Nicolas, J.; Charleux, B.; Guerret, O.; Magnet, S. Novel SG1-Based Water-Soluble Alkoxyamine for Nitroxide-Mediated Controlled Free-Radical Polymerization of Styrene and *n*-Butyl Acrylate in Miniemulsion *Macromolecules* **2004,** *37*, 4453-4463

[207] Vinas, J.; Chagneux, N.; Gigmes, D.; Trimaille, T.; Favier, A.; Bertin, D. SG1-based alkoxyamine bearing a N-succinimidyl ester: A versatile tool for advanced polymer synthesis *Polymer* **2008**, *49*, 3639–3647.

[208] Dove, A. P. Controlled ring-opening polymerisation of cyclic esters: polymer blocks in self-assembled nanostructures *Chem. Commun*. **2008**, 6446–6470.

[209] Bougard, F.; Jeusette, M.; Mespouille, L.; Dubois, P.; Lazzaroni, R. Synthesis and Supramolecular Organization of Amphiphilic Diblock Copolymers Combining Poly(*N,N*-dimethylamino-2-ethyl methacrylate) and Poly(ε-caprolactone) *Langmuir* **2007**, *23*, 2339–2345.

[210] Mespouille, L.; Coulembier, O.; Paneva, D.; Degee, P.; Rashkov,I.; Dubois, P. Amphiphilic poly(*N,N*-dimethylamino-2-ethyl methacrylate)-g-poly(ε-caprolactone) graft copolymers: synthesis and characterisation *Chem. Eur. J.* **2008**, *14*, 6369–6378.

[211] Lee, H.; Jakubowski, W.; Matyjaszewski, K.; Yu, S.; Sheiko, S. S. Cylindrical Core-Shell Brushes Prepared by a Combination of ROP and ATRP *Macromolecules* **2006,** *39*, 4983-4989.

[212] Heise, A.; Trollsas, M.; Magbitang, T.; Hedrick, J. L.; Frank C. W.; Miller, R. D. Star Polymers with Alternating Arms from Miktofunctional Initiators Using Consecutive Atom Transfer Radical Polymerization and Ring-Opening Polymerization *Macromolecules* **2001**, *34*, 2798–2804.

[213] Babin, J.; Taton, D.; Brinkmann, M.; Lecommandoux, S. Synthesis and Self-Assembly in Bulk of Linear and Mikto-Arm Star Block Copolymers Based on Polystyrene and Poly(glutamic acid) *Macromolecules* **2008**, *41*, 1384–1392.

[214] Zhang, Q.; Remsen, E.E.; Wooley, K.L. Shell Cross-Linked Nanoparticles Containing Hydrolytically Degradable, Crystalline Core Domains *J. Am. Chem. Soc.* **2000,** *122*, 3642-3651.

[215] Yagci, Y.; Tasdelen, M. A. Mechanistic transformations involving living and controlled/living polymerization methods *Progress in Polymer Science* **2006**, *31*, 1133-1170.

[216] Hawker, C. J.; Hedrick, J. L.; Malmström, E. E.; Trollsås, M.; Mecerreyes, D.; Moineau, G.; Dubois, Ph.; Jérôme, R**.** Dual Living Free Radical and Ring Opening Polymerizations from a Double-Headed Initiator *Macromolecules* **1998**, *31*, 213-219.

[217] Mecerreyes, D.; Moineau, G.; Dubois, Ph.; Jérôme, R**.**, Hedrick, J. L.; Hawker, C. J.; Malmström, E. E.; Trollsås, M. Simultaneous Dual Living Polymerizations: A Novel One-Step Approach to Block and Graft Copolymers *Angew. Chem. Int. Ed.* **1998**, *37*, 1274-1276.

[218] Karanikolopoulos, N.; Zamurovic, M.; Pitsikalis, M.; Hadjichristidi, N. Poly(DL-lactide)-*b*-poly(*N,N*-dimethylamino-2-ethyl methacrylate): Synthesis, Characterization, Micellization Behavior in Aqueous Solutions, and Encapsulation of the Hydrophobic Drug Dipyridamole *Biomacromolecules* 2010, *11*, 430–438.

[219] Bougard, F.; Jeusette, M.; Mespouille, L.; Dubois, Ph.;Lazzaroni, R. Synthesis and Supramolecular Organization of Amphiphilic Diblock Copolymers Combining Poly(*N,N*-dimethylamino-2-ethyl methacrylate)and Poly(◻-caprolactone) *Langmuir* **2007,** *23,* 2339-2345.

[220] Meyer, U.; Palmans, A.R.A., Loontjens, T.; Heise, A. Enzymatic Ring-Opening Polymerization and Atom Transfer Radical Polymerization from a Bifunctional Initiator *Macromolecules* **2002,** *35,* 2873-2875.

[221] Peeters, J.; Palmans, A.R.A.; Veld, M.; Scheijen, F.; Heise, A.; Meijer, E. W. Cascade Synthesis of Chiral Block Copolymers Combining Lipase Catalyzed Ring Opening Polymerization and Atom Transfer Radical Polymerization *Biomacromolecules* **2004,** *5,* 1862-1868.

[222] Mespouille; L.; Nederberg; F.; Hedrick; J.L.; Dubois Ph. Broadening the Scope of Functional Groups Accessible in Aliphatic Polycarbonates by the Introduction of RAFT Initiating Sites *Macromolecules* **2009**, *42*, 6319–6321.

94

[223] Iwasaki, Y. Akiyoshi, K. Design of Biodegradable Amphiphilic Polymers: Well-Defined Amphiphilic Polyphosphates with Hydrophilic Graft Chains via ATRP *Macromolecules* **2004,** *37,* 7637-7642.

[224] Tao, L.; Luan, B.; Pan, C.-Y. Block and star block copolymers by mechanism transformation. VIII Synthesis and characterization of triblock poly(L-LA-b-St-b-MMA) by combination of ATRP and ROP *Polymer* **2003**, *44* 1013–1020.

[225] Zhao, Y.; Shuai, X.; Chen, Ch.; Xi, F. Synthesis of Star Block Copolymers from Dendrimer Initiators by Combining Ring-Opening Polymerization and Atom Transfer Radical Polymerization M*acromolecules* **2004,** *37,* 8854-8862.

[226] Yang, L.; Zhou, H.; Shi, G.; Wang, Y.; Pan, C.-Y. Synthesis of ABCD 4-Miktoarm Star Polymers by Combination of RAFT, ROP and ''Click Chemistry'' *Journal of Polymer Science: Part A: Polymer Chemistry* **2008**, 46, 6641–6653.

[227] Mecerreyes, D.; Trollsås, M.; Hedrick, J. L. ABC BCD Polymerization: A Self-Condensing Vinyl and Cyclic Ester Polymerization by Combination Free-Radical and Ring-Opening Techniques *Macromolecules* **1999,** *32,* 8753-759.

[228] Gros, L.; Ringsdorf, H.; Schupp, H. Polymeric Antitumor Agents on a Molecular and on a Cellular Level *Angew Chem. Int. Ed.* **1981**, *20,* 305-325.

[229] Ringsdorf, H. Structure and properties of pharmacologically active polymers J. Polym. Sci. Polymer Symp. **1975**, *51*, 135–153.

[230] Duncan, R. Polymer conjugates as anticancer nanomedicines *Nat. Rev. Cancer* **2006**, *6* , 688–701.

[231] Vicent, M. J., Ringsdorf, H., Duncan, R. Polymer therapeutics: Clinical applications and challenges for development *Adv. Drug Del. Rev.* **2009***,* 61, 1117–1120.

[232] Liu, S.; Maheshwari, R.; Kiick, K. L. Polymer-Based Therapeutics *Macromolecules* **2009**, *42*, 3-13.

[233] Hayward, R. C.; Pochan, D. J. Tailored Assemblies of Block Copolymers in Solution: It Is All about the Process *Macromolecules* **2010**, *43*, 3577–3584.

[234] Gaucher, G.; Dufresne, M.-H.; Sant, V. P.; Kang, N.; Maysinger, D.; Leroux, J.-C. Block copolymer micelles: preparation, characterization and application in drug delivery *Journal of Controlled Release* **2005**, *109,* 169–188.

[235] Kataoka, K.; Harada, A.; Nagasakib, Y. Block copolymer micelles for drug delivery: design, characterization and biological significance *Adv. Drug Del. Rev.* **2001,** *47*, 113–131.

[236] Meng, F.; Zhong, Z.; Feijen, F. Stimuli-Responsive Polymersomes for Programmed Drug Delivery *Biomacromolecules* **2009***, 10,* 197-209.

[237] Meng, F.; Hiemstra, Ch.; Engbers, G. H. M.; Feijen, F. Biodegradable Polymersomes *Macromolecules* **2003,** *36,* 3004-3006.

[238] Mikhail, A. S.; Allen, Ch. Block copolymer micelles for delivery of cancer therapy: Transport at the whole body, tissue and cellular levels *Journal of Controlled Release* **2009**, *138,*214–223.

[239] Rapoport, N. Physical stimuli-responsive polymeric micelles for anti-cancer drug delivery *Prog. Polym. Sci.* **2007**, *32*, 962–990.

[240] Rijcken, C. J. F.; Soga, O.; Hennink, W. E.; van Nostrum, C. F. Triggered destabilisation of polymeric micelles and vesicles by changing polymers polarity: An attractive tool for drug delivery *J. Controlled Release* **2007**, *120*, 131–148.

[241] Schmaljohann, D. Thermo- and pH-responsive polymers in drug delivery *Adv. Drug. Del. Rev.* **2006**, *58*, 1655–1670.

[242] Müller, R. H.; Jacobs, C.; Kayser, O. Nanosuspensions as particulate drug formulations in therapy: Rationale for development and what we can expect for the future *Adv. Drug Delivery Rev.* **2001**, 47, 3–19.

[243] Spencer, M.; Faulds, D. Paclitaxel: A Review of its Pharmacodynamic and Pharmacokinetic Properties and Therapeutic Potential in the Treatment of Cancer *Drugs* **1994**, *48*, 794-847.

[244] Torchilin, V. P. Structure and design of polymeric surfactant-based drug delivery systems *J. Control. Release* **2001**, *73*, 137–172.

[245] Moghimi, S. M.; Hunter, A. C.; Murray, J. C. Long-circulating and target specific nanoparticles: theory to practice *Pharmacol. Rev.* **2001**, 53, 283–318.

[246] Yamamoto, Y. Nagasaki, Y.; Kato, Y.; Sugiyama, Y.; Kataoka, K. Long-circulating poly(ethylene glycol)-poly(-lactide) block copolymer micelles with modulated surface charge, *J. Control. Release* **2001**, *77*, 27–38.

[247] Lee, E. S.; Na, K.; Bae, Y. H. Polymeric micelle for tumor pH and folate-mediated targeting *J. Contr. Rel.* **2003**, *91*, 103–113.

[248] Nagasaki, Y.; Okada, T.; Scholz, C.; Iijima, M.; Kato, M.; Kataoka, K. The Reactive Polymeric Micelle Based on An Aldehyde-Ended Poly(ethylene glycol)/Poly(lactide) Block Copolymer *Macromolecules* **1998,** *31,* 1473-1479

[249] Zhang, J.; Wang, l.-Q.; Wang, H.; Tu, K. Micellization Phenomena of Amphiphilic Block Copolymers Based on Methoxy Poly(ethylene glycol) and Either Crystalline or Amorphous Poly(caprolactone-*b*-lactide) Biomacromolecules **2006,** *7*, 2492-2500.

[250] Yin, H.;Kang, S.-W.; Bae, Y. H. Polymersome Formation from AB$_2$ Type 3-Miktoarm Star Copolymers *Macromolecules* **2009**, *42*, 7456–7464.

[251] Luo; L. B.; Ranger, M.; Lessard, D. G.; Le Garrec, D.; Gori, S.; Leroux, J. C.; Rimmer, S., Smith, D. Novel Amphiphilic Diblock Copolymers of Low Molecular Weight Poly(*N*-vinylpyrrolidone)-*block*-poly(D,L-lactide): Synthesis, Characterization, and Micellization *Macromolecules* **2004,** *37,* 4008-4013.

[252] Wang, X. Y.; Xie, X. L.; Cai, C. F.; Rytting, E.; Steele, T.; Kissel, T. Biodegradable Branched Poly(ester)s Poly(vinyl sulfonate-covinyl alcohol)-graft Poly(D,L-lactic-coglycolic acid) as a Negatively Charged Polyelectrolyte Platform for Drug Delivery: Synthesis and Characterization *Macromolecules* **2008**, *41*, 2791-2799.

[253] Tsuji, H. Poly(lactide) Stereocomplexes: Formation, Structure, Properties, Degradation, and Applications *Macromol. Biosci.* **2005**, *5*, 569–597.

[254] Slager, J.; Domb, A. J. Biopolymer stereocomplexes *Adv. Drug Del. Rev.* **2003**, *55*, 549–583.

[255] Spasova, M.; Mespouille, L.; Coulembier, O.; Paneva, D.; Manolova, N.; Rashkov, I.; Dubois, Ph. Amphiphilic Poly(D- or L-lactide)-*b*-poly(*N,N*-dimethylamino-2-ethyl methacrylate) Block Copolymers: Controlled Synthesis, Characterization, and Stereocomplex Formation *Biomacromolecules* **2009,** *10,* 1217–1223.

[256] Nederberg, F.; Appel, E.; Tan, J. P. K.; Kim,S. H.; Fukushima, K.; Sly, J.; Miller, R.D.; Waymouth, R. M.; Yang, Y. Y.; Hedrick, J. L. Simple Approach to Stabilized Micelles Employing Miktoarm Terpolymers and Stereocomplexes with Application in Paclitaxel Delivery *Biomacromolecules* **2009,** *10,* 1460–1468.

[257]Kang, N.; Perron, M.; Prud'homme, R. E.; Zhang, Y.; Gaucher, G.; Leroux, J.-C. Stereocomplex Block Copolymer Micelles: Core-Shell Nanostructures with Enhanced Stability *Nano Lett.* **2005**, *5*, 315-319.

[258] Tan, J. P. K.; Kim, S. H.; Nederberg, F.; Appel, E. A.; Waymouth, R. M.; Zhang, Y.; Hedrick, J. L.; Yang, Y. Y. Hierarchical Supermolecular Structures for Sustained Drug Release *small* **2009**, 5, 1504–1507.

[259] Kim, S. H.; Tan, J. P. K.; Nederberg, F.; Fukushima, K.; Yang, Y. Y., R. M.; Hedrick, J. L. Mixed Micelle Formation through Stereocomplexation between Enantiomeric Poly(lactide) Block Copolymers *Macromolecules* **2009**, *42*, 25-29.

[260] Kwon, G. S.; Suwa, S.; Yokoyama, M.; Okano, T.; Sakurai, Y Enhanced Tumor Accumulation and Prolonged Circulation Times of Micelle-Forming Poly(Ethylene Oxide-Aspartate) Block Copolymer-Adriamycin Conjugate *J. Contol. Rel.* **1994** *,29*, 17-23.

[261] Stenzel, M. H. RAFT polymerization: an avenue to functional polymeric micelles for drug delivery *Chem. Commun.*, **2008**, 3486–3503.

[262] Giacomelli, C., Schmidt, V.; Borsali, R. Nanocontainers Formed by Self-Assembly of Poly(ethylene oxide)-*b*-poly(glycerol monomethacrylate)-Drug Conjugates *Macromolecules* **2007,** *40,* 2148-2157.

[263] Save, M.; Weaver, J. V. M.; McKenna, P.; Armes, S. P. *Macromolecules* **2002**, 35, 1152–1159. (b) Ishizone, T.; Han, S.; Okuyama, S.; Nakahama, S. *Macromolecules* **2003**, *36*, 42–49. (c) Oguchi, K.; Sanui, K.; Ogata, N. *Polym. Eng. Sci.* **1990**, *30*, 449–452. (d) Mori, H.; Hirao, A.; Nakahama, S. *Macromolecules* **1994**, 27, 35–39. (e) Pilon, L. N.; Armes, S. P.; Findlay, P.; Rannard, S. P. Langmuir 2005, 21, 3808–3813.

[264] Wang, X. S.; Lascelles, S. F.; Jackson, R. A.; Armes, S. P. Facile synthesis of well-defined water-soluble polymers *via* atom transfer radical polymerization in aqueous media at ambient temperature *Chem. Commun.*, **1999**, 1817–1818.

[265] Robinson, K. L.; de Paz-Banez, M. V.; Wang, X. S.; Armes, S. P. Synthesis of Well-Defined, Semibranched, Hydrophilic-Hydrophobic Block Copolymers Using Atom Transfer Radical Polymerization *Macromolecules* **2001**, *34,* 5799-5805.

[266] Ishizone, T.; Han, S.; Okuyama, S.; Nakahama, S. Synthesis of Water-Soluble Polymethacrylates by Living Anionic Polymerization of Trialkylsilyl-Protected Oligo(ethylene glycol) Methacrylates *Macromolecules* **2003,** *36,* 42-49.

[267] Lutz, J. F. Polymerization of Oligo(Ethylene Glycol) (Meth)Acrylates: Toward New Generations of Smart Biocompatible Materials *J. Polym. Sci. Part A: Polym.Chem.* **2008** *46*, 3459–3470.

[268] Lammers, T. HPMA copolymers: 30 years of advances *Adv. Drug Del. Rev.* **2010**, *62*, 119–121.

[269] Talelli, M.; Rijcken, C. J. F.; van Nostrum, C. F.; Storm, G.; Hennink, W. E. Micelles based on HPMA copolymers *Adv. Drug Del. Rev.* **2010**, *62*, 231–239.

[270] Yoshimoto, K.; Hirase, T.; Madsen, J.; Armes, S. P.; Nagasaki, Y. Non-Fouling Character of Poly[2-(methacryloyloxy)ethyl Phosphorylcholine]-Modified Gold Surfaces Fabricated by the 'Grafting to' Method:Comparison of its Protein Resistance with Poly(ethylene glycol)-Modified Gold Surfaces *Macromol. Rapid Commun.* **2009**, *30*, 2136–2140.

[271] Ma, I. Y. Lobb, E. J. Billingham, N. C.; Armes, S. P. Lewis, A. L. Lloyd, A. W.; Salvage, J. Synthesis of Biocompatible Polymers. 1. Homopolymerization of 2-Methacryloyloxyethyl Phosphorylcholine via ATRP in Protic Solvents: An Optimization Study *Macromolecules* **2002,** *35,* 9306-9314.

[272] Ma, Y.; Tang, Y.; Billingham, N. C.; Armes, S. P.; Lloyd, A W.; Salvage, J. P. Well-Defined Biocompatible Block Copolymers via Atom Transfer Radical Polymerization of 2-Methacryloyloxyethyl Phosphorylcholine in Protic Media *Macromolecules* **2003,** *36,* 3475-3484.

[273] Lee, H.-I.; Pietrasik, J.; Sheiko, S. S.; Matyjaszewski, K. Stimuli-responsive molecular brushes *Progress in Polymer Science* **2010,** *35*, 24–44.

[274] Lutz, J. F.; Hoth, A. Preparation of Ideal PEG Analogs with a Tunable Thermosensitivity by Controlled Radical Copolymerization of 2-(2-Methoxyethoxy)ethyl Methacrylate and Oligo(ethylene glycol) Methacrylate *Macromolecules* **2006,** *39,* 893-896.

[275] Langer, R.; Vacanti, J. P. Tissue Engineering *Science* **1993**, *260*, 920-926.

[276] Ishaug-Riley S. L., Crane-Kruger, G. M., Yaszemski, M. J., Mikos, A. G. Three-dimensional culture of rat calvarial osteoblasts in porous biodegradable polymers *Biomaterials* **1998**, *19*, 1945-1955.

[277] Peter, S. J.; Miller, M. J.; Yasko, A. W.; Yaszemski, M. J.; Mikos, A .G. Polymer Concepts in Tissue Engineering *Jour. Biomed. Mat. Res*. **1998**, *43*, 422-427.

[278] Huang, Zh.-M.; Zhang, Y.-Z.; Kotaki, M.; Ramakrishna, S. A review on polymer nanofibers by electrospinning and their applications in nanocomposites *Composites Science and Technology* **2003**, *63*, 2223–2253.

[279] Ma, Z.W.; Kotaki, M.; Inai, R.; Ramakrishna, S. Potential of nanofiber matrix as tissue-engineering scaffolds *Tissue Engineering* **2005**, *11*, 101-109.

[280] Afifi, A. M.; Nakajima, H.; Yamane, H.; Kimura, Y.; Nakano; Sh. Fabrication of Aligned Poly(L-lactide) Fibers by Electrospinning and Drawing *Macromol. Mater. Eng.* **2009**, *294*, 658–665.

[281] Barnes, C. P., Sell, S. A.; Boland, E. D.; Simpson, D. G.; Bowlin, G.L. Nanofiber technology: Designing the next generation of tissue engineering scaffolds *Advanced Drug Delivery Reviews* **2007,** 59, 1413–1433.

[282] Greiner; A.; Wendorff, J.H. Electrospinning: A Fascinating Method for the Preparation of Ultrathin Fibers Angew. Chem. Int. Ed. **2007**, *46*, 5670 – 5703.

283 Boland, E.D.; Wnek, G.E., Simpson, D.G.; Pawlowski, K.J.; Bowlin, G.L.; Tailoring tissue engineering scaffolds using electrostatic processing techniques: a study of poly(glycolic acid) electrospinning *J. Macrom. Sci.: Pure Appl. Chem.* **2001**, *38*, 1231–1243.

[284] Welle, A.; Kröger, M.; Dörning, M.; Niederer, K.; Pindel, E.; Chronakis, I.S. 2007. Electrospun aliphatic polycarbonates as tailored tissue scaffold materials *Biomaterials* **2007**, *28*, 2211–2219.

[285] Ruoslahti, E. RGD and Other Recognition Sequences for Integrins *Annu. Rev. Cell Dev. Biol.* **1996,** *12,* 697–715.

[286] Hersel, U.; Dahmen, C.; Kessler, H. RGD modified polymers: biomaterials for stimulated cell adhesion and beyond *Biomaterials* **2003**, *24*, 4385-4415.

[287] Grafahrend, D.; Calvet, J.L.; Klinkhammer, K.; Salber, J.; Dalton, P.D.; Möller, M.; Klee D. Biofunctionalized poly(ethylene glycol)-*block*-poly(ε-caprolactone) nanofibers for tissue engineering *J. Mater. Sci. A: Mater. Med*. **2008**, *19*,1479–1484.

[288] Grafahrend, D.; Calvet, J.L.; Klinkhammer, K.; Salber, J.; Dalton, P.D.; Möller, M.; Klee D. Control of Protein Adsorption on Functionalized Electrospun Fibers *Biotechnology and Bioengineering* **2008**, *101*, 609-621.

Chapter 2: Star-Shaped and Hyperbranched Poly(ester)s

2.1 Multi-Arm Star Poly(L-Lactide) with Hyperbranched Poly(glycerol) Core

Carsten Gottschalk, Florian K. Wolf and Holger Frey

Abstract

Biocompatible multi-arm star block copolymers based on poly(L-lactide) (PLLA) have been prepared by a *core-first* approach, using hyperbranched polyglycerol, a polyether-polyol, as a polyfunctional initiator.The molecular weight of the hyperbranched initiator-core was varied from 2,200 g/mol to 5,200 g/mol, molecular weights of the resulting multi-arm stars were in the range of 6,700 – 107,000 g/mol (NMR), depending on the amount of dilactide (LA) added. Various monomer/initiator ratios have been employed in the Sn-catalyzed dilactide polymerization in order to vary the length of the lactide arms from DP_n(arm) = 2 to 20 units. Detailed NMR analysis using conventional and 2D-NMR techniques (e.g., HSQC NMR) revealed that the monomer/initiator-core ratio indeed permits control of the arm length. SEC measurements showed that the narrow polydispersities of the core molecules (M_w/M_n = 1.5 and 1.6) became even lower after grafting of PLLA for the multi-arm star polymers. SEC also demonstrated that the competing homopolymerization of LA could be avoided when using suitable reaction conditions. The resulting polyglycerol-PLLA star polymers exhibited low polydispersities (M_w/M_n) between 1.15 and 1.7, depending on the length of the PLLA arms. Attachment of the hydrophobic poly(L-lactide) chains to the hydrophilic polyether structure leads to amphiphilic, core-shell type structures suitable for guest encapsulation.

Keywords: star polymers, biocompatible, polyglycerol, hyperbranched, block copolymer, poly(lactide).

Introduction

Multi-arm star polymers are three-dimensional macromolecules, in which a large number of linear arms of similar molecular weights and narrow molecular weight distribution emanates from a central core.[1] During the last decade this class of star polymers has attracted increasing interest due to their unusual bulk and solution properties.[2] Generally, two major strategies have been employed for the synthesis of star polymers: the *arm-first* approach and the *core-first* approach on the basis of a multi-functional core used as initiator. In the latter case the arm length can be tailored by the ratio of active sites to the amount of added monomer.

Linear aliphatic poly(ester)s such as poly(lactide) (PLA) and poly(ε-caprolactone) are of great interest due to their biodegradability, biocompatibility, and permeability for many drugs. These poly(ester)s have been widely used for biomedical applications in surgery, such as surgical sutures, drug delivery systems, and internal bone fixation.[3-6] PLLA is also discussed as a promising bioerodible material for a wide range of commodity applications.[7-9] However, it still represents a challenge to tailor the properties of PLA-based materials by mere structural variation. Lowering of the degree of crystallization is often achieved by copolymerization of L-lactide (LLA) with, e.g., glycolide, ε-caprolactone, meso-lactide or other comonomers resulting in linear block copolymers.[9-11] An alternative strategy to generate unusual rheological and mechanical properties combined with a modified biodegradation profile has been recognized: the design of weakly and strongly branched molecular architectures.[12-14] One interesting approach is the synthesis of star-shaped PLLA, because the variation of the molecular structure from linear to multi-arm can be expected to exert strong effects on both rheological properties and morphology.[15]

It has been shown in several recent reports that LLA can be polymerized in a controlled manner using stannous octanoate (Sn(Oct)$_2$) as catalyst in combination with initiating hydroxyl groups.[16] The Sn-catalyzed polymerization of LLA can also be employed to prepare star polymers, if suitable polyol initiators are used. This has been demonstrated by Kim et al., who used pentaerythritol as multi-functional initiator to synthesize 4-arm poly(lactide) star polymers.[17] Hedrick and co-workers prepared well-defined star poly(lactide)s with up to 12 arms, using multi-functional dendritic initiators derived from 2,2-bis(hydroxymethyl)propionic acid derivatives.[18] The synthesis of star-shaped poly(lactide)s starting from hydroxyl-terminated PAMAM dendrimer cores was reported by Xi et al.[19]

Depending on the generation of the dendrimer employed they attached between 5 and 32 arms to the dendrimer periphery.

Because of the time-consuming synthesis of dendrimers, hyperbranched polymers prepared in a one-step procedure from AB_m monomers have also been used as macroinitiators for the synthesis of multi-arm star polymers.[20] In this context, Adeli and Haag used commercial hyperbranched poly(ethylene imine) as initiator-core to prepare poly(lactide) star polymers with encapsulation properties, however, the focus of this work was on a detailed investigation of amphiphilic host-guest properties.[21]

In order to prepare well-defined multi-arm stars, hyperbranched polymers with narrow polydispersity and predictable molecular weights are required. We use hyperbranched polyglycerols (PG) with narrow polydispersity ($M_w/M_n \leq 1.5$) that are obtained via ring-opening multibranching polymerization under slow monomer addition conditions.[22] The solubility and flexibility of these polar aliphatic polyether polyols can be tailored by the attachment of oligo(propylene oxide) segments, leaving the functionality unchanged.[23] Based on these initiator-cores, poly(ethylene oxide) stars with up to 55 arms,[24] poly(ε-caprolactone) stars with up to 52 arms[25] as well as poly(tert-butyl acrylate) and poly(2-hydroxyethyl methacrylate) multi-arm star polymers with up to 90 arms have been described in recent work.[26] Another work related to this paper was recently published by Ouchi and Ohya, who described the preparation of comb-polymers based on linear polyglycerol for the grafting of PLLA.[27]

In the current paper we introduce the synthesis of multi-arm star block copolymers using well-defined, hyperbranched polyglycerols as multi-functional initiators for the $Sn(Oct)_2$-catalyzed polymerization of LLA. The central parameters arm-length and molecular weight as well as the thermal properties of the resulting multi-arm star polymers have been studied with respect to the amount of dilactide used, i.e., the linear arm length of the stars.

Experimental Part

Materials

L-lactide (98%, Aldrich Chemical Co., LLA) and stannous(II) 2-ethylhexanoate (95%, Aldrich Chemical Co., $Sn(Oct)_2$) were used as received. All solvents were of analytical grade and used as received. PG_{28} (M_n = 2200 g/mol, M_w/M_n = 1.5) and PG_{68} (M_n = 5200 g/mol, M_w/M_n = 1.6) were prepared as reported previously[22] and dried in vacuum.

Measurements

^1H and ^{13}C NMR spectra were recorded on a Bruker AC 300 spectrometer in DMSO-d_6, operated at 300 and 75.4 MHz, respectively, and the chemical shifts are given in parts per million (ppm). Size exclusion chromatography (SEC) of the samples was carried out using a PSS-System with a Shodex RI-71 detector under the following conditions: PSS-SDV columns-combination consisting of three columns (100, 1000, 10000 Å), $CHCl_3$ as the eluent at a flow rate of 1 mL/min, concentrations of 6-10 mg/mL. The calibration curve was obtained using linear polystyrene (PS) standards. All measurements were carried out at 35°C. The thermal properties were measured by differential scanning calorimetry (DSC) using a Perkin Elmer 7 Series Thermal Analysis System in the range of –50 to 200°C at heating rates of 40 K/min and 10 K/min. The melting point of indium (156°C) was used for calibration. The T_g was determined as the midpoint of the heat-capacity increase of the second heating process and T_m as the endothermal peak in the DSC curve of the second heating process.

Polymerization

The procedure is exemplified for the sample $P(G_{28}LLA_8)$ and was carried out in an analogous manner for all other star polymers prepared. PG_{28} (0.25 g, 0.12 mmol) was dried under vacuum at 120°C for at least 2 hours in the reaction vessel. LLA (2.06 g, 14.26 mmol) was added and molten at 120°C. $Sn(Oct)_2$ (0.004 mL, 0.01 mmol), as a 10 vol.-%-solution in toluene, was added to the clear melt. After 24 hours the reaction mixture was allowed to cool down to room temperature. The solid product was dissolved in $CHCl_3$ (10 mL) and poured into cold diethyl ether to precipitate the branched polymer. The product was isolated by filtration and dried in vacuum at room temperature for 48 hours to yield 1.89 g (82 %) of a white powder. ^1H NMR (DMSO-d_6): δ = 5.46 (-CH(CH$_3$)-O<u>H</u>); 5.24-5.01 (-OOC-

CH(CH$_3$)-O-), (PG-OOC-CH(CH$_3$)-O-) and (-CH-OOC- in core); 4.25-4.11 (-OOC-CH(CH$_3$)-OH) and (-CH$_2$-OOC- in core); 3.82-3.10 (PG); 1.48 (-OOC-CH(CH$_3$)-O-); 1.26 (-OOC-CH(CH$_3$)-OH).
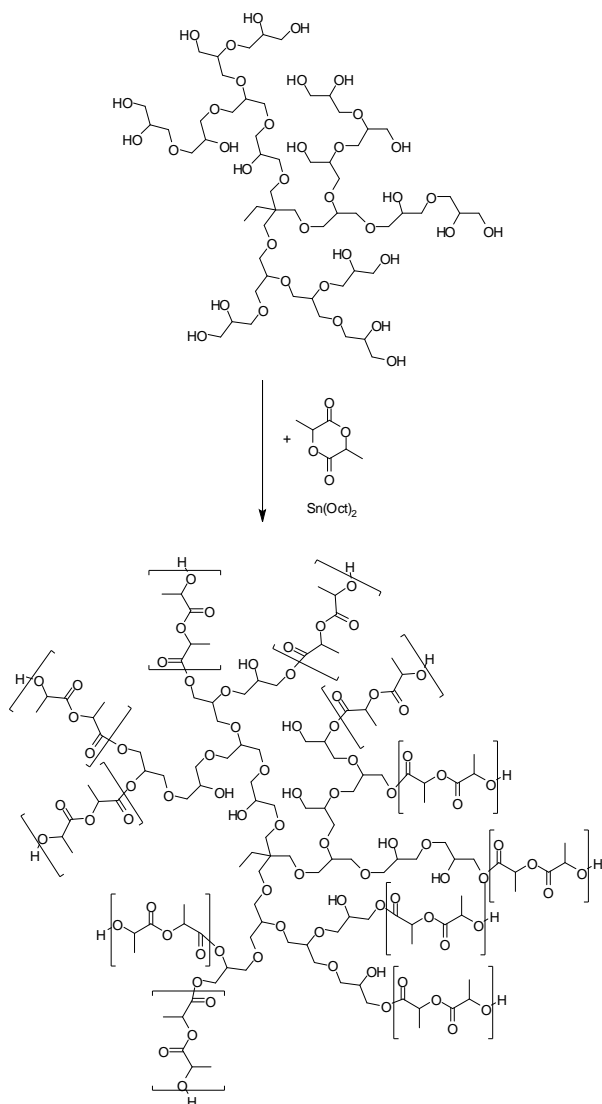
Scheme 1: Preparation of multi-arm poly(L-lactide)-star block copolymers.

Results and Discussion

In this investigation two polyol core-initiators with different molecular weight and functionality have been employed. The hyperbranched polyglycerol samples PG$_{28}$ (M$_n$ = 2200 g/mol, M$_w$/M$_n$ = 1.5) and PG$_{68}$ (M$_n$ = 5200 g/mol, M$_w$/M$_n$ = 1.6) were prepared by anionic ring-opening multibranching polymerization of glycidol in the presence of trimethylolpropane (TMP, 2-ethyl-2-(hydroxymethyl)-1,3-propanediol) as initiator-core according to previously published procedures.[22] Copolymerization of this polyol initiator with L-lactide (LLA) was carried out in the presence of catalytic amounts of Sn(Oct)$_2$, as

shown in Scheme 1. Sn(Oct)$_2$ is preferred for the bulk polymerization of lactide due to its solubility in molten lactide, high catalytic activity and the low rate of racemization of the lactide units.[9] Ring-opening polymerization of cyclic esters with this Sn-compound is generally described as a coordination-insertion mechanism, wherein hydroxyl groups act as active propagation sites. The quasi-living type of polymerization allows the control of molecular weights by the monomer/OH ratio, leading to PLLA with narrow molecular weight distribution.[16]

In the current study all polymerization experiments have been carried out in bulk (with a minimum of toluene present for transfer of the catalyst) at 120°C for 24 h with systematic variation of the lactide monomer/OH ratios. After precipitation in diethyl ether, the polymers were obtained as sticky, white powders that were soluble in a range of solvents, e.g., chloroform and DMSO. The polymers have been characterized by NMR spectroscopy and SEC, as summarized in Table 1. Careful drying of the PG-cores employed under vacuum is the crucial step for the controlled synthesis of the multi-arm star polymers, in order to avoid initiation by traces of water and methanol, which lead to concurrent homopolymerization and thus an undesired blend of linear and star poly(lactide)s.

Table 1: Characterization data of the multi-arm star block copolymers from NMR, SEC and DSC

Sample	DP_n(LLA)$_{th}$	$M_{n,th}$	NMR	SEC[a)]		T_g
			DP_n(LLA)	M_n	M_w/M_n	°C
P(G$_{28}$LLA$_2$)	2	6668	2.2	2200[b)]	1.91	11.0
P(G$_{28}$LLA$_4$)	4	11136	4.1	7300	1.33	17
P(G$_{28}$LLA$_6$)	6	15604	5.8	11900	1.23	22
P(G$_{28}$LLA$_8$)	8	20072	7.2	14300	1.16	26
P(G$_{28}$LLA$_{10}$)	10	24540	9.5	18200	1.15	37
P(G$_{68}$LLA$_2$)	2	15433	2.1	4900	1.53	21
P(G$_{68}$LLA$_4$)	4	25666	3.9	8600	1.58	23
P(G$_{68}$LLA$_6$)	6	35900	5.2	11200	1.42	27
P(G$_{68}$LLA$_8$)	8	46133	7.8	12000	1.44	30
P(G$_{68}$LLA$_{10}$)	10	56366	10.8	16000	1.34	36
P(G$_{68}$LLA$_{20}$)	20	107532	19.7	26500	1.21	45

a) Measured in CHCl$_3$ with polystyrene calibration, b) VPO: M_n = 6200 g/mol.

Most studies targeting multi-arm star structures rely on SEC as the central characterization method. In the following paragraph, we will demonstrate the usefulness of a detailed 2D NMR investigation. Two key issues were addressed in the ensuing molecular characterization: (i) can the arm-length of the multi-arm stars be controlled in the course of the grafting and (ii) can undesired homopolymerization of LA be avoided? Central parameters in the context of star polymers are both the arm length as well as the conversion of the initiating hydroxyl-groups of PG. The superposition of signals in many parts of the ^{1}H-NMR spectra makes a scrupulous NMR-characterization essential. In order to reveal and prove fundamental structure/signal coherences for this new type of star polymer and in order to answer the abovementioned questions, several 2D- NMR experiments have been performed on selected samples of the set of polymer samples. The obtained signal assignment is consistent with literature data for low molecular weight PLLA and polyglycerol (PG), which has been developed in our group.
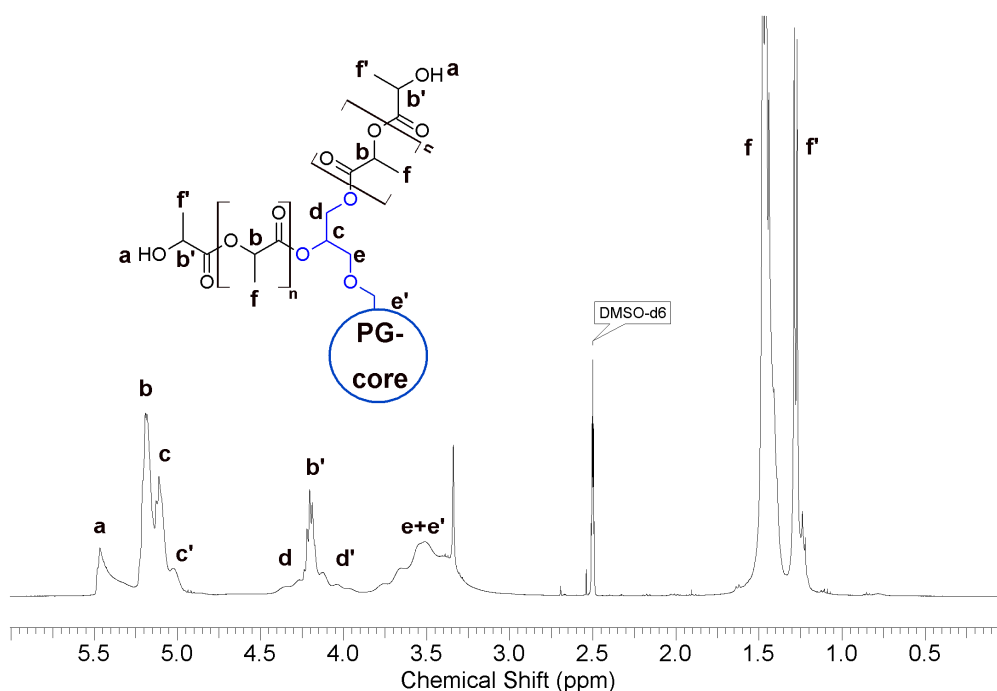
Figure 1: ^{1}H NMR spectrum of P(G$_{68}$LLA$_4$) measured in DMSO-d6.

In the following, the star copolymer P(G$_{68}$LLA$_4$) shall be used as an example for the synthesized PLLA star polymers in general. It provides a suitable model compound for NMR studies, since the signals of both PG-core and PLLA-arm occur in a balanced ratio. Figure 1 shows the ^{1}H-NMR spectrum of the star copolymer P(G$_{68}$LLA$_4$), measured in DMSO-d_6, i.e., a multi-arm star polymer with 68 glycerol units, 70 hydroxyl end groups and a targeted

average arm-length of 4 lactide units per hydroxyl end group. The spectrum exhibits a broad, featureless signal between 3.1 and 3.8 ppm for the polyether core protons, i.e. methine and methylene protons, assigned e and e'. The peaks at 5.2 ppm (**b**, 1H) and 1.4 ppm (**f**, 3H) are characteristic for the methine and methyl protons of the PLLA main chain, respectively. The terminal methine (**b'**) and methyl (**f'**) protons adjacent to the OH groups (5.5 ppm, **a**) lead to resonances at 4.2 ppm and 1.2 ppm, respectively.

The identification of the methylene (d) and methine (c) protons of the esterified primary and secondary OH-groups of the PG – core was important, since they document the successful linkage of arms and core. In this context, 2D-HSQC and COSY experiments proved to be powerful methods which confirmed our assumptions. Figure 2 shows a section of the HSQC spectrum of P(G$_{68}$LLA$_4$) with additional DEPT information (methyl/methine: red; methylene: blue), which covers all signals except for the methyl protons of the PLLA arms. The PG signals in the ^{13}C-NMR can be easily identified and distinguished from the PLLA signals due to their broad appearance - a fact explained by the long relaxation times (T$_2$) of the rather rigid PG core (neither a prolongation of the measurement up to 40h and an extension of after-pulse delay times, nor a rise of the sample temperature to 334K resulted in a significant improvement of the signal sharpness in the ^{13}C-NMR spectra). Areas A and B in Figure 2 mark the zones of a significant signal overlap of the lactide methine protons with those from esterified PG end groups. In area A the signals of b and c/c' are clearly distinguishable: While b can be assigned to the lactide arms, the ^{1}H NMR signals of c and c' reveal a correlation with the characteristic broad ^{13}C NMR signals representing the rigidified PG core. As presented in Scheme 1, linear units of PG can show 1,3- or 1,4 connections, which usually appear in an abundance of 10 and 30 % of the total amount of the repeating units, respectively, carrying primary (1,3) or secondary (1,4) hydroxyl groups.[23] While signal c can be assigned to esterified hydroxymethine groups of terminal glycerine units, c' can be ascribed to their counterparts of linear 1,4 - connected glycerine groups. Area B clearly shows the lactide methine protons b', representing the end groups of the PLLA arms. Furthermore, the HSQC investigation reveals that the broad proton signals d at δ = 3.9-4.4 ppm can be related to esterified hydroxymethyl groups (d and d'- blue) of the PG-core. As in the case of the esterified hydroxymethine protons (c/c'), differentiation between the functionalization of linear (d') and terminal (d) hydroxymethyl groups is possible. Between 4.11 and 4.25 ppm,

superposition with the rather defined signal of the terminal lactide methine protons (red) can be observed. Since chain growth, originating from hydroxyl groups of linear PG repeating units located at the center of the PG core is less likely due to steric hindrance, it is not astonishing that section C in the HSQC spectrum of Figure 1 shows signals, which can be assigned to non-esterified hydroxymethyl (g) and hydroxymethine protons (h). These could be identified according to the characteristic chemical shifts of their ^{13}C-cores.[23]

In contrast to this observation, NOE measurements with irradiation of the sample at the proton frequency of its residual water (not shown here) did not reveal the presence of significant amounts of hydroxyl groups other than those referring to terminal lactide units. This may be due to the fact that the few hydroxymethyl groups are predominantly located in the well-shielded center of the star polymer.
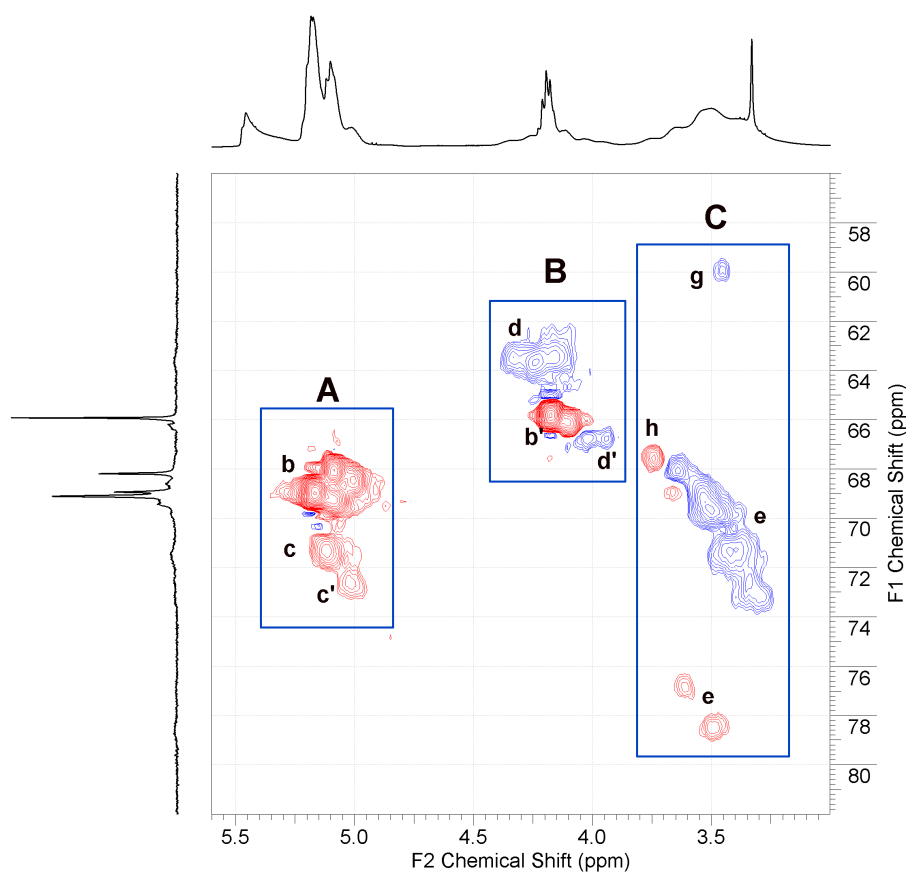
Figure 2: HSQC NMR spectrum (section) of P(G$_{68}$LLA$_4$) measured in DMSO-d$_6$.

Figure 3 shows the TOCSY NMR spectrum of P(G$_{68}$LLA$_4$), in which proton/proton coupling can be observed. The spectrum confirms the correct signal assignment of functionalized PG-hydroxyl groups. Significant cross peaks are marked with numbers from I to IV. Their origin will be explained according to the designation in Figure 1. Frame I shows the ^3J coupling of

protons c and c' with e. Further cross peaks (at chemical shifts of 3.45 and 3.70 ppm) are due to the unesterified hydroxymethyl (g) and hydroxymethine (h) protons of the linear PG units and the correlation with their hydroxyl protons. The correlation of d and c in frame II further supports the general model of adjacent, esterified primary and secondary hydroxyl groups of terminal PG units. As described above, esterification of hydroxyl groups of linear glycerol units in the core is difficult to distinguish from those of the 1,2-diols at its periphery. The fact that coupling of d only occurs with c and not with c' gives further evidence that d and c represent the esterified hydroxymethyl (d) and hydroxymethine (c) group of terminal PG units. c' can be assigned to the esterified hydroxymethine groups of the linear 1,4-connected repeating units, since these correlate exclusively with protons e. (As described, methine- and methyl protons with adjacent ether groups, representing the PG-backbone, are labelled e.) In frame III, weak coupling of the protons d and e can also be observed. This coupling over multiple bonds could only be revealed by the TOCSY NMR experiment and is not visible in the standard COSY NMR spectra. Frame IV finally shows the coupling between the hydroxy (a) and the terminal methine protons (b').
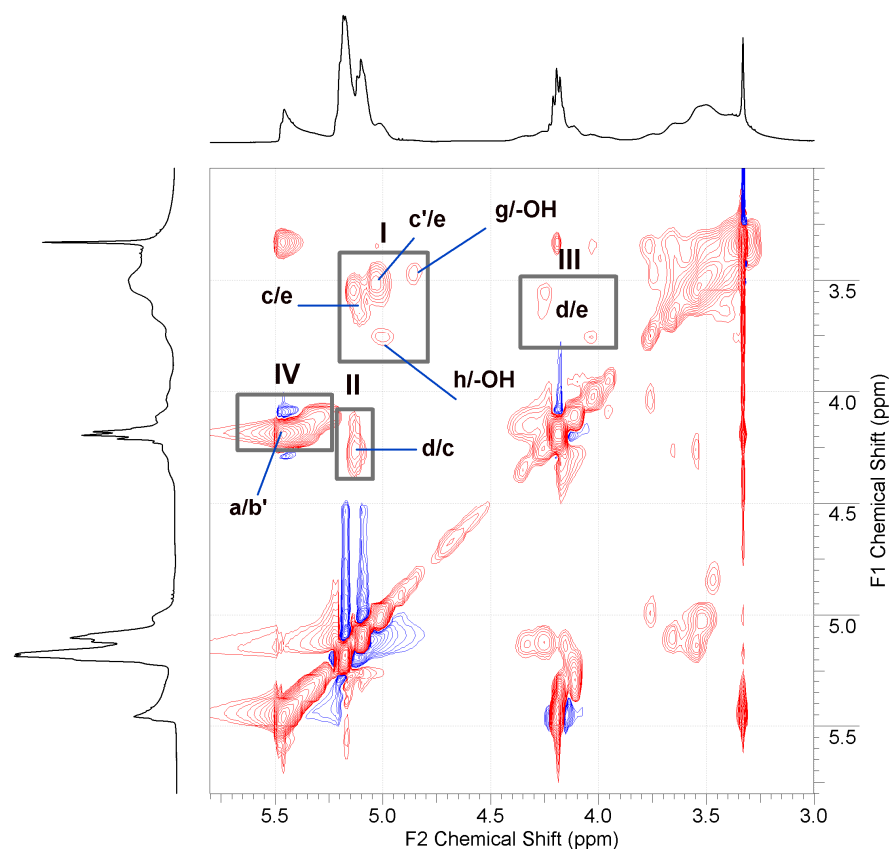
Figure 3: ^{1}H,^{1}H-TOCSY NMR spectrum (section) of P(G$_{68}$LLA$_4$) measured in DMSO-d6: Methine and methyl proton based cross peaks are plotted red - methylene blue.

Unfortunately, the methine protons of the esterified secondary hydroxyl groups (**b'**) and the methylene protons of the esterified primary hydroxyl groups (**d and d'**) of the PG core resonate at 5.2 ppm and 4.2 ppm and thus overlap with other signals. Due to this overlap, the signals of the PLLA methine protons do not provide reliable information on the structure of the star polymers and the conversion of the hydroxyl groups of the initiator. However, the observed separation of the signal for the terminal methyl protons (**f'**) permits to calculate the average PLLA arm length from the ratio of the intensities of the signals (**f**) and (**f'**). It should be noted that this calculation is based on the absence of PLLA homopolymer, which was confirmed by GPC-data, as will be discussed below.

The signal assignment as it is shown in Figure 1 can thus be confirmed by the 2D NMR experiments. The variation of similar structural elements in the complex geometry of the core resulted in a broad signal distribution of the nuclei of PG in the ^{1}H- as well as in the ^{13}C NMR spectra. Although exact signal to structure correlation was difficult to establish, differentiation between PG and lactide signals could be achieved in principle, confirming successful grafting of the LLA arms onto the PG core. Furthermore, HSQC and COSY NMR spectroscopy allowed the differentiation between functionalised linear and terminal glycerol groups of the PG-core. Unfortunately, we are not able to calculate a precise degree of functionalization of the PG cores, but it was confirmed that the majority of the functional groups, especially in the periphery of the core were esterified. A preference of primary over secondary hydroxyl groups as initiating functionalities could not be observed.

The theoretical M_n-values for all series of multi-arm stars based on the monomer/core ratio are summarized in Table 1. In the second column, the degrees of polymerization DP_n(LLA)$_{th}$ for the LLA arms per end group are listed, as calculated from the ^{1}H NMR data. A comparison of DP_n(LLA)$_{th}$ with the average DP_n(LLA) calculated from the integration of the NMR-spectra supports full conversion of the hydroxyl termini of PG and thus good control of the reaction. Therefore, the molecular weights of the resulting star-block copolymers can be estimated from the NMR experiments. However, since the spectra suggest almost complete functionalization, the maximum error will be 10-15% for the larger hyperbranched PG-core.

The molecular weight increases upon grafting as well as apparent polydispersities were studied by SEC measurements (PS standards). Figure 4 shows the typical SEC traces of a

series of multi-arm star copolymers based on the PG_{28} core. The rather symmetrical and monomodal distributions as well as the absence of signals at lower molecular weight suggest that no blend of star polymers and undesired linear homopolymer is formed. The polydispersities of the polyglycerol cores PG_{28} and PG_{68} are $M_w/M_n = 1.54$ and $M_w/M_n = 1.62$, respectively. Polydispersities generally remained low after grafting of LLA (Tab. 1; $M_w/M_n = 1.15 - 1.91$) and in most cases become even lower due to the coupling of the distributions of the PLLA chains at the star centers. It is furthermore interesting to note that – as demonstrated in Figure 4 – the molecular weight distributions of the stars become increasingly narrow with increasing amount of LLA added. This is explained by the decreasing polydispersity of the PLLA chains attached to the PG core, which leads to a lowered polydispersity due to the abovementioned coupling of the molecular weight distributions.
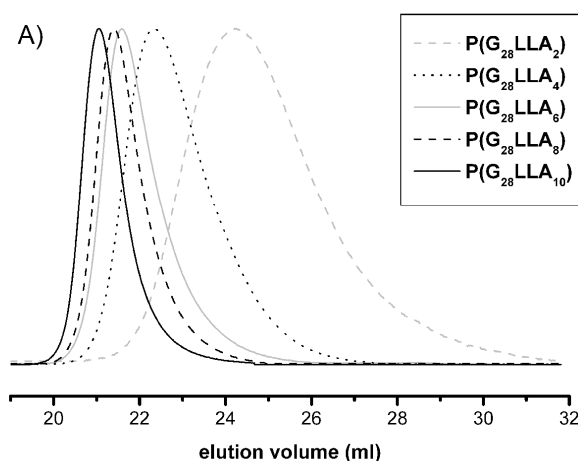
Figure 4: SEC traces of star-shaped block copolymers based on PG_{28}.

The molecular weights of the star polymers calculated from the NMR data were in the range of 6,700 to 107,500 g/mol ($M_{n,th}$, Table 1). From Table 1 it is obvious that the molecular weights of the star copolymers measured by SEC are considerably lower than the theoretical molecular weights. Generally, this is consistent with expectation and explicable with the more compact structure of star-shaped polymers in comparison with analogous linear polymer chains with identical molecular weights. In order to verify that the SEC-measurements lead to a systematic underestimation of the molecular weights of the star

polymers it is necessary to compare the data with results from other methods. Exploratory MALDI-TOF experiments suggest that the molecular weights of the star polymers indeed exceed the values obtained by SEC. For small star polymers based on PG_{28} as a core molecule, molecular weights calculated from the MALDI-TOF spectra were similar to the calculated ones.

Vapour pressure osmometry (VPO) characterization for a carefully dried sample of $P(G_{28}LLA_2)$ revealed a molecular weight of 6,200 g/mol, which was in agreement with the results of the MALDI-TOF experiments and NMR-data. This verifies the good control and pseudo-living character of the polymerization process. In addition, the calculated M_n values show a linear correlation with the data obtained under standard SEC conditions. As demonstrated in Figure 5, this is the case for both series of PLLA stars. On the one hand, this correlation is of interest for the calibration of a standard SEC set-up for such star polymers, on the other hand it shows that the underestimation of molecular weights is systematic. Interestingly, the order of magnitude of the underestimation of the molecular weights strongly depends on the functionality of the respective initiator-core, as can be seen from the slope of the lines in the diagram. In the case of the larger polyglycerol core, the increased compactness of the solution structure obviously leads to a stronger underestimation of the molecular weight by SEC.
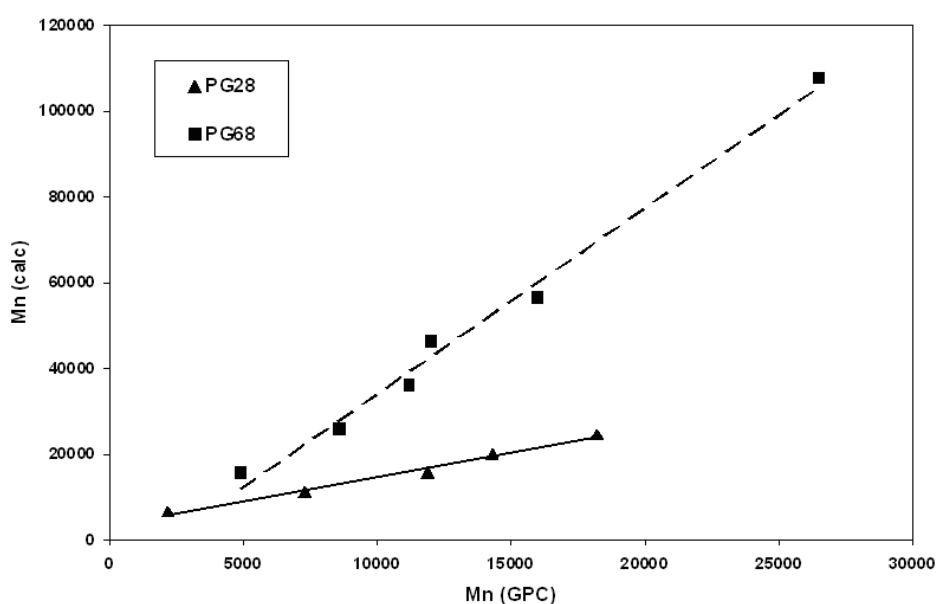
Figure 5: Correlation of theoretical M_n with M_n measured by SEC.

The thermal properties of the multi-arm star copolymers have been characterized by differential scanning calorimetry (DSC) with respect to the glass transition temperatures (T_g) and the presence of a crystalline fraction. This is a particularly intriguing point with respect to the question, to which extent the highly branched core impedes crystallization of the PLLA chains. The hyperbranched polyglycerol cores are flexible polymers with T_gs in the range of -19°C to -26°C[22], while linear PLLA exhibits a glass transition of around 60°C.[26] All values measured for the multi-arm stars are given in the last column of Table 1. For all samples, one single T_g is observed, which gradually increases with increasing length of the PLLA arms attached. In Figure 6, the glass transition is plotted versus arm length, demonstrating the linearity of this behavior. As expected, the flexibility of polyglycerol is reduced considerably by attachment of the oligo- or poly(L-lactide) blocks.

The star polymers showed no melting transitions, i.e., no crystallization was observed, except for (PG$_{68}$LLA$_{20}$) with the longest linear PLLA arms, which exhibited a melting transition at 131°C, however, with low melting enthalpy (6 J/g). This is in agreement with the expectation that crystallization of the oligo-LLA chains is only possible above a specific degree of polymerization of the arms attached. For the multiarm stars, the critical degree of polymerization appears to be in the range of 10-20.
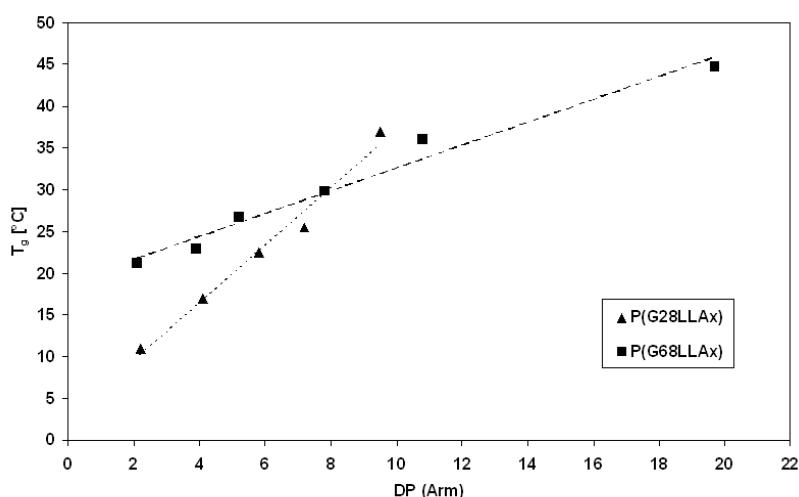
Figure 6: Correlation of the glass transition temperature (T_g) with the lactide arm length.

Attachment of the hydrophobic poly(L-lactide) chains to the hydrophilic polyether structure could lead to core-shell like reversed micelles, just like reported for polyglycerols

esterified with fatty acids as well as poly(lactide) stars with poly(ethylene imine) core.[21,29] To investigate the host-guest properties of the star-shaped block copolymers first extraction studies in the two-phase chloroform/water system have been carried out with the water-soluble dyes Methyl orange and Bengal Rose. In both cases, star polymers based on PG_{68} as core molecule extracted the dye into the chloroform phase, whereas the multi-arm stars based on PG_{28} were not capable of phase transfer. This behavior can be explained by encapsulation of the dye in the hydrophilic core of the investigated materials, which requires remaining hydroxyl groups. The host-guest properties of this biodegradable and biocompatible star-shaped block copolymers offer interesting potential for application particularly for drug delivery systems. A detailed study is in progress, aiming at a comparison with PLLA-stars published based on poly(ethylene imine) core.[21]

Conclusions

Poly(L-lactide) multi-arm star copolymers have been prepared via a *core-first* approach, using hyperbranched PG with different degree of OH-functionality as core molecules. This permitted the preparation of star polymers with varying number of arms. Several different monomer/initiator ratios were employed in the Sn-catalyzed polymerization in order to vary the length of the lactide arms [DP_n(arm) = 2 to 20]. NMR characterization revealed that the monomer/initiator ratio controls the arm length and confirmed complete or almost complete reaction of all hydroxyl end groups of the polyglycerol core. Using various 2D NMR-techniques, very detailed signal assignment was achieved. The methods employed, such as HSQC NMR, are promising for the detailed characterization of multi-arm star polymers in general. Molecular weights of the block polymers determined by SEC measurements were smaller than the predicted values due to the star-branched architecture of the samples. The moderate polydispersities of the core molecules (M_w/M_n = 1.5 to 1.6) were lowered upon grafting of the PLLA arms (M_w/M_n = 1.15 to 1.7) due to coupling of the distributions.

Due to the biocompatibility of the hyperbranched polyglycerol[30] and the biodegradability of the PLLA arms, these well-defined poly(ester) multi-arm star copolymers are attractive materials for biomedical applications.

References

(1)   S. P. Meneghetti, P. J. Lutz, D. Rein, in: *Star and Hyperbranched Polymers*, M. K. Mishra, S. Kobayashi, Eds., Marcel Dekker, New York 1999, p. 27.

(2)   (2a) J. Roovers, L.-L. Zhou, P. M. Toporowski, M. van der Zwan, H. Iatrou, N. Hadjichristidis, *Macromolecules* **1993**, *26*, 4324; (2b) B. Comanita, B. Noren, J. Roovers, *Macromolecules* **1999**, *32*, 1069.

(3)   M. Vert, *Angew. Makromol. Chem.* **1989**, *166/167*, 155.

(4)   D. Bendix, *Polymer Degradation and Stability* **1998**, *59*, 129.

(5)   U. Edlund, A.-C. Albertsson, *Advances in Polymer Sciences* **2002**, *157*, 67.

(6)   A. C. Stähelin, A. Weiler, H. Rüfenacht, R. Hoffmann, A. Geissmann, R. Feinstein, *Arthroscopy*, **1997**, *13*, 238.

(7)   R. A. Gross, B. Kalra, *Science* **2002**, *297*, 803.

(8)   E. T. H. Vink, K. R. Rábago, D. A. Glassner, B. Springs, R. P. O`Connor, J. Kolstad, P. R. Gruber *Macromol. Biosci.* **2004**, *4*, 551.

(9)   R. E. Drumright, P. R. Gruber, D. E. Henton, *Adv. Mater.* **2000**, *12*, 1841.

(10)   H. R. Kricheldorf, *Chemosphere* **2001**, *43*, 49.

(11)   (11a) M. Okada, *Prog. Polym. Sci.* **2002**, *27*, 87; (11b) A.-C. Albertsson, I. K. Varma, *Advances in Polymer Sciences* **2002**, *157*, 1.

(12)   H.-J. Sterzel, M. Laun, *DE 4321355 A1* (BASF AG, **05.01.1995**).

(13)   (13a) Y. Ohya, S. Maruhashi, T. Ouchi, *Macromol. Chem. Phys.* **1998**, *199*, 2017; (13b) Y. Ohya, S. Maruhashi, T. Ouchi, *Macromolecules* **1998**, *31*, 4662; (13c) K.Y. Cho, C.-H. Kim, J.-W. Lee, J.-K. Park, *Macromol. Rapid Commun.* **1999**, *20*, 598; (13d) T. Ouchi, T. Kontani, Y. Ohya, *J. Polym. Sci., Part A: Polym. Chem.* **2003**, *41*, 2462.

(14)   (14a) Y.X. Li, J. Nothnagel, T. Kissel, *Polymer* **1997**, *38*, 6197; (14b) M. Möller, F. Nederberg, L.S. Lim, R. Kånge, C.J. Hawker, J.L. Hedrick, Y. Gu, R. Shah, N.L. Abbott, *J. Polym. Sci., Part A: Polym. Chem.* **2001**, *39*, 3529; (14c) C. Gottschalk, H. Frey, *Macromolecules* **2006**, *39*, 1719.

(15)   D. B. Alward, D. J. Kinning, E. L. Thomas, L. J. Fetters, *Macromolecules* **1986**, *19*, 215.

(16)   (16a) H. R. Kricheldorf *Chemosphere* **2001**, *43*, 49; (16b) K. M. Stridsberg, M. Ryner, A.-C. Albertsson *Advances in Polymer Sciences* **2002**, *157*, 78; (16c) O. Dechy-Cabaret, B. Martin-Vaca, D. Bourissou *Chem. Rev.* **2004**, *104*, 6147.

(17)   (17a) S. H. Kim, Y.-K. Han, Y. H. Kim, S. I. Hong, *Makromol. Chem.* **1992**, *193*, 1623; (17b) S. H. Kim, Y.-K. Han, K.-D. Ahn Y. H. Kim, T. Chang, *Makromol. Chem.* **1993**, *194*, 3229.

(18)   (18a) B. Atthoff, M. Trollsås, H. Claesson, J. L. Hedrick, *Macromol. Chem. Phys.* **1999**, *200*, 1333; (18b) M. Trollsås, M. A. Kelly, H. Claesson, R. Siemens, J. L. Hedrick, *Macromolecules* **1999**, *32*, 4917.

(19)   (19a) Y.-L- Zhao, Q. Cai, J. Jiang, X.-T. Shuai, J.-Z. Bei, C.-F. Chen, F. Xi, *Polymer* **2002**, *43*, 5819; (19b) Y.-L- Zhao, X.-T. Shuai, C.-F. Chen, F. Xi, *Chem. Mater.* **2003**, *15*, 2836.

(20)   (20a) A. Sunder, R. Hanselmann, H. Frey *Chem. Eur. J.* **2000**, *6*, 2499; (20b) M. Jikei, M. Kakimoto *Prog. Polym. Sci.* **2001**, *26*, 1233.

(21)   M. Adeli, R. Haag, *J. Polym. Sci. Polym. Chem*. **2006**, *44*, 5740.

(22)   A. Sunder, R. Hanselmann, H. Frey, R. Mülhaupt *Macromolecules* **1999**, *32*, 4240.

(23)   A. Sunder, R. Mülhaupt, H. Frey *Macromolecules* **2000**, *33*, 309.

(24)   R. Knischka, P. J. Lutz, A. Sunder, R. Mülhaupt, H. Frey *Macromolecules* **2000**, *33*, 315.

(25)   A. Burgath, A. Sunder, I. Neuner, R. Mülhaupt, H. Frey, *Macromol. Chem. Phys.* **2000**, *201*, 792.

(26)   (26a) Z. Shen, Y. Chen, E. Barriau, H. Frey, *Macromol. Chem. Phys.* **2006**, *207*, 57; (26b) Y. Chen, Z. Shen, E. Barriau, H. Kautz, H. Frey, *Biomacromolecules* **2006**, *7*, 919.

(27)   T. Ouchi, S. Ichimura, Y. Ohya, *Polymer* **2006**, *47*, 429.

(28)   (28a) B. Kalb, A. J. Pennings *Polymer* **1980**, *21*, 607; (28b) R. Vasanthakumari, A. J. Pennings *Polymer* **1983**, *24*, 175; (28c) A. J. Ninjenhuis, D. W. Grijpma, A. J. Pennings *Polym. Bull.* **1991**, *26*, 71; M. Zuideveld, C. Gottschalk, H. Kropfinger, R. Thomann, M. Ursu, H. Frey, *Polymer* **2006**, 47, 3740.

(29)   A. Sunder, M. Krämer, R. Hanselmann, R. Mülhaupt, H. Frey *Angew. Chem.* **1999**, *111*, 3758.

(30)   R. K. Kainthan, J. Janzen, E. Levin, D. V. Devine, D. E. Brooks *Biomacromolecules* **2006**, *7*, 703.

2.2 Poly(glycolide) Multi-Arm Star Polymers: Improved Solubility via Limited Arm Length

Florian K. Wolf, Anna M. Fischer and Holger Frey

Abstract

Due to low solubility of poly(glycolic acid) (PGA), its use is generally limited to random copoly(ester)s with other hydroxy-acids, such as lactic acid or applications that permit direct processing from the polymer melt. Insolubility is generally observed for PGA with a degree of polymerization exceeding 20. Here we present a strategy which allows for the preparation of PGA-based multi-arm structures, significantly exceeding the molecular weight of processible oligomeric linear PGA (<1000 g/mol). This was achieved by the use of a multifunctional hyperbranched polyglycerol (PG) macroinitiator and the tin(II)-ethylhexanoate-catalyzed ring-opening polymerization of glycolide in the melt. This strategy permits to combine high molecular weight with good molecular weight-control (up to 16.000 g/mol, PDI= 1.4-1.7), resulting in PGA multi-arm star block copolymers containing more than 90 weight % GA. The successful linkage of PGA arms and PG core via this core first/grafting-from strategy was confirmed by detailed NMR and SEC-characterization. Various PG/glycolide ratios were employed to vary the length of the PGA arms. Besides fluorinated solvents, the materials were soluble in DMF and DMSO up to an average arm length of 12 glycolic acid units. Reductions in T_g and melting temperature compared to the homopolymer PGA promise simplified processing conditions. The findings contribute to broadening the range of biomedical applications of PGA.

Introduction

Linear aliphatic poly(ester)s such as polylactic acid (PLA) and poly(ε-caprolactone)[1] are of great interest due to their biodegradability, biocompatibility and permeability for many drugs. In contrast, poly(glycolic acid) (PGA) is scarcely used due to its high degree of crystallization and insolubility in all common solvents. However, glycolic acid is widely employed in copolymers of varying composition with the above mentioned lactone comonomers[2]. For the PGA homopolymer, peculiar processing techniques for the polymer melt are required and characterization is limited to solid state techniques[3].

In recent works, PLA and poly(ε-caprolactone)[4] have been successfully used for the synthesis of numerous star[5] and multiarm-star[6] as well as (hyper)branched polymers[7]. Although PGA-rich polymers exhibit a superior degradation rate in comparison to poly(lactide), star copolymers primarily composed of this building unit are hardly described in literature[8]. However, star copolymers in a general sense have attracted increasing interest for the fabrication of unimolecular micelles[9], in particular when they consist of a hydrophilic, hyperbranched (or dendritic) core and a hydrophobic corona[10]. Their potential lies in the ability to encapsulate and slowly release hydrophilic molecules. Particularly PEG/PLA-based copolymers have been intensely studied in this context[11,12,13]. Apart from these special application in solution, analogs of well known linear polymers with star architectures exhibit significantly altered physical properties[14,15]. This is often considered the primary motivation for the choice of this interesting polymer architecture[16].

A suitable multifunctional core molecule is required to prepare multi-arm star polymers with core-shell characteristic. Apart from dendrimers[17,18], well-defined hyperbranched polymers[19] fulfill this requirement and benefit from their accessibility via a facile one-step synthesis which makes a tedious, generation wise build up ubiquious. Besides poly(ethylene imine) (PEI)[20], hyperbranched polyglycerol[21,22,23,24,25,26] has proven to be a versatile and highly potent multifunctionial core molecule[27,28,29]. Derivatization and functionalization of the peripheral hydroxyl groups of this polyether-polyol have afforded a number of carrier systems[30,31,32,33,34], matching the concept outlined above. In contrast to dendrimers, where functional groups are exclusively located at the surface, poly(glycerol) scaffolds also contain hydroxyl groups throughout the structure. At first glimpse a disadvantage, this is in fact beneficial for the significantly hydrophilized core environment, when core-shell topologies for encapsulation are desired.

Here we present a solvent-free synthetic strategy for multi-arm star block copolymers with hyperbranched polyether core and PGA-arms, systematically varying arm length. The combination of glycolide with a multifunctional initiator studied in this paper is of a rather fundamental nature. Our primary objective is to improve the solubility of PGA in standard organic solvents and thus facilitate characterization as well as processing, while keeping the overall glycolide weight fraction high. Multi-arm star copolymers[35] should permit the combination of short average chain length and high molecular weight. Since ideally the high number of functionalities of the core molecules is translated into a matching number of arms with a respective chain end, end group effects are expected to exert a significant influence on solubility and crystallization tendency of the polymer.

Results and Discussion

The hyperbranched poly(glycerol)s (PG) with multiple poly(glycolide) arms were prepared by a straightforward two-step approach shown in Fig. 1. In the first step we polymerized glycidol anionically by the method described previously,[19] using trimethylolpropane as a trifunctional initiator. The hydroxyl groups of PG were deprotonated to an extent of 10%, before the slow addition of glycidol monomer was started. The subsequent polymerization proceeds via a ring-opening branching reaction, where branching occurs due to a fast proton exchange equilibrium, which represents a well-known phenomenon in oxyanionic polymerizations.

In the second step, the polyether-polyols were used as macroinitiators for the ring-opening polymerization of glycolide via $Sn(Oct)_2$-catalysis. All polymerization experiments have been carried out in bulk (with a minimum of toluene present for transfer of the catalyst) at 120°C for 24 h with systematic variation of the glycolide monomer/*hb*-PG-OH ratios. Since each glycidol unit leads to the formation of one additional end group after ring-opening and attachment to the growing PG, the corresponding total number of primary and secondary hydroxyl groups of the polymer n(OH) is equal to the sum of the initiator functionality f and the degree of polymerization DP_n.

n(OH) = DP_n + f   (equation 1)
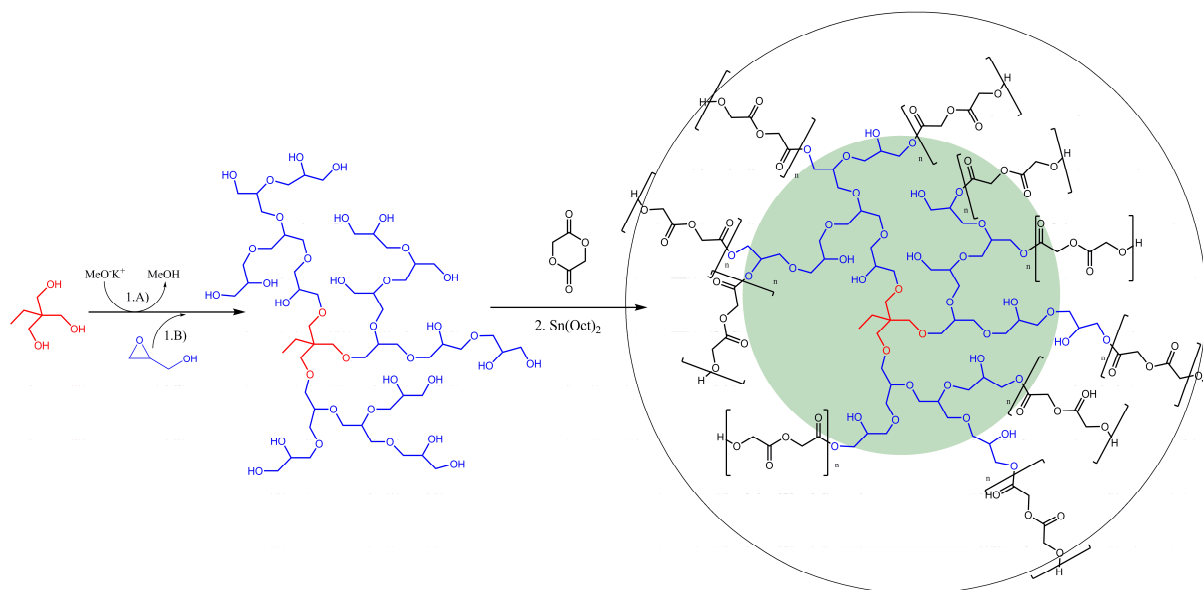
Figure 44: Synthetic route to *hb*-PG-*b*-(P)GA multi-arm star copolymers in a two step sequence. The well-established anionic ring-opening multibranching polymerization of glycidol is followed by the Sn(Oct)$_2$ mediated copolymerization of glycolide.

By variation of the initiator/monomer ratio two hyperbranched poly(glycerol) samples with different degrees of polymerization DP$_n$ were obtained. Their theoretical number of initiating hydroxyl groups was calculated from the degree of polymerization, which is available from ^{1}H NMR according to equation 1. PG$_{14}$ and PG$_{38}$ thus offer an average of 17 and 41 potential initiating moieties for the grafting-from reaction with glycolide. It should be emphasized that according to equation 1, the number of hydroxyl groups is independent of the degree of branching (DB). Typically, the poly(glycerol) macroinitiators possess primary as well as secondary –OH groups, which likely exhibit different reactivities in the initial reaction with glycolide. Since the accessibility of functional groups of PG is believed to play an important role in the properties of the resulting star block copolymer, the branched topology and the distribution of OH-groups therein are key factors that will also be addressed in the following.

Careful drying of the PG cores under vacuum is a crucial step for the controlled synthesis of the multi-arm star polymers, in order to avoid initiation by trace amounts of water, which leads to concurrent glycolide homopolymerization and thus an undesired mixture of linear and star like PGAs. In order to prevent possible precipitation from solution, the polymerization was conducted in bulk without added solvent under Sn(Oct)$_2$ catalysis with an average catalyst loading of 0.1 mol% of the glycolide feed. The mixed compounds yielded

a homogenous melt at 120°C, fulfilling a prerequisite for an efficient *grafting-from* approach. Under the employed reaction conditions and taking the high number of initiating groups into account, the conversion proceeds to high values within short reaction times. The polymers obtained show improved solubility properties compared to linear PGA and thus permit the use of common characterization methods, such as NMR in DMSO-d_6 and SEC in DMF. This is largely attributed to the high end group concentration in combination with a short average PGA chain length in the multi-arm structure.
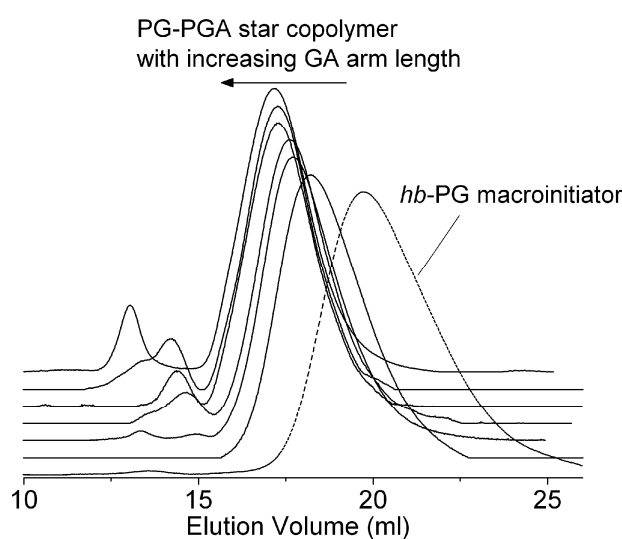
Figure 45: SEC-elugrams of the obtained multi-arm star-block copolymers derived from PG$_{38}$. The grafting of polyglycolide on the poly(glycerol) macroinitiator is accompanied by a significant decrease in elution volume.

With increasing glycolide content, a second, high molecular weight distribution mode appears together with a gradual shift of the main distribution mode to lower elution volume (Figure 45) that is in line with expectation. These apparent impurities could be caused by compounds capable of coinitiation, such as water or other hydroxyl functionalities. Table 4 illustrates the correlation between theoretical molecular weight and values obtained from SEC measurements via calibration with polyethylene glycol (PEG) standards. The obvious underestimation of the molecular weight by SEC is attributed to the peculiar spherical geometry of the multi arm star copolymer and is also observed for other star polymers. The polydispersities of the materials are in the range of 1.3-1.7 for the series of star polymers prepared, which is moderate. These values can be explained by the non-monodisperse multifunctional initiator (PDI: 1.9- 2.0), although transesterification/cyclization reactions during the synthesis cannot be completely excluded.

A detailed account of the NMR-studies aiming at determination of the PGA arm-length of the polymers will be given in the following. In this context, it should be emphasized that solubility in DMF and DMSO was generally limited to star polymers with targeted arm length of up to 12 glycolic acid units. Obviously, samples exceeding those values have not been characterized by SEC or NMR and are thus not listed in Table 4.

Table 4: Characterization data of the multi-arm star block copolymers originating from two different *hb*-PG macroinitiators from NMR and SEC.

sample	glycolide content (weight ratio)	Yield (%)	M_n (theor./NMR*)	M_n (GPC)	PDI (GPC)	average arm length (NMR)
PG_{14}	0	-	1140*	1130	2.0	-
$P(G_{14}GA_4)$	0.77	48	5000	5400	1.6	7
$P(G_{14}GA_8)$	0.87	90	8800	6500	1.5	10.6
$P(G_{14}GA_{12})$	0.91	94	-	-	-	12.1
PG_{38}	0	-	2900*	2450	1.9	-
$P(G_{38}GA_2)$	0.62	45	7600	6300	1.7	3.9
$P(G_{38}GA_4)$	0.76	72	12300	9300	1.5	5.6
$P(G_{38}GA_6)$	0.83	88	17000	11000	1.4	7.2
$P(G_{38}GA_8)$	0.87	83	21700	14300	1.5	8.6
$P(G_{38}GA_{10})$	0.89	92	26400	15600	1.4	9.5
$P(G_{38}GA_{12})$	0.91	93	31100	17000	1.3	9.8
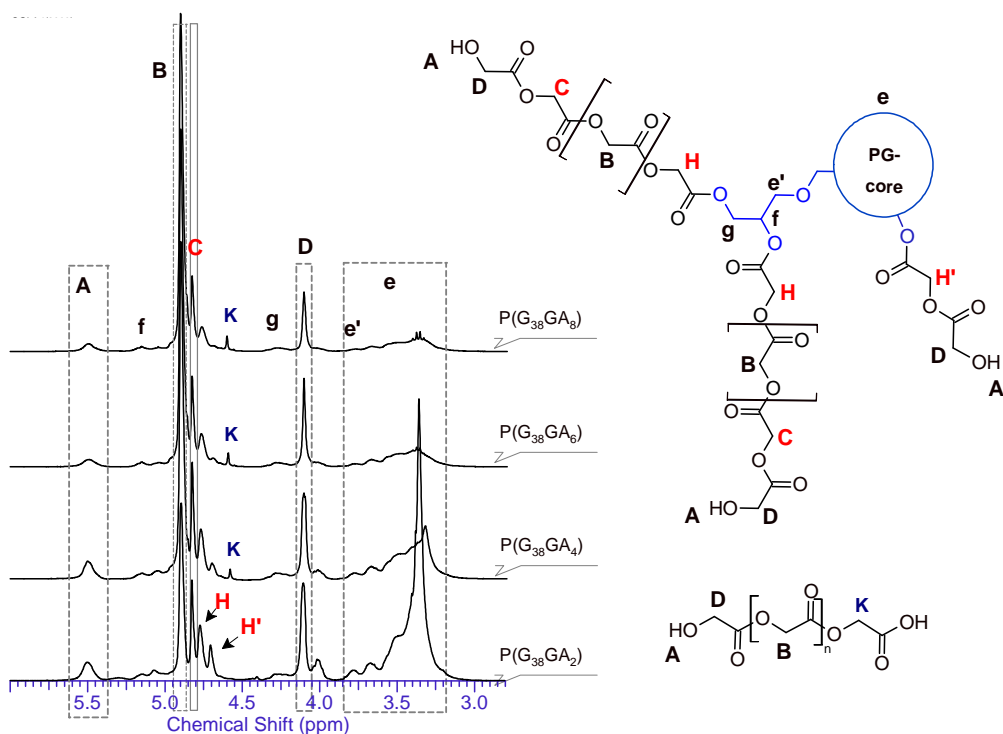
Figure 46: ^{1}H-NMR analysis of the star-block copolymers with increasing glycolide to poly(glycerol) ratio, using PG$_{38}$ as core molecule.

The ^{1}H-NMR-spectra of multi-arm polymer samples with varying composition (based on PG$_{38}$) are shown in Figure 46. As expected, an increase in the glycolide feed results in an increase of the glycolide backbone signal at 4.91 ppm (B) and a relative decrease in signal intensity of the polyglycerol (PG) core. The resonances of the core are mainly distributed between 3.1 and 3.8 ppm (e). Special attention was paid to the terminal glycolic acid unit, since this enables the determination of the average chain length of the oligoglycolide arms. The respective signal can be found at 4.12 ppm and is thus well-separated from the other glycolide-arm related signals B, C, H and H'. Furthermore, the signal denoted A at 5.5 ppm can be assigned to the terminal hydroxyl group of the arms. This important signal assignment was confirmed by a ^{1}H COSY NMR experiment (Figure 47), relying on the cross correlation of the methylene group D with the hydroxyl proton A. Verification of the assignment of methylene and methine protons of the esterified primary and secondary OH-groups of the PG core is crucial, since they evidence the successful linkage of arms and core. Unequivocal proof of attachment is obtained from the cross correlation of the methine/methylene proton of the major initiating species, the terminal glycerol units of *hb*-PG. Clear cross correlations between esterified secondary PG-OH (methine-proton) groups (f) and esterified primary-PG-OH (methylene-proton) units (g) as well as esterified secondary

PG-OH methine (f)/primary ether (e') methylene protons can be observed. In the 2D NMR spectra of the star polymers, these protons have undergone a significant downfield shift (5.0-5.4 ppm), compared to the non-functionalized *hb*-PG related signals, which are mainly found between 3.82 and 3.1 ppm. Although direct experimental proof could not be provided via 2D NMR, the signal denoted C at 4.84 ppm is assigned to the penultimate glycolic acid repeat unit. The first glycolic acid repeat unit, directly attached to the PG-core is represented by two different signals: H (4.78 ppm) or H'(4.72 ppm), While H corresponds to the first glycolic acid unit of a PGA chain, directly attached to the poly(glycerol) core, H' represents the special case of an α-unit of a glycolic acid dimer directly attached to the PG core (i.e. first and penultimate unit at the same time). Hence H` is predominantly observed for low glycolide fractions. This signal assignment is consistent with literature data for PGA-*co*-Poly(ε-caprolactone) copolymers[36,37], as well as PLLA–PG star block copolymers, which have recently been developed in our group[22].
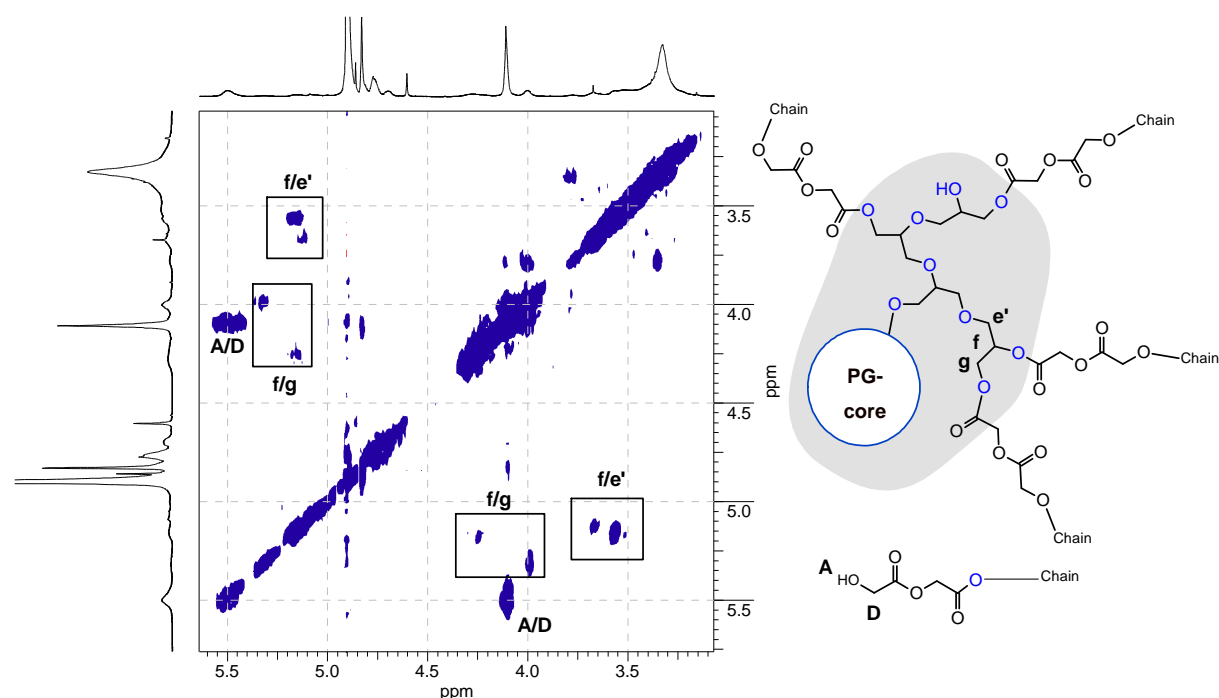
Figure 47: ^{1}H,^{1}H-Correlation COSY NMR: This experiment visualizes correlations of terminal groups with their adjacent hydroxyl groups as well as correlations within esterified glycerol units(f/g & f/e'). The most pronounced cross correlation peak can be assigned to the terminal hydroxyl-methyl group of polyglycolide at 5.5/4.12 ppm (A/D).

The ^{1}H COSY NMR spectrum further suggests that the linear and terminal glycolic acid units do not suffer from signal superposition and can thus be evaluated for the determination of

the average arm length, which was achieved by the comparison of end group- and backbone-related signals (B and D). Although a precise signal-to-structure correlation is difficult to establish, differentiation between PG and poly(glycolide) signals was achieved, confirming successful grafting of poly(glycolide) onto the PG core. Even more important, it was confirmed that the majority of the hydroxyl groups of PG, particularly in the periphery of the core was esterified.

An interesting correlation between the high molecular weight modes observed in SEC and the NMR spectra was found in the singlet, present at 4.61 ppm (K). According to literature data, this can be related to a carboxylic acid chain end of PGA homopolymer.[38] It can be observed for samples which exhibit an additional mode in SEC. This therefore supports the assumed formation of PGA homopolymer by co-initiation with water. Despite careful drying of the hygroscopic PG-macro-initiator in vacuo, contamination with water could obviously not be fully eliminated. Since glycolide has been used as received and not stored in vacuo or inert gas atmosphere, this is the most likely cause for the introduction of traces of moisture into the system.
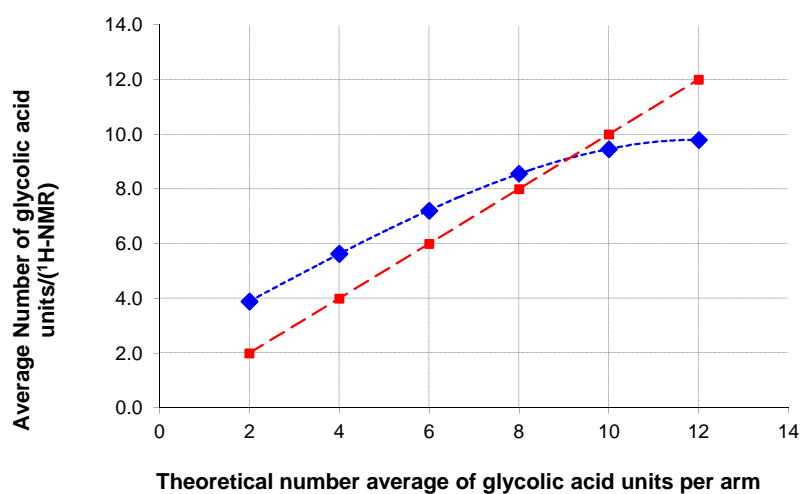
Figure 48: Comparison of average number of repeat units vs. the theoretical number based on the ratio of PG and glycolic acid. The dotted line represents the ideal case of matching numbers and was added as guide to the eyes.

The graph shown in Figure 48 relates the number of glycolic acid repeat units per arm, calculated from ^{1}H NMR for the series of PG_{38}-derived star polymers. These values are compared with the theoretical number expected from the ratio of glycolide monomer to the

sum of possible initiating sites at *hb*-PG. Indeed, an interesting trend can be observed which is most likely influenced by two concurring factors:

1. For very low and moderate numbers of GA repeat units, the observed chain length of the glycolide stars exceeds theoretical expectation. This difference can be attributed to the difference in accessibility and nature (primary/secondary) of the hydroxyl groups of the hyperbranched PG core. A certain fraction of potential initiating sites suffers from a reduced reactivity towards the employed glycolide lactone monomer. Especially the hydroxyl groups close to the core of the hyperbranched structure and/or those of a secondary nature are less active in glycolide addition. The first ring-opening step of the glycolide lactone always generates/retains a primary hydroxyl group, which is more reactive for the attachment of further glycolide monomers than the average PG-hydroxyl groups. Nevertheless, the observed yield of the precipitated star polymers (Table 4) were high enough to assume conversions exceeding 90% before the polymer melt congealed. In addition, ^{1}H NMR spectra of the samples showed no residual glycolide monomer with its distinct singulet signal at 5.06 ppm (in DMSO-d_6).

2. With increasing arm length, the observed number of units drops below the theoretical value. As stated above, we assume that water was introduced by glycolide monomer (indicated by signal K). Hence co-initiation by trace amounts of water enhances with an increase in the glycolide/macroinitiator ratio.

Since the effect discussed in the second consideration counteracts the first one, we observe the described trend from an under- to an overestimation of the chain length.

During the polymerization in the melt, continuous polymer melts with high viscosity are only observed for samples with a targeted average of up to 5-6 GA units. For longer arm lengths, the high mobility of the oligo-GA chains contributes to the consolidation of the melt via crystallization, when reaching high conversion with a lack of molten glycolide monomer that acts as a plasticizer. This is supported by the results of the DSC measurements (Figure 49) of the star copolymers *hb*-PG$_{38}$-*b*-GA$_\mathbf{4}$; -*b*-GA$_\mathbf{8}$ and -*b* −GA$_{\mathbf{12}}$, which confirm the variety of glycolide arm lengths achieved.
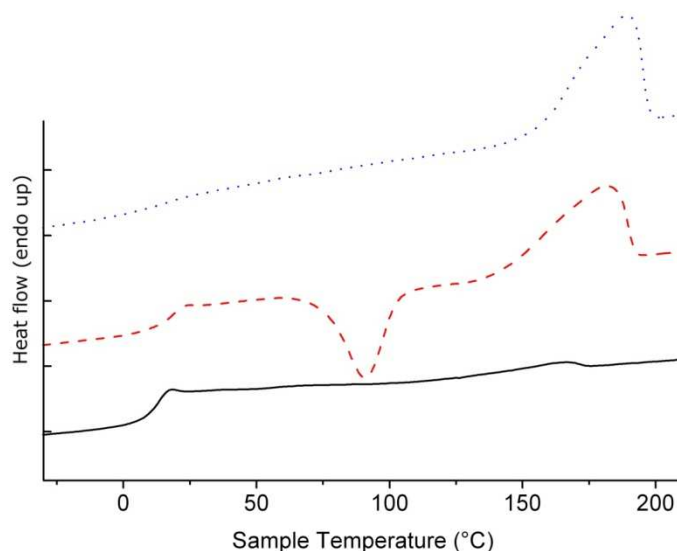
Figure 49: DSC-heating traces (second heating run at 20°C/min) for hb-PG$_{38}$-b-GA$_4$ (bottom); -b-GA$_8$(middle) and -b –GA$_{12}$(top), reflecting the increasing influence of polyglycolide chain length.

Table 5: Thermal properties of selected mulitarm-star copolymers

Samples	GA-units/arm(theor.)	GA-units/arm (found)	Tg (°C)	ΔH$_m$(J/g)	T$_m$(°C)
P(G$_{38}$GA$_4$)	4	5.6	10.13	3.1	161.4
P(G$_{38}$GA$_8$)	8	8.6	15.44	57.6	180.7
P(G$_{38}$GA$_{12}$)	12	9.8	17.5	59.9	189.5

Generally, the observed glass transition (T$_g$) of the glycolide arms for hb-PG$_{38}$-b-GA$_2$ and -b-GA$_4$ is significantly depressed (10-18°C) in comparison to literature data for PGA homopolymer[39] (approximately 40-50°C). This reflects the influence of the flexible PG core. The T$_g$ increased slightly with molecular weight, as it is also observed for most linear polymers. Both findings can be attributed to the low average number of repeat units per arm and are often observed for oligomers. This generally ensures increased chain mobility. As expected, this increased mobility enables efficient crystalline packing for a very short average chain length of 8.6 GA repeat units (for hb-PG$_{38}$-b-GA$_8$). Even for hb-PG$_{38}$-b-GA$_4$ with very low average PGA arm length a slight endothermic melting peak is visible in the DSC heating trace. The high crystallization tendency of the star block copolymers despite the generally impeded crystallization due to the strongly branched PG core is obvious from the data. An average chain length of less than 8-9 glycolic acid units is sufficient for a crystallization-induced

vitrification of the polymer melt at 120°C. The observed melting temperatures for star-shaped PGA ranged between 170 and 190°C (Table 5) and are significantly depressed compared to PGA homopolymer of comparable molecular weight. This should allow for polymer processing at lower temperatures, which is particularly advantageous for such a thermolabile material.

Conclusions

This work presents the first synthesis of star block copolymers based on glycerol and glycolide. *Hb*-PG-*b*-PGA multi-arm star copolymers have been prepared via a core-first approach, using hyperbranched poly(glycerol) with different hydroxyl-functionality as core molecules. The melt copolymerization with *hb*-PG as macroinitiator via Sn(Oct)$_2$ catalysis afforded well-defined complex polymer structures with predictable molecular weights. In contrast to their linear analogs of comparable molecular weight, the polymers exhibited superior solubility in organic solvent like DMF and DMSO. This permitted detailed characterization via 1D and 2D-NMR, SEC and DSC. It should be stressed that the multi-arm star polymers presented possess molecular weights up to 31,000 g/mol and high glycolide weight content up to approximately 91 weight%. The short chain lengths of the oligoglycolic acid chains along with the increased number of end-groups are expected to enhance hydrolytic degradability significantly, rendering the novel materials promising candidates for drug release applications.

Experimental Part

Instrumentation

^{1}H NMR spectra were recorded at 300 MHz on a Bruker AC 300. The spectra were measured in DMSO-d_6 and the chemical shifts are referenced to residual solvent signals. (^{1}H proton NMR signal: 2.50 ppm). 2D-NMR experiments were performed on a Bruker Avance-II-400 (400 MHz) equipped with an inverse multinuclear 5mm probe head and a z-gradient coil. Standard pulse sequences for gs-COSY, and gs-NOESY experiments were used. The refocusing delays for the inverse hetero-correlations were set to 3.45 and 62.5 ms, corresponding to $^1J_{C,H}$ = 145 Hz and $^nJ_{C,H}$ = 8 Hz, respectively.

For SEC measurements in DMF (containing 1 g/L of lithium bromide as an additive), an Agilent 1100 series was used as an integrated instrument, including a PSS Gral column ($10^4/10^4/10^2$ Å porosity) and RI detector. Calibration was achieved with poly(ethylene glycol) standards provided by Polymer Standards Service (PSS)/Germany. Differential scanning calorimetry (DSC) measurements were carried out on a Perkin-Elmer 7 Series Thermal Analysis System with auto sampler in the temperature range of -40 to 230 °C at a heating rate of 20 K/min. The melting points of indium (T_m=156.6 °C) and Millipore water (T_m = 0°C) were used for calibration.

Reagents

Diglyme (99%) and glycidol (Sigma Aldrich) were purified by vacuum distillation over CaH$_2$ directly prior to use. Tetrahydrofuran (THF) was refluxed with sodium/benzophenone before distillation. Glycolide was purchased from Purac®/Gorinchem (Netherlands) and used as received. Tin(II) 2-ethyl hexanoate (Sn(oct)$_2$, 97% was obtained from Acros and used as received.

The synthesis of **hb-PG** was conducted as described in previous publications, using the slow monomer addition technique.[21, 25, 26]

"Grafting from" polymerization of glycolide with hyperbranched polyglycerol-polyol as a macroinitiator. In a typical experiment, exemplified for the synthesis of star-block copolymers hb-PG$_{38}$-b-GA$_6$ 0.530 g hb-PG$_{38}$ (0.181 mmol/7.33 mmol of primary and secondary hydroxyl groups, according to equation 1) were placed in a flask immersed in an

oil bath at 120 °C and evacuated for at least 20 minutes. 2.55 g (22.0 mmol) of glycolide were charged to the flask, which was re-immersed into the oil bath. 75 ml of a 10% solution of Sn(Oct)$_2$ (= 0.022 mmol) were injected to the homogenous melt. The mixture was stirred vigorously under N$_2$ atmosphere for 24 h. After cooling down, the mixture was dissolved in hexafluoroisopropanol, and precipitated in excess diethyl ether. The precipitation/purification process was executed twice to yield pure polymer. The product was isolated by filtration and dried in vacuum at room temperature for 24 h to yield a white powder in all cases, except for the copolymer with an average targeted GA amount of 2 units per arm (P(G$_{38}$GA$_2$)), which gave a viscous, non transparent, white oil.

Acknowledgement

References

[1] Sanda, F.; Sanada, H.; Shibasaki, Y.; Endo, T. *Macromolecules* **2002**; 35:680-683.

[2] Li, Y.; Kissel, Th**.;** *Polymer;* **1998***; 39;* 4421-4427.

[3] Sekine, S.; Yamauchi, K.; Aoki, A.; Asakura, T.; *Polymer* **2009**, *50*, 6083–6090.

[4] Lu, Ch.; Liu, L.; Guo, Sh.-R.; Zhang, Y.; Li, Z., Gu; J.; *European Polymer Journal* **2007**; 43, 1857–1865.

[5] Buwalda, S.J.; Dijkstra, P.J:; Calucci, L.; Forte, C.; Feijen; J. *Biomacromolecules* **2010,** *11,* 224–232.

[6] Burgath, A.; Sunder, A.; Neuner, I.; Mülhaupt, R.; Frey, H. *Macromol. Chem. Phys.* **2000**, *201*, 792-797.

[7] Wolf, F. K., Frey, H *Macromolecules* **2009**, *42*, 9443-9456.

[8] *Joziasse, C.A.P.; Grablowitz, H.; Pennings, A. J. Macromol. Chem. Phys.* **2000**; *201***,** 107–112.

[9] Satoh, T. *Soft Matter* **2009**, *5*, 1972–1982.

[10] Jones, M.-Ch.; Gao, H.; Leroux, J.-Ch; Journal of Controlled Release **2008**, *132,* 208–215.

[11] Lemmouchi, Y.; Perry, M. C.; Amass, A. J.; Chakraborty, K.; Schacht, E. *Journal of Polymer Science: Part A: Polymer Chemistry* **2007**, *45*, 3966–3974.

[12] Jie, P.; Venkatraman, S. S.; Min, F.; Freddy; B. Y. Ch.; Huat: G. L. *Journal of Controlled Release* **2005**, *110*, 20– 33.

[13] Lapienis, G. *Prog. Polym. Sci*. **2009**; 34; 852-892.

[14] Finne; A.; Albertsson A.-Ch. *Biomacromolecules* **2002,** *3*, 684-690.

[15] Tsuji, H.; Miyase, T.; Tezuka, Y.; Saha; S. K. *Biomacromolecules* **2005,** *6*, 244-254.

[16] Nagahama, K.; Shimizu, K; Ouchi, T.; Ohya, Y. *Reactive & Functional Polymers* **2009**; *69*, 891–897.

[17] Zhao, Y.; Shuai, X.; Chen, Ch.; Xi; F. *Chem. Mater.* **2003,** *15,* 2836-2843.

[18] Zhao, Y.; Shuai, X.; Chen, Ch.; Xi; F**;** *Macromolecules* **2004,** *37,* 8854-8862.

[19] Wolf, F. K.; Frey, H. *Macromolecules*, 2009, *42*, 9443–9456.

[20] Cao, P.-F.; Xiang, R.; Liu, X.-Y.; Zhang, Ch.-X.; Cheng, F., Chen, Y. *J. Polym. Sci.: Part A: Polym. Chem.* **2009**, *47*, 5184–5193.

[21] Sunder, A.; Hanselmann, R.; Frey, H.; Mülhaupt, R. *Macromolecules* **1999**, *32*, 4240–4246.

[22] Sunder, A.; Frey, H.; Mülhaupt, R. *Macromol. Symp.* **2000**, *153*, 187–196.

[23] Sunder, A.; Mülhaupt, R.; Haag, R.; Frey, H. *Adv. Mater.* **2000**, *12*, 235–239.

[24] Wilms, D.; Wurm, F.;Nieberle, J.; Böhm, P.; Kemmer-Jonas, U.; Frey, H. *Macromolecules* **2009**, *42*, 3230-3236.

[25] Wilms, D.; Stiriba, S.-E.; Frey, H. *Acc. Chem. Res.* **2010,** *43*, 129-141.

[26] Calderón, M.; Quadir, M. A.; Sharma, K. S.; Haag, R. *Adv. Mater.* **2010**, *22*, 190-218.

[27] Knischka, R.; Lutz, P.J.; Sunder, A.;Mülhaupt, R.; Frey, H.; *Macromolecules* **2000,** *33,* 315-320

[28] Frey, H. and Haag, R. *Rev. Mol. Biotechnol*. **2002**, 90, 257.

[29] Shen, Y.; Kuang, M.; Shen; Zh.; Nieberle, J.; Duan, H.; Frey, H. *Angew. Chem. Int. Ed*. **2008**, *47*, 2227 –2230.

[30] Sunder, A.; Krämer, M.; Hanselmann, R.; Mülhaupt, R.; Frey, H. *Angew. Chem., Int. Ed*., **1999**, 38, 3552.

[31] Slagt, M. Q.; Stiriba, S.-E.; Gebbink, R.J.M; Kautz, H.; Frey, H. van Koten, G. *Macromolecules* **2002**, 35, 5734.

[32] Stiriba, S.-E.; Kautz, H.; Frey, H. *J. Am. Chem. Soc.* **2002**, *124*, 9698.

[33] Burakowska, E.; Quinn, J. R.; Zimmerman, S.C.; Haag, R. *J. Am. Chem. Soc.* **2009**, *131*, 10574–10580.

[34] Gottschalk, C.; Wolf, F.; Frey, H: *Macromol. Chem. Phys*. **2007**, *208*, 1657–1665.

[35] Chen, Y.; Shen, Z.; Barriau, E.; Kautz, H.; Frey, H. *Biomacromolecules* **2006,** *7*, 919-926.

[36] *Kasperczyk, J. Macromol. Chem. Phys.* **1999**, *200*, 903–910.

[37] Dali, S.; Lefebvre, H.; El Gharbi, R., Fradet, A. *e-polymers* **2007**, no.65

[38] Dali, S.; Lefebvre, H.; El Gharbi, R.; Fradet, A. *J. Appl. Polym. Sci: Part A: Polym. Chem.* **2006**, 44, 3025-3035.

[39] Baker, G.L.; Vogel, E. B; Smith, M. R; *Polymer Reviews* **2008**, *48*, 64–84.

2.3 Inimer-Promoted Synthesis of Branched and Hyperbranched Poly(lactide) Copolymers

Florian K. Wolf and Holger Frey

Abstract

A series of (hyper)branched poly(L-lactide)(PLLA) copolymers has been prepared by ring-opening multibranching copolymerization of L-lactide with a hydroxyl-functional (ABB') lactone inimer, 5HDON (5-hydroxymethyl-1,4-dioxane-2-on). Polymerization was conducted in bulk and solution and catalyzed either by stanneous-2-ethyl hexanoate ($Sn(Oct)_2$) or an organic base, 1,5,7-triazabicyclo[4.4.0]dec-5-ene (TBD). Precise structural characterization of the resulting branched copoly(ester) structures was accomplished by a combination of 2D NMR-techniques, relying on the comparison with model compounds. The 5HDON inimer was employed in 10% and 20% fractions and is incorporated either as a dendritic unit or as focal structure, but hardly in the linear mode. A detailed reaction mechanism was derived from kinetic investigation of the polymerization via NMR spectroscopy, preparative and analytical SEC and MALDI-TOF MS. The evolution and the extent of branching have been monitored and quantified. Both the degree of branching (DB= 2D(HDON)/2D(HDON)+L(lactide); DB=0.02-0.22) and the molecular weight (M_N=1,200-34,000 g/mol) could be tailored by variation of the monomer/inimer ratio. For $Sn(Oct)_2$ catalyzed polymerization approximately 50% of the inimer is transformed into dendritic units. In the case of TBD catalysis, the formation of dendritic units was supressed at room temperature, resulting in linear poly(lactide), functionalized with a lactone end group. The focal 5HDON-unit of the branched structures is susceptible to further functionalization, e.g., by reaction with primary hydroxyl groups, leading to branched poly(lactide) functionalized with precisely one single

dye label at the focal moiety. The formation of previously absent linear repeat units from the addition of terminal lactide units to focal 5HDON units was observed, when heating the polymers above T_g for prolonged times. This reaction was accompanied by a further increase in the molecular weight of the branched copoly(ester)s.

Keywords: Hyperbranched poly(ester), poly(lactide), ROMBP, organocatalysis, degree of branching, biodegradable poly(ester), inimer.

Introduction

Poly(L-lactide) (PLLA) is one of the most widely utilized degradable polymers in the field of biomedical materials. Excellent biocompatibility, versatile molding properties and high mechanical stability render it highly attractive for medical applications, such as drug delivery systems[1,2], tissue engineering[3,4] and surgical fixation devices[5,6]. Convenient accessibility from renewable resources and the well-understood synthesis contribute to the intense current interest for its use in commodity applications from both an environmental and an economic perspective. Tailoring of the materials properties of poly(lactide) (PLA) has become a major scientific task and has been targeted by a variety of different methods. Besides polymer blending, well established strategies have focused on the control of stereochemistry[7,8,910] and the molecular composition by copolymerization with other comonomers, e.g., ε-caprolactone[11,12] and glycolide[13]. Furthermore, innovative functional lactide derivatives have recently afforded materials with unusual characteristics.[14,15,16,17,18,19]

In recent years, variation of the architecture of PLA and aliphatic poly(ester)s in general has attracted increasing interest, particularly with respect to block-,[20] star-shaped[21,22] and branched macromolecules.[23,24,25] Hedrick and co-workers introduced the term "dendrimer like stars" for dendritic PLLA obtained by a combination of dendrimer- and star polymer synthesis, using repetitive ring-opening and coupling steps. In a "grafting from method", relying on a branched, multi-functional core, they generated multiple arms via the repetitive ring-opening polymerization (ROP) of cyclic ester monomers.[26,27] Likewise, the formation of branched PLLA structures was targeted by a combination of ring opening and condensation reactions in a one-pot procedure by the copolymerization of cyclic lactones and bis-hydroxy

acids[28,29]. This approach turned out to be suitable for the preparation of branched ε-caprolactone copolymers, however, it was limited in view of the extent of branching, when employing lactide as a comonomer, as recent, thorough studies by Cooper and Storey have shown. These authors demonstrated with detailed NMR-studies that the bishydroxy acid acted as an initiator, but further esterification of the carboxylic acid group with the secondary hydroxyl termini was inefficient.[30]

A major advantage of lactide-based poly(ester)s over other biocompatible polymers is the *in vivo* degradability into non-toxic components, which can be further adjusted for the desired medical application to control drug release rates and mechanical stability[31]. Since polymer degradation preferentially occurs in the amorphous regions of PLLA, an increase in the number of branching units (and chain ends) for branched PLAs enhances both enzymatic degradability and hydrolysis. It has also been shown that control of the degradation profile via the extent of branching is possible[32]. Since every branched unit introduces an additional end group in the polymer, branched poly(ester)s bear an increased number of hydroxyl termini, which increases the versatility of the system, particularly in view of the incorporation of biologically active ligands at the degradable poly(ester). The great versatility of a hydroxy-functional linear PLA obtained via copolymerization with a functional lactone for biomedical application has been demonstrated by Noga et al.[33].
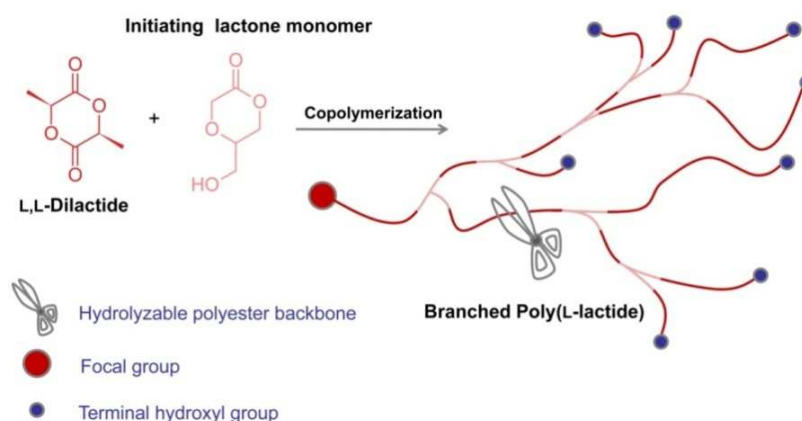
Scheme 4. Copolymerization of L-Lactide with HDON as lactone inimer, resulting in a branched poly(ester).

In recent studies, our group introduced enzymatic and metal-catalyzed copolymerizations, based on the combination of ROP and polycondensation of AB_2-monomers (bishydroxy

acids) for the synthesis of branched poly(ester)s. In order to avoid problems accruing from the polycondensation reaction with increasing bishydroxy acid content, mainly related to the removal of condensation products, we were looking for an appropriate substitute for this class of AB$_2$ comonomers. Lactones bearing an additional hydroxyl group that can act as initiator represent a promising class of cyclic "inimers". In analogy to the "self condensing vinyl polymerization" (SCVP) introduced by Fréchet et al.[34], polymerization of such inimers has been designated "self condensing cyclic ester polymerization by Trollsas et al.[35]. The SCVP has been a topic of intense theoretical and synthetic studies by Müller et. al.[36,37]. Despite these works, to date only few reports on the synthesis of branched poly(ester)s from functionalized lactones have been published. For instance, hyperbranched poly(ester)s have been obtained via polymerization of derivatives of ε-caprolactone with ABB' and AB$_2$B' structure, i.e., with additional hydroxyl groups at the lactone ring to form hyperbranched poly(ester)s in the late 1990ies.[35,38] In 2005, Zhuo et al. polymerized the six-membered lactone 6-hydroxymethyl-1,4-dioxane-2-one (6-HDON) to generate a hyperbranched, strictly alternating copoly(ester)-copolyether with a degree of branching of 0.4[39]. A variation of this monomer structure, namely the cyclic dimer of glycerol and glycolic acid 5-hydroxymethyl-1,4-dioxane-2-one (5HDON), was utilized by Rokicki et al. to generate strictly alternating hyperbranched poly(ether ester)s[40]. The same authors demonstrated that a cyclic trimethylene carbonate derivative with a pendant primary hydroxyl group can be polymerized to form hyperbranched polycarbonates via self condensing ring opening polymerization (SCROP)[41].

The concept of introducing branching points into established poly(ester) systems via copolymerization with hydroxy-functionalized lactones has found only little attention in the literature to date. Ouchi et al. utilized mevalonolactone as a branching inimer[13]. However, control over the degree of branching was difficult or even impossible and structural as well as mechanistic aspects were not investigated. In a recent work, Knauss et al. introduced branching by copolymerization of lactide with glycidol[42]. This elegant approach benefits from the commercial availability of the inimer glycidol.

In this paper we report on the ring-opening copolymerization of a reactive cyclic lactone with a pendant hydroxyl group (cyclic inimer) with lactide, targeting branched and

hyperbranched PLLA-copolymers, as shown in Scheme 4. We describe the combined AB/ABB'-type ring-opening multibranching copolymerization of L-lactide with 5HDON. We have examined the influence of different catalyst systems for the copolymerization of lactide with 5HDON and also studied the polymerization kinetics via 1D- and 2D-NMR techniques and SEC. Furthermore, we have studied the ROMBP copolymerization of lactide with 5HDON, using organo-base polymerization with 1,5,7-triazabicyclo[4.4.0]dec-5-ene (TBD)[43] in solution. We will also demonstrate that selective focal functionalization of the hyperbranched copoly(ester)s is possible, which paves the way for macromolecular architectures with hyperbranched PLLA blocks.

Results and Discussion

A. Copolymerization, detailed NMR-characterization and branching mechanism. The polymerization of lactide with Sn(Oct)$_2$ is generally described as a living coordination – insertion mechanism, with ring opening of the lactide resulting in the addition of two lactic acid units to the growing polymer chain end. Sn(Oct)$_2$ and TBD do not catalyze the polymerization of lactones without the presence of an initiator – generally amines or hydroxyl groups of primary or secondary alcohols[44]. This prerequisite permits to adjust the molecular weight of the polymer via the ratio of hydroxyl-functional initiator and also leads to selective functionalization of the polymer chain end. The synthesis of (hyper)branched PLA via copolymerization requires a cyclic lactone bearing additional reactive hydroxyl functionality, a cyclic "inimer", which can contribute to the polymer growth via two different reactions: it can participate in chain growth and initiation reactions. This synthetic approach allows the generation of a branched structure via a one-pot approach. The desired comonomer for the ROMBP of lactide has to fulfill the following requirements: (i) sufficient reactivity toward a standard acetylation-catalyst established for the synthesis of PLLA; (ii) good solubility in the lactide melt or the solvents used; (iii) a reasonable balance between initiation potential of the pendant hydroxyl groups and the reactivity of the lactone ring, which is essential for the generation of branching points; (iv) no release of condensation byproducts that would limit conversion and molecular weight.

5HDON (5-Hydroxymethyl-1,4-dioxane-2-one) is a promising comonomer candidate with respect to these requirements. High molecular weights are accessible by homopolymerization via Sn(Oct)$_2$ or DBU catalysis, as reported in literature[40]. Additionally, the synthesis of 5HDON is more feasible than for other reported inimers based on ε-caprolactone derivatives. Starting from 1,3-benzylidene-glycerol, the preparation of 5HDON can be readily accomplished in a three-pot synthesis. First developed by Broggini and Zechi[45] and modified by Rokicki et. al.[40], it relies on an acid based lactonization from the oligomeric precursor. Further optimization affords a total 5HDON yield of 79%. A problematic issue is the auto-polymerization tendency of the oily 5HDON upon storage at room temperature in bulk.

The copolymer samples prepared will be designated according to the following code in the ensuing text: PLLH XX = Poly((L-lactide)-co-(5HDON)) with a content of XX mole lactide (and thus 100-XX mole% 5HDON).

The bulk polymerization of lactide at elevated temperature and in the presence of an alcohol and Sn(Oct)$_2$ proceeds fast to high monomer conversion. The copolymerization of L-lactide and 5HDON was either carried out in bulk at 130°C with 0.1 mole% of Sn(Oct)$_2$ or in dichloromethane solution with 0.5 mol% of TBD as a catalyst. In the first part of this study, the comonomer ratio was set to 80% L-lactide and 20% 5HDON for basic structural and mechanistic studies. In the final part of this paper we summarize our results concerning copolymer composition and their impact on copolymer properties, varying the amount of branching inimer.
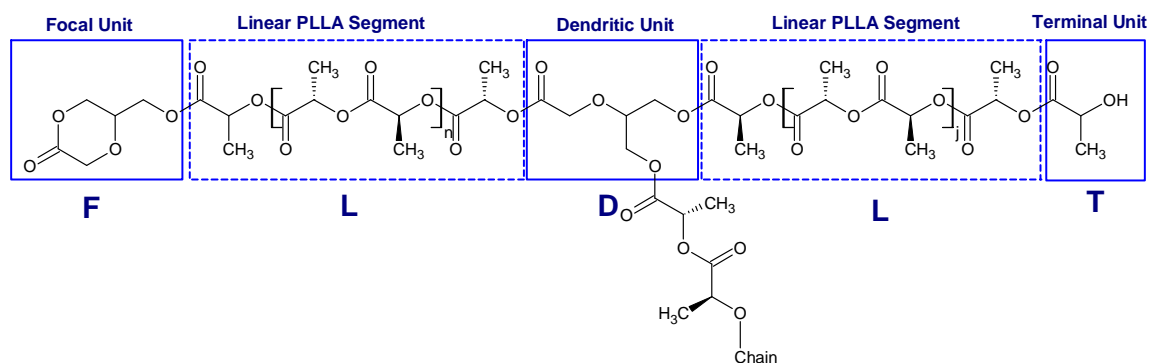
Figure 50. Major structural elements present in the branched copolymers of lactide and 5HDON

Structural characterization. Detailed NMR-spectroscopic analysis is crucial to elucidate and quantify the extent of branching in the copolymers. This involves synthesis and evaluation of model compounds mimicking the structural characteristics of the incorporated branching agent 5HDON. Due to the complexity of the ^{13}C- and ^{1}H-NMR spectra obtained for the copolymers of lactide and 5HDON, additional 2D-NMR experiments were conducted to gain further information on details of the polymer structure, which will be summarized in the following. As a consequence of this approach we were able to precisely determine the extent of branching for all copolymers, in contrast to many studies in the field of hyperbranched poly(ester)s. The conversion of lactide can be readily determined via standard ^{1}H-NMR spectroscopy in $CDCl_3$ by integration of the methyl protons of the lactide monomer and the polymer repeat units, respectively, which are sufficiently distinguishable. DMSO-d_6 was chosen as a solvent for the NMR experiments for the following reasons: It provides good spectral resolution for poly(lactide) and has already been successfully applied in the systematic investigation of poly- and oligolactides[46] and for hyperbranched poly(5HDON) [40].

Figure 51. Possible lactide and 5HDON repeat units present in the branched copolymers and the corresponding model compounds. (Respective chemical shifts are tabulated in the Supporting Information).

The first step toward identification of branching points in the PLA copolymers is the comparison of characteristic chemical shifts for model compounds resembling the structure

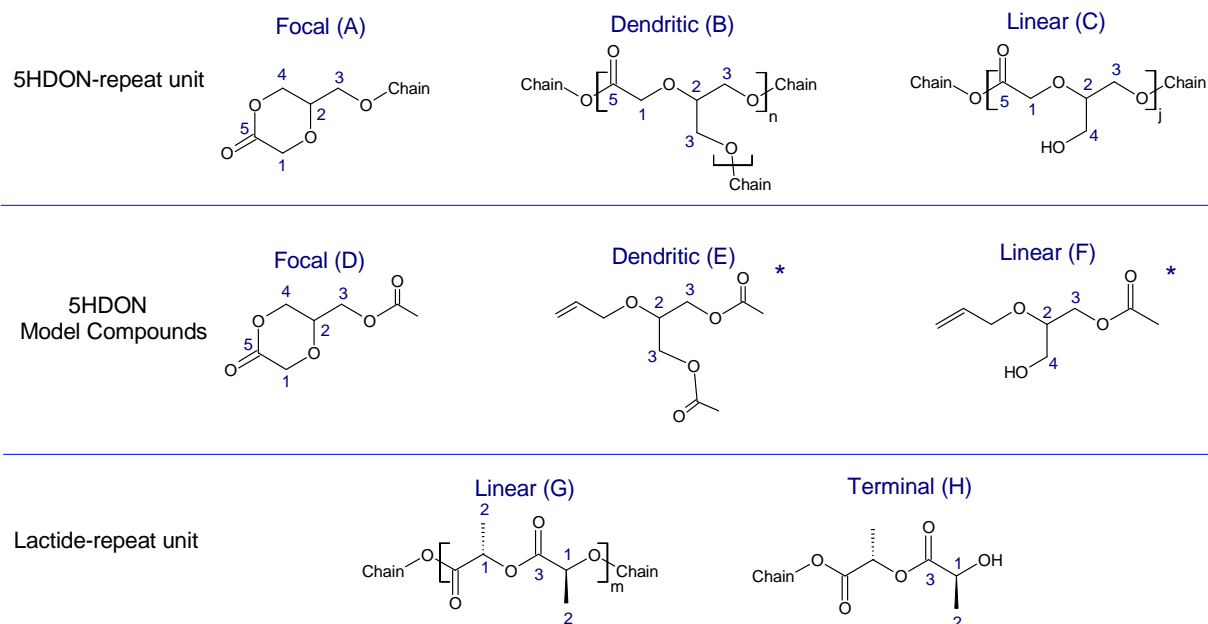of the branching units. Figure 50 shows the possible repeat units in the branched copoly(ester). The analytical pathway toward assignment of the complex NMR spectra is illustrated for one sample with high 5HDON content (20 mol%), sample PLLH 80. Although pronounced signal overlap complicates the analysis of the ^{1}H-NMR spectra, it is possible to obtain quantitative information regarding the number of end groups, the degree of branching (DB) and molecular weight. The accuracy of the implemented structure-to-signal assignment can be substantiated by a combination of ^{13}C-NMR, Hetero Nuclear Single Quantum Correlation (HSQC) and ^{1}H,^{1}H-COSY experiments. Distinct ^{13}C NMR chemical shifts of the relevant model compounds provide a reliable, but on its own insufficient base for a precise signal to structure assignment. Subsequent phase sensitive ^{1}H, ^{13}C HSQC spectroscopy allowed the fundamental transfer of structural information obtained from the model compounds to the readily available 1D ^{1}H-NMR spectra. Monomer consumption and formation of dendritic units in the course of the polymerization represent important kinetic parameters that have also been evaluated.

Model Compounds: There are four different modes of incorporation of 5HDON into the polymer backbone, as shown in Figure 51. Besides the dendritic unit (D), the difunctional character of 5HDON may lead to its transformation into focal (F), linear (L) or terminal (T) units. The most likely similar chemical shifts of these different structural elements in ^{1}H-NMR spectra inevitably complicate the quantitative characterization. Linear (L), terminal (T) and dendritic (D) units were simulated by structurally analogous glycerol 2-vinyl ethers with different degrees of acetylation, as shown by Rokicki et al.[40]. Standard decoupled ^{13}C -NMR spectroscopy results in well distinguishable signals, distinct for the direct chemical environment of the respective carbon. Particularly the methine-carbons of the linear (78.21 ppm) and branching (75.00 ppm) 5HDON units were of immediate interest, since they are clearly distinguishable from the lactide-derived methine-C signals.[46] The respective polymeric counterparts were also identified in the polymers. Furthermore, to complete the set of model compounds for the possible repeat units we prepared acetylated 5HDON in order to mimic the characteristics of a possible focal unit (Figure 52).
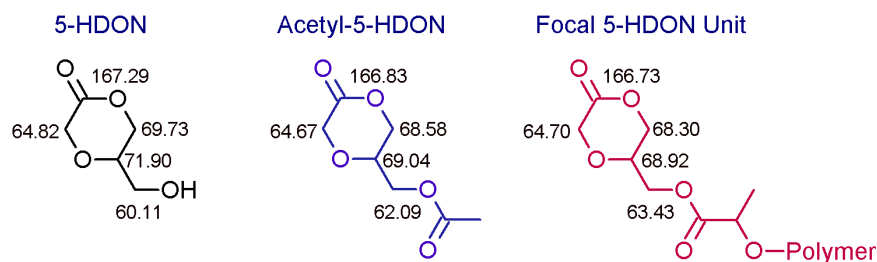
Figure 52: ^{13}C NMR hemical shifts of 5HDON, acetylated 5HDON and the focal unit, as present in branched PLLH (δ in ppm; solvent: DMSO, 400MHz).

All further clear correlations between model compounds and the polymer signals are summarized in Table 1 (Exp. Part). The ^{1}H-NMR spectrum of acetylated 5HDON is of particular interest, since it includes the characteristics of the strained lactone ring, which has significant influence on the proton-proton NMR coupling.

2D-NMR Spectroscopy: Despite the abovementioned advantages of conventional ^{13}C-NMR spectroscopy, reliable quantification of the sample composition is difficult on the basis of this method. Therefore we aimed at revealing as much information from conventional ^{1}H-NMR spectra as possible. ^{13}C, ^{1}H correlation spectroscopy has proven to be a powerful method for transferring information obtained from the examined model compounds to 1D ^{1}H-NMR spectra. The following paragraph focuses on a small area with chemical shifts in the range of 55.0 to 80.0 (^{13}C-NMR) and 3.0 to 4.6 ppm (^{1}H). These signals are related to all 5HDON repeat units of different topology and to terminal lactide units. After polymerization, 5HDON is found to be incorporated either as focal (A) or dendritic unit (B). Interestingly, the linear repeat unit C is nearly negligible (approx. 1%). Its ^{13}C/^{1}H-cross peaks are not visible in Figure 53-A, which shows the HSQC spectrum of PLLH 80 obtained from polymerization in bulk. After prolonged storage at room temperature in the NMR solvent DMSO-d$_6$ (without prior removal of the Sn-catalyst) the amount of linear units started to increase significantly, while the rest of the spectrum remained unchanged (Figure 53-B).

In the spectra given in Fig. 53 the cross peak B2 represents the methine group of the branching 5HDON unit. Cross peaks A1 to A4 can be attributed to the focal 5HDON unit. ^{13}C NMR shifts are in very good agreement with the respective values obtained from the model compound. Furthermore, the proton coupling pattern of the focal unit revealed in the two-dimensional plane is characteristic for the six-membered lactone ring of 5DHON. Its α-

methylene group shows 4 distinct (A1) peaks, also characteristic for 5HDON and acetyl 5HDON. Intriguingly, the sample, stored for 60 days at room temperature (bottom) also shows the presence of linear repeat units of 5HDON. (C1, C2, C4).
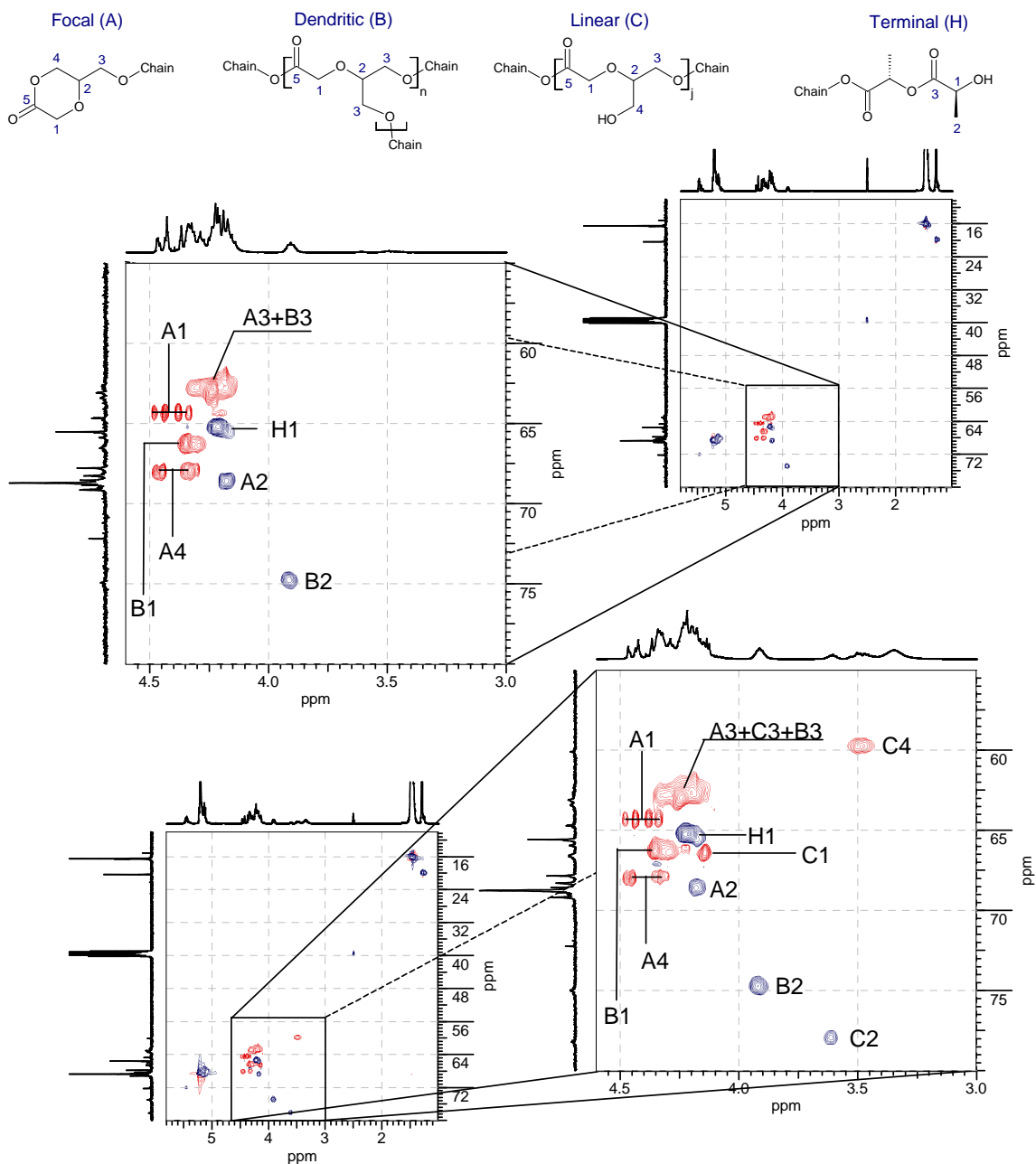

Figure 53: HSQC spectra of PLLH 80 from polymerization in bulk, catalyzed with Sn(Oct)$_2$. Phase information is given by coloration of cross peaks (red=methylene, blue=methyl, methine). Top: spectrum recorded immediately after the reaction. Bottom: after 60 days of storage at room temperature. Denotation of the cross peaks follows the code defined in Figure 51.

In order to verify the accuracy of the signal assignment presented in Fig. 4, we used ^{1}H,^{1}H-correlation spectroscopy. The assignment of linear and dendritic 5HDON units is unambiguous: While B2 revealed only one cross peak to B3, as it is expected for the symmetrically substituted branching unit, C2 couples to C3 and C4, the latter representing the non-functionalized hydroxymethyl group of the linear repeat unit. (Further NMR data can be found in the Supporting Information).

In summary, a comprehensive structural evaluation of a hyperbranched poly(lactide) copolymer obtained with 20% HDON in the monomer feed (PLLH 80) has been conducted by applying 2D-NMR in combination with the synthesis and characterization of model compounds. Quantification of crucial structural parameters, like the degree of branching DB= 2D(HDON)/2D(HDON)+L(lactide)[47,48], has been accomplished by referring to conveniently accessible ^{1}H-NMR spectra (in DMSO-d$_6$), resulting in a DB of 0.21 for the sample PLLH 80. This approach is possible, since the dendritic unit can be quantified by integration over B2. Further important quantities can be obtained directly from integration, or indirectly from superimposed ^{1}H-NMR signals.

Kinetic analysis of the polymerization. To obtain insight into details of the copolymerization process, focusing on the formation of dendritic units in the course of the polymerization, time-dependent NMR and SEC measurements were carried out. In order to cover a large time frame and to obtain sufficient resolution for the early stages of the reaction, samples were collected in logarithmically increasing intervals (after 5, 10, 20, 40, 80, 160, 320, 540, 1140, 2260 and 6690 min) either from the melt or solution and quenched thermally by rapid cooling to at least -20°C. ^{1}H-NMR spectra, measured in CDCl$_3$, revealed that lactide consumption is rapid (cf. Figure 54). The first samples were collected 5 minutes after initiation of the polymerization. Already after this stage, no unreacted 5HDON monomer was detected in the polymerization mixture. Comparison with ^{13}C-spectra of the model compound acetyl-5HDON revealed that initiation of the lactide by the primary hydroxyl groups of 5HDON proceeded fast and quantitatively. After 5 minutes, 5HDON is either incorporated as focal unit or has already been transformed into a dendritic unit. Furthermore, conversion of the lactide monomer already exceeded 70% at this point (Figure 54).
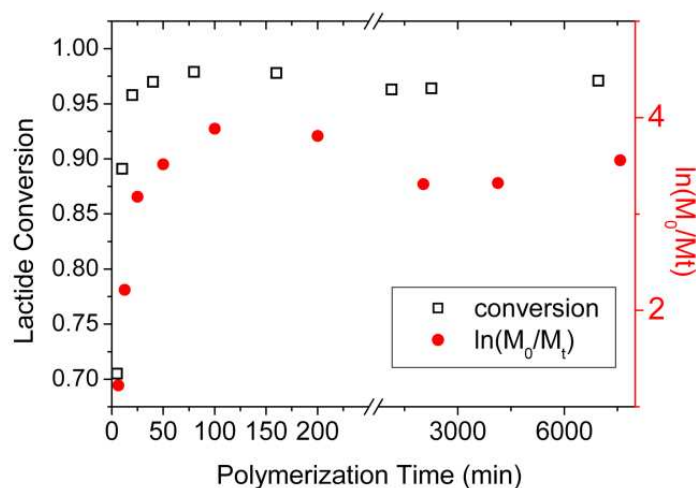
Figure 54: Time-dependent ^{1}H-NMR measurements of Sn(Oct)$_2$-catalyzed copolymerization of the 80/20 lactide/5HDON mixture (PLLH 80) in bulk (400 MHZ, CDCl$_3$). (5, 10, 20, 40, 80, 160, 320, 540, 1140, 2260 and 6690 min) The lactide concentration reaches equilibrium after a polymerization time of approximately 80 to 160 minutes.

Based on the detailed NMR-assignment one can monitor the polymerization via ^{1}H-NMR spectroscopy in DMSO-d$_6$ (Figure 55). The fraction of dendritic 5HDON units eventually approaches 51 % of the total amount of 5HDON incorporated, which corresponds to a total degree of branching (DB) of 0.21. The major fraction of these units is formed in the early stages of the polymerization, while free lactide is still present in the reaction mixture. The equilibrium distribution of 5HDON in the polymer structure can be given with 51% of dendritic, 46% of focal and approximately 3% of linear repeat units (Figure 56).
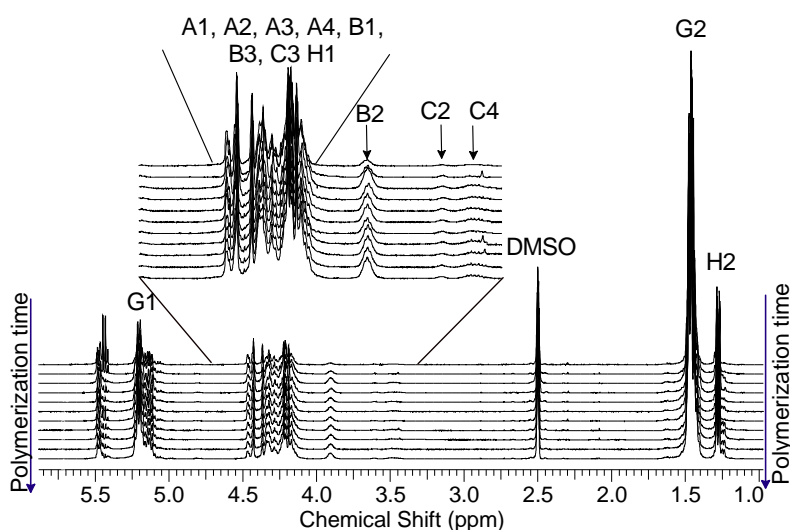
Figure 55: Time dependent ^{1}H NMR measurements of Sn(Oct)$_2$ catalyzed polymerization in bulk [II] in DMSO$_6$. Evolution of branching is visible by an increase in signal intensity of the dendritic unit (B2).

144
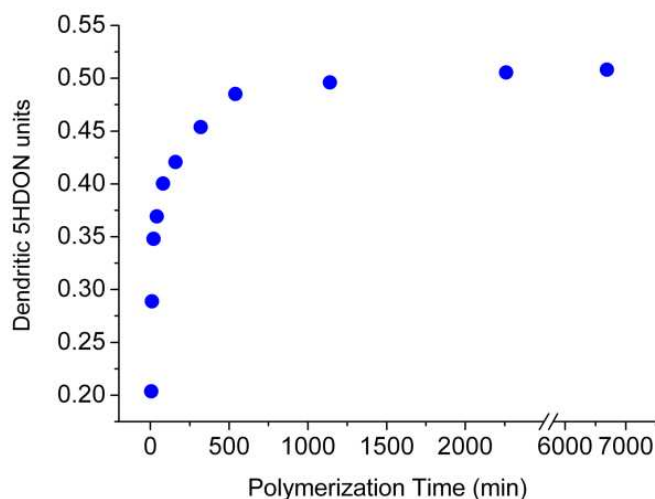
Figure 56: Development of dendritic units in the course of the polymerization. (Percentage of dendritic units with respect to the total amount of 5HDON)

Branching Mechanism. Based on the results of the detailed NMR study, a mechanistic hypothesis can be put forward that relies on the considerable difference of the reactivity of primary and secondary hydroxyl groups in the system. Figure 55 shows the lactide monomer consumption and the formation of dendritic units in the course of the polymerization. A comparison of these plots illustrates the decrease in the formation of dendritic units, as the lactide monomer approaches its equilibrium concentration (1 to 2,5 %)[49,50]. Hence, the ratio dendritic/focal 5HDON-units increases very rapidly, until the majority of lactide is consumed. Combining all observations, a reaction scheme can be derived (Scheme 2) that illustrates the mechanism of branching for the ROMBP copolymerization of lactide with the inimer 5HDON. For reasons of clarity, we have omitted details of the coordination-insertion mechanism promoted by Sn(Oct)$_2$, which can be found elsewhere[51,52,53,54,55]. The reversible aspect of lactone polymerization at elevated temperatures is taken into special account in the proposed mechanism. The primary nature of the hydroxyl group of 5HDON explains its high tendency for initiation (Scheme 5 [**1**]) in the early stages of the polymerization, as demonstrated by the NMR spectra recorded already 5 minutes after initiation. At this point the majority of the 5HDON units have been converted into focal units, i.e., initiation sites. Hence, due to the chain growth of lactide only secondary hydroxyl groups are found (Scheme 5 [**2**]) in this stage.

In the second stage of the polymerization, ring-opening of focal 5HDON groups by growing primary hydroxyl chain-ends occurs (Scheme 5 [**3A and 3B**]), and secondary hydroxyl groups are reconverted into primary ones, when HDON units are opened. If a sufficient amount of free monomer is present in the polymerization mixture, this primary hydroxyl group is quickly transformed into a dendritic unit by the addition of lactide (Scheme 5 [**4**]) at this stage. This hypothetic mechanism is supported by the observation that in the early stage of the polymerization (after 5 minutes) the lactide conversion already exceeds 65%, and no free 5HDON is present in the polymerization mixture, yet more than 2/3 of the branching points still have to be formed. This is a clear indication that the formation of branching points takes place by the reaction of terminal lactide units with focal 5HDON units in the presence of free, reactive lactide. This process is largely decelerated, when the concentration of free lactide drops. The rate-determing step in the coordination-insertion mechanism of the Sn-alkoxide species (Scheme 5 [3]) is the nucleophilic attack of an alkoxide, coordinated to the chain end on the carbonyl carbon of the monomer[55]. In this case, the formation of branching points is slowed down due to end group dilution and insufficient concentration of free lactide monomer. Therefore recyclization of the focal 5HDON unit and release of the terminal lactide group dominates in the case of low lactide concentrations, together with a simultaneous increase in melt viscosity. This context is the reason for the dramatic deceleration of the formation of branching points after the lactide monomer equilibrium concentration is reached. The higher reactivity of the primary over the secondary hydroxyl group also explains the low amount of linear units and the absence of terminal 5HDON units.

The fraction of terminal lactide units is in good agreement with the fraction of branching units according to the ^{1}H-NMR spectra measured in DMSO-d_6. Hence the amount of terminal lactide units is equal to the sum of dendritic and focal units ([T] = [D] + [F]). Since focal 5HDON units (51%) are the predominant species together with the dendritic groups (46%), the molecular weight can be controlled via the ratio of monomer to inimer, which may appear to be surprising at first glimpse. However, this is in no contradiction to the elevated molecular weights observed by Parzuchowski et al. for the homopolymerization of 5HDON to a hyperbranched poly(ester), since this system exclusively consists of one lactone type and solely primary hydroxyl groups. Ouchi and co-workers postulated that that the inimer mevalonolactone, employed for the copolymerization with lactide, acts as a latent comonomer that does not undergo initiation prior to ring opening of the lactone. However,

146

this is clearly not the case for the copolymerization with 5HDON, which is transformed quantitatively into a focal unit prior to its conversion into a dendritic unit, as it is obvious from our kinetic measurements.
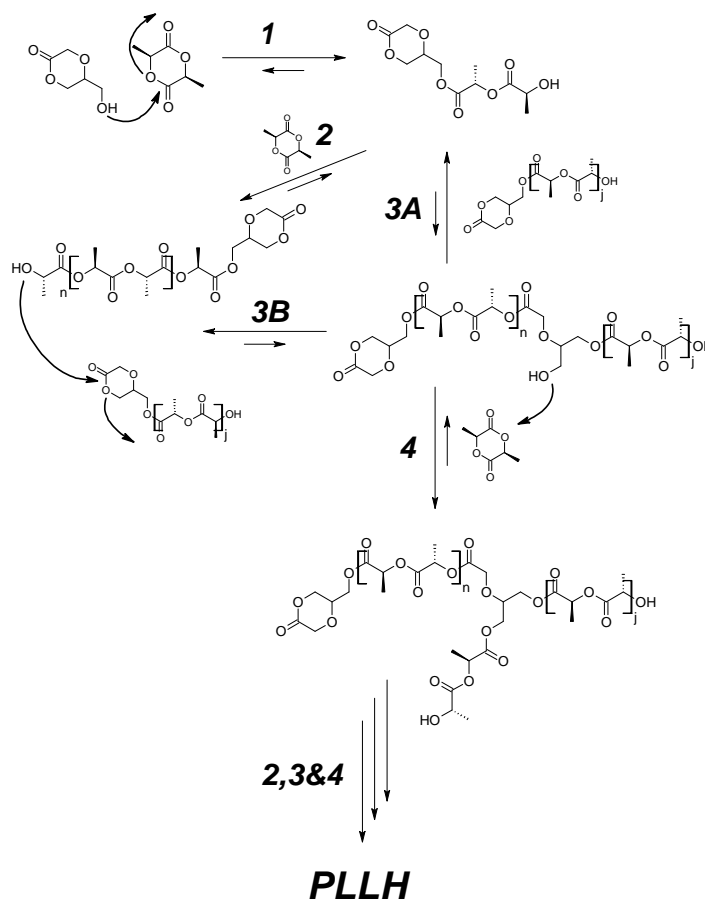
Scheme 5: Qualitative reaction scheme for ROMBP (ring-opening multibranching polymerization) of 5HDON with L-Lactide derived from kinetic measurements. 1 marks the fast initiation reaction of the primary hydroxyl group of 5HDON with L-lactide.

Alteration of the samples upon storage in DMSO solution. In Figure 53 we already addressed the formation of linear repeat units during prolonged standing of the sample PLLH 80 in DMSO-d_6 at room temperature. We assume that this rearrangement phenomenon is due to the simple transesterification reaction of hydroxyl group at a polymer chain endunit at a focal 5HDON lactone unit, resulting in linear 5HDON. This explanation can be confirmed by ^{1}H-NMR, validating the decrease of the amount of focal 5HDON groups. Furthermore, the addition reaction of two terminal groups, which only appears to be thermodynamically favored at room temperature, results in a shift of the molecular weight distribution toward

lower elution volumes and moreover to a more narrow PDI. As postulated before, regeneration of the focal cyclic 5HDON unit appears to be favored at high temperature in the absence of sufficient amounts of free lactide, while the formation of linear units only seems to be the stable form at room temperature (Scheme 5 [3A]). This is also in good agreement with the autopolymerization tendency of 5HDON stored at room temperature. The autocatalytic tendency of the inimer is explicable by the presence of high amounts of free hydroxyl groups in the sample. However, it has to be emphasized that all samples were stable in bulk and no formation of linear repeat units was observed during storage below (25°C), or above Tg (65°C).

B. Molecular weight characterization

SEC-measurements. Monitoring the polymerization process via Size Exclusion Chromatography (SEC) permitted to obtain further information regarding the polymerization, particularly with respect to the mechanistic hypothesis summarized in Scheme 5. SEC-MALLS (multi-angle laser light-scattering) characterization is not useful for these copolymers due to the poor scattering potential of the low molecular weight fractions in the rather polydisperse (PDI = 2.0 - 3.7) systems.

SEC shows that the molecular weight of the copolymer is significantly higher than expected for this initiator (inimer) to monomer ratio. This is equivalent to a rather large amount of branching units created from the focal inimer, resulting in high molecular weight. Nevertheless, the limited conversion of focal units into branching points (51%) means that adjusting the amount of 5HDON to lactide permits control over both the degree of branching *and* molecular weight. The SEC elugrams depicted in Figure 57 show a significant shift from a typical oligomer distribution obtained after several minutes to lower elution volumes in the early stages of the polymerization. Corresponding molecular weight data (Table 6) derived from calibration with polystyrene standards support the previously discussed NMR results. After 80 to 160 min, the polymerization is almost complete, as it is evident from the distribution mode of the polymer, an insignificant increase of M_N and monomer conversion (NMR). Interestingly, the increase of molecular weight is accompanied by an increase in PDI, which would be untypical for a linear chain growth of a controlled nature. Subsequently,

only a slight decrease of the oligomer fraction and a corresponding small increase of the intensity of the polymer mode are observed. A slight broadening of the molecular weight distribution is observed for extended reaction times.
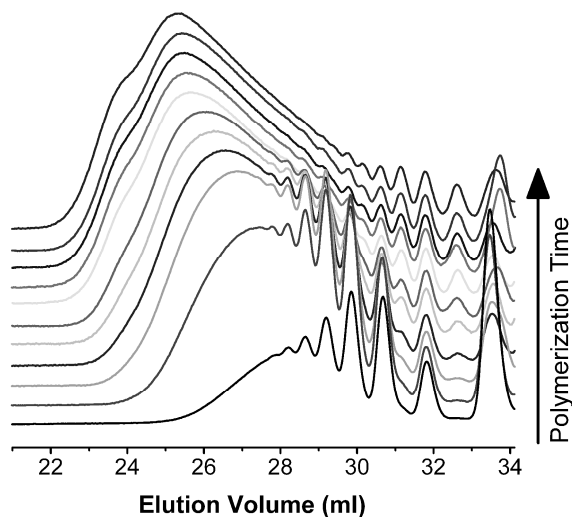
Figure 57: Evolution of the molecular weight distribution monitored by SEC (RI-detection, THF - Samples harvested and quenched after 5, 10, 20, 40, 80, 160, 320, 540, 1140, 2260 and 6690 min)

Table 6: Time-dependent development of molecular weight (M) and PDI (D) for PLLH 80.

Sample	T_P(min)[#]	M_N*	M_W*	M_W/M_N
1	5	470	920	1.98
2	10	720	1620	2.26
3	15	870	2100	2.43
4	20	960	2460	2.57
5	40	1010	2780	2.75
6	80	1090	3100	2.86
7	160	1130	3660	3.23
8	540	1190	3890	3.25
9	1140	1190	4060	3.43
10	2260	1180	4120	3.50
11	6690	1240	4620	3.73

(*SEC in THF, calibration with polystyrene standards; [#]T_P = polymerization time)

MALDI-ToF spectrometry. MALDI-ToF MS can provide valuable information regarding the incorporation of the branching inimer 5HDON into the polymer molecules formed. However,

it is well known that polydisperse samples are rather difficult to analyze, since the detection of low molar mass fractions is generally favored in terms of evaporation and ionization during the ToF- measurements (mass discrimination effect). Therefore MALDI ToF MS data are not representative for a polymer sample, when polydispersity exceeds a certain value (usually $M_w/M_n > 1.2$)[56]. In order to overcome this problem, the polymer samples were separated into fractions of narrow molecular weight distribution via preparative SEC in THF (Table 7). Figure 58 shows the MALDI-ToF spectrum of some of the separated fractions of the sample PLLH 80-6690. As it is exemplified here, incorporation of the comonomer can be observed over the entire mass range detected. The signals show a mass difference of 12 Da, which represents the mass difference of the repeating units (144 Da for lactide and 132 Da for 5HDON), evidencing incorporation of both comonomer units. Unfortunately, fractions 1 to 4, which exhibit the highest molecular weights could not be analyzed via MALDI-ToF. Fraction 5, depicted in Fig. 58, shows the presence of subdistributions for an increasing degree of branching. Each of the subdistributions is characterized by a different number of 5HDON branching units.

Table 7: SEC Data for the isolated fractions of sample PLLH 80.

fraction	Mn*	Mw*	Mw/Mn
8	220	370	1.70
7	760	1120	1.47
6	1930	2460	1.28
5	3900	4580	1.17
4	6740	7520	1.11
3	10900	11800	1.08
2	16400	17300	1.05
1	23300	24700	1.06

(*SEC in THF, calibration with polystyrene standards)

Absolute masses were calculated from the MALDI-ToF spectra for the potassium adduct of the copolymer. It is remarkable that the associated signals of the main distribution show an increment of 72 Da, which represents half of the mass of a lactide unit. This mass difference is generally observed for the polymerization of lactide under $Sn(Oct)_2$-catalysis at

elevated polymerization temperatures and prolonged reaction times (>1 h, using the described reaction conditions). This observation can be explained by Sn(Oct)$_2$ promoted transesterification-reactions in the later stages of the polymerization[57]. The most valuable information obtainable from the MALDI-ToF MS spectra is the direct correlation between the mass increase of the polymer and an increase in the number of 5HDON units, which is equal to the number of branching points.

Cyclization is a non negligible issue for branched polymers and poly(ester)s in particular[58,59]. In our case it cannot be detected by MALDI-TOF MS spectrometry, since the cyclic and non-cyclic form of the copolymer do not differ in mass (no release of a condensation product). However, according to the hypothetical mechanism for the ROMBP copolymerization (Scheme 5), a very low extent of focal cyclization is expected.
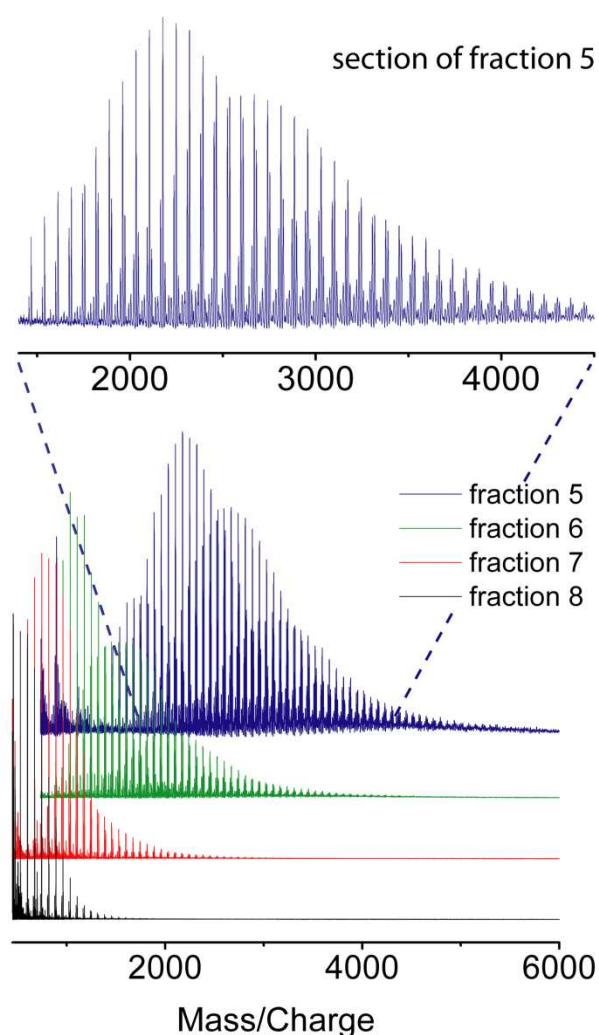
Figure 58: MALDI ToF mass spectra of SEC-separated fractions of thermally quenched sample PLLH 80 (6690 min). Fractions 5 to 8 were collected using a preparative SEC separation column.

C. Organo-base catalyzed solution copolymerization. As an extension of the Sn(Oct)$_2$ catalyzed bulk polymerization we also studied the use of TBD (1,5,7-triazabicyclo[4.4.0]dec-5-ene) for the ROMBP copolymerization with 5HDON. TBD is a powerful organo-base,[60] which is even suitable as an isotope exchange catalyst[61], but also effective for the polymerization of moderately reactive monomers like δ-valerolactone. Compared to other amidine bases like DBU, TBD shows a higher catalytic activity for poly(ester) synthesis, i.e., the lactide polymerization proceeds rapidly to high conversion at polymerization times < 1min[62]. Fig 10 shows the ^{1}H-NMR spectra of poly(lactide-*co*-HDON) copolymer samples prepared by TBD catalysis at different temperatures.
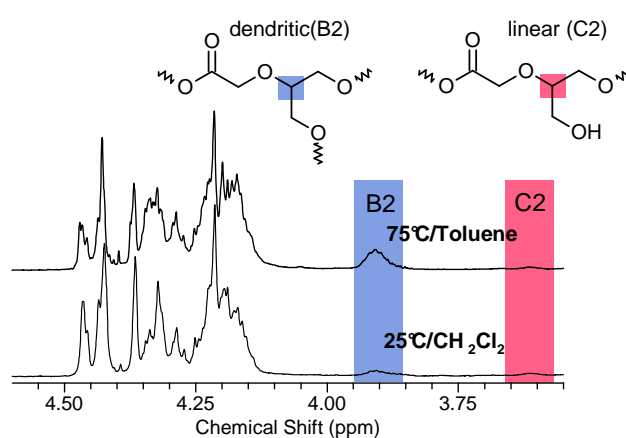
Figure 59: ^{1}H-NMR spectrum of poly(lactide-co-HDON) copolymer prepared by TBD-catalysis.

Figure 60: SEC characterization of a branched and predominantly linear copolymer of 5HDON and lactide after polymerization in solution for 60 minutes with TBD catalysis and quenching of the reaction with benzoic acid; top: synthesis at 75°C; bottom: synthesis at 25°C.

Table 8: Molecular weight data for samples obtained by TBD catalysis.

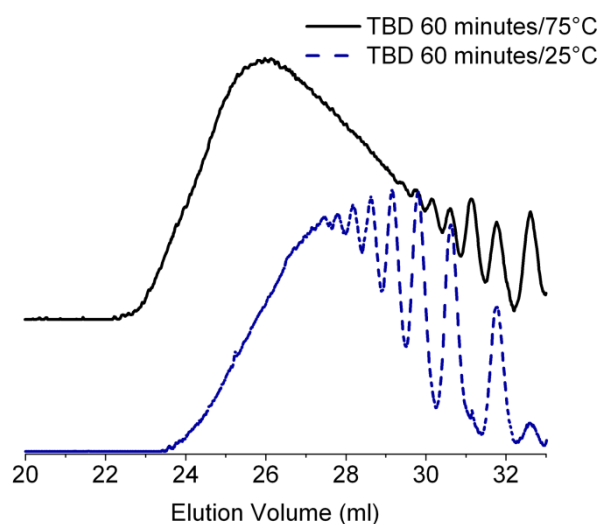| Sample	Reaction Time (min)	DB	$M_N$theo.	M_N*	M_W*	M_W / M_N
PLLH 80/TBD 25°C	60	0.01	708	690	1240	1.80
PLLH 80/TBD 75°C	60	0.22	708	1660	4100	2.47
PLLH 80/Sn(Oct)₂ 130°C	*80*	*0.21*	*708*	*1090*	*3100*	*2.86*

The synthesis of 80/20 latide/HDON copolymers with TBD-catalyst was carried out for 60 minutes. Characterization of the branched structure was accomplished in a similar manner as already described for the Sn(Oct)$_2$-catalyzed polymerizations. Fig. 60 shows the SEC-diagram for a typical copolymer sample (80/20 lactide/HDON), prepared by TBD catalysis. A strong dependence of the degree of branching DB on the reaction conditions was observed (cf. Fig. 59). The formation of dendritic units clearly depended on the polymerization temperature. At room temperature in CH$_2$Cl$_2$, 5HDON is mainly incorporated as end group (i.e., focal unit) in otherwise linear PLLA oligomers. This is obvious from the near (DB = 0.01) absence of signals of the branching units B2 in Figure 60 (bottom). The observed molecular weight matches theoretical expectation quite well, if we consider the inimer 5HDON as an initiator only (Table 8). Hence, the fraction of focal HDON units corresponds directly to the number of hydroxyl end groups. In pronounced contrast, an increase of the reaction temperature to 75°C and polymerization in toluene yielded a similar result as the melt polymerization with Sn(Oct)$_2$. NMR shows an extent of dendritic units of approx. 47% of the total fraction of 5HDON units. The amount of linear repeat units is again fairly low and corresponds to approx. 2% of the total 5HDON fraction incorporated. SEC revealed a significantly higher molecular weight, i.e., more than twice the theoretical value (Table 8). The mechanistic sequence, as depicted for the polymerization under Sn(Oct)$_2$ catalysis is believed to be valid also in this case. Control-measurements after a polymerization times of 24 and 72 h did not reveal significant changes in composition (NMR) or in shape and position of the SEC-elugram, compared to the aliquots extracted from the reaction solution and quenched by addition of benzoic acid after 60 min of polymerization time. This is also in good agreement with the previous findings that no significant chain growth occurs after full consumption of the lactide monomer.

Interestingly the two SEC elugrams shown in Figure 60 significantly differ in position and shape. The distribution maximum for the branched sample is shifted toward higher molar masses. While the linear sample shows distinguable distribution modes for the growing linear oligomers, the sample with large fraction of dendritic 5HDON units shows a considerably smoother gradient. This may be due to the overlap of subdistributions differing in the extent of branching and hence their hydrodynamic properties. In this case, kinetic studies monitoring the consumption of lactide were not possible, since the polymerization conversion of lactide rapidly proceeds to completion on the scale of seconds for the TBD promoted polymerization (>99% after 2 minutes). We assume that the divergence in reactivity for ring-opening of 5HDON compared to lactide at different temperatures is due to the different extent of dendritic units formed. Lactide is one of the most reactive monomers for the TBD-promoted polymerization at room temperature and is clearly more reactive than other cylic lactones like ε-caprolactone and δ-valerolactone. The essential condition for the formation of branching points derived in Scheme 5 was the presence of free lactide monomer leading to ring opening of the (focal) 5HDON group. This condition is tantamount to the necessity of similar reactivity ratios for the two monomers, respectively, monomer and focal lactone group. The increase in reaction temperature most likely led to a decrease of the reactivity ratio of lactide and 5HDON. In summary, the organo-base catalyzed polymerization results in branched structures with considerable fractions of dendritic units at elevated temperature. Control over the formation of linear and branched structures is achieved by polymerization temperature and solvent.

Scheme 6: 9-fluorenemethanol functionalization of the focal unit.
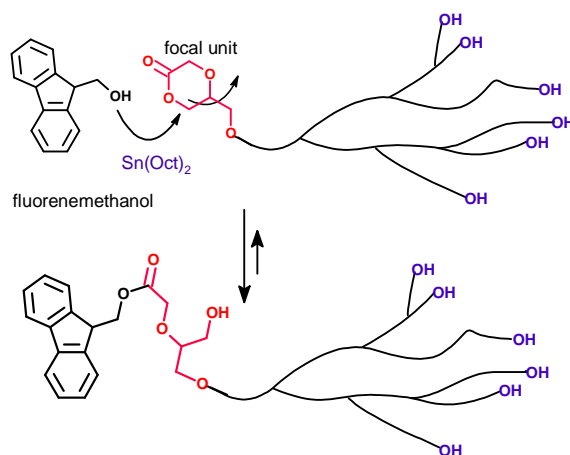
D. Selective functionalization of the focal unit.

Deliberate focal functionalization of hyperbranched structures represents an important target, since it permits to build up well-defined hyperbranched macromolecular architectures, such as block copolymers with hyperbranched block[63] or conjugate structures with biologically relevant moieties, e.g., peptides or proteins. As revealed by the previously discussed NMR-experiments, the focal unit of the polymers consists of an esterified 5HDON unit that represents a reactive cyclic lactone structure. The terminal units almost exclusively consist of secondary hydroxyl groups of the lactic acid monomer units. It was demonstrated for the melt and solution polymerization of 5HDON that terminal hydroxyl- and focal 5HDON units approach an equilibrium situation, significantly slowing down conversion and molecular weight growth. In order to investigate selective addressability of the focal 5HDON unit for polymer modification reactions, an excess of 9-fluorenemethanol was added to the thermally quenched copolymer samples, and the mixture was heated to 130°C (Scheme 3). The primary character of the added 9-fluorenemethanol is important in view of preferential reaction with the focal 5HDON unit. Furthermore, 9-fluorenemethanol was used in excess (twice the total 5HDON amount per sample).

Both SEC and MALDI-ToF MS analysis confirmed quantitative addition of 9-fluorenemethanol to the focal unit of the branched polymer samples, independent of the molecular weights of the materials. Since the branched poly(lactide) copolymer consists of a poly(ester)/ether backbone, no UV signal is detected in SEC measurements. This changes significantly with the fluorenemethanol-functionalization of the focal group. Figure 61 shows the SEC traces of sample PLLH 80 – 6690 before and after reaction with fluorenemethanol in the melt. While shape and molecular weight distribution of the retention signal remain unchanged, a strong UV-absorption trace appears for the fluorenemethanol-functionalized sample.
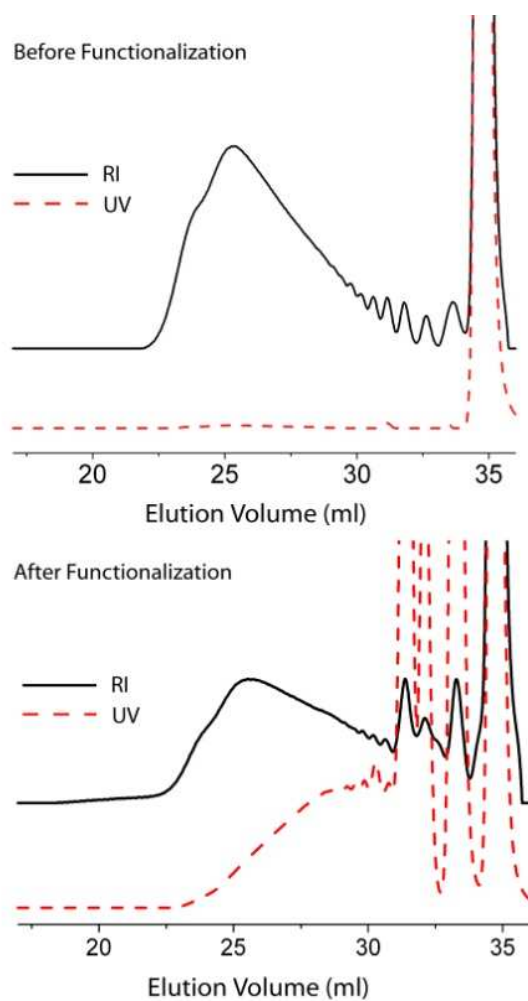
Figure 61: SEC (UV and RI traces) before (top) and after (bottom) reaction with 9-fluorenemethanol. The large peak at ~35 mL corresponds to the internal standard (toluene).
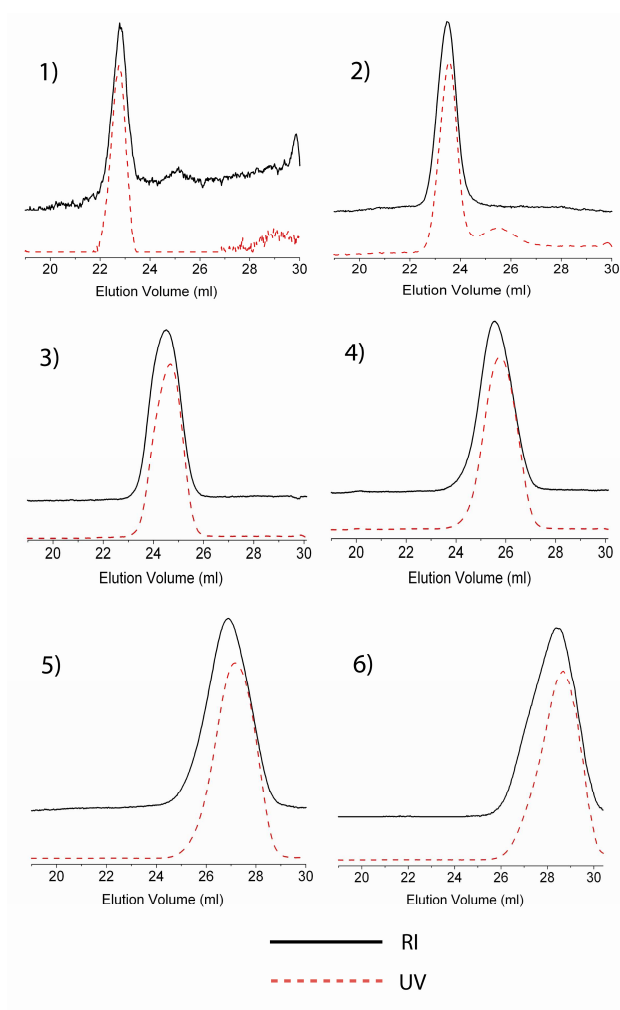
Figure 62: SEC traces of fluorenemethanol-functionalized hb-poly(lactide). The overlap of UV (dashed line) and RI signal supports the monofunctionalization over the entire mass range.

As it is obvious from Fig. 61, UV and RI signals stretch over the same range of the elution volume, but significantly differ in their shape. The UV-absorption increases with elution volume, indicating a higher amount of fluorenemethanol per mass fraction for the low molecular mass species than for the higher molecular weight fraction. This corresponds to the relative decrease of focal units that are accessible for fluorenemethanol in the higher molecular mass fractions. Since no changes in molar mass or weight distribution occurred, this supports controlled addition of fluorenemethanol, notably without random transesterification that would result in chain scission and significant broadening of the molecular weight distribution. In order to obtain additional confirmation for the successful modification of the focal group over the entire mass range, the fluorenemethanol-functionalized sample (PLLH 80) was also fractionated by preparative SEC, in analogy to the unmodified polymers. The RI and UV detector signal overlap of the fractions is obvious for all fractions of different molecular weight (Fig. 62).

157

Conclusive evidence on the well-defined focal functionalization of a hyperbranched polymer can only be obtained by mass spectrometry. Due to the lowered polydispersity of the fractions, characterization by MALDI-ToF MS up to a molecular weight of approximately 4000 g/mol was possible. The spectra obtained show exclusively the fluorenemethanol-functionalized species. Although MALDI-ToF MS is limited with regard to the quantitative analysis of synthetic polymers, the spectra recorded before and after reaction with 9-fluorenemethanol confirm mono-functionalization of each macromolecule at its focal group. Figure 63 shows two well resolved mass spectra of prep-SEC fractions of similar molecular weight, revealing addition of a single fluorenemethanol-unit per molecule over the observable molecular weight range.
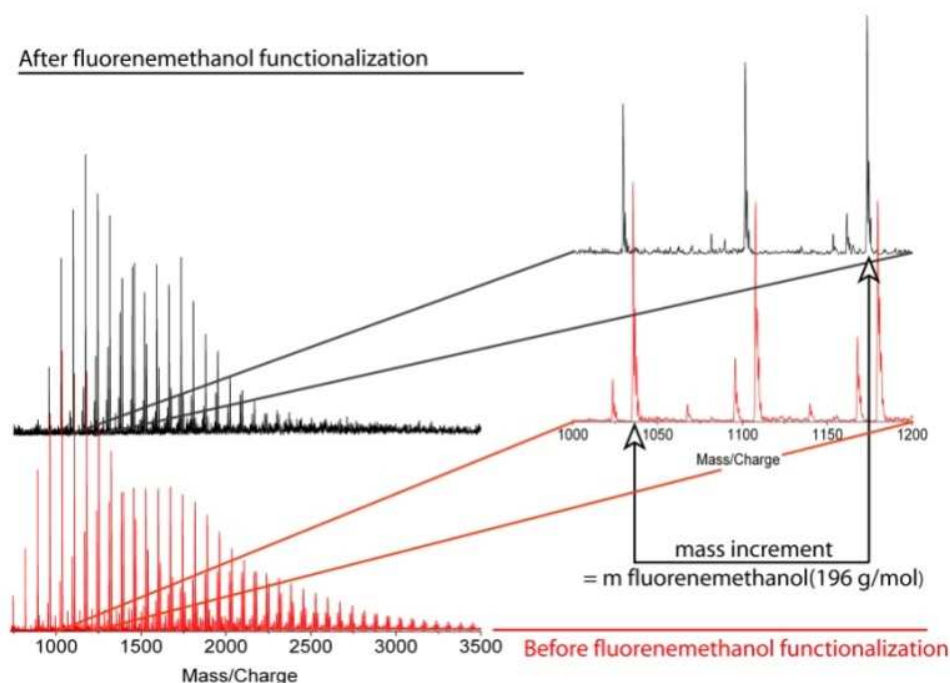
Figure 63: MALDI-TOF MS spectra of preparative SEC fractions of comparable molecular weight before (bottom) and after (top) reacting the focal unit with fluorenemethanol.

In summary we have demonstrated a facile pathway for the functionalization of *hb*PLA at the focal group, avoiding degradation caused by transesterification reactions of the monofunctional component with the polymer backbone. This renders the materials valuable for the modification of hydroxy-functional linear polymers and surfaces, since the polymer properties can be tailored via the comonomer ratio prior to functionalization. This is particularly valuable in the case of an unknown amount of functional groups.

E. Long chain branched Poly(lactide). Based on our mechanistic study on the ROMBP of lactide with the 5HDON inimer, long chain branched poly(lactide)s with lower inimer content varying between 1 and 6 % have been synthesized using $Sn(Oct)_2$ in bulk. The results of the preceding structural characterization are applicable to this set of experiments as well. NMR spectroscopy revealed a correlation between signal and structure identical to the one manifested in the first part (Figure 64). When using a lower fraction of HDON inimer, the amount of dendritic units slightly increased for most of the samples (57 % for PLLH 94; 52% for PLLH 97; unfortunately PLLH 99 was insoluble in DMSO-d_6). The resulting solubility of the samples in the eluent THF, which is commonly a poor solvent for stereoregular poly(lactide) of elevated molecular weight, is a consequence of the non linear morphology of the copoly(ester)s.

Figure 64: SEC traces (refractive index (RI) detection) of long chain branched samples derived from the copolymerization of lactide with 5HDON fractions of 6 (PLLH 94), 3 (PLLH 97) and 1 (PLLH 99) mole%.

Figure 64 shows the SEC-elugrams of the prepared long chain branched poly(lactide)s. The traces, obtained from SEC in THF revealed polydispersities below 2. Based on the
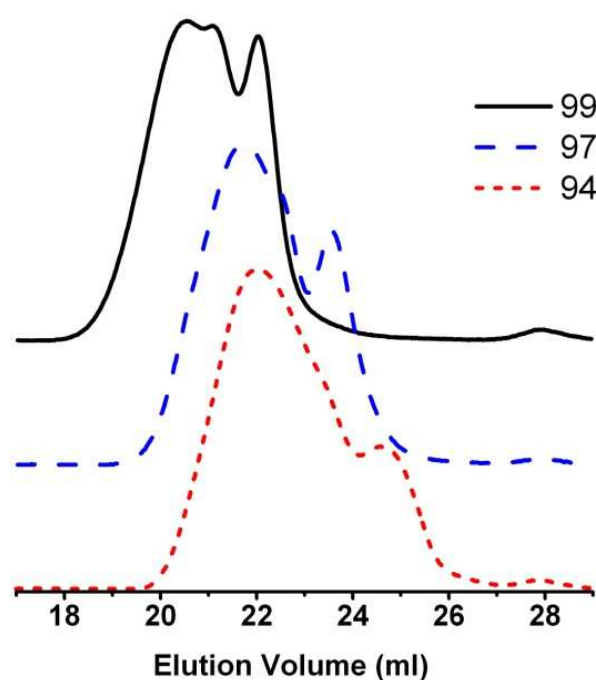
previous findings, we assume that the mechanism in fact resembles a living ring-opening copolymerization.

Table 9: SEC characterization data for the branched poly(lactide) copolymers with low HDON-fraction obtained from bulk polymerization with Sn(Oct)$_2$.

Sample	DB[#]	[M$_0$/M$_I$]	M$_N$ (theo)	M$_N$ (MALLS)	M$_W$/M$_N$ (MALLS)	α (KMH-Plot)	η$_n$ [ml/g]
PLLH 94	0.064	16	2,400	9.300	1,70	0,31	16,3
PLLH 97	0.029	32	4,800	14.400	1,63	0,41	17,8
PLLH 99	n.m.	99	14,400	34.100	1,72	0,49	35,6

([#]Degree of branching calculated from ^{1}H NMR in DMSO, n.m.= not measured, insoluble in DMSO-d$_6$)

Although limited in resolution, all SEC traces revealed non monomodal shape. This is in agreement with results obtained from MALDI-ToF MS measurements of the sample with a high 5HDON content polymer (PLLH 80). Therein, subdistributions for different degrees of branching and hence, varying number of total 5HDON units per molecule, were observed. In this case discussed above, the peak distances of the sub-distributions were uniform and a function of the monomer to inimer ratio. An increasing fraction of 5HDON incorporated as dendritic units with increasing molar mass was confirmed by separation with preparative SEC and separate NMR-analysis of the fractions, i.e., the samples reveal a polydispersity both in size and in molecular weight. Although there has been an intense debate on the precise mechanism, it is well known that Sn(Oct)$_2$ as well as the organo base TBD act exclusively as acylation-promoting catalysts and not as initiators themselves. Therefore, the molecular weight can be precisely controlled by the monomer (lactone) to initiator (alcohol) ratio: M$_{Ntheo}$=x*[M$_{Lactide}$]$_0$/[I] (1).

It has been shown by Knauss and co-workers[42] that the success of the formation of branched structures by the copolymerization of lactide with a branching inimer can be validated by comparing the obtained with the theoretical molecular weight, calculated from the monomer to initiator ratio. This is probably the most evident and striking argument for the formation of branching points. Table 9 shows that the molecular weights obtained by SEC-MALLS measurement are higher than those theoretically obtained by exclusive initiation

of the inimer. NMR characterization confirmed the presence of branching units and the excess molecular weight compared to equation (1). SEC-MALLS triple detection with viscosimetric evaluation revealed a Mark-Houwink coefficient α below 0.5, which is indicative for a non linear structure of the polymer. The Mark-Houwink coefficient α drops significantly from 0.49 to 0.31 for an increase of the inimer concentration from 1 to 6 mol%. The phenomenon of sample alteration, caused by the formation of linear units by an addition reaction of focal and terminal units upon prolonged standing at room temperature, was much less pronounced for the samples with high lactide content. This is most likely due to the increased T_g (Table 10) significantly above room temperature.

Thermal properties. DSC measurements were conducted for all polymer samples obtained by Sn(Oct)$_2$ catalysis in order to gain further information on the consequences of the branched topology of the polymer samples on crystallization. DSC thermograms of the thermally quenched PLLA samples have been obtained at a heating rate of 10°C/min (Figure 65).
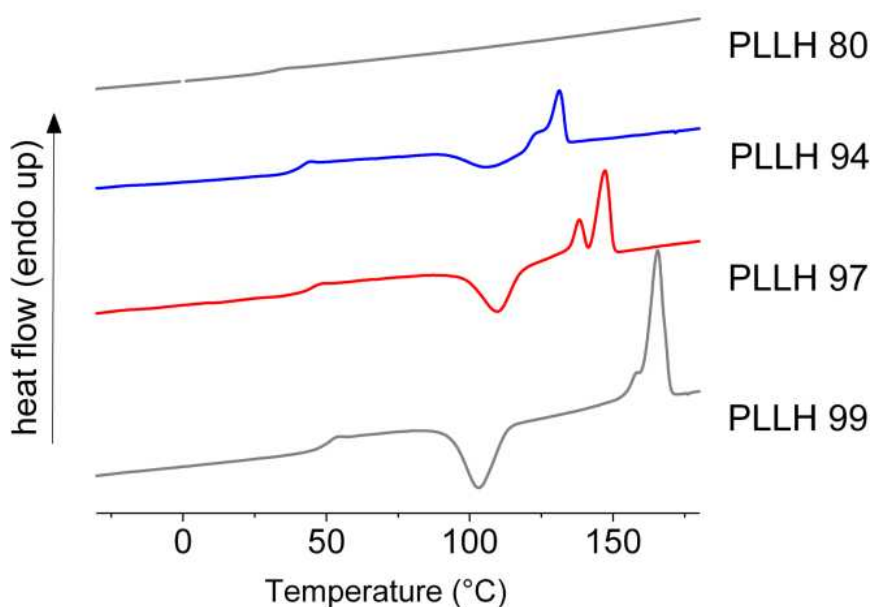

Figure 65: Differential Scanning Calorimetry (DSC) heating traces of PLLH samples with varying 5HDON content, heating rate of 10K/min (sample history: second run after previous heating to 200°C and cooling to -40 at ±10°C/min).

In addition to the glass transition, only the samples with lower inimer content show an exothermic cold-crystallization peak and an obvious melting peak. Multiple melting behavior, as observed for PLLH 97, is known for many semicrystalline polymers and is still subject of studies for stereoregular PLA[64,65]. This phenomenon is strongly dependent on the crystallization conditions. Generally, the branched polymer samples reveal a significant decrease of both T_g and melting point for increasing inimer content, as expected. The thermal characteristics are summarized in Table 10.

Table 10: Thermal properties of branched poly(lactide)s.

Sample	T_g [°C]	T_m [°C]	ΔH_m [J/g]
PLLH 80	31,2	-	-
PLLH 94	41,5	131,9	18,6
PLLH 97	44,0	145,9	41,0
PLLH 99	49,7	164,9	45,0

It is known that dendritic units randomly distributed in the polymer backbone decrease the polymers´ ability to crystallize in a regular lattice[66]. The simultaneous decrease of T_g, T_m and the melting enthalpy (ΔH_m) strongly suggests that branching points are evenly distributed in the polymer. This is consistent with the structural model derived in the previous sections. The DB linearly increases with molecular weight. It could be shown by MALDI-ToF MS (Figure 58) that the distance of the present subdistributions is regular and presumably a function of the monomer to inimer ratio. The lengthening of the period for an increase in monomer/inimer ratio was indicated by SEC measurents (Figure 64). The average linear chain length between two branching points gradually increases by a decrease of the inimer fraction. For high fractions of inimer (PLLH 80), the resulting short average linear chain length between branching points and the significantly higher amount of dendritic and terminal groups completely suppress crystallization of the polymer.

Experimental Procedures

Materials. 5-Hydroxymethyl-1,4-dioxane-2-one (5HDON) was synthesized according to modified literature procedures[40,67] and has been distilled freshly prior to use. Stanneous 2-ethyl-hexanoate (Sn(Oct)$_2$) and 9-fluorenemethanol (99%) were purchased from Acros and

used as received. 1,5,7-triazabicyclo[4.4.0]dec-5-ene (TBD) was purchased from Fluka and used without further purification. Dichloromethane as solvent was dried over P_2O_5 and freshly distilled over nitrogen. Toluene as solvent was dried over sodium and freshly distilled under nitrogen. L-Lactide was purchased from Purac (Groningen, Netherlands), recrystallized twice from toluene and stored under vacuum prior to use.

Instrumentation. NMR investigation. All ^{1}H and ^{13}C nuclear magnetic resonance spectra were recorded at 25°C using a Bruker AMX 400 (400 MHz) spectrometer or a Bruker Avance-II-400 (400 MHz) equipped with an inverse multinuclear 5mm probe head and a z-gradient coil. The spectra were measured in $CDCl_3$ and DMSO-d_6 and the chemical shifts were referred to the internal calibration on the solvents residual peak. (^{1}H proton NMR signal: 39.52 ppm for DMSO-d_6, and 77.36 ppm for $CDCl_3$, ^{13}C carbon NMR signal: 39.52 ppm for DMSO-d_6, and 77.36 ppm for $CDCl_3$)[68]. Standard pulse sequences for gs-COSY, gs-HSQC and gs-NOESY experiments were used. The refocusing delays for the inverse heterocorrelations were set to 3.45 and 62.5 ms, corresponding to $^1J_{C,H}$ = 145 Hz and $^nJ_{C,H}$= 8 Hz, respectively. Size exclusion chromatography (SEC) was performed with an instrument consisting of a Waters 717 plus autosampler, a TSP Spectra Series P 100 pump and a set of three PSS-SDV 5A columns with 100, 1000, und 10000 Å porosity. THF was used as an eluent at 30°C and at a flow rate of 1 mL min^{-1}. UV absorptions were detected by a SpectraSYSTEM UV2000. The specific refractive index increment (dn/dc) was measured at 30°C using an Optilab DSP interferometric refractometer (also RI detector) and determined with the Wyatt ASTRA IV software (Version 4.90.08). Calibration was carried out using poly(styrene) standards provided by Polymer Standards Service and performing a 3rd order polynomial fit. Online-SEC static light scattering measurements were performed via a multi-angle laser light scattering detector (MALLS) DAWN EOS laser photometer (Wyatt Technology Co.) equipped with a GaAs laser emitting at a wavelength of 685 nm. Molar masses were calculated during SEC measurements, using the Wyatt ASTRA IV software (Version 4.90.08) & ASTRA V (Version 5.1.9.1). Masses were calculated in 0.25 s intervals using the Zimm equation:

$$\frac{Kc}{R_\theta} = \frac{1}{M_w} + 2A_2 c \quad with \quad K = \frac{4\pi^2 n_0^2 \left(\frac{dn}{dc}\right)^2}{\lambda_0^4 N_A} \qquad (1)$$

n_0 is the refractive index of toluene, N_A is Avogadro's constant, λ is the laser wavelength; M_w is the apparent weight average molecular weight, A_2 is the second virial coefficient, R_θ is the Rayleigh ratio of the polymer solution at a given angle. In SEC-MALLS the second virial coefficient is small enough to be neglected at the low concentrations used in chromatographic separation. Matrix-assisted laser desorption and ionization time-of-flight (MALDI-ToF MS) measurements were performed on a Shimadzu Axima CFR MALDI-ToF MS mass spectrometer equipped with a nitrogen laser delivering 3 ns laser pulses at 337 nm. Dithranol (1,8-dihydroxy-9(10H)-Anthracetone, Aldrich 97%), was used as matrix. Potassium triflate (Aldrich, 98%) was added for ion formation. Best results were obtained for samples which were prepared from chloroform solution by mixing matrix (10 mg/mL), polymer (10 mg/mL), and salt (0.1 N solution) in a ratio of 5:1:1. A volume of 0.9 μL was deposited on the MALDI sample slide and allowed to dry at room temperature for 2 h prior to measurement. DSC measurements were carried out on a Perkin Elmer 7 Series Thermal Analysis System with auto-sampler in the temperature range of -180 C to 100°C at heating rates 10 K/minute. The melting points of indium (T_0 = 156.6 C) and Millipore water (T_0 =0°C) were used for calibration. Deuterated chloroform-d_1 and DMSO-d_6 were purchased from Deutero GmbH and dried and stored over molecular sieves. Other solvents and reagents were purchased from Acros and used as received, if not mentioned otherwise.

Modified monomer intermediate synthesis: Ethyl 2[(2-Phenyl-1,3-dioxane-5yl)oxy] acetate. 19 g (0,105 mol) trans-5-hydroxy-2-phenyl-1,3-dioxane were dissolved in 750 mL dry toluene. 0.14 mol NaH (60%dispersion in mineral oil) were slowly added under a nitrogen flow. The solution was stirred for 20 minutes, in which hydrogen development subsided. 0.13 mol ethyl bromoacetate were dissolved in 50 mL dry toluene and added to the alcoholate with a syringe pump over a period of 50 minutes while the solution was kept at 0 to 5°C. Stirring was continued for 40 minutes and slowly warmed to room temperature. After 3 h, the yellowish solution was poured in 1L of ice-water. The organic layer was separated and washed with 2x100 mL brine. Residual water was removed by stirring over $MgSO_4$/K_2CO_3 (10/1). All volatile components were removed with a rotary evaporator to yield a yellow oil. The oil was taken up in 200 ml diethyl ether from which the product crystallized on standing at -20°C. Recrystallization from diethylether yielded 21.3 g product (76%). Melting point: 78.3°C. ^{1}H NMR (300 MHz, chloroform-d_1) δ (ppm) = 1.28 (t, 3 H,

OCH$_2$CH_3), 3.54 (s, 1 H,CHO$_{cycl}$) 4.06-4.43 (m 4 H, CH_2O$_{cycl}$) 4.21 (q, 2 H, OCH_2CH$_3$) 5.53 (s, 1H OCHO$_{cycl}$) 7.33-7.52(m, 5 H, Ar)

General procedure for the Sn(Oct)$_2$ catalyzed copolymerization of L-Lactide and 5HDON in bulk. In a glove box a one necked Schlenk-flask was charged with stoichiometric amounts of Sn(Oct)$_2$, L-lactide and 5HDON. Outside the glove box, the flask was completely immersed in an oil bath and preheated to 130°C. A homogenous melt was obtained after an induction period of 40 seconds (T$_0$). All kinetic samples were taken from the melt with a small glass rod the under Ar during the polymerisation process. The samples were quenched thermally and stored at -28°C prior to examination. An aliquot of the last sample from the kinetic experiment was stored at room temperature over the period of 8 weeks prior to analysis.

Procedure for the TBD catalyzed copolymerisation of L-lactide and 5HDON in solution at room temperature. In a glove box a one neck Schlenk-flask was charged with stochiometric amounts of L-Lactide and 5HDON and sealed with a rubber septum. 2 mL/g monomer of the previously dried dichloromethane were syringed into the flask. The Schlenk-flask was immersed into a 2L water bath at 25°C, serving as temperature buffer. Polymerization was initiated by addition of the respective amount of TBD (0.5 mole %), dissolved in 100 L dichloromethane via a precision syringe. Samples for kinetic measurements were taken at the given intervals by quenching aliquots of the reaction mixture with a 5 fold excess of benzoic acid.

Procedure for the functionalization of the focal unit in the copoly(ester).
The thermally quenched sample PLLH 80 (after 6690 min reaction time), prepared by Sn(Oct)$_2$ catalyzed polymerization was charged into a Schlenk-flask and an excess of fluorenemethanol with respect to the amount of 5HDON was added. The flask was completely immersed in an oil bath, pre heated to 130°C and quenched thermally after a reaction time of 12 hours.

Synthesis of model compounds for NMR-studies: 5-acetoxymethyl-1,4-dioxan-2 -on. A mixture of 5HDON (1.2 g, 9.1 mmol), triethylamine (1.89 ml, 13.6 mmol), and DMAP (0.089g, 0.7 mmol) in 20 mL of dry dichloromethane was cooled to 1-3°C. A precooled solution of

1.28 ml (13.6 mmol) acetic anhydride in 4 mL of dichloromethane was added within 45 minutes. After one hour, the reaction was allowed to warm to room temperature within 4 hours and stirred over night. The solution was washed with 3 x 10 mL portions of 2n HCl and subsequently washed with saturated $NaHCO_3$ solution, dried over $MgSO_4$ and the solvents were evaporated in vacuum. For NMR-Analysis, the obtained product (slightly yellowish oil) was further purified via column chromatography with cyclohexane/ethyl acetate (4:3, R_f=0.6 on silica gel). (Yield: 252 mg/21%). ^{1}H NMR (400 MHz, chloroform-d_1) δ (ppm) = 2.10 (s, 3 H, $COCH_3$) 4.02 - 4.08 (m, 1 H, CH_{cycl}) 4.19 (dd, J = 4.99 Hz, 2 H, CH_2OCO) 4.32 - 4.54 (m, 4 H, $COCH_2O_{cycl}$ & CH_2O_{cycl}) ^{13}C NMR (100 MHz, DMSO-d_6) δ (ppm) = 20.56 ($COCH_3$) 62.09 ($CH_2OCOCH3$ 64.67 ($COCH_2O_{cycl}$) 68.58 (CH_2O_{cycl}) 69.04 (CH_{cycl}) 166.83 (CH_3COO) 170.19 (CH_2COO).

Conclusions

We have described the preparation of branched and hyperbranched poly(lactide)s via a new synthetic strategy, employing the ring-opening multibranching copolymerization of lactide with the cyclic inimer 5HDON. Two general synthetic strategies involving (i) $Sn(Oct)_2$ and (ii) organo base catalysis have been tested and kinetically evaluated. A structural analysis based on the synthesis of model compounds and the application of 2D-NMR techniques enabled us to monitor the formation of dendritic units in the course of the copolymerization. Based on these observations, we have derived a qualitative reaction mechanism. Unexpectedly, this mechanism is not of a condensing nature, thus, the term "self condensing cyclic ester polymerization", which derives from SCVP previously defined by Frechét, is not applicable here. Even more significantly, it could be shown that the formation of branching points occurs from the ring-opening of inimer functionalized macromonomers in the presence of lactide monomer. In general more than 50 % of the inimer are incorporated as dendritic units. Further inimer was found to be present in the polymer structures as focal group. The latter was shown to be amenable to selective functionalization with a primary alcohol. This renders the potentially biodegradable and biocompatible material useful for polymer modification reactions and surface functionalization. The formation of branching points did not occur via condensation of the macromonomers, but by a real copolymerization of the lactone structure involving lactone-functionalized oligomers.

The lactide/5HDON ring-opening branching copolymerization relies on the reactivity difference between primary and secondary hydroxyl end groups. Obviously, the presence of free lactide in the polymerization mixture is a fundamental prerequisite for the formation of dendritic units, since an increase of the molecular weight and formation of dendritic units decreases significantly when approaching the polymerization equilibrium conditions. Therefore, the ratio of incorporated dendritic to focal inimer units is believed to be a complex function of the reactivity ratio of the two lactones. Molecular weights obtained from GPC-MALLS measurements were significantly higher than expected for the employed monomer to initiator (inimer) ratio, confirming a linked and hence branched structure in agreement with our MALDI-ToF and NMR-studies. Our current efforts aim at the use of these new materials for biodegradable drug delivery constructs and biodegradable block copolymer structures with hyperbranched block and target functionalities.

Supporting Information Available: Additonal information regarding Experimental procedures, 2D NMR spectra, a complete table of all ^{1}H and ^{13}C chemical shifts of relevant for momer and polymer in DMSO-d_6 and GPC traces,. This material is available free of charge via the Internet at http://pubs.acs.org

References

[1] Berkland, C.; King, M.; Cox, A.; Kim, K. K.; Pack, D. *J. Controlled Release,* **2002,** *82*, 137–147.

[2] Ahmed, F.; Discher, D. *J. Controlled Release* **2004**, *96*, 37– 53.

[3] Lin, Y. M. Boccaccini, A. R.; Polak, J. M.; Bischop, A. E. *J. Biomaterials Appl.* **2006**, *21*, 109-118.

[4] Russias, J. Saiz, E.; Deville, S.; Gryn, K.; Liu, G.; Nalla, R. K.; Tomsia, A. P. *Journal of Biomedical Materials Research Part A* **2007,** *83A,* 434-445.

[5] Burger, C., Kabir, K.; Rangger, C.; Mueller, M.; Minor, T.; Tolba, R. H. *Arch. Orthop. Trauma Surg.* **2006,** *126*, 695–705.

[6] Stock, U. A., Mayer J.E. Jr. *J. Long Term Ev. Med. Implants* **2001**, *11*, 249–260.

[7] Chmura, A. J.; Davidson, M. G.; Jones, M. D.; Lunn, M. D.;Mahon, M. F.; Johnson, A. F.; Khunkamchoo, P.; Roberts, S.L.; Wong, S. S. F. *Macromolecules* **2006,** *39,* 7250-7257.

[8] Ovitt, T. M.; Coates, G. W. *J. Am. Chem. Soc.* **1999,** *121,* 4072-4073.

[9] Majerska, K.; Duda, A. *J. Am. Chem. Soc.* **2004**, *126*, 1026–1027.

[10] Urayama, H; Moon, S. I.; Kimura, Y. *Macromol. Mater. Eng.* **2003**, 288, 137–143.

[11] Song, C. X.; Feng, X. D. *Macromolecules* **1984,** *17*, 2764-2767.

[12] In't Veld, P. J. A.; Velner, E. M.; van De Witte, P.; Hamhuis, J.; Dijkstra, P: J.; Feijen, J. *J. Polym. Sci. Part A* **1997**, 35, 219–226.

[13] Tasaka, F.; Ohya, Y.; Ouchi, T. *Macromol. Rapid Commun.* **2001**, 22, 820-824.

[14] Simmons, T. L.; Baker, G. L. *Biomacromolecules* **2001,** *2*, 658-663.

[15] Leemhuis, M.; van Nostrum, C.F.; Kruijtzer, J. A. W.; Zhong, Z. Y.; Breteler,, M. R.; Dijkstra, P.J.; Feijen, J.; Hennink; W. E. *Macromolecules* **2006,** *39,* 3500-3508.

[16] Jing, F.; Smith, M. R.; Baker, G. L. *Macromolecules* **2007,** *40,* 9304-9312.

[17] Jiang, X.; Smith, M. R.; Baker, G. L. *Macromolecules* **2008,** *41,* 318-324.

[18] Jiang, X.; Vogel, E. B.; Smith, M. R.; Baker, G. L *Macromolecules* **2008,** *41,* 1937-1944.

[19] Jing, F.; Hillmyer, M. A.; *J. Am. Chem. Soc.* **2008**, *130*, 13826–13827.

[20] Wolf, F.; Friedemann, N.; Frey, H. *Macromolecules* **2009** , 42, 5622-5628.

[21] a) Gottschalk, C.; Wolf, F.; Frey, H, *Macromol. Chem. Phys.* **2007**, 208, 1657–1665; b) Hiemstra, C.; Zhong, Z.; Li, L.; Dijkstra, P. J.; Jan Feijen, J. *Biomacromolecules* **2006,** *7*, 2790-2795.

[22] Adeli, M. Haag, R. *J. Polym. Sci. , Part A: Polymer Chemistry*, **2006**, *44*, 5740–5749.

[23] Malmström, E.; Johansson, M.; Hult, A**.** *Macromolecules* **1995**, *28*, 1698-1703.

[24] Magnusson, H.; Malmström, E.; Hult, A *Macromolecules* **2000,** *33,* 3099-3104.

[25] Yim, S.H.; Huh, J. ;Ahn, C. H.; Park, T. G. *Macromolecules* **2007**, 40, 205-210.

[26] Trollsås, M.; Hedrick, J. L. *J. Am. Chem. Soc.* **1998**, *120*, 4644.

[27] Trollsås, M.; Claesson, H.; Atthoff, B.; Hedrick, J. L. *Angew. Chem., Int. Ed.* **1998**, *37*, 3132.

[28] Skaria, S.; Smet, M.; Frey, H. *Macromol. Rapid Commun.* **2002**, *23*, 292-296.

[29] Neuner I. T.; Ursu, M.; Frey, H. *ACS symposium series: Polymer biocatalysis and biomaterials* **2005**, 900, 354-365.

[30] Cooper, T. R; Storey, R. F. *Macromolecules* **2008,** *41,* 655-662.

[31] Ha, C.S., Gardella, J.A. Jr. *Chem. Rev.* **2005,** 105, 4205-4232.

[32] Numata, K.; Srivastava, R. K. ; Finne-Wistrand, A.; Albertsson, A. C.; Doi, Y; Abe, H. *Biomacromolecules* **2007,** 8, *3115-3125.*

[33] Noga, D. E. ; Petrie, T. A. ; Kumar, A. ;Weck, M. ; García, A. J. Collard, D. M. *Biomacromolecules* **2008,** *9,* 2056–2062.

[34] Fréchet, J. M.; Hemi, M; Gitsov, Ivan, G.; Sadahito, S; Leduc, M. R.; Grubbs, R. B. *Science* **1995**; 269, 5227-5231.

[35] Trollsås, M.; Löwenhielm, P.; Lee, V. Y.; Möller, M.; Miller, R.D.; Hedrick, J. L. *Macromolecules* **1999,** *32,* 9062-9066.

[36] Yan, D.; Wulkov, M.; Müller, A.H.E. *Macromolecules* **1997**, *30*, 7015-7023.

[37] Matyjaszewski, K.; Gaynor. S. C.; Müller, A.H.E. *Macromolecules* **1997,** *30,* 7034-7041.

[38] Liu, M.; Vladimirov, N.; Fréchet, J. M. J. *Macromolecules* **1999,** *32,* 6881-6884.

[39] Yu, X.; Feng, J.; Zhuo, R. *Macromolecules* **2005,** *38,* 6244-6247.

[40] Parzuchowski, P. G.; Grabowska, M.; Tryznowski, M.; Rokicki, G. *Macromolecules* **2006,** *39,* 7181-7186.

[41] Parzuchowski, P.G.; Jaroch, M.; Tryznowski, M.; Rokicki, G. *Macromolecules* **2008**, *41*, 3859-3865.

[42] Pitet, L. M.; Hait, S. B.; Lanyk, T. J.; Knauss, D. M. *Macromolecules* **2007,** *40,* 2327-2334.

[43] Pratt, R. C.;Bas, G. G.; Lohmeijer, D. A.; Long, D. A.; Waymouth, R. M.; Hedrick, J. L *J. Am. Chem. Soc.* **2006**, *128*, 4556-4557.

[44] Dechy-Cabaret, O.; Martin-Vaca, B.; Bourissou, D. *Chem. Rev.* **2004,** 104, 6147-6176.

[45] Broggini, G.; Zecchi, G. *Organic Preparations and Procedures International* **1991,** *23,* 762-764.

[46] Espartero, J. L.; Rashkov, I.; Li, S. M.; Manolova, N. ; Vert, M. *Macromolecules* **1996,** *29,* 3535-3539.

[47] Hölter, D.; Burgath, A.; Frey, H. *Acta Polym.* **1997**, *48,* 30.

[48] a) Hölter, D.; Frey, H. *Acta Polym.* **1997***, 48,* 298; b) Frey, H.; Hölter, D. *Acta Polymer.* **1999,** *50,* 67.

[49] Narayan, R., Kolstad, J. J.; Witzke, D. R. *Macromolecules* **1997,** *30,* 7075-7085.

[50] Yin, M.; Baker, G. L. *Macromolecules* **1999**, *32*, 7711-7718.

[51] Kowalski, A.; Duda, A. ;Penczek, S. *Macromolecules* **2000,** *33,* 689-695.

[52] Kowalski, A.; Duda, A. Libiszowski, J.; Majerska, K.; Biela, T.; Penczek, S.; *Macromol. Symp.* **2000** 157, 61–70.

[53] Kowalski, A.; Duda, A. ;Penczek *Macromolecules* **2000,** *33,* 7359-7370.

[54] Kowalski, A.; Libiszowski, J.; Majerska, K.;Duda, A.; Penczek, S. *Polymer* **2007,** 48, 3952-3960.

[55] Ryner, M.; von Schenck, H.; Stridsberg, K. ; Albertsson, A. C.; Svensson, M., *Macromolecules* **2001,** *34,* 3877-3881

[56] Michelle Byrd; H. C. M.; McEwen, C. N. *Anal. Chem*. **2000,** *72*, 4568-4576

[57] de Jong,S. J.; van Dijk-Wolthuis, W. N. E.; van den Bosch, J. J. K.; Schuyl, P. J. W.; Hennink, W. E. *Macromolecules* **1998***, 31,* 6397-6402

[58] Kricheldorf, H. R.; Stoeber, O. *Macromolecules* **1995,** *28*, 2118-2126.

[59] Burgath, A.; Sunder, A. ; Frey, H. *Macromol. Chem. Phys,* **2000,** *201,* 782–791.

[60] Kamber, N. E.; Jeong, W.; Waymouth, R. M.; Pratt, R. C.; Lohmeijer, B. G. G.; Hedrick, J. L. *Chem. Rev.* **2007,** *107*, 5813-5840.

[61] Sabot, C.; Kumar, K. A.; Antheaume, C.; Mioskowski, C *J. Org. Chem.* **2007**, *72*, 5001-5004.

[62] Lohmeijer, B. G. G.; Pratt, R. C.; Leibfarth, F.; Logan, J. W.; Long, D. A.; Dove, A. P.; Nederberg, F.; Choi, J.; Wade, J.; Waymouth, R. M.; Hedrick, J. L. *Macromolecules* **2006,** *39,* 8574-8583.

[63]Wurm, F.; Schüle, H.; Frey, H. *Macromolecules*, **2008**, *41*, 9602–9611.

[64] Di Lorenzo, M. L. *J. Appl. Polym. Sci.* **2006**, *100*, 3145.

[65] Pan, P.; Kai, W.; Zhu, B.; Dong, T.;Inoue; Y. *Macromolecules* **2007,** *40,* 6898-6905.

[66] Baker, G. L.; Vogel, Erin, B. V.; Smith, M. R. *Polymer Reviews* **2008,** *48,* 64-84.

[67] Broggini, G.; Zecchi, G. *Organic Preparations and Procedures International* **1991,** *23,* 762-764.

[68] Gottlieb, H. E.; Kotlyar, V.; Nudelman, A. *J. Org. Chem.* **1997,** *62,* 7512-7515.

Supporting Information

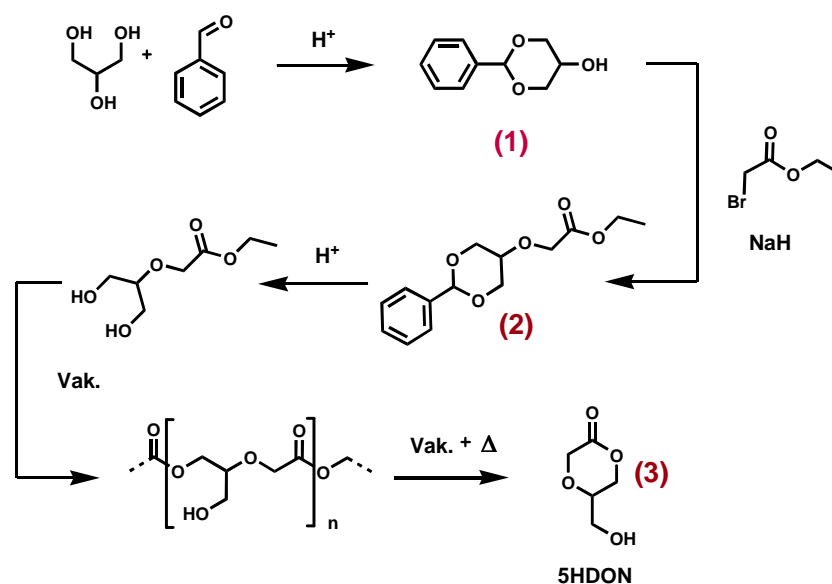## Inimer-Promoted Synthesis of Branched and Hyperbranched Poly(lactide) Copolymers

Florian K. Wolf and Holger Frey

Table of Contents

I.   Supporting Experimental Section:

S.I. 1: Reaction scheme for the synthesis of 5HDON

Modified monomer intermediate synthesis:

**Ethyl 2[(2-Phenyl-1,3-dioxane-5yl)oxy] acetate (2).**

19 g (0,105 mol) trans-5-hydroxy-2-phenyl-1,3-dioxane were dissolved in 750 mL dry toluene. 0.14 mol NaH (60%dispersion in mineral oil) was slowly added under a nitrogen flow. The solution was stirred for a period of 20 minutes, in which hydrogen development subsided. 0.13 mol ethyl bromoacetate were dissolved in 50 mL dry Toluene and added to the alkoxide with a syringe pump over a period of 50 minutes, while the solution was kept at 0° to 5°C. Stirring was continued for 40 minutes and then slowly warmed to room temperature. After 3 h, the yellowish solution was poured in 1L of ice-water. The organic layer was separated and washed twice with100 mL brine. Residual water was removed by stirring over $MgSO_4/K_2CO_3$ (10/1). All volatile components were removed with a rotary evaporater to yield a yellow oil. The oil was taken up in 200 mL diethyl ether, from which the product crystallized on standing at -20°C. Recrystallization from diethyl ether afforded 21.3 g product (76%). Melting point: 78.3°C. ^{1}H NMR (300 MHz, chloroform-d_1), ▯ (ppm) = 1.28 (t, 3 H, OCH$_2$CH_3), 3.54 (s, 1 H,CHO$_{cycl}$) 4.06-4.43 (m 4 H, CH_2O$_{cycl}$) 4.21 (q, 2 H, OCH_2CH$_3$) 5.53 (s, 1H OCHO$_{cycl}$) 7.33-7.52(m, 5 H, Ar).

II.   Supporting NMR Data:

S.I. 2: Summary of NMR data for model compounds and the structural repeat units derived thereof (400MHz, DMSO-d_6).

		5HDON-r.u.			**5HDON -** model compounds			**Dilactide-r.u.**	
		focal (A)	dendr. (B)	linear (C)	focal (D)	dendr. (E)	linear (F)	linear (G)	term. (H)
δ^1H (ppm)	1	4.30-4.47	4.25-4.35	4.11-4.16				5.10-5.23	4.15-4.25
	2	4.14-4.20	3.85-3.95	3.57-3.65				1.43-1.50	1.27-1.31
	3	4.10-4.32	4.10-4.32	4.10-4.32					
	4	4,28		3.42-3.54					
δ^{13}C (ppm)	1	64.70	66.52	66.62	64.67			68.75	65.67
	2	68.92	75.00	78.21	69.04	74.40[#]	77.70[#]	16.50	20.38
	3	63.43	63.10	63.10	62.09	63.30[#]	64.00[#]	169.29-169.36	174.13
	4	68.30		60.09	68.58		60.70[#]		
	5	166.73	169.52-169.67		166.83				

([#]Chemical shifts as reported in literature *(*Rockicki et. al., *Macromolecules* **2006** ,Vol. 39, No. 21„ 7181-7186*).*
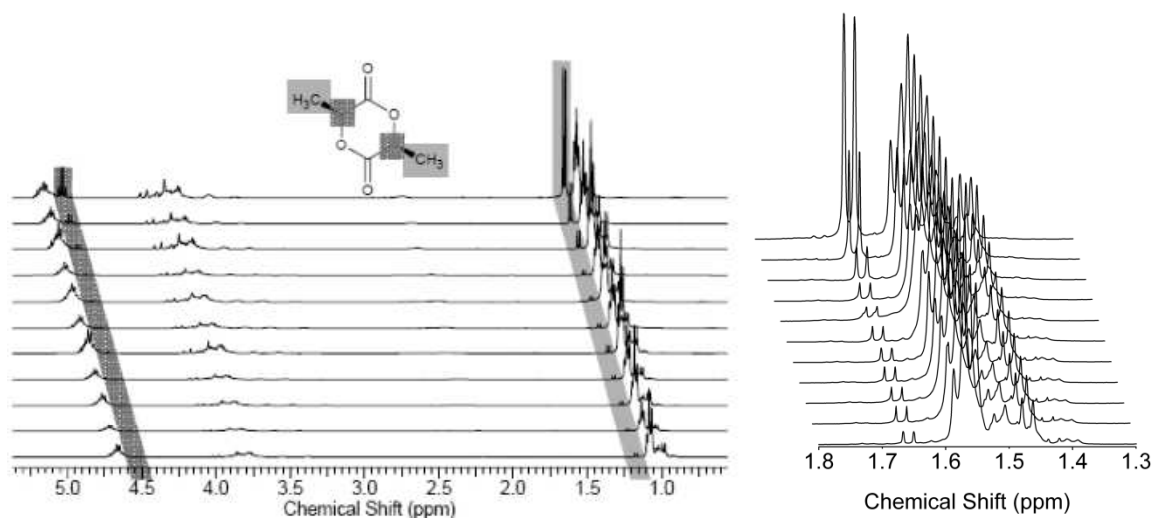
S.I. 3: Kinetic ^{1}H-NMR measurements of Sn(Oct)$_2$ catalyzed copolymerization of the 80/20 dilactide/5HDON mixture in bulk (400 MHZ, CDCl$_3$). (top to bottom: 5, 10, 20, 40, 80, 160, 320, 540, 1140, 2260 and 6690 min) The dilactide concentration reaches equilibrium after a polymerization time of approx. 80 minutes.
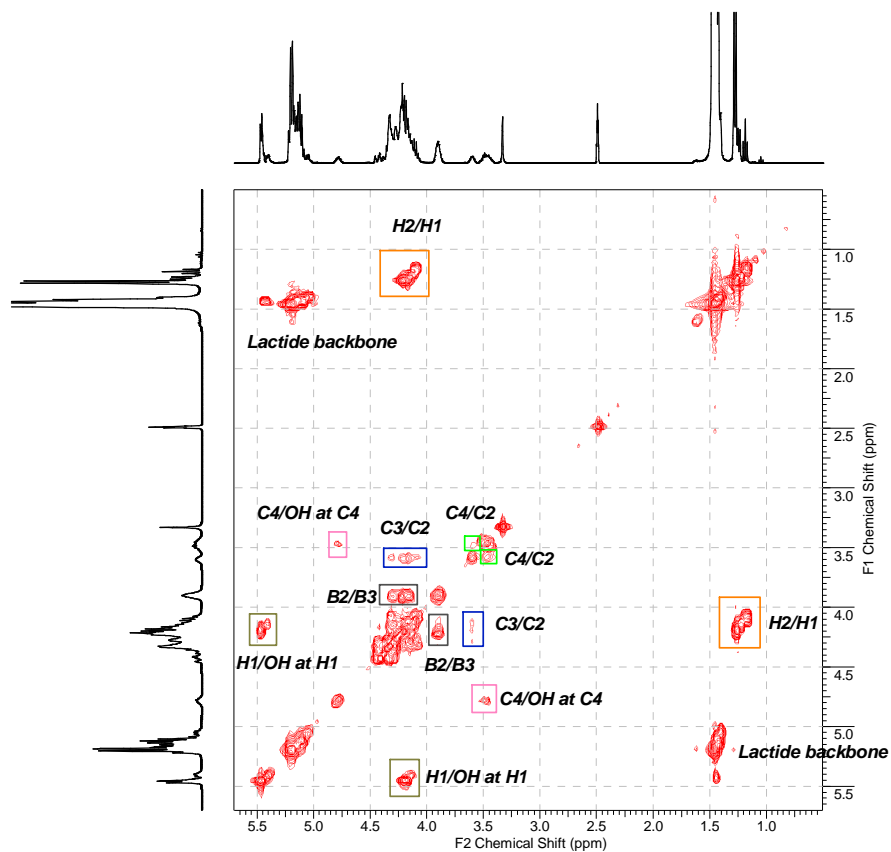
S.I. 4: ^{1}H COSY for PLLH 80 after prolonged standing at room temperature in DMSO-d$_6$ at 400 MHz.
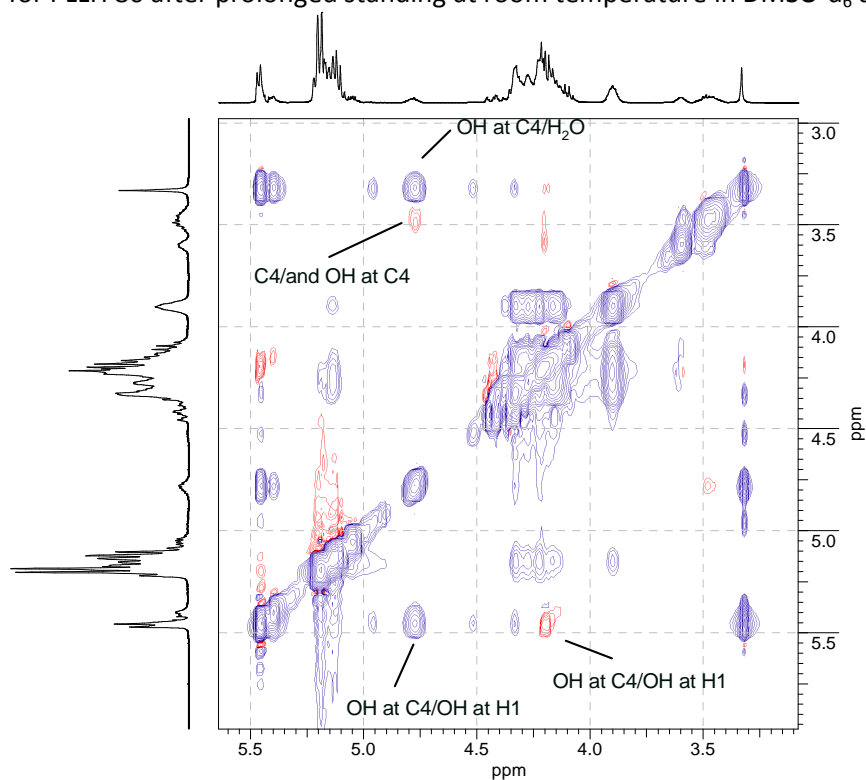
S.I. 5: NOESY (Nuclear Overhauser Enhancement Spectroscopy) of PLLH 80 after prolonged standing at room temperature in DMSO-d$_6$ at 400 MHz. NOE cross peaks of the same phase as the diagonal

arise from chemically exchanging protons (blue – positive NOE). Negative NOE (red) indicate an increased mobility of the chain ends.
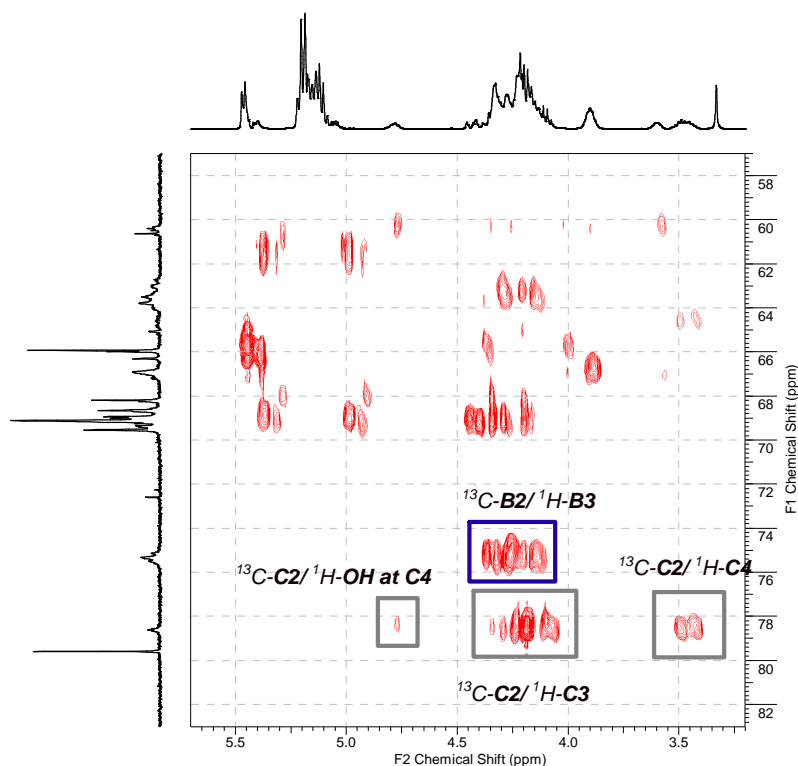
S.I. 6: Heteronuclear Multiple-Band Correlation Spectroscopy (HMBC) revealing proton-carbon connectivities through couplings over multiple bonds.
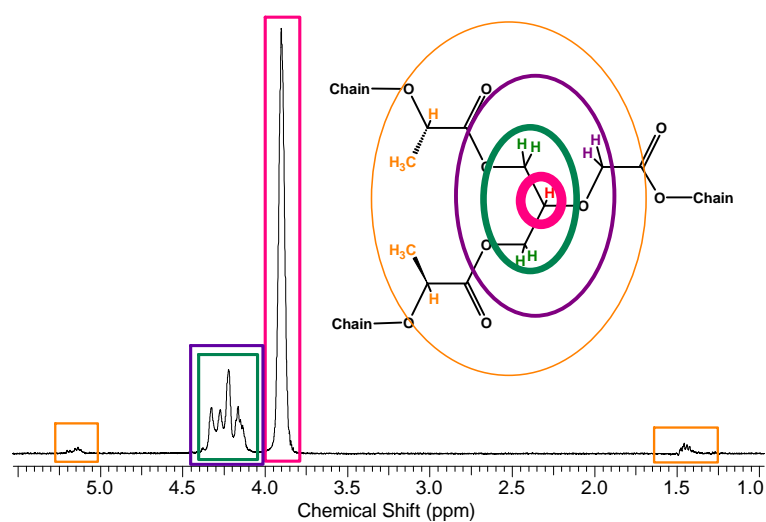
S.I. 7: [1]H-NOE experiment with excitation on the frequency corresponding to 3.9 ppm (i.e. the dendritic methine proton at B2). Spin coupling leads to excitation of vicinal protons. This spectrum indicates, that the alpha methine proton of lactic acid repeat units, directly attached to a dendritic unit are slightly shifted upfield ([1]H=5.14 ppm) compared to the quartet of lactic acid units (δ[1]H=5.21 ppm).

175
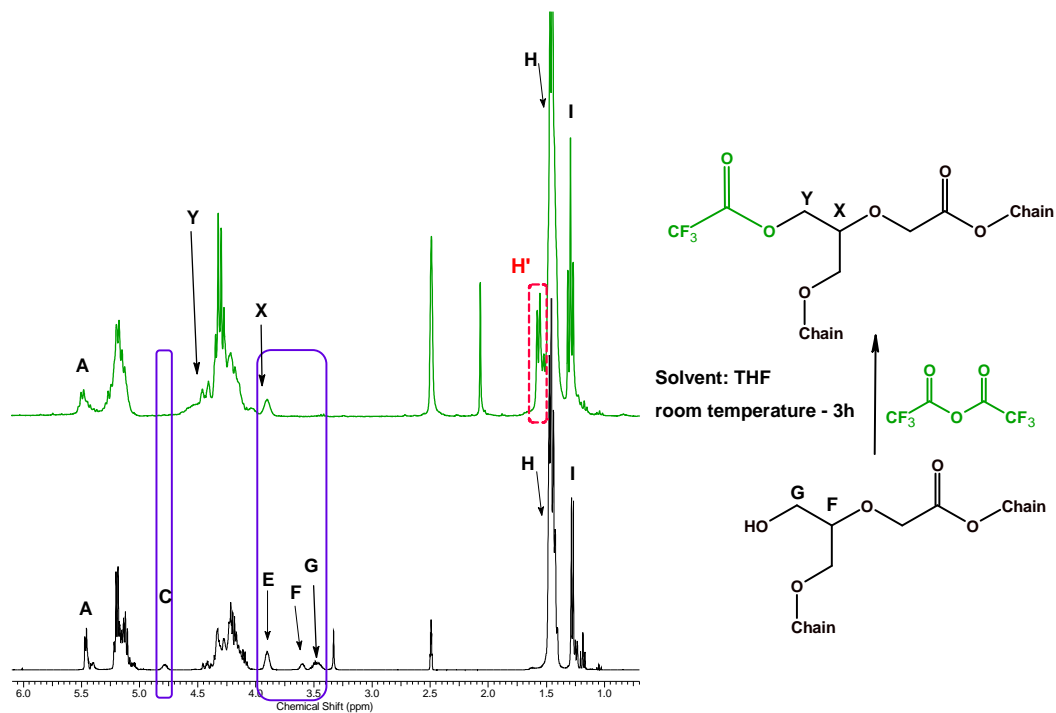
S.I. 8: Functionalization of linear 5HDON units (which appeared after prolonged storage) with TFA anhydride. Dissappearance/shift of proton signals related to G and F. Superposition of new peak X with previously present peak E.

III.   SEC Data
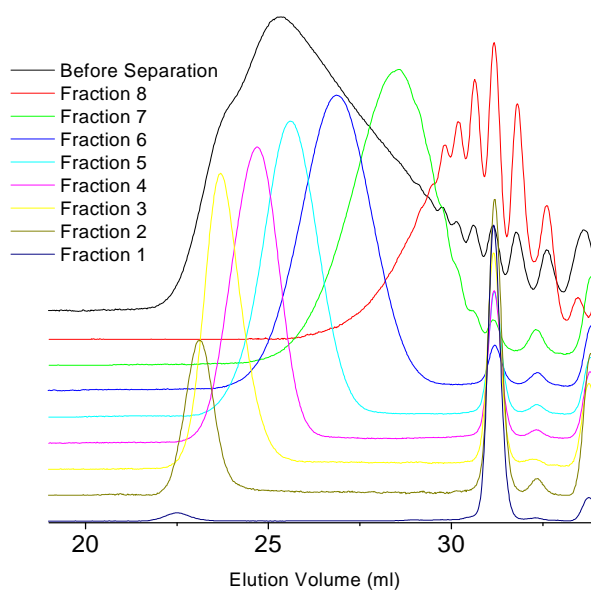
S.I. 9: SEC traces of PLLH 80 before and after separation into 8 fractions by preparative SEC in THF.

IV.   Schemes

S.I. 10: Polymerization products that can be excluded for the copolymerization of dilactide with 5HDON. (1) linear copoly(ester) by exclusive ring-opening; (2) comb like poly(ester) by subsequent homopolymerization of the focal 5HDON units of macromonomers.

Linear Copolymer   Comb like Copolymer
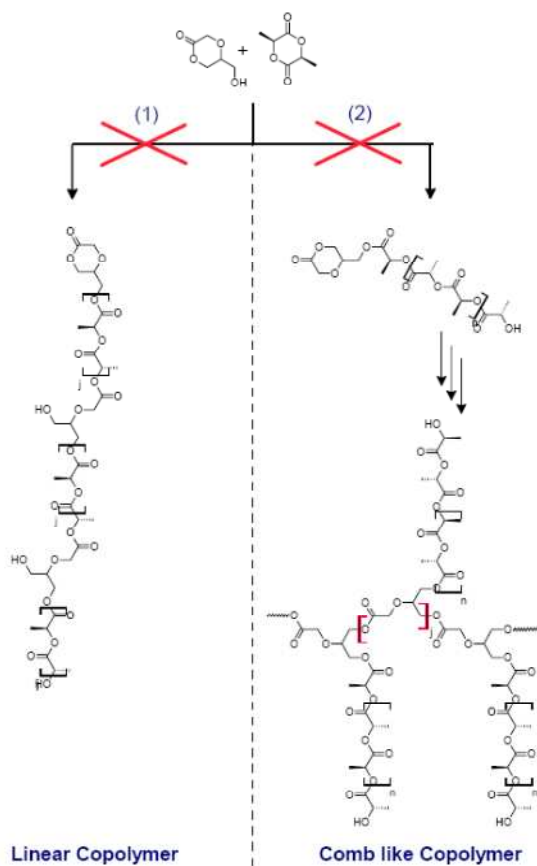
Chapter 3: Amphiphilic Poly(ester) −*b*-Poly(methacrylate)

Copolymers for Medical Applications

3.1 Poly(lactide)-*block*-Poly(HEMA) Copolymers: An Orthogonal One-Pot Combination of ROP and ATRP, Using a Bifunctional Initiator

Florian K.Wolf, Nora Friedemann and Holger Frey

Abstract

We describe an orthogonal polymerization strategy for the preparation of amphiphilic poly(lactide)-*block*-poly(2-hydroxyethylmethacrylate) (PLA-*b*-PHEMA) copolymers with a partially biodegradable and a potentially biocompatible polymer backbone segment. The strategy is based on an orthogonal polymerization from a double-headed initiator, which has been realized in a rapid one-pot or in a two-pot route. The "lactide first" strategy permits exclusive chain growth from the hydroxyl-group of the initiator 2-hydroxyethyl 2-bromo-2-methylpropanoate**.** 2-Hydroxy-ethylmethacrylate (HEMA) was polymerized in a second step without the use of hydroxyl-protecting groups by controlled radical polymerization (ATRP). Due to the heterogeneous character of the two blocks, ATRP had to be conducted in dimethylsulfoxide at 80°C, granting both sufficient solubility for the stereoregular, semicrystalline poly(lactide) block and permitting fast chain growth of the Poly(HEMA) block. The PLLA/PDLA macroinitiators were synthesized using Sn(Oct)$_2$ as a catalyst in solution (PDI=1.07-1.17; M$_n$=2,000-9,000g/mol). NMR spectroscopy and MALDI-ToF MS confirmed complete terminal functionalization with the bifunctional initiator 2-hydroxyethyl 2-bromo-2-methylpropanoate. Fast growth (<10 min, 45-60% conversion) of the poly(HEMA) block was achieved with a CuCl/bipyridine or CuCl/CuCl$_2$/bipyridene system. SEC measurements

indicated complete attachment of the second block resulting with narrow polydispersity of 1.2 to 1.3 (M_n=5,000-9,000). Developing the concept further, removal of residual lactide monomer and Sn(Oct)$_2$ catalyst has been proven to be redundant by a variation in the synthetic procedure. In consistence with new AGET (activators generated by electron transfer) ATRP methods, grafting of free lactide monomer onto the HEMA backbone could be prevented by oxidative deactivation of Sn(Oct)$_2$ by small amounts of copper(II), obtaining the PLA-*b*-PHEMA block copolymers in one single step. DSC measurements demonstrate phase segregation of the blocks after cooling from the melt as well as isolation from solution.

Keywords: Poly(HEMA), Poly(lactide), AGET, ATRP, biocompatible poly(ester), orthogonal polymerization, amphiphilic block copolymer.

Introduction

Acrylate- and lactone-based materials find application in the fabrication of polymer systems for a variety of biomedical application. While the former group offers access to non degradable, but readily tunable systems in terms of e.g. hydrophilicity[1,2], pH- and temperature-induced phase behavior[3] as well as loading with therapeutic agents[4] by simple variation of the acrylate substituent, the latter often offers access to a hydrophobic poly(ester) backbone, which is *in vivo* degradable to non-toxic components. This feature renders copolymers consisting of these blocks highly interesting for a number of biomedical applications, ranging from controlled release systems in drug delivery applications[5] to the fabrication of degradable surgical implants. Further advantages of the combination of these blocks include the selective introduction of large amounts of functional groups via the polyacrylate block, the generation of amphiphilic block copolymers[6] and partially biodegradable structures[7].

Nevertheless, only few examples for the synthesis of poly(ester)-block-polyacrylate copolymers via ROP of a lactone and controlled radical polymerization of an acrylate have been described in the literature so far[8,9,10,11]. From the vast number of potential comonomer combinations, lactide and 2-hydroxyethyl-methacrylate (HEMA) based polymers have not been combined to block copolymer systems to date, although each of these polymers

represents successfully employed and important materials with respect to biomedical applications. While poly(HEMA) exhibits excellent blood compatibility[12] and is furthermore widely used in the fabrication of intra ocular- and soft contact lenses, poly(lactic acid) is fully biocompatible and biodegradable[13].

However, combinations of poly(HEMA) and poly(ester) systems in general are not completely unknown and have been realized in a few works in different approaches. Copolymerization via α-ω-heterobifunctional acrylate macromonomers[14] with HEMA was exploited for the formation of degradable hydrogels. Ratner et. al. have synthesized these materials for tissue engineering applications from oligo(caprolactone) macromonomers, relying on ATRP copolymerization with 2-hydroxyethylmethacrylate[15]. Furthermore, poly(HEMA) homo- and block copolymers have proven to be suitable for grafting poly(caprolactone) and poly(lactide) onto the primary hydroxyl groups[16,17,18,19,20].

Examples for the use of poly(lactide)s as macroinitiators are rare. To date, the combination of ROP and ATRP has been applied successfully in the synthesis of star-block copolymers[21,22;23]. Recently, we reported on the synthesis of biocompatible multiarm star block copolymers based on a hyperbranched polyglycerol macroinitiator with 56 to 90 poly(HEMA) arms[24]. Storey et. al. were the first to use (α,ω)-chloride functionalized PLA as macroinitiators in an ATRP-based acrylate polymerization leading to triblock copolymers[25]. A first step toward the synthesis of linear poly(acrylate)/poly(ester) block copolymers with intended application in drug delivey was presented by Wulff et. al. and Guillaume et. al. in the form of poly(methyl methacrylate)-poly(vinyl sugars)[26] and poly(methyl methacrylate)-poyl(caprolactone)[8] block copolymerss. Unlike the synthetic strategy presented in this paper, the poly(ester) macroinitiators used in these works were obtained by postpolymerization modification of the poly(ester) end groups, resulting in a procedure comprising at least three synthetic steps. An elegant route to ATRP/ROP based A_2B_2 PCl/acrylate miktoarm polymers involving a double-headed, tetrafunctional initiator was presented by Hadjichristidis et. al.[27]. We modified the concept using a heterofunctional initiator[10] to combine dilactide and HEMA in a block copolymer without the use of hydroxyl protecting groups (Figure 66).

In this work we present the first example of a one-pot synthesis of a poly(lactide)-poly(HEMA) block copolymers by a synthetic two step ROP/ATRP strategy, involving a double-headed initiator. We demonstrate that the synthesis can be carried out in one pot without intermediate work-up.
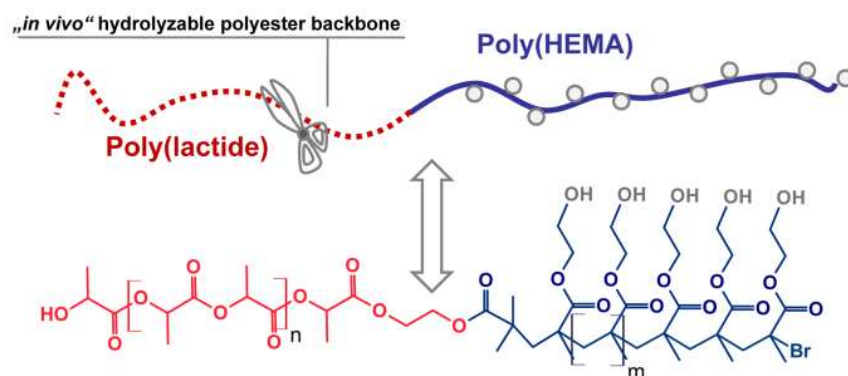
Figure 66: Poly(lactide)-*block*-poly(HEMA) copolymer structure, illustrating the potential use as, e.g., drug carrier.

Experimental Part

Instrumentation

NMR investigation: All ^{1}H and ^{13}C nuclear magnetic resonance spectra were recorded at 25°C, using a Bruker AC 300 (300MHz) or a Bruker AMX 400 (400 MHz) spectrometer. The spectra were measured in CDCl$_3$ and DMSO-d$_6$ and the chemical shifts are referred to the internal calibration on the solvents´ residual peaks. (^{1}H proton NMR signal: 2.50 ppm for DMSO-d$_6$, and 7.26 ppm for CDCl$_3$, ^{13}C carbon NMR signal: 39.52 ppm for DMSO-d$_6$, and 77.36 ppm for CDCl$_3$). For SEC measurements in DMF (containing 1 g/L of lithium bromide as an additive), an Agilent 1100 series system was used as an integrated instrument including three HEMA-based-columns ($10^5/10^3/10^2$ Å porosity) from MZ-Analysentechnik GmbH, a UV (275 nm) and a RI detector. Calibration was achieved with poly(styrene) standards provided by Polymer Standards Service (PSS). (MALDI-ToF MS) measurements were performed on a Shimadzu Axima CFR MALDI-ToF MS mass spectrometer, equipped with a nitrogen laser delivering 3 ns laser pulses at 337 nm. Dithranol (1,8-dihydroxy-9(10*H*)-Anthracetone, Aldrich 97%), was used as a matrix. Potassium triflate (Aldrich, 98%) was added for ion formation. The best results were obtained for samples prepared from chloroform solution by mixing matrix (10 mg/mL), polymer (10 mg/mL), and salt (0.1 N solution) in a ratio of 5:1:1. A volume of 0.9 μL sample solution was deposited on the MALDI target and allowed to dry at room temperature for 2 h prior to the measurement. Differential scanning calorimetry (DSC) measurements were carried out on a Perkin-Elmer 7 Series Thermal Analysis System with

auto sampler in the temperature range of 0 to 200 °C at a heating rate of 10 K/min. The melting points of indium (T_m=156.6 °C) and Millipore water (T_m=0 °C) were used for calibration.

Materials

All solvents were of analytical grade. In order to remove the stabilizer, THF used for dialysis was freshly distilled prior to use. HEMA was purified according to literature procedures prior to polymerization[24]. Stanneous 2-ethyl-hexanoate (Sn(Oct)$_2$) (99%) was purchased from Acros and used as received. Deuterated chloroform-d$_1$ and DMSO-d$_6$ were purchased from Deutero GmbH and dried and stored over molecular sieves. DMSO and DMSO-d$_6$ were degassed by 3 freeze pump thaw cycles without previous drying of the solvent. Dilactide was purchased from Purac®/Gorinchem (Netherlands) and recrystallized 3 times from dry toluene and stored under vacuum prior to use. Dialysis of block copolymers was performed with Cellu Sep®H1 membranes with a molecular weight cutoff of 1000 g/mol.

Initiator Synthesis

2-Hydroxyethyl 2-bromo-2-methylpropanoate (HBMP):

93.06g (1.50 mol) of dry glycol and 6.48 g (0.064 mol) of dry triethylamine were placed in a 500 mL round bottom flask, kept under a nitrogen atmosphere. Within 2 hours, 14.6 g (0.063 mol) of 2-bromo-isobutyryl bromide were added at 0-5°C. After an additional hour the reaction mixture was slowly warmed to room temperature and stirred over night. The mixture was warmed to 50°C for 15 minutes. 200 mL of water were added and extracted with 3x80 mL of chloroform. The organic phase was subsequently washed with 50 mL of 1n hydrochloric acid, saturated sodium carbonate solution and brine. After drying over magnesium sulfate, the solvent was evaporated and the product was purified by distillation in vacuum (83°C/0.1mbar). 7.79 g (58%) of a colorless oil were obtained. ^{1}H-NMR (CDCl$_3$, 300MHz) δ^1H/ppm: 1.85 (s, 1H, -OH); 1,97 (s, 6H, -CH_3); 3,89 (t, ^3J =4.5Hz, 2H, -CH_2OH); 4.33 (t, ^3J=4.5Hz, -OCH_2-)

General Procedures for the Synthesis of the first block:

Poly(L-lactide)/Poly(D-lactide) macroinitiators (Route A) via a two-step approach.

2-hydroxyethyl 2-bromo-2-methylpropanoate and lactide were charged to a Schlenk-tube at predetermined molar ratio (see Table 11), sealed with a rubber septum and repeatedly flashed with argon after evacuation. Freshly distilled toluene (2 mL/g dilactide) was added via a syringe and the tube was immersed in an oil bath heated to 120°C. Polymerization was initiated after 2 minutes by injecting a 5% solution of the catalyst $Sn(Oct)_2$ in toluene corresponding to 0.1% of the monomer. Polymerization was quenched after 18 h by cooling to room temperature. An aliquot of the sample for conversion analysis was harvested prior to precipitation in excess methanol. The polymer was collected by centrifugation or filtration and taken up in CH_2Cl_2 for a second precipitation in diethyl ether. ^{1}H-NMR ($CDCl_3$, 400MHz) δ^1H/ppm: 1.57 (d, ^3J =7.0 Hz CHCH_3, poly(lactide) chain); 1.91 (s, BrC(CH_3)$_2$; 4.34 (q, ^3J =7.0 Hz HOCH(CH$_3$)); 4.31-4.46 (m, -OCH_2CH_2O-); 5,15 (q, ^3J =7.0 Hz CH(CH$_3$), poy(lactide) chain).

General Procedures for the Synthesis of the second block:

ATRP of HEMA in DMSO (Route A) via a two step approach.

In a typical polymerization, poly(lactide) macroinitiator (MI) (0,5 g), bipyridine[L] and HEMA[M] were placed in a Schlenk tube in the ratio of MI[1]:L[2]:M[50] and subsequently dissolved in 4 mL of DMSO. Argon was bubbled through the mixture for 20 minutes, followed by degassing in three freeze pump thaw cycles. The mixture was immersed in an oil bath and heated to 80°C. The polymerization was initiated by adding an equivalent of CuCl(I) under argon counter flow. The reaction vessel was subsequently sealed with a rubber septum. Polymerization was quenched rapidly by cooling by immersing the tube in an ice bath (upon which the polymer remained soluble). The mixture was diluted with THF and flashed over a short column with neutral aluminum oxide to remove the copper catalyst. Residual HEMA monomer was removed by precipitation in methanol. To remove traces of low molecular weight compounds for DSC analysis, the block copolymer was dialyzed in $CHCl_3$/MeOH (1:1) or THF for 2 days with a molecular weight cutoff of 1000 g/mol. After drying in vacuum, a white solid was obtained. ^{1}H-NMR (DMSO-d$_6$, 400MHz) δ^1H/ppm: 0.70-1.10 (m, C(CH_3)(COOCH$_2$CH$_2$OH)); 1.28 (d, ^3J =7.0 Hz HOCH(CH_3), poly(lactide) *term. unit*); 1.46 (d, ^3J = 7.0 Hz OCH(CH_3), poly(lactide) chain), 1.70-2.05 (m, -CH_2C(CH$_3$)(COOCH$_2$CH$_2$OH)); 3.58 (s, -COOCH$_2$CH_2OH); 3.89 (s, -COOCH_2CH$_2$OH); 4.20 (p, ^3J =7.0 Hz HOCH(CH$_3$); poly(lactide) *term.*

unit); 4.82 (s, -COOCH_2CH_2OH); 5.20 (q, ^3J =7.0 Hz CH(CH$_3$); poy(lactide) chain); 5.48 (d, ^3J =6.0 Hz HOCH(CH$_3$), poly(lactide) *term. unit*).

Modification of the synthetic route to a one pot procedure (Route B):

General Procedure for the ROP of Lactide with subsequent ATRP of HEMA in DMSO.

The polymerization of lactide (0.5g) was conducted in a rubber sealed Schlenk tube, as described above. After 18h the polymerization was quenched and toluene, which was used as the polymerization medium, was removed by freeze drying. Subsequently, bipyridine[L] and HEMA[M] were added in a ratio of MI[1]:L[2]:M[50] and subsequently dissolved in 4 mL of DMSO-d$_6$. After degassing the mixture by three freeze-pump thaw cycles, a mixture of Cu(I)Cl[1]:Cu(II)Cl$_2$ [0.05]was added to the preheated reaction mixture (80°C) under an argon stream. Polymerization and work-up of the samples were carried out as described above.

Results and Discussion

Poly(HEMA) and Poly(lactide) represent two highly established polymer materials in the field of biocompatible polymers for medical and healthcare applications. Despite many interesting implications of such a topology, these polymers have not yet been combined to block copolymers. ATRP of acrylates and ROP of cyclic esters are fully orthogonal polymerization methods, which motivated us to combine both techniques. 2-Hydroxyethyl-2-bromo-2-methylpropanoate (HBMP), which was introduced by Matyjaszewski et. al.[8], was chosen as an asymmetric bifunctional initiator for our block copolymer synthesis. The primary nature of the hydroxyl group and the tertiary alpha-carboxy-halogen ensures fast initiation for both ROP and ATRP, respectively, rendering the compound suitable as a double-headed initiator. The advantage of this approach lies in the redundance of protective groups for the poly(HEMA) backbone, when starting with a poly(lactide)-first strategy that gives access to an α-hydroxy, ω-bromoester-telechelic macroinitiator for ATRP. Limited solublity of the poly(lactide)-based macroinitiator in polar solvents and solvent mixtures like water/methanol, methanol[28], 1-propanol/MEK[29] necessitated substitution of these conventional solvents known to be suitable for ATRP of HEMA. DMSO is a rarely used, but represents a good solvent for the ATRP of HEMA. It guarantees both sufficient solubility of

the stereoregular poly(*L*-lactide) (PLLA)/poly(*D*-Lactide) (PDLA) macroinitiator and good reactivity for the polymerization of HEMA.

Scheme 7: Synthesis of Poly(lactide)-*block*-Poly(HEMA) copolymers by ring-opening polymerization of lactide initiated from the hydroxyl moiety of the initiator and subsequent ATRP of HEMA, initiated by the isobutyryl bromide part of the α-haloester.[a]
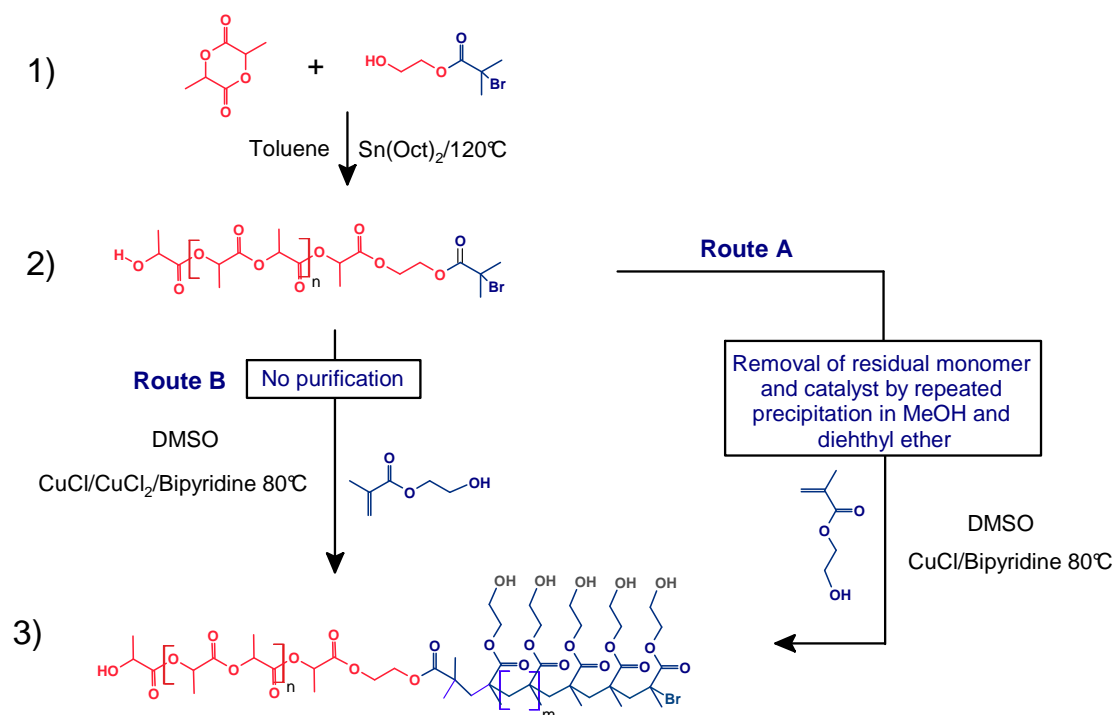
[a]Two routes, with (route A) and without prior work-up of the macroinitiator (route B), have been employed successfully in the synthesis of block copolymers. Molecular characterization data of the polymers obtained are summarized in Table 1.

The use of a protective group (e.g., the trimethyl silyl group (TMS)[30]), which would permit performing the polymerization in a less polar solvent, would require further synthetic steps that were avoided in this manner. Both synthetic approaches developed in the current paper are shown in Scheme 7. The two-pot approach involving purification of the PLLA-block will be discussed first (route **A**) in the ensuing paragraph, since it permitted detailed characterizion of the telechelic PLLA-block precursor with respect to full terminal functionalization. Subsequently, it will be demonstrated that the polymerization can also be carried out in one reaction vessel, omitting the intermediate purification step (route **B**, Scheme 11).

A) Two-Pot approach; Route A

MALDI-ToF spectrometry is a crucial method to support quantitative functionalization of all polymer chains formed and thus to monitor the first step of the block copolymer synthesis. A typical MALDI-ToF spectrum, obtained after formation of the PLLA-block, is presented in Figure 67. The spectrum indicates complete attachment of the bromoisobutyryl group to the PLA backbone. This is also confirmed by comparison of NMR-signal intensities from the α– with the ω-telechelic endgroup of the PLA formed. The extent of transesterification was minimized by thermal quenching of the reaction mixture before reaching the polymer/monomer equilibrium. Consequently, narrow PDIs (1.09-1.17, Table 11) and only a minor subdistribution of PLLA species with a non-even number of lactic acid repeat units is observed in the MALDI-ToF spectrum. As can be shown by ^{1}H-NMR spectra and is also indicated by the MALDI-ToF data, molecular weights of the linear poly-*L*-lactide macroinitiators were overestimated by SEC in DMF (calibrated with polystyrene standards). A correction factor of 0.81 for molecular weights determined by SEC appears to be appropriate for the analyzed mass range (2000-8000 g/mol), assuming that the MALDI-ToF values are representative of the actual molecular weights and molecular weight distribution. This is not unreasonable in our case, since the PLA-samples possess narrow molecular weight distribution and the MALDI-ToF spectrum (Fig. 2) is symmetrical.

In the usual procedure (Scheme 7: Route A), prior to polymerization of the second block, poly(lactide)s were precipitated in 1) methanol and 2) diethyl ether to remove residual (lactide) monomer and catalyst.
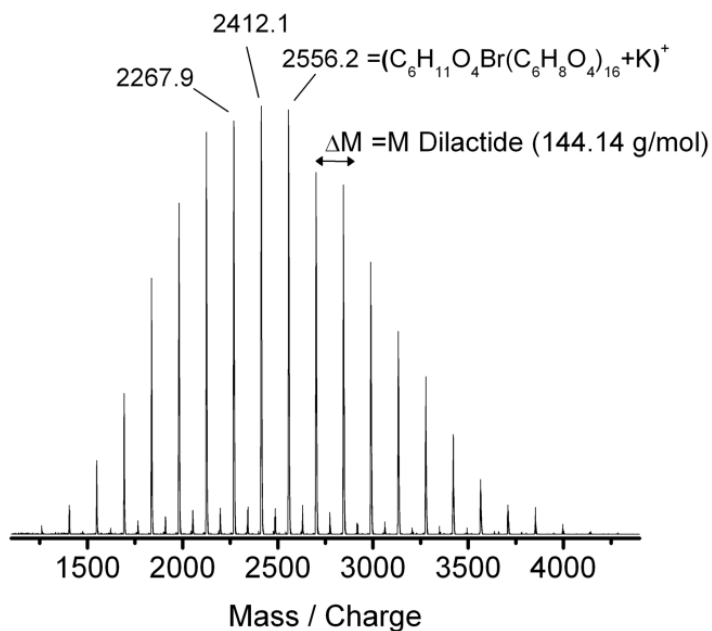
Figure 67. MALDI-ToF spectrum of PLLA-MI 2, supporting quantitative attachment of the bifunctional initiator to the PLA block.

To promote fast initiation and quantitative attachment of HEMA to the poly(lactide) macroinitiator, we used the mixed halide exchange technique, changing from bromine to chlorine[31]. ATRP conducted with CuCl(I) instead of CuBr(I) in DMSO was sufficiently fast to guarantee short polymerization times, as could be shown by a time-dependent conversion analysis in DMSO-d_6 (Figure 68). In fact, we were not able to monitor the onset and early phase of the polymerization and the first value obtained after 5 minutes already revealed a conversion of 32-34% which is fairly high compared to a total conversion of aprox. 39 % (90 min). Although we assume polymerization kinetics of living nature in the early phase of the reaction, the polymerization rate significantly decreases in the examined period as the $\ln([M_0]/[M_t])$ vs conversion plot in Figure 68 indicates. Apart from bi-or monomolecular termination reactions, aerial oxidation, unintentionally introduced during sample harvesting, can not totally be precluded. It is important to note that the polymer nature of the PLA-macroinitiator had no effect on the ATRP reaction rate, which is a consequence of its excellent solubility in DMSO at 80°C, i.e., at the polymerization conditions employed for the synthesis of the poly(HEMA) block. Thus, we were able to use the well-established combination of Cu(I)Cl and 2,2'-bipyridine as ATRP-mediating transition metal complex. Although no copper (II) salt was added as regulating deactivator at the beginning of the

polymerization, polydispersities could be kept low (Mw/Mn = 1.21 to 1.30; cf. Table 11) and no significant amount of prematurely terminated macroinitiator was detected.
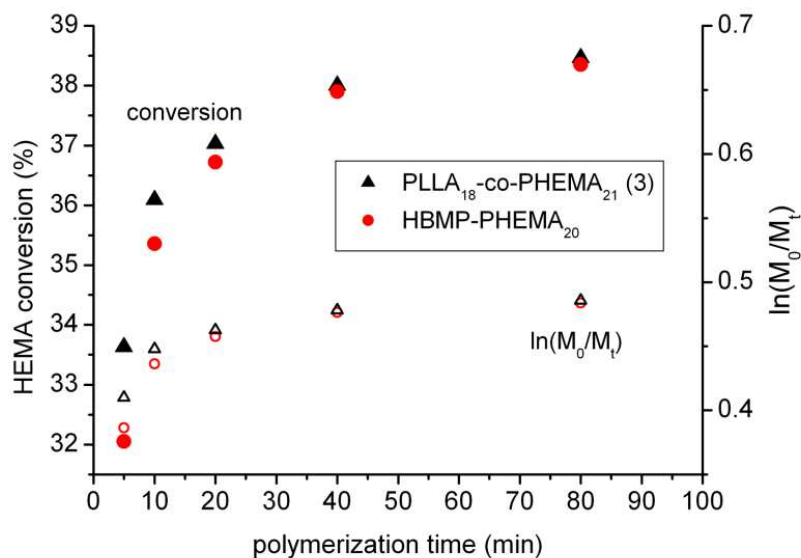

Figure 68: Development of HEMA-conversion and $\ln([M_0]/[M_t])$ in the course of the ATRP, using 2-hydroxyethyl-2-bromo-2-methylpropionate (HBMP) (circles) and a PLLA-HBMP-macroinitiator (triangles).
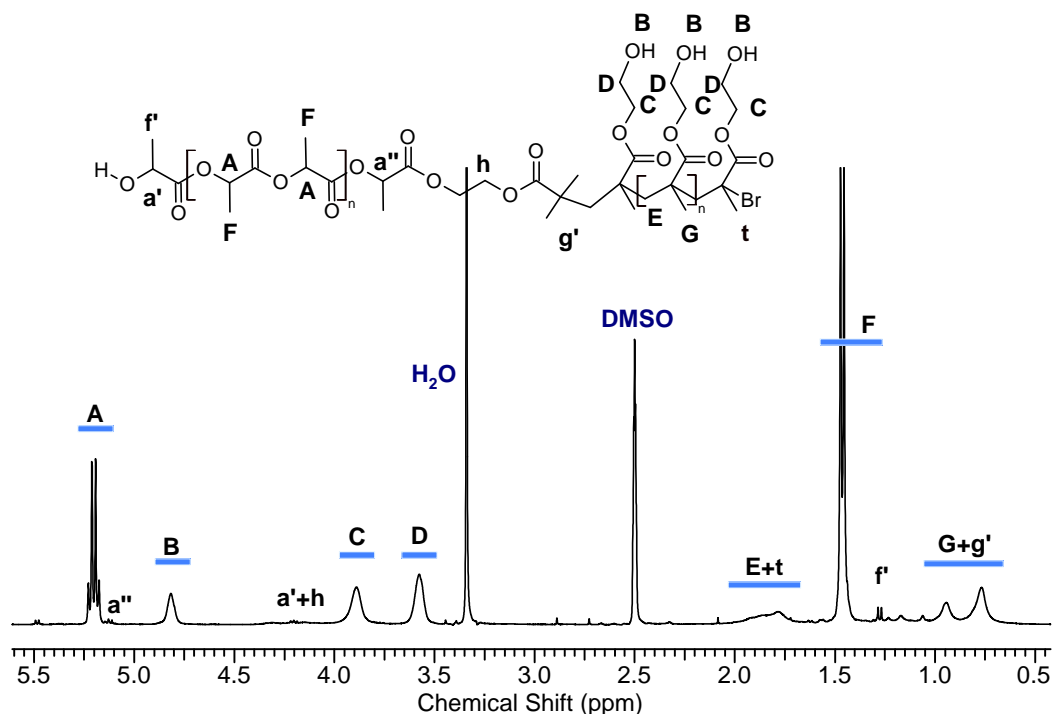

Figure 69: ^{1}H-NMR spectrum (400MHz) of PDLA$_{30}$-b-PHEMA$_{33}$ in DMSO-d$_6$ (after purification by dialysis).
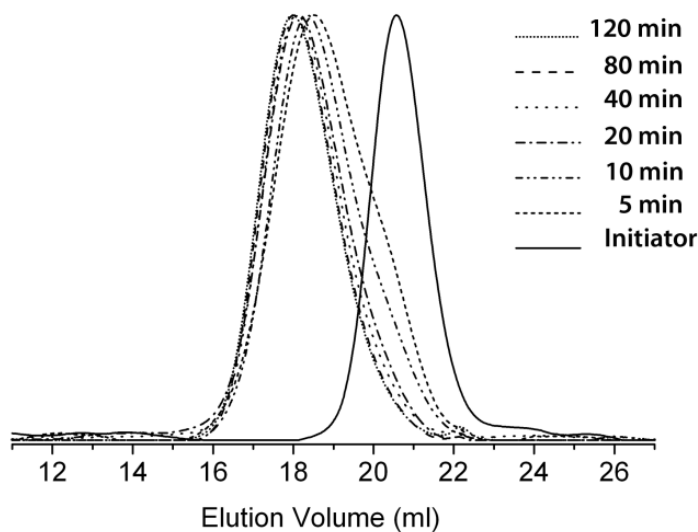
Figure 70. Kinetic study of the chain growth of PLLA-MI 2 to $PLLA_{18}$-*b*-$PHEMA_{xx}$(5).

SEC data confirm complete attachment of the second block to the PLA macroinitiators (PLA-MI) with a symmetrical, monomodal molar mass distribution of the block copolymers. Figure 70 shows a clean shift of the distribution mode toward lower elution volumes. Only the first samples harvested (after 5, respectively 10 min polymerization time) show a small shoulder toward higher elution volumes (lower molecular weights). Since we employed the mixed halide exchange technique to prevent slow initiation, we assume that this phenomenon is attributed to a slow propagation immediately after initiation. This could be explained by an enhancement in the reactivity of the chain ends with increasing amount of HEMA units attached, since the reaction media DMSO is presumably a better solvent for PHEMA (homopolymer is readily soluble in DMSO at room temperature) than for poly(iso-lactide) which is only poorly soluble in DMSO (at room temperature and regarding the molecular mass range presented). Hence, this effect is strongest in the early phase of the reaction where poly(lactide)s with only few HEMA units attached are still present. Nevertheless it can be concluded that no undesired homopolymer is present. Molar mass evaluation by SEC (in DMF, calibration with polystyrene standards), shows an overestimation of molecular weights of the PLA-PHEMA block copolymerss compared to the more reliable results obtained from ^{1}H-NMR spectra which exhibits well distinguishable signals from both block copolymers The ^{1}H NMR structure/signal assignment is shown in Figure 69. The terminal Groups of the poly(lactide) are well distinguishable from the backbone signals in this well resolved

spectrum (the respective chemical shifts are available in the experimental section). Furthermore, no residual HEMA and dilactide monomer could be observed after work up.

B) One-Pot approach; Route B

Since the introduction of the initiator for both blocks in the first step avoids a post polymerization functionalization with an ATRP initiator, it is an intriguing issue, whether one can further simplify the synthesis to a two step, yet *one-pot* procedure, in which a prior purification of the poly(lactide) macroinitiator is redundant. As has been pointed out before, the Sn(Oct$_2$) promoted ring-opening polymerization is known to be accompanied by side reactions like inter- and intramolecular transesterifications, since Sn(Oct$_2$) acts as a transesterification catalyst, when approaching the polymer/monomer equilibrium. Therefore, quenching of the polymerization prior or close to completion of the monomer consumption is crucial to obtain well-defined PLA. In order to circumvent the intermediate purification step, it was essential, that residual lactide monomer and Sn(Oct)$_2$ catalyst would not be reactive during the ATRP of HEMA. This represents a particular challenge in this case, since it has been shown in numerous works that the hydroxyethyl group of HEMA enabled facile and even simultaneous grafting and polymerization of lactones onto the poly(acrylate) backbone.[16-20] In other words, for the synthesis of block copolymers, further reaction of residual lactide monomer during the ATRP of HEMA by active Sn(Oct)$_2$ species has to be prevented.
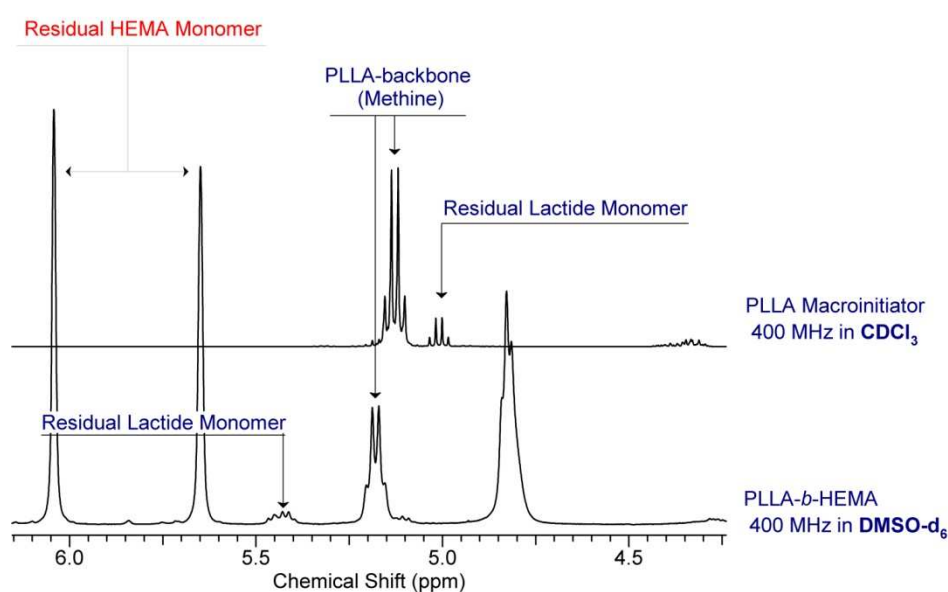

Figure 71: ^{1}H NMR Spectra PLLA-MI 6 of and the corresponding block copolymer PLLA$_{18}$-b-PHEMA$_{29}$ prepared thereof.

Sn(Oct)$_2$ itself has been discovered to act as an active reducing agent in the special AGET ATRP[10,32,33] polymerization, which permits the use of very small amounts of copper. In classic AGET ATRP, Cu(II), which is generated by oxidation throughout the reaction, is reduced by Sn(II) and thereby regenerates the active Cu(I) species. In our approach, we employed the AGET principle in a reverse manner to oxidatively deactivate the Sn(II) species by addition of Cu(II) in slight excess (2-3 times) to the employed amount of Sn(Oct)$_2$ (cf. Scheme 11: Route B). Detailed NMR studies show that in this case the amount of residual lactide monomer does not decrease throughout the ATRP of HEMA. Figure 6 shows the lactide/PLLA methyl group related groups of protons, which both appear as a quartet and are well distinguishable in the NMR solvent employed (δ^1H/ppm of dilactide OCOC*H*(CH$_3$) (1. CDCl$_3$ = 5.03; 2. DMSO-d$_6$= 5.44). Furthermore, no signals characteristic for the grafting of lactide onto the PHEMA backbone were observed.

SEC evidenced (Figure 72) that chain extension of the PHEMA block from the PLLA macroinitiator proceeded smoothly in the one-pot case, without the presence of unreacted PLLA macroinitiator via route B. Both conversions and polydispersities are low (1.18-1.27), and comparable to those obtained via route A after removal of residual monomer/catalyst by precipitation (Table 11).
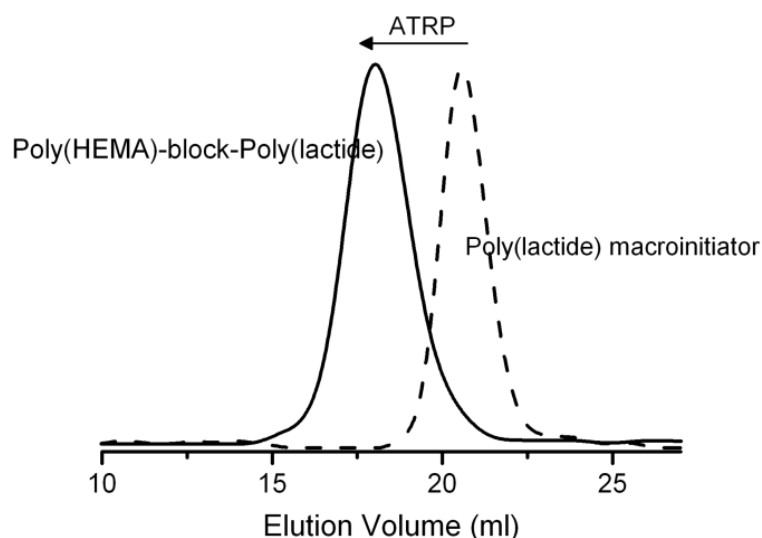

Figure 72: SEC-elugram of: (A) PLLA-MI 2 which is converted into PLLA$_{18}$-*b*-PHEMA$_{29}$ in a one-pot reaction.

In general all polymers, regardless of the discussed synthetic pathway were obtained as white powders. This indicates complete removal of the copper salts used in the ATRP by filtration and/or dialysis.

Table 11: Molecular weights and composition data for PLA based macroinitiators and the resulting PLLA-*b*-PHEMA block copolymers

Polymer	Initiator (I)	Monomer (M)	M/I	M_N theo. (100% conv.)	M_N (NMR)	Polym. Time	Conv. (NMR)	M_N (SEC)	PDI	Composition (NMR)
PLLA-MI 1	2-HBMP	*L*-Lactide	20	3100	2980	18 h	0.91	3500	1.17	PLLA$_{19}$
PLLA-MI 2	2-HBMP	*L*-Lactide	20	3100	2620	18 h	0.85	3200	1.09	PLLA$_{17}$
PLLA-MI 3	2-HBMP	*L*-Lactide	50	7420	6910	18 h	0.93	8600	1.17	PLLA$_{46}$
PDLA-MI 4	2-HBMP	*D*-Lactide	30	4540	4500	18 h	0.99	6500	1.15	PDLA$_{30}$
PLLA-MI 5	2-HBMP	*L*-Lactide	40	5980	5320	18 h	0.89	5800	1.08	PLLA$_{37}$
PLLA-MI 6	2-HBMP	*L*-Lactide	20	3090	2780	18 h	0.90	3400	1.07	PLLA$_{27}$
PHEMA#	2-HBMP	HEMA	50	6930	2750	80 min	0.4	5900	1.25	PHEMA$_{20}$
PLLA-*b*-PHEMA 1	PLLA-MI 1	HEMA	50	9490	6510	320 min	0.54	10800	1.30	PLLA$_{19}$-*b*-PHEMA$_{26}$
PLLA-*b*-PHEMA 2*	PLLA-MI 2	HEMA	50	9130	6150	47 h	0.53	10200	1.27	PLLA$_{18}$-*b*-PHEMA$_{29}$
PLLA-*b*-PHEMA 3#	PLLA-MI 2	HEMA	50	9130	5100	80 min	0.38	8400	1.21	PLLA$_{18}$-*b*-PHEMA$_{21}$
PLLA-*b*-PHEMA 4	PLLA-MI 2	HEMA	50	9130	5140	160 min	0.38	8400	1.28	PLLA$_{18}$-*b*-PHEMA$_{21}$
PLLA-*b*-PHEMA 5	PLLA-MI 3	HEMA	100	19900	---	7 h	---	13200	1.32	PLLA$_{46}$-*b*-PHEMA$_{XX}$
PLLA-*b*-PHEMA 6	PLLA-MI 2	HEMA	50	9130	---	7 h	---	9700	1.28	PLLA$_{18}$-*b*-PHEMA$_{XX}$
PDLA-*b*-PHEMA 7	PDLA-MI 4	HEMA	70	13600	8750	320 min	0.46	13100	1.27	PDLA$_{30}$-*b*-PHEMA$_{33}$
PLLA-*b*-PHEMA 8*	PDLA-MI 5	HEMA	140	23500	14900	80 min	0.51	22000	1.24	PLLA$_{37}$-*b*-PHEMA$_{74}$
PLLA-*b*-PHEMA 9*	PDLA-MI 6	HEMA	70	11900	6550	80 min	0.41	9100	1.18	PLLA$_{18}$-*b*-PHEMA$_{29}$

* synthesized without prior work-up of the macroinitiator in a one pot reaction

polymerization in DMSO-d$_6$ with conversion analysis

DSC-Analysis

Differential scanning calorimetry was conducted with a selected block copolymer sample with nearly equal block ratios of stereoregular PDLA and PHEMA, i.e., PDLA$_{30}$-*b*-PHEMA$_{33}$. The behavior of this material with two strongly incompatible blocks was of particular interest

in this study in order to obtain information on phase segregation. Furthermore, the corresponding PLA macroinitiators have also been examined. In case of the block copolymer, solvent and monomer free samples were obtained by careful drying after dialysis in THF, while the PDLA macroinitiator was examined after purification by repeated precipitation in 1. methanol and 2. diethyl ether and subsequent drying in vacuum. The theoretical enthalpy of fusion (ΔH_f) for a pure PDLA crystal (100% degree of crystallization) was calculated to be 93.7 J/g by extrapolation by Fischer et. al.[34]. The crystalline PDLA macroinitiator exhibits a distinct melting peak at 156°C (Figure 73) and an initial enthalpy of fusion of 59 J/g, which could be increased to 67 J/g by keeping the sample at 120 °C for extended periods. This represents a high degree of crystallization. These results are in good agreement with the high mobility of the relatively short polymer chains (M_N=4.500g/mol), resulting in a high crystallization rate that is typical for low molecular weight PDLA and PLLA[35].
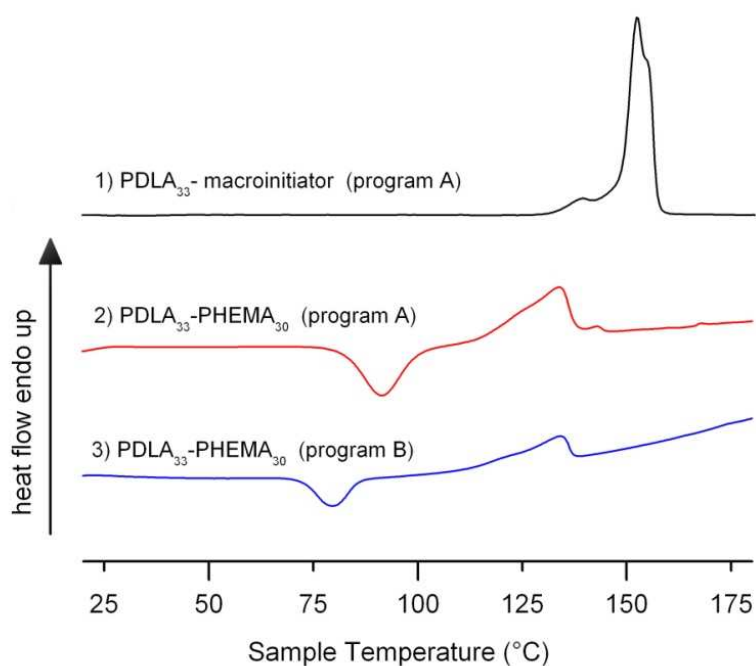
Figure 73: Heating traces (2nd heat run) of PDLA macroinitiator 1) and the PDLA$_{30}$-PHEMA$_{33}$ block copolymers 2) & 3).

The block copolymer was examined employing two different temperature programs. Program A (Table 12) involved a tempering step at 120 °C to promote crystallization, while program B was conducted by direct heating and cooling at 10°C/min for comparison (Figure 73). The heating trace of the macroinititor does not exhibit a recrystallization peak in the heating run, suggesting completion of the crystallization during the previous cooling scan. This is not the case for the block copolymer which shows recrystallization exotherms during

the heating process at A) 91.4 °C and B) 79.5°C with matching crystallization/melting enthalpies.

Table 12: Thermal properties of the the $PDLA_{30}$-b-$PHEMA_{33}$ block copolymer

Polymer Sample	Program	Run	T_m (°C)	$\Delta H_{m'}$ (J/g)	ΔH_m (J/g PDLA)	X_m [§]
$PDLA_{30}$-MI	$A^{(+)}$	1	156.1	59.0	59.0	0.63
		2	152.4	67.9	67.9	0.72
		3	152.6*	65.6	65.6	0.70
$PDLA_{30}$-b-$PHEMA_{33}$	$A^{(+)}$	1	137.4	28.5	51.9	0.61
		2	133.7	20.1	36.6	0.43
		3	134.1	21.1	38.4	0.45
$PDLA_{30}$-b-$PHEMA_{33}$	$B^{(\#)}$	1	135.0	31.3	57.0	0.67
		2	134.3	18.3	33.3	0.39
		3	135.2	16.9	30.8	0.36

*Double melting peak/middle of two melting peaks

[+]1) Program A: heat from 0°C to 200°C @20°C/min 2) cool from 200 to 120 °C @10°C/min 3) hold @120 for 15 min 4) cool from 120°C to 0°C

[#]1) Program B: heat from 0°C to 200°C @10°C/min 2) cool from 200 to 0 °C @10°C/min

[§]degree of crystallization

The initial (first heat run) degrees of crystallization (X_m) (61 %) of the PDLA block copolymer correspond to the macroinitiator homopolymer. Interestingly Tgs were not observed for the examined homo and block copolymerss under employed reaction conditions. The $PDLA_{30}$-MI showed a significant endothermic thermal relaxation peak during the first heating run at 56.1°C but no step change in heat capacity could be observed in the second or third. As expected, the PDLA-PHEMA block copolymer melts over a broader range (113-138 °C) and at a lower temperature compared to the macroinititor, which exhibits a rather sharp melting peak at around 134 °C. In case of the blockcopolymers, a glass transition of the PHEMA block might be obscured by the early onset of the endothermic melting peak of the poly(lactide)-block. Since PHEMA is a noncrystalline polymer, the crystallization enthalpy can be fully attributed to the PDLA block, which represents 50.2 wt. % of the total block copolymer in this case. The degree of crystallization of the block

copolymer samples from the second and third heating run still leads to rather high melting enthalpies corresponding to a degree of crystallization of the poly(lactide) block of 36 to 45 %. In view of the special structure of the present blockcopolymer, compromising a cleavable poly(ester)backbone on one hand and a polyacrylate backbone with a large number primary hydroxyl groups on the other, transesterification during thermal treatment (up to 200°C) is a non-negligible issue. In this case, sample PDLA$_{30}$-*b*-PHEMA$_{33}$ revealed a significant broadening in the molecular weight distribution (M$_n$: 8750; PDI: 1.27 → M$_n$: 7300; PDI: 2.65 (monomodal)) after 3 heating/cooling cycles. Nevertheless these results confirm that the novel PLA-*b*-PHEMA block copolymers are poorly miscible and thus present in a phase-segregated state in the solid at room temperature. Detailed studies on the thermal properties of the series of novel block copolymers are in progress.

Conclusions

We have developed a rapid two-step, one pot strategy to new poly(lactide)-*block*-poly(HEMA) block copolymers, combining two highly established biocompatible materials. The amphiphilic, well-defined AB diblock structures are obtained by the use of a hetero-bifunctional initiator, combining two controlled, fundamentally different polymerization techniques: (i) ROP of dilactide and (ii) ATRP of HEMA, resulting in low polydispersities (1.18-1.3). To the best of our knowledge, such block copolymers have not been prepared to date.

Chain extension of the poly(lactide) macroinitiator with poly(HEMA) without prior work-up and removal of residual Sn(Oct)$_2$ catalyst and unreacted lactide monomer was possible by oxidative deactivation of the Sn-catalyst with small amounts of Cu(II) salts in analogy to the AGET principle. In a more general sense, this work demonstrates that the use of poly(lactide)-based macroinitiators for the ATRP of a monomer of a very different polarity is possible without additional protection/deprotection steps. Therefore this method represents a new, general approach for the synthesis of hydrophobic poly(ester)/hydrophilic polyacrylate copolymers in a convenient two step sequence.

As expected from the different chemical nature of the blocks, phase segregation is observed, leading to crystalline domains of the apolar PLA in the hydrophilic poly(HEMA) matrix. The novel amphiphilic block copolymer structures can be used for the transport and release of therapeutic agents, covalently bound to the functional polymer backbone in a

poly(lactide) matrix. This could result in a release behavior superior to plain incorporation by physical mixing of the biodegradable polymer matrix and the therapeutic agent.

References

[1] Amado, E.; Augsten, Ch.; Mäder, K.; Blume, A.; Kressler, J *Macromolecules* **2006,** *39,* 9486-9496

[2] Save, M.; Weaver, J. V. M.; Armes, S. P.; McKenna, P. *Macromolecules,***2002,** *35,*1152-1159

[3] Feil, H.; Bae, Y. H. Feijen, J.; Kim, S. W. Macromolecules **1993***, 26,* 2496-2500

[4] Barz, M.; Tarantola, M. Fischer, K.; Schmidt, M.; Luxenhofer, R.; Janshoff, A.; Theato, P. Zentel, R. *Biomacromolecules* **2008,** *9,* 3114–3118

[5] Jeong, B.; Bae, Y.H.; Lee,' D.S.; Kim, S. W. *Nature* **1997**, **388**, 860-862

[6]. Weaver, J. V. M; Bannister, I.; Robinson, K. L.; Bories-Azeau, X.; Smallridge, M; McKenna; P.; Armes, S. P. *Macromolecules* **2004,** *37,* 2395-2403

[7] Noga, D. E. ; Petrie, T. A. ; Kumar, A. ;Weck, M. ; García, A. J. Collard, D. M. *Biomacromolecules* **2008,** *9,* 2056–2062

[8] Jakubowski, W.; Lutz, J. F.; Slomkowski, S.; Matyjaszewski K. *J. Polym. Sci. A: Polym. Chem* **2005**, *43*, 1498–1510

[9] Schappacher, M.; Fur, N.; Guillaume, S. M.; *Macromolecules* **2007,** *40,* 8887-8896

[10] Jakubowski, W.; Matyjaszewski; K. *Macromol. Symp.* **2006**, 240, 213–223

[11] Messman,J. M.; Scheuer, A. D.; Storey, R. F.; *Polymer* **2005**, *46*, 3628-3638

[12] Prasitsilp, M.; Siriwittayakorn, T.; Molloy, R.; Suebsanit, N.; Siriwittayakorn, P; Veeranondha, S. *Journal of Material Science: Materials in Medicine* **2003**, 14, 595-600

[13] Vert, M.; Li. S. M.; Spenlehauer, G.; Guerin, P. *Journal of Material Science: Materials in Medicine* **1992**, 3, 432-446

[14] Barakat, I.; Dubois, Ph. Jérôme. R.; Teyssié, Ph.; Goethals, E.; *J. Polym. Sci. A: Polym. Chem.* **1994**, 32, 2099-2110

[15] Atzet, S.; Curtin, S.; Trinth, P.; Bryant, S.; Ratner, B. *Biomacromolecules* **2008**, 9 3370-3377

[16] Ydens, I.; Degee, P.; Dubois, P.; Libiszowski, J.; Duda,A: Penczek, S. *Macromol. Chem. Phys.* **2003**, 204, 171–179

[17] Lee, H.; Matyjaszewski, K.; Yu-Su, S.; Sheiko S.S. *Macromolecules* **2008**, *41*, 6073-6080

[18] Zhao, C.; Wu, D.; Huang, N.; Zhao, H. *J. Polym. Sci. A: Polym. Phys.* **2008**, 46, 589-598

[19] Wu, D.; Yang, Y.; Cheng, X.; Liu, L.; Tian, J.; Zhao, H. *Macromolecules* **2006**, 39, 7513-7519

[20] Hellaye, M. L.; Lefay, C.; Davis, T. P.; Stenzel, M. H.; Barner-Kowollik, Ch. *J. Polym. Sci. A: Polym. Chem.* **2008**, *46*, 3058–3067

[21] Hedrick, J. L.; Trollsas, M.; Hawker, C. J.; Atthoff, B.; Claesson, H.; Heise, A; Miller, A.D.; Mecerreyes, D.; Jérome, R.; Dubois, Ph. *Macromolecules* **1998**,31 8691-8705

[22] Johnson, R. M.; Fraser, C.L. *Macromolecules* **2004,** *37,* 2718-2727

[23] Zhao, Y.; Shuai, X.; Chen, Ch.; Xi, F**.** *Macromolecules* **2004,** *37,* 8854-8862

[24] Chen, Y.; Shen, Z.; Barriau,E.; Kautz,H.; Frey, H. *Biomacromolecules* **2006,** *7*, 919-926

[25] Messman,J. M.; Scheuer, A. D.; Storey, R. F.; *Polymer* **2005**, *46*, 3628-3638

[26] Chen, Y. M.; Wulff, G. *Macromol. Rapid Commun.* **2002**, *23*,59-63

[27] Priftis, D.; Pitsikalis, M.; Hadjichristidis, N. *J. Polym. Sci. A: Polym. Chem.* **2007,** *45*, 5164–5181

[28] Robinson, K.L.; Khan, M. A.; de Paz Báñez, M.V.; Wang, X.S.; Armes, S. P. *Macromolecules* **2001,** *34,* 3155-3158

[29] Beers, K. L.; Boo, S.; Gaynor, S. G.; Matyjaszewski, K. *Macromolecules* **1999,** *32,* 5772-5776

[30] Beers, K. L.; Gaynor, S. G. Matyjaszewski, K.; Sheik, S. S.; Möller, M. *Macromolecules* **1998,** *31,* 9413-9415

[31] Matyjaszewski, K.; Shipp, D. A.; Wang, J.L.; Grimaud, T.; Patten, T.E**.** *Macromolecules* **1998,** *31,* 6836-6840

[32] Jakubowski, W.; Min, K.; Matyjaszewski, K. *Macromolecules*, **2006**, *39*, 39–45

[33] Min, K.; Gao, H.; Matyjaszewski, K. *J. Am. Chem. Soc.* **2005**, *127*, pp 3825–3830

[34] Fischer, E. W., Sterzel, H. J.; Wegner, G. *Kolloid Z. Z.Polym.* **1972***, 251,*980-990

[35] Pan, P.; Kai, W.; Zhu, B.; Dong, T.; Inoue, Y. *Macromolecules* **2007,** *40,* 6898-6905

3.2 Poly(isoglycerol methacrylate)-*b*-poly(D- or L-lactide) Copolymers: A Novel Hydrophilic Methacrylate as Building Block for Supramolecular Aggregates

*Florian K. Wolf, Anna M.Hofmann and Holger Frey*

Abstract

On the basis of a new acetal-protected glycerol monomethacrylate monomer (cis-1,3-benzylidene glycerol methacrylate/BGMA) a series of potentially biocompatible and partially biodegradable homo- and block copolymers were synthesized. ATRP polymerization of BGMA yielded well-defined polyacrylates with pendant benzylidene acetal groups and high glass transition temperatures (115-130 °C).This hydrophobic poly(cis-1,3-benzylidene glycerol methacrylate) could be readily transformed into the hydrophilic and water-soluble poly(1,3-dihydroxypropyl methacrylate), referred to as poly(isoglycerol methacrylate) (PIGMA). It exclusively contains primary hydroxyl groups and therefore differs significantly from the commonly known poly(glycerol methacrylate) (PGMA). Block copolymer systems based on poly(lactide) and BGMA were realized via two orthogonal living polymerization techniques starting from a bifunctional initiator, employing first atom transfer radical polymerization (ATRP) of BGMA and in the second step organo-base catalyzed polymerization of L- or D-lactide. This route provides well-defined block copolymers of low polydispersity (PDI 1.12-1.17) and molecular weights in the range of 7000 to 30 000 g/mol (NMR). Rapid and highly selective acetal hydrolysis of the PBGMA block resulted in the release of the hydrophilic and water-soluble poly(1,3-dihydroxypropyl methacrylate) (poly(isoglycerol methacrylate), PIGMA). Acidic hydrolysis of the acetal protecting groups of poly(BGMA)-b-poly(lactide) copolymers proceeded smoothly to amphiphilic structures, notably without affecting the potentially labile poly(ester) block. The novel PIGMA-b-PLLA

copolymers are capable of supramolecular self-assembly to spherical aggregate structures in aqueous environment. The polymers generally exhibited low aggregation constants (CAC: 8-20 mg/L). Because of the unique feature of stereocomplex formation of poly(lactide), the corresponding aggregate morphology could be adjusted by mixing two nearly identical PIGMA-b-PLA copolymers with enantiomeric poly(lactide blocks) in a 1:1 ratio. In this case the uniformly shaped micelles (20 nm) changed to large vesicles with diameters ranging from 600 to 1400 nm. These features render this new type of amphiphilic block copolymers promising for drug delivery applications.

Introduction

Biodegradable poly(ester)s are among the best established, but also most promising materials in current Polymer Science for the design of "smart" biomedical devices, such as drug delivery and controlled release systems in the form of nanoparticles,[1] micelles and polymersomes.[2] Amphiphilic block copolymers are currently subject of intense research with respect to their potential application as encapsulation devices of therapeutic agents exhibiting triggered release.[3] Linear aliphatic poly(ester)s represent excellent building blocks for the formation of hydrophobic domains because of their established *in vivo* degradability and non-toxicity. Poly(lactide) (PLA) has been successfully combined with poly(ethylene glycol) (PEG) and other hydrophilic blocks.[4] Among biocompatible and biodegradable poly(ester)s, poly(lactide) exhibits the unusual feature of stereocomplex-formation of enantiomeric, homo-chiral chains. This is not only accompanied by a strong increase of the melting temperature by approximately 50 °C, but can also be exploited for the kinetic and thermodynamic stabilization of block copolymer aggregates in aqueous environment.[5] Hedrick and co-workers have shown in elegant recent work that stereocomplex-driven association between PEG-*b*-PDLA and PNIPAM-*b*-PLLA leads to the formation of mixed micelles.[6]

Scheme 8: The new poly(isoglycerol methacrylate) (PIGMA) can be localized in a family of hydrophilic methacrylates /methacrylamides, which represent suitable building blocks for biomedically motivated copolymers. Abbreviations: PHPMA (poly(2-hydroxypropyl methacrylamide))[7], POEGMA (poly(oligoethylene glycol methacrylate))[8], PGMA (poly(glycerol methacrylate))[22, 32, 33, 35].
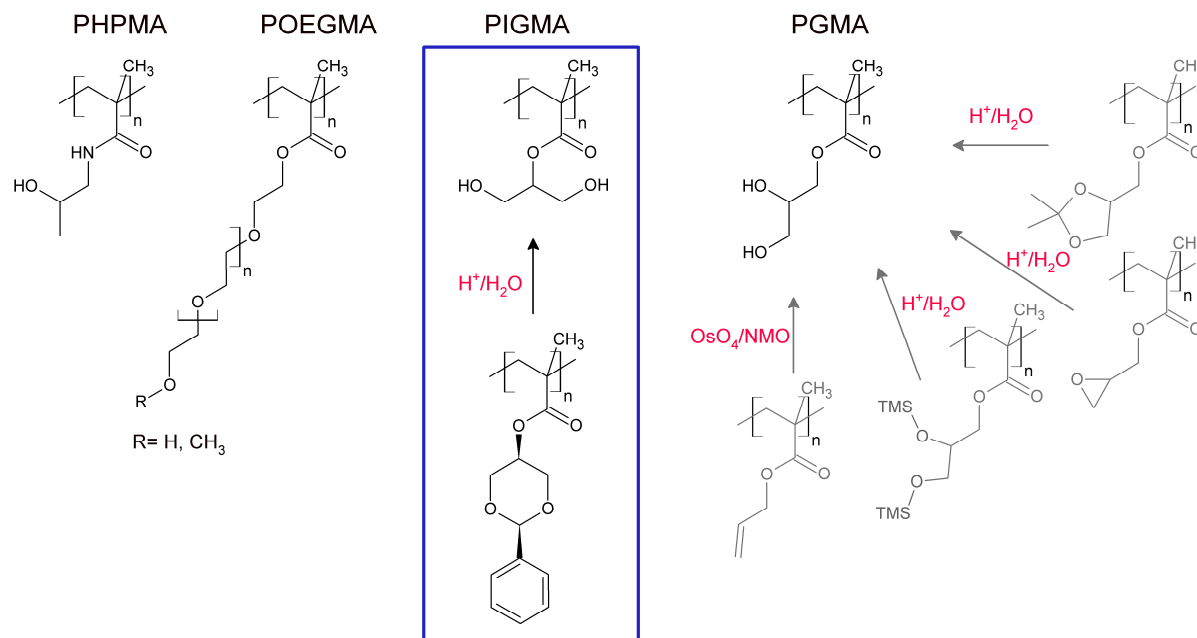

Generally, copolymers of PEG and PLA have been in the focus of interest in the aggregate-promoted application as drug delivery vehicles.[9] This is at least partially attributed to their facile synthesis, which relies on commercially available mono-methyl ether PEGs. Nevertheless PEG-based systems show some disadvantages, such as the lack of further functionality and toxicity of the gaseous monomer ethylene oxide. In less academic circles, the ill-founded fear of product contamination by trace amounts of ethylene oxide in PEG-based products is currently developing a market pull for suitable alternatives.

In this context, we have directed our focus on poly(methacrylate)-based polymers, which possess a functional moiety that can easily be adjusted by simple esterification reaction of the respective alcohol with methacrylic acid. In general, poly(methacrylate)s provide access to non degradable, but readily tunable systems in terms of e.g., hydrophilicity,[10] pH- and temperature-induced phase behavior[11] as well as loading with therapeutic agents[12] by simple variation of the substituent, as demonstrated in Scheme 8. Via ATRP single and multiheaded initiators can be conveniently obtained and introduced in polymers with low synthetic effort.[13,14,15] Block copolymers are accessible by an acrylate- or lactone-first[16,17,18,19,20,21,22] strategy or even by simultaneous growth of the two blocks under

optimized conditions.[23] Very recently, Trimaille et al. have succeeded in combining NMP of *n*-butyl acrylate and the ROP of ε-caprolactone in a one step procedure, starting from a bifunctional, SG1-nitroxide functionalized initiator, yielding well-defined block copolymers.[24] In a previous work, we have introduced a straightforward one-pot procedure to poly(lactide)-*b*-poly(HEMA) copolymers.[25] This system represents one of only few examples describing the combination of a hydrophobic, aliphatic poly(ester) with a hydrophilic poly(acrylate), carrying pendant hydroxyl groups.[26,27,28] Although these block copolymers could be prepared without additional protective groups from plain HEMA, they were not capable of aggregation into stable polymeric aggregates in aqueous solution due to the insufficient water solubility of the poly(HEMA) block.[29] Structurally similar methacrylate monomers are well-known and provide similar (2-hydroxypropyl methacrylate) and superior (glycerol methacrylate, 2-hydroxypropyl methacrylamide) hydrophilicity in their respective polymeric forms.[30,31] An obvious approach to enhance the hydrophilicity of HEMA relies on the increase of the number of hydroxyl groups per repeating unit. To date, this has been realized by poly(2,3-dihydroxypropyl methacrylate), which is commonly known under the name poly(glycerol methacrylate) (PGMA). The synthesis of PGMA is often based on its ketal-protected form: solketyl methacrylate (2,3-isopropylidene glycerol methacrylate), which was first realized in 1990.[32] The PGMA block can either be deprotected in an additional pre- or in a post polymerization step by acid-catalyzed hydrolysis.[33] Nevertheless, alternative pathways have been subject of past and current research. Borsali and co-workers recently employed silylated glycerol monomethacrylate (2,3-bistrimethylsilyloxypropyl methacrylate) to yield amphiphilic block copolymers with poly(ε-caprolactone) block after deprotection.[26] Ruckenstein et al. used the postpolymerization osmylation-reaction for the oxidative introduction of PGMA´s bis-hydroxyl group in poly(styrene)-*b*-poly(allyl methacrylate)s, which was obtained by successive carbanionic polymerization.[34] Davis and co-workers recently obtained poly(glyceryl methacrylate)-*block*-poly(pentafluorostyrene) by hydrolysis of the less polar poly(glycidyl methacrylate) precursor after RAFT polymerization.[35] The increased hydrophilicity and functionality of PGMA[36] and its suitability for drug delivery systems,[37,38,39] hydrogels for soft contact lenses[40] or antifouling coatings[41] lead to an increasing commercial interest in this kind of polymer.

Scheme 9: Synthesis of benzylidene glycerol methacrylate (2) in two steps
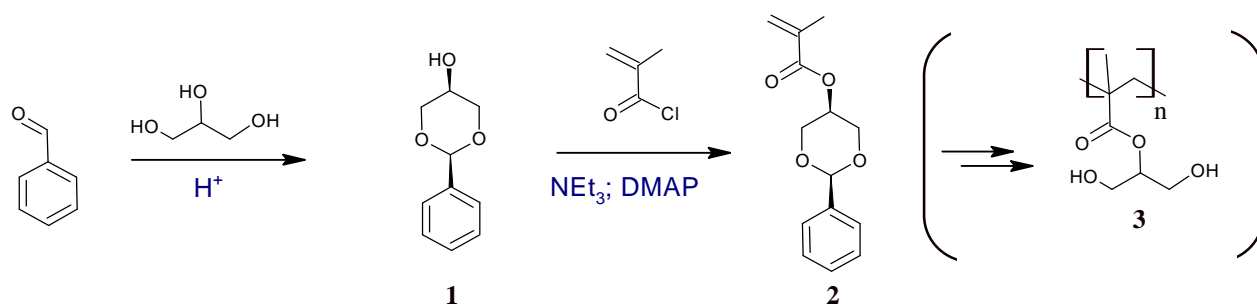
Considering glycerol methacrylate (GMA), the synthetic methods published to date only offer access to the 2,3-dihydroxypropyl isomer, which provides a primary and a secondary hydroxyl functionality. Depending on the purity of the employed solketal, the methacrylate synthesized in this manner may contain impurities of up to 8% of the 2,3-isopropylidene glycerol isomer of GMA. This results in random incorporation of 1,3-dihydroxyisopropyl methacrylate in the polymer backbone in the respective ratio after polymerization and deprotection.[29] However, poly(1,3-di-hydroxyisopropyl methacrylate)* has not been obtained in its pure form yet. In this work, we describe the synthesis and ATRP-polymerization of a new methacrylate monomer (2), granting access to the 1,3- dihydroxy form of poly(glycerol monomethacrylate) (3) (Scheme 2). Furthermore, we present a series of well-defined block copolymers of poly(isoglycerol methacrylate) and poly(lactide) segments and describe their aggregation behavior in aqueous solution with respect to the stereochemistry of the PLA blocks employed.

Experimental Part

Instrumentation

NMR investigation: All ^{1}H and ^{13}C nuclear magnetic resonance (NMR) spectra were recorded at 25°C, using a Bruker AMX 400 (400.1/100.67 MHz) spectrometer. The spectra were measured in CDCl$_3$ and THF-d_8, and the chemical shifts are assigned by internal calibration on the solvents residual peaks. (^{1}H proton NMR signal: 1.73 ppm for THF-d_8, and 7.26 ppm for CDCl$_3$, ^{13}C carbon NMR signal: 25.37 ppm for THF-d_8, and 77.00 ppm for CDCl$_3$). Size

---

* For reasons of simplicity and clarity, the new poly(1,3- di-hydroxyisopropyl methacrylate) will be refered to as poly(*iso*-glycerol (mono)methacrylate) (PIGMA) which exhibits two primary hydroxyl-groups in contrast to the commonly employed isomer poly(glycerol methacrylate) (PGMA).

exclusion chromatography (SEC) was performed with an instrument consisting of a Waters 717 plus auto-sampler, a TSP Spectra Series P 100 pump and a set of three PSS-SDV 5A columns with 100, 1000, and 10000 Å porosity. THF was used as an eluent at 30 °C and at a flow rate of 1 mL/min. UV absorptions were detected by a SpectraSYSTEM UV2000. The specific refractive index increment (dn/dc) was measured at 30°C, using an Optilab DSP interferometric refractometer (also RI detector) and determined with the Wyatt ASTRA IV software (Version 4.90.08). Calibration was carried out using poly(styrene) standards provided by Polymer Standards Service and performing a third order polynomial fit. MALDI-ToFMSmeasurements of poly(lactide) macroinitiators were performed on a Shimadzu Axima CFR MALDI-ToF MS mass spectrometer, equipped with a nitrogen laser delivering 3 ns laser pulses at 337 nm. Dithranol (1,8-dihydroxy-9(10H)-anthracetone, Aldrich 97%), was used as a matrix. Potassium triflate (Aldrich, 98%) was added for ion formation. Good results were obtained for samples prepared from THF solution by mixing matrix (10 mg/mL), polymer (10mg/mL), and salt (0.1Nsolution) in a ratio of 5:1:1. A volume of 0.9 μL sample solution was deposited on the MALDI target and allowed to dry at room temperature for 2 h prior to the measurement. Differential scanning calorimetry (DSC) measurements were carried out on a Perkin-Elmer 7 Series Thermal Analysis System with auto sampler in the temperature range of 0 to 200 °C at a heating rate of 20 K/min. The melting points of indium (Tm = 156.6 °C) and Millipore water (T_m = 0 °C) were used for calibration. In order to visualize the X-ray diffraction information obtained for BGMA we used the basic version of Mercury Crystal Structure Visualization and Exploration software (version 2.2) available free of charge at http://www.ccdc.cam.ac.uk/mercury.

Materials

All solvents were of analytical grade and purchased from Acros Organics. Methylene chloride was refluxed over phosphorous pentoxide and distilled immediately prior to use. 1,8-Diazabicyclo[5.4.0]undec-7-ene (DBU) was obtained from Acros Organics (98%) and distilled from CaH_2 prior to use. Glycerol (25 kg; 99.5%) of plant origin was kindly donated by Caldic (Germany). Deuterated chloroform-d$_1$ and THF-d$_8$ were purchased from Deutero GmbH, dried and stored over molecular sieves. Lactide was purchased from Purac® (Gorinchem, NL), recrystallized 3 times from dry toluene and stored under vacuum prior to use. 2-Hydroxyethyl 2-bromo-2-methylpropanoate (HBMP) was synthesized as described

previously.[25] 5-Hydroxy-2-phenyl-1,3-dioxane was prepared with a standard rotary evaporator and isolated from cold diethyl ether on a multi 100 gram scale according to a procedure adapted from Aasbø et al. [42] Dialysis of the micellar solution was performed with Cellu Sep®H1 membranes (Membrane Filtration Products, Inc.) with a molecular weight cutoff of 1000 g/mol.

Monomer Preparation: 2-Phenyl-1,3-dioxan-5yl-methacrylate (BGMA)

32 g (0.18 mol) 5-hydroxy-2-phenyl-1,3-dioxane, 21 g (0.21 mol, 28.5 ml) of triethyl amine and 50 mg of N,N-dimethyl amino pyridine were dissolved in 400 mL of dry dichloromethane in a 1L flask equipped with a 250 mL dropping funnel and an argon balloon. Subsequently a solution of 20 g (0.19 mol) of methacryloyl chloride in 150 mL of dry dichloromethane was added drop-wise under constant cooling (0-5 °C) over a period of 2 h. The solution was slowly allowed to warm to room temperature and stirred for an additional 72 h. The solution was extracted twice with water and twice with saturated potassium carbonate solution (50 ml each). The organic phase was dried over a 1/10 mixture of anhydrous potassium carbonate and magnesium sulfate. After evaporation of the solvents, the crude product was taken up in 20 mL of THF and poured into 200 mL of a 1:1 mixture of diethyl ether and hexanes. The product crystallized in colorless needles upon standing at -25°C for 48 h (34.8 g/78%). ^{1}H NMR (CDCl$_3$, 400MHz) δ^1H/ppm: 2.01 (s, 3H, CCH_3); 4.18-4.35 (m, CHCH_2O); 4.77 (s, 1H, -OCH(CH$_2$O)$_2$); 5.58 (s, 1H; -OCHO); 5.65 (s, 1H, C=CH_2 (E)), 6.30 (s, 1H, C=CH_2 (Z)); 7.36-7.53 (m, 5H- aromat.). ^{13}C NMR (CDCl$_3$, 100 MHz) δ^{13}C/ppm): 18.23 (CCH$_3$); 66.10 (-OCH(CH$_2$O)$_2$-); 69.00 (-OCH(CH$_2$O)$_2$-); 101.30 (CH$_2$O$_{cycl}$); 126.05 (CH$_{aromat}$ 2+6); 126.54 (CCH$_2$); 128.31 (CH$_{aromat}$ 3+5); 129.12 (CH$_{aromat}$ 4); 137.93 (C_{aromat} 1); 167.16 (CCOOCH).

Density$_{X-Ray}$: 1.284 g/cm^3

Crystallographic Data:

- Space group: P-1 (triclinic);
- Lattice constants:
  - a = 6.0518 Å, α = 74.93 °
  - b = 9.8632 Å, β = 87.07 °
  - c = 11.1612 Å, β = 87.68 °

Procedure for the Synthesis of the First Block: ATRP of BGMA

(Exemplified for PBGMA-MI 4 with a monomer/alkyl halide/copper/ligand ratio of [100]:[1]:[1]:[1]) A 2:1 mixture of benzene and methanol was pre-degassed by 3 freeze-pump-thaw cycles. Monomer and initiator were charged into an argon-flushed Schlenk-tube, dissolved in a benzene/methanol mixture and degassed in three freeze pump thaw cycles. The ligand, hexamethyl triethylenetetramine (HMTETA) (2-fold excess) was charged in a separate Schlenk tube, dissolved in 10 mL of benzene/methanol 2:1 and degassed as described above. Then 5 mL of the ligand solution were injected into a pre-evacuated Schlenk-tube, containing the desired amount of CuCl. The tube was flushed with argon and sonicated for 10 min, upon which a nearly colorless solution of the copper-complex formed. Polymerization was initiated upon injecting the copper/HMTETA complex to the monomer/initiator solution, preheated to the reaction temperature of 80 °C. Polymerization was quenched after 5 h by removal of the reaction vial from the oil bath followed by exposure to air. A sample was harvested for conversion analysis. Since the block copolymer partially precipitated from the reaction mixture upon cooling, benzene was added and the solution was left to stand to evaporate excess methanol. The less polar environment facilitated catalyst removal via filtration over a short column filled with neutral aluminum oxide (10 mL/g polymer). Further work-up including complete removal of residual monomer was achieved by precipitation in excess methanol (150 mL/g polymer). After filtration, the block copolymer was obtained as a white powder in a yield reflecting the respective conversion.

^{1}H NMR (CDCl$_3$, 400 MHz) δ^1H/ppm: 0.94-1.46 (m, C(C*H$_3$*)(COOCH(CH$_2$O-)$_2$); 1.80-2.34 (m,-C*H$_2$*C(CH$_3$)(COOCH(CH$_2$O-)$_2$); 3.56-4.33 (COOCH(C*H$_2$*OH)$_2$); 4.20-4.57 (COOC*H*(CH$_2$O-)$_2$); 5.27-5.49 (COOCH(CH$_2$O-)$_2$C*H*C$_6$H$_5$); 7.16-7.54 (COOCH(CH$_2$O-)$_2$CHC$_6$*H$_5$*).

Polymerization of Lactide:

The ω-hydroxyl-PBGMA macroinitiator and lactide of the respective D- or L-configuration were charged into a Schlenk-tube at predetermined molar ratios (Table 14). The tube was sealed with a rubber septum and repeatedly flushed with argon after evacuation. Freshly distilled dichloromethane (4 mL/g lactide) was added via a syringe. Polymerization was initiated after 2 minutes by injecting a 10% (weight) solution of DBU corresponding to 1 mol% of the monomer. Polymerization was quenched after 20 minutes by injecting 1 mL of

methanol. A small sample was removed for conversion analysis prior to precipitation in an excess of methanol. The polymer was collected by filtration.

^{1}H NMR (CDCl$_3$, 400 MHz) δ^1H/ppm: 0.94-1.46 (m, C(CH$_3$)(COOCH(CH$_2$O-)$_2$); 1.57 (d, ^3J =7.0 Hz CHCH$_3$, poly(lactide)), 1.80-2.34 (m,-CH$_2$C(CH$_3$)(COOCH(CH$_2$O-)$_2$); 3.56-4.33 (COOCH(CH$_2$OH)$_2$); 4.20-4.57 (COOCH(CH$_2$O-)$_2$); 5,15 (q, ^3J =7.0 Hz CH(CH$_3$), poy(lactide)); 5.27-5.49 (COOCH(CH$_2$O-)$_2$CHC$_6$H$_5$); 7.16-7.54 (COOCH(CH$_2$O-)$_2$CHC$_6$H$_5$).

Acetal Cleavage: Kinetics via ^{1}H NMR

20 mg of the block copolymer were dissolved in 0.82 mL of deuterated THF and charged into a standard NMR tube. The probe head was preheated to 37°C prior to injection of 0.15 mL of a 1n HCl/DCl solution. Spectra were measured in intervals of 15 minutes with 4 scans each (approx. 30 seconds/experiment)' the first scan 1 minute after the injection. ^{1}H NMR (first spectrum obtained)(82% THF-d_8, 18% 1n HCl/DCl; 400 MHz) δ^1H/ppm: 0.90-1.22 (m, C(CH$_3$)(COOCH(CH$_2$OH)$_2$); 1.46 (d, ^3J = 7.0 Hz OCH(CH$_3$), poly(lactide)); 1.85-2.20 (m,-CH$_2$C(CH$_3$)(COOCH(CH$_2$OH)$_2$); 3.69-3.81 (COOCH(CH$_2$OH)$_2$); 4.65-4.77 (-COOCH(CH$_2$OH)$_2$); 5.15 (q, ^3J =7.0 Hz CH(CH$_3$); poy(lactide)); 5.48 (d, ^3J =6.0 Hz HOCH(CH$_3$), poly(lactide) *term. unit*).

Preparation of Micelles.

10 to 15 mg of the block copolymer was dissolved in 2.7 mL of THF, and 0.5 mL of 1n hydrochloric acid were added. The vial was sealed with a rubber septum and the content stirred at 37 °C for 8 h. Subsequently 10 mL of water were added drop-wise under vigorous stirring over a period of 4 h. Samples were dialyzed against 3x1 L of water for a total of 48 h. The first dialysis solution was buffered with 0.1 mg of sodium acetate. The aggregate morphologies were studied using a transmission electron microscope (TEM). The TEM samples were prepared by drop casting the above mentioned aggregate solution (c = 1-1.5 mg/mL) on a plasma treated carbon coated copper grid. The samples were allowed to dry at room temperature under a slight nitrogen flux for at least 16 h prior to examination.

Fluorescence Measurements

The extremely hydrophobic pyrene is preferentially solubilized in the hydrophobic interior of the aggregate. This can be readily observed in the fluorescence excitation spectra of the probe at an emission wavelength of 372 nm.[43] In the concentration range of aqueous micellar solutions, a shift of the excitation band in the 335 nm region toward higher wavelength is observed for the employed block copolymers. The ratio of the fluorescence intensities at 339 and 335 nm was used to validate the shift of the broad excitation band. The critical aggregation concentrations (CAC) were determined from the crossover point in the low concentration range. Pyrene-containing samples were prepared by continuous dilution of the aggregate solution with a saturated pyrene stock solution. The mixtures were allowed to equilibrate for 48 to 64 h prior to investigation by fluorescence spectroscopy.

Results and Discussion

Monomer synthesis

The synthetic strategy for benzylidene glycerol methacrylate (BGMA) is shown in Scheme 1. The monomer was readily obtained on a multigram scale via a two-step route, starting from the acetal formed by glycerol and benzaldehyde with subsequent esterification of the secondary hydroxyl group with methacryloyl chloride.

In comparison to ketones, as employed in solketyl methacrylate synthesis, benzaldehyde and its derivates show a strong preference for the formation of six-membered cyclic acetals due to the energetically favored equatorial position in the chair conformation of the ring. This acetal protecting group provides excellent stability in neutral and basic environment and is conveniently cleaved under slightly acidic conditions. The isolation of 2-phenyl-5-hydroxyphenyl-1,3-dioxane (1) relies on a crystallization step, which exclusively yields the *cis*-isomer of the compound in very high purity (Figure 74).

The coupling reaction with methacryloyl chloride was conducted in dichloromethane in the presence of stoichiometric amounts of triethylamine (TEA) and catalytic amounts of dimethylaminopyridine (DMAP). The novel monomer (2) could be readily obtained in 78% yield by crystallization from THF/diethyl ether/hexanes (1:10:10), and the white crystals exhibited a melting point of 65.7 °C. This methacrylate significantly differs from 2-phenyl-(1,3-dioxane-4-yl)methyl methacrylate, which was previously described and obtained by an

elaborate synthesis from solketyl methacrylate via 2,3-dihydroxypropyl methacrylate and subsequent reprotection as benzylidene acetal.[44]
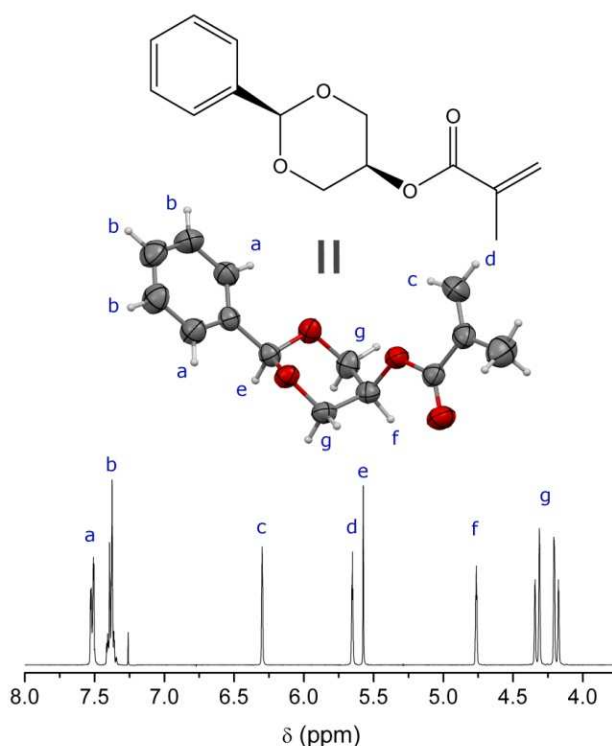

Figure 74: ^{1}H NMR analysis and crystal structure derived from the X-ray diffraction pattern of BGMA.

Considering the bifunctional initiator used for the synthesis of the targeted block copolymers and the quantitative protection of the hydroxyl groups of the monomer, two different synthetic routes appeared to be viable: (A) synthesis of a poly(lactide) macroinitiator and subsequent chain extension with poly(lactide), or (B) preparation in reverse manner, that is, ATRP of BGMA with subsequent chain extension by ROP of lactide (cf. Scheme 10). Both pathways have been tested. To ensure fast initiation, ATRP was conducted with the mixed halide exchange technique,[45] starting from highly reactive isobutyryl-bromide, using copper(I) chloride in combination with stoichiometric amounts of HMTETA. A suitable solvent system providing good polymerization control for the ATRP of BGMA, while offering sufficient solubility for BGMA and lactide based homopolymers, was found with a 1:2 mixture of methanol and benzene. The low polarity of the PBGMA based polymers also ensures convenient removal of the Cu complex after polymerization. Column filtration over neutral aluminum oxide with a low polarity solvent (e.g., benzene) permitted excellent retention of the colored Cu-species. Furthermore, PBGMA and poly(L-lactide) as

well as their block copolymers of arbitrary composition ratios can be readily purified by (a single) precipitation in their common nonsolvent methanol. A change in block copolymer composition was not observed in this step. Residual monomer and catalyst (DBU-benzoate salt as well as Cu-complex) were removed by this procedure. Generally speaking, the benzylidene acetal of BGMA not only contributes to an increase in the monomer and polymer solubility in commonly employed, apolar organic media, but also gives access to other controlled polymerization methods (e.g., living anionic polymerization), which show far less tolerance toward the presence of functional groups than ATRP. Obviously, block copolymer synthesis involving two or more orthogonal polymerization methods, employing monomers of different functionality and/or polarity necessitates masking of their functional groups.
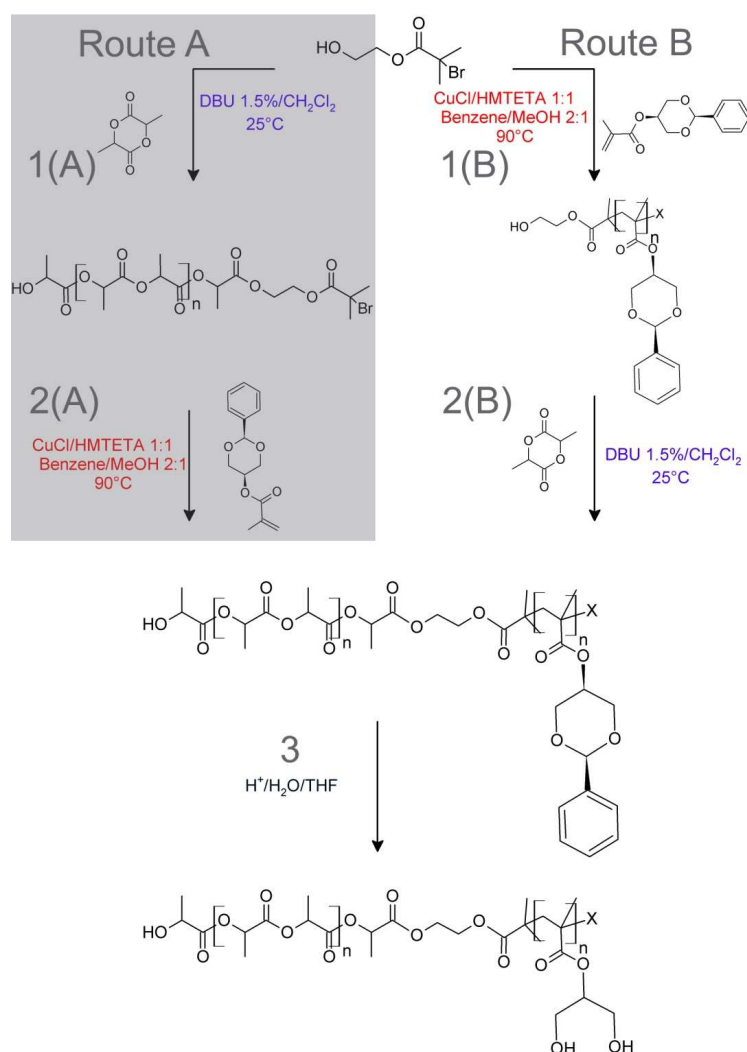
Scheme 10: Two alternative synthetic pathways to poly(*iso* glycerol (mono)methacrylate)-*b*-poly(lactide) block copolymers (A) lactide first; (B) BGMA first. While Route B resulted in well-defined block copolymers, route A showed inefficient block formation and was not further pursued.

ATRP of BGMA:

ATRP was the obvious method of choice for the preparation of a narrow polydispersity block of the novel monomer. The semilogarithmic plot of the kinetic polymerization data derived from ^{1}H NMR shows a nearly linear correlation throughout the major part of the polymerization, with a small decrease toward high conversion. Hence, the reaction can be considered living with a close to constant radical concentration during the polymerization. The slight flattening of the plot can be explained by traces of oxygen, which might have been introduced during sample harvesting, although all syringes were carefully purged with argon prior to the process. The kinetically evaluated sample reached a conversion of only 66%.

Table 13: Molecular characterization data for the preparation of PBGMA macroinitiators. SEC in THF, evaluation with polystyrene standards.

	Polymer	Initiator	Monomer	M/I	M_N theo. (100% conv.)	M_N (NMR)	Time (min)	Conv. (NMR)	M_N (SEC)	PDI	Composition (NMR)
	PBGMA-MI 1	2-HBMP	**BIGMA**	25	6400	5480	300	0.85	3830	1.23	PBGMA$_{21}$
	PBGMA-MI 2	2-HBMP	**BIGMA**	40	9900	9520	300	0.96	5700	1.26	PBGMA$_{38}$
1. ATRP of BGMA	PBGMA-MI 3	2-HBMP	**BIGMA**	55	13600	11700	300	0.86	6300	1.30	PBGMA$_{47}$
	PBGMA-MI 4	2-HBMP	**BIGMA**	100	24800	20200	300	0.80	11700	1.20	PBGMA$_{80}$
	PBGMA-MI 5	2-HBMP	**BIGMA**	110	27500	22400	300	0.81	11900	1.18	PBGMA$_{89}$
	PBGMA-MI 6	2-HBMP	**BIGMA**	200	49700	35800	300	0.72	18700	1.15	PBGMA$_{144}$
	PBGMA-MI 7	2-HBMP	**BIGMA**	400	99300	65900	360	0.66	24400	1.24	PBGMA$_{266}$

The evolution of molar mass correlated linearly with conversion (Figure 75). The monodisperse SEC traces observed revealed narrow molecular weight distributions (PDI 1.18-1.30), characteristic for well-controlled CRP/ATRP processes. The decrease in PDI was very pronounced during the earlier stages of the polymerization and became significant after 60 minutes. We assume that this point is indicative of complete consumption of the initiator, followed by exclusive propagation with constant chain growth. This goes along with the appearance of a non-zero extrapolation of the linear fit and can be explained by the use of the mixed halide exchange technique and hence a significantly faster initiation than propagation reaction, which results in slightly faster monomer consumption at the onset of the polymerization. First DSC studies showed a rather high T_g of the PBGMA homopolymer (120-135°C depending on M_n), which is due to the high rotational barrier introduced by the bulky benzylidene acetal substituents at the methacrylate polymer chain. We will report in

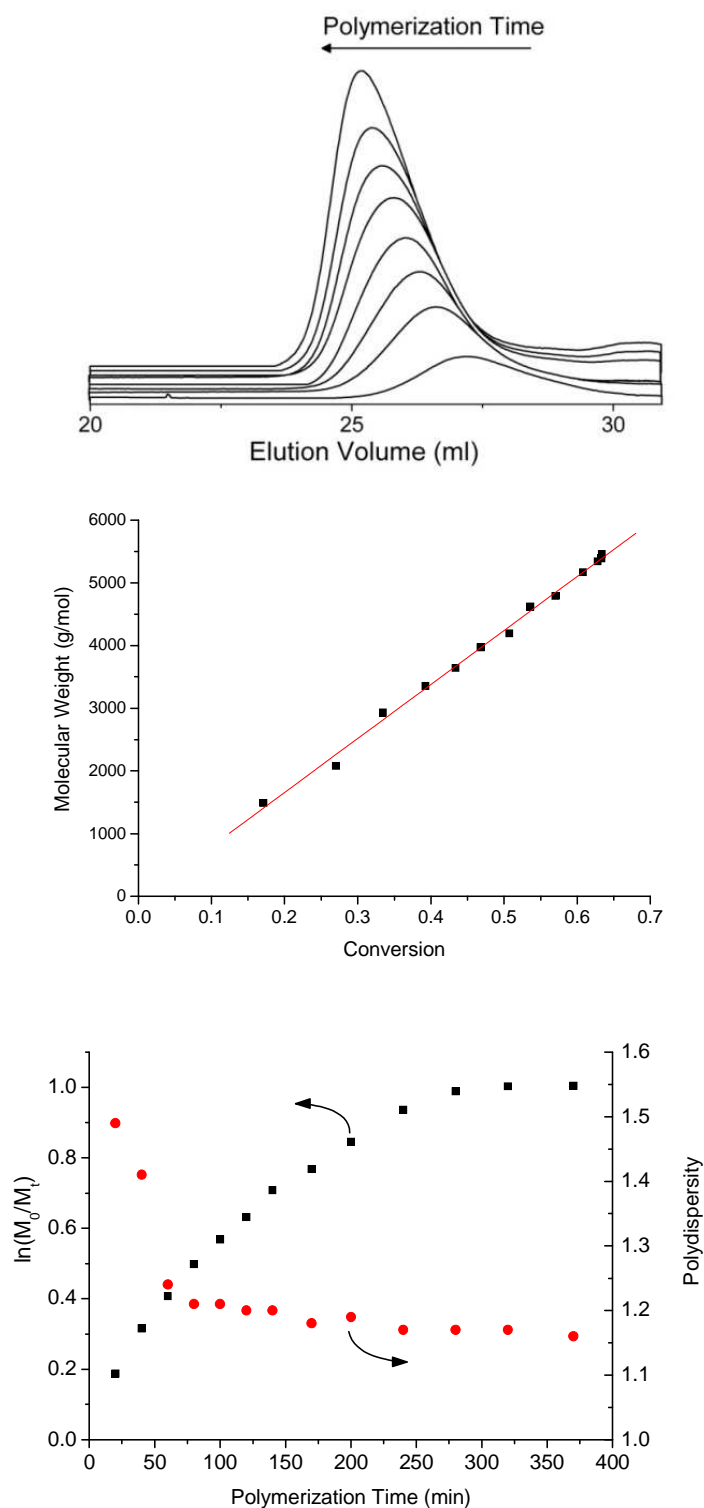detail on the interesting thermal properties of PBGMA-based polymers in a subsequent publication.

Figure 75: Kinetics of the polymerization of BGMA: SEC traces (top, plotted for 20-170 min) show a clean shift toward lower elution volumes in the course of the polymerization; middle: linear correlation of molecular weights (SEC$_{THF}$ data), derived from PS standards with conversion; bottom: ln(M_0/M_t) vs polymerization time.

Chain extension with Poly(lactide)

Since the poly(isoglycerol methacrylate) hydroxyl groups are fully protected, the lactide chain growth commences from the single hydroxyl moiety of the bifunctional macroinitiator. Ring-opening polymerization was conducted under organo-base catalysis with DBU (1,8-diazabicyclo[5.4.0]undec-7-ene), which has proven to work excellent for lactide ring-opening[46] on a laboratory or semibatch scale. It provides superb end group-fidelity, good polymerization control and fast kinetics, even at room temperature. The polymerization time for the samples prepared was kept between 15 and 45 minutes, depending on the monomer/initiator ratio and resulted in conversion ranging from 85 to 99% (1.5 mol% catalyst loading).
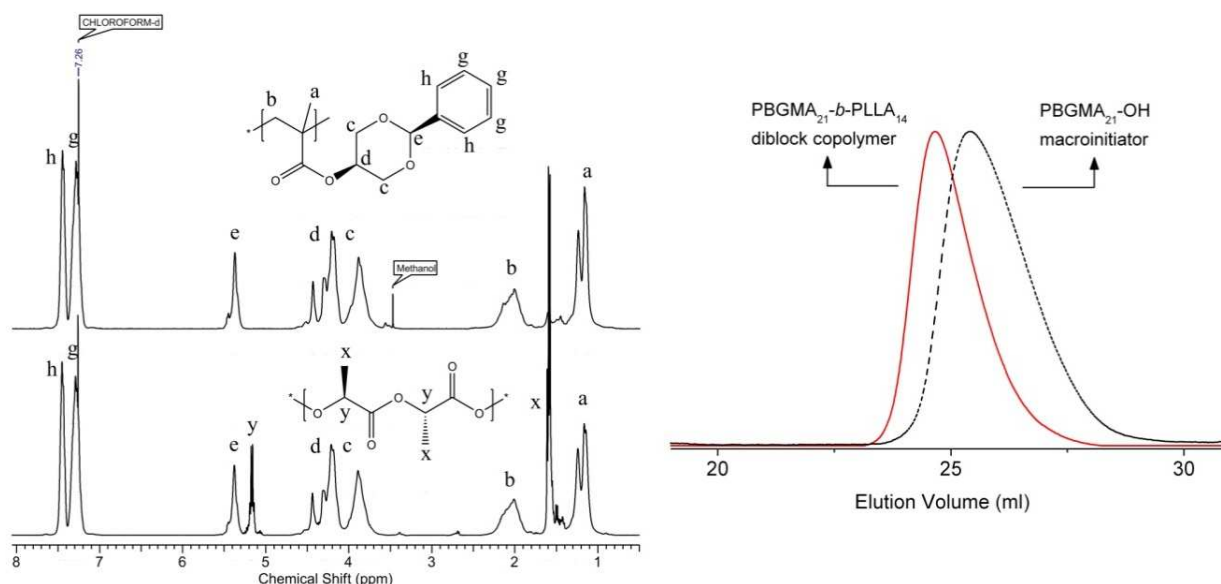

Figure 76: Chain extension of the PBGMA-macroinitiator with poly(lactide) depicted in the form pre/post NMR (left) and SEC (right) measurements. Although the sample chosen is composed of few lactide repeating units (i.e. DP=14), it shows clean chain extension. This fact is attributed to the high initiating potential of the primary hydroxyl group of the PBGMA prepolymer.

While route B (cf. Scheme 10) resulted in well-defined block copolymers (Table 2), the pathway A led to the formation of less defined structures, presumably composed of a mixture of homo and block copolymers. This was indicated by a change in composition (depletion of the lactide block, sometimes even complete disappearance) after precipitation in a nonsolvent for both blocks and broader molecular weight distributions. This is astonishing, since the poly(lactide) macroinitiators were completely functionalized (single distribution in MALDI-ToF spectra) and chain extension of these macroinitiators via ATRP has

already been conducted successfully with HEMA (in DMSO with CuCl/biPyridyl), as recently described by the authors.[37] However, route B results in the formation of well-defined block copolymerss and is slightly more practical, since diversification of the macroinitiator is possible, using the synthetically more convenient ROP of L-lactide (polymerization at room temperature, polymerization time < 15 min, no oxygen free environment necessary). In this case, all samples were monomodal and their block ratios remained unchanged during the purification process (filtration, precipitation), as was verified by ^{1}H NMR and SEC (Figure 3).

Table 14: Molecular charachterization data for the chain extension of the PBGMA macroinitiators with lactide. *SEC in THF, evaluation with polystyrene standards. #M = Monomer(L-/D-LA = L-/D-Lactide).

	Polymer	Initiator	M#	M/I	M_N theo. (100%conv.)	M_N NMR	Time (min)	Conv. (NMR)	M_N (SEC*)	Composition (NMR)
2. ROP of Lactide	PBGMA-PLA 1	PBGMA$_{89}$ (MI 5)	L-LA	35	27400	26100	20	0.74	15200	PBGMA$_{89}$-PLLA$_{27}$
	PBGMA-PLA 2	PBGMA$_{89}$ (MI 5)	D-LA	35	38300	29500	20	0.45	13600	PBGMA$_{89}$-PDLA$_{16}$
	PBGMA-PLA 3	PBGMA$_{47}$ (MI 3)	L-LA	30	16000	15400	45	0.86	9770	PBGMA$_{47}$-PLLA$_{26}$
	PBGMA-PLA 4	PBGMA$_{47}$ (MI 3)	D-LA	30	16000	15700	45	0.92	9970	PBGMA$_{47}$-PDLA$_{28}$
	PBGMA-PLA 5	PBGMA$_{21}$ (MI 1)	L-LA	15	7600	7550	20	0.96	6100	PBGMA$_{21}$-PLLA$_{14}$
	PBGMA-PLA 6	PBGMA$_{21}$ (MI 1)	D-LA	15	7600	7550	20	0.96	6270	PBGMA$_{21}$-PDLA$_{14}$
	PBGMA-PLA 7	PBGMA$_{80}$ (MI 4)	D-LA	46	28600	27900	30	0.88	16900	PBGMA$_{80}$-PDLA$_{40}$

For the chain extension with poly(lactide) the respective degrees of polymerization were targeted by adjusting the monomer/initiator molar ratio, affording hydroxyl-functional PBGMA homopolymer precursors of varying chain lengths. Because of pronounced underestimation of molecular weight by SEC (PS standards) absolute molecular weights were estimated from the monomer/initiator ratio, considering the specific conversion of the sample calculated from NMR in the case of the PBGMA-macroinitiator. This underestimation is explained by the bulkiness of the substituents along the polymethacrylate backbone. In general, the use of the bifunctional initiator made post polymerization reactions redundant and the completely functionalized macroinitiators allowed quantitative chain extension with lactide.

Cleavage of the Acetal Protecting Group

The formation of the hydrophilic PIGMA from its protected precursor PBGMA was investigated via ^{1}H NMR. We observed that the rate of the acetal hydrolysis depends significantly on the reaction temperature. Screening of suitable time/temperature deprotection conditions was conducted by exposing the initial test sample to 3 different temperatures (A) 19 °C for 23 h (24%), (B) 4 °C for 12 h (6%) and (C) 27 °C, 12 h (100%). The first reaction mixture was composed of 90% THF and 9% D_2O and 1% 10 N HCl (0.1 mol/L). Upon completion of the acetal cleavage during the last deprotection sequence, the polymer precipitated from the reaction mixture and was redissolved by increasing the water/HCl content of the mixture to 18%. These results indicate that acetal cleavage at slightly increased (30-40 °C) temperatures should result in shorter reaction times, which are still tolerable for the poly(ester) backbone of the second block.[47] This was confirmed and monitored via NMR analysis in THF-d_8/1 N DCl in the respective ratio (Figure 77).
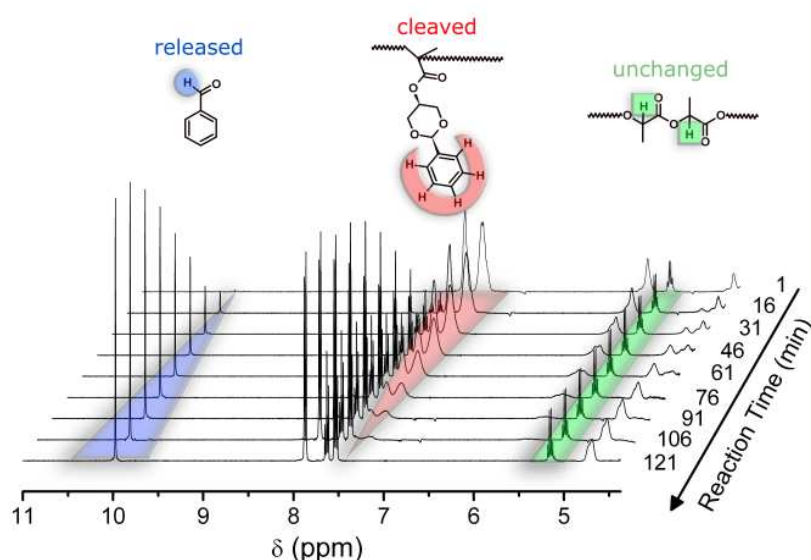

Figure 77: Deprotection of the benzylidene-acetal groups of the diblock copolymer, monitored by ^{1}H NMR in THF-d_8.

As expected, the pronounced amphiphilic nature of the block copolymers did not permit SEC measurements in THF after deprotection. Nevertheless, DMF offers sufficient solubility for homo- and block copolymerss of the employed components before as well as after acetal hydrolysis. In Figure 79 monomodal SEC traces with DMF as an eluent reveal narrow monomodal molecular weight distributions and illustrate the successful 3-step process to

the amphiphilic block copolymers, free of detrimental side reactions. Remarkably, the block copolymers exhibit a significantly decreased elution volume after deprotection (Table 15).
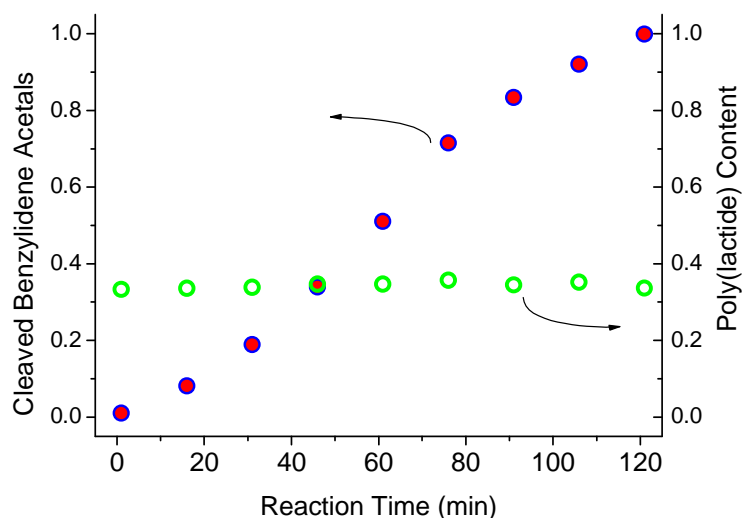

Figure 78: Evaltuation of the NMR results: While the poly(lactide) backbone remains unaffected, the benzylidene protecting groups of the polymer are fully cleaved within only 2 h at 37 °C.

This is in good agreement with the observed underestimation in molecular weight for polymers consisting of PBGMA by evaluation with calibration standards like PEG, PS and PMMA, which were at hand. PBGMA homopolymers were cleavable under the same conditions and could be redissolved in water (D_2O) after solvent evaporation.

Table 15: Comparison of SEC data for the PBGMA-PLA based block copolymers before and after deprotection. The apparent increase in molecular weight after hydrolysis is noticeable, despite a nominal weight loss of 40% for the transformation of PBGMA to PIGMA (SEC in DMF; evaluation was achieved with poly(ethylene glycol) standards).

before deprotection				*after deprotection*			
Composition (NMR)	M_N theo.	M_N (SEC)	PDI	M_N (theo)	M_N (SEC)	PDI	Composition
PBGMA$_{21}$	5480	3800	1.15	3330	5800	1.22	PIGMA$_{21}$
PBGMA$_{89}$	22400	11500	1.18	14300	18300	1.25	PIGMA$_{89}$
PBGMA$_{89}$-*b*-PLLA$_{27}$	26100	8400	1.17	18100	13900	1.27	PIGMA$_{89}$-*b*-PLLA$_{27}$
PBGMA$_{47}$-*b*-PLLA$_{26}$	15400	8200	1.17	11300	11900	1.26	PIGMA$_{47}$-*b*-PLLA$_{26}$
PBGMA$_{47}$-*b*-PDLA$_{28}$	15700	8500	1.16	11600	11800	1.27	PIGMA$_{47}$-*b*-PDLA$_{28}$
PBGMA$_{47}$-*b*-PLLA$_{26}$ + PBGMA$_{47}$-PDLA$_{28}$	s.a.	s.a.	s.a.	11400	12500	1.31	PIGMA$_{47}$-*b*-PLLA$_{26}$ + PIGMA$_{47}$-b-PDLA$_{28}$
PBGMA$_{21}$-*b*-PLLA$_{14}$	7550	5300	1.12	5400	7450	1.24	PIGMA$_{21}$-*b*-PLLA$_{14}$
PBGMA$_{80}$-*b*-PDLA$_{40}$	27900	13700	1.17	18900	20700	1.18	PIGMA$_{80}$-*b*-PDLA$_{40}$
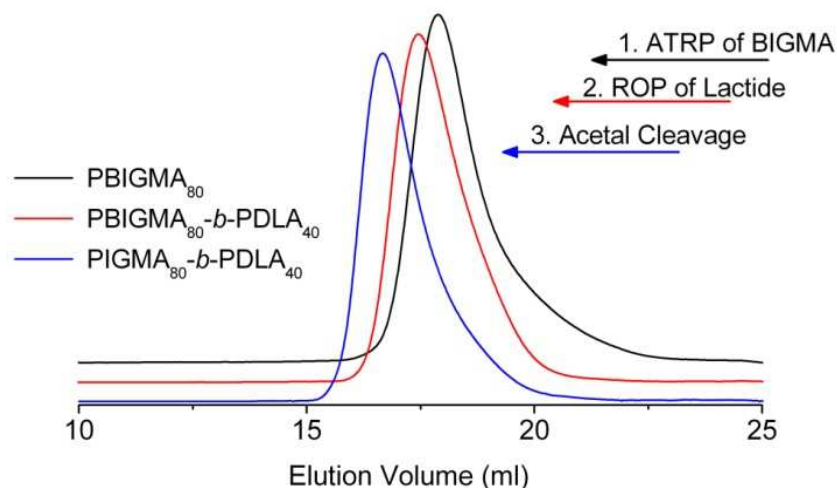
Figure 79: SEC traces (DMF): (1) PBGMA$_{80}$ (right); (2) PBGMA$_{80}$-b-PDLA$_{40}$; (3) PIGMA$_{80}$-b-PDLA$_{40}$.

The shelf life of the block copolymers under the acidic conditions of the deprotection reaction was found to be remarkable. Even for times representing a multitude of those required for complete acetal cleavage, no degradation of poly(lactide) or isomerization of the poly(isoglycerol methacrylate) could be observed. This is supported both by ^{1}H NMR and by the constant ratio of lactide and cleaved benzaldehyde-related signals (Figure 80). Furthermore, SEC traces measured 24 and 96 h after deprotection strongly resemble each other.
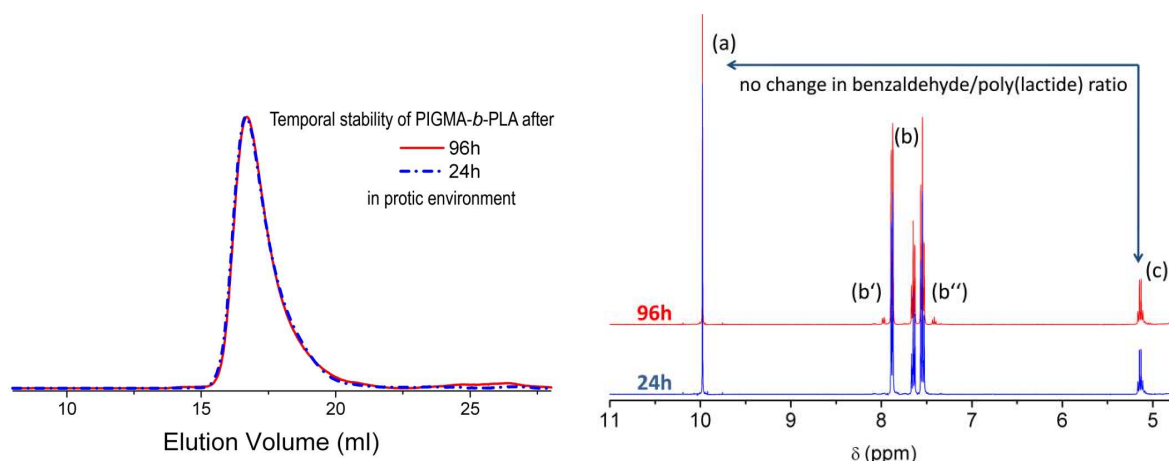

Figure 80: The stability of the amphiphilic PIGMA-b-PLA copolymer in acidic environment beyond the timeframe required for deprotection of the acetal is indicated by consistent elugrams (left) and unchanged signal ratios in ^{1}H NMR (right).

Aggregate Formation of the PIGMA-PLLA Block Copolymers

Using the so-called indirect dissolution method with subsequent dialysis, well-defined micelles were formed upon self-organization of PIGMA-*b*-PLA. The acetal protecting groups of the double hydrophobic PBGMA-*b*-PLA copolymers were cleaved prior to the aggregation studies without isolation from solution, as described in the previous section. First of all the critical aggregation concentration (CAC) has been examined. Fluorescence measurements with pyrene as fluorescent probe are an excellent method to obtain information concerning aggregate formation. The ratio of the fluorescence intensities at 339 and 335 nm was used to evaluate the shift of the excitation spectra. The ratio remained constant below a certain concentration, but changed substantially above a critical concentration reflecting the partitioning of pyrene between the aqueous solution and aggregated phases. It has to be emphasized that the micellar aggregates formed by enantiomerically pure block PLA block copolymers already possess high thermodynamic stability in aqueous solution and may perform as favorable drug carriers themselves[48]. Nevertheless, the special stereochemistry of poly(lactide) provides access to non covalent stabilization via stereo-complexation of two isotactic and enantiomeric poly(lactide) chains. This was achieved by dissolving equal amounts of two block copolymers of similar composition with enantiomeric poly(lactide) blocks prior to hydrolysis of the acetal goups.
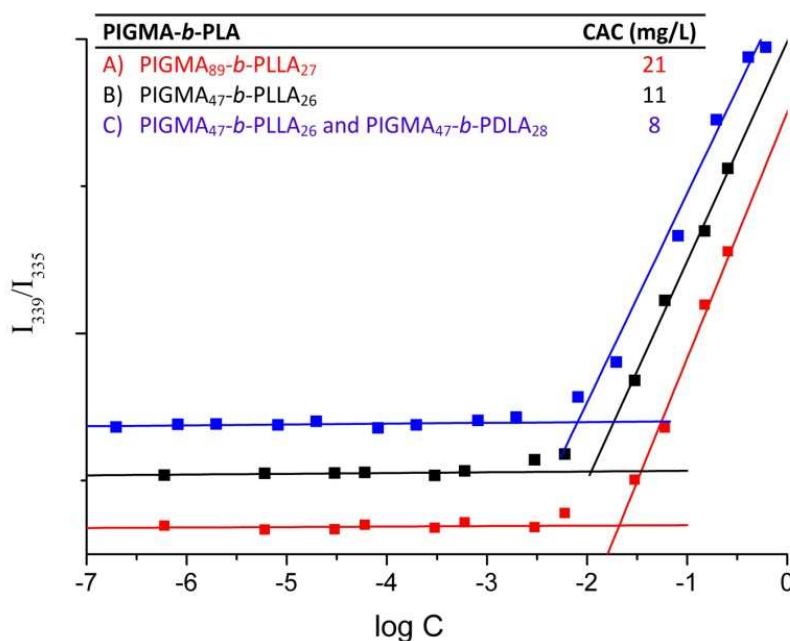

Figure 81: CAC measurements using pyrene fluorescence excitation spectra at an emission wavelength of 372 nm. (A) (red) $PIGMA_{89}$-*b*-$PLLA_{27}$ (B) (black) $PIGMA_{47(7500)}$-$PLLA_{26(3800)}$ (C) (blue) $PIGMA_{47(7500)}$-$PLLA_{26(3800)}$ and $PIGMA_{47(7500)}$-$PDLA_{28(4000)}$ (1:1)..

From the set of synthesized polymers we focused on those with an approximate block ratio of 2:1. (i.e., $PIGMA_{47}$-b-$PLLA_{26}$ and $PIGMA_{47}$-b-$PDLA_{28}$). Since it is known that crystallization occurs in enantiomeric (1:1) blends at PLA chain lengths shorter than their isotactic counterparts, we aimed at keeping the PLA block length below the critical limit of 30 repeating units. At this chain length (and even below), stabilization by crystalline stereocomplexes in amphiphilic block copolymers based on poly(lactide) is possible.[49] They generally crystallize in a triclinic unit cell, in which the chains exhibit a characteristic 3_1 helical conformation. Figure 81 shows the apparent CAC values obtained for the different amphiphilic block copolymers. The CAC lies in the same order of magnitude being approximately twice as high for the $PIGMA_{47}$-b-$PLLA_{26}$ block copolymer compared to the PEG_{123}-b-$PLLA_{29}$ sample (from ref. 5). This indicates an increase in hydrophilicity and hence stabilization potential of PIGMA compared to PEG in aqueous solution. Therefore, an increase of the PIGMA chain length at nearly constant PLLA chain lengths resulted in an increase of the CAC by a factor of approx. 2 ($PIGMA_{47}$-b-$PLLA_{26}$ to $PIGMA_{89}$-b-$PLLA_{27}$). Generally speaking, the low CAC permits application of the block copolymers in highly dilute systems, such as the blood plasma.

The influence of the assumed stereocomplexation (mixture of $PIGMA_{47}$-b-$PLLA_{26}$ and $PIGMA_{47}$-b-$PDLA_{28}$) on the CAC was small, confirming results obtained by Leroux et al.[5] for PEG-PLA block copolymers. Intriguingly, the diastereomeric mixing of two block copolymers of very similar composition has a strong influence on the aggregates´ morphology. As pointed out, the chosen block lengths had a positive hydrophilic to hydrophobic ratio between 3.5 and 2 (e.g. $PIGMA_{47}$-b-$PLLA_{26}$), which clearly explains the formation of spherical micelles with an approximate diameter of 20 to 30 nm (Figure 82, top).

Although block copolymers with a crystallizable hydrophobic block show a tendency toward the formation of nonspherical wormlike micelles a fact that can be attributed to the lamellar packing of the crystallizable chains - X-ray diffraction studies of PEG-PLLA-based polymeric micelles performed by Leroux et al. [5] showed that the stereoregular poly(lactide) does not crystallize, if the block length remains below 30 repeating units. In the case of mixtures of similar PIGMA-b-PLA block ratios with enantiomeric poly(lactide) blocks an entirely different morphology was found. Surprisingly, TEM images of the aggregates prepared from mixed solutions (1/1 mixture) of the diasteromeric block copolymers showed the formation of vesicular aggregates, i.e., "polymersomes" with average diameters

between 600 and 1400 nm (Figure 82, bottom). For the hydrophilic to hydrophobic volume ratio chosen, spherical micelles or cylindrical aggregates would have been expected from a conventional point of view, especially since it is known that crystalline domains in the hydrophobic block of an aggregate can promote the formation of cylinders with a small length/width aspect ratio.[50]
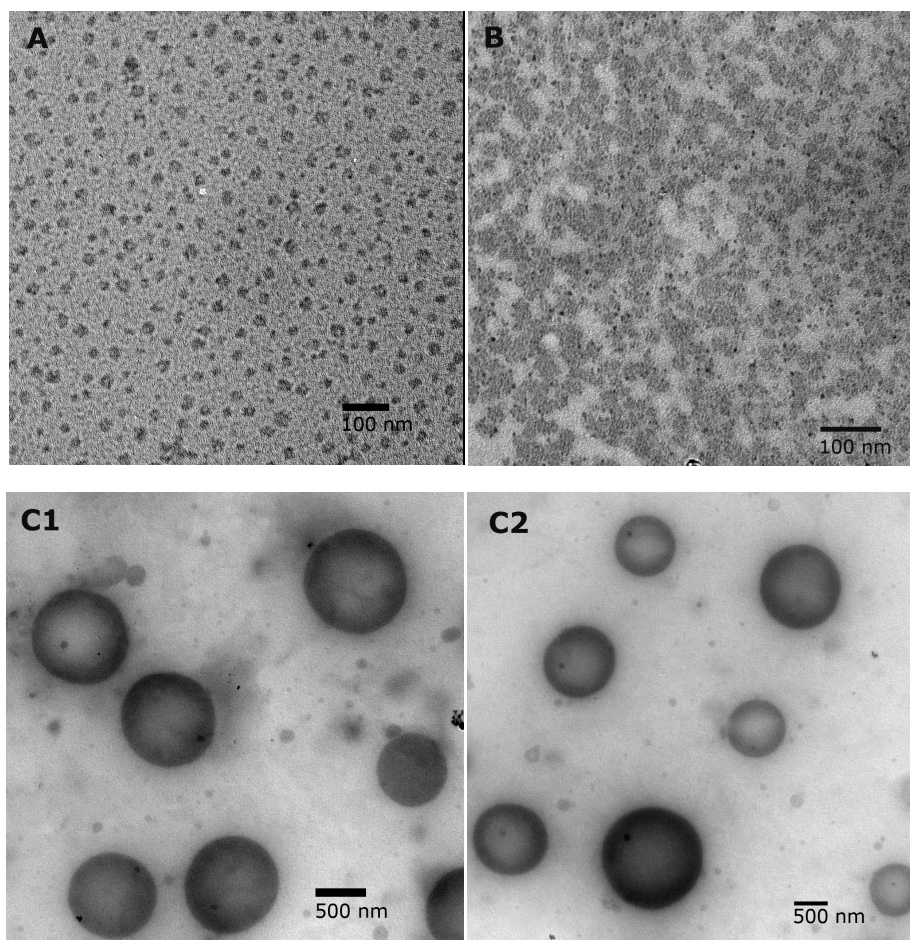

Figure 82: TEM image of (A) PIGMA$_{47}$-*b*-PLLA$_{26}$ and (B) PIGMA$_{47}$-*b*-PDLA$_{28}$[†] micellar aggregates with an average diameter of 20 to 30 nm. Sample preparation was carried out under identical conditions with a 1:1 mixture of PIGMA$_{47}$-*b*-PLLA$_{26}$ and PIGMA$_{47}$-*b*-PLLA$_{28}$ afforded large polymersomes (C1 and C2) with a diameter between 600 and 1400 nm (bottom).

[†] In the case of sample preparation of the PIGMA$_{47}$-*b*-PDLA$_{28}$, the copper grids were not hydrophilized by argon/oxygen plasma treatment because of an equipment failure. This fact impaired the spreading of the sample on the grid and thus caused higher local aggregate concentrations.

Since our block copolymers show a significantly increased hydrophilic to hydrophobic ratio, polymersome formation[9] is unlikely and indeed not observed for aggregate solutions with a single homochiral PLA component (Figure 82, top). Since all other parameters remained unchanged during aggregate preparation, stereocomplexation can be considered to be a very likely cause for the change in the aggregate morphology. Here, the question arises, how bilayer formation, as a prerequisite for polymersome formation, is triggered. Since the thermodynamic parameters are not known for this new block copolymer system, we can only argue with the sum of poly(lactide)s´ known characteristics[51] to put forward a conclusive explanation. Due to its stereoregular methyl substituent in alpha-position, poly(D/L- lactide) represents a rather stiff hydrophobic part of the block copolymer with a low conformational degree of freedom, resulting in a rather high T_g , i.e., 30-40 K above room temperature. This stiffness is generally known to promote the formation of planar bilayer structures. Although this behavior is obviously not sufficiently pronounced for non crystalline poly(L-lactide), as expected for the employed average number of repeating units (26 and 28), the formation of stereocomplex-induced crystallization appears to be important for the mixed block copolymers. Antonietti and Förster concluded that "*planar assemblies are spontaneously formed in a much broader range in phase space, if there is a tendency of the tecton* (in this case a block copolymer) *to exhibit at least nematic order*"[52]. The additional 3-dimensional positional order of the 3_1 helical conformation in the α-form, in which the stereo-complexed poly(lactide) "tecton" is packed in a parallel fashion[53] is based on nocovalent secondary valences and most likely promotes the formation of planar assemblies and hence represents the reason for the formation of polymersome-type structures. We believe that the preparation technique employed via the indirect dissolution[54] from THF with water is an important factor to obtain the defined aggregates we observed. THF is a good solvent for stereoregular PLA of moderate molecular weight and a poor solvent for crystalline, stereocomplexed PLA. This ensured sufficient chain mobility upon aggregate formation, while not endangering the formation of stable crystalline domains, which are not formed unless a controlled amount of water as poor solvent for the inner PLA-block is added.

This is further supported by an SEC examination (DMF, from THF/HCl solution) of the freshly prepared 1:1 mixture of $PIGMA_{47}$-*b*-$PLLA_{26}$ and $PIGMA_{47}$-*b*-$PDLA_{28}$ prior to selective dissolution. Intriguingly, the SEC trace of this mixture was monomodal and showed no

aggregate formation. Evaluation with PS-standards provided a sample of similar molecular weight and polydispersity resembling those obtained for their homopolymers (

Table 15). A more detailed report on the intriguing topic of stereocomplex-induced changes in block copolymer aggregate morphology in solution will be subject of a forthcoming publication.

An additional interesting feature of the prepared aggregates is the high number of primary hydroxyl groups at their periphery. This provides interesting potential for the block copolymer in targeted drug delivery, since the abundance of hydroxyl groups at the corona allows attachment of (multiple) distinct piloting/targeting functions to the micelle corona by straightforward chemistry. Stereocomplex-induced crystallization knowingly contributes to an enhanced kinetic and thermodynamic stability of aggregates. In their potential application as sustained release devices, stereocomplexation could thus increase plasma circulation time of PIGMA-*b*-PLA copolymers, facilitating their accumulation at the target site.

Conclusions

This work presents the first synthesis of poly(*cis*-benzylidene isoglycerol methacrylate) (PBGMA), a polymer which exhibits interesting materials properties and can easily be transformed into poly(isoglycerol methacrylate), which exclusively contains primary hydroxyl-groups along the backbone. This was realized by selective acetal protecting chemistry in form of the new glycerol based methacrylate monomer BGMA (benzylidene glycerol methacrylate). The monomer is suitable for the preparation of poly(ester) based block copolymers with a bifunctional initiator via (i) ATRP and (ii) ring-opening polymerization of lactide. Selective acetal cleavage of the benzylidene groups yielding the amphiphilic poly(isoglycerol methacrylate)-*b*-(poly (L-lactide)), which was capable of self assembly in micellar solution. Structural similarity is obvious for the recently investigated poly(glyceryl glycerol), which is accessible from oxyanionic polymerization, employing either osmylation chemistry or release from its acetonide protecting group.[55]

Illustrating the aggregation potential of the block copolymerss, we have been able to demonstrate that PIGMA is a potential alternative for PEG as hydrophilic component in biocompatible block copolymers with promising attributes for drug delivery systems. In combination with poly(lactide), micelles with low CAC could be obtained. Their morphology

could be adjusted from micellar to polymersome type aggregates by changing the physiochemical cross-linking with enantiomeric poly(lactide) blocks via stereocomplexation.

With this work we aim at further exploration of the field of amphiphilic poly(ester)/polyacrylate based block copolymers suitable for biomedical purposes.

References

[1] Jacobson, G. B.; Shinde, R.; Contag, Ch. H. Zare, R. N. *Angew. Chem.* **2008**, *120*, 7998 –8000.

[2] Meng, F.; Zhong, Z.; Feijen, J. *Biomacromolecules* **2009**, *10,* 197-209.

[3] Liu, S.; Maheshwari, R.; Kiick, K. L. Macromolecules **2009**, *42*, 3-13.

[4] Meng, F.; Hiemstra, Ch.; Engbers, G. H. M.; Feijen, J. *Macromolecules* **2003**, *36,* 3004-3006.

[5] Kang, N.; Perron, M.-E.; Prud'homme, R. E.; Zhang, Y.; Gaucher, G.; Leroux, J.-C. *Nano Lett.* **2005**, *5*, 315-319.

[6] Kim, S. H.; Tan, J. P. K.; Nederberg, F.; Fakushima, K.; Yang, Y. Y.; Waymouth, R. M.; Hedrick, J. L. *Macromolecules,* **2009,** *42*, 25-29.

[7] Kopeček, J.; Bažilová, H. *Eur. Polym. J.* **1973**, *9,* 7-14.

[8] Robinson, K. L.; de Paz-Bánẽz, M. V.;Wang, X. S.; Armes, S.P**.** *Macromolecules* **2001,** *34,* 5799-5805.

[9] Yin, H.; Kang, S.-W. Bae, Y. H. *Macromolecules* **2009**, 42, 7456–7464.

[10] Save, M.; Weaver, J. V. M.; Armes, S. P.; McKenna, P. *Macromolecules* **2002**, *35,*1152-1159.

[11] Feil, H.; Bae, Y. H. Feijen, J.; Kim, S. W. *Macromolecules* **1993***, 26,* 2496-2500.

[12] Barz, M.; Tarantola, M. Fischer, K.; Schmidt, M.; Luxenhofer, R.; Janshoff, A.; Theato, P. Zentel, R. *Biomacromolecules* **2008,** *9,* 3114–3118.

[13] Hu, F.; Neoh, K. G.; Kang, E.-T. *Macromol. Rapid Commun.* **2009**, 30, 609–614.

[14] Hawker, C. J.; Hedrick, J. L.; Malmström, E. E.; Trollsås, M.; Mecerreyes, D.; Moineau, G.; Dubois, Ph.; Jérôme, R**.** *Macromolecules* **1998,** *31*, 213-219.

[15] Mecerreyes, D.; Moineau, G.; Dubois, Ph.; Jérôme, R**.**, Hedrick, J. L.; Hawker, C. J.; Malmström, E. E.; Trollsås, M. *Angew. Chem. Int. Ed.* **1998**, *37*,1274-1276.

[16] Chen, Y. M.; Wulff, G. *Macromol. Rapid Commun.* **2002**, *23*, 59-63.

[17] Jakubowski, W.; Lutz, J. F.; Slomkowski, S.; Matyjaszewski K. *J. Polym. Sci. A: Polym. Chem* **2005**, *43*, 1498–1510.

[18] Schappacher, M.; Fur, N.; Guillaume, S. M.; *Macromolecules* **2007,** *40,* 8887-8896.

[19] Jakubowski, W.; Matyjaszewski; K. *Macromol. Symp.* **2006**, 240, 213–223.

[20] Messman,J. M.; Scheuer, A. D.; Storey, R. F.; *Polymer* **2005**, *46*, 3628-3638.

[21] Hales, M., Barner-Kowollik, Ch., Davis, Th. P.; Stenzel, M. H. *Langmuir,* **2004**, *20*, 10809-10817.

[22] Spasova, M.; Mespouille, L.; Coulembier, O.; Paneva, D.; Manolova, N; Rashkov, I.; Dubois, Ph. *Biomacromolecules* **2009,** *10,* 1217–1223.

[23] Jakubowski, W.; Matyjaszewski, K. *Macromol. Symp.* **2006**, *240*, 213–223.

[24] Chagneux, N.; Trimaille, Th.; Rollet, M. Beaudoin, E.; Gerard, P.; Bertin, D.; Gigmes, D. *Macromolecules* **2009**, 42, 9435–9442.

[25] Wolf, F.; Friedemann, N.; Frey, H. *Macromolecules*, **2009**, *42*, 5622–5628.

[26] Giacomelli. C.; Borsali R. *Macromol. Rapid Commun*. **2008**, *29*, 573–579.

[27] Bougard, F.; Giacomelli, C. Mespouille, L.; Borsali, R. Dubois, Ph.; Lazzaroni, R *Langmuir* **2008**, *24,* 8272-8279.

[28]Clément, B.; Trimaille, T; Alluin, O.; Gigmes, D.; Mabrouk, K. ; Féron, F.; Decherchi, P.; Marqueste, T.; Bertin, D. *Biomacromolecules* **2009,** *10,* 1436–1445.

[29] Weaver, J. V. M; Bannister, I.; Robinson, K. L.; Bories-Azeau, X.; Smallridge, M; McKenna; P.; Armes, S. P. *Macromolecules* **2004,** *37,* 2395-2403.

[30] Save, M.; Weaver, J. V. M; McKenna, P; Armes, S.P. *Macromolecules* **2002,** *35,* 1152-1159.

[31] Ishizone, T.; Han, S.; Okuyama, S.; Nakahama, S. *Macromolecules* **2003,** *36,* 42-49.

[32] (a) Oguchi, K.; Sanui, K.; Ogata, N.; *Polym. Eng. Sci.* **1990**, *30*, 449-452 (b) Mori, H.; Hirao, A.; Nakahama, S. *Macromolecules* **1994**,*27*, 35-39.

[33] Pilon, L. N.; Armes, S. P.; Findlay, P.; Rannard, S. P.; *Langmuir* **2005,** *21,* 3808-3813.

[34] Zhang, H.; Ruckenstein, E. *Macromolecules* **2000**, *33,* 4738-4744.

[35] Gudipati, Ch. S.; Tan, M. B. H.; He, Ch.; Davis, T. P. *Macromol. Rapid Commun.* **2008**, *29*, 1902–1907.

[36] Amado, E.; Augsten, Ch.; Mäder, D.; Blume, A.; Kressler, J *Macromolecules* **2006,** *39,* 9486-9496.

[37] Giacomelli, C.; Schmidt, V.; Borsali, R. *Langmuir* **2007,** *23,* 6947-6955.

[38] Jones, M.-Ch.; Gao, H.; Leroux, J.-Ch. *J. Contr. Rel.* **2008**, *132,* 208–215.

[39] Giacomelli, C.; Schmidt, V. Borsali, R. *Macromolecules* **2007**, *40*, 2148-2157.

[40] Mequanint, K.; Patel, A.; Bezuidenhout, D. *Biomacromolecules* **2006,** 7, 883-891.

[41] Patrucco, E.; Ouasti, S.;Vo, C. D.; De Leonardis, P.; Pollicino, A.; Armes, S. P.; Scandola, M.; Tirelli, N. *Biomacromolecules* **2009**, *10,* 3130–3140.

[42] Carlsen, P.H.J.; Sørbeye, K.; Ulven, T.; Aasbø, K. *Acta Chemica Scandinavica* **1996**, *50*, 185-187.

[43] Wilhelm. M.; Zhao C.-L.; Wang, Y.; Xu, R.; Winnik, M. A.; Mura, J.-L.; Riess, G.; Croucher, M. D. *Macromolecules* **1991**, *24*, 1033-1040.

[44] Coskun, M.; Ilter, Z.; Ozdemir E.; Demirelli, K.; Ahmedzade, M. *Polym. Degrad. Stab.* **1998**, *60,* 185-193.

[45] Matyjaszewski, K.; Shipp, D. A.; Wang, J. L.; Grimaud, T.; Patten, T. E. *Macromolecules* **1998**, *31*, 6836–6840.

[46] (a) Dove, A. P.; Pratt, R. C.; Lohmeijer, B. G. G.; Waymouth, R. M.; Hedrick, J. L. *J. Am. Chem. Soc.* **2005**, *127*, 13798–13799. (b) Pratt, R. C.; Lohmeijer, B. G. G.; Long, D. A.; Lundberg, P. N. P.; Dove, A. P.; Li, H. B.; Wade, C. G.; Waymouth, R. M.; Hedrick, J. L. *Macromolecules* **2006**, *39*, 7863–7871.

[47] Sosnowski, S. *J. Polym. Sci,. Part A: Polym. Chem*. **2008**, *46*, 6978–6982.

[48] Zhang, J.; Wang, L.-Q.; Wang, H.; Tu, K. *Biomacromolecules* **2006,** *7*, 2492-2500.

[49] Kim, S. H.; Tan, J. P. K.; Nederberg, F.; Fakushima, K.; Yang, Y. Y.; Waymouth, R. M.; Hedrick, J. L. *Macromolecules* **2009,** *42*, 25-29.

[50] Lazzari, M.; López-Quintela, M. A. *Macromol. Rapid. Commun.* **2009,** *31,* 1785-1791

[51] Slager, J.; Domb, A. J. *Adv. Drug Delivery Rev.,* **2003** *55*, 549–583.

[52] Antonietti, A., Förster, S. *Adv. Mater.***2003,** *15*, 1323-1333.

[53] Okihara, T.; Tsuji, M.; Kawaguchi, A.; Katayama, K.;Tsuji, H.; Hyon, S.-H.; Ikada, Y. *J. Macromol. Sci. -Phys.* **1991**, *B30*, 119-140.

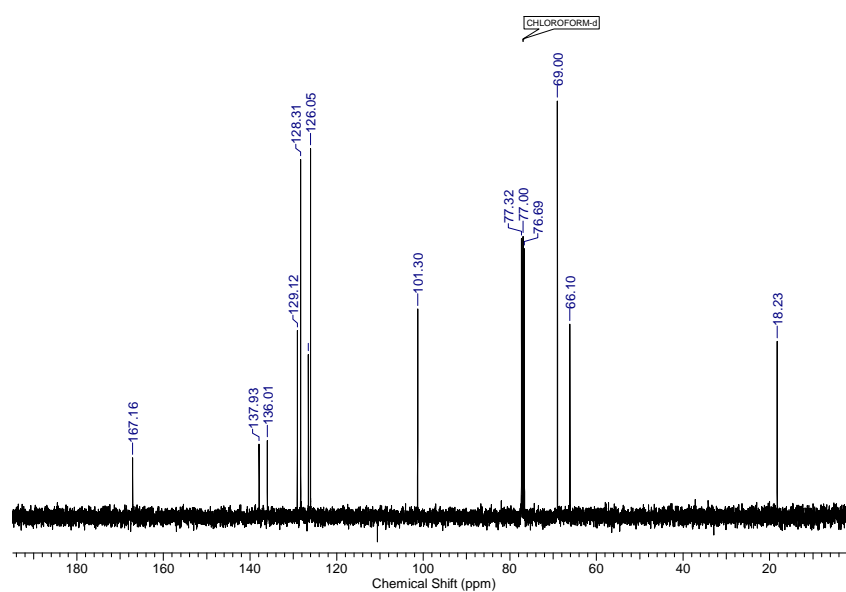[54] Zhang,L.; Eisenberg, A. *Science* **1995**, *268*, 1728-1731.

[55] Wurm, F.; Nieberle, J.; Frey H. *Macromolecules* **2008,** *41,* 1909-1911.
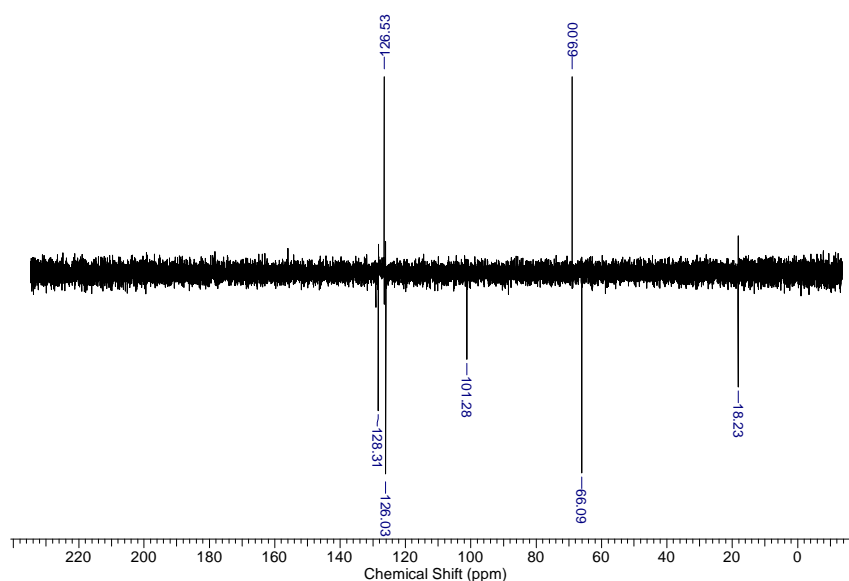
Supporting Information

Poly(isoglycerol methacrylate)-*b*-poly(D- or L-lactide) Copolymers: A Novel Hydrophilic Methacrylate as Building Block for Supramolecular Aggregates

Florian K. Wolf, Anna M.Hofmann and Holger Frey

^{13}C-NMR-Characterization of BGMA

S.I.1: ^{13}C NMR spectrum (CDCl$_3$ 100 MHz)

S.I.2: ^{13}C DEPT NMR spectrum of BGMA (CDCl$_3$ 100 MHz)

3.3 pH-Responsive Aggregates From Amphiphilic Block-Copolymers Based on Poly(ethylene glycol) and Poly(*cis*-1,3-benzylidene glycerol methacrylate)

Florian K. Wolf and Holger Frey*

Abstract

We describe the synthesis, self-assembly behavior, and the pH-triggered release properties of amphiphilic block copolymers with a benzylidene acetal-bearing poly(*iso*-glycerol methacrylate) (PIGMA) hydrophobic block. Two well-defined amphiphilic poly(ethylene glycol)-block-poly(*cis*-1,3-benzylidene glycerol methacrylate) (PEG-*b*-PBGMA) copolymers with different hydrophilic/hydrophobic balances (HLB = 0.3 and 2.0) were realized by atom transfer radical polymerization (ATRP) with a PEG-based macroinitiator (Mn 5200 g/mol). PEG_{111}-*b*-$PBGMA_{62}$ (HLB = 0.33) was subsequently used for the formation of pH-sensitive aggregates that exhibited an interesting worm like shape (TEM). This system was used to encapsulate the hydrophobic fluorescent dye and model payload nile red. Hydrolysis of the pendant acetal groups of the block copolymer was investigated using UV/VIS spectroscopy, confirming the disintegration of the aggregates by hydrolysis of the benzylidene acetal and formation of benzaldehyde. Fluorescence spectroscopy of the encapsulated nile red allowed to monitor the release of a hydrophobic model payload in acidic aqueous environment under the disintegration of the aggregates. These in vitro studies showed pH-dependent release behavior. Significantly faster dye release was observed at a pH of 4.0 compared to pH 5.0 or physiological pH.

Results and Discussion

Polymeric micelles and nanocapsules, formed by aggregation of amphiphilic block copolymers are considered to be promising for a large variety of applications. The most interesting examples could be the delivery/release of various substances (drugs and cosmetically active substances are especially interesting in this context), biomineralization,[1] the use as nanoreactors[2] or stabilizers in heterogeneous catalysis[3] and as dispersants for insoluble materials[4,5]. Generally, the controlled disintegration of polymeric aggregates as a consequence of an external trigger is highly desirable, for instance in the controlled delivery of therapeutic agents. A variety of mechanisms to accomplish this transition seem plausible. The chemical structure of the core-forming block can be utilized to render polymer micelles susceptible to external stimuli, such as changes in pH,[6] temperature or strong mechanical forces (e.g., due to ultrasound).[7]

In contrast to block copolymer aggregates composed of polymer blocks or components containing ionizable groups that undergo structural changes or destabilization by pH in a reversible manner,[8] the cleavage of hydroxyl-masking groups represents a practically irreversible transformation.[9] Besides ortho-esters[10], acetal groups[11,12] represent a cleavable link of choice to induce a permanent polarity change of a polymer. This has been exploited in various acid sensitive linkages in polymer- drug conjugates that have been developed to take advantage of pH changes as release trigger.[13,14] In 2005, Fréchet and coworkers presented a strategy towards pH-sensitive aggregates via linear and linear-dendritic architectures with pendant acetal groups. Zhong and coworkers very recently constructed drug release systems based on poly(ethylene glycol) (PEG) and poly(mono- or trimethoxy-benzylidene-pentaerythritol carbonate) (PMBPEC)/(PTMBPEC)[15]. Micelles incorporating the therapeutic agent were degraded under loss of their amphiphillic character due to a polarity change of the hydrophobic polycarbonate block. This was achieved by cleavage of the benzylidene acetal group at pH 5 on a time scale of several hours. These studies show that the structural motif of the cyclic benzylidene acetals is particularly attractive as acid sensitive moiety, since the hydrophobic aromatic ring efficiently masks the high polarity of copolymer linked 1, 3 – diol groups. This has recently been demonstrated by Grinstaff et. al. in methacrylate-based microparticles produced via mini-emulsion polymerization[16].

In this Communication we present a new block copolymer system, which is based on the very recently introduced *cis*-benzylidene *iso*-glycerol methacrylate (BGMA) monomer[17] and

realized by a straightforward living radical polymerization from a PEG-macroinitiator. Acid catalyzed cleavage of the apolar, acetal-protected PBGMA block leads to release of the hydrophobic payload.
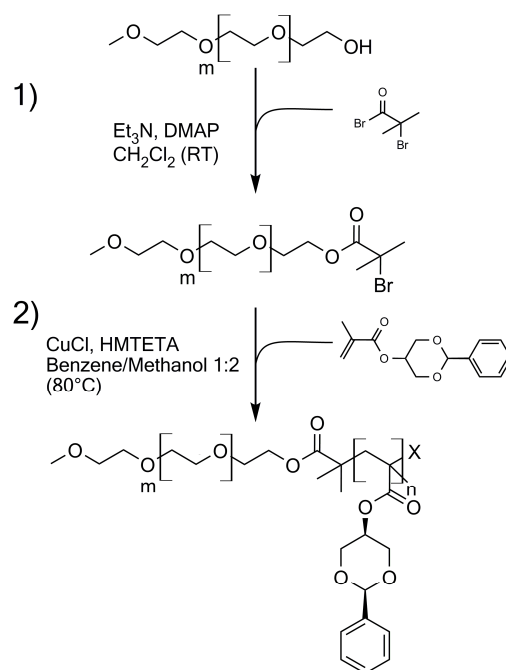

Figure 83: Synthetic route to PEG-*block*-PBGMA copolymers. The formation of the PEG macroinitiator is followed by ATRP of BGMA, affording the amphiphilic block copolymers.

Monomer and polymer design. The advantage of the recently introduced *cis*-benzylidene glycerol methacrylate (BGMA) and the respective polymer[17,18] lies in their simple synthesis and the predictability of the acidic cleavage products, i.e. benzaldehyde and the glycerol ester of methacrylic acid. The monomer preparation is based on (i) the formation of the 1,3-benzyl acetal of glycerol, followed by (ii) esterification of the free secondary hydroxyl-function of the acetal. This pathway enables the synthesis of the raw material in high quantities and allows facile variation of the substituents at benzaldehyde. The hydrolysable acetal group of the glycerol derivative attached to a methacrylate functionality of the block copolymer permits convenient assembly of the block structure via an established controlled living radical polymerization method. ATRP was considered the method of choice, since it had already shown good performance for the polymerization of BGMA[17]. Major drawbacks of previously reported benzylidene acetal carrying copolymer systems, like the challenging polymerization of *N*-carboxy anhydrides initiated from PEO-NH$_2$[19] or the elaborate,

generation wise build up of the dendritic block in acetal bearing linear-dendritic block copolymers[20] can thus be circumvented.

In order to create an amphiphilic block structure in a convenient 2 step process (Figure 83), commercially available PEG monomethyl-ether (mPEG) with a molecular weight of 5000 g/mol was chosen as an established hydrophilic segment, which exhibits high solubility in water, no immunogenicity, antigenicity, and toxicity.[21] Esterification with 2-bromoisobutyryl bromide yielded an ATRP macroinitiator (S.I. 1), which could be chain-extended to form well-defined block copolymers (Figure 85). To ensure a high initiation rate and thus realize complete conjugation of the second block we employed the mixed halide exchange technique, using a CuCl/HMTETA system. These ATRP polymerization conditions were adopted from a procedure previously introduced for the copolymerization of PBGMA - poly(lactide) block copolymers. Although ATRP showed incomplete conversion (51 and 69%, respectively), block copolymer precipitation from cold acetone yielded pure block copolymer in the respective yields.
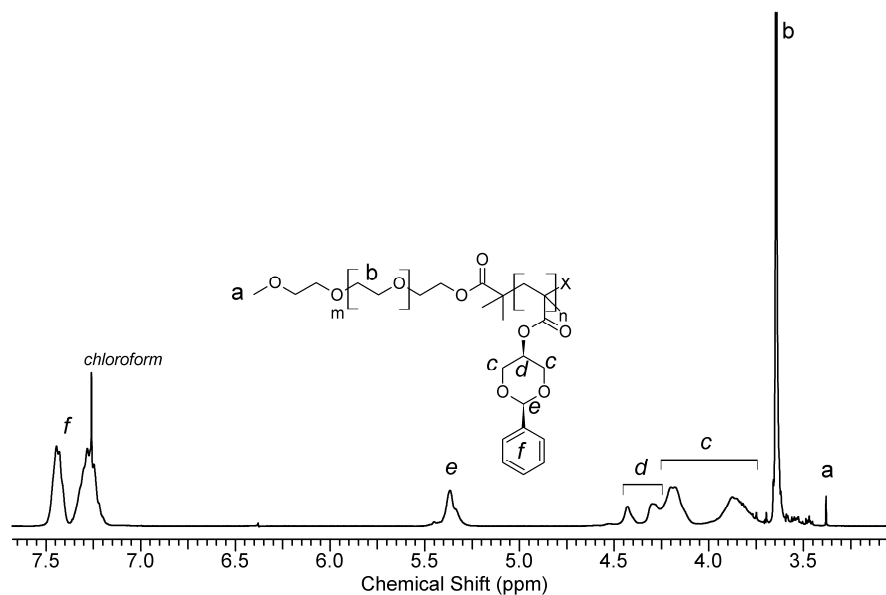

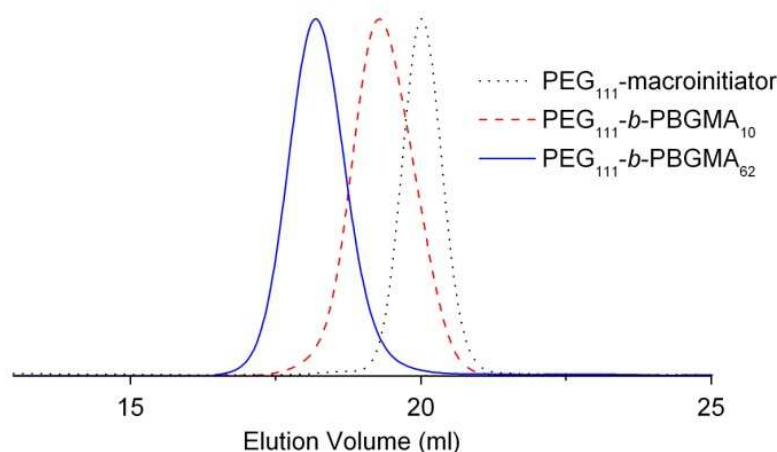Figure 84: ^{1}H NMR spectrum of the PEG$_{111}$-$block$-PBGMA$_{62}$ (P3) block copolymer.

Figure 85: SEC-traces (DMF+0.5% LiBr) for the PEG-macroinitiator and the block copolymers derived thereof.

As described recently, molecular weight determination of PBGMA and PBGMA-*b*-PLA based polymers via SEC in THF or DMF with PEG standards resulted in a significant underestimation of molecular weight[11] - a fact that could also be observed here. The number-average molecular weights (M_n) and the polydispersity indices (M_w/M_n) of the corresponding block copolymers deduced from both SEC and ^{1}H NMR as well as the CAC values (critical aggregation concentration) together with the hydrophilic-lipophilic balance values (HLB) are listed in Table 1. Although the proximity of the different linear combinations of the block copolymer limits resolution of single polymer masses, MALDI-ToF spectroscopy (cf. S.I. 2) of PEG$_{111}$-*b*-PBGMA$_{62}$ shows a monomodal mass distribution around 23,000 g/mol and therefore supports the molecular weight determined by NMR spectroscopy (Figure 84).

Table 16: Molecular characterization data for the PEG-*b*-PGMA block copolymer samples

Sample	Compostion	M_n (NMR)	M_n (SEC)*	M_w/M_n (SEC)*	M_n (cleaved)♣	HLB#	CAC (mg/L)§
P1	PEG$_{111}$-macroinitiator	5200	4800	1.03	-	-	-
P2	PEG$_{111}$-*b*-PBGMA$_{10}$	7500	6400	1.07	6600	2.01	4.3
P3	PEG$_{111}$-*b*-PBGMA$_{62}$	20400	10900	1.08	14900	0.33	1.6

* = (g/mol), determined via SEC in DMF/evaluation with PEG standards

\# = hydrophilic/lypophilic balance

§ = critical aggregation concentration (CAC) as determined by pyrene fluorescence spectroscopy

♣ = theoretical molecular weight after complete acetal cleavage based on the molecular composition determined via ^{1}H NMR

In the following, we will focus on the examination of the aggregation and release behavior of PEG$_{111}$-*b*-PBGMA$_{62}$ (P3) upon acetal cleavage. The combination of long PBGMA chain length and a low HLB promises the formation of kinetically stable aggregates with good loading capacity for potential hydrophobic guest molecules.

Aggregation in aqueous environment: The amphiphilic PEG-*b*-PBGMA copolymers were not directly soluble in water. Due to the apolar nature and high T_g (i.e. 120-130°C) of the PBGMA-block, the copolymer micelles had to be prepared by first dissolving a certain amount of block copolymer in THF, which is a co-solvent for both blocks. Deionized water was then added drop-wise under vigorous stirring within 2 hours. Samples were transferred to dialysis tubing, sealed, and dialyzed against 10 mM pH 7.3 buffer. Removal of the nonselective organic solvent by dialysis against water together with the high T_g of the core forming block most likely resulted in frozen micelles, as it is known from copolymer systems with polystyrene as the hydrophobic block[22]. Determination of the critical aggregation concentration was conducted by fluorescence spectroscopy, using pyrene.[23] With values between 1.6 and 4.3 mg/L they were sufficiently low for application as drug delivery systems. TEM images of a dried aggregate solution (P3), which were previously stained by exposure to OsO$_4$ vapor to increase the contrast, are shown in Figure 86.

PEG$_{111}$-*b*-PBGMA$_{62}$ possesses a dominant hydrophobic block and exhibits an interesting worm-like structure with a long persistence length in the micrometer range, as judged from TEM-image inspection (Figure 86, right). This behavior is quite remarkable for PEG-based diblock copolymers in aqueous solution, since the formation of worm like micelles outside the HLB range of 0.45 to 0.55 (compared to 0.33 in the present case) is rarely observed.[24] The lower part of the HLB range is particularly populated by species with higher molecular weight hydrophobic chains.[25] Following this trend, an extrapolation of the aqueous morphology phase diagrams determined by Bates[26] or Maskos[27] renders the present morphology highly plausible, although these values have been determined for PEG block copolymers with highly flexible, low Tg, poly(butadiene) as a hydrophobic segment. The micelle preparation technique for the structurally rigid, high Tg material PBGMA is believed to influence the aggregate geometry as it has been observed for other amphiphilic block

copolymers.[28] Hence we can not preclude the formation of "kinetically trapped" aggregate morphologies which do not necessarily represent equilibrium forms.[29]
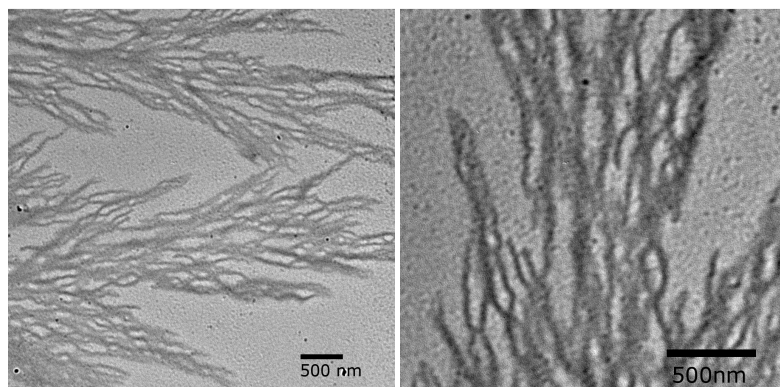

Figure 86: TEM-images of the block copolymers aggregate solutions (P3- stained with OsO$_4$)

Nevertheless, this worm like morphology may be advantageous for flow intensive applications, as encountered in the human blood stream.[30] Furthermore, cylindrical aggregates have shown enhanced permeation into porous tissue compared to spherical aggregates of similar dimensions.[31]

pH-dependent aggregate disintegration and Nile Red release: The PEO-*b*-PBGMA block copolymers have been designed such that upon hydrolysis of each acetal group at the poly(*cis*-benzylidene glycerol methacrylate) (PBGMA) block an aliqout of glycerol-diol functionality is released. Thereby the core-forming block becomes increasingly hydrophilic upon exposure to a sufficiently acidic environment. This leads to an increasing destabilization/disintegration of the micelle and should enable the release of the drug from its hydrophobic compartment into the environment (cf. Scheme 11).
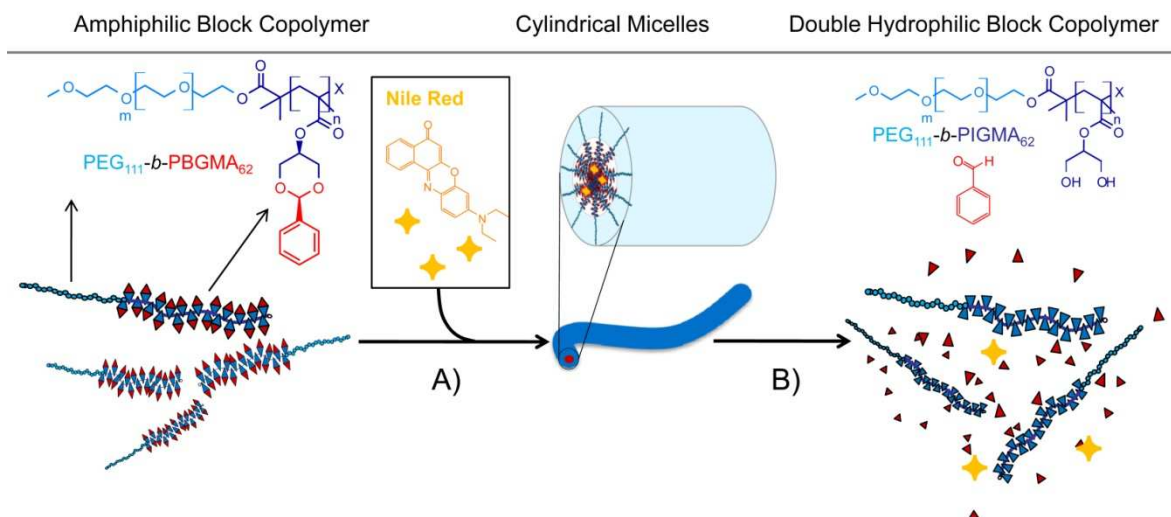
Scheme 11: General mode of action for the aggregation and controlled disassembly of the PEG-*b*-PBGMA block copolymers. A) The hydrophobic fluorescence dye Nile Red is loaded into the hydrophobic micellar core of the benzylidene acetal bearing poly(methacrylate) block. B) Upon exposure to an acidic environment, the benzylidene groups are hydrolyzed. The polarity change of the core causes a disintegration of the micelle, which is accompanied by a release of the hydrophobic model payload (i.e. the dye).

After following the above described preparation procedure of the dye-loaded aggregates the sample was separated into three aliquots, and for two samples the pH was adjusted to 4.0 or 5.0 by addition of a small volume of concentrated pH acetate buffer of the respective pH. The third sample was adjusted to the same salt concentration by adding additional phosphate buffer. Hydrolysis of the acetal groups of the polymethacrylate structure within the micellar cores was investigated for each copolymer aggregate solution at 37 °C and at different pH values. In the case of monomethoxy- or trimethoxy-benzaldehyde, acetal hydrolysis can be followed by UV/vis spectroscopy by comparing the absorbance intensity of the aldehyde hydrolysis products at 279 and 290 nm, respectively, with that of the polymer-linked acetals. The present system of the rather electron deficient benzaldehyde/benzylacetal exhibits UV-absorption maxima that are shifted towards lower wavelengths. While free benzaldehyde is characterized by an absorption maximum at approx. 250 nm in the aqueous system, the respective glycerol acetal (5-hydroxy-2-phenyl-1,3-dioxane) shows significant signal overlap with the water-related absorption below 210 nm (Figure 87, right). Corresponding UV-absorption behavior was observed for the polymer bound acetal (Figure 87, left). Although this fact impedes a precise quantitative evaluation, as conducted in studies dealing with 1,3,5 trimethoxybenzaldehyde derivatives, the general

disappearance of PBGMA-acetal related absorption bands could be followed (Figure 87, left). It was accompanied by the appearance of a band at approx. 248-250 nm, which is related to the successful segregation of benzaldehyde at pH 4 within 18h. At pH 5 and physiological pH, no change in the absorption behavior could be observed for this sample and significant amounts of benzaldehyde were not formed within the examined time range.
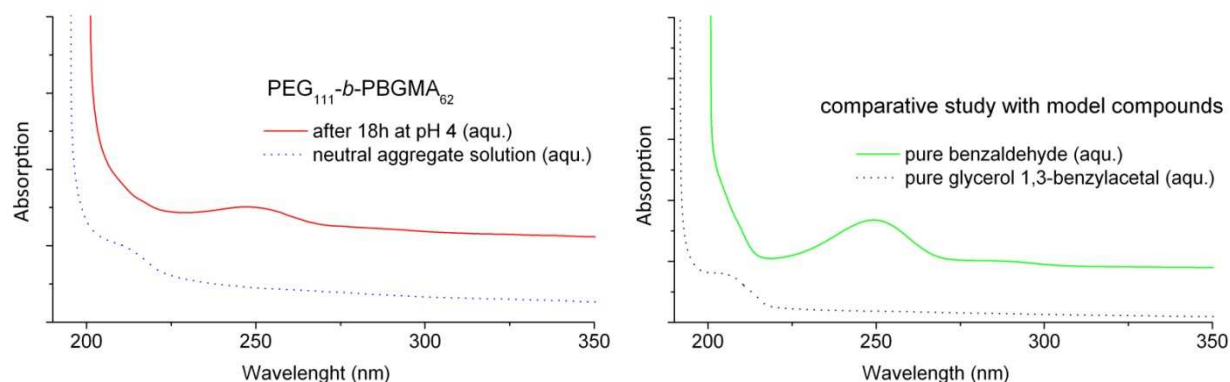

Figure 87: Release of benzaldehyde throughout the process of acetal cleavage monitored via UV-vis spectroscopy at pH 4.

To monitor the disintegration process over time and to evaluate the release profile, we investigated the change in fluorescence intensity of a hydrophobic model payload. Nile Red was chosen for this purpose, since it is a hydrophobic dye with a negligible fluorescence in aqueous solution. Nevertheless its fluorescence increases strongly in a non-polar environment. It has thus proven to be a good tracer compound to study the disintegration of cellular membranes and supramolecular aggregates in aqueous environment and can furthermore be considered a model payload emulating hydrophobic therapeutic agents[32]. A transition from the hydrophobic micellar core environment to the aqueous solution can conveniently be examined by fluorescence spectroscopy via the Nile Red emission intensity at approx. 580 nm. A significant decrease in fluorescence intensity could indeed be observed for an aqueous solution of Nile Red-loaded PEG$_{111}$-b-PGMA$_{62}$ (**P3**) at pH 4 (37°C) (Figure 88). The steady decrease indicates a consistent release, which is presumably related to a slow disintegration of the hydrophobic core without the characteristics of an undesired burst release (Figure 88). After 11 hours, only 25% of the initial fluorescence remain (S.I. 4) - A significant fluorescence decay above pH 4 is not observed. This behavior resembles the

results obtained by Grinstaff et al.,[10] who tested both plain benzyl acetals as well as trimethoxy-substituted benzyl-acetals for the fabrication of Paclitaxel®-loaded nanopartices. In this case significant release at pH 5 was only observed for the trimethoxy-substituted benzyl acetal. Only slight fluorescence decay is observable in less acidic/neutral environment. We assume that this is caused by dye diffusion out of the micellar core without significant polarity change by acetal cleavage.
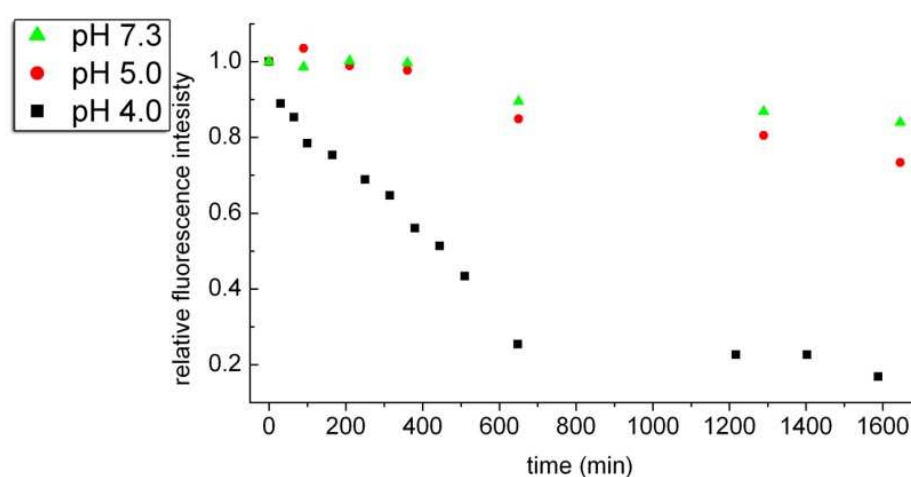

Figure 88: Nile Red fluorescence profile of as a function of pH and time at 37°C for PEG_{111}-b-$PGMA_{62}$.

During the deprotection step at pH 4 the previously slightly opaque aggregate solution of PEG_{111}-b-$PGMA_{62}$ became almost completely transparent, and the characteristic smell of benzaldehyde was noticeable.

Acetal cleavage results in the transformation to a double hydrophilic block copolymer composed of poly(ethylene glycol) and a poly(iso-glycerol methacrylate) backbone with pendant glycerol units. The calculated molecular weights of the released PEG-b-PIGMA copolymers are clearly below the renal exclusion value after full acetal cleavage (Table 16). In the case of in vivo application this should ensure efficient renal elimination from the body. The presented results indicate that these block copolymer aggregates are stable beyond the margins of the desired site of action. The rigid character of PBGMA based aggregates as well as the increased stability of the aggregates at pH > 4 could render PBGMA based block copolymers interesting for applications in cancer therapy.[33] Premature release of the payload in the extracellular matrix before the potential internalization might be prevented and thus allow for a specific targeting of lysosomes (pH 4-5) in malignant cells.[8,34] A broader

range of block ratios and especially the preparation and behavior of spherical micelles will be examined in the near future.

In summary, we have realized a novel, well-defined amphiphilic block copolymer system in a simple two-step procedure. First a poly(ethylene glycol) macroninitiator was prepared and then chain-extended via the controlled radical polymerization of *cis*-1,3-benzylidene glycerol methacrylate with CuCl/HMTETA. Aggregation in aqueous environment was achieved via the controlled dissolution method from THF. The disintegration of the aggregates could be qualitatively examined via UV/vis spectrometry of the backbone pendant benzylidene acetal and free benzaldehyde. The disintegration kinetics at different, physiologically relevant pH values was followed indirectly by the fluorescence studies of a formerly encapsulated hydrophobic guest species (Nile Red). Compared to reported linear and linear-dendritic block copolymers with trimethoxy-substituents, the PEG-*b*-PBGMA based aggregates/nanoparticles require slightly lower pH for disintegration. At physiological pH or pH 5 the aggregates are stable and do not - or only slowly release the encapsulant (depending on the molecular weight of the core forming block). A further decrease to pH 4 hydrolyses the benzylidene protecting group within a few hours and liberates the primary hydroxyls, which causes the desired hydrophobic to hydrophilic transformation and continuous disintegration of the aggregate. Currently, substituted benzylidene glycerol methacrylate derivates and random copolymer combinations thereof are being studied and appear to be promising for further tailoring of the release profiles.

Supporting Information Available: Employed methods and materials, ^{1}H NMR spectroscopy with end-group analysis of PEG macroinitiator, detailed synthetic procedures, UV-vis and fluorescence spectroscopy data. This material is available free of charge via the Internet at http://pubs.acs.org.

References

[1] Mann, S. *Nature* **1993**, *365*, 499 - 505

[2] Nardin, *C.;* Thoeni, *S.;* Widmer, *J.;* Winterhalter*, M.* Meier, W**.** *Chem. Commun.* **2000**, 1433–1434

[3] Astruc, D.; Lu, F.; Aranzaes, J. R. *Angew. Chem. Int. Ed*. **2005**, *44*, 7852 – 7872

[4] Shin, H.Min, B.G.; Jeong, W.; Park, Ch. *Macromol. Rapid. Commun.* **2005**, 26, 1451–1457

[5] Zorn, M.; Bae, W. K.; Kwak, J.; Lee, H.; Lee, Ch.; Zentel, R.; Cha, K. *ACS Nano* **2009**, *3*, 1063-1068

[6] Oh, K.T.; Yin, H.; Seong, E.; Bae, Y. H. *J. Mater. Chem.*, **2007**, *17*, 3987–4001

[7] Schmaljohann, D. *Adv. Drug Del. Rev.* **2006**, *58*, 1655–1670

[8] Lee, E. S. Gao, Zh.; Bae, Y. H. *J. Contr. Rel.* **2008**, 132, 164–170

[9] Rijcken, C. J. F.; Soga, O.; Hennink, W. E.; van Nostrum, C. F. *J. Contr. Rel.* **2007**, *120*, 131–148.

[10] (a) Huang, X. N.; Du, F. S.; Ju, R.; Li, Z. C. *Macromol. Rapid Commun.* **2007**, *28*, 597–603. (b) Huang, X. N.; Du, F. S.; Liang, D. H.; Lin, S. S.; Li, Z. C. *Macromolecules* **2008**, *41*, 5433–5440. (c) Huang, X. N; Du, F. S.; Cheng, J.; Dong, Y.; Liang, D.; Ji, S.; Lin, S. S.; Li, Z. C. *Macromolecules* **2009**, *42*, 783-790.

[11] Morinaga, H.; Morikawa, H.; Wang, Y.; Sudo, A.; Endo T**.** *Macromolecules* **2009**, *42*, 2229-2235

[12] Zou, Y.; Brooks, D. E.; Kizhakkedathu, J. N.; *Macromolecules* **2008**, *41*, 5393-5405

[13] Ulbrich, K.; Subr, V. *Adv. Drug Del. Rev.* **2004**, *56*, 1023– 1050

[14] Giacomelli, C.; Schmidt, V.; Borsali, R. *Macromolecules* **2007,** *40,* 2148-2157

[15] Chen, Wei; Meng, F.; Li, F.; Ji, S.-J.; Zhong, Z *Biomacromolecules* **2009,** *10,* 1727–1735.

[16] Griset, A. P.; Walpole, J.; Liu, R.; Gaffey, A.; Colson,Y. L.; Grinstaff, M.W. *J. Am. Chem. Soc.* **2009**, *131*, 2469–2471

[17] Wolf, F. K.; Hofmann, A. M.; Frey, H. *Macromolecules* **2010**, *43*, 3314–3324

[18] Lu, J.; Li, N.; Xu, Q.; Ge, J.; Lu, J.; Xia, X.; *Polymer* **2010**, 51, 1709–1715

[19] (a)Yokoyama, M.; Kwon, G. S.; Okano, T.; Sakurai, Y.; Seto, T.; Kataoka, K.; *Bioconjugate Chem.*, **1992**, *3*, 295. (b) Gillies, E. R.; Fréchet, J. M. J. *Chem. Commun.* **2003**, 1640-1641

[20] Gillies; E. R.; Jonsson, T. B.; Fréchet, J.M.J *J. Am. Chem. Soc.* **2004,** 126, 11936-11943. (b) Gillies; E. R.; Fréchet, J.M.J; *Bioconjugate Chem*. 2005, 16, 361-368

[21] *Poly(ethylene glycol) Chemistry: Biotechnical and Biomedical Applications;* Harris, J. M., Ed.; Plenum Press: New York, 1992.

[22] Zhang, L.; Barlow, R. J.; Eisenberg, A. *Macromolecules* **1995**, *28*, 6055–6066.

[23] Wilhelm. M.; Zhao C.-L.; Wang, Y.; Xu, R.; Winnik, M. A.; Mura, J.-L.; Riess, G.; Croucher, M. D. *Macromolecules* **1991**, *24*, 1033-1040

[24] Won, Y. Y.; Brannan, A. K.; Davis, H. T.; Bates, F. S. *J. Phys. Chem. B* **2002,** *106,* 3354-3364

[25] Jain, S.; Bates, F. S. *Macromolecules* **2004,** *37,* 1511-1523

[26] Jain, S.; Bates, F. S. *Science* **2003,** *300*, 460-464

[27] Maskos, M. *Polymer* 2006, *47,* 1172–1178

[28] Lazzari, M.; López-Quintela, M. A. *Macromol. Rapid Commun*. 2009, 30, 1785–1791

[29] Henselwood, F.; Liu, G**.** *Macromolecules* **1997,** *30,* 488-493

[30] Dalhaimer, P.; Bates, F.S.; Discher, D. E. *Macromolecules* **2003,** *36,* 6873-6877

[31] Kim, Y.; Dalhaimer, P.; Christian, D.A. Discher, D. E. *Nanotechnology* **2005**, 16, 484-491

[32] Krishna, M. M. G. *J. Phys. Chem. A* **1999***, 103,* 3589-3595

[33] Ganta, S.; Devalapally, H.; Shahiwala, A.; Amiji, M. *Journal of Controlled Release* **2008**, 126, 187–204

[34] Duncan, R. *Anti-Cancer Drugs* **1992,** *3*, 175–210

Experimental Section

Instrumentation

NMR investigation: All ^{1}H and ^{13}C nuclear magnetic resonance (NMR) spectra were recorded at 25°C, using a Bruker AMX 400 (400.1/100.67 MHz) spectrometer. The spectra were measured in $CDCl_3$ and the chemical shifts are referenced to the internal calibration on the solvents′ residual peaks. ([1]H: 7.26 ppm for $CDCl_3$, [13]C: 77.00 ppm for $CDCl_3$). For SEC measurements in DMF (containing 0.5 g/L of lithium bromide as an additive), an Agilent 1100 series was used as an integrated instrument including a PSS Gral column combination (with $10^4/10^4/10^2$ Å porosity) and a RI detector. Calibration was carried out using poly(ethylene glycol) standards provided by Polymer Standards Service and performing a 3rd order polynomial fit. UV/vis spectroscopy was performed with a JASCO V-630 UV-VIS spectrophotometer and fluorescence was measured on a JASCO PL6200 spectrofluorometer. MALDI-ToF MS measurements were performed on a Shimadzu Axima CFR MALDI-ToF MS mass spectrometer, equipped with a nitrogen laser delivering 3 ns laser pulses at 337 nm. Dithranol (1,8-dihydroxy-9(10*H*)-anthracetone, Aldrich 97%), was used as a matrix. Potassium triflate (Aldrich, 98%) was added for ion formation. Good results were obtained for samples prepared from THF solution by mixing matrix (10 mg/mL), polymer (4 mg/mL), and salt (0.1 N solution) in a ratio of 5:1:1. A volume of 2 μL sample solution was deposited on the MALDI target and allowed to dry at room temperature for 2 h prior to the measurement.

Materials

All solvents were of analytical grade and purchased from Acros Organics. Methylene chloride was refluxed over phosphorous pentoxide and destilled immediately prior to use. 2-Bromo-2-methylpropionyl bromide was obtained from Acros Organics and used as received. Triethylamine was refluxed over CaH_2 and distilled freshly prior to use. PEG-5000 mono-methyl ether was purchased from Aldrich and used as received. The monomer preparation of 2-phenyl-1,3-dioxan-5yl-methacrylate (BGMA) was conducted as described recently.[17]

Functionalization of PEG with an ATRP initiator-head group

5 g of PEG 5000 mono-methyl ether and a 25 fold molar excess of triethyl amine were dissolved in 50 ml of dry CH_2Cl_2. The flask was immersed in an ice bath and a 20 fold molar excess of 2-bromo isobutyryl bromide was added in 8 shots via a syringe through a rubber septum. The reaction was allowed to warm slowly to room temperature and stirred for 48 h. The reaction mixture was then precipitated in 700 ml of diethyl ether to yield the crude product, which was harvested by filtration. Trace-contamination free polymer was harvested by re-precipitation from 400 ml of cold (-25°C) acetone over night. NMR spectrometry (S.I. 1) confirmed a complete mono-functionalization of the PEG precursor. The average degree of polymerization of the PEG was determined via ^{1}H NMR spectroscopy by comparison of the methoxy-end group singlet (3.34 ppm - with the PEG-backbone signal (3.64 ppm) and was determined to be approx. 111 units by this means. ^{1}H NMR ($CDCl_3$, 400MHz) δ(ppm): 1.90 (s, C(CH_3)$_2$Br); 3.34 (s, CH_3-O-PEG); 3.60 (bs, CH_2CH_2O-); 4.28 (q, -CH$_2$CH_2OOCC(CH$_3$)$_2$Br)
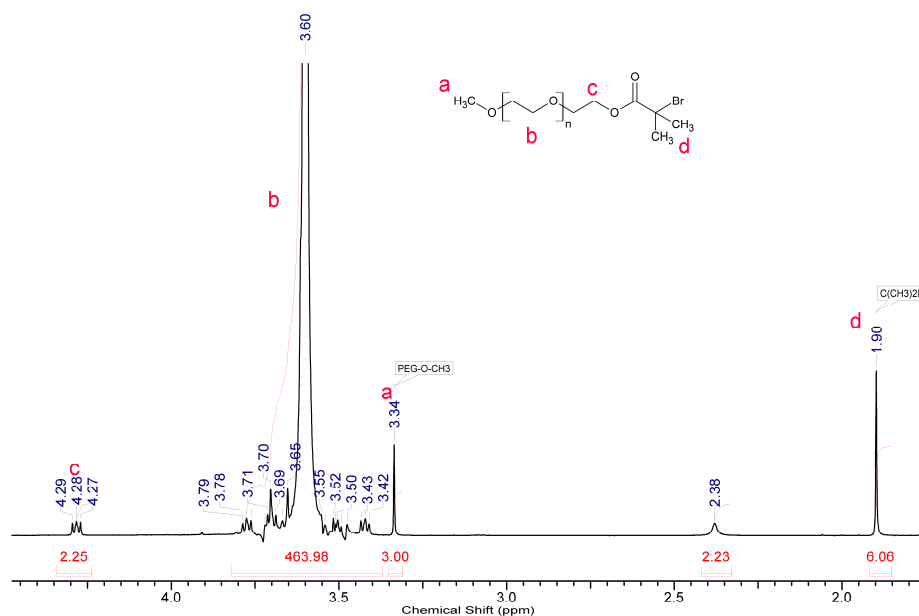
S.I. 11: NMR spectrum of the M-PEG-2 bromo-isobutyryl-bromide macroinitiator.

General procedures for the synthesis of the 2nd block: ATRP of BGMA

For PEG$_{111}$-*b*-PBGMA$_{62}$ (P3) the total composition of the sample had a monomer/PEG-alkyl halide/copper/ligand ratio of [90]:[1]:[1]:[1]) using CuCl/HMTETA. The polymerization was conducted according to a similar procedure described earlier.[17] Work-up of the sample was conducted as follows: After polymerization, the sample was exposed to air and the solvent (methanol/benzene; 2:1)) was removed in a rotary evaporator and a conversion analysis was performed via ^{1}H NMR in CDCl$_3$ (i.e. 69% for P3). The block copolymer was taken up in chloroform and filtered over neutral aluminum-oxide to remove the copper complex. Thereafter, chloroform was evaporated in vacuo and the crude product was taken up in 100 ml of acetone and precipitated there from upon standing at -25°C over night. The colorless polymer was collected via filtration, washed with cold diethylether (-25°) and dried in vacuo (yield: 65 %).

^{1}H NMR (CDCl$_3$, 400MHz) δ (ppm): 0.94-1.46 (m, C(C*H$_3$*)(COOCH(CH$_2$O-)$_2$); 1.80-2.34 (m,-C*H$_2$*C(CH$_3$)(COOCH(CH$_2$O-)$_2$); 3.34 (s, C*H$_3$*-O-PEG); 3.60 (bs, C*H$_2$*C*H$_2$*O-); 4.20-4.57 (COOC*H*(CH$_2$O-)$_2$); 5.27-5.49 (COOCH(CH$_2$O-)$_2$C*H*C$_6$H$_5$); 7.16-7.54 (COOCH(CH$_2$O-)$_2$CHC$_6$*H$_5$*).
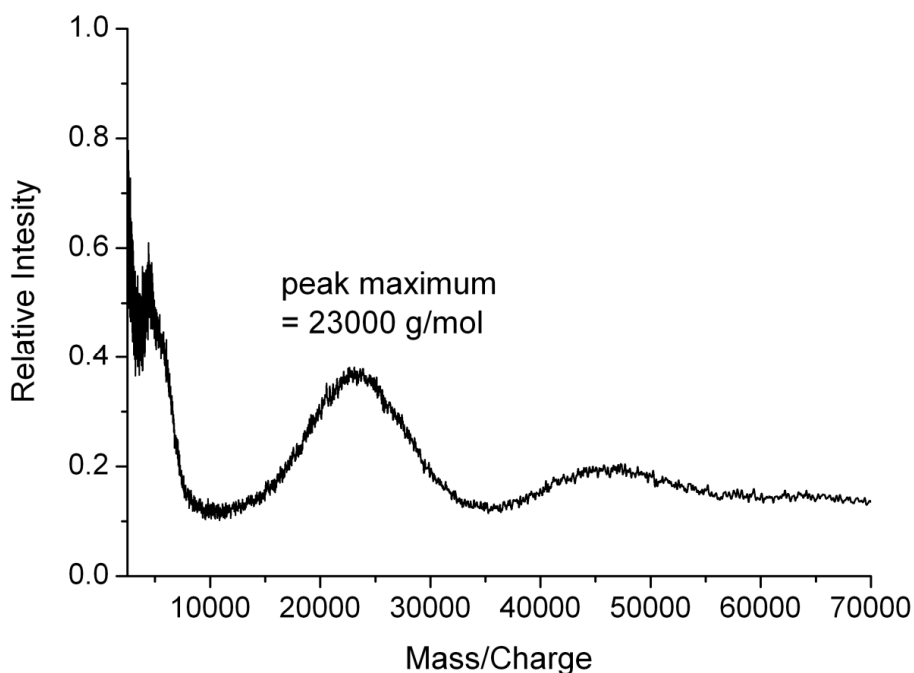
S.I. 12: MALDI-ToF spectrum of PEG$_{111}$-b-PGMA$_{62}$ which shows a peak maximum of approx. 23,000 g/mol. This corresponds well to the molecular weight determined by NMR in CDCl$_3$ and (i.e. 20,400 g/mol). Due to the elevated laser power required for this mass range, fragmentation of the polymer can also be observed in the mass range up to 7000g/mol. The presence of a second mode at twice the molecular weight of the main distribution is addressed to ionization artifacts, since SEC (Figure 3) clearly revealed a monomodal distribution.

Aggregate preparation and CAC measurements via Fluorescence spectroscopy. Since the glass-transition temperature (T$_g$) of the core-forming block hampers ordered self organization in solution, a co-solvent for the induction of the self-assembly process was needed. 10 to 15 mg of the block copolymer were dissolved in 2.7 mL of THF. Subsequently, 10 mL of water were added drop-wise under vigorous stirring over a period of 4 h. Samples were dialysed against water for 2 hours which was then replaced by a 10 mmol pH 7.3 phosphate buffer. The aggregate morphologies were studied using transmission electron microscopy (TEM). The TEM-samples were prepared by drop casting the above mentioned aggregate solution (c = 1-1.5 mg/mL) on a plasma treated carbon coated copper grid. The samples were allowed to dry at room temperature under a slight nitrogen flux for at least 16 h prior to staining with OsO$_4$ vapour from a 1% OsO$_4$ solution in water. A significant change of the aggregate morphology is not expected throughout the drying process at room temperature (high Tg of the core forming block).

For aggregation studies via fluorescence spectroscopy the concentration of block copolymer was varied from 6.6×10^{-7} to 1.0 mg/mL, and the concentration of pyrene was fixed at 1.0 μM. The extremely hydrophobic pyrene is preferentially solubilized in the hydrophobic interior of the aggregate. This can be readily observed in the fluorescence excitation spectra of the probe at an emission wavelength of 372 nm. In the concentration range of aqueous micellar solutions a shift of the excitation band in the 335 nm region towards higher wavelength is observed for the employed block copolymers. The ratio of the fluorescence intensities at 339 and 335 nm was used to validate the shift of the broad excitation band. The critical aggregation concentrations (CAC) were determined from the crossover point in the low concentration range. Pyrene-containing samples were prepared by continuous dilution of the aggregate solution with a saturated pyrene stock solution. The mixtures were allowed to equilibrate for 48 to 64 h prior to investigation by fluorescence spectroscopy. The micellar solution (2 mg/mL)prepared as above-mentioned was divided into four aliquots and adjusted to pH 4.0, 5.0 and 7.3, respectively, by addition of 50 μL of 4.0 M pH 4.0 or 5.0 acetate buffer or 7.3 phosphate buffer, while keeping identical salt concentrations.
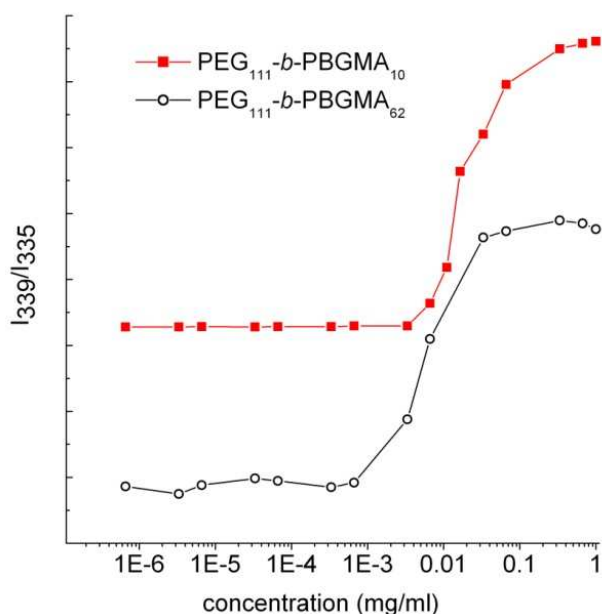
S.I. 13: CAC measurements using pyrene fluorescence excitation spectra at an emission wavelength of 372 nm. The ratio of the fluorescence intensities at 339 and 335 nm was used to evaluate the shift of the excitation spectra. The ratio remained constant below a certain concentration, but changed substantially above a critical concentration, reflecting the partitioning of pyrene between the aqueous solution and aggregated phases.

Encapsulation and Release of Nile Red. Nile Red was encapsulated in the micelles by adding 20 μL of 1 mM Nile Red in acetone to 0.4 mL of copolymer solution in THF (5 mg/mL), followed by drop-wise addition of 10 mL phosphate buffer (10 mM, pH 7.3). To completely evaporate THF and acetone, the solution was stirred overnight and then vacuumed for 1 h. The aggregate solutions should therefore have a concentration of 0.2 mg/mL and contain 2.0 μM of Nile Red. The solution was divided into three aliquots of approx. 3 ml and adjusted to the respective pH by adding sodium acetate buffer. The samples were stirred at 37 °C and the fluorescence intensity was measured at the desired time points. Spectra were collected in the emission mode between 500 and 680 nm with a band width of 20 nm. The sample was excited at a wavelength of 488 nm (at a bandwidth of 5 nm).
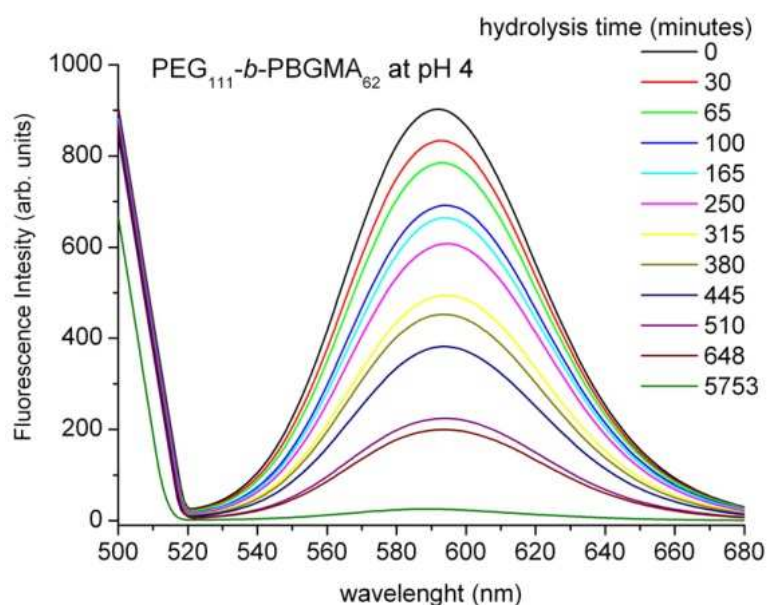
S.I. 14: Decay of the fluorescence intensity over time.

UV/vis-measurements. In order to confirm the release of benzaldehyde throughout the aggregates exposure to acidic pH at 37°C, we examined a reference sample without additional dye loading via UV/vis spectroscopy before and after the experiment. According to the absorption intensity of the analytes, the samples were prepared according to the procedure described above but with only a third of the concentration (i.e. 0.066 mg/mL and therefore still above the CAC). The same concentration was chosen for benzaldehyde and 5-hydroxy-2-phenyl-1,3-dioxane which were used for reference spectra in phosphate buffer at pH 7.3. While benzaldehyde exhibits an absorption maximum at approx. 250 nm, the

corresponding glycerol acetal is shifted towards lower wavelengths. Its maximum is situated at approx. 205 nm. A precise determination is difficult due to the increasing absorption coefficient of water at this wavelength.

3.4 Synthesis, Characterization and Evaluation of P(LLA)-*block*-P(HPMA) Copolymers: A New Type of Functional Biocompatible Block Copolymer

Matthias Barz, Florian K. Wolf, Fabiana Canal,[*] Kaloian Koynov[†], Maria J. Vicent,[*] Holger Frey and Rudolf Zentel

Abstract

We describe a synthetic pathway to functional poly(*L*-Lactide)-*block*-poly(2-Hydroxypropyl methacrylamide) copolymers. The synthesis relies on a combination of ring-opening polymerization of L-lactide, conversion into a chain transfer agent (CTA) for the RAFT polymerization of pentafluorophenyl methacrylate. A series of block copolymers was prepared that exhibited molecular weights M_n ranging from 7600 g/mol to 34300 g/mol, with moderate PDI between 1.3 and 1.45. These reactive precursor polymers have been transformed into biocompatible P(LLA)-block-P(HPMA)copolymers and their fluorescently labeled derivatives by facile replacement of the pentafluorophenyl groups. The fluorescence label was used to study cellular uptake as well as aggregation behavior of this new type of partially degradable amphiphilic block copolymer by fluorescence correlation spectroscopy (FCS).

[*] Centro de Investigacion Principe Felipe, Avda Autopista el Saler 16/3, ES-46012 Valencia, Spain

[†] Max-Planck-Institute for Polymer Research, Ackermannweg 10, D-55128 Mainz, Germany

Introduction

Since publication of the seminal concept for polymers as therapeutic agents in the 1970s by Ringsdorf et al.[1], there has been tremendous progress in polymer based nanomedicine.[2,3,4,5,6] In recent decades, polymers have been widely investigated as carrier systems for drugs. In the ideal case, the drug is selectively and exclusively transported to the desired site of action, increasing the drug efficacy and minimizing undesired side effects. Masking the active agent for circulation in healthy tissue and organs can either be achieved by polarity-driven encapsulation in a polymer based aggregate/physical matrix or by covalent attachment to the polymer itself. The first polymers designed to fulfill these demands entered clinical trials approximately a decade ago and have been subjected to extensive research ever since.[7,8,9] A pioneering step for a synthetic polymer in clinical approval was achieved by a drug conjugate based on the N-(2-hydroxypropyl)-methacrylamide (HPMA) in the 1980s.[7] Most other systems with clinical approval are based on poly(ethylene glycol) (PEG), e.g., protein polymer conjugates,[10,11] antibody polymer conjugates[12,13] and polymeric micelles with a drug encapsulated or covalently attached to the hydrophobic part of the block copolymer.[14,15,16,17]

In contrast to difunctional PEG based systems, acrylate and acrylamide based polymers provide access to a plethora of different functionalities and reactive groups at the polymer backbone, e.g., activated esters or alkyne ester attached to the polymer main chain, since they are readily obtained by straightforward synthetic chemistry.[18,19,20,21] Particularly in biological or medical applications multi-functional systems are desired, as they offer control of functionality, hydrophilicity, pH-induced phase behavior and charge density. However, the major drawback of all systems obtained previously by free radical polymerization is the lack of control over molecular weight and weight distribution. Currently, modern controlled radical polymerization techniques such as ATRP, RAFT or NMP,[22,23,24,25,26,27] provide means to tackle this issue and can also be employed to generate unprecedented block copolymer structures. In this respect, various multi-functional systems have been used for biological or medical applications. [28,29,30,31,32,33]

The synthesis of amphiphilic block copolymers is often challenging, especially when the expected window for common solvents for both blocks is narrow. Successful approaches to this problem either rely on the cleavage of silane [34] or acetal[35] based protecting groups, the oxidation of vinyl functionalities or hydrolysis of epoxides. In this respect the activated ester

approach[19] offers a useful tool in the synthesis of multi-functional and amphiphilic block copolymers. In addition, the transformation of fluorinated activated ester groups, such as pentafluorophenol esters can be precisely monitored by ^{19}F NMR spectroscopy.

The block copolymer systems explored at present are based on non-degradable backbone structures, which are expected to represent a drawback for long-term therapeutic applications. Therefore it is highly desirable to combine both a degradable and a functional segment in one block copolymer. This concept is particularly attractive, if eventual degradation of one block leads to well-known building blocks, like it would be the case for a combination of P(HPMA) with the biodegradable poly(L-lactide) (PLLA).

In this context, we have developed functional P(LLA)-block-P(HPMA)copolymers by combining ring-opening polymerization (ROP) and subsequent RAFT polymerization. PLLA is well-known to be degradable under *in vivo* conditions and is widely used in biomedical polymer technology, compromising applications in drug delivery,[36] tissue engineering,[37] surgical sutures, etc.[38,39] However, one of the most interesting properties reported for PEG-*block*-PLLA block copolymers is their stability in blood described by Kataoka et al. in 2001.[36] This is a crucial prerequisite that renders PLLA-based block copolymer systems a promising platform for *in vivo* transport. Particularly the stereoregular P(LLA) blocks retain their integrity due to their thermodynamic and kinetic stability and hence should allow for a targeted delivery prior to their excretion or degradation.

Surprisingly, only few examples combining ROP with a controlled radical polymerization technique are known in literature.[40,41,42,43] To date, none of them has capitalized on the activated ester approach to generate reactive precursor block copolymers, which can be precisely characterized and afterwards transformed into functional P(HPMA) based block copolymers. In the approach presented here, well-defined poly(L-lactide)s are reacted to a macro chain transfer agent (CTA). These compounds are used for chain extension with pentafluorophenol methacrylates via the RAFT polymerization method. In the following polymer modification step the pentafluorophenyl groups of the reactive precursor were exchanged with Oregon Green 488 cadaverine and 2-hydroxypropylamine. This approach[33] afforded a dye-labeled HPMA block copolymer. Additionally, in this work we have studied micelle formation in solution by fluorescence correlation spectroscopy (FCS) and present a first biological evaluation, focusing on cellular uptake and toxicity of the aggregates.

Experimental Part

Materials

All chemicals were reagent grade, obtained from Aldrich and used without further purification, unless indicated otherwise. All solvents were of analytical grade. Pentafluorophenol was obtained from Fluorochem (Great Britain, UK) and distilled prior to use. Dioxane, dimethylsulfoxide (DMSO) and dichloromethane were dried and freshly destilled. 2,2'-Azobis(isobutyronitrile) (AIBN) was recrystallized from diethyl ether and stored at -7°C. DBU (1,8-Diazabicyclo[5.4.0]undec-7-ene) (99%) was purchased from Acros and distilled from calcium hydride. Deuterated chloroform-d_1 and DMSO-d_6 were purchased from Deutero GmbH. DMSO-d_6 was dried and stored over molecular sieves (4Å). L-lactide was purchased from Purac/Gorinchem (Netherlands), recrystallized three times from dry toluene and stored under vacuum prior to use. Dialysis of block copolymers was performed with Cellu SepH1® membranes (Membrane Filtration Products, Inc.) with a molecular weight cutoff of 1000 g/mol and Spectra/Por® membranes (Roth) with a molecular weight cutoff of 3500 g/mol. The 4-cyano-4-((thiobenzoyl) sulfanyl)pentanoic acid (CTA),[44] the PFMA[45] and the poly(L-lactide) were synthesized according to literature procedures.[46,47] The dithiobenzoate end group was removed according to the procedure reported by Perrier et al.[48] (for detailed information see supplementary information).

Characterization

^{1}H-, ^{13}C- and ^{19}F-NMR spectra were obtained at 300 or 400 MHz using a FT-spectrometer from Bruker and analyzed using the ACDLabs 9.0 software. The polymers were dried at 40°C over night under vacuum and subsequently characterized by size exclusion chromatography (SEC). For SEC measurements in DMF containing 1 g/L of lithium bromide as an additive, an Agilent 1100 series system was used with a flow rate of 1 mL min^{-1} at 30°C as an integrated instrument, including three HEMA-based-columns (10^5/10^3/10^2 Å porosity) from MZ-Analysentechnik GmbH, a UV (275 nm) and a RI detector. Size-exclusion chromatography with THF as an eluent was performed at 25°C and at a flow rate of 1 mL min^{-1} with an instrument consisting of a Waters 717 plus autosampler, a TSP Spectra Series P 100 pump, and a set of three PSS-SDV 5-l columns with porosities of 100, 1000, and 10000 Å and a refractive index detector, respectively. A detailed description of the FCS experiments can be found in the supplementary information. Calibration was achieved with well-defined

poly(ethylene glycol)/DMF or poly(styrene)/THF standards, provided by Polymer Standards Service (PSS)/Mainz Germany.

End group modification of PLLA to ω-CTA macroinitiator for RAFT polymerization

1.0 g 4-Cyano-4-((thiobenzoyl) sulfanyl)pentanoic acid was dissolved under nitrogen in 100mL CH_2Cl_2. The solution was cooled in an ice bath and 0.5 g of dicyclohexylcarbodiimide (DCC) were added. After 10 minutes a solution of 0.02 g 4-(dimethylamino)-pyridine (DMAP) in 5 mL CH_2Cl_2 was slowly added. 3.3 g of the poly(L-lactide) in 20 mL CH_2Cl_2 were added to the activated acid. The reaction was allowed to proceed over night. Finally the solution was concentrated and the functionalized polymer was precipitated twice in cold methanol, once in diethyl ether, dried in high vacuum and a reddish powder was obtained. Yield: 3.06 g, 91%, degree of functionalization 69 % (NMR).^{1}H NMR (300 MHz, CDCl$_3$): δ ^{1}H/[ppm] 0.92 (s, C(CH_3)$_3$; 1.57 (d, ^3J =7.0 Hz CHCH_3, PLLA chain); 1.92 (s, CR$_2$CH_3, CTA); 2.50 2.75 (m, -CH$_2$CH$_2$, CTA); 3.78-3.89 (m, -OCH_2C(CH$_3$)$_3$); 4.34 (q, ^3J =7.0 Hz HOCH(CH$_3$)); 5,15 (q, ^3J =7.0 Hz CH(CH$_3$), poly(lactide) chain); 7.38 (t, J =1.0 Hz CH=CH, CTA); 7.56 (t, J =1.0 Hz CH=CH, CTA); 7.89 (d, J =1.0 Hz CH=CH, CTA)

Synthesis of P(PFMA)-*block*-P(LLA) copolymers

RAFT polymerization of PFMA using the poly(L-lactide) macroinitiator was performed in a Schlenk tube. The reaction vessel was loaded with 3.5 mg 2,2'-azobis(isobutyronitrile (AIBN) (0.02 mmol), 0.2 g poly(L-lactide) macro CTA and 1.58 g of PFMA (12 mmol) (example for P2R) in 5 mL of dioxane. Following three freeze–vacuum–thaw cycles, the tube was immersed in an oil bath at 80 °C for 12 h. Subsequently, the block copolymer was once precipitated in ethanol and twice in hexane, isolated by centrifugation and dried at 30 °C under high vacuum for 12 hours. The block copolymer was obtained as a slightly red powder. Yield: (59 %). ^{1}H-NMR (CDCl$_3$, 400MHz) δ^{1}H/[ppm]: 0.92 (s, C(CH_3)$_3$; 1.42 (s, CRCH_3, poly(PFMA) chain); 1.57 (d, ^3J =7.0 Hz CHCH_3, poly(lactide) chain); 2.07 (s, -CH$_2$- poly(PFMA) chain) 3.78-3.89 (m, -OCH_2C(CH$_3$)$_3$); 4.34 (q, ^3J =7.0 Hz HOCH(CH$_3$)); 5,15 (q, ^3J =7.0 Hz CH(CH$_3$), poly(lactide) chain). ^{19}F NMR (CDCl$_3$): δ ^{19}F/[ppm] -165.0 (br), -159.7 (br), -153.1 (br)

Removal of the dithioester endgroup.

The dithiobenzoate end group was removed according to the procedure reported by Perrier et al.. Typically 200 mg of polymer, (Mn = 23000 g/mol), and 80 mg of 4,4'-azobis(4-cyanovaleric acid) (30 times excess in relation to the polymer end group) were dissolved in 3 mL of anhydrous dioxane. The solution was heated to 80 °C for 3 h. Finally the copolymer was precipitated 3 times in 100 mL of diethyl ether and collected by centrifugation. In the case of the block copolymer, the crude product was first precipitated in ethanol twice and than once in diethyl ether. The copolymer was dried in vacuo for a period of 24 h and a colorless product was obtained (yield: 90 %). The absence of the dithiobenzoate end group was confirmed by UV-Vis spectroscopy with the absence of the peak at 302 nm wavelength.

Synthesis of P(LLA)-*block*-P(HPMA) copolymers

In a typical reaction 100 mg of **P(PFMA)-*block*-P(LLA)** without ditihioester end group was dissolved in 2 mL abs. dioxane and 0.5 mL dried DMSO. A colorless solution was obtained. Subsequently 20 mg of triethylamine (TEA) and 15 mg of hydroxypropylamine were added. The mixture was kept at 30 °C for 24 h. Finally, a second aliquot of 15 mg of hydroxypropylamine and 20 mg triethylamine was added to the reaction, which was then allowed to proceed under the abovementioned conditions for 4 h. The solution was concentrated in vacuum, precipitated twice in diethyl ether, mixed with water and dialyzed against water using Spectra/Por$^{®}$ membranes with a molecular weight cutoff of 3500 g/mol. In a last purification step a preparative SEC (Sephadex G-25) was used to purify the final product and remove remaining traces of the unmodified P(LLA) (see figure 1b). The solution of the product was lyophilized, yielding 30 mg of a colorless polymer. ^{1}H NMR (DMSO-d_6): δ ^{1}H/[ppm] 0.92 (s, C(CH_3)$_3$; 0.7-1.42 (CR$_3$CH_3, C$H3$CHOH poly(HPMA) chain); 1.57 (d, ^{3}J =7.0 Hz CHCH_3, poly(lactide) chain); 1.2-2.1 (s, -CH_2- poly(HPMA) chain); 2.6-3.2(CHOH, poly(HPMA) chain); 3.72 (CH_2NH, poly(HPMA) chain); 5.15 (q, ^{3}J =7.0 Hz CH(CH$_3$), poly(lactide) chain).

Synthesis of dye labeled P(LLA)-*block*-P(HPMA) copolymers

The polymer modification reaction was carried out under the same conditions as mentioned above, but a small fraction of Oregon Green 488 cadaverin dye was used in addition (Table 2). In a typical reaction 150 mg of P(PFMA)-block-P(LLA) (Mn = 25000 g/mol) without ditihioester end group were dissolved in 2 mL abs. dioxane and 0.5 mL dried DMSO.

A colorless solution was obtained. In a typical reaction 2.5 mg Oregon Green 488 cadaverin and 20 mg triethylamine were added and the reaction was allowed to proceed at 30 °C for 4 h. In the next step 40 mg of TEA and 25 mg of hydroxypropylamine were added. The mixture was kept at 30 °C for 24 h, and finally additional 25 mg of hydroxypropylamine and 30 mg TEA were added. The reaction was allowed to proceed for another 4 h. The solution was concentrated under vacuum, precipitated twice in diethyl ether, carefully mixed with water and dialyzed against water using Spectra/Por® membranes with a molecular weight cutoff of 3500 g/mol. In a last purification step a preparative SEC (HiTrap™ Desalting Column, Sephadex G-25 superfine) was used to purify the final product and remove remaining traces of the unmodified P(LLA) (see figure 1b). The solution of the purified product was lyophilized, yielding a yellowish polymer. Yield: 30 mg. ^{1}H NMR (DMSO-d_6): δ [ppm] 0.92 (s, C(CH_3)$_3$; 0.7-1.42 (CR$_3$CH_3, C$H3$CHOH poly(HPMA) chain); 1.57 (d, ^3J =7.0 Hz CHCH_3, PLLA chain); 1.2-2.1 (s, -CH_2- poly(HPMA) chain); 2.6-3.2(CHOH, poly(HPMA) chain); 3.72 (CH_2NH, poly(HPMA) chain); 5.15 (q, ^3J =7.0 Hz CH(CH$_3$), poly(lactide) chain).

Cell cultures

HeLa (human cervix adenocarcinoma cells) were grown in DMEM medium supplemented with 10% v/v of heat-inactivated fetal bovine serum (FBS). Cells were maintained at 37°C in an atmosphere of 5% carbon dioxide and 95% air and underwent passage twice weekly.

Cells viability assay

The cytotoxicity of the conjugates synthesized was evaluated using the MTT (3-(4,5-dimethyltiazol-2-yl)-2,5-diphenyl-tetrazolium bromide) cell viability assay (72 h incubation) with HeLA cells. Cells were seeded into sterile 96-well microtitre plates (seeding density 2.2x10^4 cell/mL). Cells were allowed to settle for 24 h before the unlabeled polymer P1 (0.2 µm filter-sterilized) was added. A series of stock solutions of conjugates dissolved in DMSO, with different concentrations ranging from 1 mg/mL to 300 mg/mL, were prepared and the cells were treated with 1 µL of each stock solution, in such a manner that the final polymer concentrations range from 0,01 mg/mL to 3 mg/mL with a final DMSO concentration of 1% (v/v). In control experiments, DMSO-solvent toxicity was evaluated in the absence of

conjugates under otherwise identical conditions. 100% cell viability was assigned to control cells (1% DMSO). After a further 68 h of incubation, MTT (20 μL of a 5 mg/mL solution in PBS) was added to each well, and the cells were incubated for 4 h. After removal of the medium, the precipitated formazan crystals were dissolved in optical grade DMSO (100 μL), and the plates were read spectrophotometrically at 570 nm after 30 min using a Victor Wallace plate reader. [2]

Live cell confocal fluorescence microscopy

Cells were seeded on glass placed into 10 cm^2 Petri plates at a concentration of 2×10^5 cells/mL. After 24 h of incubation the cells were treated with 10 μL of Oregon Green-labeled conjugate solution. The final polymer concentration was 0.1 mg/mL. Pulse and chase experiments were performed: after 1 h or 2 h of incubation at 37°C, the medium was replaced with fresh one and cells were incubated at 37°C for further 1 h or 2 h. Then cells were washed twice with PBS supplemented with 10% (v/v) of fetal bovine serum (3 mL) and the glass was removed and set on the microscope. Images were captured with a confocal Leica microscope equipped with a l-blue 63 oil immersion objective and handled with a TCS SP2 system, equipped with an acoustic optical beam splitter (AOBS). Excitation of the dye was achieved with an argon laser (548, 476, 488, 496 and 514 nm) and a blue diode (405 nm). Images were captured at an 8-bit gray scale and processed with LCS software Version 2.5.1347 (Leica, Germany) containing multicolor, macro and 3D components.

Results and Discussion

Synthesis of P(LLA)-*block*-P(HPMA) Copolymers

The synthesis of the P(HPMA)-*block*-PLLA block copolymers was carried out in 4 steps (see Scheme 1) by combining the ring opening polymerization of L-lactide with the RAFT technique. This strategy is motivated by the idea to create a reactive ester block copolymer that can be used as a versatile platform for subsequent polymer modification. The induction of an amphiphilic character as well as the attachment of a drug or/and traceable markers in the hydrophilic block section are realized in a single reaction step. 2-Hydroxypropylamine and the drug/marker simultaneously replace the pentafluorophenyl functionalities in the desired stochiometry. Further functionalization would of course be impossible with a P(LLA)-*block*-P(HPMA) block copolymer prepared directly. In the initial step, PLLA was prepared by

controlled ring-opening polymerization (ROP) with the organo-base 1,8-diazabicyclo-[5.4.0]undec-7-ene (DBU), which has been introduced recently as highly efficient transesterification catalyst by Hedrick and coworkers.[47,48] In a second step the hydroxyl end group of the P(LLA) block was coupled with the well known chain transfer agent 4-cyano-4-((thiobenzoyl)sulfanyl)pentanoic acid by DCC-mediated esterification. The ensuing RAFT polymerization was carried out under the recently reported conditions for the controlled radical polymerization of PFMA.[30,32,49]

Scheme 1. Synthesis of functional poly(L-lactide)-*block*-poly(HPMA) copolymers by a combination of ROP and RAFT polymerization, using the activated ester approach.
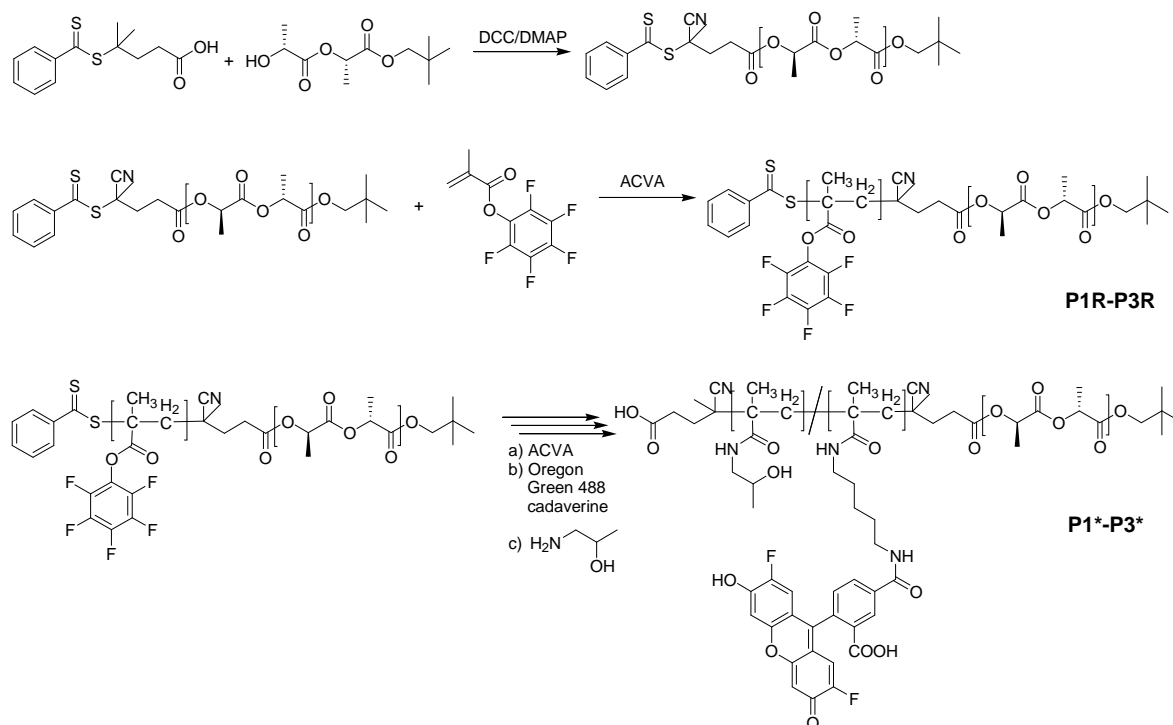
Despite its localization at the ω- position of the PLLA-chain the chemical structure of the chain transfer agent remains unaffected. Therefore, it is reasonable to assume that the polymerization kinetics are comparable to those of the PFMA homopolymerization, reported previously by Theato et al.[49] and Klok et al..[32] Following this procedure we were able to prepare a series of block copolymers differing in the block length of the P(PFMA) block (see Table 1). These reactive block copolymers possess molecular weights in the range of 7 600 g/mol to 34 300 g/mol (M_n) and moderate PDIs from 1.3 to 1.45 (determined by GPC in THF), confirming well-defined block structures. The degree of polymerization of the P(PFMA) block

was varied from 10 up to 117 in order to study the amphiphilic behavior of the materials systematically.

With the intention of avoiding undesired side reactions of the dithiobenzyl ester end group, for instance disulfide or thiolactone formation, the method of Perrier et al. was employed for its modification, using 4,4'-azobis(4-cyanovaleric acid).[46] In this approach a 20 to 30-fold excess of the azo compound is used, converting the dithiobenzyl ester end group into a 4-cyanovaleric acid end group by a radical substitution reaction. The carboxylic acid functionality was chosen due to its hydrophilic character, which is favorable for the end group of the water soluble PHPMA-block.
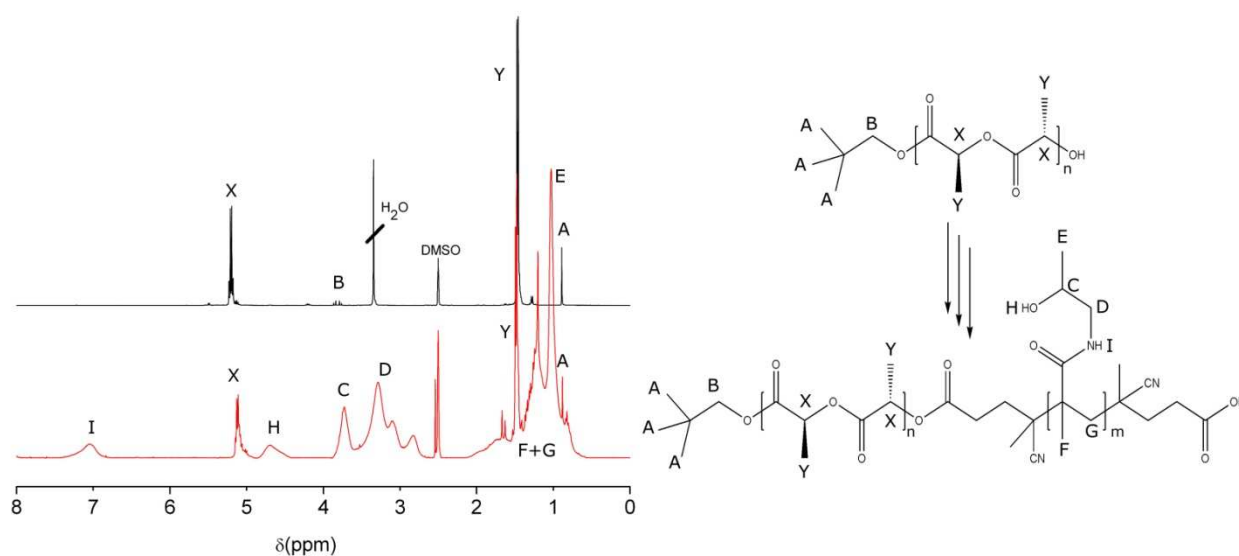
Figure 1: ^{1}H NMR spectra of PLLA (top) and final P(LLA)-block-P(HPMA)copolymer (**P2***, bottom**)** in DMSO-d_6.

In the final step (see Scheme 1) the activated ester units of the precursor block copolymer were aminolysed in a postpolymerization modification reaction, using 2-hydroxypropylamine. The polymer modification reaction was carried out at a stoichiometric ratio of PFMA units in the polymer to amine, which was found to be tolerable for the poly(ester) structure, since amide formation of the activated ester structures proceeded significantly faster than ester aminolysis of the P(LLA) block, which was not observed.
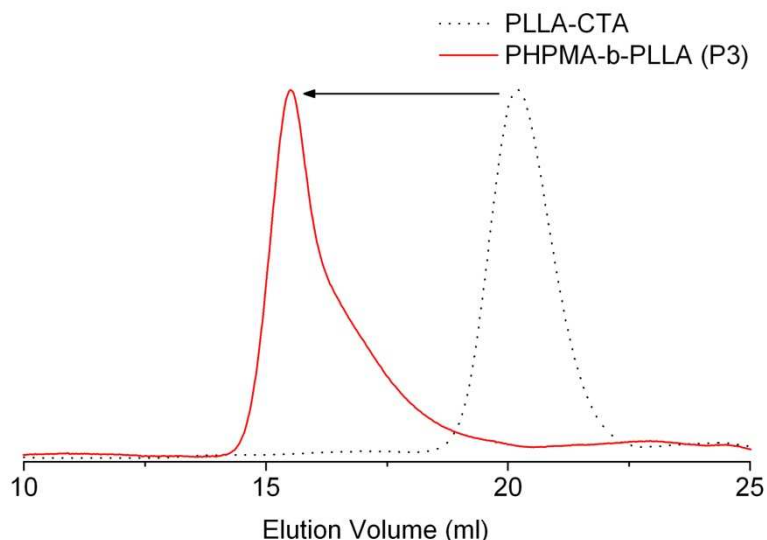
Figure 2: SEC elugrams of the P(LLA)-macro CTA (GPC$_{DMF}$) and final purified P(PFMA)-*block*-P(LLA) block copolymer **P3** (GPC$_{DMF}$) ensuring the removal of unmodified PLLA (RI-detection).

After 24 h reaction time, the remaining reactive ester groups were quenched at 40 °C with a small amount of amine, until full conversion was confirmed by ^{19}F-NMR. Following this procedure, aminolysis of the P(LLA) could be avoided, which is confirmed by the ratio of the signal intensity of the methine proton in PLLA at 5.1 ppm to the intensity of the tertiary proton of the HPMA units at 3.7 ppm (Figure 1). According to the determined molecular weights this ratio has to be 0.54 for **P2.** This ratio was confirmed by ^{1}H-NMR (ratio of 0.53). The slight differences between calculated and experimentally derived values are in the range of measuring accuracy. The absence of signals from P(LLA) degradation products and the constant ratio of P(LLA) to acrylate based signals confirm the stability of the P(LLA) block during the transformation of the P(PFMA) block to P(PHPMA). Although not integratable due to signal overlap with the polymer backbone, the singlet (A) at 0.89 ppm originating from the neopentyl initator at the α-chain end is still clearly visible. Integration of Lactide (X) and HPMA signals (C and D) allowed the validation of the achieved block length ratios via proton NMR. All synthesized block copolymers are compiled in Table 1.

Table 1: Characteristics of reactive ester P(PFMA)-*block*-P(LLA) block copolymer precursors **P1R**, **P2R** and **P3R**. The molecular weight of the PLLA was determined to Mn = 3.0 kg/mol with a PDI = 1.1.

Polymer	Average block ratio (HPMA/L-lactide)[a]	Dye content % (Oregon Green 488)	$M_{n,calc}$[b] kg/mol	M_n kg/mol	PDI
P1R	-	-	10	7.6[c]	1.31[c]
P2R	-	-	30	22.8[c]	1.45[c]
P3R	-	-	50	34.3[c]	1.43[c]
P1	10/42	-		5.4[a]	1.31[a]
P2	78/42	-		14.2[a]	1.45[a]
P3	124/42	-		20.7[a]	1.43[a]
P1[*]	9/42	10		5.8[a]	1.31[a]
P2[*]	77/42	1.3		15.9[a]	1.45[a]
P3[*]	123/42	0.8		22.1[a]	1.43[a]

a)   As determined by ^{1}H NMR spectroscopy after aminolysis with hydroxypropylamine with respect to the molecular weight of the precursor polymer **P1R**-**P3R**.

b) $M_{n,calc} = [M]/[CTA] \times conv \times MW_M + MW_{CTA}$

c)   As determined by by GPC in THF as solvent for the reactive polymers **P1R**-**P3R**.

Prior to the aminolysis using 2-hydroxypropylamine, a small fraction of Oregon green cadaverine dye can be coupled with the activated ester in order to fluorescently label the block copolymers. Subsequently the above mentioned polymer modification procedure was applied to obtain the dye containing P(HPMA) block.

The final block copolymers were first precipitated from diethyl ether (1x) and EtOH (2x). Subsequently, dialysis against water and preparative SEC (Sephadex G-25) was applied to remove all side products of the postpolymerization modification. At this stage also remaining traces of unmodified PLLA are efficiently removed (see Figure 1b). At this stage it is however difficult to find a good solvent for both polymers (PLLA and P(HPMA)-block-P(PLLA)). DMF is a compromise in which only slight aggregation may occur. In addition this explaines the slight tailing of the SEC-trace as it is visible in Figure 2. To this respect, the molecular weight of the block copolymers was calculated from the reactive Precursors **P1-R**, **P2-R** and **P3-R**. After the last step the aqueous polymer solution was lyophilized yielding the final block

copolymer. A pure product is of crucial importance for both fluorescence correlation spectroscopy and for biological evaluation. In this respect, yields of approx. 60 % after purification for the polymer modification reaction are more than acceptable. The block copolymers prepared are listed in *Table 1* with the respective characterization data. Similar to the precursor materials, the P(HPMA) block copolymers also exhibited monomodal SEC traces (DMF: PDI 1.3 to 1.45), suggesting that chain scission of the PLLA block had not occurred.

P(LLA)-*block*-P(HPMA)Copolymers: Aggregation, Cellular Uptake and Toxicity

Aiming at applications for drug transport or molecular imaging, the study of the aggregates formed by the amphiphilic block copolymer structures in buffer solutions and a first evaluation in cell cultures represents an important issue of this work. Due to the amphiphilic character of the block copolymers, the formation of various aggregates in aqueous solution is expected (e.g., micelles, compound micelles or polymersomes). Particularly for biological studies regarding cellular uptake and intracellular distribution, the aggregation behavior is highly important. For example Sahay et al. recently reported that the uptake route of Pluronic P85 switches from caveolae mediated endocytosis to uptake through clathrin coated pits when the concentration of the copolymer is increased from below to above the critical micelle concentration (cmc).[50] In this respect, we have investigated the superstructure formation in isotonic aqueous solution by applying fluorescence correlation spectroscopy (FCS) to the polymer **P2***.[51] Details of the set-up and the evaluation process can be found in the supporting information. The DP_n of the non-degradable P(HPMA) block within block copolymer **P2*** is still below the renal exclusion value, which ensures elimination from the body. This design principle is fundamental whenever actual therapeutic applications are targeted. In contrast to light scattering, where absorption of the laser light by the particles studied is undesirable, the FCS technique measures and correlates fluctuations of the fluorescence signal in order to determine diffusion coefficients. Thus, fluorescently labeled compounds have to be used. Since the diffusion of the labeled polymer is the primary variable of interest in FCS, it is possible to work under conditions also required for experiments in cellular biology. Hence it is possible to work in an environment more suitable for biologically relevant issues, as long as the absorption maximum of the dye differs from that of the surrounding medium.[51]

For the FCS measurements the block copolymer **P2*** (P(HPMA)$_{77}$-*block*-P(LLA)$_{42}$) (see Table 1) was dissolved in DMSO at a concentration of 10 mg/mL. This solution was slowly mixed with PBS buffer (pH = 7.2) to obtain a concentration of 1 mg/mL. For the final measurements the solution was further diluted, resulting in a concentration of 0.1 mg/mL. We assume that this concentration significantly exceeds the critical micelle concentration (CMC) of the block copolymer, as is observed for other lactide based amphiphilic block structures.[52] Furthermore, this concentration is suitable for further cell studies that will be described in the following paragraph.

Table 2: Characterization of fluorescently labeled (Oregon green 488 cadaverine) P(LLA)-block-P(HPMA)block copolymer in PBS buffer (pH = 7.2) by fluorescence correlation spectroscopy (FCS)

Concentration of Polymer P2*		Fluorescence Correlation Spectroscopy Data		
mg/mL	mol/L	τ_Δ $\mu\sigma$	D m^2/s	D$_h$ nm
0.1	6.50×10^{-06}	221	2.67×10^{-11}	17.0
0.01	6.50×10^{-07}	172	3.42×10^{-11}	13.2
0.001	6.50×10^{-08}	152	3.87×10^{-11}	11.6

From the diffusion time of the fluorescently labeled block copolymer aggregate we evaluated a hydrodynamic radius (R$_H$) of 8.5 nm. Thus, block copolymer micelles with an average diameter of 17 nm and nonpolar PLLA core were present in neutral PBS buffer. These findings are comparable to the results of Saeed et al., who very recently observed aggregates of around 20-30 nm for related P(EGMA)-*block*-P(PLGA) block copolymers.[52] We have also studied solutions with lower concentrations of **P2***. The results summarized in Table 2 show aggregates with slightly lower hydrodynamic diameters formed at concentrations of 0.001 mg/mL. A concentration of 0.1 mg/mL was therefore considered to be adequate for a thorough cellular study of the aggregates.

Cell toxicity assay and intracellular localization of P(LLA)-*block*-P(HPMA) copolymers in human cervical cancer cells (HeLa cells)

The synthesized P(LLA)-*block*-P(HPMA)block copolymers are designed for *in vitro* as well for *in vivo* applications. Considered separately, the building blocks of the copolymer are

known to be non-toxic at the concentrations of interest as well as highly biocompatible. Nevertheless, it has to be proven that the new block copolymer itself is non-toxic as well. For this purpose, we carried out MTT tests on the block copolymer **P2**. The MTT assay is a standard colorimetric assay for the evaluation of the cell viability by evaluating the mitochondrial activity. We investigated the concentration dependent influence of the block copolymer **P2** on cell viability over periods of 24 and 72 h. At both times very high cell viability levels close to 100% with respect to control samples were observed. Those findings ensure non toxic behavior of the block copolymers for concentrations up to 3 mg/mL.
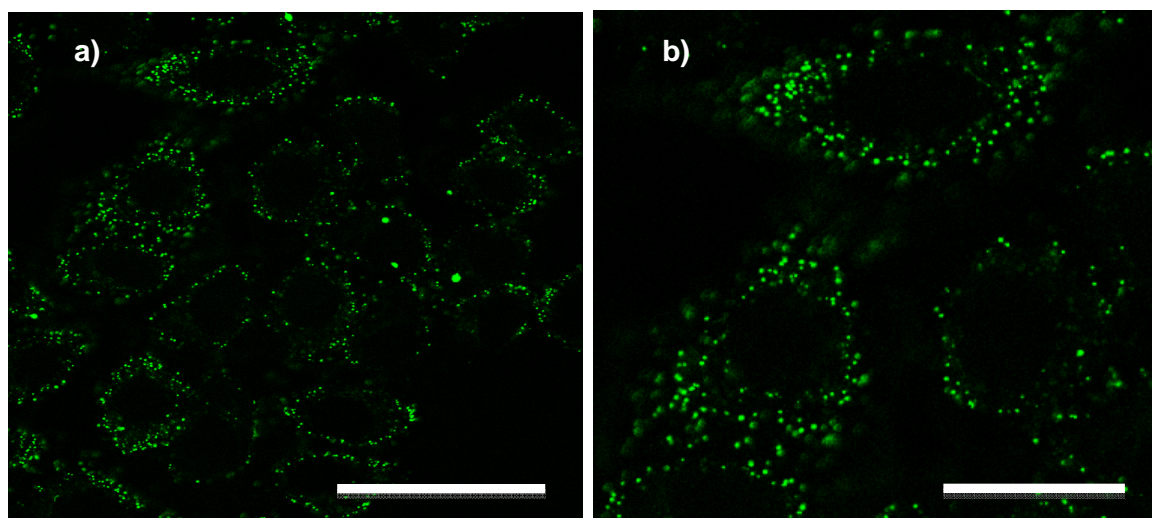
Figure 3: Confocal microscopy images taken from live HeLa cells after 1 h of incubation with the Oregon green 488 cadaverine labeled P(LLA)-*block*-P(HPMA)copolymer at a polymer concentration of 0.1 mg/mL. (scale bar = 50 µm (a) and 25 µm (b)).

Of course the data derived from the MTT test could also be explained by an inefficient or non-existent cellular uptake. In order to lend further support to cellular uptake of the block copolymer micelles, live cell confocal fluorescence microscopy was employed. Preliminary uptake studies were performed at a block copolymer concentration of 0.1 mg/mL. As mentioned above, this concentration significantly exceeds the assumed CMC-range. Thus, we can expect micelles interacting with the cell membrane. The confocal microscopy image shown in Figure 3 was taken after 1 h incubation time. Both images show a uniform distribution of fluorescently labeled aggregates within the cells, keeping in mind that the focal plane was set to be on intracellular level (see DIC microscopy image). In addition, the aggregates were well separated from each other and no agglomeration was observed. These findings are promising and warrant further biological evaluation with a view towards drug

encapsulation. From the confocal microscopy results it can be concluded that pronounced cellular uptake of the block copolymers took place. Thus, we could ensure non toxic behavior for the sample **P2***, leading to the reasonable assumption, that this new type of polymer is generally non toxic for imaging purposes as well as therapeutic applications. This conclusion is promising, since HPMA and PLLA are both well-established for biomedical use. Further studies regarding the uptake kinetics, precise intracellular location and degradation studies are currently under investigation in our laboratories. In addition, we are studying the encapsulation capability of these block copolymer micelles for in vitro as well as in vivo applications.

In summary, these first results on cellular uptake and toxicity clearly underline the potential of P(LLA)-block-P(HPMA)copolymers for further application in biological systems.

Conclusions

To the best of our knowledge, the highly biocompatible, polar P(HPMA) and the biodegradable P(LLA) structures have not been combined to block-like structures yet. This is probably attributed to the entirely different mechanisms for the controlled polymerization of the respective monomers. In this work we have established a combination of these building blocks by ring opening of LLA and successive RAFT-polymerization of PFMA P(PFMA), resulting in reactive ester precursor block copolymers. The molecular weight (Mn) of the block copolymers could be controlled in the range of 7 600–34 300 g/mol and well-defined (PDI¼1.30–1.45) reactive block copolymers were obtained. These materials represent a versatile platform for further functionalization via attachment of drugs, target moieties, and labels due to the activated ester block of P(PFMA) by polymer modification reaction. The postpolymerization modification reactions were shown to proceed without any apparent degradation and side reactions to the basic poly(ester) structure as evidenced by ^{1}H NMR with all modified polymers, achieving the desired block ratios. The synthetic pathway established here resulted in the formation of amphiphilic P(HPMA)-b-P(LLA) copolymers. The aggregation behavior of a carefully purified block copolymer sample (P(HPMA)77-b-P(LLA)42) was studied by FCS, demonstrating the formation of micellar structures with a hydrodynamic diameter of 17nm at a concentration of 0.1mg/mL. We have also been able to confirm the expected non-toxic behavior of this new type of block copolymer at concentrations up to 3mg/mL for P(HPMA)$_{77}$-b-P(LLA)$_{42}$. Furthermore, by

confocal fluorescence microscopy we have shown that the block copolymersare taken up by HeLa cells. These findings demonstrate that the novel P(HPMA)-b-P(LLA) copolymers are a potential platform for micellar drug-delivery applications. Further experiments regarding the detailed cellular uptake mechanism as well as detailed intracellular distribution for the whole series of block copolymers are currently carried out in our laboratories.

References

[1] Ringsdorf, H. *J. Polym. Sci. Polym. Symp.* **1975**, *51*, 135.

[2] Ferrari, M. *Nat. Rev. Cancer* **2005**, *5*, 161.

[3] Duncan, R. *Nat. Rev. Cancer* **2006**, *6*, 688.

[4] a) Haag, R. Kratz, F. *Angew. Chem. Int. Ed.* **2006**, *45*, 198; b) Liu, S.; Maheshwari, R.; Kiick, K. L. *Macromolecules* **2009**, *42*, 3.

[5] Duncan, R. *Pharm. Sci. Technol. Today* **1999**, *2*, 441.

[6] Duncan, R. *Nat. Rev. Drug Discovery* **2003**, *2*, 347.

[7] R. Duncan, J. K. Coatsworth, S. Burtles, *Hum. Exp. Toxicol.* **1998**, *17*, 93.

[8] Vasey, P.A.; Kaye, S. B.; Morrison, R.; Twelves, C.; Wilson, P.; Duncan, R.; Thomson, A. H.; Murray, L. S.; Hilditch, T. E.; Murray, T.; Burtles, S.; Fraier, D.; Frigerio, E.; Cassidy, J. *Clin. Cancer Res.* **1999**, *5*, 83.

[9] Hopewell, W.; Duncan, R.; Wilding, D.; Chakrabarti, K. *Hum. Exp. Toxicol.* **2001**, *20*, 461.

[10] Matsumura, Y.; Maeda, H. *Cancer Res.* **1986**, *46*, 6387.

[11] Pasut, G.; Veronese, F. M. *Adv. Drug Del. Rev.* **2009**, *61*, 1177–1188.

[12] Baka, S.; Clamp, A. P.; Jayson, G. C. *Expert Opin. Ther. Targets* **2006**, *10*, 867.

[13] Kaushik, V. V.; Moots, R. J. *Expert Opin. Biol. Ther.* **2005**, *5*, 601-606.

[14] Matsumura, Y.; Kataoka, K. *Cancer Sci.* **2009**, *100*, 572.

[15] Nishiyama, N.; Kataoka, K. *Pharmacol. Ther.* **2006**, *112*, 630.

[16] Batrakova, E.V.; Kabanov, A.V.; *J. Control. Release* **2008**, *130*, 98.

[17] Kabanov, A.V.; Alakhov, V.; *Crit. Rev. Ther. Drug. Carr. Syst.* **2002**, *19*, 1.

[18] Gauthier, M. A.; Gibson, M. I.;Klok, H. A. *Angew. Chem., Int. Ed.* **2009**, *48*, 48.

[19] Theato, P. J. *Polym. Sci. Part A: Polym. Chem.* **2008**, *46*, 6677.

[20] Binder, W. H.; Sachsenhofer, R. *Macromol. Rapid Commun.* **2008**, *29*, 952.

[21] Batz, H. G.; Franzmann, G.; Ringsdorf, H. *Angew. Chem., Int. Ed.* **1972**, *11*, 1103.

[22] Matyjaszewski, K.; Gnanou, Y.; Leibler, L. *Macromolecular Engineering Vol. 1*. WILEY-VCH Verlag GmbH & Co, Weinheim, **2007.**

[23] Tsarevsky, N .V.; Matyjaszewski, K.; *Chem. Rev.* **2007**, *107*, 2270.

[24] Moad, G.; Rizzardo, E. L.; Thang, S. H. *Polymer* **2008**, *49*, 1079.

[25] Stenzel, M. *Chem. Commun.* **2008**, 3486.

[26] Boyer, C.; Bulmus, V.; Davis, T. P.; Ladmiral, V.; Liu, J.; Perrier, S. *Chem. Rev.* **2009,** *109,* 5402–5436.

[27] Hawker, C. J.; Bosman, A. W.; Harth, E. *Chem. Rev.* **2001**, *101*, 3661.

[28] York, A. W.; Scales, C. W.; Huang, F.; Mc Cormick, C. L. *Biomacromolecules* **2007**, *8*, 2337.

[29] Konak, C.; Matyjaszewski, K.; Kopeckova, P., Kopecek, J.*Polymer* **2002**, *43*, 3735.

[30] Barz, M.; Tarantola, M.; Fischer, K.; Schmidt, M.; Luxenhofer, R.; Janshoff, A.; Theato, P.; Zentel, R. *Biomacromolecules* **2008**, *9*, 3114.

[31] Herth, M.; Barz, M.; Moderegger, D.; Allmeroth, M.; Jahn, M.; Thews, O.; Zentel, R.; Rösch, F. *Biomacromolecules* **2009**, *10*, 1697.

[32] Gibson, M. I.; Fröhlich, E.; Klok, H. A. *J. Polym. Sci. Part A: Polym. Chem.* **2009**, *47*, 4332.

[33] Barz, M.; Luxenhofer, R.; Zentel, R.; Kabanov, A. V. *Biomaterials* **2009**, *30*, 5682.

[34] Du, J.; Chen, Y. *Macromolecules* **2004,** *37,* 6322.

[35] Mori, H.; Hirao, A.; Nakahama, S.; *Macromolecules* **1994**, *27*, 35.

[36] Yamamoto, Y. Nagasaki, Y.; Kato, Y.; Sugiyama, Y.; Kataoka, K. *J. Control. Release* **2001**, *77*, 27.

[37] Murphy, W. L.; Peters, M. C.; Kohn, D. H. Mooney, D. J. *Biomaterials* **2000**, *21*, 2521.

[38] Jain, R. A. *Biomaterials* **2000**, *21*, 2475-

[39] Gupta, B.; Revagade, N.; Hilborn, J. *Prog.Polym. Sci.*, **2007,** *32*, 455.

[40] Hales, M.; Barner-Kowollik, C., Davis, T. P.; Stenzel, M. H. *Langmuir* **2004**, *20*, 10809.

[41] You, Y.; Hong, C.; Wang, W.; Lu, W.; Pan, C. *Macromolecules* **2004**, *37*, 9761.

[42] Messman, J. M.; Scheuer, A. D.; Storey, R. F. *Polymer* **2005**, *46*, 3628.

[43] Wolf, F. K.; Friedemann, N.; Frey, H. *Macromolecules* **2009**, *42*, 5622.

[44] Chong, Y. K.; Moad, G.; Rizzardo, E.; Tang, S. H. *Macromolecules*, **1999**, *32*, 2071.

[45] Eberhardt, M.; Mruk, R.; Zentel, R.; Theato, P. *Eur Polym J* **2005**, *41*, 1569.

[46] Dove, A. P.; Pratt, R. C.; Lohmeijer, B .G. G.; Waymouth, R. M.; Hedrick, J. L. *J. Am. Chem. Soc.* **2005**, *127*, 13798.

[47] Pratt, R. C.; Lohmeijer, B. G. G.; Long, D. A.; Lundberg, P. N. P.; Dove, A. P.; Li, H. B.; Wade, C. G.; Waymouth, R. M.; Hedrick, J. L *Macromolecules* **2006**, *39*, 7863.

[48] Perrier, S.; Takolpuckdee, P.; Mars, C. A. *Macromolecules* **2005**, *38*, 2033.

[49] Eberhardt, M.; Theato, P. *Macromol. Rapid Commun.* **2005**, *26*, 1488.

[50] Sahay, G.; Batrakova, E. V.; Kabanov, A. V. *Bioconjugate Chem* **2008**, *19*, 2023.

[51] Rigler, R.; Elson, E. S. *Fluorescence Correlation Spectroscopy*, Springer: New York, **2001**.

[52] Saeed, A. O.; Dey, S.;Howdle, S. M.; Thurecht, K. J.; Alexander, C. *J. Mater. Chem.* **2009**, *19*, 4529.

Supporting Information

Synthesis, Characterization and Evaluation of P(LLA)-block-P(HPMA)Copolymers: A New Type of Functional Biocompatible Block Copolymer

Matthias Barz, Florian K. Wolf, Fabiana Canal,[*] Kaloian Koynov[†], Maria J. Vicent,[*] Holger Frey and Rudolf Zentel

Removal of the dithioester endgroup

The dithiobenzoate end group was removed according to the procedure reported by Perrier et al.[46] Typically 200 mg of polymer, (M_n = 23.000 g/mol), and 80 mg of 4,4'-azobis(4-cyanovaleric acid) (~30 times excess in relation to the polymer end group) were dissolved in 3 mL of anhydrous dioxane. The solution was heated to 80 °C for 3 h. Finally the copolymer was precipitated 3 times in 100 mL of diethyl ether and collected by centrifugation. In the case of the block copolymer, the crude product was first precipitated in ethanol twice and then once in diethyl ether. The copolymer was dried in vacuum for a period of 24 h and a colorless product was obtained (yield: 90 %). The absence of the dithiobenzoate end group was confirmed by UV-Vis spectroscopy with the absence of the peak at 302 nm wavelength.

[*] Centro de Investigacion Principe Felipe, Avda Autopista el Saler 16/3, ES-46012 Valencia, Spain

[†] Max-Planck-Institute for Polymer Research, Ackermannweg 10, D-55128 Mainz, Germany

Characterization of reactive block copolymers by GPC
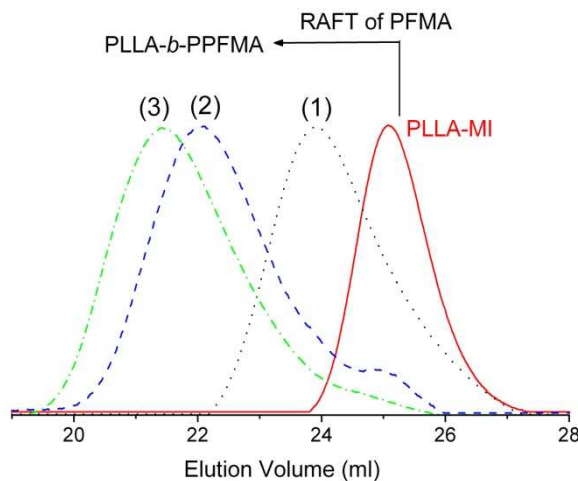
S.I. 1.   a) SEC elugrams of the P(LLA)-macro CTA (GPC$_{THF}$/polystyrene based calibration, M$_n$ = 4600 g/mol, M$_n$ (NMR) = 3000 g/mol; PDI = 1.08) and the respective P(PFMA)-*block*-P(LLA) block copolymers P1, P2 and P3 prepared in THF (RI-detection).

In Figure S.I. 1 the SEC elugrams (solvent THF; RI-detection) of the P(LLA)$_{42}$ macroinitiator as well as the P(PFMA)-*block*-P(LLA) reactive ester block copolymer derived thereof are shown. The obvious shift towards lower elution volumes in SEC indicates an increase in hydrodynamic volume of the sample and thus successful chain extension. The small shoulder for the block copolymer is most probably related to residual P(LLA) homopolymer, which is consistent with NMR-measurements, from which a degree of functionalization with the CTA of 69 % was observed. However, the contamination with homopolymer can be removed during work-up of the subsequent reaction steps (as demonstrated in Figure 3).

Characterization of block copolymers in solution by fluorescence correlation spectroscopy (FCS)

Fluorescence correlation spectroscopy experiments were performed using a commercial FCS setup (Zeiss, Germany) consisting of the module ConfoCor 2 and an inverted microscope model Axiovert 200 with a Zeiss C-Apochromat 40 ×/1.2 W water immersion objective. The fluorophores were excited by an Argon laser (λ = 488 nm) and the emission was collected after filtering with a LP505 long pass filter. For detection, an avalanche photodiode that

enables single-photon counting was used. Eight-well, polystyrene-chambered cover glass (Laboratory-Tek, Nalge Nunc International) was used as sample cell. The dye-labeled P(LLA)-*block*-P(HPMA)*block* copolymer was dissolved in DMSO (c = 20 mg/mL) and PBS buffer (pH = 7.2) was slowly added to obtain a final concentration of 0.1 mg/mL. The solution was kept at room temperature over 24 h prior to the measurements. For each solution, 10 measurements with a total duration of 5 min were performed. The time-dependent fluctuations of the fluorescence intensity $\delta I(t)$ were recorded and analyzed by an autocorrelation function $G(t)=1+<\delta I(t') \, \delta I(t'+t)>/<I(t')>^2$. As has been shown theoretically for an ensemble of m different types of freely diffusing fluorescence species, $G(t)$ has the following analytical form:[51]

$$G(t) = 1 + \left[1 + \frac{f_T}{1 - f_T} e^{-t/\tau_T} \right] \frac{1}{N} \sum_{i=1}^{m} \frac{f_i}{\left[1 + \dfrac{t}{\tau_{Di}} \right] \sqrt{1 + \dfrac{t}{S^2 \tau_{Di}}}} \qquad \text{(Equation S.I. 1)}$$

Here, N is the average number of diffusing fluorescence species in the observation volume, f_T and τ_T are the fraction and the decay time of the triplet state, τ_{Di} is the diffusion time of the *i-th* species, f_i is the fraction of component i, and S is the so-called structure parameter, $S = z_0/r_0$, where z_0 and r_0 represent the axial and radial dimensions of the confocal volume, respectively. Furthermore the diffusion time, τ_{Di}, is related to the respective diffusion coefficient, D_i, through [k1] $D_i = r_0^2/4 \, \tau_{Di.}$ The experimentally obtained $G(t)$ can be fitted with eq. 1, yielding the corresponding diffusion times and subsequently the diffusion coefficients of the fluorescent species. Finally, the hydrodynamic radii R_h can be calculated (assuming spherical particles) using the Stokes-Einstein relation: $R_h = k_B T/6\pi\eta D$, where k_B is the Boltzmann constant, T is the temperature, and η is the viscosity of the solution. As the value of r_0 depends strongly on the specific characteristics of the optical setup a calibration was done using a reference standard with known diffusion coefficient, i.e., Rhodamine 6G. Typical autocorrelation curves and the corresponding representation using eq. 1 are shown in Fig. S.I. 2.
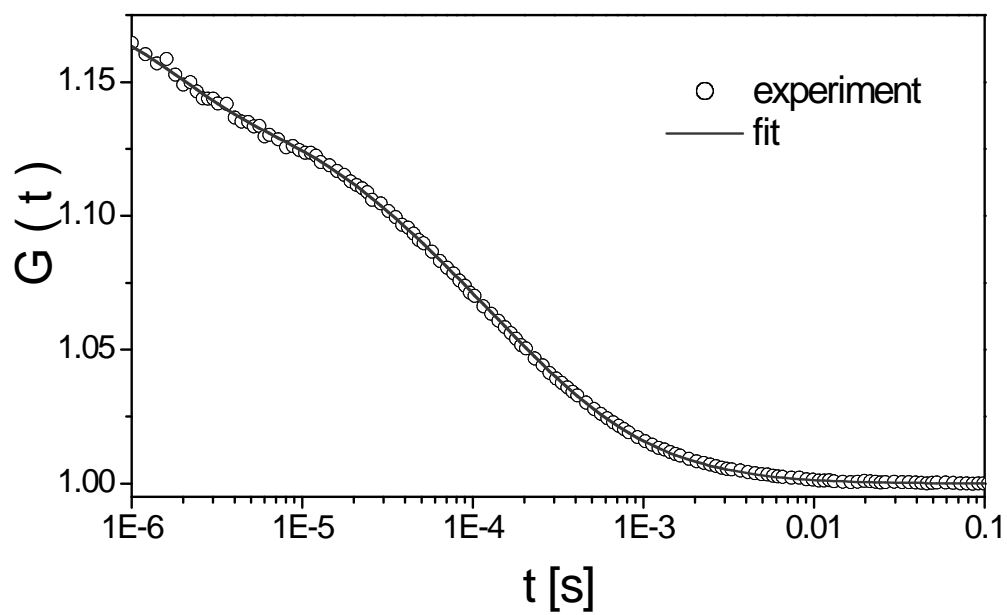
Figure S.I.2: Experimental autocorrelation curve determined by fluorescence correlation spectroscopy (FCS) for fluorescently labeled P(LLA)-*block*-P(HPMA)**P2***** (c = 0.1 mg/ml in PBS buffer (pH = 7.2)) and the corresponding fit with eq.1.

4.0 Ongoing Projects and Future Work

4.1 Influence of Poly(lactide)s Tacticity on Micellization, Cellular Uptake Kinetics and Intracellular Localization in HeLa Cells of PLA-*block*-PHPMA Copolymers

This study represents the continuation of work presented in Chapter 3.4

Matthias Barz, Florian K. Wolf, Fabiana Canal,[*] Kaloian Koynov,[†] Maria J. Vicent,[*] Holger Frey and Rudolf Zentel

In this pursuing study we investigate the influence of poly(lactide) tacticity on the micellization as well as the biological fate of formed micelles of poly(lactide)-*block*-poly(2-hydroxypropyl methacrylamide) (PLA-*block*-PHPMA) copolymers. The physical properties of poly(lactide) can be altered by stereochemical manipulation. This study focuses on the influence of poly(lactide) tacticity on micellization and endocytosis of HPMA based block copolymers in a human cervix adenocarcinoma (HeLa) cell line. The kinetics of cellular uptake and intracellular fate of HPMA based copolymers represent additional important parameters.

Therefore we synthesized and investigated PLA-*block*-PHPMA copolymers of comparable molecular weights and block length ratios, differing in the tacticity of the hydrophobic poly(lactide) block. Isotactic PHPMA-*block*-PLLA and atactic PHPMA-*block*-PDLLA copolymers were prepared by (1) ROP of lactide, (2) RAFT of the active ester monomer pentafluorophenol methacrylate and (3) applying the activated ester approach as described in the previous section 3.4 (where further details concerning the preparation are presented). Molecular characterization data is available in tables 1&2. In this context, pure PLA-*block*-PHPMA block copolymers and fluorescently labeled analogs were synthesized, exhibiting molecular weights M_n around 20,000 g/mol with moderate polydispersities M_w/M_n of 1.4.

---

[*] Centro de Investigacion Principe Felipe, Avda Autopista el Saler 16/3, ES-46012 Valencia, Spain

[†] Max-Planck-Institute for Polymer Research, Ackermannweg 10, D-55128 Mainz, Germany

Table 1: Reactive ester PLA-*block*-PFMA copolymer precursors.

Polymer	PLA-CTA (M_n)	$M_{n,calc}$ [b] kg/mol	M_n kg/mol	PDI
P1R	PLLA 3000	30	22.8	1.45
P2R	PDLLA 3200	30	23.7	1.34

The synthesized polymers differ only in the tacticity of the poly(lactide) block. All other parameters, e.g. block length and degree of polymerization, remain unchanged.

Table 1: Reactive ester PLA-*block*-PHPMA copolymers derived from P1R and P2R and their fluorescently labeled derivatives (P1* and P2*)

Polymer	PLA composition	Average block ratio (HPMA/L-lactide)[a]	Dye content % (Oregon Green 488)	M_n kg/mol	PDI
P1	*L*	78/42	-	14.2	1.45
P2	*D,L*	74/42	-	14.8	1.34
P1*	*L*		1.3	14.9	1.47
P2*	*D,L*		1.3	15.3	1.34

The aggregation in solution was investigated for the dye labeled copolymers in isotonic aqueous solution, applying fluorescence correlation spectroscopy (FCS). The normalized autocorrelation curves measured for 0.1 mg/mL PBS buffer solutions of **P1*** and **P2*** and the corresponding fit are shown in Figure 1.
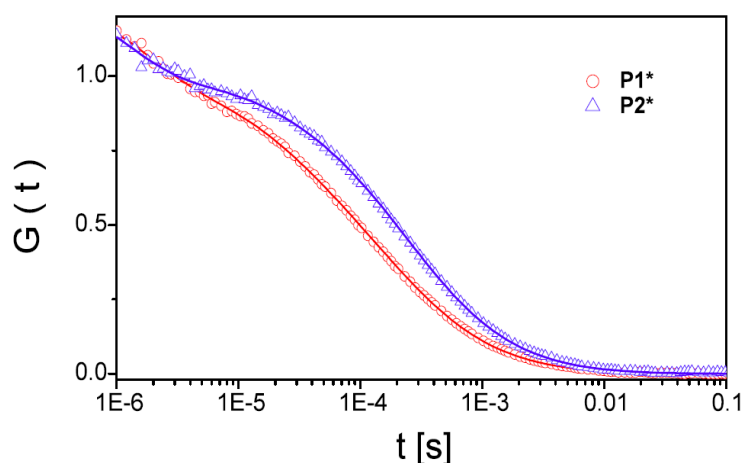
Figure 1: Normalized autocorrelation curves determined by fluorescence correlation spectroscopy for **P1*** (○) and **P2*** (△)**.** The solid lines represent the corresponding fits with eq. S.I. 1 from chapter 3.4.

In addition to the slowly diffusing aggregates also fast diffusing species, i.e. residual amounts of free dye molecules, were present in the solutions. From the diffusion time of the slow component we evaluated hydrodynamic radii (R_H) of around 8.5 nm and 10.2 nm for **P1*** and

P2*, respectively (0.1 mg/L). These values are significantly higher than the single polymer chain hydrodynamic radius and we hence conclude that micelles with average diameters (2x R_H) of 17 nm and 20.4 nm have been formed (pH 7.2 PBS buffer).

Cellular toxicity

No toxic side effects of P1 or P2 could be observed towards a HeLa cell lines (tested for 24 and 72h of exposure at concentrations up to 3 mg/mL).

Cellular uptake

Time-dependent as well as concentration dependent studies on the uptake of polymer micelles in HeLa cells were conducted.

The time-dependent experiments were carried out at two different temperatures (37 °C and 4 °C) in order to prove the energy-dependent mechanism of internalization. The HeLa cells were exposed to a 0.1 mg/mL polymer solution for different time periods, ranging from 5 min to 5 h. The cellular internalization profile of **P1* (PLLA)** augmented with increasing incubation time approximating a saturation concentration. In the case of **P2***, the maximum uptake was registered after 1 h of incubation, followed by a decrease after 2 and 5 h. This kind of uptake could be related to an exocytosis process or represents a dye quenching phenomenon which would be supported by the high accumulation of the fluorescent polymer inside the cells. Also degradation of the P(DLLA) block, effecting the endosomal department cannot be excluded.
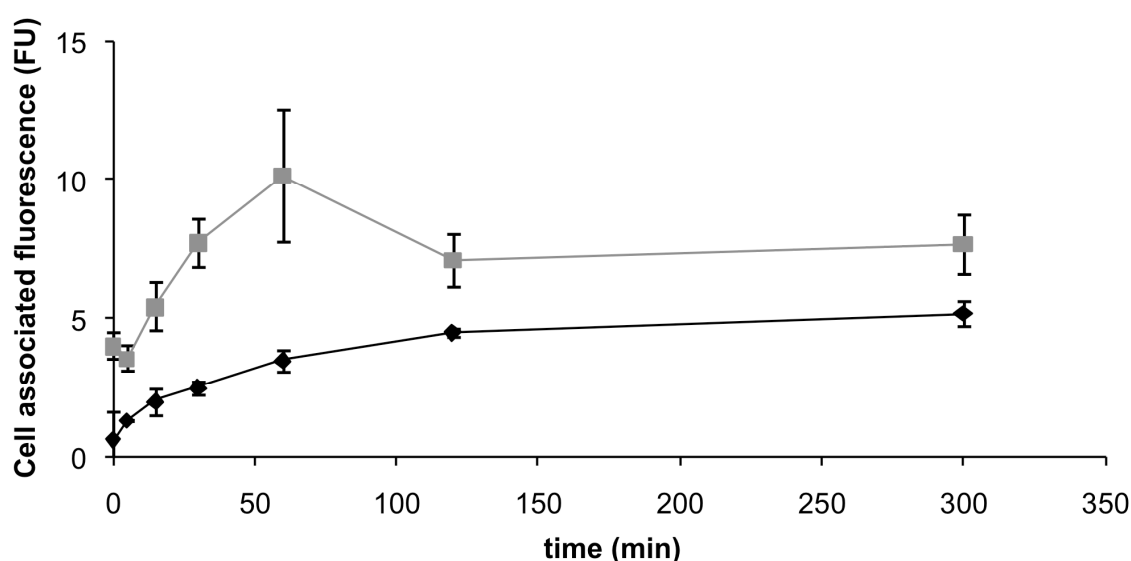
Figure 2: Time-dependent cellular uptake of **P1*** (bottom) and **P2*** (top) with standard deviations, conducted at 37°C.

The significantly lower uptake for both polymer types at 4°C (not shown) is indicative for an energy depended uptake process and therefore a strong argument for an endocytotic pathway of internalization. All experiments were conducted in duplicate and the observed standard deviations observed for the PDLLA based sample visualized the necessity for additional experiments. In general PDLLA based micelles experienced an increased time-dependent cellular uptake compared to their isotactic analogs.
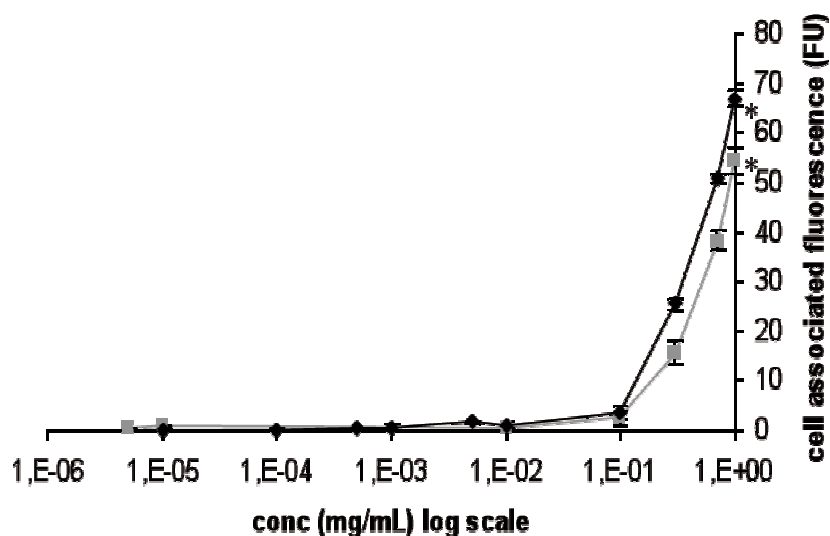
Figure 3: Concentration-dependent internalization profiles of **P1*** and **P2***after 1 h of incubation at 37°C.

Further studies showed that for both polymer systems, the cellular internalization increased with an increase in concentration. Experimentally, a minimum polymer concentration of 0.1 mg/mL was required to trace cellular uptake. In this case PLLA based - **P1*** showed a slightly increased uptake performance, compared to the PDLLA based - **P2*** (67 FU at 1 mg/mL for **P1*** and 1 mg/mL of 54 FU registered for **P2***).

The localization of the polymers inside the cells was followed by live cell confocal fluorescence microscopy, incubating the cells with 0.1 mg/mL polymer solutions at different times. Since the highest internalization was detected after 1 to 2 hours of incubation (for **P1*** and **P2*)**, as reported above, 2 h can be expected to be a suitable time frame for the investigation of the cellular fate of the aggregates. Furthermore, we applied a lysosomal marker (Dextrane Texas Red) to study the intracellular localization of the copolymers. In the case of the PLLA-*b*-PHPMA copolymer, no direct colocalization of marker and polymer can be

observed and **P1*** is exclusively present in the cytosol. In the case of PHPMA-*block*-PDLLA copolymers a low extent of colocalization was found (Figure 4). Since aggregates are still located in the cytosol, this indicates lysosomal internalization of the PDLLA copolymer **P2***.
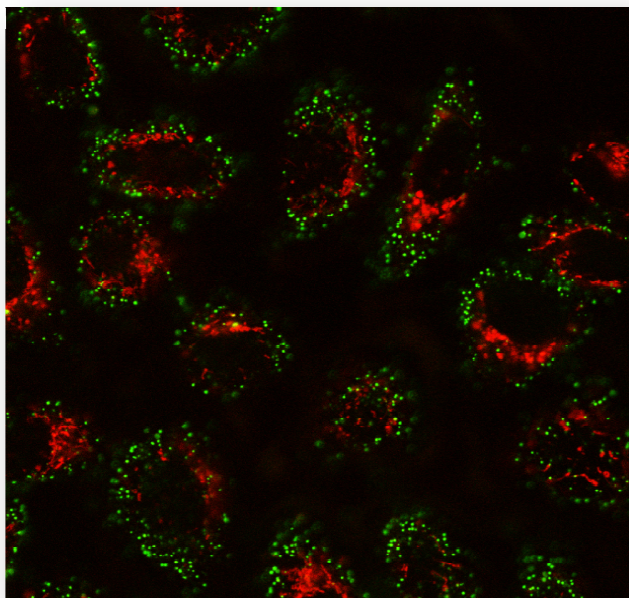
Figure 4: Representative fluorescence image of the intracellular localization of P2* (green) and Dextran Texas Red in the cell (red).

The absence (**P1***)/low degree (**P2***) of colocalization could be related to a slower intracellular delivery, which means that the block copolymer aggregates may need longer than 2 hours to be internalized by the lysosomes. This requires further studies involving longer time frames. The current observations indicate a primary localization of **P1*** and **P2*** in the golgi apparatus and/or the endoplasmic reticulum.

In summary, we have collected initial information indicating a direct influence of the polymer tacticity of the poly(lactide) block on cellular uptake as well as on intracellular localization. In the confocal laser scanning microscopy images, no colocalization of the polymer with a lysosomal marker (Dextrane Texas Red) could be observed even after 5 h incubation. These findings are suggestive of an endosomal escape. Supplementary data is needed to verify the uptake kinetics as well as the endosomal escape hypothesis. In this respect, additional biological studies will be carried out by the collaboration partners in the near future.

Experimental Part

Poly(D,L-lactide) Synthesis

The synthesis was carried out as described for PLLA in section 3.4. Due to the amorphous character of poly(D,L-lactide), the sample was precipitated repeatedly (3x) in cold (-25°C) diethyl ether after quenching with an equimolar amount of benzoic acid. 1H-NMR (CDCl$_3$, 400MHz) δ^1H/ppm): 0.92 (s, C(CH$_3$)$_3$; 1.50- 1.60 (m, CHCH$_3$, poly(lactide) chain); 3.78-3.89 (m, -OCH$_2$C(CH$_3$)$_3$); 4.34 (q, *3J* =7.0 Hz HOCH(CH$_3$)); 5.11-5.21 (m CH(CH$_3$), poly(lactide) chain).

Cellular uptake by fluorescent activated cell sorting (FACS)

Cells were seeded at a density of 2x105 cells/mL in a sterile 6-well plate. After 48 h incubation, cells were treated with 10 µL of OG-labeled polymers **P1*** and **P2*** solution in PBS with 10% v/v of DMSO. In the time-dependent experiment the final polymer concentration was 0.1 mg/mL, while in the concentration-dependent experiments the polymer concentration ranged from 1,E-06 to 1 mg/mL. The experiments were carried out in triplicate; some wells were untreated and used as control. In the time-dependent experiments, cells were incubated for times of 0, 5, 30 min, 1, 2 and 5 h at 37°C, afterwards the plates were put in ice, the medium was removed and cells were washed trice with 1 mL of cold PBS and scraped. Cell associated fluorescence was then analyzed using a Cytomics FC 500 (Beckman Coulter Inc.) equipped with an argon laser (405 nm) and an emission filter for 455 nm. Data collection involved 15000 counts per sample and was analyzed with Beckman Coulter CXP software. The experiments were also carried out at 4°C, placing the plates at 4°C 30 min before the experiment started and then following the same procedure as described above. The concentration-dependent experiments were carried out incubating the cells for 1 h at 37°C with different polymer concentrations and then following the same procedure as reported above.

Please see **Chapter 3.5** for additional experimental details on:
- Materials/Methods,
- End group modification of PLLA to ω-CTA macroinitiator for RAFT polymerization
- Synthesis of P(PFMA)-*block*-P(LLA) copolymers
- Synthesis of P(LLA)-*block*-P(HPMA) copolymers
- Synthesis of dye labeled P(LLA)-*block*-P(HPMA) copolymers
- Cell cultures
- Removal of the dithioester endgroup
- Cells viability assay
- Live cell confocal fluorescence microscopy

4.2   Amphiphilic, Star-Shaped PLA-Multiblock Copolymers

Florian K. Wolf, Daniel Wilms, and Holger Frey

This study aims at the synthesis of biocompatible multiarm star copolymers. The individual arms shall be composed of amphiphilic multi block segments of low individual and total polydispersities. Generally, the geometric layout shall exhibit the characteristics of a multilayer system. Ideally, the hydrophilic middle block is composed of a degradable poly(ester) segment, i. e., poly(lactide) or poly(ε-caprolactone), granting a degradability of the high molecular weight monomolecular micelles into compounds sufficiently small for renal elimination (i.e., < 20,000 g/mol).

The synthesis is based on a "grafting from" approach, using a multi-hydroxyl functional initiator which can be partially deprotonated by, e.g. potassium alkoxides and used for the ROP of a hydroxyl-functional epoxide. Of course, the latter requires a protecting group which is stable under the employed basic conditions. EEGE (ethoxy ethyl glycidyl ether),[1] which features a hydrolyzable acetal was chosen for this purpose.[2] Post-polymerization acidic hydrolysis affords linear poly(glycerol).[3,4]

In a subsequent step, the polyether arms are extended via ring-opening polymerization of lactide, using a suitable transesterification catalyst. DBU was chosen due to its good performance and easy handling, generally granting nearly complete monomer conversion. Next, the terminal poly(ester) group is reacted with an initiator for ATRP of the final poly(methacrylate) shell. 2-Bromo isobutyrylbromide is an appropriate reagent for this purpose. Prior to ATRP, the acetal groups of the inner PEEGE core are cleaved by stirring the polymer with 10 vol. % of 1n HCl in THF. Suitable monomers for the formation of the optional hydrophilic outer shell could be OEGMA (oligo ethylene glycol methacrylate) or GMA (glycerol methacrylate).

Scheme 1: General design of a monomolecular micelle with the underlying structural motive of multi-arm star – multi block copolymers. An interesting review which concentrates on the synthesis of straight forward star shaped poly(ether)s and especially PEOs has been recently published by Lapienis.[5]

1) Hydrophilic poly(ether) core:
   Anionic ring-opening polymerization of epoxides

2) Hydrophobic poly(ester) sub shell:
   Ring-opening polymerization of lactones

3) Optional hydrophilic corona:
   Living radical polymerization of methacrylates
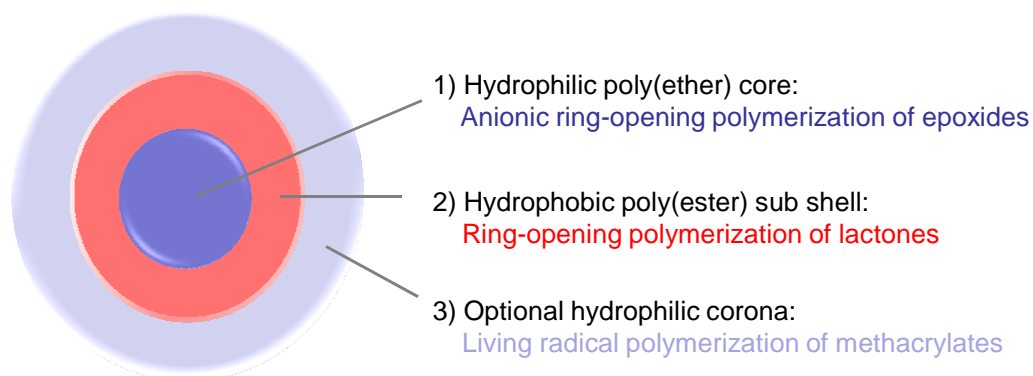
Hitherto, we have concentrated on combining the abovementioned monomers to obtain linear copolymers by using the simple, bifunctional initiator diethylene glycol. In the first part of this section, the general feasibility of the individual steps of the synthetic route described above were tested before targeting a star-shaped structure.

In the second part, we concentrated on the synthesis of two interesting new polyolic initiator systems with six and eight primary hydroxyl groups, respectively, of equal reactivity. The latter is based on a highly interesting porphyrine derivative, which could allow for the introduction of a photosensitive moiety in the micelles core. Generally, these polyols represent first generation dendrons and have been realized via a divergent approach.

In the following, the current state of the project is summarized and future steps are briefly addressed.

Block Copolymer Synthesis:

The synthetic process to the desired triblock copolymers starts with the polymerization of EEGE using a bifunctional initiator (Scheme 2). Straightforward deprotonation of diethylene glycol with potassium methanolate was the method of choice. Methanol can be removed easily in vacuo (at 60 °C). This process is facilitated by the use of a dispersing solvent, taking

into account the specific polarity of the initiator. DMF, DMSO and diglyme were successfully applied. A degree of deprotonation between 35 and 40 % per OH group proved to be highly efficient and MALDI-ToF spectrometry showed the diethylene glycol functionalized species of PEEGE exclusively (Figure 2). On account of the aggravated proton abstraction from an already onefold deprotonated diethylene glycol molecule, higher degrees of deprotonation, especially those exceeding 50 %, were omitted due to the low molecular weight and the bifunctional nature of the initiator. EEGE was injected as a 40-50 vol. % solution in dioxane, heated to 80 °C and stirred over night after an induction period of 10 minutes. In general, Schlenk-tubes with a low diameter/volume ratio are highly effective for this process since the dispersed initiating potassium salts often adhere to the side walls of the tube. A complete coverage by a high monomer/solvent fill level is thus guaranteed.

Polymerization over night was sufficient to achieve full monomer conversion. Addition of 5-10 vol. % of ethanol finally quenched the reaction. Subsequently, excess dioxane was removed in vacuo and a vol. equivalent of dichloromethane was added. The slightly opaque slurry was filtered over a short neutral aluminium oxide column to remove residual salts (eluted with excess dichloromethane). After removal of the solvent in vacuum, transparent, slightly yellowish PEEGE was obtained in nearly quantitative yield.
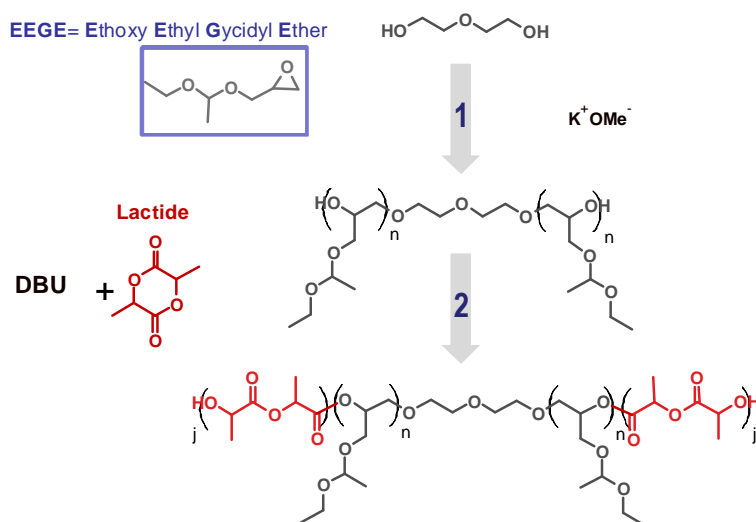
Scheme 2: Initial strategy to PEEGE-*b*-PLA copolymers.

The chain extension with lactide was conducted under the conditions previously described[6] using the organo base DBU in dichloromethane. However, attempts with different monomer/macroinitiator ratios yielded block copolymers with relatively poor PDI values.

Significant tailing and the presence of shoulders at the low molecular weight flank of the signals could be observed (Figure 1). The bimodal character indicated the presence of free macroinitiator in the solution. In summary, these facts indicate that in the present system, propagation is faster than initiation. The secondary nature of the PEEGE hydroxyl endgroup was assumed to be the main reason for this observation.

In order to (re)create the primary character of the poly(ether backbone) and thus facilitate the initiation of lactide polymerization, we investigated the chain extension from PEEGE with ethylene oxide (EO). This strategy requires no intermediate isolation of PEEGE or a significant change of reaction conditions. A solution of EO was added to the living PEEGE chains. The vessel with the PEEGE/dioxane solution was evacuated upon cooling with a dry ice/ethanol bath. After warming to room temperature, a 35 vol% solution of EO in THF was injected into the evacuated Schlenk tube and stirred for 30 minutes before slow heating to 60 °C. After 24 to 48 h, work up of the P(EO-*b*-EEGE-*b*-EO) was conducted as described above for plain PEEGE samples.

SEC (DMF)

M_n 12 100   PDI 1.43

M_n 8 750   PDI 1.79

Slow initiation due to secondary nature of the hydroxyl group:

M_n 19 600   PDI: 1.40

M_n 15 200   PDI:1.64
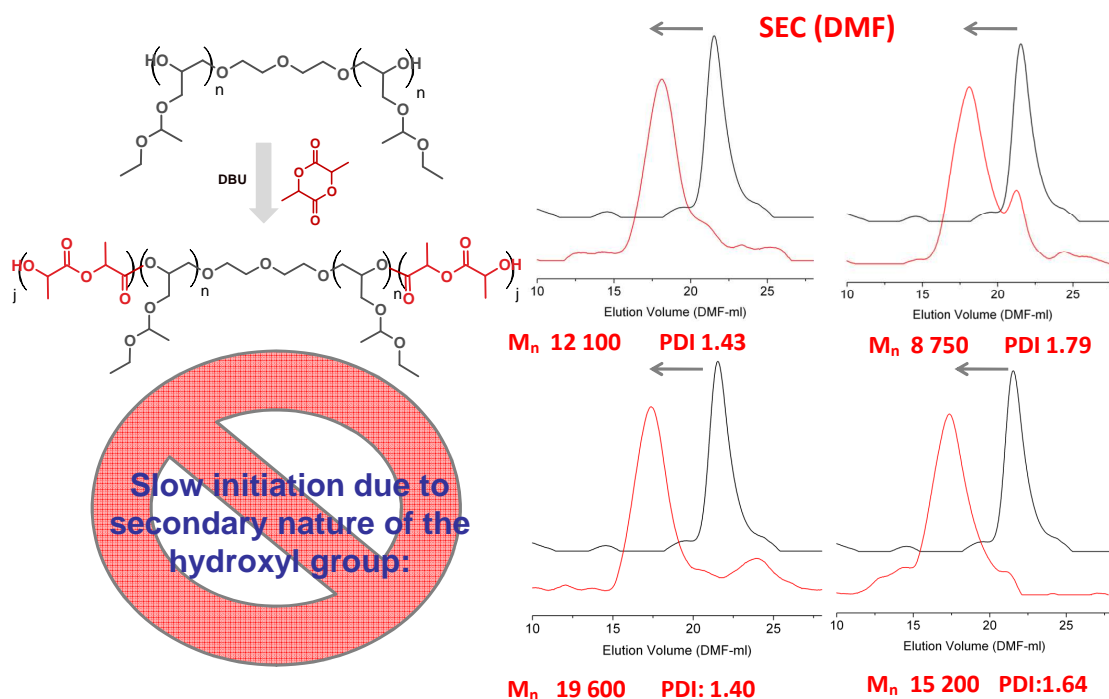
Figure 1: Broad and/or bimodal SEC (in DMF, cal. with PEG standards) traces after chain extension with lactide. Presumably due to $k_I < k_P$

MALDI-ToF mass spectroscopy of the PEEGE precursor and the chain extended triblock copolymer illustrated a quantitative end-capping of the terminal groups with at least 7 EO

units per chain. This value was obtained for the densest populated PEEGE species (as evaluated from MALDI-ToF), i.e., $C_4H_{10}O_3(C_7H_{14}O_3)_{13}$ $(C_2H_4O)_n$. No species with $n<7$ could be identified in the spectrum depicted in Figure 2. The selected ratio of 25 EO units/diethylene glycol unit should hence be sufficient to guarantee a quantitative end capping with EO. This would correspond to an average weight gain of only 44 x 12.5 = 550 g/mol per arm.
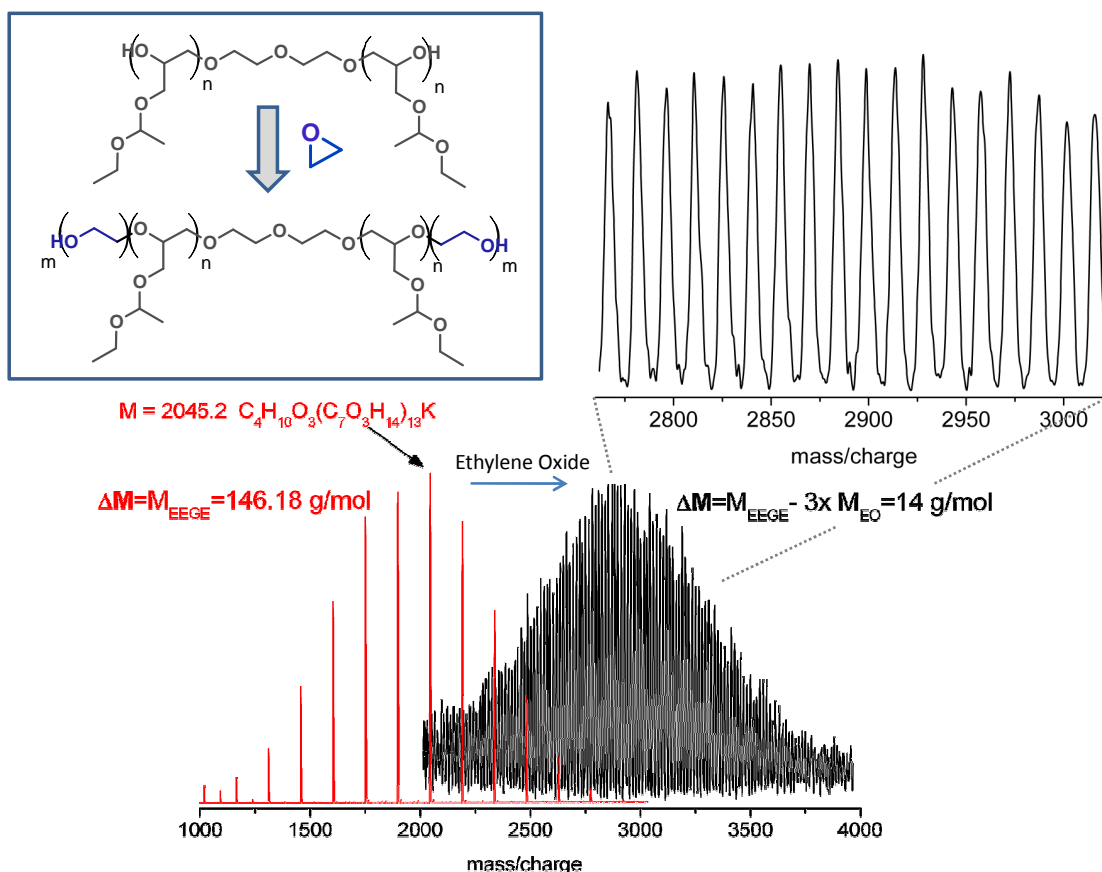
Figure 2: Chain Extension of PEEGE with EO visualized via MALDI-ToF MS.

In addition to MALDI-ToF analysis, a simple evaluation of a quantive "end capping" of PEEGE terminal units with ethylene oxide can be conducted more conveniently via routine ^{1}H NMR analysis (Figure 3). The absence of a distinct signal related to the terminal methine proton at 3.84 ppm (CDCl$_3$, 400 MHz) is very characteristic. This peak is well separated from the other backbone signals (up to 3.75 ppm) and can be evaluated quantitatively.

After end capping with EO, the chain extension with lactide afforded much better results and the PDIs of the resulting multi-block copolymers were found to be between 1.08 (SEC in DMF, PEG standard) and 1.14 (SEC in THF, PS standard) (Figure 4). Three different copolymers with nearly identical molecular parameters could be realized on the base of

P(EO$_{12.5}$-*b*-EEGE$_{10}$-*b*-EO$_{12.5}$). They only differ in their relative chain tacticities: isotactic and enantiomeric PLLA and PDLA as well as the atactic PDLLA were targeted. While PLLA and PDLA block copolymers could be readily precipitated from methanol and/or diethyl ether, work-up of PDLLA based systems was conducted via dialysis in THF/methanol (4:1).
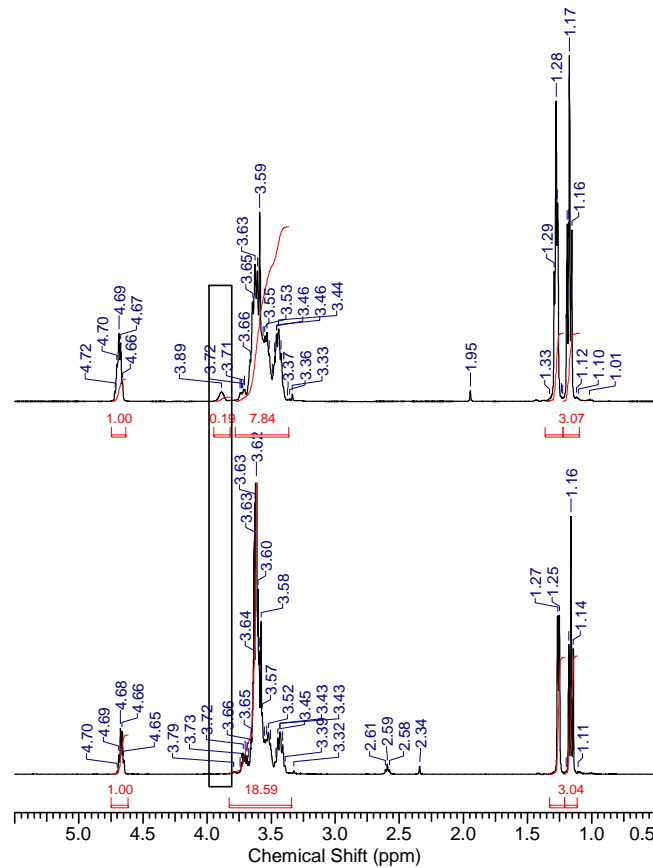
Figure 3: ^{1}H NMR spectra (400 MHz, CDCl$_3$) of PEEGE$_{10}$ (top) and P(EO$_{12.5}$-*b*-PEEGE$_{10}$-*b*-EO$_{12.5}$) (bottom).The quantitative end-capping of the terminal PEEGE group is illustrated by the disappearance of the signal at 3.89 ppm and the strong increase of the 3.3 -3.7 ppm integral.
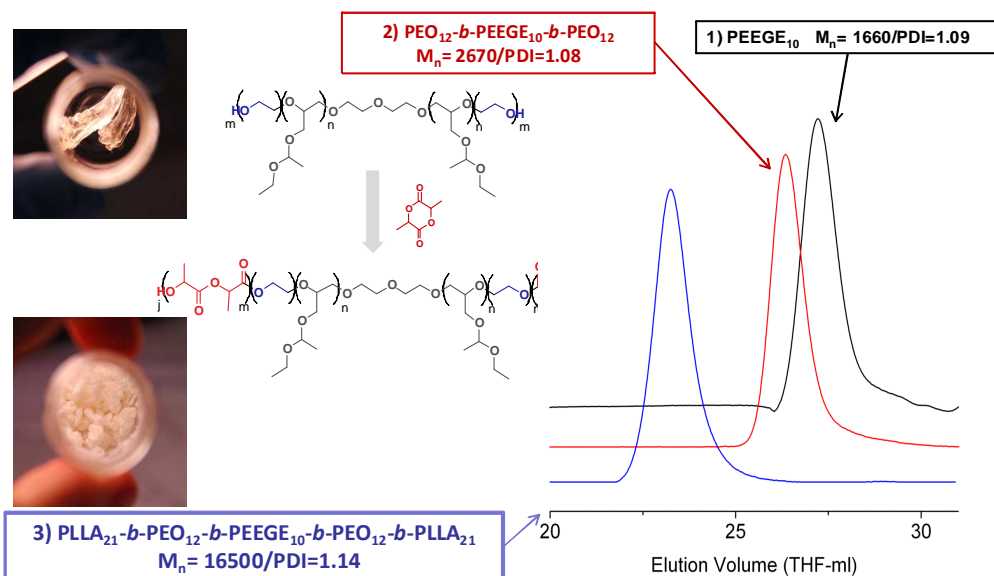
Figure 4: SEC (in THF, PS standards). Pictures: The character of the sample changes from viscoelastic, to crystalline and brittle upon PLLA grafting.

Table 1: Molecular characterization data of the successive steps of the block copolymer build-up.

PEEGE	P(EO-*b*-EEGE-*b*-EO)	P(LA-*b*-EO-*b*-EEGE-*b*-EO-LA)	P(LA-*b*-EO-*b*-*lin*PG-*b*-EO-*b*-LA)
		⟹ 14300 g/mol, PDI: 1.09 (PLLA)	⟹ 12300 g/mol, PDI: 1.12 (PLLA)
2800 g/mol, PDI: 1.09	⟹ 4400 g/mol, PDI: 1.11	⟹ 14700 g/mol, PDI: 1.08 (PDLA)	⟹ 11900 g/mol, PDI: 1.11 (PDLA)
		⟹ 13900 g/mol, PDI: 1.08 (PDLLA)	⟹ 11400 g/mol, PDI: 1.09 (PDLLA)

The acetal groups of the middle section of the P(LA-*b*-EO-*b*-EEGE-*b*-EO-LA) copolymers could be readily cleaved in THF with 10 vol.% of 1N HCl without detrimental deterioration of the other segments as could be evidenced by SEC and NMR (Figure 4, left). Table 1 illustrates the development of the separate steps of the block copolymer build up.

The reaction of the PLA end groups with a 1.4-fold excess of 2-bromo isobutyrylbromide in dichloromethane resulted in a quantitative functionalization. The presence of a 1.5-fold excess of triethylamine guaranteed the stability of the acid sensitive acetal groups. An interesting detail, which can be observed for the 2-bromo-isobutyryl end group at the PLA chain is the separate appearance of its two methyl groups in the ^{1}H NMR spectrum which can be found at 1.94 and 1.97 ppm, respectively (Figure 5, right). This can be explained by the chiral character of the ultimate lactide unit in combination with the high rotational

barrier caused by the bulky bromine substituent. It should be noted, that acetal cleavage after reaction with 2-bromo-isobutyryl-bromide was successful as well. Generally, purification is conducted by precipitation or dialysis as described above.
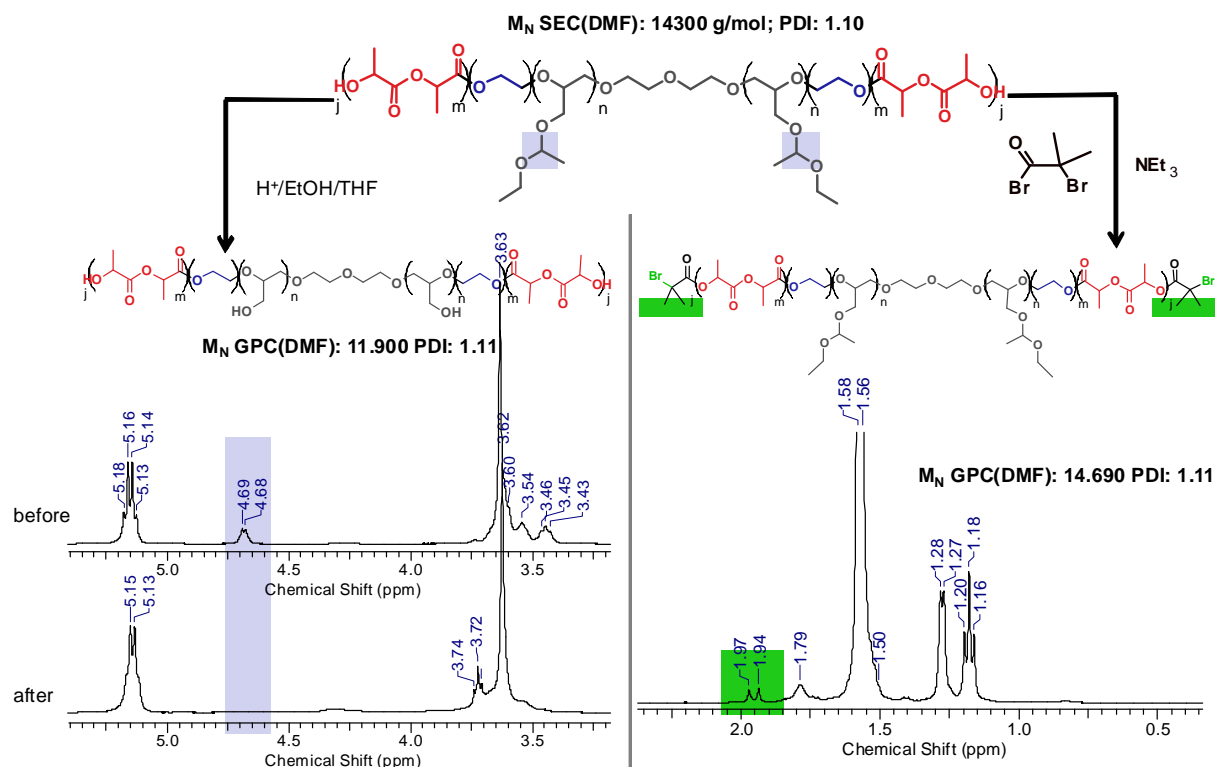
Figure 5: Post-polymerization modification of the P(LA-*b*-EO-*b*-EEGE-*b*-EO-*b*-LA) copolymers via acetal cleavage of the middle block (left), or end group modification with 2-bromo-isobutyrylbromide (right).

Future work comprises a study of the ATRP polymerization of hydrophilic methacrylates or their precursors initiated from the multi block copolymers' chain ends and a transfer of the synthetic concept to the multi-functional initiators which will be briefly introduced in the following.

Multi-functional Initiator:

Several requirements for the design of the multi-functional initiator have to be met. Most important is the high and equal reactivity of all hydroxyl groups in the initiation process of an oxy-anionic epoxide polymerization. This requires a high symmetry of the system, which is not given by short chains with pendant groups like linear poly(glycerol) or hyperbranched

poly- or oligo-(glycerol)s. They feature primary and secondary hydroxyl groups and are generally polydisperse. First generation dendrimers are considered ideal for our purpose for a number of reasons: They permit access to compounds with high core symmetry and an end group number between 6 and 8. Furthermore, the core motive can be readily varied. In our case, a strong UV absorption was a fundamental requirement to analyze and record the initiators incorporation via a UV SEC detector. The polymer backbone (aliphatic esters, ethers and poly(alkyl) segments) hardly show any absorption and thus allows for a simple proof of initiator incorporation in dependence of the molecular weight.

The coupling reaction should yield a structure with a backbone that is not susceptible to cleavage or other side reactions under the employed reaction conditions. Furthermore, the OH group density should be moderate. Otherwise, solubility could be impaired in the monomer/solvent mixture, especially in the deprotonated state. This particularly holds true for a multi-deprotonated, polyfunctional initiator.

Tris(4-hydroxyphenyl)ethane represents a commercially available product and has proven to be a versatile synthon in dendrimer and star polymer synthesis which matches the required symmetry criteria. In order to multiply the number of available initiating sites per molecule, we were looking for a suitable AB_2 monomer to construct a first generation dendrimer. Thereby, **B** should represent two symmetric, primary hydroxyl groups. **A** ought to exhibit good performance as a leaving group which should allow facile etherification with a phenolate.

In 1995, Gnanou and coworkers[7] described the synthesis of PEO-based dendrimers. They used an acetal protected TMP derivatized with a pendant tosylate[*] or alkylchloride[†] group. The dendritic structure was obtained by repetitive end capping of living PEO with the AB_2 compound, cleavage of the acetal group and reinitiation of EO polymerization. 1,1,1-Tris(hydroxymethyl)propane is the ideal building block for this purpose (Scheme 4). The two hydroxyl groups can be readily protected as acetonide (1), while the third one can be transformed into a leaving group via tosylation (2). In order to allow purification via distillation, we exchanged the tosylate with a bromine (3). Scheme 2 shows a full schematic

---

[*] 2,2-dimethyl-5-ethyl-5-methyltosyl-1,3-dioxane
[†] 2,2-dimethyl-5-ethyl-5-chloromethyl-1,3-dioxane

methodology for the synthesis of the alkyl bromide precursor which has been designed according to these criteria and has not been described to date (Scheme 3).

Scheme 3: Synthesis of 2,2-dimethyl-5-ethyl-5-bromomethyl-1,3-dioxane
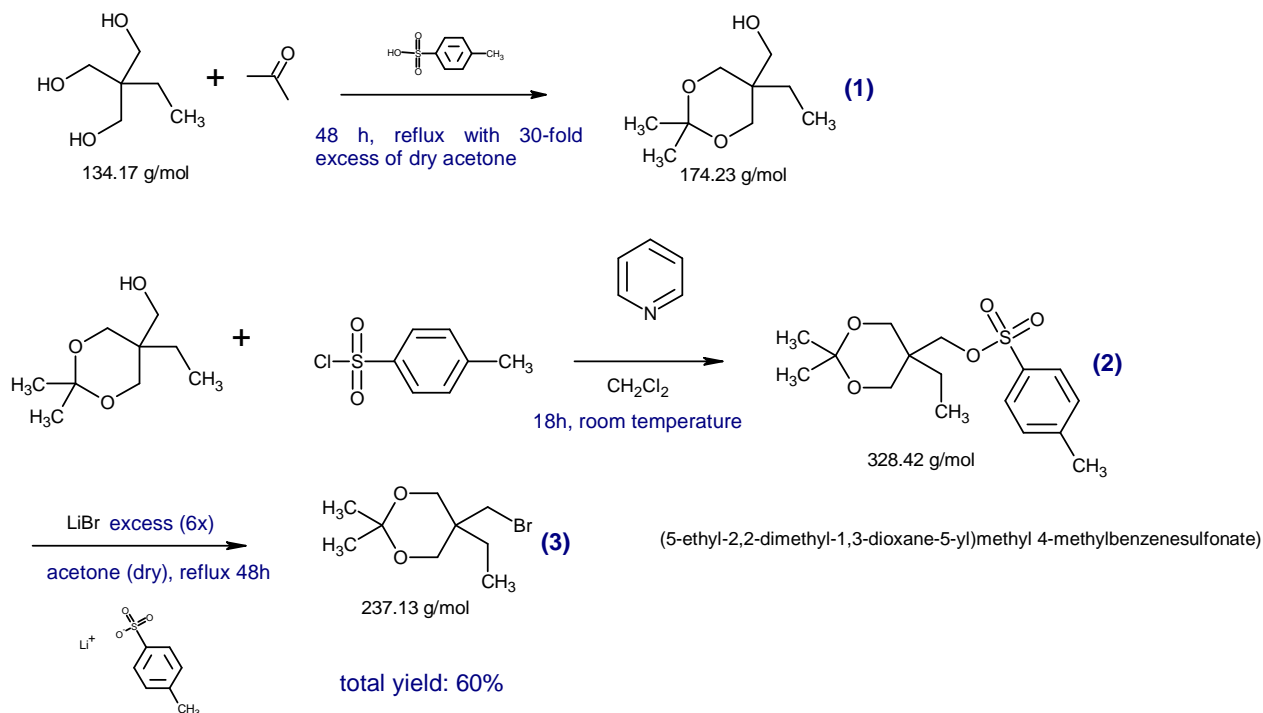
Tris(4-hydroxyphenyl)ethane should be exchangeable with an even more elaborate, functional core molecule. The porphyrin motive is highly interesting in terms of the photochemical and redox properties. Especially the combination of targeted drug delivery with photodynamic therapy could be highly promising. Photodynamic therapy is based on the delivery of a photosensitizer to the malignant tissue in which highly reactive singlet oxygen generated by laser photoirradiation causes oxidative destruction of the target tissue. Incorporation of porphyrine in the core of a monomolecular micelle of the composition described above could yield nanoreactors with high potential in polymer based therapeutics.[8] The interesting photochemical characteristic of porphyrine should be retained or even improved since self-quenching should be largely suppressed. The use of porphyrine derivates as initiators in anionic polymer synthesis has not been reported yet. Tetrakis(p-hydroxyphenyl) porphyrin is the porphyrin derivates that is most amenable to further modification due to its free hydroxyl groups.

Scheme 4: Tris(4-hydroxyphenyl)ethane (a) and Tetrakis(p-hydroxyphenyl) porphyrin are interesting precursors (generation 0) for first generation dendritic initiators .
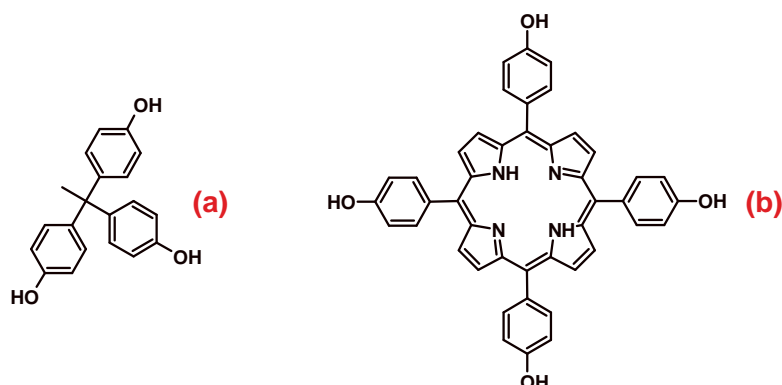
Nevertheless, porphyrine centered star polymers are not unknown. Tetrakis(p-hydroxyphenyl) porphyrin has been "PEGylated" to yield 4-arm stars polymers. These have been prepared by reaction between tetrakis(p-hydroxyphenyl) porphyrin and chlorinated poly(ethylene glycol) methyl ethers.[9] In a straight forward approach, Penfold and coworkers used ATRP of MMA or styrene from a modified porphyrin to increase the porphyrins solubility and dispersibility in polymer thin films.[10] Thermoresponsive stars with LCST behavior were obtained by RAFT of N,N-diethylacrylamide.[11] We want to transform tris(4-hydroxyphenyl)ethane (Scheme 3, a) and tetrakis(p-hydroxyphenyl) porphyrin (Scheme 3, b) into highly efficient initiators for the ROP of epoxides using the dioxane derivative (3), as depicted in Scheme 2. The synthesis of the multi-functional initiator was achieved by the efficient Williamson coupling between tris(4-hydroxyphenyl)ethane and 5-bromomethyl-5-ethyl-2,2-dimethyl-dioxane in analogy to the *"dendrimac"* synthesis recently described by Hutchings et al. (Scheme 4).[12,13] This reaction is most efficient if cesium carbonate is used in combination with highly polar DMF or DMAc as reaction medium.

Potassium carbonate may also be used in combination with chelating 18-crown-6 to guarantee sufficient nucleophilicity of the phenolate. Hence, no significant exess of the alkylbromide was necessary to obtain fully dendronized (4) after 48-72 h at 60°C. Integration of the ^{1}H NMR spectrum in Figure 6 reveals the proper stochiometry between tris(4-hydroxyphenyl)ethane and dioxane related signals.

Scheme 4: Synthesis of the multi-functional initiator via Williamson coupling and acetal hydrolysis.
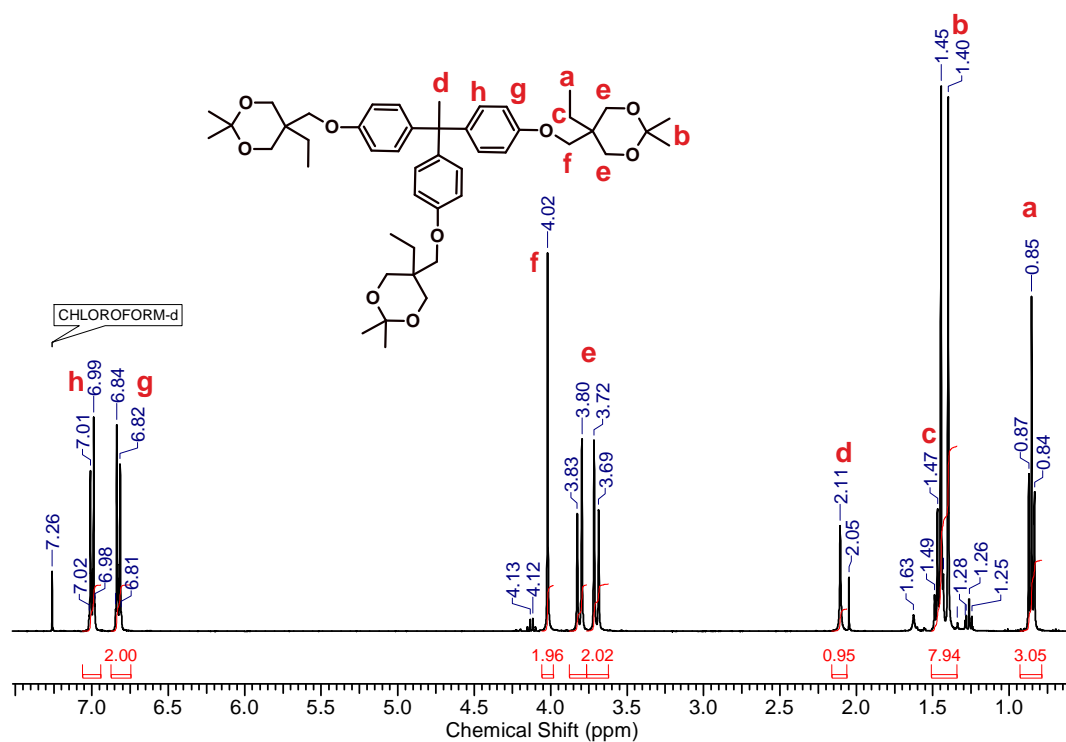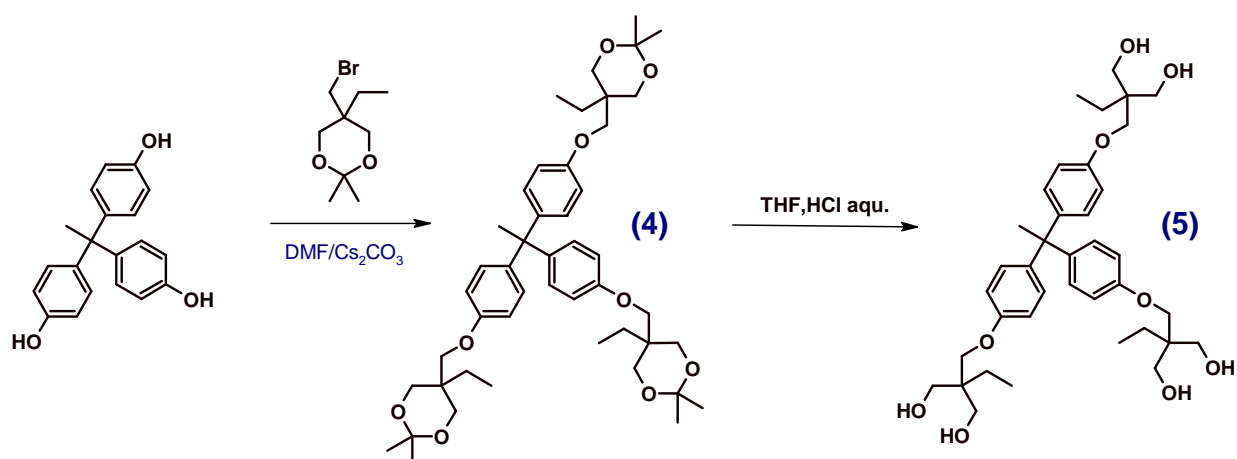
Figure 6: ^{1}H NMR of the initiator precursor.

The acid catalyzed cleavage of the acetal protecting group of (4) proceeded quantitatively and (5) could be used directly after removal of solvent and HCl in vacuum.
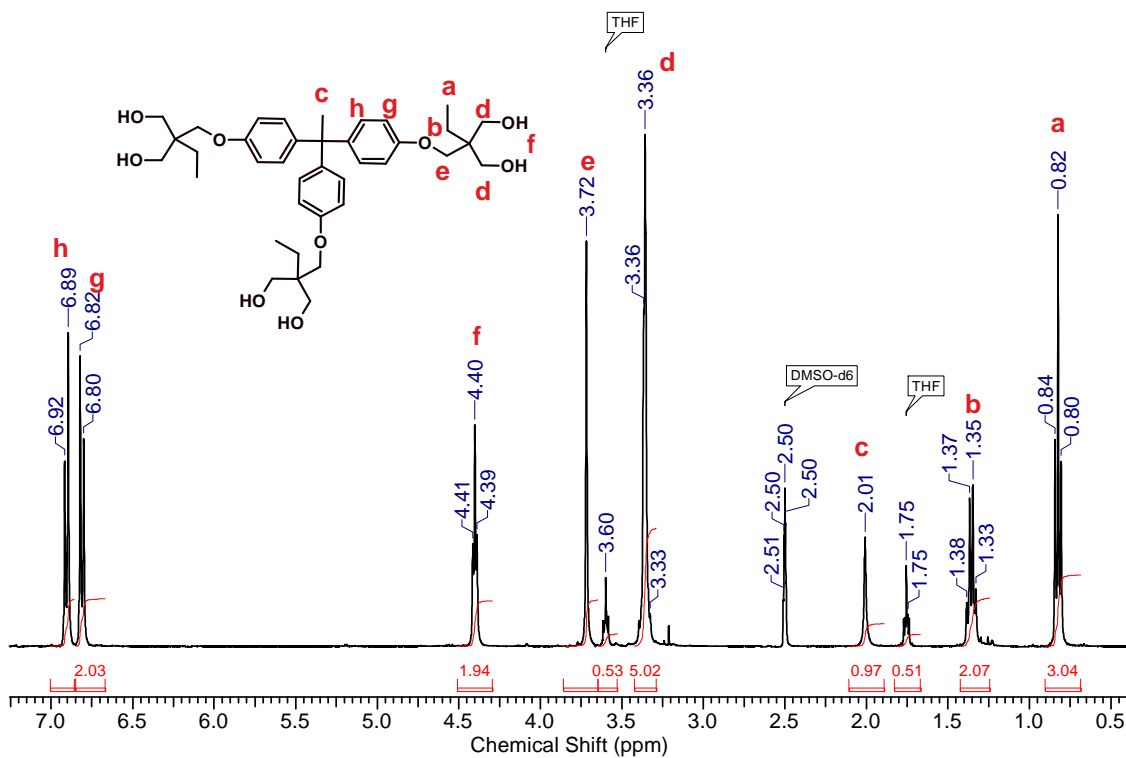
Figure 6: ^{1}H NMR of the hexafunctional initiator.

Scheme 5: Synthesis of the multi-functional initiator via Williamson coupling and acetal hydrolysis from 4-hydroxyphenyl-porphyrin.
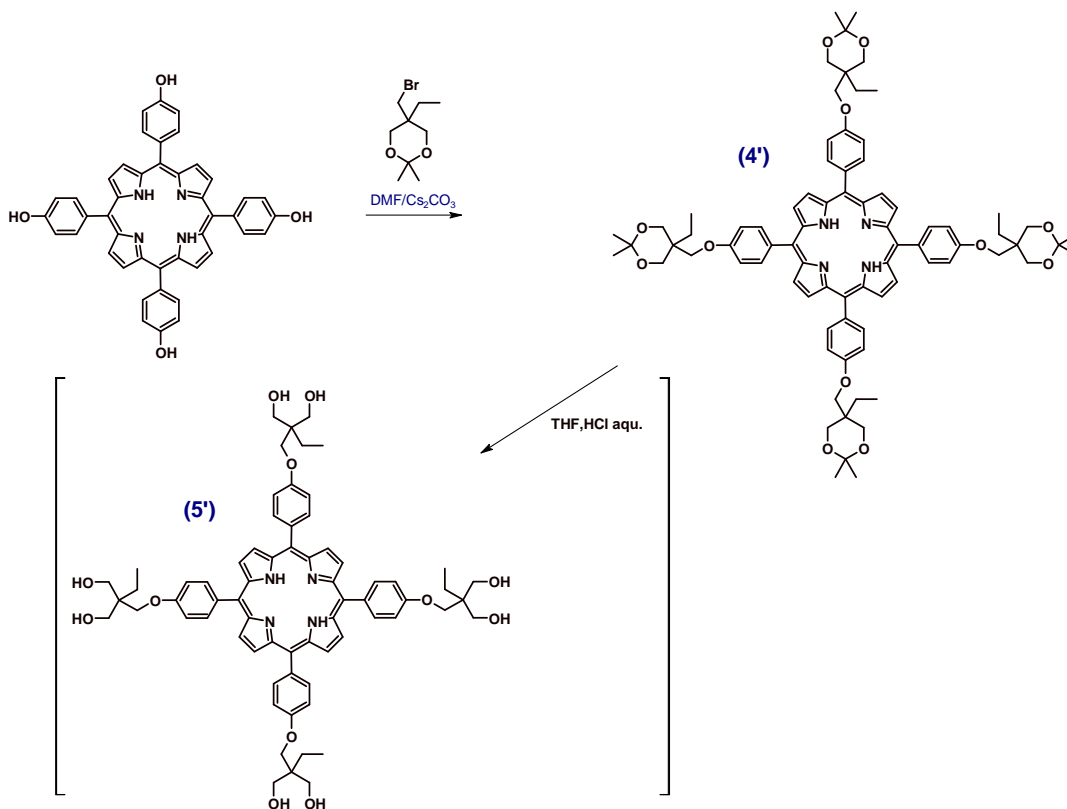
A transfer of these reaction conditions to 4-hydroxyphenyl-porphyrin was initially unsuccessful and only trace amounts of fully-functionalized porphyrin could be obtained (Scheme 5). However, an increase of the reaction temperature to 125°C in combination with an excess (two fold) of the alkyl bromide yielded the desired product in 32% yield. Excess dioxane acetal (3) was removed via column chromatography. Yet, the formation of partially functionalized porphyrins was not observed. We hence assume a cooperative effect in the form of enhancement of reactivity with increasing degree of substitution for the Williamson coupling.

The success of the etherification could be readily monitored via NMR (Figure 8) and SEC. In Figure 7, the shift of the elution volume and a PDI of 1.02 are indicative for a successful dendronization.
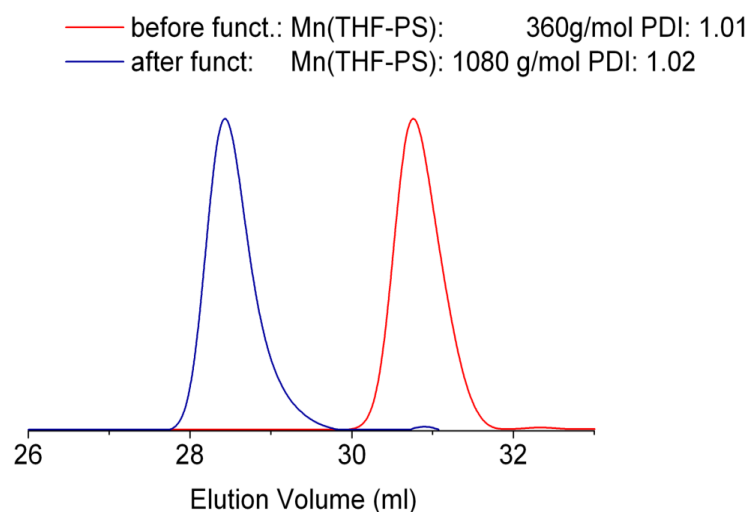
Figure 7: SEC (RI, DMF) traces of the porphyrin phenol precursor and the completely functionalized **4'**.

Deprotection of the porphyrine derivative was problematic. Upon contact with an acidic environment, the protonated version of the Porph-G1 dendron (4') was formed instantaneously (color change from deep purple to green). It exhibited a very poor solubility in all tested solvents (DMF, ethanol, water, THF, and mixtures of these). Nevertheless, the educt could be partially recovered by treatment with triethylamine and separation of the phases between ether and water. However, a facilitated oxidation in this environment cannot be precluded.

293
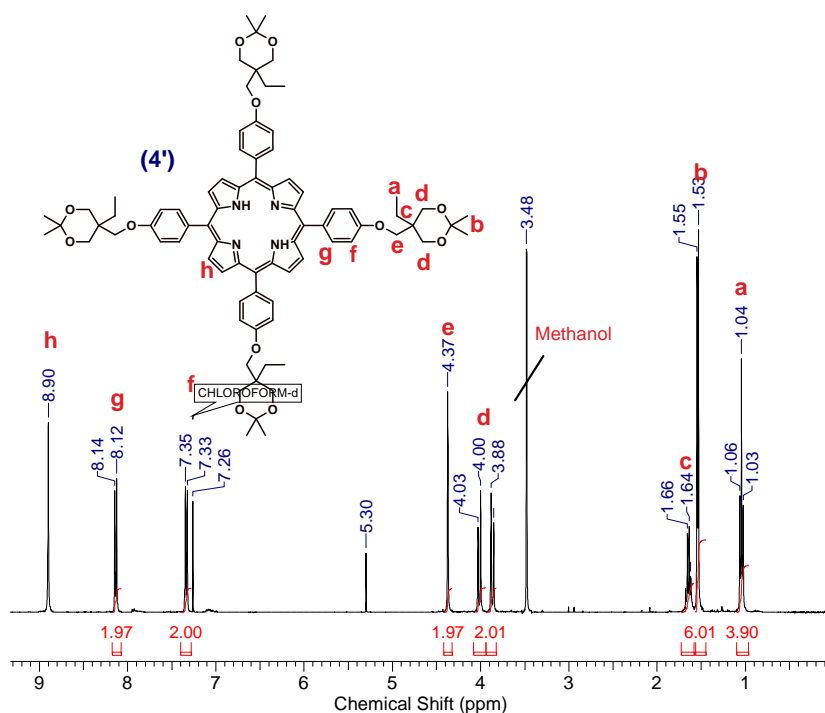
Figure 8: ^{1}H-NMR of the porphyrin initiator precursor.

Synthesis of Mulitarm Star Block Copolymers

Until now, first studies have been conducted concerning the ROP of EEGE and EO, initiated by the above presented G1-dendron.

Scheme 6: First step in the synthesis of multiarm star block copolymers: Deprotonation and polymerization of epoxides.
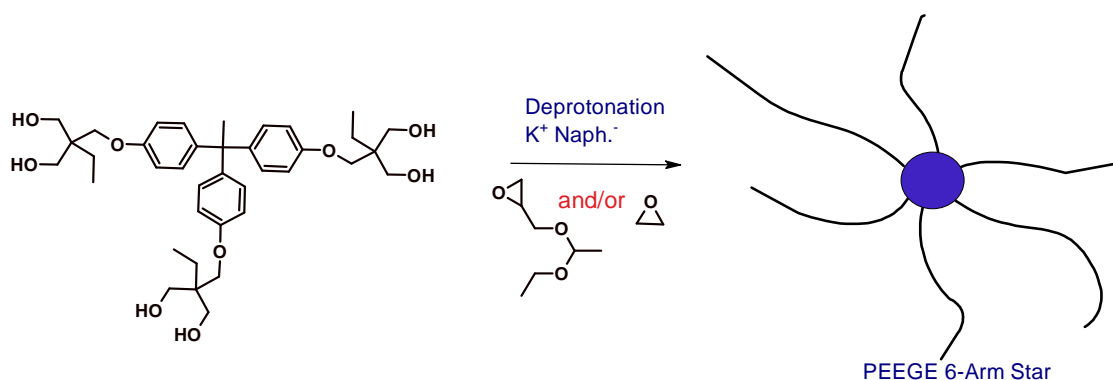
Deprotonation of the initiator with potassium naphtalide helped to suppress co-initiation from other alkoxides like potassium methylate which have also been used as deprotonating agents. Generally, the presence of the aromatic triphenyl-methyl systems significantly

facilitated the analysis of initiator incorporation. Comparative evaluation of UV and RI derived traces in SEC measurements allowed a molecular weight dependent estimation of initiator incorporation. SEC traces of the initial attempts to realize EEGE or EO homo star polymers from the multi-functional initiator are shown in Figure 9.
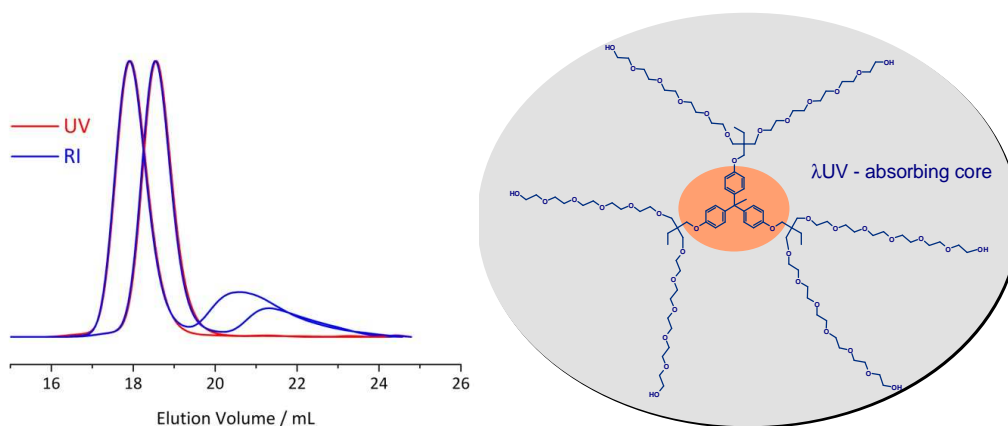
Figure 9: SEC traces (left) and scheme (right) of PEO star polymers with different intiator/monomer ratios.

While RI traces (blue) show a bimodal distribution, UV-detection, which is primarily sensitive to the aromatic system of the multi-functional initiator, exhibits a monomodal shape. Hence, the bimodal character has to be related to mono- or bifunctional impurities, capable of co-initiation like alcohols or water. These show no significant UV absorption and would explain the lower molecular weight, compared to the 6-arm star. Evaluation of the UV traces with PEG standards gave PDIs below 1.05. The problem of co-initiation was addressed by a more careful drying procedure of the initiator by repetitive addition and evaporation of toluene and the avoidance of metal alkoxides as deprotonating agents. Potassium naphthalide, which cannot initiate polymerization itself, was used instead. Figure 10 shows a good correspondence between UV and RI related trace detection and only a minor second mode for the latter, indicating the success of the applied measures.
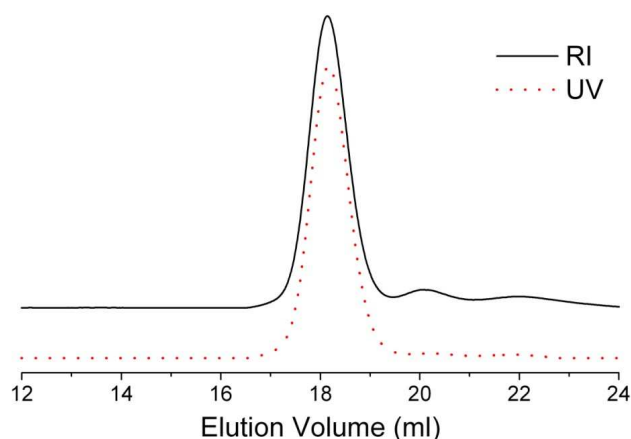
Figure 10: SEC- traces of $(PEEGE_{25})_6$-star polymer: Underestimation of molecular weight compared to ^{1}H NMR (M_n = 11400 g/mol, PDI: 1.04; DMF_{UV}, PEG-standard).

The evaluation of the initiator incorporation and even the average chain length via NMR is possible by integration of the aromatic proton signals between 6.70 and 6.92 ppm ($CDCl_3$) (Figure 11). The observed 155 total units correspond well to the targeted value of 25 repeating units/arm. Nevertheless, this would also mean a significant underestimation of molecular weight compared to the evaluation via SEC with PEG-standards due to the more compact nature of the star polymer. However, the degrees of deprotonation examined so far correspond to only 20 % of the OH groups. Compared to the linear block copolymers, the targeted EEGE arm length/OH group was increased from 5 to 25. This could explain a lower conversion of EEGE under similar reaction conditions. The amount of residual EEGE monomer for the sample presented above was as low as 1 %.

Future work will tie up at this point. Especially the block copolymer synthesis of star polymers will be addressed. ATRP of water solubility mediating methacrylates is a central issue. The selective conjugation of drugs to the polyfunctional core should be examined. Regarding the synthesis of the porphyrine based initiator the exchange of the acetonide protecting group with a p-methoxy benzylacetal could allow access to an alternative deprotection pathway via hydrogenation.
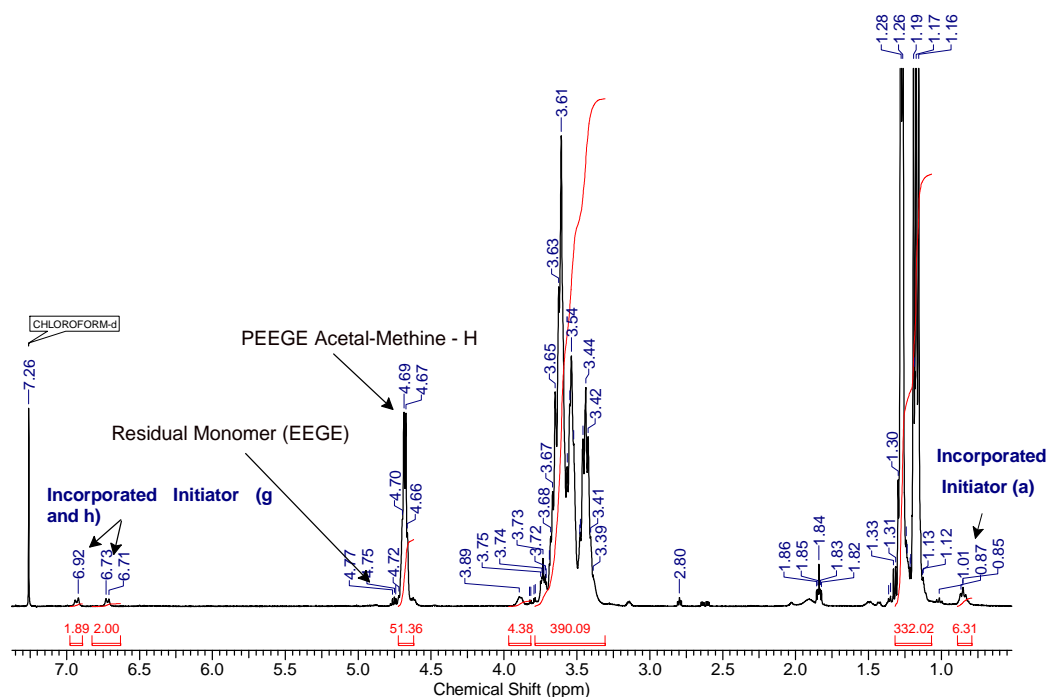
Figure 11: ^{1}H-NMR of a (PEEGE$_{25}$)$_6$-star polymer.

Additional Experimental Procedures

1) 5-Hydroxyethyl-5-ethyl-2,2-dimethyldioxane (1)

(Rec. literature: Ouchi, M.; Inoue, Y.; Wada, K.; Iketani, S.; Hakushi, T.; Weber, E. *J. Org. Chem.* 1987,52, 2420-2427)

2-(Hydroxymethyl)-2-methyl-1,3-propanediol (200 g, 1.5 mol) and p-toluenesulfonic acid (200 mg) were dissolved in acetone (2 L, previously dried by stirring and subsequent distillation over P$_2$O$_5$), and the mixture was stirred for 2 days at room temperature. The solution was neutralized by adding 5 g of K$_2$CO$_3$, filtrated, and evaporated to give the crude product which was further purified by distillation in vacuum; b.p. 75°C (0.3 mbar) (256 g, 96%): NMR (400 MHz, CDCl$_3$) δ^1H/ppm: CH$_2$C*H$_3$* 0.84 (t, *J*=7.63 Hz, 3 H); C*H$_2$*CH$_3$ 1.30 (q, *J*=7.63 Hz, 2 H); CC*H$_3$* 1.39 (s, 3 H); CC*H$_3$* 1.42 (s, 3 H); CH$_2$O*H* 1.81 (t, *J*=5.58 Hz); C*H$_2$*O 3.66 (d, *J*=4.89 Hz, 2 H); C*H$_2$*O 3.75 (d, *J*=5.48 Hz, 2 H) **IR** λ(cm^{-1}) 3420, 2964, 2865, 1453, 1370, 1255, 1200, 1153, 1044,829, 520.

NMR spectrum with peaks labeled:
- M07(m), M06(d), M08(d): 3.75, 3.74, 3.67, 3.65, 3.62 (integration 4.05)
- M05(t): 1.83, 1.82, 1.80, 1.72 (integration 0.19)
- M03(s), M04(s): 1.42, 1.39, 1.31, 1.29, 1.27 (integration 3.02, 2.10)
- M01(t): 0.86, 0.84, 0.82 (integration 3.00)

Chemical Shift (ppm)
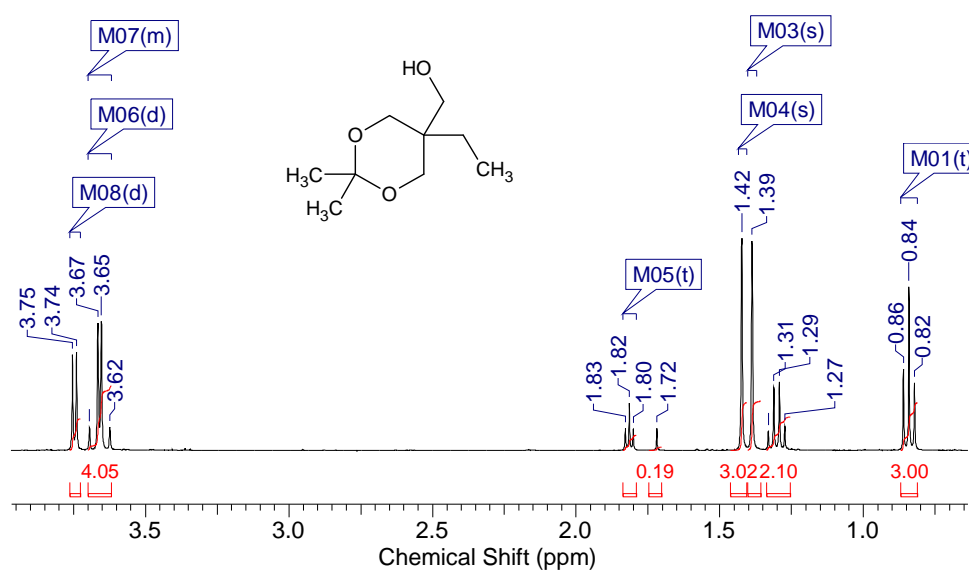
2,2-Dimethyl-5-ethyl-5-methyltosyl-1,3-dioxane (2)

(Rec. Literature: *Chem. Commun.*, 1998, 2341–2342)

120 g 5-hydroxyethyl-5-ethyl-2,2-dimethyldioxane were dissolved in 1 L of dry dichloromethane. After adding 100 ml of dry pyridine, the solution was cooled to 0°C and 0.756 mol (144.13 g) of pTSA-Cl, dissolved in 500 ml of dry dichloromethane, were added via a dropping funnel within 2 hours. The solution was slowly allowed to warm to room temperature and stirred over night. Conversion was validated by thin layer chromatography (hexanes/EtAc 1:1). In case of completion of the reaction, the solvent was reduced to 10% of the original amount and the precipitating salt was removed by filtration. The filter cake was washed with 100 ml of hexanes and the filtrate was concentrated with a rotary evaporator. A small aliquot of the crude product was purified by filtration over a short silica column for characterization. The residue can be used in the next step without further purification. However, purification is possible via (re-)crystallization of the product from THF(1)/diethylether(5)/hexanes(5) in the fridge.

5-Bromomehtyl-5-ethyl-2,2-dimethyl-dioxane (3)

(Rec. Literature: Veeravagu, P.; Arnold, R. T.; Eigenmann E. W. *J. Am Chem Soc.* **1964**, *86*, 3072-3075)

115 g (1,3 mol) of lithium bromide were added to a solution of 0.6 mol of (2) in dry acetone and refluxed for 48 hours. Finally, the solution was concentrated to approx. 150 ml and poured into 500 ml of water. The product was extracted with 3x100 ml of diethylether and subsequently washed with 2x50 ml brine. The organic phase was then dried over $MgSO_4/K_2CO_3$ (10/1) and evaporated after filtration. The product was obtained as colorless oil after distillation in vacuum (0.5 mbar/ bp. 45-47 °C). Yield: 59 g/73%. ^{1}H NMR (400 MHz, $CDCl_3$) δ/ppm: CH_2CH_3 0.83 (t, *J*=7.63 Hz, 3 H); CH_2CH_3 1.36 (q, *J*=7.04 Hz, 2 H) ; CCH_3 1.40 (s, 3 H); CCH_3 1,42 (s, 3 H); CH_2Br 3.66 (s, 2 H); CH_2O 3.71 (s, 4 H). ^{13}C NMR (100 MHz, $CDCl_3$) δ/ppm: CH_2CH_3 6.46; CCH_3 19.96; CCH_2CH_3 24.66; CCH_3 27.20; CCH_2CH_3 36.28; CCH_2Br 37.25; CH_2O 66.00; $C(CH_3)_2$ 98.37) **IR** λ (cm^{-1}) 2966, 2865, 1451, 1371, 1244, 1203, 1104, 1048, 970, 930, 828, 655, 521.
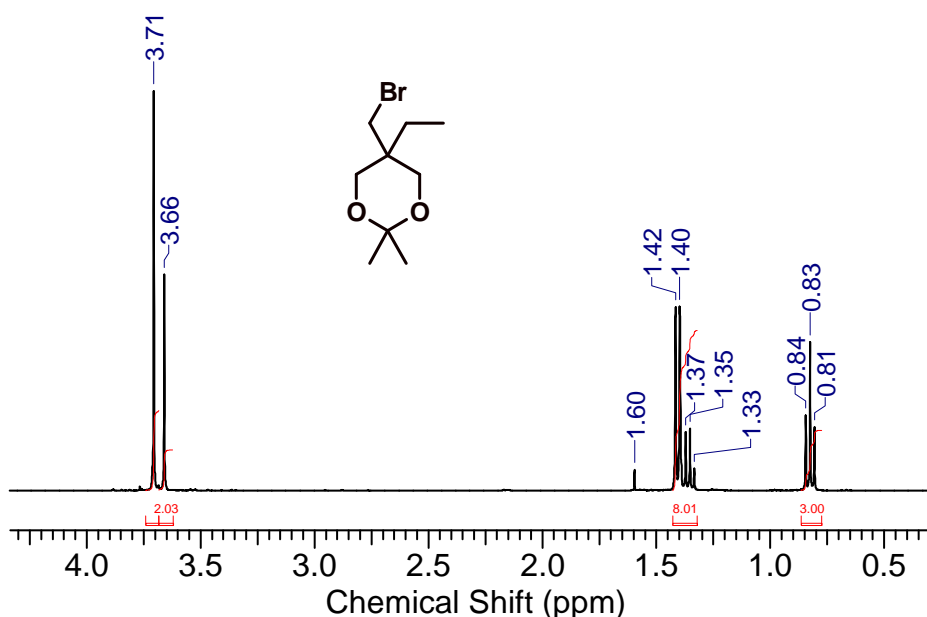
[1]H spectrum (400 MHz, $CDCl_3$)
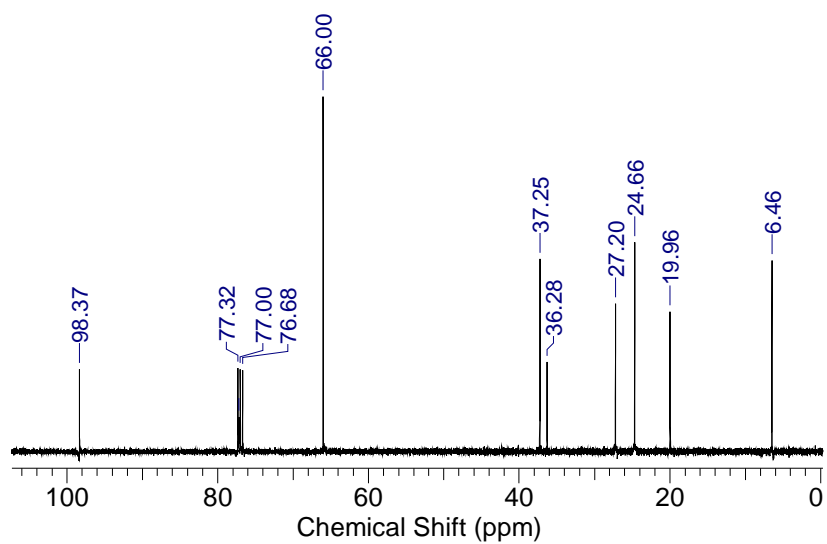
^{13}C NMR spectrum (100 MHz, CDCl$_3$)
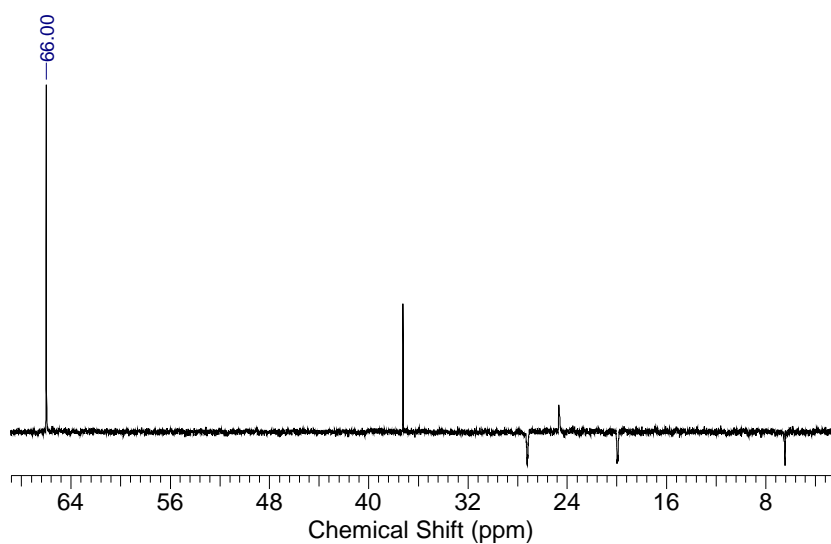
^{13}C DEPT spectrum (100 MHz, CDCl$_3$)

References

[1] Fitton, A. O.; Hill, J.; Jane, D. E.; Millar, R. *Synthesis* **1987**, 1140.

[2] Taton, D.; Le Borgne, A.; Sepulchre, M.; Spassky, N*. Macromol. Chem. Phys.* **1994** 195, *139-148.*

[3] Mangold, C.; Wurm, F.; Obermeier, B.; Frey, H. *Macromol. Rapid Comm.* **2010**, *31*, 258-264.

[4] Keul, H.; Möller, M. *J. Polym. Sci. A: Polym. Chem.* **2009**, *47*, 3209–3231.

[5] Lapienis, G. *Progress in Polymer Science* **2009**, *34,* 852–892.

[6] Wolf, F. K.; Hofmann, A. H., Frey, H *Macromolecules* **2010**, *43*, 3314-3324.

[7] Six, J.L., Gnanou, Y. Macromolecular Symposia **1995**, *95*, 137-150.

[8] Dai, X.-H.; Dong, C.-M.; Fa, H.-B.; Yan, D.; Wei, Y. *Biomacromolecules* **2006,** *7*, 3527-3533.

[9] Mineo, P.; Scamporrino, E.; Vitalini, D. *Macromol. Rapid Commun.* **2002**, *23*, 681–687.

[10] High, L .R. H.; Holder, S. J.; Penfold, H. V. *Macromolecules* **2007,** *40,* 7157-7165.

[11] YUSA, S. I.; Endo, T.; Ito, M. *Journal of Polymer Science: Part A: Polymer Chemistry* **2009**, 47, 6827–6838.

[12] Hutchings, L. R.; Roberts-Blemings, S. J. *Macromolecules* **2006**, *39*, 2152.

[13] Kimani, S. M.; Hutchings, L. R. *Macromol. Rapid Commun.* **2008**, *29*, 633–637.

4.3 Vinyloxyethylmethacrylate: A Precursor to Covalent, Acid Labile Polymer Conjugates?

Florian K. Wolf and Holger Frey

Since the outline of the general concept of drug polymer conjugates by H. Ringsdorf almost 30 years ago,[1] excellent work on its realization has been conducted by R. Duncan and many other researchers. Especially polymer-protein (e.g. PEGylated α-interferons, SMANCS) and polymer-cancer drug congjugates (various compounds are in clinicial trials) are in the focus of interest. The covalent conjugation to specially designed polymers shall facilitate the drugs transport to tumour cells and away from sites of toxicity, and/or to maintain drugs at a therapeutic concentration over long periods of time.[2]

Their accumulation in tumor tissue is additionally supported by the EPR-(enhanced permeation and retention) effect.[3] The water-soluble polymer backbone thus acts as a molecular shuttle with covalently attached active agents and optional targeting vectors. The conjugation helps to overcome drug resistance and eventually a poor watersolublity of a hydrophobic drug. To achieve a high drug loading, multiple conjugations per polymer chain are desirable. In order to be pharmaceutically active, the drug/polymer link has to be selectively cleavable at the desired site of action. The two most common release pathways are enzymatic or acid catalyzed hydrolysis. Especially the latter is attractive and has been realized in the form of trityl, hydrazone, acetal and imino groups.

The concept of polymerization of a drug carrying monomer is particularly attractive for methacrylates, since they can be readily functionalized. In addition, a plethora of functional groups is tolerant towards radical polymerization which is thus the method of choice for the polymerization of the drug conjugated monomer. Our target is to synthesize and explore a universal methacrylate synthon which can be used to flexibly bind active agents, markers or targeting vectors via an acid sensitive acetal group to the polymer backbone. Our strategy is

302

hence based on the facile acetal formation beween a vinyl ether and a primary hydroxyl group. This reaction has already been exploited in the formation of Ethoxy Ethyl Gylcidyl Ether (EEGE) (Scheme 1, (1)). An epoxide monomer which allows for the construction of linear poly(glycerol) via anionic polymerization and acid catalyzed acetal cleavage.

Scheme 1: Formation of formyl-acetals via vinyl ethers and primary alcohols and the exploitation in monomer design and synthesis.
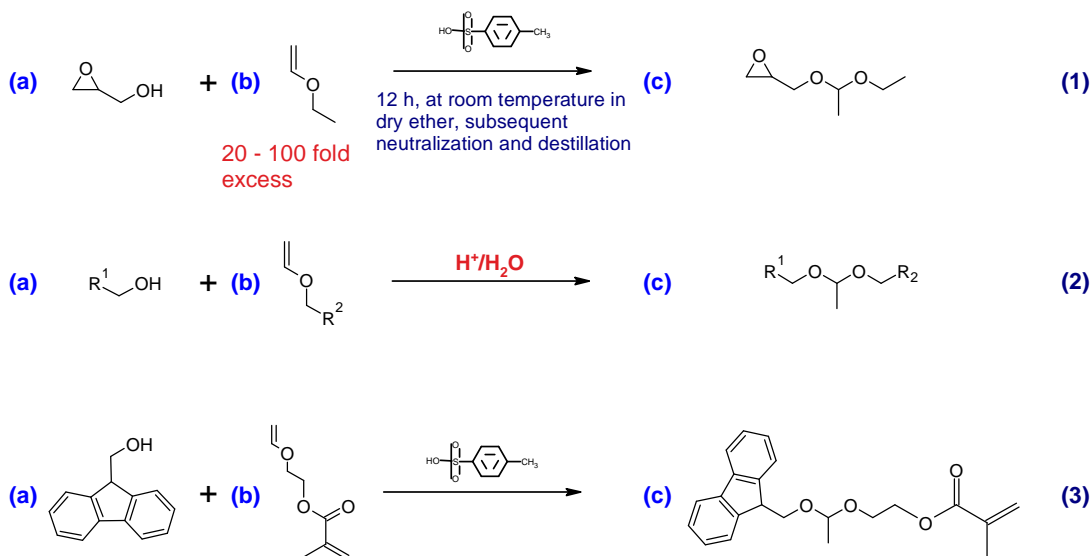
This example prompted us to examine the general conjugation between an active agent (R^1/and a monomer R^2; via a formyl-acetal as depicted in Sheme 1 (2). Hence, a vinyl ether carrying (methacrylate) monomer was required. Almost 10 years ago, Ruckenstein et al. introduced vinyloxyethyl methacrylate (VEMA) to generate a vinyloxy-functional polymethacrylate. Back then, the vinyl group served as protecting moiety for the hydroxyl group of HEMA (2-hydroxy ethylmethacrylate) which was later released.[4] VEMA is available via a facile synthesis based on 2-chlorovinylether and sodium methacrylate which rendered it highly attractive for our purposes. An even more striking argument for its use is the release of the biocompatible poly(HEMA) motive after polymerization and acetal cleavage (Scheme 2).
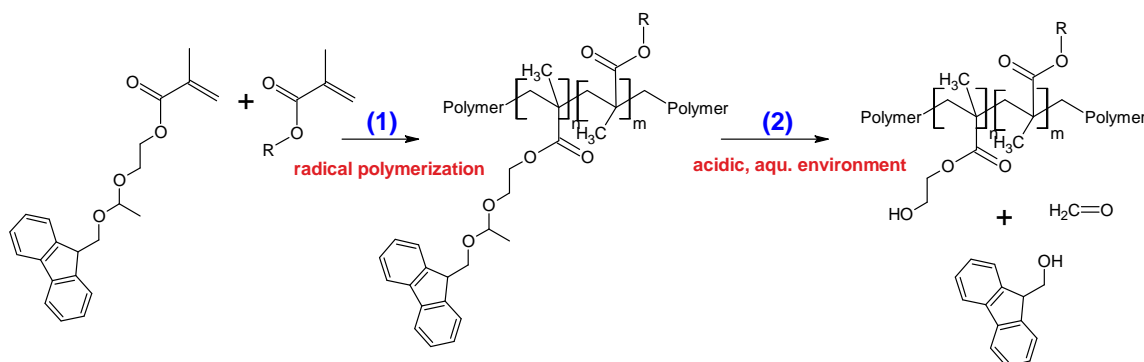
Until now, we succeeded in the synthesis of a suitable acetal model compound. In a first experiment we successfully "clicked" 2-fluorenemethanol to the vinyl ether group of VEMA (1:1 molar ratio, p-TSA catalysis; Scheme 1 (3)). Fluorenemethanol was the model payload of choice because it facilitates to trace the fate of monomer and acetal moiety during synthesis and polymerization. Although the formation of biproducts could be observed, product could be isolated in sufficient purity by automated column chromatography (gradient: hexanes/ethyl acetate) in 28 % yield (Figure 1).
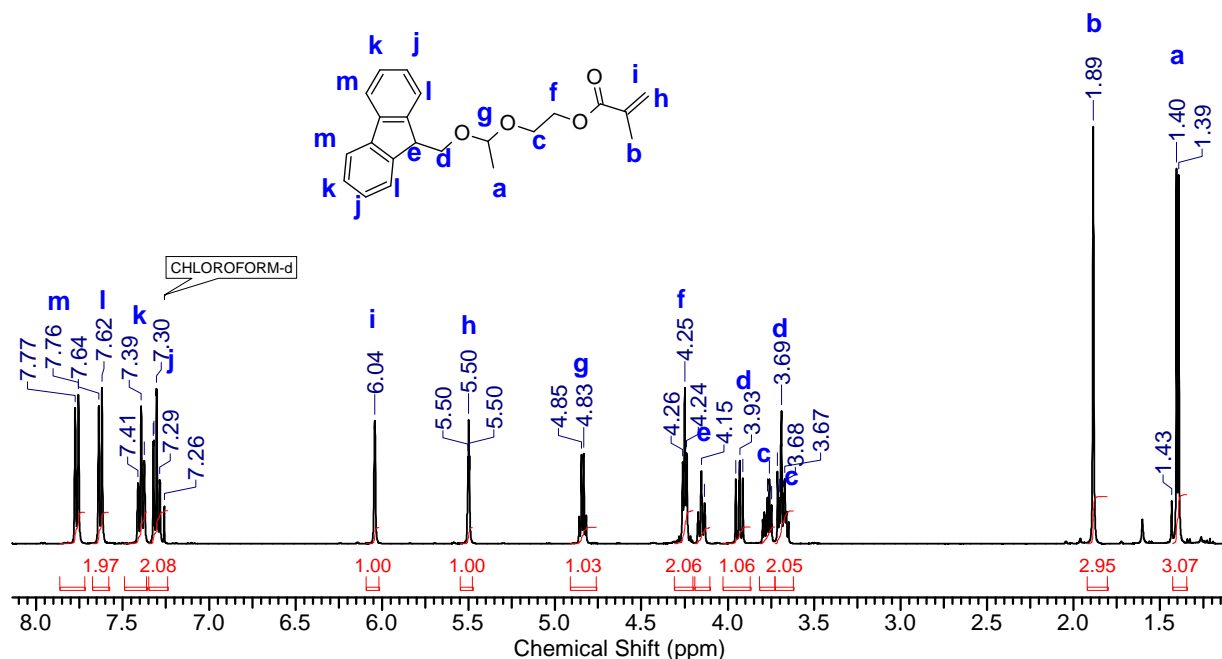
Figure 1: ^{1}H NMR of formyl-acetal bridged fluorenemethanol-hydroxyethyl methacrylate: 2-[1-(9*H*-fluoren-9-ylmethoxy)ethoxy]ethyl methacrylate

As a byproduct, the di(fluorenemethanol) could be isolated and identified (Figure 2). Consequentially, the formation of bis HEMA formyl-acetal and the corresponding hemi-

acetals is expected. The formation of these biproducts most likely could have been prevented by an excess of the vinyl compound (in analogy to the EEGE synthesis) [5] and/or the *in situ* removal of water by e.g. molecular sieves. However 50% of the amount of acetal formed can be related to the product by an evaluation of an ^{1}H NMR of the raw mixture as depicted in Figure 3 (comparison of the integral at 1.39 ppm (dublett of **a**) with the general acetal methine (**g**) at 4.83 ppm).
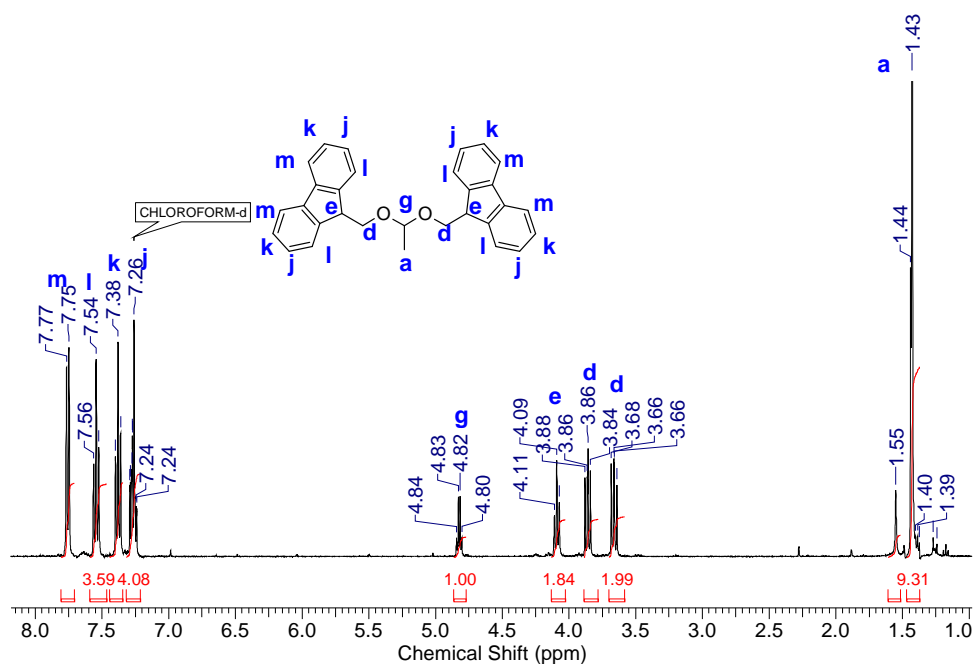
Figure 2: ^{1}H NMR of the biproduct di(fluorenemethanol) formyl-acetal.
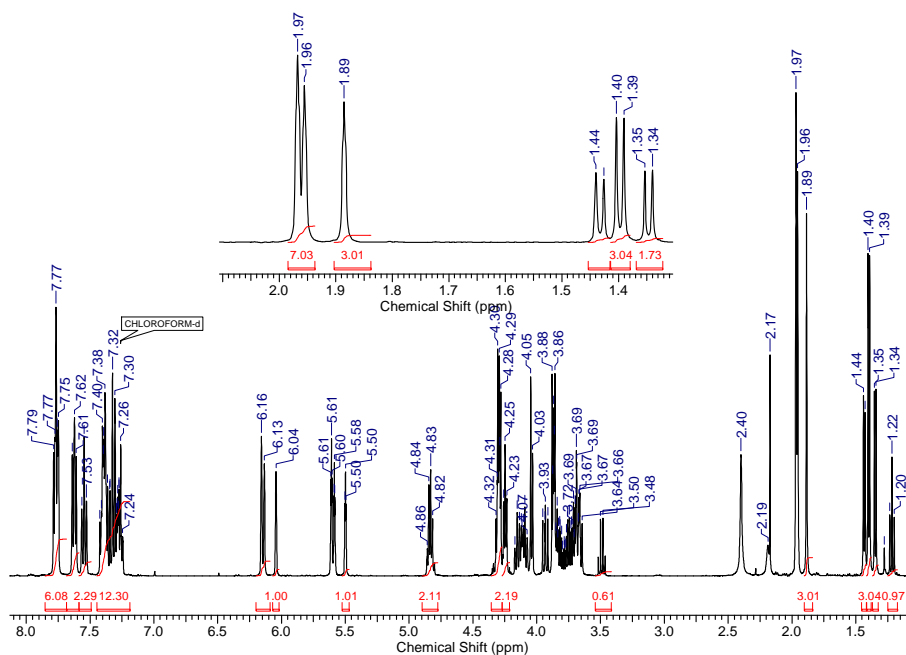
Figure 3: ^{1}H-NMR of the raw reaction mixture.

Future Work:

In general, monomer synthesis should be optimized with regard to the acetal formation step to avoid purification by column chromatographie. Apart from the points stated above, the universality of the alcohol compound in the coupling step should be examined. It would be highly interesting to analyze the differences with regard to the priority of the hydroxyl group. After successful (co-) polymerization, the release kinetics should be examined in dependence of the pH and temperature with a primary focus on physiological relevant conditions.

References

[1] Ringsdorf, H. *J. Polymer Sci. Polymer Symp.* **1975***, 51, 135–153.

[2] Duncan, R. *Nature Reviews Cancer* **2006,** *6*, 688-701.

[3] Matsumura, Y.; Maeda, H. *Cancer Res.* **1986**, *6*, 6387–6392.

[4] Ruckenstein, E.; Zhang, H. *Polymer Bulletin* **2001***, 47*, 113–119.

[5] Fitton, A. O.; Hill, J.; Jane, D. E.; Millar, R. *Synthesis* **1987**, 1140.

4.4 Oligo(glycerol methacrylate)

Florian K. Wolf, Anja Thomas and Holger Frey

Graft copolymers containing oligo- and poly(ethylene oxide) (OEO and PEO) as side chains attached to the backbone have attracted significant interest because of their unique properties. They have expanded a class of materials important for material science and biomedicine. In particular, they are interesting for applications in nanotechnology (nanosized structures), lithium battery preparation (ionic conductivity), elastomer fabrication (viscoelasticity), drug delivery systems (biocompatible carriers) and biomedical implants (coating materials).[1] Many of these systems with 2 to 10 EO units exhibit an interesting LCST behavior which can be fine tuned in a physiologically relevant temperature range between 20 and 60°C.[2]

Scheme 1: Classification of the new hydrophilic POGMA.
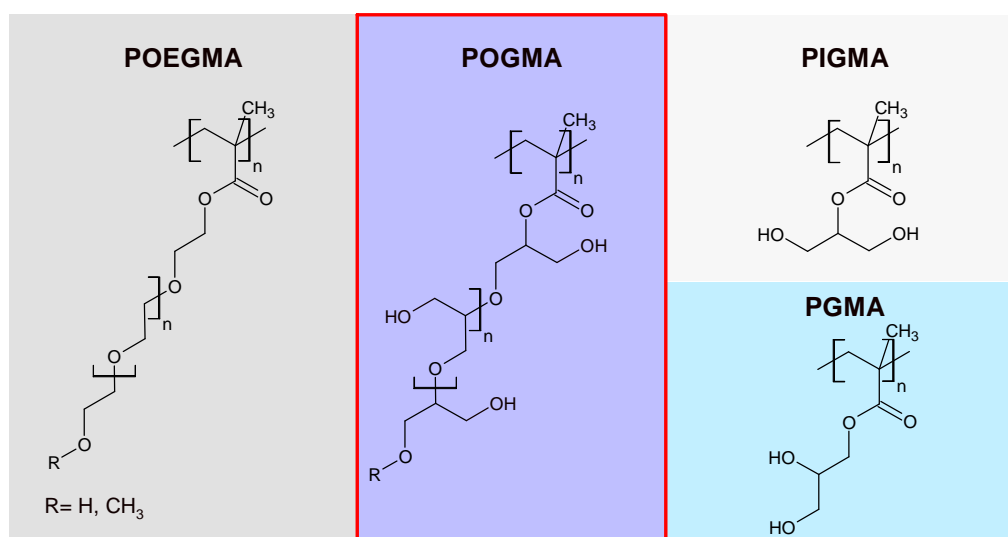
Poly(methacrylate)s represent the most important type of OEO and PEO side chain carrying backbone materials. They first appeared in the 1980s and have even gained industrial significance since then.[3,4] However, controlled radical polymerization of OEGMA

has not been described until 1999 (group of S. P. Armes).[5,6] Well-defined molecular brush polymers are thus accessible via a "grafting through" process.

The hydrophilic PEG chains render POEGMA based polymers highly interesting for biomedical applications. The high degree of hydration in water is the basis for good antifouling properties.[7,8] However, POEGMA offers a maximum of one functional group per side chain. The LCST behavior, which is observed for short chain length, furthermore illustrates that the hydrophilicity could be further enhanced. This is particularly attractive if the brush density shall be reduced by copolymerization with hydrophobic standard or specialty monomers. The latter might be loaded with an active agent and could thus represent monomer conjugates with drugs, proteins, targeting vectors, labeling dyes, photochromes, etc..

Scheme 2: Synthesis of POGMA: Oligomerization of EEGE with subsequent end-capping with a methacryloyl derivative. The polymerization and deprotection sequence should be commutable.
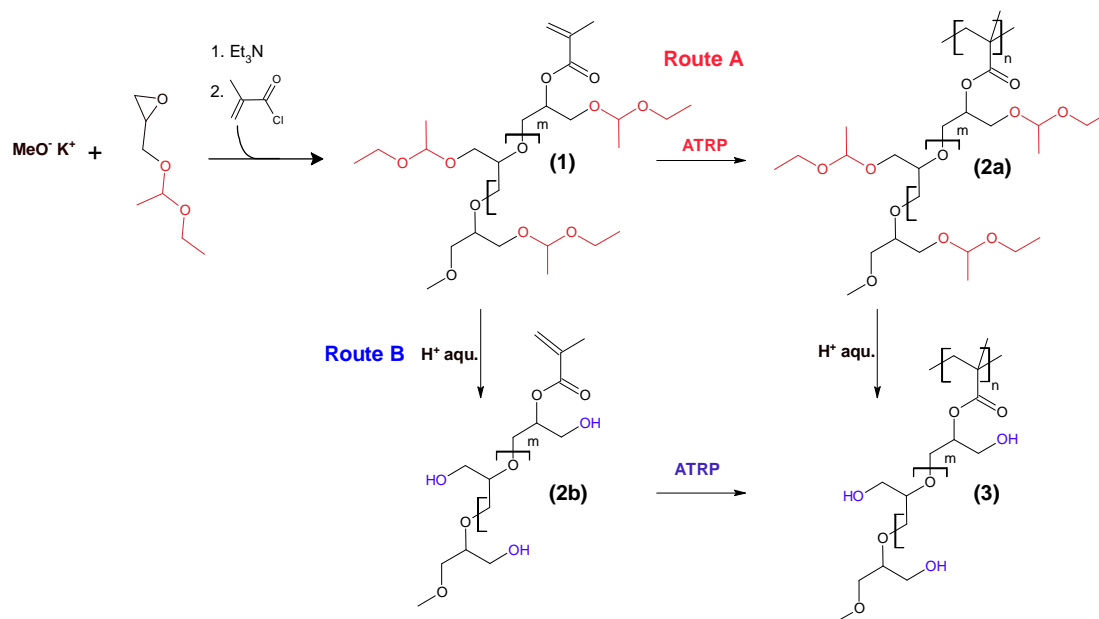
Our strategy to overcome these shortcomings is the variation of the PEG - polymer brush structure. Apart from PEG, linear (and hyperbranched) poly(glycerol)s have attracted increasing attention which can be attributed to a good biocompatibility and an additional hydroxyl group along the polymer backbone.[9,10] This prompted us to investigate the synthesis and polymerization of linear oligo- and poly(glycerol) methacrylate macromonomers and their protected equivalents. The first results shall be briefly described in the following.

The straightforward synthesis is based on the oligomerization of EEGE (ethoxy ethyl glycidyl ether) via anionic ring-opening from e.g. potassium methanolate (Scheme 2). After quantitative conversion, the terminal unit is esterified with methacrylic acid chloride or anhydride in the presence of triethylamine. Reaction for 12-24 h hours yields the completely functionalized Oligo(EEGE)methacrylate (OEEGMA) macromomers **(1)**.
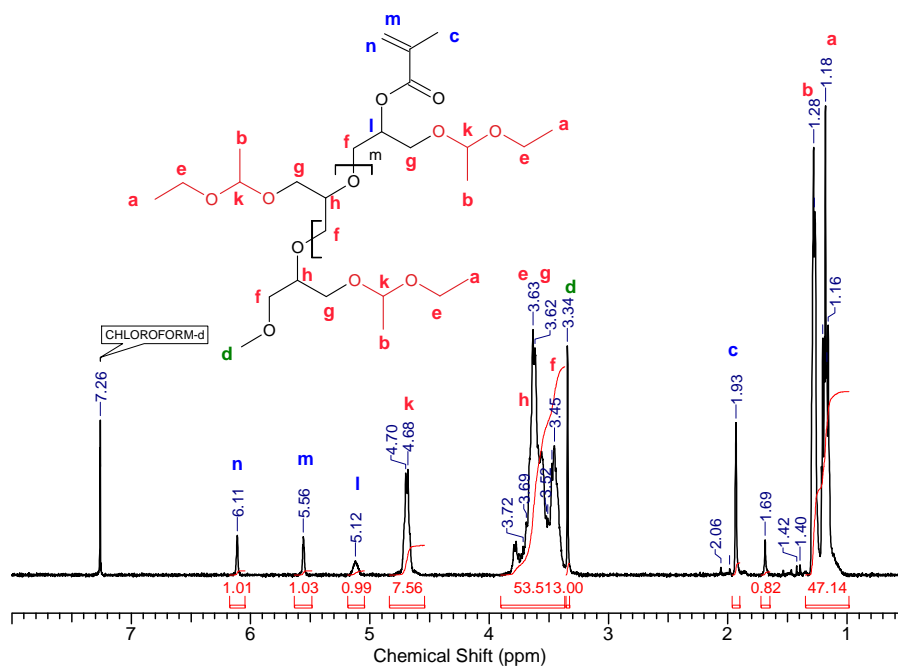

Figure 2: ^{1}H NMR of OEEGEMA$_{7.5}$ illustrates the proper end group stochiometry (c/d/l/m = 3/3/1/1).
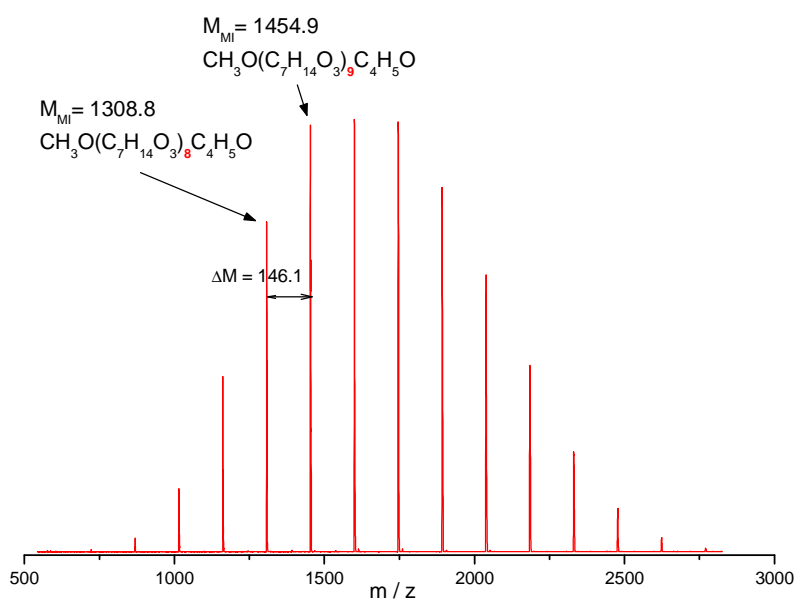
Figure 1: MALDI-ToF spectrum of an O(EEGE)-methacrylate macromonomer: In this mass range, the peak maxima represents the most abundant monoisotopic (MI) species. Quantitative α-methoxy/ω-methacrylate functionalization without the presence of side products is thus confirmed.

The stoichiometric presence of methoxy and acrylate endgroups could be proven by MALDI-ToF and NMR measurements (Figures 1 and 2). The mass increment of the MALDI-ToF spectrum shown in Figure 1 corresponds to the EEGE (146 g/mol) repeat unit. The most abundant peak can be assigned to the species with 10 EEGE units. Purification from reaction side products and excess acid was conducted by extraction with water from an organic solvent and filtration over a short neutral aluminum oxide column (with excellent retention of the residual acrylate salt in EtAc)

OEEGMA: 1.200 g/mol, PDI = 1.05

P(OEEGMA): 7.200 g/mol, PDI = 1.19

Elution Volume (ml)
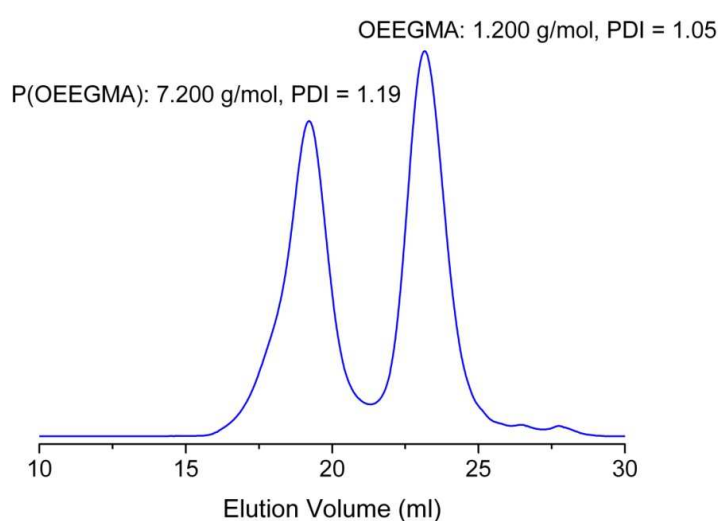
Figure 2: Elugram of an ATRP raw reaction mixture, showing brush-polymer (left) and macromonomer (right) with a conversion of 49% after SEC evaluation.

Future Work:

SEC proved the well-defined nature of the macromonomers and polydispersities below 1.1 were generally obtained. First attempts to polymerize OEEGEMA via ATRP (PMDETA, CuCl in 1-propanol/toluene 1:2) were successful and yielded well-defined (PDI = 1.19) brush polymers **(2a)** (Figure 2). As Scheme 2 points out, polymerization of acetal protected and "free" poly(glycerol) macromoners should be possible. Hence, the flexible use of the macromonomers **1** and **2b** should enhance synthetic versatility and flexibility. Controlled radical polymerization in water of **2b** is highly attractive for the functionalization of proteins via a grafting from approach. Especially polymerization of the readily available OGMA **(2b)** with 5 -15 glycerol units should hence be pursued. Polymerization of OEEGMA **(1)** is particularly interesting for the formation of amphiphilic block copolymers with hydrophobic

building blocks. **(1)** guarantees a more facile preparation and analysis because the amphiphilic character of the block copolymer is not revealed until the final reaction step via acetal cleavage.

References

[1] Neugebauer, D. *Polym. Int.* **2007***, 56*, 1469–1498.

[2] Lutz, J.-F. *J. Polym. Sci. Part A: Polym Chem*. **2008**, 46, 3459–3470

[3] Masson, P.; Beinert, G.; Franta, E.; Rempp, P. *Polym. Bull.* **1982**, *7*, 17–22.

[4] Ito, K.; Tsuchida, H.; Hayashi, A.; Kitano, T.; Yamada, E.; Matsumoto, T. *Polym. J.* **1985**, *17*, 827–839.

[5] Wang, X.-S.; Lascelles, S. F.; Jackson, R. A.; Armes, S. P. *Chem Commun* **1999**, 1817–1818.

[6] Wang, X.-S.; Armes, S. P. *Macromolecules* **2000**, *33*, 6640–6647.

[7] Prime, K. L.; Whitesides, G. M. J Am Chem Soc **1993**, *115*, 10714–10721.

[8] Ma, H. W.; Hyun, J. H.; Stiller, P.; Chilkoti, A. *Adv. Mater*. **2004**, *16*, 338–341.

[9] Keul, H.; Möller, M. *J. Polym. Sci. A. Polym. Chem.* **2009,**

[10] Kainthan, R. K., Brooks D. E. *Biomaterials* **2007**, 28, 4779-4787

4.5 Hydroxy-functional Lactones and Cyclic Carbonates: From Inimers to Water Soluble Poly(ester)s

Florian K. Wolf and Holger Frey

In Chapter 1.1, the preparation and polymerization of a variety of functional lactones and cyclic carbonates have been discussed. Especially their hydroxy-functional representatives are fascinating components since they hold out the prospect for the preparation of hydrophilic poly(ester)s, which have rarely been described so far. In view of the fact that the hydroxyl group can act as initiator in combination with most catalysts in ROP of lactones and cyclic carbonates, this functionality needs to be protected during the synthesis of linear poly(ester)s. Generally, this strategy would allow access to polyfunctional, hydrophilic, and degradable polymers (Scheme 1, top). Alternatively, polymerization without such a protecting group yields hyperbranched structures exhibiting unique and fascinating properties (Scheme 1, bottom). This concept of an initiating inimer has already been applied successfully in Chapter 2.3.
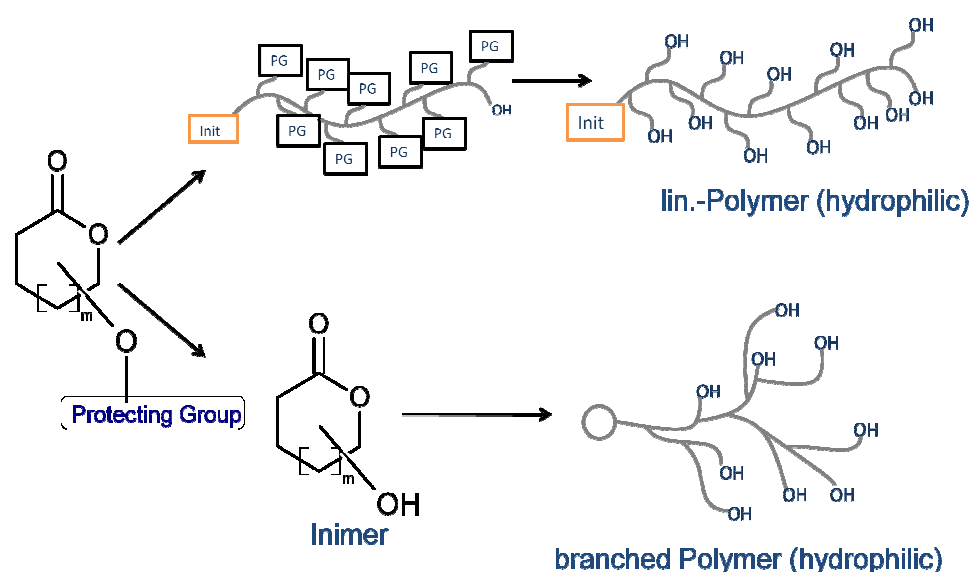
Scheme 1: A lactone with protected hydroxyl group as versatile building block for linear and branched poly(ester)s (PG = Protecting Group).

The most crucial parameter regarding the definition and the degree of branching of the resulting polymer is the inimers balance between rate of initiation and propagation. Lactone based inimers are slightly more complex in design and synthesis, unlike, e.g., functional vinyl-based inimers for SCVP where the molecular separation of the two reactive groups allows for a simple fine-tuning of the rate ratio by selecting the respective components from a "molecular toolkit". The initiating substituent and the site of polymerization, i.e., the cyclic lactone frame, are strongly intertwined. The conspicuous absence of systematic studies on inimer reactivities in ROMBP has prompted us to synthesize and investigate new hydroxyl functional lactones and carbonates. Futhermore, a systematic comparison between branched and linear polymers should be interesting. Therefore, the synthesis of linear poly(ester)s and poly(carbonate)s from protected inimer precursors will also be addressed.

Bis(hydroxymethyl) glycolide

During the search for an interesting inimer system applicable in the ROMBP copolymerization of lactide, the concept of a hydroxyl functional lactide derivate emerged. Ever since, realization was only pursued *en passant* since the original project was conducted with the readily available 5HDON lactone inimer (see chapter 2.3). A lactide derivative with a benzyloxy-protected hydroxyl group had been realized in 2006 bei Leemhuis *et. al.*[1] as well as the group of Collard[2]. This approach uses 2-bromopropionyl bromide as coreactant of the α-hydroxyl acid and thus allows for a two step cyclization via 1) dimerization via esterification and 2) lactonization by replacement of the α-bromine. However, we soon realized that bis(hydroxymethyl) glycolide would be best accessible via a partially protected glycerol acid used in the above mentioned works via the acid catalyzed dimerization in organic media at low concentration. Leemhuis *et al.*[1] as well as Gerhardt *et al.*[2] used 3-benzyloxy-2-hydroxy-propionic acid, which was obtained from the expensive, enantiomerically pure, *O*-benzyl-serin via a diazotation strategy. Hence, we were looking for an alternative pathway to the α–hydroxyl acid which allows for a less expensive scale-up of this important building block. We adapted a synthetic procedure from Zwick and coworkers (from 1958)[3] and obtained the hydroxyl acid from 2-bromo-3-benzyloxy-proponic acid (semi

concentrated potassium carbonate solution, reflux, 4 h) in a multi 100 gr. scale (Scheme 1, top).

In 2008, Collard and coworkers[4] published the synthesis of the desired 3,6-(benzyloxymethyl)-1,4-dioxane-2,5-dione, which had also been realized by us at this time. In addition, they demonstrated the successful copolymerization with lactide and the subsequent deprotection (PdC/H$_2$) and functionalization with biotin via maleinic acid anhydride. However, the comonomer concentration did not exceed 5 mol%. Neither homopolymerization nor polymerization after removal of the protecting groups from 3,6-(benzyloxymethyl)-1,4-dioxane-2,5-dione (i.e., as inimer) were investigated in this publication.

Scheme 2: Synthesis of 3,6-(benzyloxymethyl)-1,4-dioxane-2,5-dione via 3-benzyloxy-2-hydroxy-propionic acid (IV.1)

3,6-(Benzyloxymethyl)-1,4-dioxane-2,5-dione

Racemo - Compounds

Meso - Compound

314
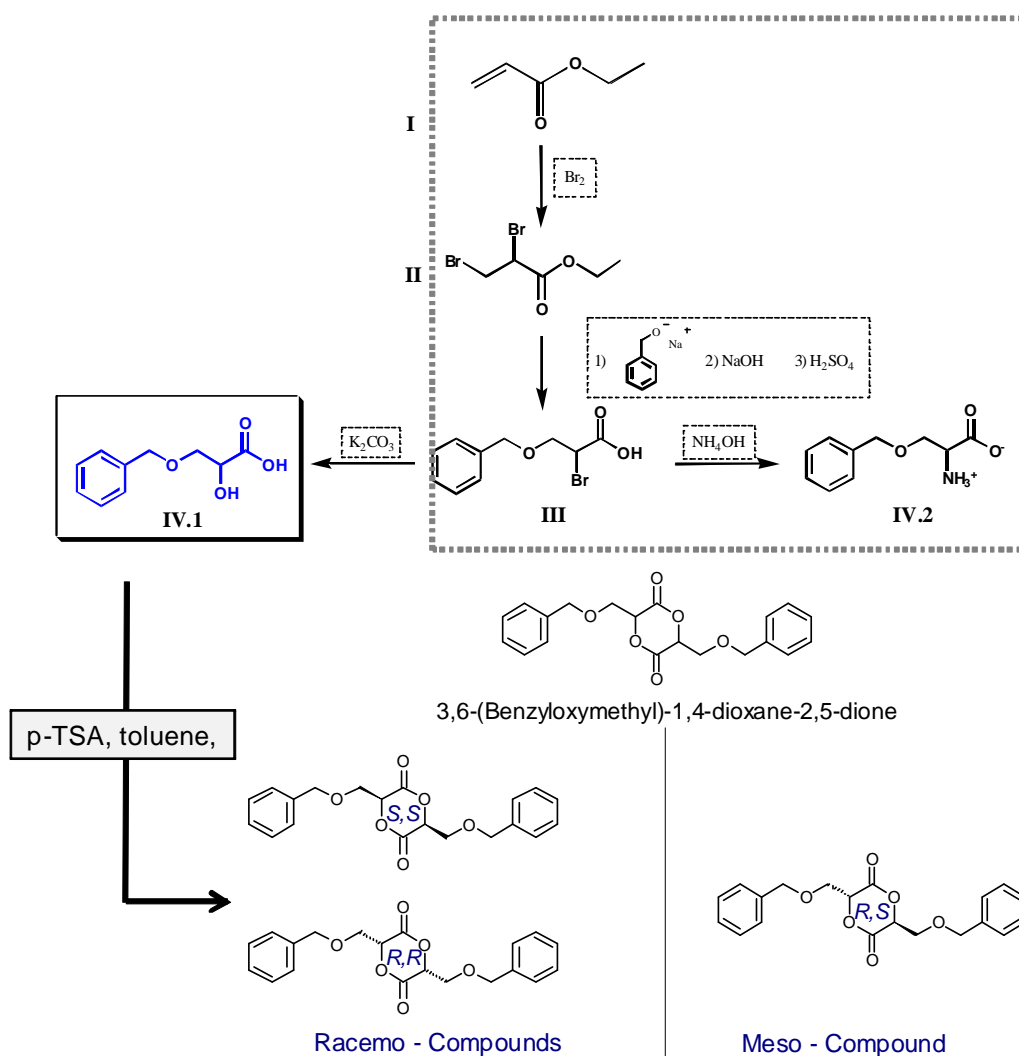
After realization of 3,6-(benzyloxymethyl)-1,4-dioxane-2,5-dione from a racemic mixture of 3-benzyloxy-2-hydroxy-propionic acid (Scheme 2, bottom), cyclocondensation in a dilute toluene solution afforded a mixture of the *racemo* and the *meso* compound. Subsequent neutralization and extraction with sodium hydrogen carbonate yielded the crude product.

The purification of the monomers was significantly aggravated by a side product which could be related to educt contamination with benzyl alcohol. It could be identified as 3-benzyloxy-2-hydroxy-benzyl propionate (Figures 1 & 2). Purification was further pursued via column chromatography. Two different eluents were tested on silica plates:

1. Hexanes 18/EtAc 2: RF_{racemo}: 0.27 , RF_{meso}: 0.18 , $RF_{contam.}$: 0.29

2. Benzene 19/EtAc 1: RF_{racemo}: 0.29 , RF_{meso}: 0.20 , $RF_{contam.}$: 0.19
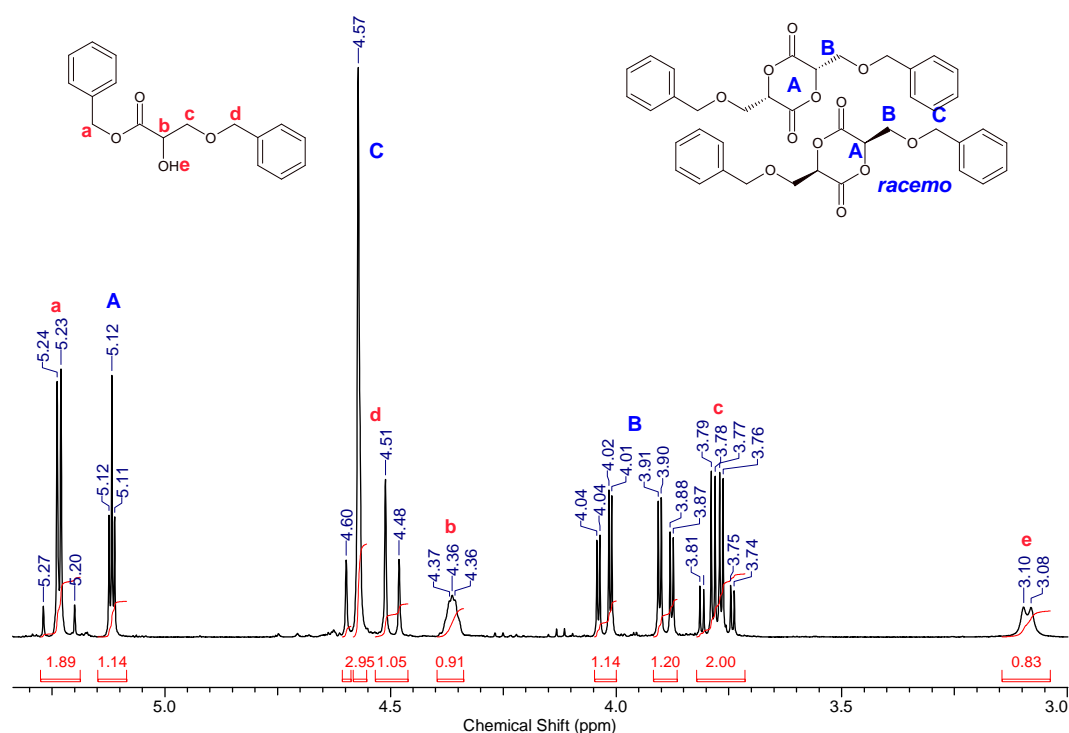
Figure 1: ^{1}H NMR spectrum (CDCl$_3$, 400 MHz) of a mixture of the contamination (3-benzyloxy-2-hydroxy-benzyl propionate) and the *racemo*-lactone.

NMR spectrometry of the fractionated crude product confirmed its assumed composition. The first relevant fractions contain a mixture of the 3-benzyloxy-2-hydroxy-benzyl propionate and the *racemo* compound. The structure/signal assignment of Figure 1 was validated via a ^{1}H,^{1}H COSY NMR experiment (Figure 2).
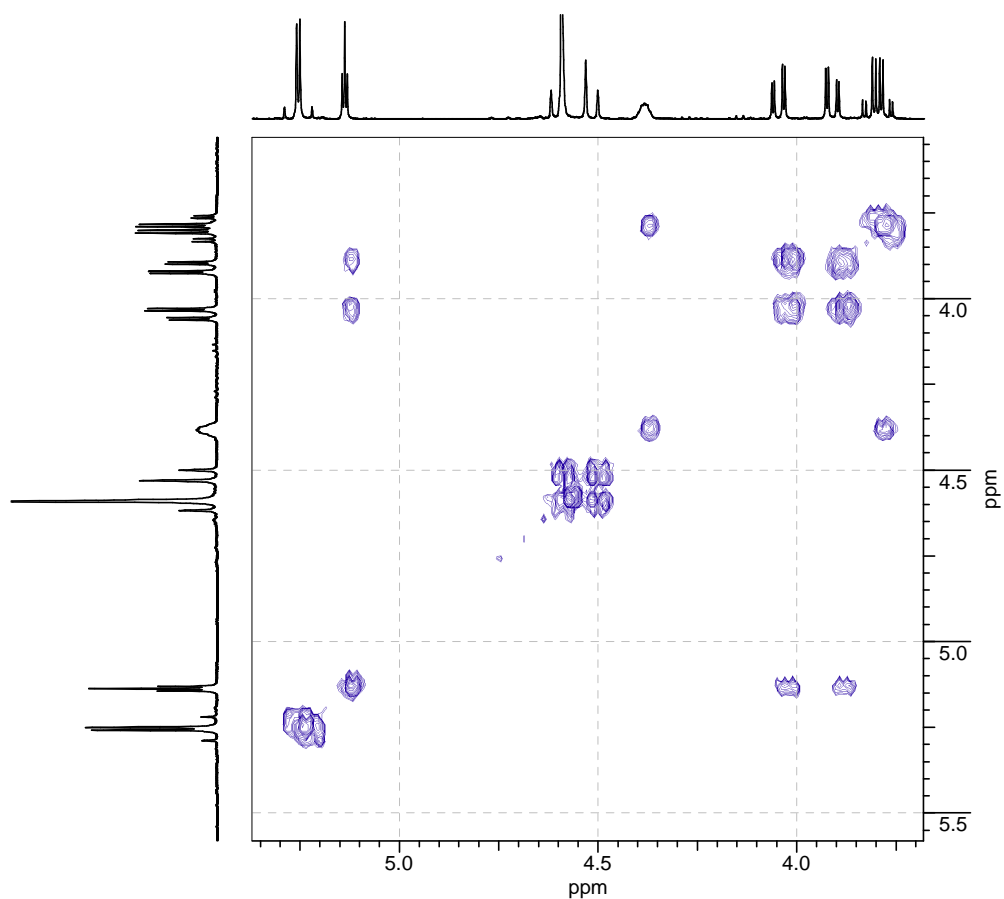
Figure 2: ^{1}H,^{1}H COSY NMR spectrum (CDCl$_3$, 400 MHz) of a mixture of the contamination (3-)and the *racemo*-lactone.
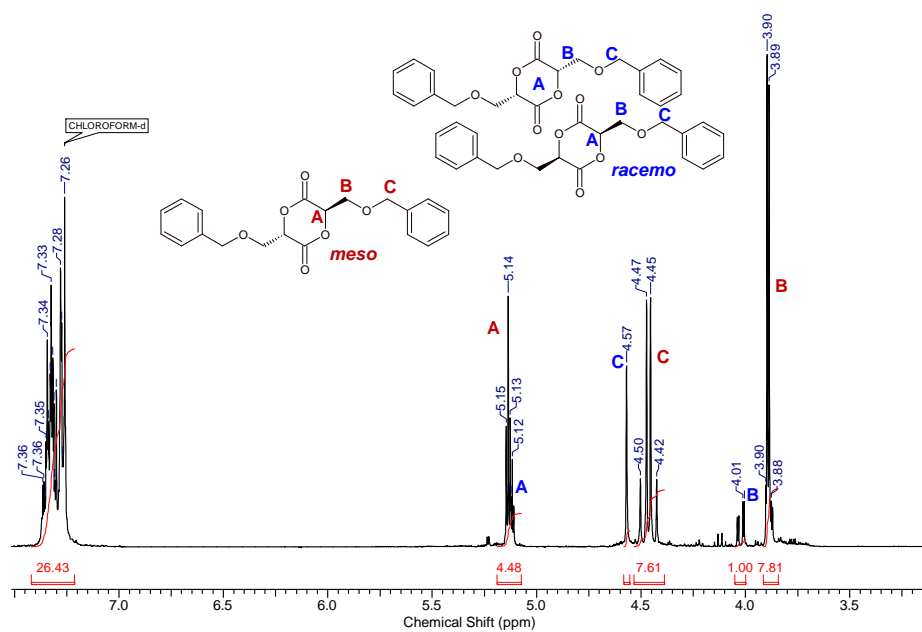

Figure 3: ^{1}H NMR (CDCl$_3$, 400MHz) a mixture of the *meso* and the *racemo* diasteromers (obtained from column chromatography: mid fraction).
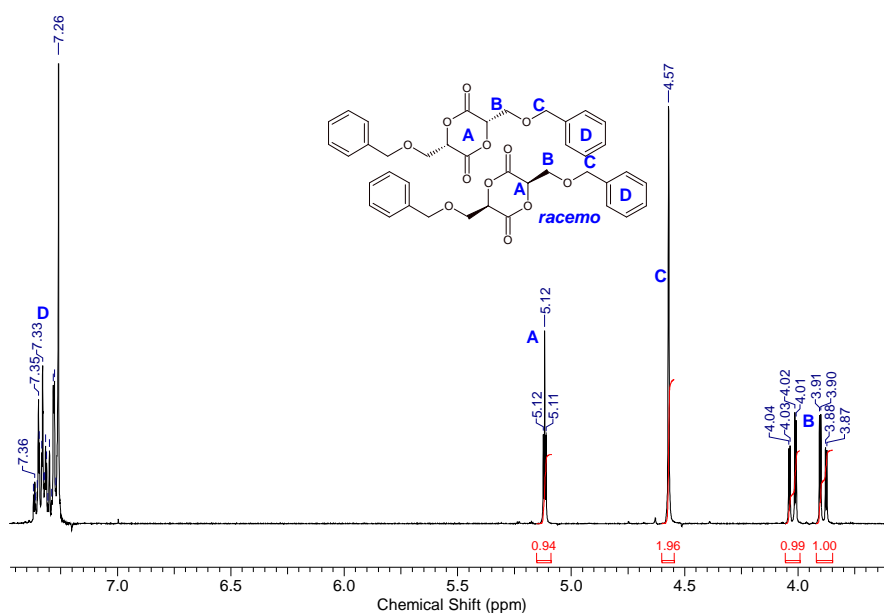
Figure 4: ^{1}H NMR (CDCl₃, 400MHz) of the pure racemo compound, obtained via crystallization from ether/hexanes.

While the *racemo* compound (*R,R* and *S,S*) eluted ahead of the *meso* compound the contamination either co-eluted with the *racemo*, or the *meso* compound, depending on the composition of the eluent. After separation from the crude reaction products, crystallization from diethylether/hexanes (2:1) at 4 °C exclusively afforded the *racemo* compound in high purity (Figure 2) (total yield: 8 %; mp = 55.2 °C, compared to a mp = 70.2-73.2 °C for the pure *S,S* enatiomer as determined by Collard *et al.*[4]).
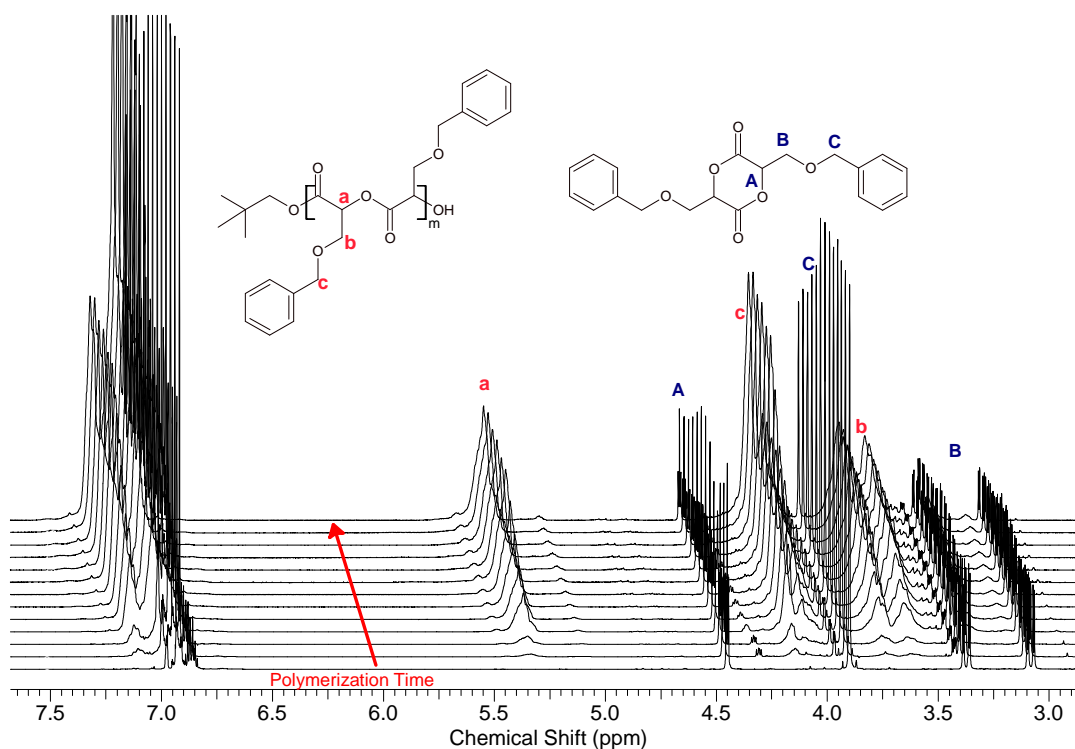
Figure 5: Collected ^{1}H NMR (400 MHz, benzene-d_6) spectra for the ROP of *rac*-3,6-(benzyloxymethyl)-1,4-dioxane-2,5-dione M(50):I(1):C(2) with DBU.
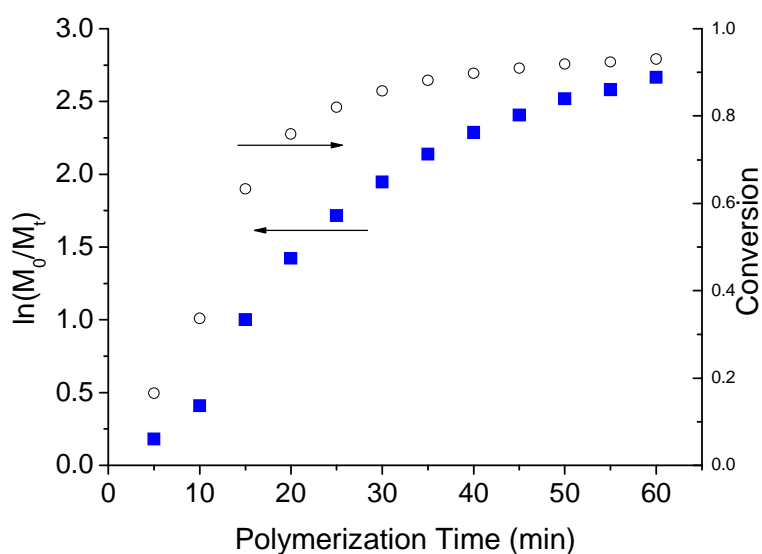

Figure 6: Kinetic plot as derived from ^{1}H NMR measurements.

Polymerization

In order to evaluate the general reactivity of the monomer/catalyst system (DBU) a preliminary kinetic study was conducted. Especially the large benzyloxymethyl substituent attached to the dioxanone scaffold could significantly hamper the monomer/catalyst interaction. ROP experiments conducted with other substituted glycolide derivatives seemed to be promising.[5,6,7] However studies on the polymerization of glycolides with sterically demanding substituents via solution polymerization with organocatalysts have not been reported yet. Hence we examined the ROP via polymerization under NMR observation in benzene-d_6 with isopentyl-alcohol as initiator in a total stoichiometry of monomer(40):initiator(1):catalyst(2) ($m_M = 50$ mg) at room temperature. Polymerization was initiated by injection of a DBU solution in benzene-d_6. Spectra were collected in 5 minute intervals with four scans per spectrum within 1h after initiation. Polymerization proceeded rapidly within this time frame and a total conversion of 93% was reached (Figure 6).

Polymerization kinetics appear to be of first order in respect to the monomer. However, flattening of the curve for high conversions is a typical characteristic for the increasing reversibility of the poly(ester) formation. SEC analysis of the NMR sample of the

318

poly(benzyloxy lactide) (after quenching with benzoic acid) revealed a relatively broad molecular weight distribution (Figure 7) and a significant underestimation of molecular weight compared to the adjusted monomer/initiator ratio (40:1).
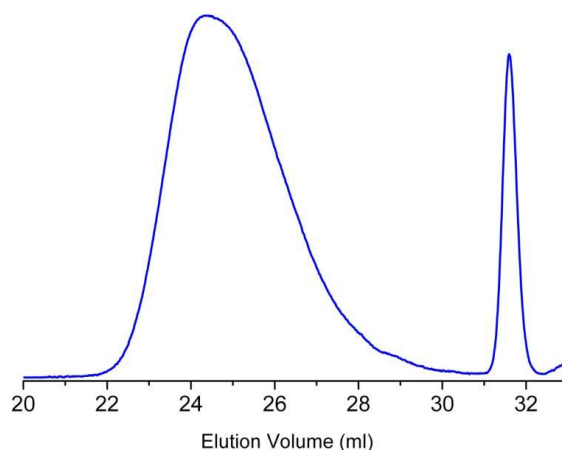

Figure 7: SEC in THF (PS standards) reveals a broad molecular weight distribution as well as residual monomer (Mn = 5500, PDI = 1.55). HPLC evaluation of this RI trace gave a conversion of 89.5%.

Further analysis via MALDI-ToF spectrometry revealed the presence of cycles as well as two different linear species with neopentyl **(B)** and benzyloxy-2-hydroxy-benzyl propionate **(C)** endgroups[*] (α-chain end) (Figure 8). The high intensity of the peaks attributed to the cyclic species is most likely caused by a structural effect as well as a mass discrimination effect. Thus it does not represent the quantitative composition of the sample. This overestimation of cyclic, compared to linear species can be explained by their reduced tendency towards chain entanglement, which generally hampers a good ionization of polymers im MALDI-ToF MS. Their desorption/ionization is thus highly favored in comparison to the linear analogs.[†] However, the presence of transesterification reactions is indicated by a balanced ratio of chains with odd and even numbers of 3-benzyloxy-2-hydroxypropionic acid repeat units (Figure 8). The presence of endgroup **C** can be attributed to monomer contamination with 3-

---

[*] With mass spectrometry poly(benzyloxymethyl glycolide) carrying the 3-benzyloxy-2-hydroxy-benzyl propionate is not distinguishable from that functionalized with plain benzylalcohol. This is due to the fact that a subunit of it corresponds to the smallest repeat unit in the polymer chain.

[†] In general, many studies which report high cyclic fractions obtained from thermodynamically controlled (or at least influenced) polymerizations (i.e. polycondensation and ring-opening polymerization) exclusively settle their quantitave evaluation on mass spectrometric evidence. The possibility of a highly different desorption/ionization behavior of the cyclic and non cyclic species is hardly considered. (e.g. works by Kricheldorf et. al.).

benzyloxy-2-hydroxy-benzyl propionate which was obviously not completely removed by the crystallization step described above. However, this problem should be readily overcome by the use of pure 3-benzyloxy-2-hydroxypropionic acid in monomer synthesis.

Purification of the polymer was conducted successfully via precipitation from methanol and collection via centrifugation (yield: 38 mg).
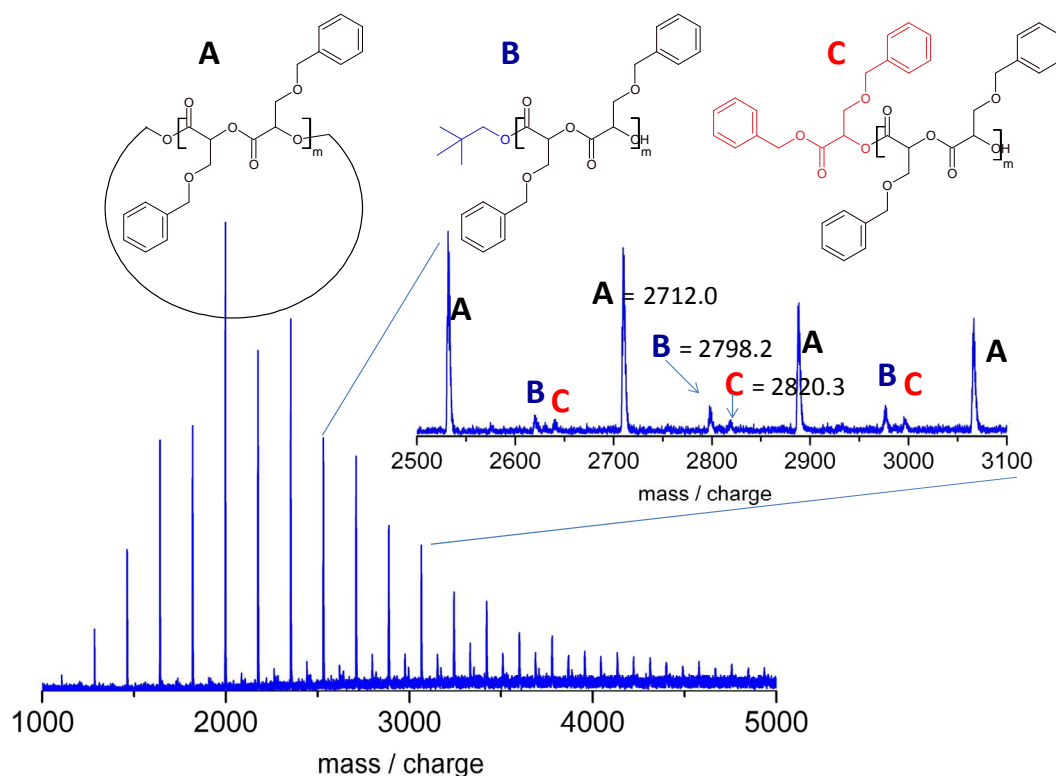

Figure 8: MALDI-ToF spectrum (Matrix: Dithranol) of the 60 minute sample of the kinetic investigation. Potassium adducts of cyclic **(A)** as well as linear poly(benzyloxy lactide) with neopentyl **(B)** and 3-benzyloxy-2-hydroxy-benzyl propionate **(C)** endgroups.

Benzyl Ether Cleavage

Collard *et al.*[4] reported the successful cleavage of the benzylether in poly(lactide) polymers containing small amounts of 3,6-(benzyloxymethyl)-1,4-dioxane-2,5-dione repeat units. In a first test we subjected the prepared poly(benzyloxy lactide) sample (38 mg) to a similar catalytic hydrogenation procedure (15 mg Pd/C in 2,5 ml THF-d_8). Subsequent MALDI-ToF MS and NMR spectroscopy (Figure 9) revealed full deprotection of the benzylether groups, accompanied by the release of the poly(glycerol acid) structure. MALDI-ToF MS confirmed

the retention of the cyclic nature of the low molecular weight fraction (Figure 10). Further testing was not conducted due to the small reaction scale.
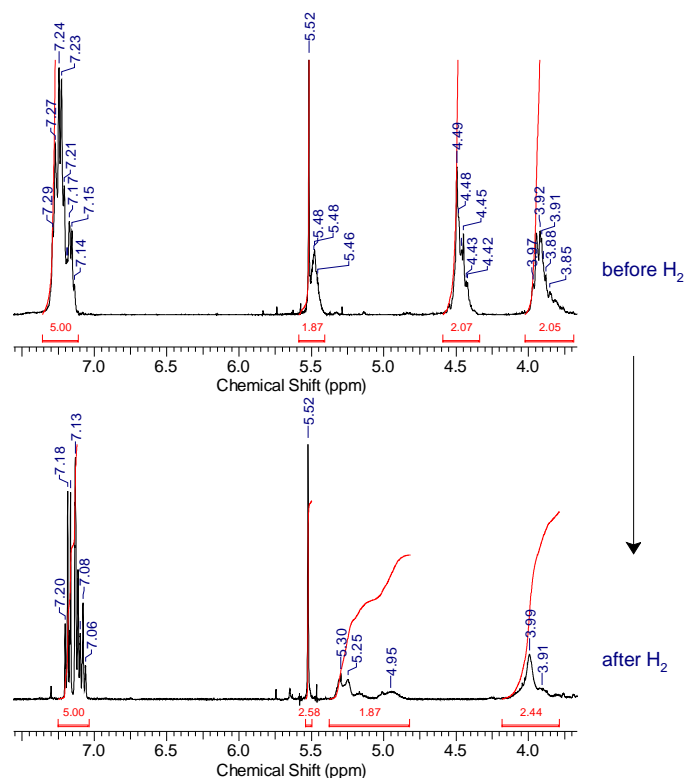

Figure 9: ^{1}H NMR spectra (400 MHz, THF-d_8) before (top) and after (bottom) hydrogenolytic cleavage of the benzylether groups.
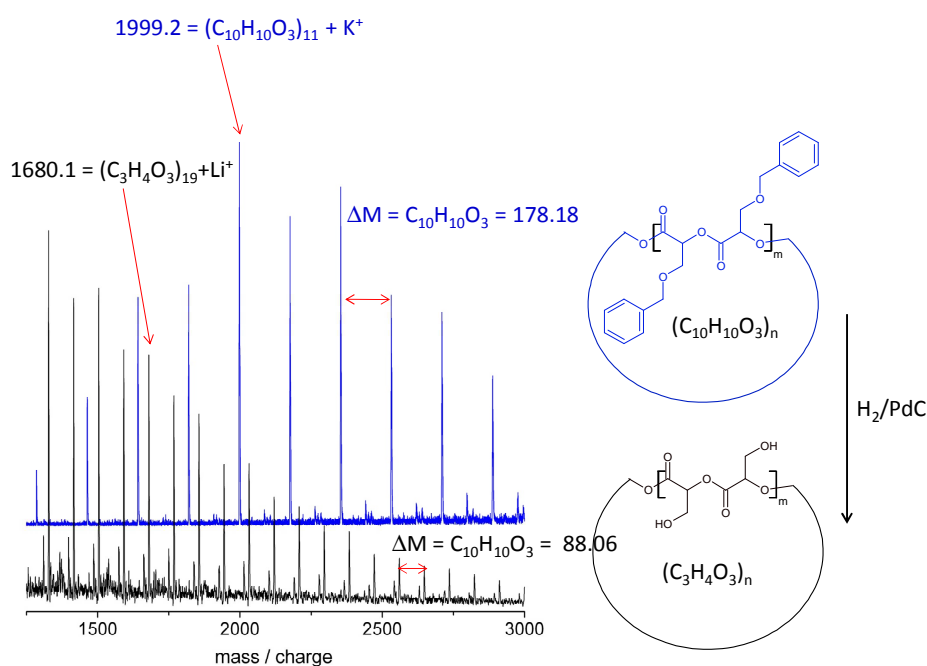

Figure 10: MALDI-ToF MS spectra collected before (top, blue) and after hydrogenation (bottom, black). The dominant distribution reflects the cyclic, low molecular mass fraction of the sample.

The disappearance of the neopentyl terminated species in the MALDI-ToF MS spectrum can be explained by a peak superposition with cyclic structures (Figure 10), e.g., $(C_3H_4O_3)_{29}$ Li^+ (2560.8 g/mol) $\approx C_5H_{10}O(C_3H_4O_3)_{28}$ Li^+ (2558.8 g/mol). Because of an average half width at full maximum of 3.5 g/mol, the minor component (i.e. the neopenty alcohol terminated species) cannot be detected separately.

Conclusions and Future Work

To date, we have succeeded in the preparation of 1,2-connected poly(glycerol acid). This polymer represents a new member of the scarce species of hydrophilic poly(ester)s. It was realized by preparation and successful homopolymerization of 3,6-(benzyloxymethyl)-1,4-dioxane-2,5-dione, which we refer to as bis(benzyloxymethyl) glycolide. Minor problems in monomer and polymer purity are related to benzyl alcohol contamination in the lactone formation step. A higher purity of the starting component 3-benzyloxy-2-hydroxy-propionic acid should guarantee higher monomer yields. Since this linear polymer structure is a highly promising candidate for medical applications, biocompatibility and degradability characteristics should be examined.

Scheme 3: Targeted deprotection of bis(benzyloxymethyl) glycolide to bis(hydroxymethyl) glycolide and possible isomerization products.
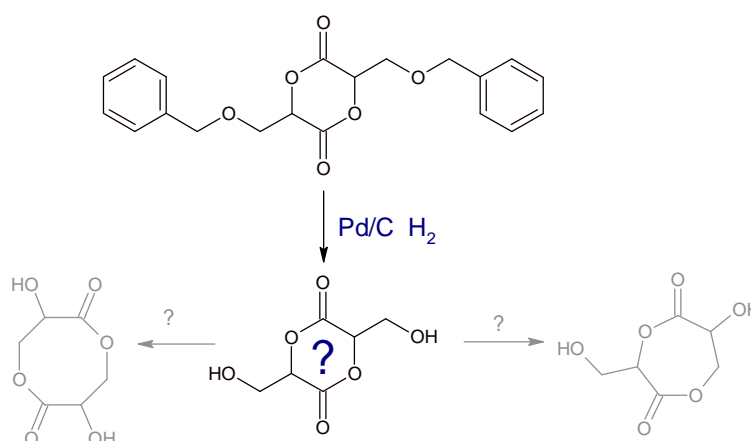

A key issue will represent the deprotection of bis(benzyloxymethyl) glycolide to bis(hydroxymethyl) glycolide (Scheme 3). Especially the danger of isomerization into another, non-strained lactone form has to be evaluated during the investigation of the inimers' potential in ROMBP.

1,3-Glycerol Carbonate

As pointed out in chapter 1, cyclic six-membered carbonates are highly interesting precursors to biodegradable polymers. Compared to lactones, they are more amenable towards functionalization since cyclization of 2-substituted 1,3-diols affords the product in high yields. The functional group is localized at the most distant point from the carbonate moiety and polymerization kinetics are less dependent on the substituent's size. Hence, the introduction of hydroxyl groups or their precursors represents an interesting alternative to lactone-based inimers. Up to now, only one example for a six-membered cyclic carbonate inimer has been described in the literature: 5-{3-[(2- hydroxyethyl)thio]propoxy}-1,3-dioxan-2-one has been successfully applied for the ROMBP of a hyperbranched poly(carbonate) by Rockiki and co-workers.[8]

In principle, a simpler cyclic carbonate inimer is imaginable: 5-Hydroxy-1,3-dioxan-2-one (1,3-glycerol carbonate). However, a straightforward synthesis is impossible since a simple reaction of glycerol and alkylcarbonates or phosgene derivates would yield a crude product mixture with the thermodynamic stable 1,2-carbonate. If used in slight excess, dimethylcarbonate allows the fabrication of pure 1,2-carbonate, as shown by Rockiki *et. al.*[9] Due to its low ring strain, this isomer is not a suitable candidate for ROP.

Scheme 4: Synthesis of 5-benzyloxy- 1,3-dioxan-2-one as described by Grinstaff.
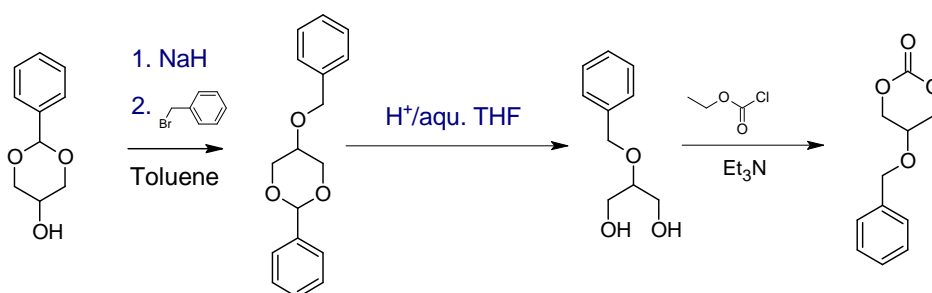
In 2003, Grinstaff et al. realized linear poly(glycerol carbonate)s by ring-opening polymerization of a benzyloxy protected 1,3 glycerol carbonate (5-benzyloxy- 1,3-dioxan-2-one) and subsequent cleavage of the benzyl ether via catalytic hydrogenation (Scheme 4). The protecting group prevents coinitiation during ROP and strictly linear poly(carbonate)s are obtained.

However, deprotection of the monomer prior to polymerization and its subsequent use as latent AB$_2$ monomer has not been investigated yet. The perspective of highly biocompatible hyperbranched polycarbonate prompted us to do so. As pointed out in Chapter 2.3 and supported by theoretical studies by Müller et al., the reactivity ratio between initiation and propagation is highly interesting in terms of polydispersity[10] and degree of branching[11]. The combination of a secondary alcohol with a reactive carbonate ring should very interesting in comparison to 5-hydroxymethyl 1,4- dioxin-2-on (5HDON), which was investigated in chapter 2.3.

However, isolation and stability of the 1,3 –glycerol carbonate had to be ensured first. 5-Benzyloxy- 1,3-dioxan-2-one could be deprotected by catalytic hydrogenation (PdC/H$_2$, 7 bar in THF) without the appearance of the 1,2-isomerization product. Grinstaff et al. used Sn(Oct)$_2$ as catalyst for the polymerization of 5-benzyloxy- 1,3-dioxan-2-one. In order to evaluate a sufficient activity of the organo base DBU towards this carbonate, we conducted a basic kinetic study via polymerization in an NMR tube (CD$_2$Cl$_2$, room temperature). Conversions at 20 and 150 minutes were measured and 89% were reached within this time frame (Figure 11).
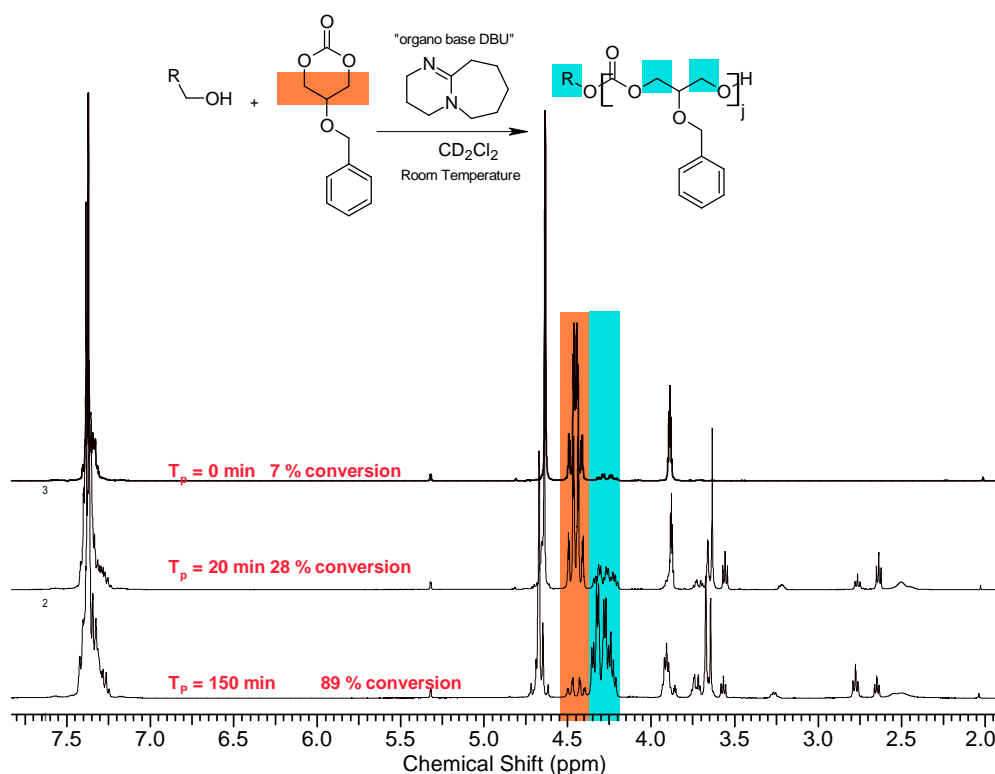

Figure 11: Basic ^{1}H NMR study of the polymerization of 5-benzyloxy- 1,3-dioxan-2-one (400 MHz, CD$_2$Cl$_2$).

A preliminary polymerization attempt was conducted under NMR surveillance in THF-d_8 using a 1 wt. % loading of DBU as transesterification catalyst (Figure 12). A complete isomerization of the 1,3-glycerol carbonate into the 1,2-form could be observed within a time frame of approx. 13 minutes (residual 1,3 monomer content < 0.4%). Clues of a successful polymerization could not be found.
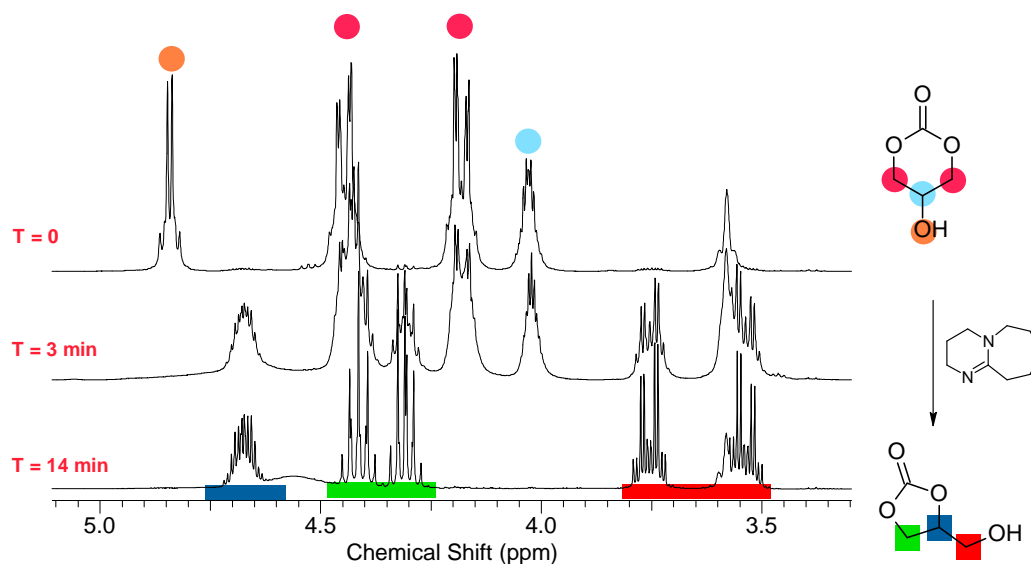

Figure 12: Isomerization of 1,3-gylcerol carbonate into the 1,2-form in the presence of 1 wt. % of DBU (RT, THF-d_8 at 400 MHz)

Future Work

The exploration of 1,3-glycerol carbonate has to be pursued. Other catalyst and reaction conditions should be in the focus of interest. However, isomerization to the energetically favoured 1,2-form in the presence of a transesterification catalyst is not surprising. The success of the ROMBP will significantly depend on the balance between the rate constants $k_{initiation}$, $k_{isomerization}$ and $k_{propagation}$.

Scheme 5: Possible reaction pathways of 1,3-Carbonate in the presence of lactide as comonomer.
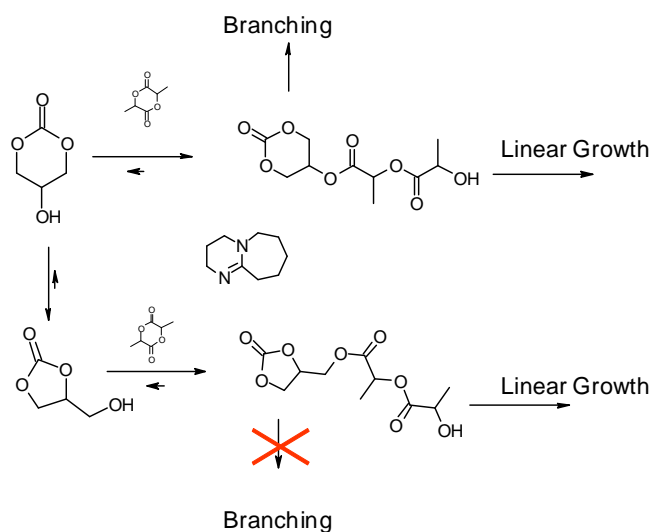
Especially the copolymerization with lactones could be highly interesting to prevent isomerization. This scenario is depicted in the upper section of Scheme 5. A fast intiation ($k_{initiation,}$ > $k_{isomerization}$) with a highly reactive comonomer such as glycolide or lactide would "cap" the hydroxyl group and thus prevent isomerization (Scheme 5). This strategy could be supplemented by the slow addition of comonomer.

References

[1] Leemhuis, M.; van Nostrum, C. F.; Kruijtzer, J. A. W.; Zhong, Z. Y.; ten Breteler, M. R.; Dijkstra, P. J.; Feijen, J.; Hennink, W. E. *Macromolecules* **2006,** *39,* 3500-3508.

[2] Gerhardt, W. W.; Noga, D. E.; Hardcastle, K. I.; Garcia, A. S.; Collard, D. M.; Weck, M. *Biomacromolecules* **2006,** *7*, 1735-1742.

[3] Grassmann W.; Wünsch, E.; Deufel, P.; Zwick, A. *Chemische Berichte-Recuil* **1958**, *93*, 538-541.

[4] Noga, D. E.; Petrie, T. A.; Kumar, A.; Weck, M.; Garcia, A. J.; Collard, D. M. *Biomacromolecules* **2008**, *9,* 2056-2062.

[5] Jiang, X.; Vogel, E. B.; Smith III, M. R.; Baker. G. L. *J. Polym. Sci. A: Polym. Chem.* **2007,** *45*, 5227–5236.

[6] Jing, F.; Smith, III, M. R., Baker, G. L. *Macromolecules* **2007,** *40,* 9304-9312.

[7] Jiang, X.; Smith III, M. R.; Baker, G. L. *Macromolecules* **2008,** *41,* 318-324.

[8] Parzuchowski, P. G.; Jaroch, M.; Tryznowski, M.; Rokicki, G**.** *Macromolecules* **2008**, *41*, 3859-3865.

[9] Rokicki, G.; Rakoczy, P.; Parzuchowski, P.; Sobiecki, M.; *Green Chem.* **2005**, *7*, 529–539.

[10] Müller, A.H.E.; Yan, D.; Wulkow, M. *Macromolecules* **1997**, *30,* 7015-7023.

[11] Yan, D. Y.; Müller, A. H. E.; Matyjaszewski, K. *Macromolecules* **1997,** *30*, 7024–7033.

Appendix

A.1: Curriculum Vitae

A.2: List of Publications

Journal Articles

1) High Aspect Ratio Surface Relief Structures by Photoembossing
Ko Hermans, <u>Florian K. Wolf</u>, Jolke Perelaer, Rene A. J. Janssen, Ulrich S. Schubert, and Cees W. M. Bastiaansen, *Applied Physics Letters* **2007**, *91*, 174103 (1-3)

2) Multi-Arm Star Poly(L-lactide) with Hyperbranched Poly(glycerol) Core
Carsten Gottschalk, <u>Florian K. Wolf</u>, Holger Frey**,** *Macromolecular Chemistry and Physics* **2007**, *208*, 1657–1665

3) Poly(lactide)-*b*-Poly(HEMA) Block Copolymers: An Orthogonal One-Pot Combination of ROP and ATRP, Using a Bifunctional Initiator
<u>Florian K. Wolf</u>, Nora Friedemann, Holger Frey, *Macromolecules* **2009**, *42*, 5622–5628

4) Inimer-Promoted Synthesis of Branched and Hyperbranched Poly(lactide) Copolymers
<u>Florian K. Wolf</u> and Holger Frey, *Macromolecules* **2009**, *42*, 9443–9456

5) Poly(isoglycerol methacrylate)-*b*-Poly(lactide) Copolymers: A Novel Hydrophilic Methacrylate as Building Block for Supramolecular Aggregates
<u>Florian K. Wolf</u>, Anna M. Hofmann, Holger Frey, *Macromolecules* **2010**, *43,*3314-3324

6) Polymilchsäure – ein Vielseitiges Material für Anwendungen in der Medizin
<u>Florian K. Wolf</u>, Holger Frey *Natur und Geist –Das Forschungsmagazin der Johannes Gutenberg-Universität Mainz* **2010***, 26* (1)*,* 12-16

7) Synthesis, Characterization and Evaluation of P(HPMA)-*block*-P(LLA) Copolymers: A New Type of Functional Biocompatible Block Copolymer
Matthias Barz, <u>Florian K. Wolf</u>, Fabiana Canal, Kaloian Koynov, Maria J. Vicent, Holger Frey, Rudolf Zentel, *Macromolecular Rapid Communications* **2010***, in press*

8) Hyperbranched Poly(glycerol) with Poly(glycolide) Corona: Improving Solubility by Limiting Chain Length
<u>Florian K. Wolf</u>, Anna M. Fischer Holger Frey *Beilstein Journal of Organic Chemistry* **2010**, *accepted*

9) pH-Responsive Aggregates of Amphiphilic Block Copolymers Based on Poly(ethylene glycol) and Poly(*cis*-1,3-benzylidene glycerol methacrylate)
<u>Florian K. Wolf</u> and Holger Frey, *submitted*

10) Synthesis of Hyperbranched Poly(D,L-lactide)s by Self-Condensation of AB$_2$-Macromonomers
Anna M. Fischer, <u>Florian K. Wolf</u>, Holger Frey, **2010**, *in preparation*

A.3: Conference Contributions

Synthesis of Hyperbranched Poly(lactide)s by Self Condensing Ring-Opening Branching Polymerization
Florian K. Wolf, Holger Frey, *Polymer Preprints of the 235th ACS National Meeting,* New Orleans*, USA*, **2008**

Poly(lactide)-*b*-Poly(HEMA) Block Copolymers: An Orthogonal One-Pot Combination of ROP and ATRP, Using a Bifunctional Initiator
Florian K. Wolf, Holger Frey, *Frontiers in Polymer Science,* Mainz*, Germany* **2009**

Poly(isoglycerol methacrylate)-*b*-Poly(lactide) Copolymers: New Block Copolymers for Biomedical Applications
Florian K. Wolf, Anna M. Hofmann, Holger Frey *APME-Conference,* Dresden*, Germany* **2010**